J. exp. Biol. **117**, 181–191 (1985)
Printed in Great Britain © *The Company of Biologists Limited 1985*

OCULOMOTOR FUNCTION AT LOW TEMPERATURE: ANTARCTIC *VERSUS* TEMPERATE FISH

J. C. MONTGOMERY AND J.A. MACDONALD
Department of Zoology, University of Auckland, Auckland, New Zealand

Accepted 4 December 1984

SUMMARY

The peripheral oculomotor system can be modelled as a first order linear system (Montgomery, 1983), and hence specified by its characteristic frequency and 'd.c.' gain. These parameters can be determined by recording eye movements produced by stimulation of the abducens nerve with sinusoidally modulated pulse trains, and compare well with those independently derived from the relationship between motoneurone firing and spontaneous eye movement. Characteristic frequency and gain of the peripheral oculomotor system were determined for two species of antarctic teleost and one temperate species, to examine temperature compensation within a complete motor output pathway. Compared with low temperature function in temperate fish, the characteristic frequency is clearly temperature compensated in antarctic fish, which explains in part the observed temperature compensation of their rapid eye movement. The 'd.c.' gain of the peripheral oculomotor system is inversely related to temperature, providing an automatic compensation for possible reductions in central nervous system output and sensory gain at low temperature.

INTRODUCTION

For several million years antarctic fish have inhabited the world's coldest marine environment, where the mean annual sea temperature is as low as $-1{\cdot}9\,^{\circ}C$ (Littlepage, 1965). For a temperate fish, cooling to this degree would be lethal; even if the body fluids remained supercooled and did not freeze, CNS motor programmes would cease (respiration: Friedlander, Kotchabhakdi & Prosser, 1976; eye movement: Montgomery, McVean & McCarthy, 1983), peripheral nerve conduction would fail (Macdonald, 1981) as would muscle function (McCarthy, 1982), and the activity of many enzyme systems would be drastically reduced (Clarke, 1983). The ability of antarctic fish to survive at $-1{\cdot}9\,^{\circ}C$ depends on a range of adaptations which enable their vital systems to function. For example, their body fluids are prevented from freezing by an antifreeze component (DeVries, 1980) and the activity of many of their biochemical systems is partially temperature compensated. That is: the activity of these systems exceeds their activity in temperate species lowered to near freezing, but does not match that of temperate fishes at warm temperature (see Clarke, 1983).

Key words: Antarctic fish, oculomotor system, temperature.

Cold adaptation of enzymes and membranes occurs in the nervous system, allowing adequate function of the neuronal elements (Prosser & Nelson, 1981). In antarctic fish, there is temperature compensation of both peripheral nerve conduction (Macdonald, 1981) and neuromuscular function (Macdonald & Montgomery, 1982), though in comparison with temperate fish, obvious functional deficits remain. For example, nerve conduction velocity in antarctic fish is less than half that of temperate fish, and the refractory period of peripheral nerves is around 15–25 ms (Macdonald & Montgomery, 1982). The implications of these differences within the context of a functioning motor control system are explored in this study. The problem addressed is how fish maintain integrated activity at low temperature.

Choice of the oculomotor system for study offers considerable advantages: it is one of the best understood vertebrate motor control systems, eye movements include components of accuracy (visual stabilization) and speed (saccades), and detailed mechanical analyses can be made. It is a system in which the potent techniques of control systems analysis have proved to be particularly useful, and where despite its apparent complexity, a single first order model of the peripheral oculomotor system provides a satisfactory description for most purposes (Robinson, 1981). The parameters of the model can be derived from a study of eye movements elicited by abducens nerve stimulation (Montgomery, 1983), and this approach has been used to quantify the effects of acute temperature change on the oculomotor system (Montgomery & Paulin, 1984). A comparison of the peripheral oculomotor system of antarctic and temperate fish provides the opportunity to study genetically controlled temperature compensation within a complete motor output pathway.

MATERIALS AND METHODS

Experiments were performed on three species of teleost fish. The temperate eurythermal *Girella tricuspidata* was caught in hand nets at night by divers using SCUBA, and kept in tanks of circulating sea water at 24 °C. The two species of antarctic fish, *Pagothenia borchgrevinki* and *Dissostichus mawsoni*, were caught on hand lines in the vicinity of Scott Base (77°51′S, 166°48′E), and experiments were carried out in a fish hut on the sea ice.

In fish anaesthetized with Tricaine, the cranium was opened and the brain removed leaving the stumps of the cranial nerves accessible intracranially (Fig. 1). Bleeding was controlled by cautery, and the fish were maintained in a tank by passing sea water at the appropriate ambient temperature over the gills. The stump of the abducens nerve (cranial nerve VI) was secured in a suction electrode, and the cranial cavity filled with Ringer. Electrical stimuli were trains of supramaximal square wave pulses (0·5 ms, 1·5–2 V). Two types of pulse trains were used to stimulate the nerve: constant frequency trains in the range 0–50 Hz for antarctic fish and 0–200 Hz for *G. tricuspidata*, or trains in which the pulse frequency was sinusoidally modulated at modulation frequencies in the range 0·04–8 Hz.

Eye movements produced by electrical stimulation of the abducens nerve were recorded by an opto-electronic movement detector (Helversen & Elsner, 1977), in which a reflected light spot was focused on a Schott barrier photodiode mounted in

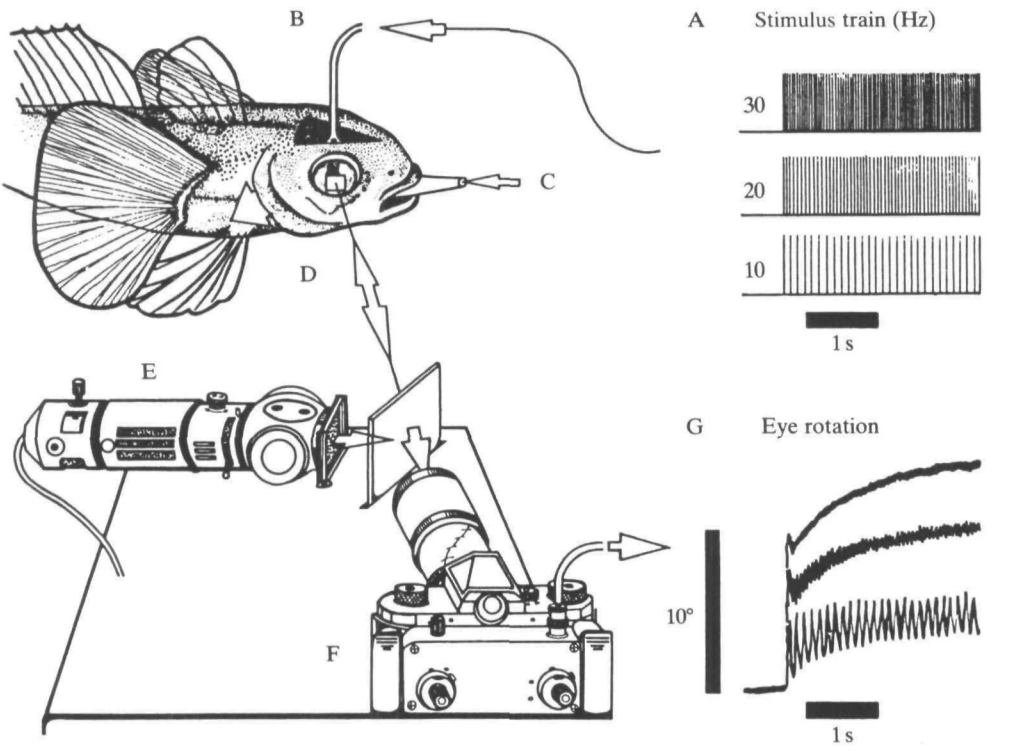

Fig. 1. Experimental procedure. (A) Stimulus pulse trains (0·5 ms, 2 V) were applied to the stump of the VI nerve *via* a suction electrode (B), in a fish (in this case the antarctic fish *Pagothenia borchgrevinki*) from which the brain had been removed, but in which the circulation was still intact and the gills perfused with sea water (C). A retroreflective eye patch was attached to the eye (D) and illuminated (E) through a half-silvered mirror. Eye rotation was recorded by an opto-electronic movement detector mounted in the film plane of a camera (F). (G) Eye movement response to trains of pulses at 10, 20 and 30 Hz.

a single lens reflex camera body. Further details of the method are described elsewhere (Montgomery *et al.* 1983).

The force required to produce and maintain a given eye deviation was measured with a calibrated strain gauge connected to the surface of the eye. Force was applied tangentially to the eye surface to produce a movement in the same plane as that produced by abducens nerve stimulation. Deflection of the eye was measured both with a protractor positioned above the eye and with the opto-electronic movement detector.

These teleost preparations did not show the remarkable stability reported for the carpet shark (Montgomery, 1983). Some preparations exhibited little or no drop in response over the course of an experiment (e.g. Fig. 4), whereas others declined during the long periods of stimulation required for the low frequency sine waves. Gain measurements from such declining preparations were adjusted in proportion to the response to a standard stimulus pulse train. At the conclusion of the experiment good responses were still obtained from other extraocular muscles in the same preparation, indicating that any drop in responsiveness was due to fatigue of the activated muscle.

Table 1. *Eye movement parameters*

	Pagothenia borchgrevinki	*Dissostichus mawsoni*	*Girella tricuspidata*
Temperature (°C)	−2	−2	24
Mean fish size (g)	89	38 000	750
Twitch contraction time (ms)	25	85	•
Mean latency (ms; ± S.D.; $N = 3$)	22 ± 2.9	43 ± 3.6	21 ± 2.3
Gain (slope stimulus response)	0.32	0.6	0.07
Gain [amplitude ratio (× ± S.D.; $N = 3$)	0.35 ± 0.05	0.78 ± 0.15	0.07 ± 0.02
Characteristic frequency (Hz; ± 95 CI)	0.54 ± 0.16	0.56 ± 0.09	1.4 ± 0.2
Elastic coefficient (g per degree)	0.06	1.25	0.02

• No twitch response.

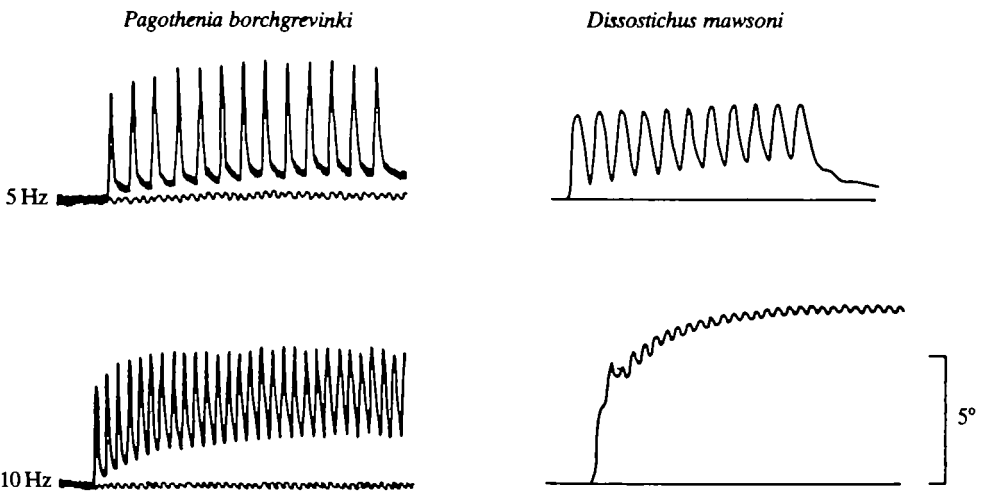

Fig. 2. Eye movement records of *Pagothenia borchgrevinki* and *Dissostichus mawsoni* to supramaximal stimulation of the abducens nerve with constant frequency pulse trains (5 and 10 Hz). Note the slower twitch of *D. mawsoni*, and consequent increased summation at 10 Hz.

RESULTS

The most dramatic difference between antarctic fish and *Girella tricuspidata* was the efficacy of low frequency stimulation at the colder temperature. Single supramaximal pulses in both *Pagothenia borchgrevinki* and *Dissostichus mawsoni* produced large eye movements (Fig. 2). Twitch contraction time, the rate of relaxation and response latency were all longer in *D. mawsoni* (Fig. 2; Table 1). Maximal eye deviation in the antarctic species *P. borchgrevinki* and *D. mawsoni* (about 15° and 20° respectively) was produced at 50 Hz stimulation. In the temperate fish however, single stimulus pulses produced no observable eye movement, and stimulus frequencies of around 50 Hz were required to produce a threshold response (Fig. 3). The eye movement response in this species was still increasing at impulse frequencies of 200 Hz.

In all three species of fish, when eye rotation was plotted as a function of impulse

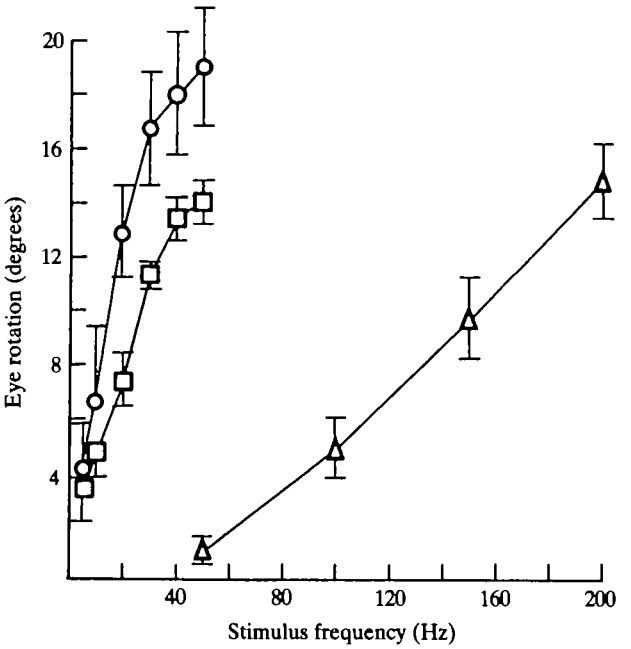

Fig. 3. Stimulus response curves for constant frequency pulse trains. Circles: *Dissostichus mawsoni*; squares: *Pagothenia borchgrevinki*; triangles: *Girella tricuspidata*. Error bars indicate ± S.E.

frequency, there was an approximately linear section of the stimulus response curve, below saturation (Fig. 3). This region corresponds to the natural operating range of the oculomotor system (Montgomery, 1983; Zuber, 1968). The 'd.c.' gain (output/input) of the oculomotor system can be specified by the slope of the stimulus response curve, and was highest in *D. mawsoni* and least in *G. tricuspidata* (Fig. 3; Table 1). A second, independent, estimate of gain can be obtained from the ratio of the amplitude of eye movement to the amplitude of sinusoidal modulation of the stimulus pulse train at low modulation frequencies (e.g. Fig. 5). Estimates of gain derived in this way agreed well with the values determined from the slopes of the stimulus response curves (Table 1).

Pulse trains, sinusoidally modulated between 0 and 40 Hz for antarctic fish and 0–160 Hz for *G. tricuspidata*, were used to determine the frequency response of the oculomotor systems. As modulation frequency was decreased, the resulting eye rotation increased in amplitude, as shown for *G. tricuspidata* (Fig. 4). Maximum and minimum stimulus pulse frequencies were unchanged. The response to a standard constant frequency pulse train preceding each sine wave stimulus remained constant throughout the stimulus sequence in this example.

The sinusoidal nature of the eye movement response to a modulated pulse train in the antarctic fish may be seen with the expanded time scale of Fig. 5. Responses to single stimulus pulses were evident, and the low frequency of the modulating input sine wave allowed direct comparison of the stimulus and response wave forms. Amplitude of the modulated response was determined by averaging the trough-to-peak excursion of a series of modulated cycles.

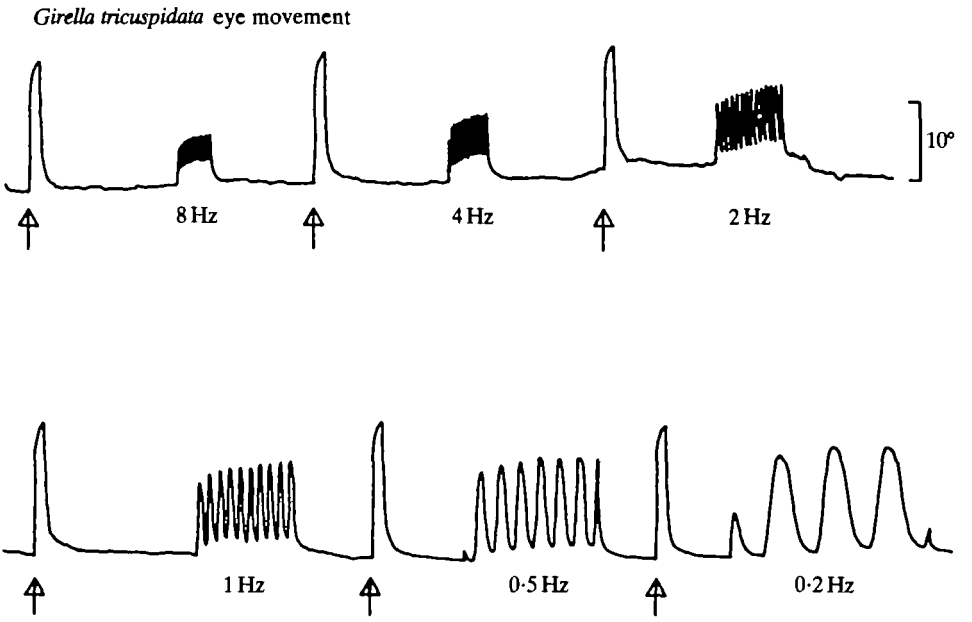

Fig. 4. Eye movement record of *Girella tricuspidata* during presentation of a series of sinusoidally modulated pulse trains. Modulation frequency is shown below each stimulus presentation (peak-to-peak 0–160 Hz in all cases). Arrows mark the onset of a standard 200 Hz, 200 pulse constant frequency pulse train, showing the responsiveness of the preparation is unchanged. Note the decreased gain at modulation frequencies above 1 Hz.

Relative gain at each modulation frequency was calculated as the ratio between gain at the chosen frequency and maximum (d.c.) gain. A Bode plot (log relative gain *versus* log modulation frequency, Fig. 6) shows that within this frequency range, the peripheral oculomotor system behaves very much as a linear first order system. The characteristic frequency (half power frequency; frequency at which response has dropped by 3 dB) of each group of fish was determined using a non-linear regression technique (Helwig & Council, 1979) to fit the best first order model of the form:

$$G(f) = \frac{1}{\sqrt{1 + (f/f_c)^2}},$$

where G is gain, f_c is characteristic frequency and f is modulation frequency. As the characteristic frequencies for the two antarctic species were not significantly different (Table 1) the relative gains for both have been combined and plotted in Fig. 6 along with the best-fit model. The temperate species had a significantly higher characteristic frequency, and the mean relative gain at each modulation frequency was plotted along with the best-fit model for these points.

There was an approximately linear relationship between force (applied tangential to the eye surface) and angular deviation of the eye. The slope of this relationship was taken as an estimate of the elastic coefficient of the peripheral oculomotor system (Table 1). The elastic coefficient tended to increase with low temperature and with

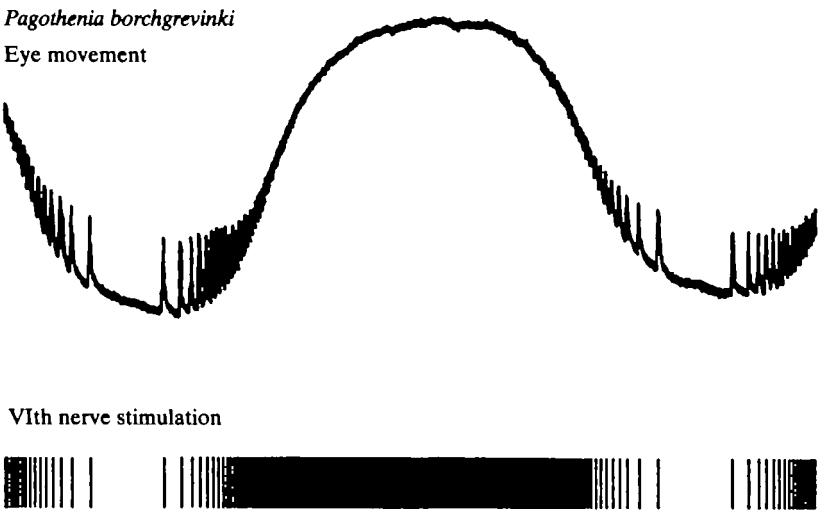

Fig. 5. Eye movement record of *Pagothenia borchgrevinki* during presentation of a sinusoidally modulated pulse train. The expanded time base of this record, and the pronounced single twitches allow comparison of the eye movement response with the reconstructed stimulus pulse train (lower trace).

increased size, so that the tension required for a given eye deviation was greater in both antarctic fish, but considerably greater in the large *D. mawsoni*.

Preliminary experiments were performed on the effects of acute temperature change on the characteristic frequency of the peripheral oculomotor system of *G. tricuspidata*. The characteristic frequency was strongly temperature dependent, decreasing from 1·4 Hz at 24 °C to 0·8 Hz at 16 °C and 0·25 Hz at 12 °C in a 24 °C-acclimated fish.

DISCUSSION

Models of the oculomotor system

The approach adopted in this paper has been to study the relationship between supramaximal stimulation of the abducens nerve and resulting eye movement. It has been suggested that the response characteristics obtained in this way will be dominated by the fast motor units (Montgomery, 1983). Teleost fish present a unique opportunity to test this hypothesis, for, unlike other vertebrates, the extraocular muscles are composed of two discrete regions of red and white muscle fibres, and the abducens motoneurones are correspondingly divided into two subgroups (Sterling, 1977). The motoneurones of the caudal subgroup have a characteristic phasic-tonic activity during eye movements and are thought to innervate the white muscle, whereas the activity of rostral motoneurones is related only to eye position, and these

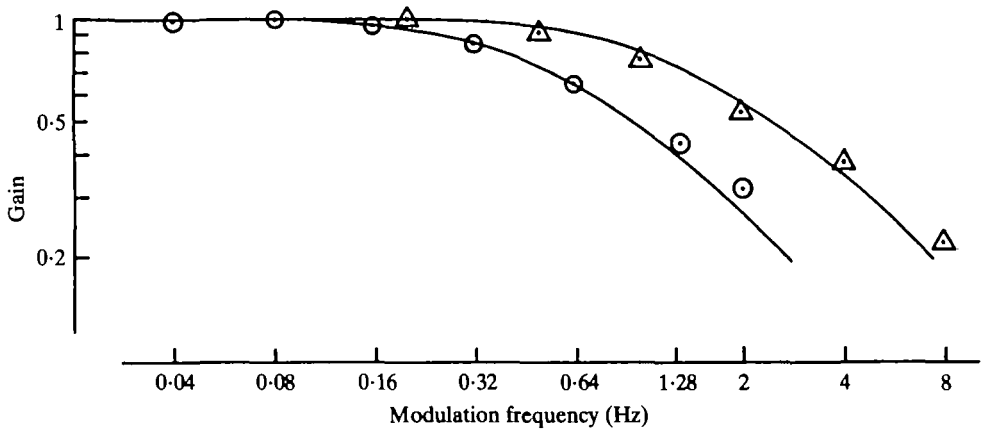

Fig. 6. Normalized gain *versus* modulation frequency. Open circles: the combined mean response of the two antarctic fish. Open triangles: mean response of *Girella tricuspidata*. Solid lines are best fit theoretical models (characteristic frequencies 0·55 and 1·4 Hz respectively).

units are thought to innervate the red fibres (Gestrin & Sterling, 1977).

From information provided by Gestrin & Sterling (1977) it is possible to calculate the transfer function which relates eye movement to the firing of the phasic-tonic, or fast motor units. The modulation of discharge rate of the 'average motoneurone' (ΔR) is related to eye position (E) and eye velocity (dE/dt) by the following equation (Robinson, 1981):

$$\Delta R = kE + r(dE/dt),$$

where k and r are constants. The constant k can be evaluated for goldfish from the slope of the line relating tonic frequency to eye position (Fig. 8 in Gestrin & Sterling, 1977). Assuming total eye deviation to equal 40°, k has an average value of 3·4 (± S.D. of 1·8; $N = 14$). Linear regression of burst frequency against saccade velocity (Fig. 7 in Gestrin & Sterling, 1977) for saccades initiated from middle positions yields a value for the constant r of 0·58 (S.E. of regression coefficient = 0·12). Robinson (1981) also shows that the transfer function [G(S)] derived from the preceding differential equation is of the form:

$$G(s) = \frac{1}{Ts + 1},$$

where the time constant $T = r/k = 0{\cdot}17$ s, and hence the characteristic frequency $f = (2\pi T)^{-1} = 0{\cdot}94$ Hz. This value for the goldfish is similar to the characteristic frequency of the parore oculomotor system reported in this study: 1·4 ± 0·2 Hz (± 95 % confidence interval). Temperature affects the characteristic frequency of the peripheral oculomotor system in dogfish (Montgomery & Paulin, 1984) and parore (this study); assuming the recordings in goldfish were around 18–20 °C (actual recording temperatures are not given by Gestrin & Sterling, 1977), the slightly higher characteristic frequency found in parore may be due to a higher recording temperature (24 °C).

Parameters of the model of the peripheral oculomotor system determined from

J. exp. Biol. 117, 69–86 (1985)
Printed in Great Britain © *The Company of Biologists Limited 1985*

THE MECHANICAL PROPERTIES OF THE AUTOTOMY TISSUES OF THE HOLOTHURIAN *EUPENTACTA QUINQUESEMITA* AND THE EFFECTS OF CERTAIN PHYSICO-CHEMICAL AGENTS

BY MARIA BYRNE*

Department of Biology, University of Victoria, Victoria, B.C. V8W 2Y2, Canada

Accepted 26 November 1984

SUMMARY

Evisceration in the holothurian *Eupentacta quinquesemita* (Selenka) results from a rapid softening of autotomy structures comprised of connective tissue. The mechanical properties of two autotomy tissues, the introvert and the retractor muscle tendon, were tested to investigate their function in the non-evisceration state and their behaviour during autotomy. The results show that these structures do not have a pre-existing mechanical weakness to account for their rapid failure during evisceration. The autotomy response was mimicked *in vitro* by increasing K^+ concentration. The introvert exhibited viscous behaviour and the absence of Ca^{2+} and Mg^{2+} decreased introvert viscosity, whereas excess Ca^{2+}, and low and high pH, increased viscosity. These agents may influence the mechanical properties of the autotomy structures by directly affecting connective tissue ionic interactions and may induce proteoglycan conformational changes. K^+ may also exert an indirect effect through responses of cells controlling connective tissue tensility. The most likely mechanism of autotomy is through an alteration of connective tissue ionic interactions.

INTRODUCTION

The phenomenon of variable tensility in echinoderm connective tissue is associated with two types of change. Echinoderm catch ligaments exhibit reversible stiffening/softening tensility changes, whereas autotomy ligaments undergo an irreversible sudden reduction in tensility leading to loss of body parts. The echinoid spine catch apparatus is the classic example of an echinoderm catch ligament. When in catch, the connective tissue ring surrounding the spine base holds the spine in place so firmly that it is impossible to move the spine without tearing the apparatus (von Uexküll, 1900; Takahashi, 1967). Similar changes in tensility have been described for holothuroid, asteroid and crinoid connective tissues (Lindemann, 1900; Jordan, 1914; von Uexküll, 1926; Serra-von Buddenbrock, 1963; Meyer, 1971; Stott, Hepburn, Joffe & Heffron, 1974; Freinkel & Hepburn, 1975; Eylers, 1976*a*,*b*; Wilkie,

* Present address: Smithsonian Marine Station at Link Port, Route 1, Box 194-C, Fort Pierce, Florida 33450, U.S.A.

Key words: Holothurian autotomy, connective tissue, mechanical properties.

1983). The mechanical properties of echinoderm catch ligaments have been examined in numerous studies and it appears that variable tensility is associated with the viscous behaviour of the connective tissue matrix and is effected by a change in the connective tissue environment (Takahashi, 1967; Eylers, 1976*b*, 1982; Biglow, 1981; Motokawa, 1981, 1982, 1983, 1984*a,b*; Wilkie, 1983, 1984; Hidaka, 1983; Hidaka & Takahashi, 1983).

The ability to autotomize body parts is characteristic of echinoderms (Emson & Wilkie, 1980), but the mechanical properties of autotomy connective tissues have received relatively little attention. Two autotomy structures that have been studied are the holothurian retractor muscle tendon and the ophiuroid intervertebral ligament (Smith & Greenberg, 1973; Wilkie, 1978).

Evisceration in the dendrochirote holothurian *Eupentacta quinquesemita* is associated with sudden softening of three autotomy connective tissues: (1) the tendon (P-L tendon) connecting the pharyngeal retractor muscle (PRM) to the longitudinal body wall muscle (LBWM), (2) the intestine-cloacal junction and (3) the introvert, the anterior extensible portion of the body wall (Byrne, 1982). Autotomy of the P-L tendon usually occurs within 30 s and that of the introvert takes approximately 3 min but took up to 5 min in some specimens (Byrne, 1983). During evisceration the introvert changes from a firm opaque structure to one that is soft and translucent. It becomes distended as it is filled with coelomic fluid and autotomized organs propelled anteriorly by contraction of the body wall muscles. Autotomy results from changes within the connective tissue and internal hydrostatic pressure plays a role in the eventual detachment of the introvert. In this study, the mechanical properties of the P-L tendon and the introvert were examined to correlate their mechanical properties *in vitro* with their function in the non-evisceration state and with their behaviour during autotomy. The introvert is comprised predominantly of connective tissue and creep tests were used to quantify its mechanical properties. Muscle fibres dispersed in the introvert connective tissue occupy 1–4 % of the introvert cross-sectional area and do not appear to influence introvert autotomy (Byrne, 1983). The connective tissue of the P-L tendon is intimately associated with PRM muscle bundles making it impossible to isolate the tendon (Byrne, 1982) and so entire PRM preparations were used for tests. The PRMs were extended under a constant load to examine the mechanical properties of the tendon and PRM, especially for the position of failure.

Variable tensility of echinoderm connective tissues can be mimicked *in vitro* by altering the pH and cation composition of test solutions (Wilkie, 1978,1983,1984; Biglow, 1981; Smith, Wainwright, Baker & Cayer, 1981; Eylers, 1982; Motokawa, 1982, 1983, 1984*a,b*; Hidaka, 1983) and similar experiments were used to investigate the mode of action of physico-chemical agents used in other studies on the autotomy structures of *E. quinquesemita*.

MATERIALS AND METHODS

Tissue samples

Specimens of *Eupentacta quinquesemita* were collected subtidally near Victoria, B.C. and near the Friday Harbor Laboratories, Washington, and acclimated in an ambient sea water system for at least 24 h before use in experiments. They were

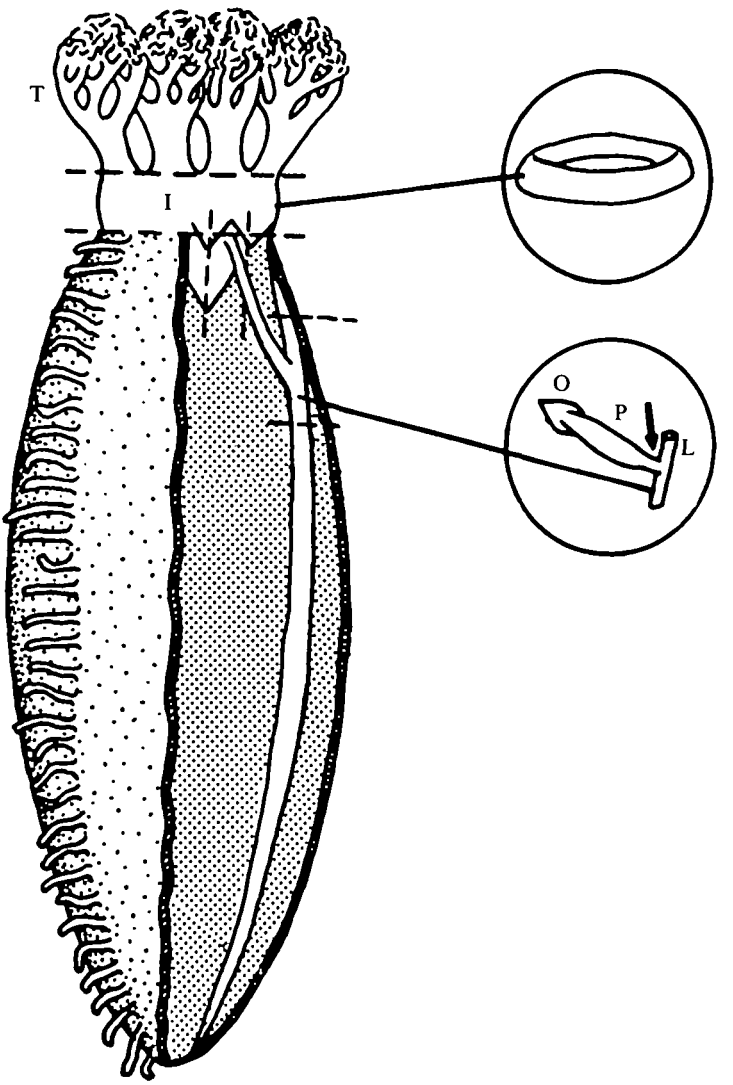

Fig. 1. Diagram showing the dissection and isolation of the introvert (I) and the pharyngeal retractor muscle (P) of *Eupentacta quinquesemita* (Selenka). Incisions indicated by the broken lines. O, ossicle; L, longitudinal body wall muscle; T, tentacle; arrow, P-L tendon.

relaxed in 6·7 % $MgCl_2$ or 0·1 % propylene phenoxetol (PPOX) in sea water for 3–5 h before dissection. The introvert was dissected as follows (Fig. 1): it was cut along its posterior margin where it joins the body wall, the tentacles were cut off at their bases and the body wall muscle tissue was removed. For ease of handling, circumferential rings were used for all tests. The PRMs were isolated from relaxed specimens by dissection around their junction with the LBWM and at their anterior insertion into the ossicle (Fig. 1). Surgical silk thread was tied at either end of the preparations and thread loops were made to facilitate connections of the PRMs to the testing apparatus (see below). Before testing, the preparations were washed in sea water for 3–5 h.

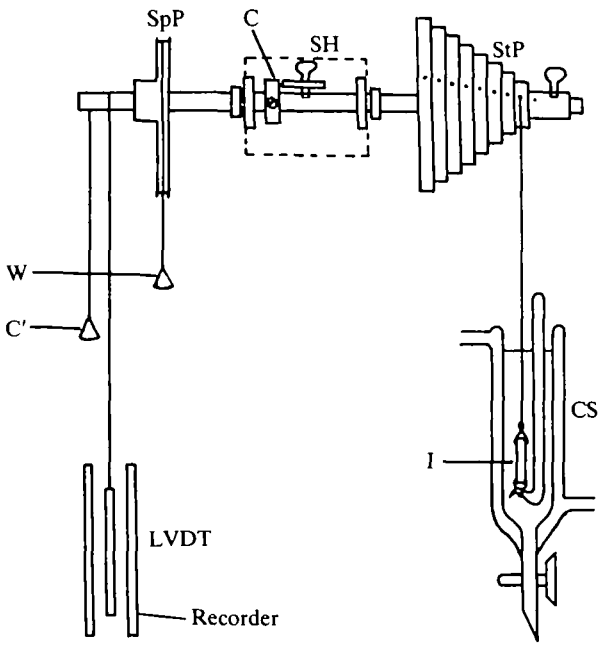

Fig. 2. The constant stress creep-testing machine, modified from Vogel & Papanicolaou (1983). The introvert (I) is in a bathing solution and is attached to the 'step' of the step pulley (StP) with a diameter closest to the original length of the specimen. C, counterweight for the step pully; C', counterweight for the LVDT core rod; CS, cooling sleeve; LVDT, linear variable differential transformer, measures specimen elongation and is connected to a chart recorder; SH, shaft holder; SpP, spiral pulley; W, applied weight, when multiplied by the moment arm of the spiral pulley, gives the force on the specimen.

Introvert

A constant stress creep machine (Fig. 2) was used to quantify the mechanical properties of the introvert. Stress (σ) is $= F/A$, where F = force and A = cross-sectional area of the specimen. It was assumed that the volume of the introvert remained constant during tests. The rationale behind the creep machine's design and construction is described in Vogel & Papanicolaou (1983). The machine has two essential features: a circular step pulley with steps of different radii and a spiral pulley, both of which are on the same shaft. The specimen is attached to that step of the step pulley with a diameter nearest to the initial length of the specimen. The spiral pulley is designed so that the product of specimen length and the pulley lever arm is constant, i.e. the lever arm length decreases directly in proportion to specimen elongation, keeping stress constant. The stress on the specimen is given by: $\sigma = F'Ro'/RSo$, where F' = applied weight, Ro' = initial lever arm length, R = radius of the step pulley chosen and So = initial cross-sectional area of the specimen. Shaft rotation was measured by a linear variable differential transformer (LVDT) and provided a measure of specimen length, which was required to calculate strain. The introvert proved to be a highly extensible tissue, therefore natural or true strain; $e = \ln(L/Lo)$ was used, where L = actual length and Lo = original length of the tissue (Wainwright, Biggs, Currey & Gosline, 1976). The introvert rings were held between two heart

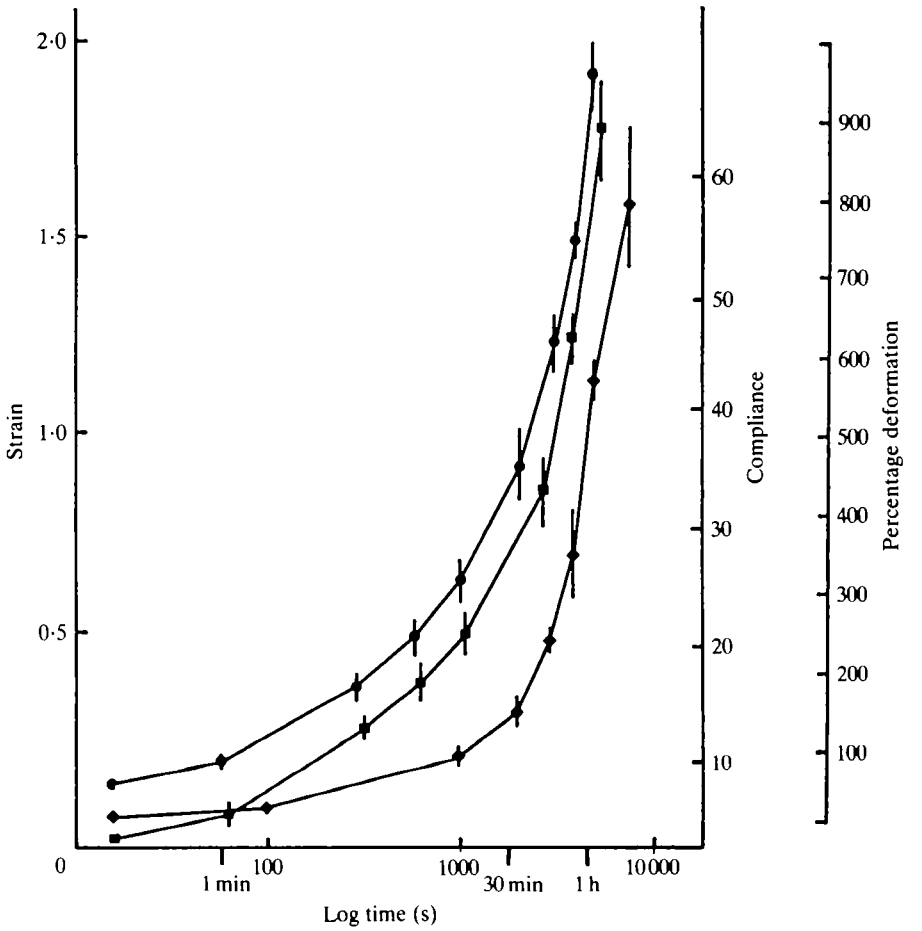

Fig. 4. Creep curve (—●—), compliance (—■—) and percentage deformation (—◆—) of introvert tissue tested in ASW. $N = 9$ at t_o, $N = 6$ at $t = 3500$ s, $N = 4$ at $t = 6000$ s. Means ± S.E.M.

Experimental solutions

Creep tests were done while the introvert was bathed in artificial sea water (ASW), Ca^{2+}-free sea water (CaFSW), MgFSW, or CaMgFSW, made according to M.B.L. Formulae (Cavanaugh, 1956). The salinity of local sea water varies between 28 and 32 ‰. Solutions containing various concentrations of K^+ were made by adding isosmotic KCl (0·45 mol l^{-1}) to 0·45 mol l^{-1} NaCl (KNaASW), i.e. ASW containing the cations K^+ and Na^+ only. Isosmotic KCl and solutions of other monovalent cations, Rb^+ (0·45 mol l^{-1} RbCl) and Na^+ (0·45 mol l^{-1} NaCl), were used to examine the K^+ response specificity. Isosmotic $CaCl_2$ (0·30 mol l^{-1}) was also tested. To test the effect of anaesthetics on the K^+ response, tissues were tested without recovery from anaesthesia. Buffer solutions, pH 2–12, were used to test the effect of pH on introvert viscosity. For pH 4–10, Tris buffers were made with appropriate amounts of Tris-HCl and Trisma base (Sigma). For pH 2, McIlvaine's buffer was used (Pearse, 1968) and 0·1 mol l^{-1} NaOH was used for pH 12. The effect of experimental

solutions on the PRM was tested while the tissue was attached to the lever maintained in position by a light load (F/A at $t_o = 0{\cdot}98 \times 10^4\,N\,m^{-2}$).

RESULTS

Introvert

The introvert was creep-tested in ASW to examine the mechanical properties of the tissue in a solution approximating to physiological conditions. The combined creep curve for nine specimens shows that the tissue deformed at a slow and constant rate until failure (Fig. 4). When strain is plotted against log time, the creep curve is exponential due to the constant creep rate. The creep curve between 600 and 4000 s was used to calculate viscosity. This was to avoid the influence of initial slack in the tissue and after 4000 s the sample size decreased (Fig. 4). Introvert compliance increased as the creep test progressed (Fig. 4) and deformations at failure were up to 900 % relative to the original length of the tissue (Fig. 4). The introvert is very viscous and deformations beyond approximately the first 10 min were irreversible. Specimens in creep tests arrested after 10 min did not return to their original dimensions before eventually degenerating. During the first 5–10 min the introvert appeared relatively stiff when manipulated and examined directly. The introvert cross-sectional area appeared to decrease uniformly during creep tests. Narrowing or necking of the tissue was not observed even as the introvert approached failure. Introvert viscosity in ASW tests was of the order of $10^8\,N\,m^{-2}\,s$ (Table 2).

Pharyngeal retractor muscle

Eight PRMs were placed on the lever and two were loaded with $0{\cdot}98 \times 10^4\,N\,m^{-2}$ and six with $4{\cdot}9 \times 10^4\,N\,m^{-2}$. Strains at failure were similar for all tests despite the different initial stresses (Fig. 5). Six PRMs broke at or near the ossicle but two of the PRMs at the higher load broke at the tendon.

Table 1. *Introvert compliance D(t) at t = 300 s, D(t) = e(t)/σ*

Solution	D(t)*	S.E.	*N*
ASW	1·2	0·09	9
CaFSW	2·7	0·46	9
MgFSW	1·5	0·18	5
CaMgFSW	4·3	0·29	2
0·45 mol l^{-1} KCl	2·5	0·29	3
0·25 mol l^{-1} KCl	1·8	0·36	2
0·15 mol l^{-1} KCl	1·2	0·06	5
0·075 mol l^{-1} KCl	1·2	0·15	4
0·45 mol l^{-1} NaCl	1·0	0·20	2
$MgCl_2$–KCl†	1·9	–	1‡
PPOX–KCl‡	0·7	0·05	4

* All values $\times 10^{-5}\,N^{-1}\,m^2$.
† Anaesthetized tissue tested in 0·45 mol l^{-1} KCl without recovery in sea water.
‡ Only one of three specimens lasted 300 s before failure.
PPOX, propylene phenoxetol.

Table 2. *Introvert viscosity* (η) *in test solutions*, $\eta = \sigma/\dot{e}$

Solution	η*	N	r^2
ASW	10·0	9	1·0
CaFSW	6·0	9	1·0
MgFSW	5·0	5	1·0
CaMgFSW	1·25	2	1·0
0·45 mol l^{-1} KCl	2·08	3	0·89
0·45 mol l^{-1} RbCl	1·07	2	0·97
0·25 mol l^{-1} KCl	5·6	2	0·96
0·15 mol l^{-1} KCl	7·5	5	0·9
0·075 mol l^{-1} KCl	10·0	4	0·97
0·45 mol l^{-1} NaCl	12·0	2	0·87
$MgCl_2$–KCl†	0·9	3	1·0
PPOX–KCl†	10·0	4	1·0

* All values $\times 10^7$ N m^{-2} s.

† Anaesthetized tissue tested in 0·45 mol l^{-1} KCl without recovery in sea water.

r^2, coefficient of determination. The regressions were calculated for the creep curves, see Figs 4, 6 and 8 for standard errors.

PPOX, propylene phenoxetol.

Effect of experimental solutions

Introvert

The softening of the introvert observed during evisceration was mimicked *in vitro* by increasing the K^+ concentration in the bathing solution. Excess K^+ ions induced an increase in compliance and decrease in viscosity (Fig. 6; Tables 1, 2). Isosmotic KCl had the greatest effect with rapid failure at low strain values (Table 3). The

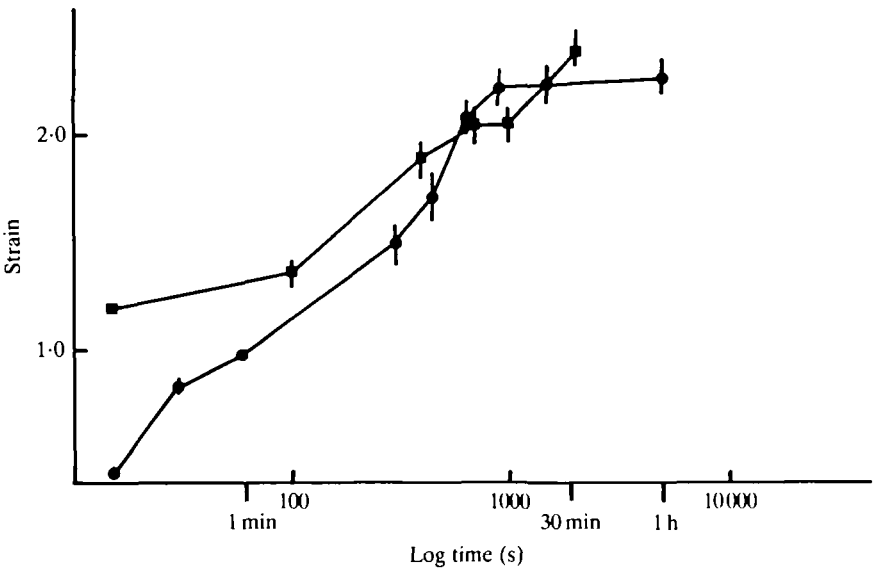

Fig. 5. Elongation of the PRMs extended with a constant load while bathed in ASW. Strains resulting from the two initial stresses, (—●—) $\sigma = 0{\cdot}98 \times 10^4$ N m^{-2} ($r^2 = 0{\cdot}92$) and (—■—) $\sigma = 4{\cdot}9 \times 10^4$ N m^{-2} ($r^2 = 0{\cdot}97$), were similar. Means ± S.E.M.

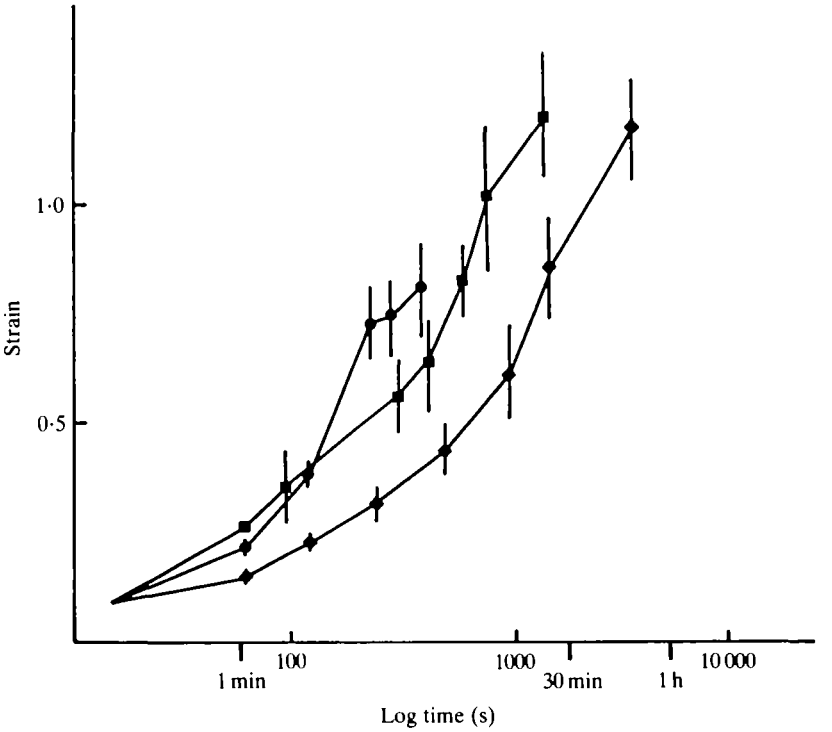

Fig. 6. The influence of K^+ on introvert creep behaviour. 0·45 mol l^{-1} KCl (—●—) induced a rapid creep rate and failure ($N = 3$). 0·25 mol l^{-1} KCl (—■—) ($N = 2$). 0·075 mol l^{-1} KCl (—◆—) tests resembled controls ($N = 4$). Means ± S.E.M.

influence of the ion decreased as the concentration was lowered and 0·15 mol l^{-1} KCl was the lowest concentration tested that affected introvert viscosity. For tissues tested in 0·075 mol l^{-1} KCl, the creep curves were similar to controls. The concentration of K^+ in the coelomic fluid of *Eupentacta quinquesemita* is 0·012 mol l^{-1} (Byrne, 1983). Isosmotic RbCl produced results similar to those with KCl and 0·45 mol l^{-1} NaCl tests were similar to controls (Tables 2, 3). The decrease in compliance induced by 0·45 mol l^{-1} KCl was arrested when the bathing solution was replaced with isosmotic $CaCl_2$ (Fig. 7). Excess Ca^{2+} stiffened the introvert and the tissue did not fail in tests.

Anaesthetized tissues tested without prior recovery exhibited variable responses to K^+. $MgCl_2$ did not interfere with K^+-induced softening, but PPOX inhibited the response and may have had a stiffening influence. PPOX-anaesthetized tissues had viscosity values similar to controls and the creep tests had a similar duration, although the breaking strains were lower than those of controls (Tables 2, 3). Introvert preparations that were anaesthetized in $MgCl_2$ or PPOX, and then washed in sea water for 3–5 h before testing, had similar responses to those tested in excess K^+.

The initial stiff period apparent in control tissue when handled directly was not present in tissues treated with divalent-cation-free sea water. Introvert preparations

Table 3. *Breaking strain and failure times for introvert creep tests*

Solution	Breaking strain (S.E.)	Time (s) (S.E.)	*N*
ASW	1·52 (0·25)	4200 (800)	9
CaFSW	1·93 (0·08)	2455 (470)	9
MgFSW	1·33 (0·18)	1520 (345)	5
CaMgFSW	1·46 (0·11)	350 (70)	2
0·45 mol l^{-1} NaCl	1·53 (0·08)	6000 (1180)	2
0·45 mol l^{-1} KCl	0·83 (0·08)	350 (54)	3
0·45 mol l^{-1} RbCl	1·00 (0·03)	390 (30)	2
0·25 mol l^{-1} KCl	1·19 (0·13)	1250 (250)	2
0·15 mol l^{-1} KCl	1·10 (0·20)	1720 (186)	5
0·075 mol l^{-1} KCl	1·40 (0·17)	3400 (1300)	4
$MgCl_2$–KCl*	0·63 (0·14)	130 (78)	3
PPOX–KCl*	1·00 (0·19)	3125 (315)	4

* Anaesthetized tissue tested in 0·45 mol l^{-1} KCl without recovery in sea water.
PPOX, propylene phenoxetol.

soaked for 2 h and tested in CaFSW, MgFSW or CaMgFSW deformed at a faster rate than ASW controls, with decreased viscosity and increased compliance (Fig. 8; Tables 1, 2). The lack of Ca^{2+} made the tissue more compliant and deformations at failure were higher than those of ASW controls (Table 3). The lack of Mg^{2+} hastened failure and at strains similar to controls (Table 3). The lack of both ions elicited the greatest increase in compliance and decrease in viscosity with a rapid failure at strains similar to controls (Fig. 8; Tables 1–3). In contrast, excess Ca^{2+} (isosmotic $CaCl_2$) induced stiffening and the tissue did not fail in tests.

Manipulation of pH affects introvert viscosity. The viscosity value was lowest at pH 7·0, similar to that of ASW tests, and increased sharply at either side of this pH (Fig. 9). The pH of *E. quinquesemita* coelomic fluid is 7·0 (Byrne, 1983).

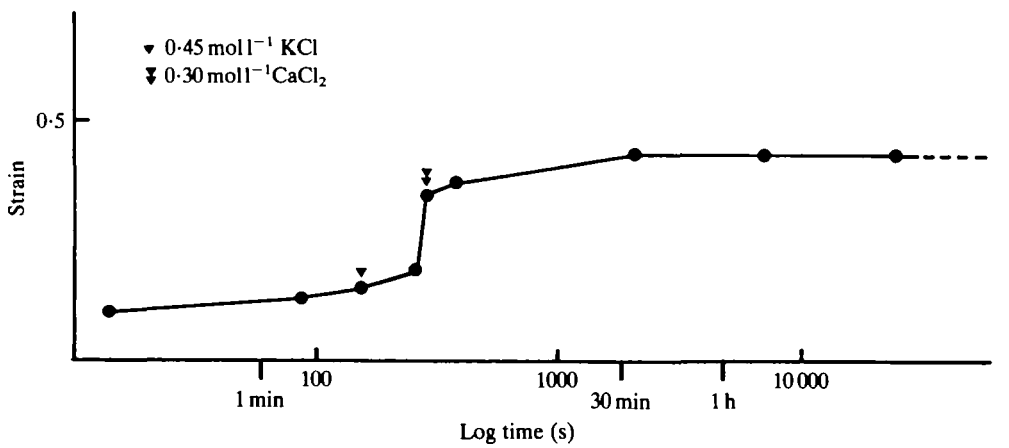

Fig. 7. Antagonistic interaction of K^+ and Ca^{2+} on introvert creep behaviour. The increased compliance induced by 0·45 mol l^{-1} KCl is arrested if the bathing solution is replaced with 0·30 mol l^{-1} $CaCl_2$. The tissue remained stiff in $CaCl_2$ for the duration of the test and did not fail.

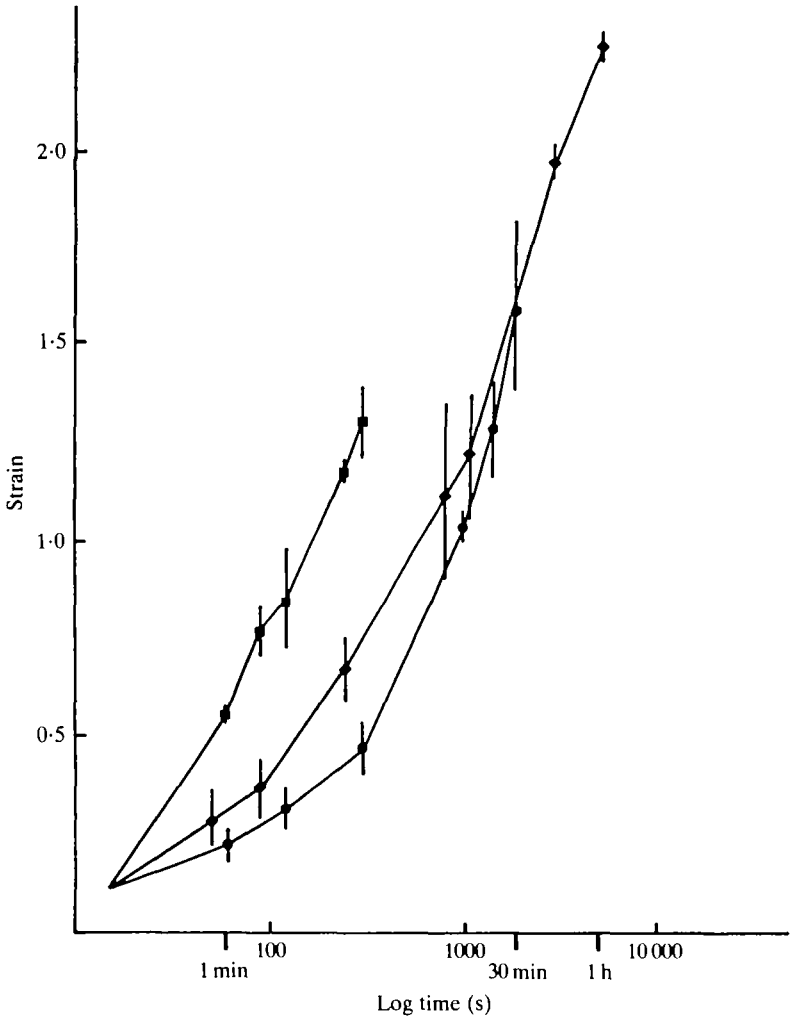

Fig. 8. Creep curve of introvert tissue bathed in cation-free ASW. CaFSW (—◆—) induced a decrease in viscosity, and deformations at failure were greater than controls ($N = 9$). MgFSW (—●—) also decreased introvert viscosity and hastened failure at strains similar to ASW tests ($N = 5$). The lack of both ions (—■—) elicited the greatest increase in compliance and rapid failure ($N = 2$). Means ± S.E.M.

Pharyngeal retractor muscle

Muscle preparations tested in ASW and 0·45 mol l^{-1} NaCl did not fail in tests (Table 4). KCl and RbCl were most effective in eliciting tendon autotomy. These solutions induced muscle contraction, tendon softening and a rapid separation of the PRM and LBWM (Table 4). $MgCl_2$ did not block these responses but PPOX inhibited K^+-induced autotomy. Tendon failure occurred with other solutions, but the response times were considerably longer (Table 4) and the results cannot be reliably compared with the rapid tendon autotomy *in vivo* during evisceration. Excess Ca^{2+} induced muscle contraction resulting in a narrow neck at the P-L tendon and

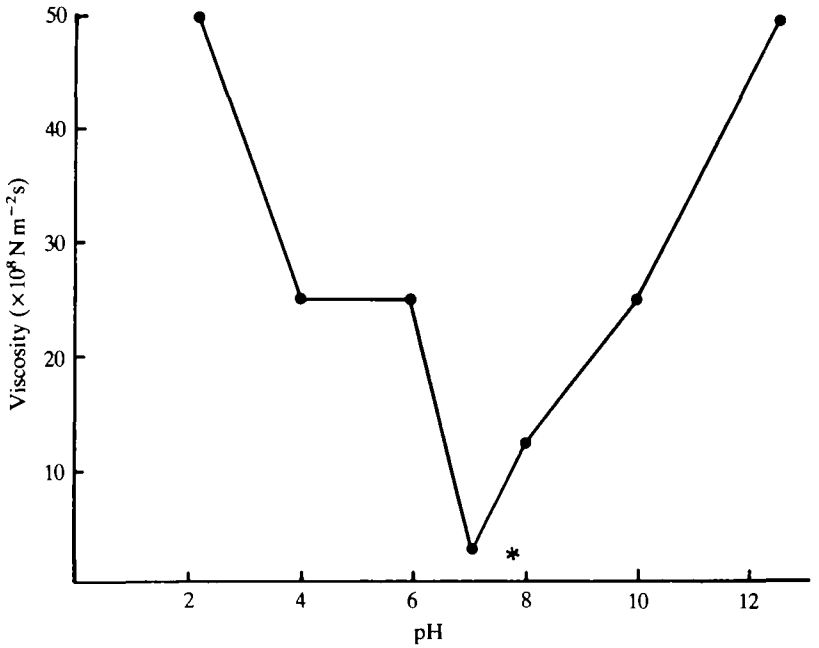

Fig. 9. The influence of pH on introvert viscosity. The asterisk marks introvert viscosity in ASW (pH 7·8) tests.

concentration of stress forces at the neck may have caused eventual tendon rupture. Muscle contraction induced by KCl and RbCl may also have resulted in stress concentration, but the rapid response of the P-L tendon suggests that these agents also affected the connective tissue. CaFSW induced muscle relaxation and uniform cross-sectional area along the PRMs and they did not fail in CaFSW tests. Most of the PRMs tested in MgFSW broke at the tendon.

Table 4. *Response of PRM preparations to test solutions*

Solution	*N*	P-L tendon failure, *N*	Response time (s) (S.E.)
ASW	5	0	
0·45 mol l^{-1} NaCl	5	0	
0·45 mol l^{-1} KCl	10	10	102 (12)
0·45 mol l^{-1} RbCl	9	9	90 (130)
0.30 mol l^{-1} $CaCl_2$	5	5	4806 (570)
CaFSW	5	0	
MgFSW	9	7	4800 (1038)
$MgCl_2$–KCl*	5	5	126 (60)
PPOX–KCl*	7	1	90

* Anaesthetized tissue tested in 0·45 mol l^{-1} KCl without recovery in sea water.
PPOX, propylene phenoxetol.

DISCUSSION

The compliant properties of the introvert correlate with the extensibility it exhibits during suspension feeding in association with tentacle protraction and retraction and with the characteristic infolding of the introvert that occurs when the tentacular crown is withdrawn. In comparison, the body wall posterior to the introvert was considerably less extensible in mechanical tests (M. Byrne, unpublished results). The introvert is comprised of a dense connective tissue layer containing collagen fibrils and matrix and a predominant layer of loose connective tissue containing matrix and occasional small unstriated fibrils (Byrne, 1983). Morphologically and histochemically the introvert appears to be comprised predominantly of glycosaminoglycan (GAG) (Byrne, 1983, 1985) which probably accounts for its viscous properties *in vitro* and its extensible behaviour *in vivo*. Other echinoderm connective tissues have been shown biochemically to possess a high GAG and proteoglycan content (Junqueira *et al.* 1980; Minafra *et al.* 1980; Bailey, Gathercole, Dlugosz & Voyle, 1982).

The creep curves in ASW were similar for all introvert preparations although they differed in duration, which suggests that some specimens were stiffer than others. The proportion of loose and dense connective tissue in the introvert varies between specimens (Byrne, 1983) and may be a source of creep test variability. The introvert may also have catch properties as described for the holothurian body wall (Motokawa, 1984*b*) and so the test tissues may have been in various states of catch. The introvert creep rate appears to be less variable than that of the body wall (Motokawa, 1984*b*). Introvert creep curves are similar to those obtained for other echinoderm connective tissues (Takahashi, 1967; Eylers, 1976*a*, 1982; Wilkie, 1978; Motokawa, 1981; Smith *et al.* 1981) and for sea anemone mesogloea (Alexander, 1962; Koehl, 1977). As for other echinoderm connective tissues the introvert exhibited viscoelastic properties. Assuming that introvert collagen fibrils are similar to vertebrate tendon collagen, relatively inextensible and of high tensile strength (Harkness, 1961), the large deformations obtained during creep tests indicate that the collagen fibrils are discontinuous, as suggested for holothurian dermis and mesogloea (Gosline, 1971; Motokawa, 1981).

Initially during creep tests, the collagen fibrils may act as tensile elements with the matrix transferring the load from fibre to fibre. As deformation continues, the collagen fibrils must slip past each other perhaps associated with a decrease in fibre-matrix adhesion. This may be associated with an alteration in the GAG-collagen electrostatic interactions (see below) and a decrease in matrix viscosity. The interfibrillar slippage results in a decrease in stiffness and increase in compliance. During the final stages of the creep tests, matrix proteoglycan molecules may be pulled upon directly, with possible breakage of intermolecular ionic bonds and subsequent tissue failure. Initial reinforcement by fibrillar elements followed by viscous behaviour dominated by matrix proteoglycans is similar to that described for sea anemone mesogloea and insect cuticle (Gosline, 1971; Reynolds, 1975).

Introvert compliance and its viscous matrix are central to its function *in vivo* where introvert extension and inversion are generated by the tentacle muscles, the PRMs and the body wall musculature. During tentacle protraction and retraction, introvert collagen fibrils may slip past each other, but it is unlikely that the tissue is extended

to the point where the collagen fibrils no longer overlap. In the non-evisceration state the introvert does not approach failure and so it is unlikely that matrix proteoglycans are ever pulled upon directly, as is suggested to occur in the latter portion of the creep tests.

During evisceration, the introvert serves as a specialized autotomizing structure. The sudden softening characteristic of the introvert during autotomy was not observed in control tests in ASW, suggesting that the tissue does not have a pre-existing mechanical weakness to account for its failure during evisceration and that autotomy involves a physiological change in the tissue. Ultrastructural examination of autotomizing introvert revealed that changes in the connective tissue matrix caused interfibrillar slippage resulting in complete fibril disarray and that the subsequent viscid flow was followed by autotomy (Byrne, 1985).

The P-L tendon serves as a connection between the PRM and LBWM and as an autotomizing structure. The tendon is comprised of collagenous connective tissue associated with PRM muscle fibres and it functions in conjunction with the PRM (Byrne, 1982). Consequently, the test results largely reflect PRM properties. The tendon was found to be as strong or stronger than associated muscle tissue and it thus forms a strong connection between the PRM and LBWM. PRM failure usually occurred at or near the anterior insertion into the ossicle but not at the tendon. Similar results were obtained for the P-L tendon of *Sclerodactyla briareus,* which also autotomizes during evisceration (Smith & Greenberg, 1973).

Introvert and P-L tendon autotomy during evisceration was mimicked *in vitro* by elevated K^+, especially with isosmotic KCl. Introvert compliance also increased in the absence of divalent cations. The results of ion experiments may be a function of the connective tissue chemistry. Connective tissue polysaccharides in solution undergo reversible conformational changes induced by altering ion concentrations (Cael, Winter & Arnott, 1978) and their polyanionic nature creates potential for GAG-GAG and collagen-GAG electrostatic interactions (Obrink, 1975; Comper & Laurent, 1978; Lindahl & Höök, 1978). Experimental alteration of ion concentrations may have affected introvert viscosity by changing these interactions or by inducing proteoglycan conformational change. Manipulation of the ionic milieu has been used with similar results for other echinoderm connective tissues (Wilkie, 1978; Biglow, 1981; Smith *et al.* 1981; Eylers, 1982; Hidaka, 1983). Viscosity changes induced by altering K^+ and Ca^{2+} concentrations were obtained in solutions of holothurian dermis where cellular inclusions were completely disrupted (Biglow, 1981). The effect of K^+ may involve the masking of GAG anionic sites, thereby reducing collagen-GAG and GAG-GAG ionic interactions, as suggested for other echinoderm connective tissues (Wilkie, 1978; Biglow, 1981; Eylers, 1982). K^+ and Rb^+ reduced introvert viscosity and induced P-L tendon autotomy, but Na^+ did not, perhaps because K^+ and Rb^+ have similar ionic characteristics, both are larger than Na^+ (Masterton & Slowinski, 1973).

Excess Ca^{2+} stiffened the introvert, perhaps by acting as a divalent cross-linker; that is, as an ionic bridge facilitating ionic interactions. Conversely, the lack of Ca^{2+} would have a softening effect. Treatment with CaFSW decreased introvert viscosity, as has been found for other echinoderm connective tissues (Biglow, 1981; Smith *et al.* 1981; Eylers, 1982; Hidaka, 1983). MgFSW also decreased introvert viscosity and

hastened failure compared with ASW controls. This solution had a similar effect in other studies (Wilkie, 1978, 1983; Smith *et al.* 1981). The lack of both Mg^{2+} and Ca^{2+} had the greatest influence on the introvert with results similar to those from isosmotic KCl tests. Both Mg^{2+} and Ca^{2+} appear to play a stabilizing role in the connective tissue, as suggested in other investigations (Wilkie, 1978, 1983; Smith *et al.* 1981), although excess Mg^{2+} lowered the viscous resistance of the echinoid catch apparatus (Hidaka, 1983). The response of the introvert to altering ion concentrations suggests that the mechanism of autotomy may involve a change in the ionic environment *in vivo*.

Besides the potential effect of K^+ on ionic interactions, there is evidence that the action of K^+ may be indirect through cellular mediation, especially in studies where low concentrations of K^+ were tested (Table 5). Wilkie (1983) found that the K^+ response that makes crinoid cirral ligaments more pliant is Ca^{2+}-dependent and is inhibited by Mg^{2+}. Concentrations of 0·075–0.1 mol l^{-1} KCl in KNaASW had no discernible effect on the introvert, perhaps due to the absence of other cations. In studies where K^+ was tested with an appropriate decrease in Na^+ and where other sea water cations were balanced, K^+ was found to have a stiffening or a relaxing effect depending on the tissues tested (Table 5). Inconsistent responses were observed for the ophiuroid oral plate ligament which stiffens or softens in response to isosmotic KCl (Wilkie, 1984). The influence of K^+, especially at low concentrations, may not be due to a direct physico-chemical effect and at high concentrations the ion potentially exerts direct and indirect effects. The inconsistent effect of K^+ suggests that the K^+ response may be tissue-specific, perhaps involving cells controlling variable tensility.

Introvert mechanical properties were influenced by pH. Viscosity was lowest at pH 7·0 and increased sharply with increasing pH (8–12) and decreasing pH (pH 6–2). The ophiuroid intervertebral ligament and the echinoid catch apparatus were also

Table 5. *The effect of K^+ on the mechanical properties of echinoderm connective tissues*

Class and species	Tissue	$[K^+]$ (mol l^{-1})	Response	Reference
Crinoidea				
Antedon bifida (Pennant)	cirral ligament•	0·015–0·05	softening	Wilkie (1983)
Echinoidea				
Anthocidaris crassispina (A. Aggassiz)	catch apparatus•	0·1	hardening	Takahashi (1967)
Diadema setosum Leske	spine central ligament•	0·1	hardening	Motokawa (1983)
Holothuroidea				
Sclerodactyla briareus (Lesueur)	P-L tendon†	0·1	softening	Smith & Greenberg (1973)
Stichopus chloronotus Brandt	dermis•	0·05–0·1	hardening	Motokawa (1981)
Eupentacta quinquesemita (Selenka)	introvert‡	0·075	no effect	present study

• KASW, † KCl, ‡ KNaASW.

influenced by pH, but the viscosities and tensile strength of these tissues were lowest at pH 10 and 5 respectively (Wilkie, 1978; Hidaka, 1983). These different experimental results may reflect differences in tissue physiology, perhaps associated with matrix composition. They may also be influenced by the different test solutions employed. Wilkie (1978) also used a series of buffer solutions while Hidaka (1983) used buffered ASW where the presence of other sea water cations may have influenced the results. Altering pH may influence the mechanical properties of echinoderm connective tissues by changing the net surface charge of the matrix and thereby affect connective tissue ionic interactions, as suggested by Hidaka (1983). Although *in vitro* tests demonstrated that the introvert stiffens at low and high pH, the sensitivity of the tissue to pH change suggests that the mechanism of autotomy may involve an alteration of tissue pH.

The results of ion and pH experiments have been used to suggest that the mechanism of variable tensility involves ion or pH changes that alter electrostatic interactions within the connective tissue, thereby causing tensility change (Wilkie, 1979; Motokawa, 1981, 1982, 1983; Eylers, 1982; Hidaka, 1983). Large ionic or pH changes are unlikely *in vivo* and the results of experiments described here and elsewhere involving ion concentrations and pH values above or below physiological levels may be *in vitro* artifacts reflecting proteoglycan conformational changes. Although ion and pH change are potential mechanisms, their physiological role in variable tensility of echinoderm connective tissues has yet to be established.

Anaesthetic antagonism of the K^+ response has been taken as evidence to suggest that variable tensility is neurally controlled (Wilkie, 1978, 1983). The influence of anaesthetics on the introvert and P-L tendon was variable. $MgCl_2$ did not block K^+-induced softening, perhaps because Mg^{2+} is a muscle relaxant and it may have a limited effect on connective tissue, especially in competition with a high concentration of K^+ ions. $MgCl_2$ partially blocked the response of the ophiuroid intervertebral ligament to excess K^+ (Wilkie, 1978). Propylene phenoxetol inhibited the K^+ response as shown in other studies (Wilkie, 1978, 1983), but its mode of action has not been established and it may have exerted a direct stabilizing influence on the connective tissue.

In general, the mechanical properties of echinoderm connective tissues that exhibit variable tensility appear to be associated with changes in the matrix, not with collagen or muscle events. At present, the most likely mechanism of variable tensility is through an alteration of connective tissue ionic interactions, but how this is brought about is not known. There is evidence for neural control of evisceration autotomy and for the presence of an endogenous evisceration factor in *Eupentacta quinquesemita* and this evidence will be presented in a following report (M. Byrne, in preparation).

I thank Professor A. R. Fontaine for his enthusiastic supervision of my research. Dr M. LaBarbera and Dr S. Vogel provided helpful comments and equipment. I am grateful to Dr I. C. Wilkie and Dr S. Vogel for reading earlier versions of this manuscript. Ms J. Piraino also read the manuscript. I thank Dr A. O. D. Willows, director of the Friday Harbor Laboratories for use of facilities. The work was supported by a University of Victoria Graduate Fellowship and this report is Smithsonian Marine Station contribution no. 133.

REFERENCES

ALEXANDER, R. McN. (1962). Visco-elastic properties of the body wall of sea anemones. *J. exp. Biol.* **39**, 373–386.

BAILEY, A. J., GATHERCOLE, L. J., DLUGOSZ, J. & VOYLE, C. A. (1982). Proposed resolution of the paradox of extensive crosslinking and low tensile strength of cuvierian tubule collagen from the sea cucumber *Holothuria forskali*. *Int. J. biol. Macromolec.* **4**, 329–334.

BIGLOW, C. E.(1981). Investigation of variable tensility in echinoderm connective tissue. B.Sc. thesis, University of Victoria.

BYRNE, M. (1982). Functional morphology of a holothurian autotomy plane and its role in evisceration. In *International Echinoderms Conference, Tampa Bay,* (ed. J. M. Lawrence), pp. 65–68. Rotterdam: A. A. Balkema.

BYRNE, M. (1983). Evisceration and autotomy in the holothurian *Eupentacta quinquesemita* (Selenka). Ph.D. thesis, University of Victoria.

BYRNE, M. (1985). Ultrastructural changes in the autotomy tissues of *Eupentacta quinquesemita* (Selenka) (Echinodermata: Holothuroidea) during evisceration. In *International Echinoderms Conference, Galway*, (ed. B. F. Keegan). Rotterdam: A. A. Balkema (in press).

CAEL, J. J., WINTER, W. T. & ARNOTT, S. (1978). Calcium chondroitin 4-sulphate molecular conformation and organization of polysaccharide chains in a proteoglycan. *J. molec. Biol.* **125**, 21–42.

CAVANAUGH, G. M. (1956). *Formulae and Methods,* Vol. V, pp. 83–88. Marine Biological Laboratory, Woods Hole.

COMPER, W. D. & LAURENT, T. C. (1978). Physiological function of connective tissue polysaccharides. *Physiol. Rev.* **58**, 255–315.

EMSON, R. H. & WILKIE, I. C. (1980). Fission and autotomy in echinoderms. *Oceanogr. mar. Biol. A. Rev.* **18**, 155–250.

EYLERS, J. P. (1976*a*). Mechanical properties of holothurian body wall. *Thal. Jugos.* **12**, 111–115.

EYLERS, J. P. (1976*b*). Aspects of skeletal mechanics of the starfish *Asterias forbesii*. *J. Morph.* **149**, 353–367.

EYLERS, J. P. (1982). Ion-dependent viscosity of holothurian body wall and its implications for the functional morphology of echinoderms. *J. exp. Biol.* **99**, 1–8.

FREINKEL, W. D. & HEPBURN, H. R. (1975). Dermal stiffness and collagen cross-linking in a sea cucumber (Holothuroidea). *S. Afr. J. Sci.* **71**, 280–281.

GOSLINE, J. M. (1971). Connective tissue mechanics of *Metridium senile*. II. Visco-elastic properties and macromolecular model. *J. exp. Biol.* **44**, 775–795.

HARKNESS, R. D. (1961). Biological functions of collagen. *Biol. Rev.* **36**, 399–463.

HIDAKA, M. (1983). Effects of certain physico-chemical agents on the mechanical properties of the catch apparatus of the sea-urchin spine. *J. exp. Biol.* **103**, 15–29.

HIDAKA, M. & TAKAHASHI, K. (1983). Fine structure and mechanical properties of the catch apparatus of the sea-urchin spine, a collagenous connective tissue with muscle-like holding capacity. *J. exp. Biol.* **103**, 1–14.

JORDAN, H. (1914). Über 'reflexarme' Tiere. IV. Die Holothurien. I Mitteilung. Die Holothurien als hohlorganige Tiere und die Tonusfunktion ihrer Muskulatur. *Zool. Jb. (Zool.)* **34**, 365–436.

JUNQUEIRA, L. C. U., MONTES, G. S,. MOURÃO, P. A. S., CARNEIRO, J., SALLES, L. M. M. & BONETTI, S. S. (1980). Collagen-proteoglycans interaction during autonomy in the sea cucumber *Stichopus badionotus*. *Revue can. Biol.* **39**, 157–164.

KOEHL, M. A. R. (1977). Mechanical diversity of connective tissue of the body wall of sea anemones. *J. exp. Biol.* **69**, 107–125.

LINDAHL, U. & HÖÖK, M. (1978). Glycosaminoglycans and their binding to biological macromolecules. *A. Rev. Biochem.* **47**, 385–417.

LINDEMANN, W. (1900). Ueber einige Eigenschaften der Holothurienhaut. *Z. Biol.* **39**, 18–36.

MASTERTON, W. L. & SLOWINSKI, E. J. (1973). *Chemical Principles*. London: W. B. Saunders.

MEYER, D. L. (1971). The collagenous nature of problematical ligaments in crinoids (Echinodermata). *Mar. Biol.* **9**, 235–241.

MINAFRA, S., GALANTE, R., D'ANTONI, D., FANARA, M., COPPOLA, L. & PUCCI-MINAFRA, I. (1980). Collagen associated protein-polysaccharide in the Aristotle's lanternae of *Paracentrotus lividus*. *J. submicrosc. Cytol.* **12**, 255–265.

MOTOKAWA T. (1981). The stiffness change of the holothurian dermis caused by chemical and electrical stimulation. *Comp. Biochem. Physiol.* **70**C, 41–48.

MOTOKAWA, T. (1982). Factors regulating the mechanical properties of holothurian dermis. *J. exp. Biol.* **99**, 29–41.

MOTOKAWA, T. (1983). Mechanical properties and structure of the spine-joint central ligament of the sea urchin, *Diadema setosum* (Echinodermata, Echinoidea). *J. Zool., Lond.* **201**, 223–235.

MOTOKAWA, T. (1984*a*). Connective tissue catch in echinoderms. *Biol. Rev.* **59**, 255–270.

MOTOKAWA, T. (1984*b*). The viscosity change of the body-wall dermis of the sea cucumber *Stichopus japonicus* caused by mechanical and chemical stimulation. *Comp. Biochem. Physiol.* **77**A, 419–423.

OBRINK, B. (1975). Polysaccharide-collagen interactions. In *Structures of Fibrous Biopolymers*, (eds E. D. T. Atkens & A. Keller), pp. 81–92. London: Butterworths.

PEARSE, A. G. E. (1968). *Histochemistry Theoretical and Applied*. London: Churchill Livingstone.

REYNOLDS, S. E. (1975). The mechanical properties of the abdominal cuticle of *Rhodnius* larvae. *J. exp. Biol.* **62**, 69–80.

SERRA-VON BUDDENBROCK, E. (1963). Études physiologiques at histologiques sur le tégument des holothuries (*Holothuria tubulosa*). *Vie Milieu* **14**, 55–70.

SMITH, D. S., WAINWRIGHT, S. A., BAKER, J. & CAYER, M. L. (1981). Structural features associated with movement and 'catch' of sea urchin spines. *Tissue Cell* **13**, 299–320.

SMITH, G. N., JR. & GREENBERG, M. J. (1973). Chemical control of the evisceration process in *Thyone briareus*. *Biol. Bull. mar. biol. Lab., Woods Hole* **144**, 421–436.

STOTT, R. S. H., HEPBURN, H. R., JOFFE, I. & HEFFRON, J. J. A. (1974). The mechanical defense of a sea cucumber. *S. Afr. J. Sci.* **70**, 46–48.

TAKAHASHI, K. (1967). The catch apparatus of the sea-urchin spine. II. Response to stimuli. *J. Fac. Sci. Tokyo Univ.* **11**, 121–130.

VOGEL, S. & PAPANICOLAOU, M. N. (1983). A constant stress creep testing machine. *J. Biomechanics* **16**, 153–156.

VON UEXKÜLL, J. (1900). Die Physiologie des Seeigelstachels. *Z. Biol.* **39**, 73–112.

VON UEXKÜLL, J. (1926). Die Sperrmuskulatur der Holothurien. *Pflüg. Arch. ges. Physiol.* **212**, 1–14.

WAINWRIGHT, S. A., BIGGS, W. D., CURREY, J. D. & GOSLINE, J. M. (1976). *Mechanical Design in Organisms*. London: Edward Arnold Ltd.

WILKIE, I. C. (1978). Nervously mediated change in the mechanical properties of a brittlestar ligament. *Mar. Behav. Physiol.* **5**, 289–306.

WILKIE, I. C. (1979). The juxtaligamental cells of *Ophiocomina nigra* (Abildgaard) (Echinodermata: Ophiuroidea) and their possible role in mechano-effector function of collagenous tissues. *Cell Tissue Res.* **197**, 515–530.

WILKIE, I. C. (1983). Nervously mediated change in the mechanical properties of the cirral ligaments of a crinoid. *Mar. Behav. Physiol.* **9**, 229–248.

WILKIE, I. C. (1984). Variable tensility in echinoderm collagenous tissues: a review. *Mar. Behav. Physiol.* **11**, 1–34.

J. exp. Biol. 117, 69–86 (1985)
Printed in Great Britain © *The Company of Biologists Limited 1985*

THE MECHANICAL PROPERTIES OF THE AUTOTOMY TISSUES OF THE HOLOTHURIAN *EUPENTACTA QUINQUESEMITA* AND THE EFFECTS OF CERTAIN PHYSICO-CHEMICAL AGENTS

BY MARIA BYRNE*

Department of Biology, University of Victoria, Victoria, B.C. V8W 2Y2, Canada

Accepted 26 November 1984

SUMMARY

Evisceration in the holothurian *Eupentacta quinquesemita* (Selenka) results from a rapid softening of autotomy structures comprised of connective tissue. The mechanical properties of two autotomy tissues, the introvert and the retractor muscle tendon, were tested to investigate their function in the non-evisceration state and their behaviour during autotomy. The results show that these structures do not have a pre-existing mechanical weakness to account for their rapid failure during evisceration. The autotomy response was mimicked *in vitro* by increasing K^+ concentration. The introvert exhibited viscous behaviour and the absence of Ca^{2+} and Mg^{2+} decreased introvert viscosity, whereas excess Ca^{2+}, and low and high pH, increased viscosity. These agents may influence the mechanical properties of the autotomy structures by directly affecting connective tissue ionic interactions and may induce proteoglycan conformational changes. K^+ may also exert an indirect effect through responses of cells controlling connective tissue tensility. The most likely mechanism of autotomy is through an alteration of connective tissue ionic interactions.

INTRODUCTION

The phenomenon of variable tensility in echinoderm connective tissue is associated with two types of change. Echinoderm catch ligaments exhibit reversible stiffening/softening tensility changes, whereas autotomy ligaments undergo an irreversible sudden reduction in tensility leading to loss of body parts. The echinoid spine catch apparatus is the classic example of an echinoderm catch ligament. When in catch, the connective tissue ring surrounding the spine base holds the spine in place so firmly that it is impossible to move the spine without tearing the apparatus (von Uexküll, 1900; Takahashi, 1967). Similar changes in tensility have been described for holothuroid, asteroid and crinoid connective tissues (Lindemann, 1900; Jordan, 1914; von Uexküll, 1926; Serra-von Buddenbrock, 1963; Meyer, 1971; Stott, Hepburn, Joffe & Heffron, 1974; Freinkel & Hepburn, 1975; Eylers, 1976*a*,*b*; Wilkie,

* Present address: Smithsonian Marine Station at Link Port, Route 1, Box 194-C, Fort Pierce, Florida 33450, U.S.A.

Key words: Holothurian autotomy, connective tissue, mechanical properties.

1983). The mechanical properties of echinoderm catch ligaments have been examined in numerous studies and it appears that variable tensility is associated with the viscous behaviour of the connective tissue matrix and is effected by a change in the connective tissue environment (Takahashi, 1967; Eylers, 1976*b*, 1982; Biglow, 1981; Motokawa, 1981, 1982, 1983, 1984*a,b*; Wilkie, 1983, 1984; Hidaka, 1983; Hidaka & Takahashi, 1983).

The ability to autotomize body parts is characteristic of echinoderms (Emson & Wilkie, 1980), but the mechanical properties of autotomy connective tissues have received relatively little attention. Two autotomy structures that have been studied are the holothurian retractor muscle tendon and the ophiuroid intervertebral ligament (Smith & Greenberg, 1973; Wilkie, 1978).

Evisceration in the dendrochirote holothurian *Eupentacta quinquesemita* is associated with sudden softening of three autotomy connective tissues: (1) the tendon (P-L tendon) connecting the pharyngeal retractor muscle (PRM) to the longitudinal body wall muscle (LBWM), (2) the intestine-cloacal junction and (3) the introvert, the anterior extensible portion of the body wall (Byrne, 1982). Autotomy of the P-L tendon usually occurs within 30 s and that of the introvert takes approximately 3 min but took up to 5 min in some specimens (Byrne, 1983). During evisceration the introvert changes from a firm opaque structure to one that is soft and translucent. It becomes distended as it is filled with coelomic fluid and autotomized organs propelled anteriorly by contraction of the body wall muscles. Autotomy results from changes within the connective tissue and internal hydrostatic pressure plays a role in the eventual detachment of the introvert. In this study, the mechanical properties of the P-L tendon and the introvert were examined to correlate their mechanical properties *in vitro* with their function in the non-evisceration state and with their behaviour during autotomy. The introvert is comprised predominantly of connective tissue and creep tests were used to quantify its mechanical properties. Muscle fibres dispersed in the introvert connective tissue occupy 1–4 % of the introvert cross-sectional area and do not appear to influence introvert autotomy (Byrne, 1983). The connective tissue of the P-L tendon is intimately associated with PRM muscle bundles making it impossible to isolate the tendon (Byrne, 1982) and so entire PRM preparations were used for tests. The PRMs were extended under a constant load to examine the mechanical properties of the tendon and PRM, especially for the position of failure.

Variable tensility of echinoderm connective tissues can be mimicked *in vitro* by altering the pH and cation composition of test solutions (Wilkie, 1978,1983,1984; Biglow, 1981; Smith, Wainwright, Baker & Cayer, 1981; Eylers, 1982; Motokawa, 1982, 1983, 1984*a,b*; Hidaka, 1983) and similar experiments were used to investigate the mode of action of physico-chemical agents used in other studies on the autotomy structures of *E. quinquesemita*.

MATERIALS AND METHODS

Tissue samples

Specimens of *Eupentacta quinquesemita* were collected subtidally near Victoria, B.C. and near the Friday Harbor Laboratories, Washington, and acclimated in an ambient sea water system for at least 24 h before use in experiments. They were

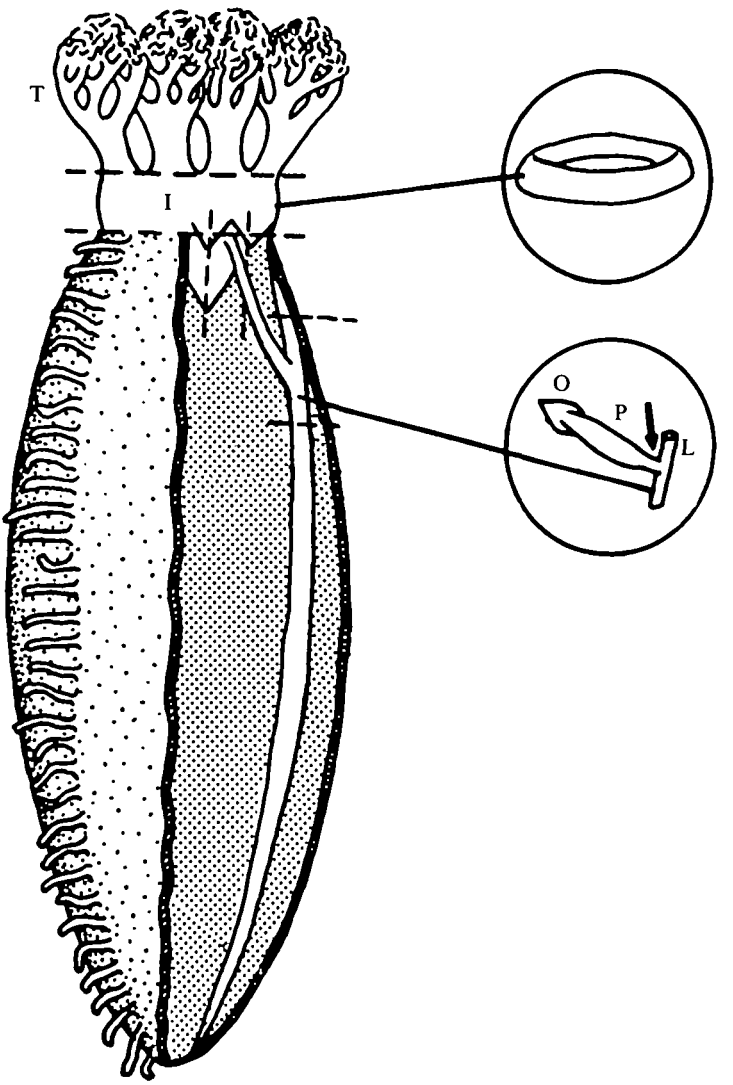

Fig. 1. Diagram showing the dissection and isolation of the introvert (I) and the pharyngeal retractor muscle (P) of *Eupentacta quinquesemita* (Selenka). Incisions indicated by the broken lines. O, ossicle; L, longitudinal body wall muscle; T, tentacle; arrow, P-L tendon.

relaxed in 6·7 % $MgCl_2$ or 0·1 % propylene phenoxetol (PPOX) in sea water for 3–5 h before dissection. The introvert was dissected as follows (Fig. 1): it was cut along its posterior margin where it joins the body wall, the tentacles were cut off at their bases and the body wall muscle tissue was removed. For ease of handling, circumferential rings were used for all tests. The PRMs were isolated from relaxed specimens by dissection around their junction with the LBWM and at their anterior insertion into the ossicle (Fig. 1). Surgical silk thread was tied at either end of the preparations and thread loops were made to facilitate connections of the PRMs to the testing apparatus (see below). Before testing, the preparations were washed in sea water for 3–5 h.

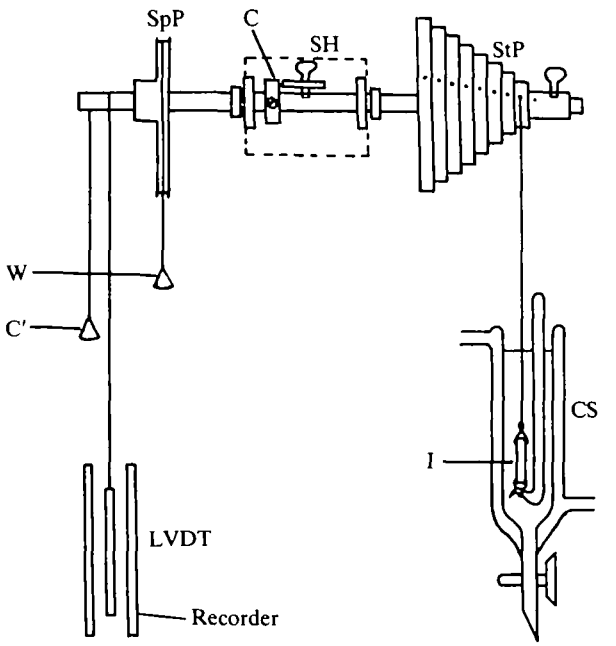

Fig. 2. The constant stress creep-testing machine, modified from Vogel & Papanicolaou (1983). The introvert (I) is in a bathing solution and is attached to the 'step' of the step pulley (StP) with a diameter closest to the original length of the specimen. C, counterweight for the step pully; C', counterweight for the LVDT core rod; CS, cooling sleeve; LVDT, linear variable differential transformer, measures specimen elongation and is connected to a chart recorder; SH, shaft holder; SpP, spiral pulley; W, applied weight, when multiplied by the moment arm of the spiral pulley, gives the force on the specimen.

Introvert

A constant stress creep machine (Fig. 2) was used to quantify the mechanical properties of the introvert. Stress (σ) is $= F/A$, where F = force and A = cross-sectional area of the specimen. It was assumed that the volume of the introvert remained constant during tests. The rationale behind the creep machine's design and construction is described in Vogel & Papanicolaou (1983). The machine has two essential features: a circular step pulley with steps of different radii and a spiral pulley, both of which are on the same shaft. The specimen is attached to that step of the step pulley with a diameter nearest to the initial length of the specimen. The spiral pulley is designed so that the product of specimen length and the pulley lever arm is constant, i.e. the lever arm length decreases directly in proportion to specimen elongation, keeping stress constant. The stress on the specimen is given by: $\sigma = F'Ro'/RSo$, where F' = applied weight, Ro' = initial lever arm length, R = radius of the step pulley chosen and So = initial cross-sectional area of the specimen. Shaft rotation was measured by a linear variable differential transformer (LVDT) and provided a measure of specimen length, which was required to calculate strain. The introvert proved to be a highly extensible tissue, therefore natural or true strain; $e = \ln(L/Lo)$ was used, where L = actual length and Lo = original length of the tissue (Wainwright, Biggs, Currey & Gosline, 1976). The introvert rings were held between two heart

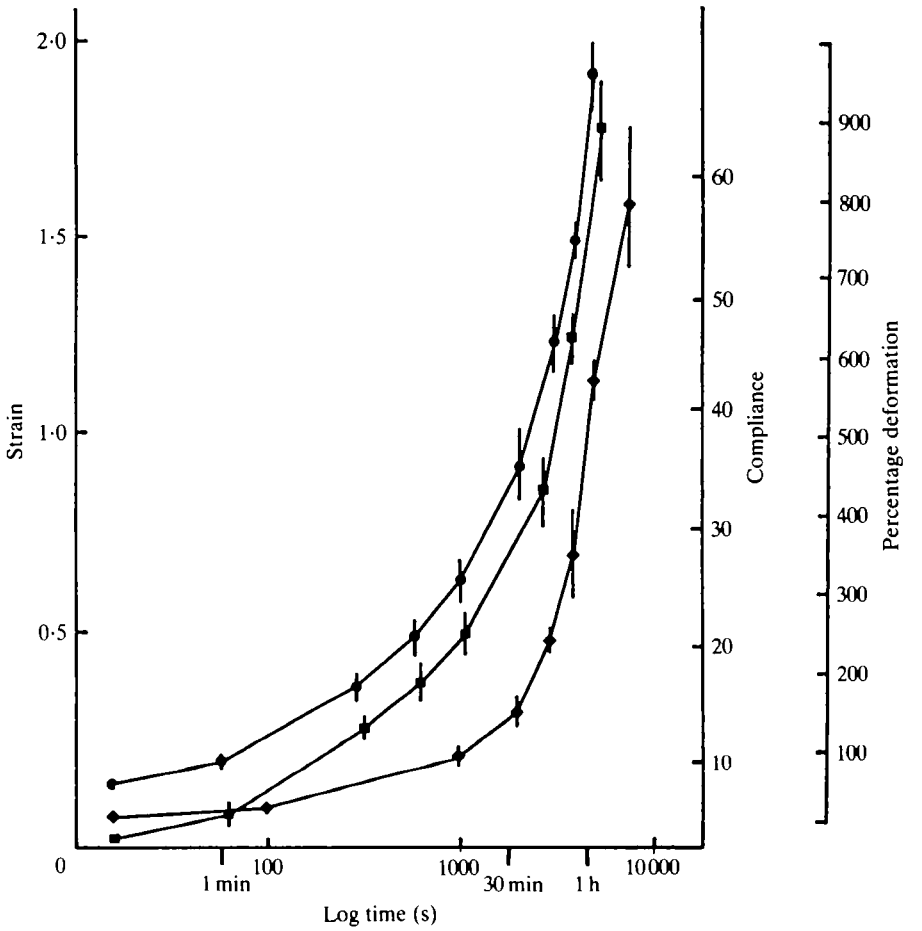

Fig. 4. Creep curve (—●—), compliance (—■—) and percentage deformation (—◆—) of introvert tissue tested in ASW. $N = 9$ at t_o, $N = 6$ at $t = 3500$ s, $N = 4$ at $t = 6000$ s. Means ± S.E.M.

Experimental solutions

Creep tests were done while the introvert was bathed in artificial sea water (ASW), Ca^{2+}-free sea water (CaFSW), MgFSW, or CaMgFSW, made according to M.B.L. Formulae (Cavanaugh, 1956). The salinity of local sea water varies between 28 and 32 ‰. Solutions containing various concentrations of K^+ were made by adding isosmotic KCl (0·45 mol l^{-1}) to 0·45 mol l^{-1} NaCl (KNaASW), i.e. ASW containing the cations K^+ and Na^+ only. Isosmotic KCl and solutions of other monovalent cations, Rb^+ (0·45 mol l^{-1} RbCl) and Na^+ (0·45 mol l^{-1} NaCl), were used to examine the K^+ response specificity. Isosmotic $CaCl_2$ (0·30 mol l^{-1}) was also tested. To test the effect of anaesthetics on the K^+ response, tissues were tested without recovery from anaesthesia. Buffer solutions, pH 2–12, were used to test the effect of pH on introvert viscosity. For pH 4–10, Tris buffers were made with appropriate amounts of Tris-HCl and Trisma base (Sigma). For pH 2, McIlvaine's buffer was used (Pearse, 1968) and 0·1 mol l^{-1} NaOH was used for pH 12. The effect of experimental

solutions on the PRM was tested while the tissue was attached to the lever maintained in position by a light load (F/A at $t_o = 0{\cdot}98 \times 10^4\,N\,m^{-2}$).

RESULTS

Introvert

The introvert was creep-tested in ASW to examine the mechanical properties of the tissue in a solution approximating to physiological conditions. The combined creep curve for nine specimens shows that the tissue deformed at a slow and constant rate until failure (Fig. 4). When strain is plotted against log time, the creep curve is exponential due to the constant creep rate. The creep curve between 600 and 4000 s was used to calculate viscosity. This was to avoid the influence of initial slack in the tissue and after 4000 s the sample size decreased (Fig. 4). Introvert compliance increased as the creep test progressed (Fig. 4) and deformations at failure were up to 900 % relative to the original length of the tissue (Fig. 4). The introvert is very viscous and deformations beyond approximately the first 10 min were irreversible. Specimens in creep tests arrested after 10 min did not return to their original dimensions before eventually degenerating. During the first 5–10 min the introvert appeared relatively stiff when manipulated and examined directly. The introvert cross-sectional area appeared to decrease uniformly during creep tests. Narrowing or necking of the tissue was not observed even as the introvert approached failure. Introvert viscosity in ASW tests was of the order of $10^8\,N\,m^{-2}\,s$ (Table 2).

Pharyngeal retractor muscle

Eight PRMs were placed on the lever and two were loaded with $0{\cdot}98 \times 10^4\,N\,m^{-2}$ and six with $4{\cdot}9 \times 10^4\,N\,m^{-2}$. Strains at failure were similar for all tests despite the different initial stresses (Fig. 5). Six PRMs broke at or near the ossicle but two of the PRMs at the higher load broke at the tendon.

Table 1. *Introvert compliance D(t) at t = 300 s, D(t) = e(t)/σ*

Solution	D(t)*	S.E.	*N*
ASW	1·2	0·09	9
CaFSW	2·7	0·46	9
MgFSW	1·5	0·18	5
CaMgFSW	4·3	0·29	2
0·45 mol l^{-1} KCl	2·5	0·29	3
0·25 mol l^{-1} KCl	1·8	0·36	2
0·15 mol l^{-1} KCl	1·2	0·06	5
0·075 mol l^{-1} KCl	1·2	0·15	4
0·45 mol l^{-1} NaCl	1·0	0·20	2
$MgCl_2$–KCl†	1·9	–	1‡
PPOX–KCl‡	0·7	0·05	4

* All values $\times 10^{-5}\,N^{-1}\,m^2$.
† Anaesthetized tissue tested in 0·45 mol l^{-1} KCl without recovery in sea water.
‡ Only one of three specimens lasted 300 s before failure.
PPOX, propylene phenoxetol.

Table 2. *Introvert viscosity* (η) *in test solutions*, $\eta = \sigma/\dot{e}$

Solution	η*	N	r^2
ASW	10·0	9	1·0
CaFSW	6·0	9	1·0
MgFSW	5·0	5	1·0
CaMgFSW	1·25	2	1·0
0·45 mol l^{-1} KCl	2·08	3	0·89
0·45 mol l^{-1} RbCl	1·07	2	0·97
0·25 mol l^{-1} KCl	5·6	2	0·96
0·15 mol l^{-1} KCl	7·5	5	0·9
0·075 mol l^{-1} KCl	10·0	4	0·97
0·45 mol l^{-1} NaCl	12·0	2	0·87
$MgCl_2$–KCl†	0·9	3	1·0
PPOX–KCl†	10·0	4	1·0

* All values $\times 10^7$ N m^{-2} s.

† Anaesthetized tissue tested in 0·45 mol l^{-1} KCl without recovery in sea water.

r^2, coefficient of determination. The regressions were calculated for the creep curves, see Figs 4, 6 and 8 for standard errors.

PPOX, propylene phenoxetol.

Effect of experimental solutions

Introvert

The softening of the introvert observed during evisceration was mimicked *in vitro* by increasing the K^+ concentration in the bathing solution. Excess K^+ ions induced an increase in compliance and decrease in viscosity (Fig. 6; Tables 1, 2). Isosmotic KCl had the greatest effect with rapid failure at low strain values (Table 3). The

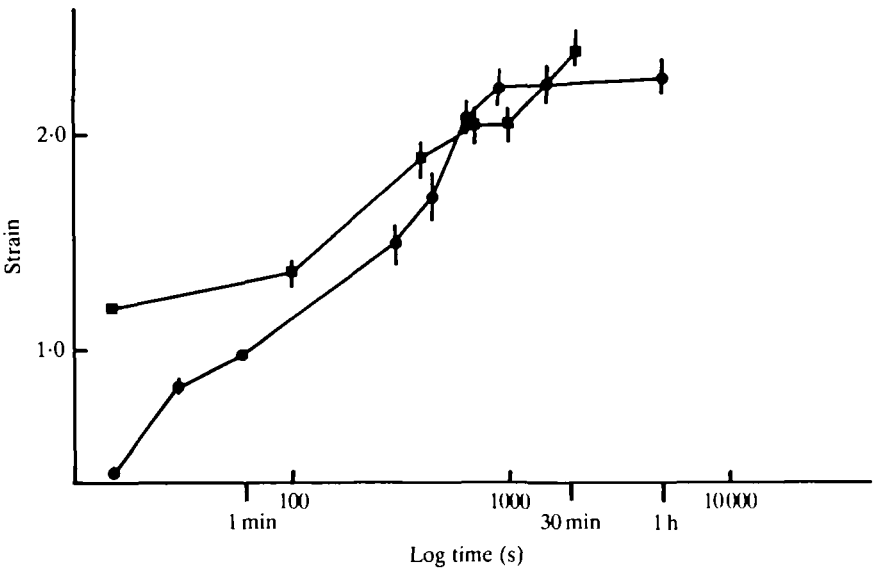

Fig. 5. Elongation of the PRMs extended with a constant load while bathed in ASW. Strains resulting from the two initial stresses, (—●—) $\sigma = 0{\cdot}98 \times 10^4$ N m^{-2} ($r^2 = 0{\cdot}92$) and (—■—) $\sigma = 4{\cdot}9 \times 10^4$ N m^{-2} ($r^2 = 0{\cdot}97$), were similar. Means ± S.E.M.

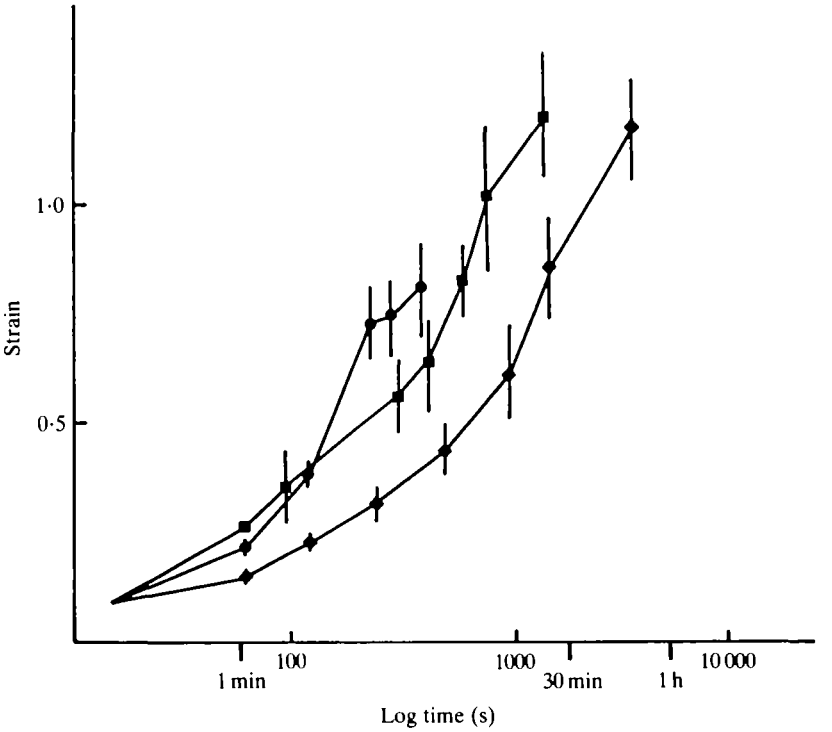

Fig. 6. The influence of K^+ on introvert creep behaviour. 0·45 mol l^{-1} KCl (—●—) induced a rapid creep rate and failure ($N = 3$). 0·25 mol l^{-1} KCl (—■—) ($N = 2$). 0·075 mol l^{-1} KCl (—◆—) tests resembled controls ($N = 4$). Means ± S.E.M.

influence of the ion decreased as the concentration was lowered and 0·15 mol l^{-1} KCl was the lowest concentration tested that affected introvert viscosity. For tissues tested in 0·075 mol l^{-1} KCl, the creep curves were similar to controls. The concentration of K^+ in the coelomic fluid of *Eupentacta quinquesemita* is 0·012 mol l^{-1} (Byrne, 1983). Isosmotic RbCl produced results similar to those with KCl and 0·45 mol l^{-1} NaCl tests were similar to controls (Tables 2, 3). The decrease in compliance induced by 0·45 mol l^{-1} KCl was arrested when the bathing solution was replaced with isosmotic $CaCl_2$ (Fig. 7). Excess Ca^{2+} stiffened the introvert and the tissue did not fail in tests.

Anaesthetized tissues tested without prior recovery exhibited variable responses to K^+. $MgCl_2$ did not interfere with K^+-induced softening, but PPOX inhibited the response and may have had a stiffening influence. PPOX-anaesthetized tissues had viscosity values similar to controls and the creep tests had a similar duration, although the breaking strains were lower than those of controls (Tables 2, 3). Introvert preparations that were anaesthetized in $MgCl_2$ or PPOX, and then washed in sea water for 3–5 h before testing, had similar responses to those tested in excess K^+.

The initial stiff period apparent in control tissue when handled directly was not present in tissues treated with divalent-cation-free sea water. Introvert preparations

Table 3. *Breaking strain and failure times for introvert creep tests*

Solution	Breaking strain (S.E.)	Time (s) (S.E.)	*N*
ASW	1·52 (0·25)	4200 (800)	9
CaFSW	1·93 (0·08)	2455 (470)	9
MgFSW	1·33 (0·18)	1520 (345)	5
CaMgFSW	1·46 (0·11)	350 (70)	2
0·45 mol l^{-1} NaCl	1·53 (0·08)	6000 (1180)	2
0·45 mol l^{-1} KCl	0·83 (0·08)	350 (54)	3
0·45 mol l^{-1} RbCl	1·00 (0·03)	390 (30)	2
0·25 mol l^{-1} KCl	1·19 (0·13)	1250 (250)	2
0·15 mol l^{-1} KCl	1·10 (0·20)	1720 (186)	5
0·075 mol l^{-1} KCl	1·40 (0·17)	3400 (1300)	4
$MgCl_2$–KCl*	0·63 (0·14)	130 (78)	3
PPOX–KCl*	1·00 (0·19)	3125 (315)	4

* Anaesthetized tissue tested in 0·45 mol l^{-1} KCl without recovery in sea water.
PPOX, propylene phenoxetol.

soaked for 2 h and tested in CaFSW, MgFSW or CaMgFSW deformed at a faster rate than ASW controls, with decreased viscosity and increased compliance (Fig. 8; Tables 1, 2). The lack of Ca^{2+} made the tissue more compliant and deformations at failure were higher than those of ASW controls (Table 3). The lack of Mg^{2+} hastened failure and at strains similar to controls (Table 3). The lack of both ions elicited the greatest increase in compliance and decrease in viscosity with a rapid failure at strains similar to controls (Fig. 8; Tables 1–3). In contrast, excess Ca^{2+} (isosmotic $CaCl_2$) induced stiffening and the tissue did not fail in tests.

Manipulation of pH affects introvert viscosity. The viscosity value was lowest at pH 7·0, similar to that of ASW tests, and increased sharply at either side of this pH (Fig. 9). The pH of *E. quinquesemita* coelomic fluid is 7·0 (Byrne, 1983).

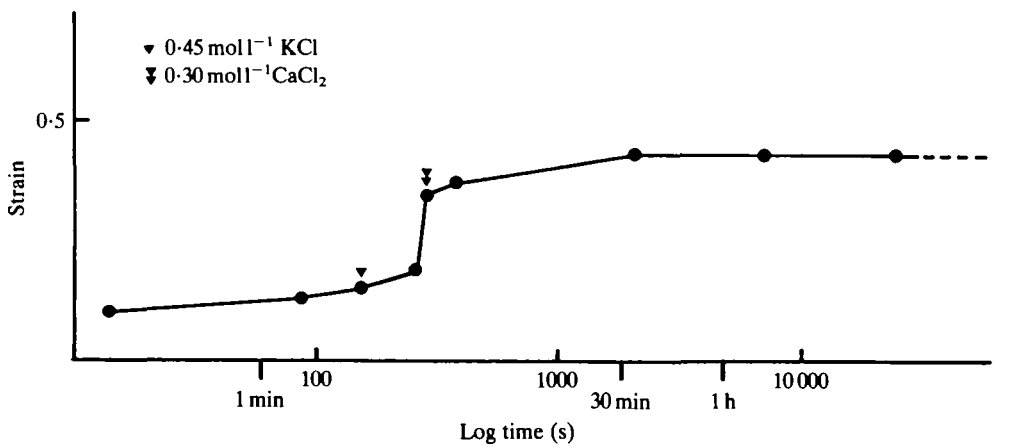

Fig. 7. Antagonistic interaction of K^+ and Ca^{2+} on introvert creep behaviour. The increased compliance induced by 0·45 mol l^{-1} KCl is arrested if the bathing solution is replaced with 0·30 mol l^{-1} $CaCl_2$. The tissue remained stiff in $CaCl_2$ for the duration of the test and did not fail.

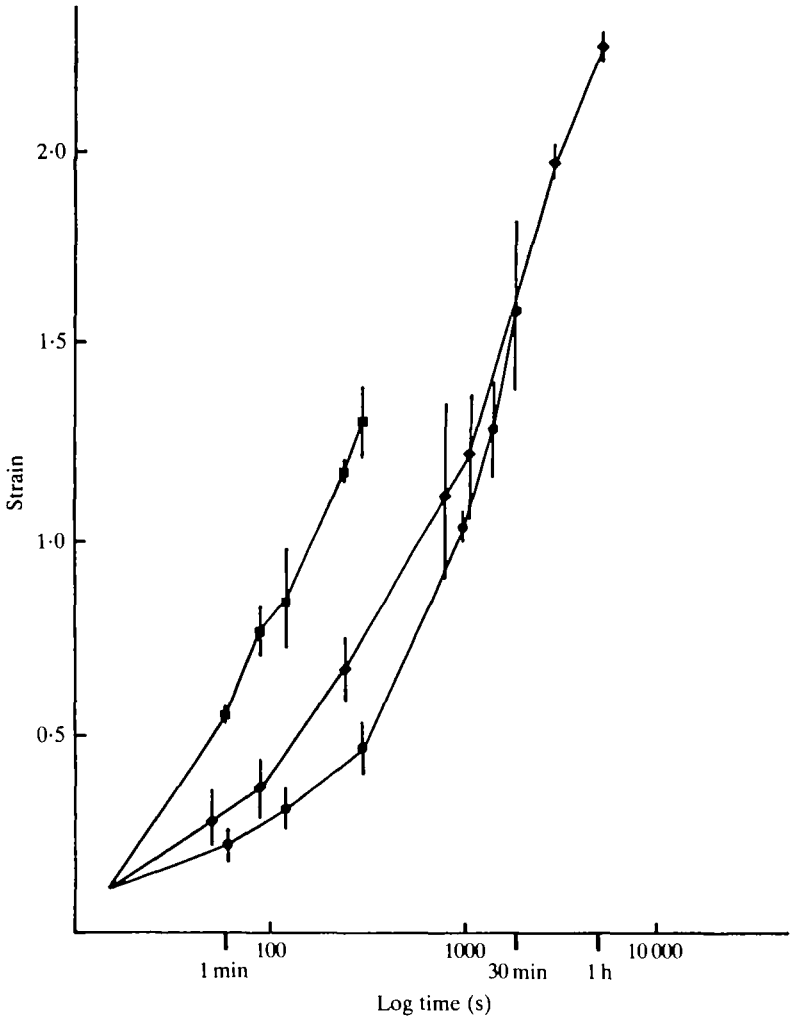

Fig. 8. Creep curve of introvert tissue bathed in cation-free ASW. CaFSW (—◆—) induced a decrease in viscosity, and deformations at failure were greater than controls ($N = 9$). MgFSW (—●—) also decreased introvert viscosity and hastened failure at strains similar to ASW tests ($N = 5$). The lack of both ions (—■—) elicited the greatest increase in compliance and rapid failure ($N = 2$). Means ± S.E.M.

Pharyngeal retractor muscle

Muscle preparations tested in ASW and 0·45 mol l^{-1} NaCl did not fail in tests (Table 4). KCl and RbCl were most effective in eliciting tendon autotomy. These solutions induced muscle contraction, tendon softening and a rapid separation of the PRM and LBWM (Table 4). $MgCl_2$ did not block these responses but PPOX inhibited K^+-induced autotomy. Tendon failure occurred with other solutions, but the response times were considerably longer (Table 4) and the results cannot be reliably compared with the rapid tendon autotomy *in vivo* during evisceration. Excess Ca^{2+} induced muscle contraction resulting in a narrow neck at the P-L tendon and

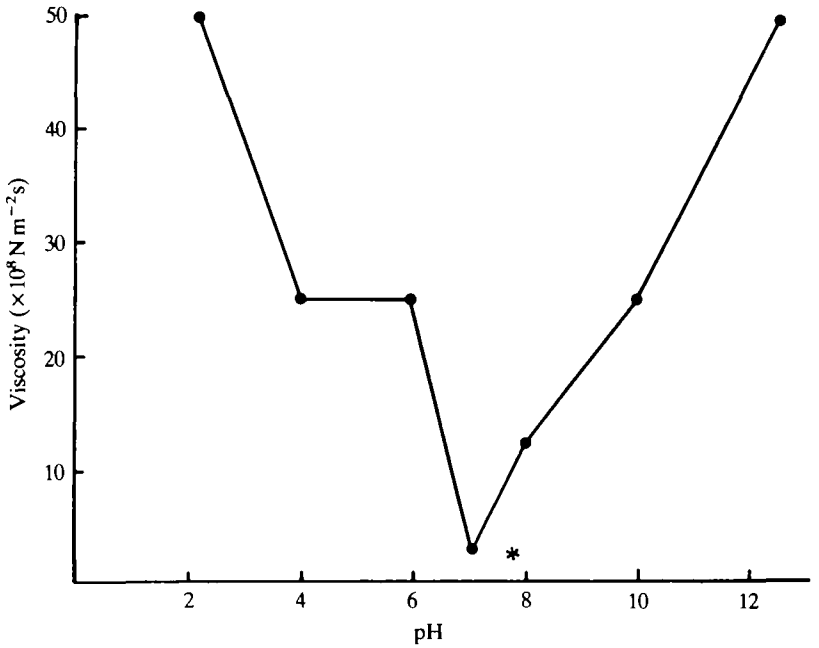

Fig. 9. The influence of pH on introvert viscosity. The asterisk marks introvert viscosity in ASW (pH 7·8) tests.

concentration of stress forces at the neck may have caused eventual tendon rupture. Muscle contraction induced by KCl and RbCl may also have resulted in stress concentration, but the rapid response of the P-L tendon suggests that these agents also affected the connective tissue. CaFSW induced muscle relaxation and uniform cross-sectional area along the PRMs and they did not fail in CaFSW tests. Most of the PRMs tested in MgFSW broke at the tendon.

Table 4. *Response of PRM preparations to test solutions*

Solution	*N*	P-L tendon failure, *N*	Response time (s) (S.E.)
ASW	5	0	
0·45 mol l^{-1} NaCl	5	0	
0·45 mol l^{-1} KCl	10	10	102 (12)
0·45 mol l^{-1} RbCl	9	9	90 (130)
0.30 mol l^{-1} $CaCl_2$	5	5	4806 (570)
CaFSW	5	0	
MgFSW	9	7	4800 (1038)
$MgCl_2$–KCl*	5	5	126 (60)
PPOX–KCl*	7	1	90

* Anaesthetized tissue tested in 0·45 mol l^{-1} KCl without recovery in sea water.
PPOX, propylene phenoxetol.

DISCUSSION

The compliant properties of the introvert correlate with the extensibility it exhibits during suspension feeding in association with tentacle protraction and retraction and with the characteristic infolding of the introvert that occurs when the tentacular crown is withdrawn. In comparison, the body wall posterior to the introvert was considerably less extensible in mechanical tests (M. Byrne, unpublished results). The introvert is comprised of a dense connective tissue layer containing collagen fibrils and matrix and a predominant layer of loose connective tissue containing matrix and occasional small unstriated fibrils (Byrne, 1983). Morphologically and histochemically the introvert appears to be comprised predominantly of glycosaminoglycan (GAG) (Byrne, 1983, 1985) which probably accounts for its viscous properties *in vitro* and its extensible behaviour *in vivo*. Other echinoderm connective tissues have been shown biochemically to possess a high GAG and proteoglycan content (Junqueira *et al.* 1980; Minafra *et al.* 1980; Bailey, Gathercole, Dlugosz & Voyle, 1982).

The creep curves in ASW were similar for all introvert preparations although they differed in duration, which suggests that some specimens were stiffer than others. The proportion of loose and dense connective tissue in the introvert varies between specimens (Byrne, 1983) and may be a source of creep test variability. The introvert may also have catch properties as described for the holothurian body wall (Motokawa, 1984*b*) and so the test tissues may have been in various states of catch. The introvert creep rate appears to be less variable than that of the body wall (Motokawa, 1984*b*). Introvert creep curves are similar to those obtained for other echinoderm connective tissues (Takahashi, 1967; Eylers, 1976*a*, 1982; Wilkie, 1978; Motokawa, 1981; Smith *et al.* 1981) and for sea anemone mesogloea (Alexander, 1962; Koehl, 1977). As for other echinoderm connective tissues the introvert exhibited viscoelastic properties. Assuming that introvert collagen fibrils are similar to vertebrate tendon collagen, relatively inextensible and of high tensile strength (Harkness, 1961), the large deformations obtained during creep tests indicate that the collagen fibrils are discontinuous, as suggested for holothurian dermis and mesogloea (Gosline, 1971; Motokawa, 1981).

Initially during creep tests, the collagen fibrils may act as tensile elements with the matrix transferring the load from fibre to fibre. As deformation continues, the collagen fibrils must slip past each other perhaps associated with a decrease in fibre-matrix adhesion. This may be associated with an alteration in the GAG-collagen electrostatic interactions (see below) and a decrease in matrix viscosity. The interfibrillar slippage results in a decrease in stiffness and increase in compliance. During the final stages of the creep tests, matrix proteoglycan molecules may be pulled upon directly, with possible breakage of intermolecular ionic bonds and subsequent tissue failure. Initial reinforcement by fibrillar elements followed by viscous behaviour dominated by matrix proteoglycans is similar to that described for sea anemone mesogloea and insect cuticle (Gosline, 1971; Reynolds, 1975).

Introvert compliance and its viscous matrix are central to its function *in vivo* where introvert extension and inversion are generated by the tentacle muscles, the PRMs and the body wall musculature. During tentacle protraction and retraction, introvert collagen fibrils may slip past each other, but it is unlikely that the tissue is extended

to the point where the collagen fibrils no longer overlap. In the non-evisceration state the introvert does not approach failure and so it is unlikely that matrix proteoglycans are ever pulled upon directly, as is suggested to occur in the latter portion of the creep tests.

During evisceration, the introvert serves as a specialized autotomizing structure. The sudden softening characteristic of the introvert during autotomy was not observed in control tests in ASW, suggesting that the tissue does not have a pre-existing mechanical weakness to account for its failure during evisceration and that autotomy involves a physiological change in the tissue. Ultrastructural examination of autotomizing introvert revealed that changes in the connective tissue matrix caused interfibrillar slippage resulting in complete fibril disarray and that the subsequent viscid flow was followed by autotomy (Byrne, 1985).

The P-L tendon serves as a connection between the PRM and LBWM and as an autotomizing structure. The tendon is comprised of collagenous connective tissue associated with PRM muscle fibres and it functions in conjunction with the PRM (Byrne, 1982). Consequently, the test results largely reflect PRM properties. The tendon was found to be as strong or stronger than associated muscle tissue and it thus forms a strong connection between the PRM and LBWM. PRM failure usually occurred at or near the anterior insertion into the ossicle but not at the tendon. Similar results were obtained for the P-L tendon of *Sclerodactyla briareus,* which also autotomizes during evisceration (Smith & Greenberg, 1973).

Introvert and P-L tendon autotomy during evisceration was mimicked *in vitro* by elevated K^+, especially with isosmotic KCl. Introvert compliance also increased in the absence of divalent cations. The results of ion experiments may be a function of the connective tissue chemistry. Connective tissue polysaccharides in solution undergo reversible conformational changes induced by altering ion concentrations (Cael, Winter & Arnott, 1978) and their polyanionic nature creates potential for GAG-GAG and collagen-GAG electrostatic interactions (Obrink, 1975; Comper & Laurent, 1978; Lindahl & Höök, 1978). Experimental alteration of ion concentrations may have affected introvert viscosity by changing these interactions or by inducing proteoglycan conformational change. Manipulation of the ionic milieu has been used with similar results for other echinoderm connective tissues (Wilkie, 1978; Biglow, 1981; Smith *et al.* 1981; Eylers, 1982; Hidaka, 1983). Viscosity changes induced by altering K^+ and Ca^{2+} concentrations were obtained in solutions of holothurian dermis where cellular inclusions were completely disrupted (Biglow, 1981). The effect of K^+ may involve the masking of GAG anionic sites, thereby reducing collagen-GAG and GAG-GAG ionic interactions, as suggested for other echinoderm connective tissues (Wilkie, 1978; Biglow, 1981; Eylers, 1982). K^+ and Rb^+ reduced introvert viscosity and induced P-L tendon autotomy, but Na^+ did not, perhaps because K^+ and Rb^+ have similar ionic characteristics, both are larger than Na^+ (Masterton & Slowinski, 1973).

Excess Ca^{2+} stiffened the introvert, perhaps by acting as a divalent cross-linker; that is, as an ionic bridge facilitating ionic interactions. Conversely, the lack of Ca^{2+} would have a softening effect. Treatment with CaFSW decreased introvert viscosity, as has been found for other echinoderm connective tissues (Biglow, 1981; Smith *et al.* 1981; Eylers, 1982; Hidaka, 1983). MgFSW also decreased introvert viscosity and

hastened failure compared with ASW controls. This solution had a similar effect in other studies (Wilkie, 1978, 1983; Smith *et al.* 1981). The lack of both Mg^{2+} and Ca^{2+} had the greatest influence on the introvert with results similar to those from isosmotic KCl tests. Both Mg^{2+} and Ca^{2+} appear to play a stabilizing role in the connective tissue, as suggested in other investigations (Wilkie, 1978, 1983; Smith *et al.* 1981), although excess Mg^{2+} lowered the viscous resistance of the echinoid catch apparatus (Hidaka, 1983). The response of the introvert to altering ion concentrations suggests that the mechanism of autotomy may involve a change in the ionic environment *in vivo*.

Besides the potential effect of K^+ on ionic interactions, there is evidence that the action of K^+ may be indirect through cellular mediation, especially in studies where low concentrations of K^+ were tested (Table 5). Wilkie (1983) found that the K^+ response that makes crinoid cirral ligaments more pliant is Ca^{2+}-dependent and is inhibited by Mg^{2+}. Concentrations of 0·075–0.1 mol l^{-1} KCl in KNaASW had no discernible effect on the introvert, perhaps due to the absence of other cations. In studies where K^+ was tested with an appropriate decrease in Na^+ and where other sea water cations were balanced, K^+ was found to have a stiffening or a relaxing effect depending on the tissues tested (Table 5). Inconsistent responses were observed for the ophiuroid oral plate ligament which stiffens or softens in response to isosmotic KCl (Wilkie, 1984). The influence of K^+, especially at low concentrations, may not be due to a direct physico-chemical effect and at high concentrations the ion potentially exerts direct and indirect effects. The inconsistent effect of K^+ suggests that the K^+ response may be tissue-specific, perhaps involving cells controlling variable tensility.

Introvert mechanical properties were influenced by pH. Viscosity was lowest at pH 7·0 and increased sharply with increasing pH (8–12) and decreasing pH (pH 6–2). The ophiuroid intervertebral ligament and the echinoid catch apparatus were also

Table 5. *The effect of K^+ on the mechanical properties of echinoderm connective tissues*

Class and species	Tissue	$[K^+]$ (mol l^{-1})	Response	Reference
Crinoidea				
Antedon bifida (Pennant)	cirral ligament•	0·015–0·05	softening	Wilkie (1983)
Echinoidea				
Anthocidaris crassispina (A. Aggassiz)	catch apparatus•	0·1	hardening	Takahashi (1967)
Diadema setosum Leske	spine central ligament•	0·1	hardening	Motokawa (1983)
Holothuroidea				
Sclerodactyla briareus (Lesueur)	P-L tendon†	0·1	softening	Smith & Greenberg (1973)
Stichopus chloronotus Brandt	dermis•	0·05–0·1	hardening	Motokawa (1981)
Eupentacta quinquesemita (Selenka)	introvert‡	0·075	no effect	present study

• KASW, † KCl, ‡ KNaASW.

influenced by pH, but the viscosities and tensile strength of these tissues were lowest at pH 10 and 5 respectively (Wilkie, 1978; Hidaka, 1983). These different experimental results may reflect differences in tissue physiology, perhaps associated with matrix composition. They may also be influenced by the different test solutions employed. Wilkie (1978) also used a series of buffer solutions while Hidaka (1983) used buffered ASW where the presence of other sea water cations may have influenced the results. Altering pH may influence the mechanical properties of echinoderm connective tissues by changing the net surface charge of the matrix and thereby affect connective tissue ionic interactions, as suggested by Hidaka (1983). Although *in vitro* tests demonstrated that the introvert stiffens at low and high pH, the sensitivity of the tissue to pH change suggests that the mechanism of autotomy may involve an alteration of tissue pH.

The results of ion and pH experiments have been used to suggest that the mechanism of variable tensility involves ion or pH changes that alter electrostatic interactions within the connective tissue, thereby causing tensility change (Wilkie, 1979; Motokawa, 1981, 1982, 1983; Eylers, 1982; Hidaka, 1983). Large ionic or pH changes are unlikely *in vivo* and the results of experiments described here and elsewhere involving ion concentrations and pH values above or below physiological levels may be *in vitro* artifacts reflecting proteoglycan conformational changes. Although ion and pH change are potential mechanisms, their physiological role in variable tensility of echinoderm connective tissues has yet to be established.

Anaesthetic antagonism of the K^+ response has been taken as evidence to suggest that variable tensility is neurally controlled (Wilkie, 1978, 1983). The influence of anaesthetics on the introvert and P-L tendon was variable. $MgCl_2$ did not block K^+-induced softening, perhaps because Mg^{2+} is a muscle relaxant and it may have a limited effect on connective tissue, especially in competition with a high concentration of K^+ ions. $MgCl_2$ partially blocked the response of the ophiuroid intervertebral ligament to excess K^+ (Wilkie, 1978). Propylene phenoxetol inhibited the K^+ response as shown in other studies (Wilkie, 1978, 1983), but its mode of action has not been established and it may have exerted a direct stabilizing influence on the connective tissue.

In general, the mechanical properties of echinoderm connective tissues that exhibit variable tensility appear to be associated with changes in the matrix, not with collagen or muscle events. At present, the most likely mechanism of variable tensility is through an alteration of connective tissue ionic interactions, but how this is brought about is not known. There is evidence for neural control of evisceration autotomy and for the presence of an endogenous evisceration factor in *Eupentacta quinquesemita* and this evidence will be presented in a following report (M. Byrne, in preparation).

I thank Professor A. R. Fontaine for his enthusiastic supervision of my research. Dr M. LaBarbera and Dr S. Vogel provided helpful comments and equipment. I am grateful to Dr I. C. Wilkie and Dr S. Vogel for reading earlier versions of this manuscript. Ms J. Piraino also read the manuscript. I thank Dr A. O. D. Willows, director of the Friday Harbor Laboratories for use of facilities. The work was supported by a University of Victoria Graduate Fellowship and this report is Smithsonian Marine Station contribution no. 133.

REFERENCES

ALEXANDER, R. McN. (1962). Visco-elastic properties of the body wall of sea anemones. *J. exp. Biol.* **39**, 373–386.

BAILEY, A. J., GATHERCOLE, L. J., DLUGOSZ, J. & VOYLE, C. A. (1982). Proposed resolution of the paradox of extensive crosslinking and low tensile strength of cuvierian tubule collagen from the sea cucumber *Holothuria forskali*. *Int. J. biol. Macromolec.* **4**, 329–334.

BIGLOW, C. E.(1981). Investigation of variable tensility in echinoderm connective tissue. B.Sc. thesis, University of Victoria.

BYRNE, M. (1982). Functional morphology of a holothurian autotomy plane and its role in evisceration. In *International Echinoderms Conference, Tampa Bay,* (ed. J. M. Lawrence), pp. 65–68. Rotterdam: A. A. Balkema.

BYRNE, M. (1983). Evisceration and autotomy in the holothurian *Eupentacta quinquesemita* (Selenka). Ph.D. thesis, University of Victoria.

BYRNE, M. (1985). Ultrastructural changes in the autotomy tissues of *Eupentacta quinquesemita* (Selenka) (Echinodermata: Holothuroidea) during evisceration. In *International Echinoderms Conference, Galway*, (ed. B. F. Keegan). Rotterdam: A. A. Balkema (in press).

CAEL, J. J., WINTER, W. T. & ARNOTT, S. (1978). Calcium chondroitin 4-sulphate molecular conformation and organization of polysaccharide chains in a proteoglycan. *J. molec. Biol.* **125**, 21–42.

CAVANAUGH, G. M. (1956). *Formulae and Methods,* Vol. V, pp. 83–88. Marine Biological Laboratory, Woods Hole.

COMPER, W. D. & LAURENT, T. C. (1978). Physiological function of connective tissue polysaccharides. *Physiol. Rev.* **58**, 255–315.

EMSON, R. H. & WILKIE, I. C. (1980). Fission and autotomy in echinoderms. *Oceanogr. mar. Biol. A. Rev.* **18**, 155–250.

EYLERS, J. P. (1976*a*). Mechanical properties of holothurian body wall. *Thal. Jugos.* **12**, 111–115.

EYLERS, J. P. (1976*b*). Aspects of skeletal mechanics of the starfish *Asterias forbesii*. *J. Morph.* **149**, 353–367.

EYLERS, J. P. (1982). Ion-dependent viscosity of holothurian body wall and its implications for the functional morphology of echinoderms. *J. exp. Biol.* **99**, 1–8.

FREINKEL, W. D. & HEPBURN, H. R. (1975). Dermal stiffness and collagen cross-linking in a sea cucumber (Holothuroidea). *S. Afr. J. Sci.* **71**, 280–281.

GOSLINE, J. M. (1971). Connective tissue mechanics of *Metridium senile*. II. Visco-elastic properties and macromolecular model. *J. exp. Biol.* **44**, 775–795.

HARKNESS, R. D. (1961). Biological functions of collagen. *Biol. Rev.* **36**, 399–463.

HIDAKA, M. (1983). Effects of certain physico-chemical agents on the mechanical properties of the catch apparatus of the sea-urchin spine. *J. exp. Biol.* **103**, 15–29.

HIDAKA, M. & TAKAHASHI, K. (1983). Fine structure and mechanical properties of the catch apparatus of the sea-urchin spine, a collagenous connective tissue with muscle-like holding capacity. *J. exp. Biol.* **103**, 1–14.

JORDAN, H. (1914). Über 'reflexarme' Tiere. IV. Die Holothurien. I Mitteilung. Die Holothurien als hohlorganige Tiere und die Tonusfunktion ihrer Muskulatur. *Zool. Jb. (Zool.)* **34**, 365–436.

JUNQUEIRA, L. C. U., MONTES, G. S,. MOURÃO, P. A. S., CARNEIRO, J., SALLES, L. M. M. & BONETTI, S. S. (1980). Collagen-proteoglycans interaction during autonomy in the sea cucumber *Stichopus badionotus*. *Revue can. Biol.* **39**, 157–164.

KOEHL, M. A. R. (1977). Mechanical diversity of connective tissue of the body wall of sea anemones. *J. exp. Biol.* **69**, 107–125.

LINDAHL, U. & HÖÖK, M. (1978). Glycosaminoglycans and their binding to biological macromolecules. *A. Rev. Biochem.* **47**, 385–417.

LINDEMANN, W. (1900). Ueber einige Eigenschaften der Holothurienhaut. *Z. Biol.* **39**, 18–36.

MASTERTON, W. L. & SLOWINSKI, E. J. (1973). *Chemical Principles*. London: W. B. Saunders.

MEYER, D. L. (1971). The collagenous nature of problematical ligaments in crinoids (Echinodermata). *Mar. Biol.* **9**, 235–241.

MINAFRA, S., GALANTE, R., D'ANTONI, D., FANARA, M., COPPOLA, L. & PUCCI-MINAFRA, I. (1980). Collagen associated protein-polysaccharide in the Aristotle's lanternae of *Paracentrotus lividus*. *J. submicrosc. Cytol.* **12**, 255–265.

MOTOKAWA T. (1981). The stiffness change of the holothurian dermis caused by chemical and electrical stimulation. *Comp. Biochem. Physiol.* **70**C, 41–48.

MOTOKAWA, T. (1982). Factors regulating the mechanical properties of holothurian dermis. *J. exp. Biol.* **99**, 29–41.

MOTOKAWA, T. (1983). Mechanical properties and structure of the spine-joint central ligament of the sea urchin, *Diadema setosum* (Echinodermata, Echinoidea). *J. Zool., Lond.* **201**, 223–235.

MOTOKAWA, T. (1984*a*). Connective tissue catch in echinoderms. *Biol. Rev.* **59**, 255–270.

MOTOKAWA, T. (1984*b*). The viscosity change of the body-wall dermis of the sea cucumber *Stichopus japonicus* caused by mechanical and chemical stimulation. *Comp. Biochem. Physiol.* **77**A, 419–423.

OBRINK, B. (1975). Polysaccharide-collagen interactions. In *Structures of Fibrous Biopolymers*, (eds E. D. T. Atkens & A. Keller), pp. 81–92. London: Butterworths.

PEARSE, A. G. E. (1968). *Histochemistry Theoretical and Applied*. London: Churchill Livingstone.

REYNOLDS, S. E. (1975). The mechanical properties of the abdominal cuticle of *Rhodnius* larvae. *J. exp. Biol.* **62**, 69–80.

SERRA-VON BUDDENBROCK, E. (1963). Études physiologiques at histologiques sur le tégument des holothuries (*Holothuria tubulosa*). *Vie Milieu* **14**, 55–70.

SMITH, D. S., WAINWRIGHT, S. A., BAKER, J. & CAYER, M. L. (1981). Structural features associated with movement and 'catch' of sea urchin spines. *Tissue Cell* **13**, 299–320.

SMITH, G. N., JR. & GREENBERG, M. J. (1973). Chemical control of the evisceration process in *Thyone briareus*. *Biol. Bull. mar. biol. Lab., Woods Hole* **144**, 421–436.

STOTT, R. S. H., HEPBURN, H. R., JOFFE, I. & HEFFRON, J. J. A. (1974). The mechanical defense of a sea cucumber. *S. Afr. J. Sci.* **70**, 46–48.

TAKAHASHI, K. (1967). The catch apparatus of the sea-urchin spine. II. Response to stimuli. *J. Fac. Sci. Tokyo Univ.* **11**, 121–130.

VOGEL, S. & PAPANICOLAOU, M. N. (1983). A constant stress creep testing machine. *J. Biomechanics* **16**, 153–156.

VON UEXKÜLL, J. (1900). Die Physiologie des Seeigelstachels. *Z. Biol.* **39**, 73–112.

VON UEXKÜLL, J. (1926). Die Sperrmuskulatur der Holothurien. *Pflüg. Arch. ges. Physiol.* **212**, 1–14.

WAINWRIGHT, S. A., BIGGS, W. D., CURREY, J. D. & GOSLINE, J. M. (1976). *Mechanical Design in Organisms*. London: Edward Arnold Ltd.

WILKIE, I. C. (1978). Nervously mediated change in the mechanical properties of a brittlestar ligament. *Mar. Behav. Physiol.* **5**, 289–306.

WILKIE, I. C. (1979). The juxtaligamental cells of *Ophiocomina nigra* (Abildgaard) (Echinodermata: Ophiuroidea) and their possible role in mechano-effector function of collagenous tissues. *Cell Tissue Res.* **197**, 515–530.

WILKIE, I. C. (1983). Nervously mediated change in the mechanical properties of the cirral ligaments of a crinoid. *Mar. Behav. Physiol.* **9**, 229–248.

WILKIE, I. C. (1984). Variable tensility in echinoderm collagenous tissues: a review. *Mar. Behav. Physiol.* **11**, 1–34.

supramaximal abducens nerve stimulation are in good agreement with the parameters determined from the firing patterns of phasic-tonic motoneurones. The slow motoneurones would not be expected to make a substantial contribution to the eye movement dynamics but would contribute to the low frequency gain, and may introduce a degree of phase lag in the response to low frequency sine wave stimulation (Montgomery, 1983).

Effects of temperature on the parameters of the model

The characteristic frequency of the peripheral oculomotor system is determined by the visco-elastic coupling of the globe to the orbit (Collins, 1971). Increasing viscosity will lower the characteristic frequency, as will decreasing elasticity. The combined effect of temperature on these two variables results in a very strong temperature dependence of characteristic frequency in the temperate fish. For *G. tricuspidata* acclimated to 24 °C the characteristic frequency measured at 12 °C is already considerably lower than that of the antarctic fish, indicating a degree of temperature compensation in the mechanical coupling of globe to orbit in antarctic fish. Connective tissue sheaths on the extraocular muscles of antarctic fish (J. C. Montgomery & J. A. Macdonald, unpublished observation) may provide the increased elasticity.

For a first order system, the lower the characteristic frequency the slower the response is to a given step input. Thus saccade velocity may be related to characteristic frequency, and for a given burst rate in the motoneurones a lower characteristic frequency would result in a reduced saccade velocity. The changes in characteristic frequency with temperature may thus explain some of the observed effects of temperature on saccade velocity. Saccade velocity decreases with decreasing temperature for *G. tricuspidata* (Montgomery *et al.* 1983), but is clearly temperature compensated in antarctic fish (Montgomery & Macdonald, 1983). Presumably changes in burst rates of oculomotor neurones with temperature will also contribute to the observed effects of temperature on rates of rapid eye movement.

Changes in the characteristic frequency of the peripheral oculomotor system will also affect the degree of central processing required to produce slow compensatory eye movements. Over the working range of the vestibulo-ocular reflex, afferent input from semicircular canals is in phase with head velocity. This signal must be integrated to produce eye movements in phase with head position in order to stabilize the visual field (Carpenter, 1977). For frequencies of head movement above the characteristic frequency of the peripheral oculomotor system, this integration step can be performed by the sluggish response of the motor pathway, while at lower frequencies, this integration must be performed by the central nervous system. At present insufficient is known about the frequency match between natural head movements, vestibular input and frequency response characteristics of the oculomotor system to assess adequately the relative importance of the contribution of oculomotor dynamics to the production of accurate compensatory eye movements.

The gain of the peripheral oculomotor system is inversely related to temperature (Montgomery, 1984), both for acute temperature change within one species and for fish adapted to different temperatures. The gain of the peripheral oculomotor system in the two antarctic species at $-1{\cdot}5$ °C is considerably higher than the gain of the temperate fish. The increase in gain at low temperature can be explained in terms of

J. exp. Biol. 117, 171–179 (1985)
Printed in Great Britain © *The Company of Biologists Limited 1985*

A PASSIVE TWO LAYER PERMEABILITY-WATER CONTENT MODEL FOR *PERIPLANETA* CUTICLE

BY J. MACHIN AND G. J. LAMPERT

Department of Zoology, University of Toronto, Toronto, Ontario, Canada M5S 1A1

Accepted 23 November 1984

SUMMARY

Two layers in *Periplaneta* pronotum, endocuticle and combined epicuticle and exocuticle were functionally distinguished by their permeabilities and water affinities. A passive model combining the permeabilities of these layers and the water content of the endocuticle was designed to predict pronotal water contents in a variety of ambient activities at 20 °C.

The model predicted cuticle water contents with acceptable accuracy above ambient activities of 0·56 but overestimated them in drier conditions. Despite universally high water activities in the endocuticle, differences in water content related to ambient activity were predicted. Cuticle water contents below haemolymph equilibrated values, represented in the literature as evidence of active water regulation, were largely attributed to passive activity gradients combined with evaporation errors.

INTRODUCTION

Mass gains, observed when excised cuticle samples are exposed to atmospheres of the same water activity as the haemolymph, have been put forward as evidence that the insect epidermis is capable of actively regulating cuticle water content (Winston & Beament, 1969). We suggest that Winston & Beament's (1969) active model might have arisen from faulty assumptions about the influence of water activity gradients on cuticle hydration, especially the inner, water-rich layers. Since the mass gains in question are small and the standard errors are relatively high, Winston & Beament could also have underestimated the importance of evaporative loss during preparation of cuticle samples, by dismissing the time taken as 'only a few seconds'.

It is therefore appropriate to examine the evidence supporting a greater epidermal role more closely. Both the data in the preceding paper (Machin, Lampert & O'Donnell, 1985) and those of Winston & Beament (1969) are suitable for this purpose because these studies employed essentially the same methods of preparing *Periplaneta* pronotal discs. However they came to widely differing conclusions about the forces governing the distribution of cuticular water.

Resolution of these diverging interpretations will rest on two different

Key words: *Periplaneta* cuticle, water content, permeability, passive model.

investigations. First, by reconstructing Winston & Beament's (1969) cuticle excision procedures, it has been possible to assess the magnitude of evaporation errors and their impact on subsequent rehydration. Second, the need to understand the forces governing the distribution of cuticular water at a quantitive level has led to the development of a passive model determined by ambient activity and the water affinities and permeabilities of component layers of the cuticle. The model interprets the water-holding characteristics of the cuticle components *in vitro* measured at equilibrium, in such a way that intact cuticular water content could be predicted for the range of water activity gradients experienced by living cockroaches. Most importantly the model can be used to simulate Winston & Beament's (1969) key experiment by predicting the amount of water the cuticle would possibly gain when returned to an atmosphere of the same water activity as the haemolymph.

METHOD AND RESULTS

Assessment of evaporation errors

The phases of preparing epidermis-free discs of cuticle from *Periplaneta* pronotum described by Machin *et al.* (1985) were timed with a stopwatch. As far as can be judged the technique was virtually identical to that used by Winston & Beament (1969), except that they wrapped their samples in foil prior to weighing on a torsion balance. To estimate the evaporative losses prior to wrapping, the masses of freshly excised discs were continuously recorded on a Mettler ME22 microbalance for several minutes. Air activity in the room was either 0·85 or 0·925 at a temperature of 22 °C. Winston & Beament prepared their cuticle samples in a humidified chamber with activities between 0·85 and 0·90. They are not clear on this point, but it seems likely that the chamber was at room temperature, presumably not greatly different from 22 °C.

Representative preparation times together with typical disc mass loss curves are shown in Fig. 1. The exponential equations best describing these curves are also indicated. Such equations were used to extrapolate the mass at the beginning of evaporation, considered to be the point at which epidermal and associated tissues were removed. As a result of our experience we estimate that the delay from the start of evaporation to the foil wrapping was probably between 20 and 40 s. This delay would account for a subsequent mass gain over Ringer to a minimum error (at 20 s delay at $0{\cdot}90a_w$) (a_w, water activity) of 0·70 and a maximum (at 40 s delay at $0{\cdot}85a_w$) of 1·83 % initial wet mass. Such gains represent a significant proportion of the gains interpreted by Winston & Beament (1969) as evidence of active regulation of cuticular water.

A passive model of cuticle water relations

Epidermal permeability has been shown to be insignificant so the model will concentrate on cuticle alone and is based on the two cuticular layers distinguished as endocuticle and combined exocuticle and epicuticle (Machin *et al.* 1985). The water content of any layer depends on its water affinity, expressed in terms of mass or volume, and the prevailing water activity. Water activity is determined, in turn, by the permeability of given layer in relation to the permeabilities of the others. If the

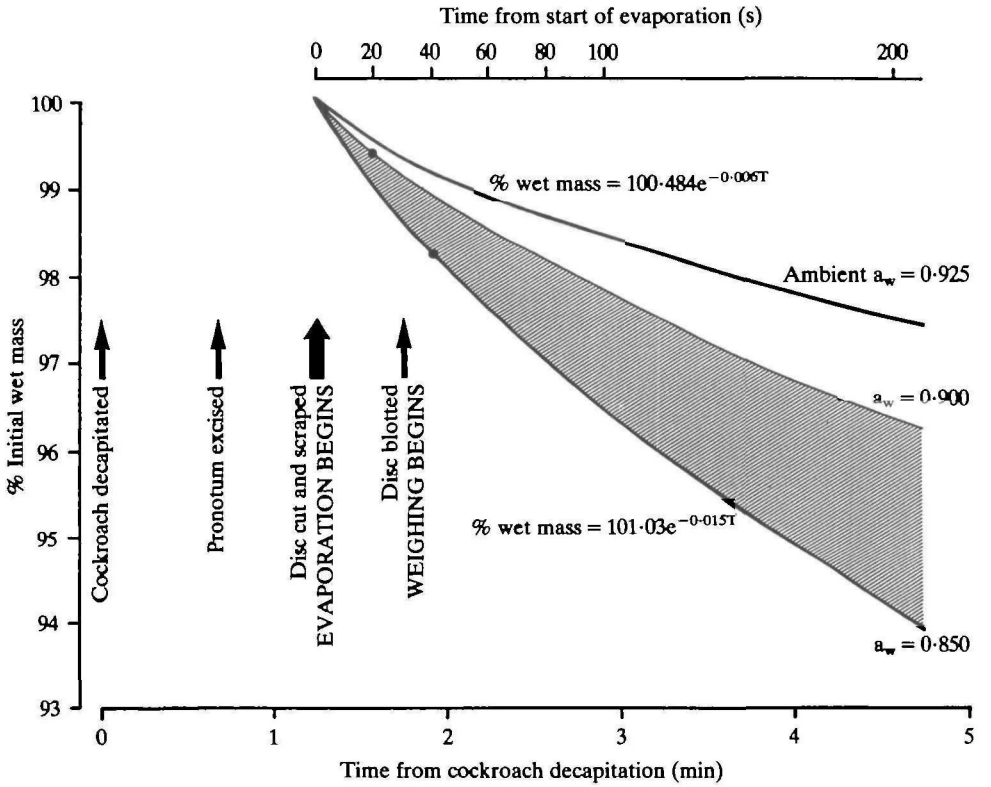

Fig. 1. Diagram to show the timing of the phases of disc preparation superimposed on observed pronotal water loss curves (heavy lines) at ambient water activities of 0·85 and 0·925 at 22 °C. Initial wet mass refers to fully hydrated cuticle discs. The parts of the curves preceding weighing were extrapolated using the least squares fitted exponential equations as indicated. The curves were used to construct a third (thin line) for 0·90 activity. The estimated range of potential evaporation error in conditions used by Winston & Beament (1969) is indicatd by the shaded area. The closed circles indicate minimum and maximum errors at 20 and 40 s delay in weighing, respectively.

properties within each of the two layers are uniform, the driving force of water flux, assumed to be vapour pressure or activity (a_w), would fall linearly across each layer.

For systems containing two barriers in series, the following general relationship enables a component permeability (P_2) to be calculated, knowing the overall permeability (P_O) and the permeability of the other component, (P_1):

$$\frac{1}{P_O} = \frac{1}{P_1} + \frac{1}{P_2}. \tag{1}$$

The gradients (Δa_w) for each layer in any conditions can then be obtained from their permeabilities by rearrangement of Fick's equation describing passive diffusion:

$$\Delta a_w = \frac{J}{PA}, \tag{2}$$

where J is equal to the total flux across the cuticle, A the area and P the permeability

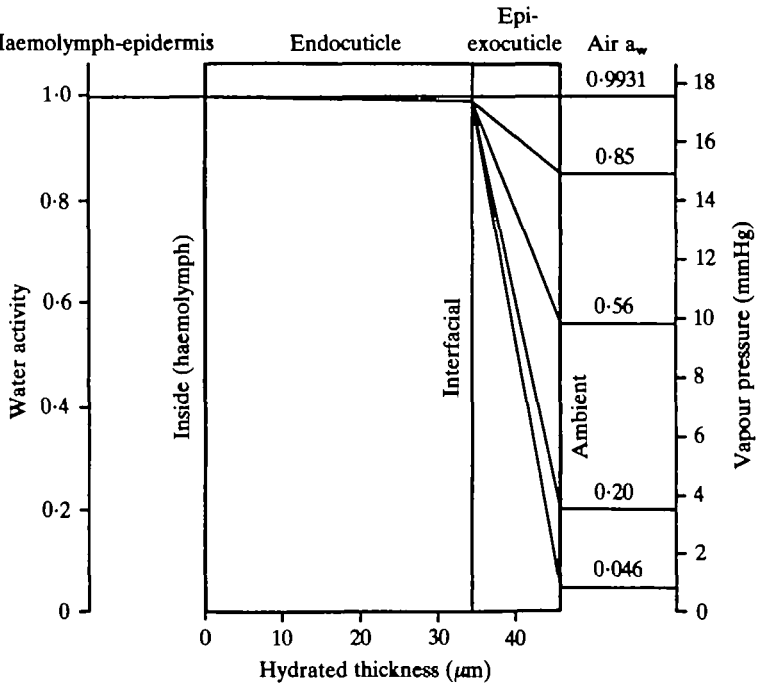

Fig. 2. Diagram showing steady state, *in vitro* water activity gradients across the cuticle in different ambient activities. The gradients were constructed by drawing straight lines between three fixed activities. Inside and ambient activities were measured and the steady state interfacial value between the two layers compatible with equal fluxes was calculated by progressive approximation.

of the layer in question. The total water held by the cuticle is then obtained by integrating water contents over the activity range existing in each layer.

Component permeabilities

Unfortunately, construction of a model is rather more difficult than the above account suggests because of the complex interdependence of permeability, water

Table 1. *Modelled* in vitro, *steady state permeabilities and interfacial vapour pressures at different ambient activities*

Water activity		Permeabilities ($mg\,h^{-1}\,cm^{-2}\,mm\,Hg^{-1}$)		
Ambient	Interfacial	Endocuticle	Epi-exocuticle	Total
0.85	0.9929	74.283	0.127	0.127
0.56	0.9927	72.692	0.067	0.067
0.20	0.9925	70.771	0.053	0.053
0.046	0.9924	69.873	0.050	0.050

Inside a_w was 0.9931, vapour pressure = 17.427 mmHg.

J. exp. Biol. **117**, 111–117 (1985)
Printed in Great Britain © *The Company of Biologists Limited 1985*

DEVELOPMENTAL CHANGES IN THE INTERFERENCE REFLECTORS AND COLORATIONS OF TIGER BEETLES (*CICINDELA*)

BY T. D. SCHULTZ AND M. A. RANKIN

Department of Zoology, University of Texas, Austin, Texas 78712, U.S.A.

Received 4 December 1984

SUMMARY

Samples of cicindelid cuticle were examined at various stages of adult ecdysis. The multilayered potential reflector was secreted in the initial stages of the moult, verifying that it is not tectocuticle and supporting the contention that it is a form of inner epicuticle. At early stages of ecdysis, the electron-dense layers were visible only when the section was post-stained. During post-ecdysial colour development, the dense layer increased in inherent electron density. Concurrently, the reflector increased in refractive index and the interference coloration increased in intensity and wavelength of maximum reflectance. Black pigment was also deposited simultaneously within the outer portion of the cuticle. It is proposed that electron-dense material was deposited *in situ* within the inner epicuticle after ecdysis, thereby increasing the wavelength and reflectance of interference colour.

INTRODUCTION

Schulze (1913) and Stegemann (1930) described the iridescent colour-producing layer of tiger beetle (Cicindelidae) cuticle as a 'Sekretschicht' or secretory layer produced by epidermal glands after ecdysis. This layer appeared as a superficial, thin, dark layer in cross-sections of elytra under optical microscopy (Stegemann, 1930). A gradual increase in thickness of this dark layer was interpreted as the discharge of a pigmented fluid over the surface of the pharate exoskeleton. Subsequently, the 'Sekretschicht' has been assumed to be a form of tectocuticle (Richards, 1951) or cement layer (Wigglesworth, 1972).

Detailed observations of post-ecdysial colour changes in cicindelids were made by Shelford (1917) and Willis (1967). In all of the species studied, the interference colours of the cuticle progressed from short to long wavelength colours during a 48-h period following emergence from the pupal exuvia. Simultaneously, the cuticle became pigmented and opaque to transmitted light. Histological or ultrastructural changes were not considered in these two studies.

Key words: Interference colour, epicuticle, *Cicindela*.

Schultz & Rankin (1985) identified the source of structural colours in tiger beetle (*Cicindela*) integument as epicuticular by virtue of its location, ultrastructure and reaction to solvents. The inner epicuticle consists of alternating layers of electron-dense and electron-lucent material which serve as a multilayer interference reflector. The reflective cuticle is located in the outer 2 μm of the exoskeleton. Cuticular layers below the reflective cuticle exhibit exocuticular characteristics.

In this study, the development of the cuticular reflector was investigated. Since the reflected colour directly relates to the optical thickness of the reflecting layers, development of these layers may be observed through the development of the interference coloration. The ultrastructure of developing cuticle was examined at different stages of colour development by transmission electron microscopy. The time of deposition of the reflecting layers also served to identify the layer according to current concepts of cuticle development and structure.

MATERIALS AND METHODS

Populations of larval and adult *C. scutellaris* Vaurie and *C. splendida* Hentz were counted over a period of 2 years (1979–1980) in Bastrop State Park, Texas. The approximate date of pupation was determined by census data and observations of larval activity.

Third instar larvae and pupae were excavated from their burrows and reared to adulthood in the laboratory. Larvae were placed in glass tubes, 70 cm × 30 mm. The extreme length was necessary for *C. scutellaris* whose burrows often exceed 50 cm. Tubes were packed with specific soils from oviposition sites in the field (Patilo soils for *C. scutellaris*, Axtell soils for *C. splendida*), and were placed vertically in a growth chamber with a photoperiod of 12·5 h light and 11·5 h dark. The sand was moistened every 6 days from the top of the tube. Larvae were fed *Tenebrio* larvae and adult *Tribolium confusum*.

Pupae were placed in opaque plastic cups. Each cup was padded with cotton, which formed an artificial pupal chamber. The artificial chamber was critical in ensuring that the imago would shed the pupal exuvia successfully. The cotton was moistened periodically with a solution of 1·5 % H_2O_2 to prevent mould developing. The development of adult colour was observed under a dissecting microscope.

Elytral cuticle was cut from developing *C. scutellaris* 4 days before ecdysis (10 days after pupation), 12 h after ecdysis, and 14 days after the moult. Strips of cuticle were prepared for transmission electron microscopy (TEM) as described previously (Schultz & Rankin, 1985). Sections of pharate and adult cuticle were both post-stained and left unstained. Post-staining consisted of 5 min in 1 % uranyl acetate in 50 % ethanol, followed by 5 min in lead citrate. All samples were examined under a Zeiss 10CA transmission electron microscope. Thin sections were also observed under optical microscopy.

RESULTS

The colour development of the tiger beetles, *C. splendida* and *C. scutellaris*, showed a progressive increase in peak reflected wavelength to the mature adult colour. Since the reflector is composed of multiple layers (Schultz & Rankin, 1985), there

must be either a gradual addition of layers which reflect longer wavelengths, or a gradual increase in the optimal thickness of the layers themselves. Electron microscopy, coordinated with observations of colour development, supported the latter interpretation. Since the ultimate colour of *C. splendida* is red, the sequence of colour development was longer, but essentially the same as that of *C. scutellaris*. For the sake of brevity, only the observations of *C. scutellaris* will be described.

The pharate elytron, 4 days prior to ecdysis, was pale white or cream with a slight violet iridescence. Electron micrographs revealed that the presumptive epicuticle (region *A*), and part of the exocuticle (region *B*), had already been deposited by this time (Fig. 1). The epicuticle was already composed of a full complement of bands, but the presumptive dense bands were thinner (15–40 nm thick) than they appear in mature cuticle, and were revealed only by post-staining (see Methods). In unstained sections, light 'negative shadows' appeared within the boundaries of the dark bands (layer *D* in Fig. 1). These could be distinguished from the grainy appearance of the potential electron-lucent bands (layer *L*). With post-staining, however, these areas appeared very dense, black and finely grained (Fig. 2). An electron-dense strip, 30 nm thick, was present in both stained and unstained sections at the outer border of the cuticle. The entire thickness of the epicuticle at this stage was 50–60 % thinner than in mature cuticle. No evidence of pigmentation was observable in optical cross-sections of the pharate elytron.

By the completion of ecdysis, the elytral colour had not changed substantially. Over the next 8 h, the basic colour of the cuticle darkened from white to a golden straw. The elytra were not yet pigmented, but displayed a distinctive violet hue. From 8 to 12 h after ecdysis, the iridescence became predominantly blue, and spread spatially over the elytron from base to apex. Simultaneously, the elytron blackened and became opaque. Pigmentation progressed through the elytron from base to apex, enhancing the lustre of the iridescence. By the 12th hour, all but the apical quarter of the elytron was pigmented, and it reflected a rich, blue colour. The apex was still violet and somewhat transparent.

Micrographs of cuticle 12 h after ecdysis showed that the epicuticle had assumed its surface microsculpture (Schultz & Rankin, 1985), and the outer exocuticle was fully formed (layers *A* and *B* in Fig. 3). Underlying layers of exocuticle (layer *C* in Fig. 3) were evident, but the formation of 'plywood' mesocuticle was yet to be initiated. The limits of the dense epicuticular bands were defined more clearly and expanded to approximately 80 % of their eventual thickness. However, they lacked the very dark granularity apparent in mature cuticle. Electron density decreased from outer to inner layers.

The elytra were entirely blue and pigmented 24 h after shedding the pupal exuvium. Over the following 6 h to 5 days the iridescent hue became progressively more green. All areas of the beetle became fully pigmented. The resistance of the elytron to superficial tears increased during this period, but the elytron did not become rigid and hardened for several days. In the field, this occurs after the adult has emerged from its pupal chamber. Drying undoubtedly facilitates elytral hardening. By the 14th day, the elytra and colour were developed fully.

Electron micrographs of mature cuticle show fully formed epicuticle, outer exocuticle and procuticular layers (Fig. 4). Although post-staining enhances the resolution

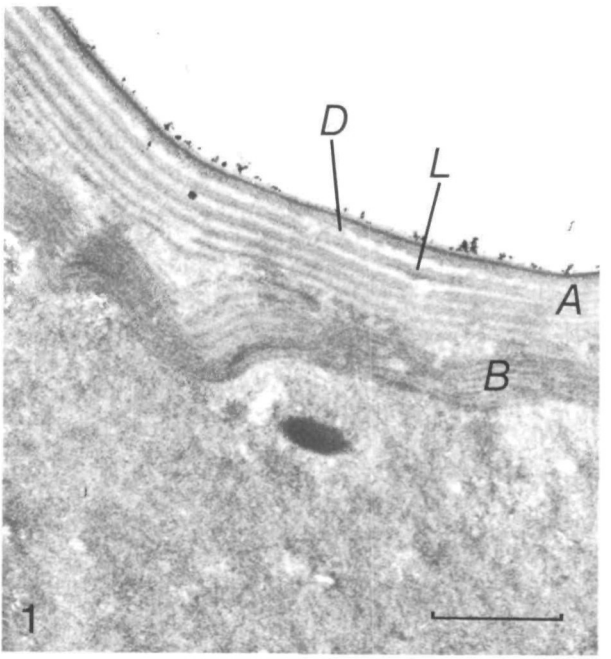

Fig. 1. Transmission electron micrograph of cross-section of pharate elytral cuticle 10 days after pupation. This section was not post-stained. The epicuticle (*A*) has been deposited and exhibits a multilayered ultrastructure. If not post-stained, the potential dense layers (*D*) appear less dense than the potential *L* layers. The outer exocuticle (*B*) has been partially deposited. Scale bar, 1 μm.

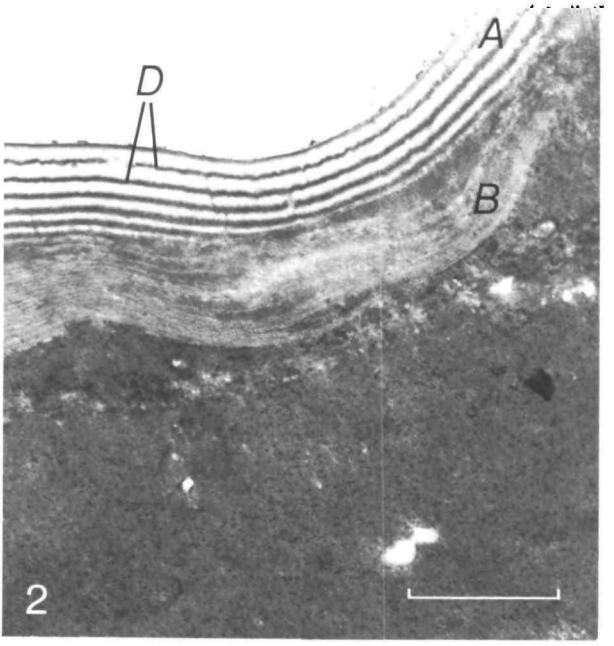

Fig. 2. Transmission electron micrograph of cross-section of pharate elytral cuticle 10 days after pupation. This section was taken from the same tissue as was the section in Fig. 1, but was post-stained with lead citrate and uranyl acetate. Structural features are the same, except that the potential *D* layers appear very dense and granulate. *A*, epicuticle; *B*, outer exocuticle. Scale bar, 1 μm.

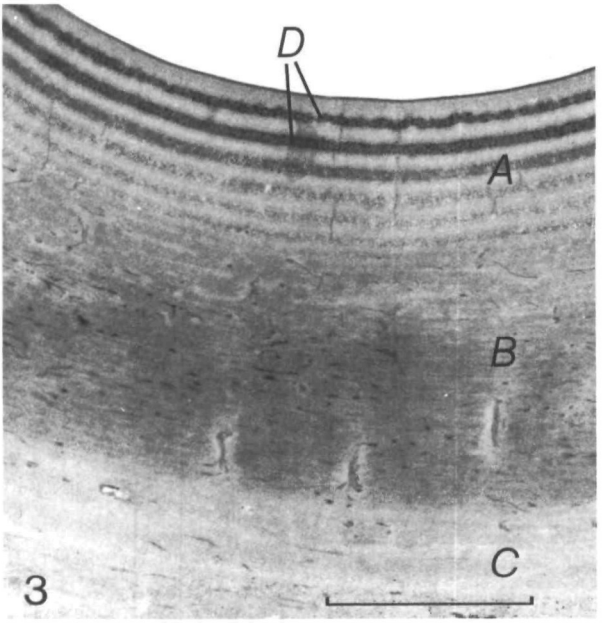

Fig. 3. Transmission electron micrograph of cross-section of elytral cuticle 12 h after ecdysis. The epicuticle (*A*) and outer exocuticle (*B*) are fully deposited. The inner exocuticle (*C*) is partially formed. The epicuticular *D* layers appear denser at this stage. Section was not post-stained. Scale bar, 1 μm.

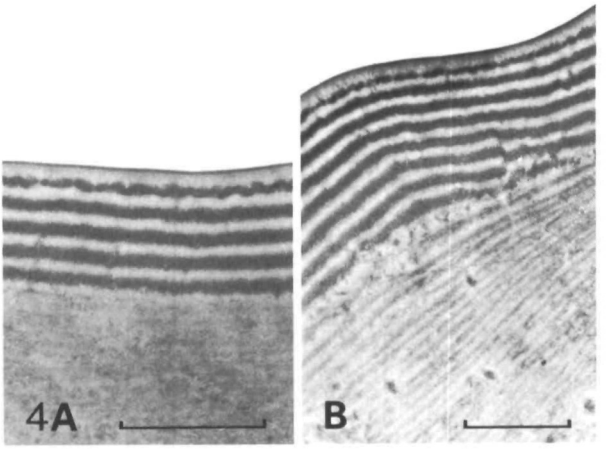

Fig. 4. Transmission electron micrograph of cross-sections of elytral cuticle 14 days after ecdysis. Epicuticular layers are fully developed and the electron density of the *D* layers is apparent in both unstained and post-stained sections. (A) Unstained; (B) post-stained. Scale bars, 1 μm.

of dense layers in the epicuticle (Fig. 4B), their high electron density is also apparent in micrographs of unstained sections (Fig. 4A).

DISCUSSION

The present study indicates that the potential cuticular reflector is formed prior to ecdysis, and therefore, cannot be considered as a dermal gland product. The early

deposition and location of the reflective layers indicate they are epicuticular. The first layer formed during a moult cycle is the cuticulin layer, followed by the inner epicuticle (Filshie, 1982). In pre-ecdysial samples of *C. scutellaris*, the potential reflective layers constitute the outer portion of newly formed cuticle, and display a thin, dense outer border, suggestive of a cuticulin layer. A partially deposited exocuticle appears below these layers and exhibits a helicoidal orientation of fibrils.

Micrographs of developing cuticle, and the continuity of dense layers produced by adjacent cells, indicate that a substrate or precursor is deposited during the initial formation of the epicuticle. The change in electron density of the dense layers suggests that a change in molecular chemistry occurs during the moult cycle. Either electron-dense material is deposited after formation of the epicuticle, or endogenous material within these layers is converted to compounds of higher electron density or affinity for OsO_4. Simultaneously, the colour of the newly emerged imago progresses from shorter to longer wavelengths, while dark pigmentation forms behind the reflecting layers. Although associated changes in refractive index cannot be determined, the increase in optical thickness of these layers must be responsible for the increasing wavelength of maximum reflectance observed during development.

In situ impregnations of developing cuticle have been reported previously. Wigglesworth (1976) described the spreading of a proteinaceous secretion within the epicuticle associated with sclerotization or melanization. It is generally assumed (Hackman, 1974) that a phenolic precursor of melanin is located in the integument at the site of pigmentation, perhaps as a by-product of sclerotization. This substrate is then assumed to be converted to melanin by an enzyme transported to this site *via* the pore canals.

Cicindelid pore canals contain materal substantially denser than the areas of exocuticle they traverse (Schultz & Rankin, 1985). Smaller extensions of the canals within the epicuticle possess electron-lucent lumina whose borders are dense. The dense contents of the pore canals may be substrates or enzymes dispersed in the exocuticle and epicuticle for sclerotization or pigmentation. If the dense epicuticular layers of cicindelids are melanoproteins formed *in situ*, the reaction entails a simultaneous increase in absorptivity and electron density.

These observations of colour development agree with those of Shelford (1917) and Willis (1967) for several *Cicindela* species. Shelford mistakenly assumed that the reflector was a single, thin layer containing materials with the properties of aniline dyes. He attributed the changing colours to changes in the chemical composition of the layer. While chemical characteristics of the reflector do appear to change during ecdysis, these changes occur within a multilayered ultrastructure that is formed during the initial stages of the adult moult.

The authors thank Susan Houghton of the Marine Biological Laboratory, Woods Hole, MA, for her considerable skill in sectioning and photographing this difficult material. Permission for the collection of specimens was provided by the Texas Department of Parks and Wildlife. This study was supported partially by graduate student subvention funds provided by the University of Texas and NSF Grant 2610711250.

REFERENCES

FILSHIE, B. (1982). Fine structure of the cuticle of insects and other arthropods. In *Insect Ultrastructure*, Vol. 1, (eds R. C. King & M. Akai), pp. 281–312. New York: Plenum Press.

HACKMAN, R. H. (1974). Chemistry of insect cuticle. In *The Physiology of Insecta*, Vol. 6, (ed. M. Rockstein), pp. 216–270. New York: Academic Press.

RICHARDS, A. G. (1951). *The Integument of Arthropods*. St. Paul: University of Minnesota Press.

SCHULZE, P. (1913). Chitin und andere Cuticularstrukturen bei Insekten. *Verh. dt. zool. Ges.* p. 165.

SCHULTZ, T. D. & RANKIN, M. A. (1985). The ultrastructure of the epicuticular interference reflectors of tiger beetles (*Cicindela*). *J. exp. Biol.* **117**, 87–110.

SHELFORD, V. E. (1971). Color and color pattern mechanisms of tiger beetles. *Illinois biol. Monogr.* **3**, 4.

STEGEMANN, F. (1930). Die Flugeldecken der Cicindelidae. Ein Beitrag zur Kenntnis der Insektcuticula. *Z. Morph. Ökol. Tiere* **18**, 1–73.

WIGGLESWORTH, V. B. (1972). *The Principles of Insect Physiology*. London: Chapman & Hall.

WIGGLESWORTH, V. B. (1976). The distribution of lipid in the cuticle of *Rhodnius*. In *The Insect Integument*, (ed. H. R. Hepburn), pp. 89–106. New York: Elsevier Scientific Publishing Co.

WILLIS, H. (1967). Bionomics and zoogeography of tiger beetles of saline habitats in the central United States. *Univ. Kansas Sci. Bull.* **47**, 145–313.

content and activity gradient in each of the layers (Machin *et al.* 1985). We would expect activity gradients within each of the layers to lead automatically to local differences in water content, and presumably permeability. Steady state conditions of regional equality of water flux would therefore require the activity gradient to be curved not linear. A workable solution to these problems appears to be offered by empirical permeability equations which take no account of the complexities within each layer. To determine how the properties of component layers combine in the intact cuticle, it is first necessary to determine the interfacial activity at the border of the endocuticle and epi-exocuticle so that the gradients across each layer can be determined separately. A calculator programme was used to determine which interfacial activity was compatible with a steady state from a series of approximations starting from any arbitrarily chosen value. The programme then averaged high and low interfacial values progressively until equality between endocuticle and epi-exocuticle water fluxes was reached. Fluxes, calculated from equation 2, were considered equal when they agreed to within 1 %. Under these steady state conditions no further changes to the water content of a layer or its permeability could take place.

The calculations were based upon the following empirical equations relating endocuticle and whole cuticle permeability with the reciprocal of vapour pressure lowering ($vp_s - vp_a$) at different ambient activities, obtained by Machin *et al* (1985):

$$\text{endocuticle } P = -0.892 + \frac{9.424}{vp_s - vp_a} \tag{3}$$

$$\text{epi-exocuticle } P = 0.0355 + \frac{0.263}{vp_s - vp_a}. \tag{4}$$

In vitro interfacial activities and component permeabilities calculated in this way are summarized in Table 1. Note that the very high endocuticle permeabilities are consistent with rapid, short-term evaporative loss in excised samples. In Fig. 2, which illustrates the corresponding linear activity gradients, it can be seen that all activity gradients in the endocuticle which fall within the width of the drawn line, are very close to the Ringer equilibrated ($a_w = 0{\cdot}9931$) line. Since interfacial activities are based directly on empirical results they are known with some certainty.

It is worth noting that the model confirms the traditional arrangement of an external water barrier maintaining the inner endocuticle in a hydrated state (Beament, 1961). Endocuticle hydration exaggerated the permeability difference of the two layers to a factor of between 550 and 1400. Beament (1961) speculated that lipid removal from the cuticle might result in a 100- to 300-fold permeability increase. The higher values for endocuticle are presumably due to corrections for unstirred layers which have not been made previously.

Water contents

Cuticle water contents (per gram dry mass of cuticle or per 0·633 g endocuticle) were calculated from endocuticle gradients alone since no significant difference was found between the water affinities of whole cuticle and of endocuticle (Machin *et al.* 1985). In Fig. 3 the calculated water affinity regression line for the whole cuticle, together with the data on which it was based, has been re-drawn with water activity

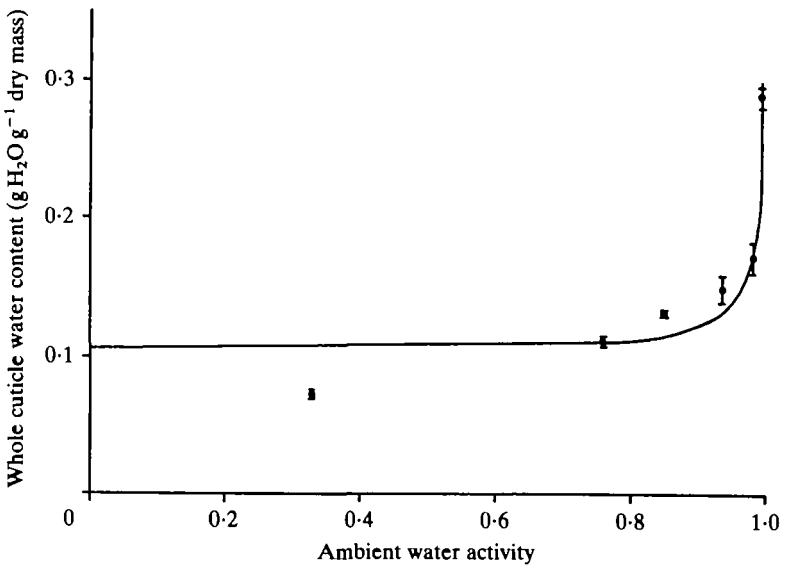

Fig. 3. Graph showing the relationship between whole cuticle water content and ambient water activity for *Periplaneta* pronotum at equilibrium. The line is the best least squares fit to the data of Machin, Lampert & O'Donnell (1985).

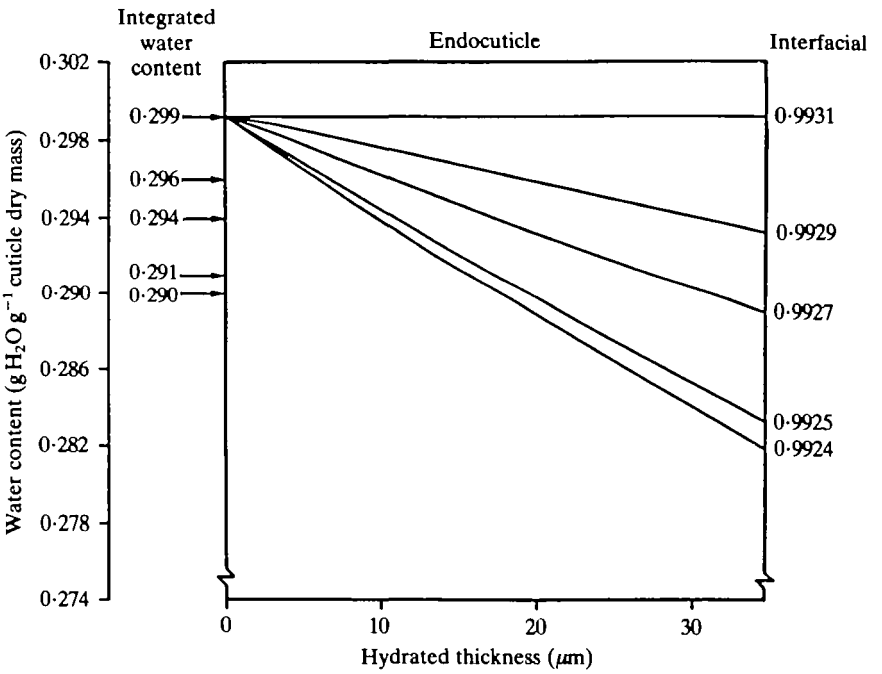

Fig. 4. Diagram demonstrating that endocuticle *in vitro* shows water content deficits even though activity gradients are very slight. The integrated total water contents determined by the model are also indicated on the left.

in place of the reciprocal of vapour pressure lowering on the abscissa. Total cuticle water contents were obtained by integrating the water content over the activity range existing across the endocuticle using the linear form of the water affinity relationship:

$$\text{whole cuticle water content (g g}^{-1}\text{ dry mass)} = 0.106 + \frac{0.0234}{vp_s - vp_a}. \quad (5)$$

When the actual distribution of water across the endocuticle is obtained from activity gradients (Fig. 4) it can be seen that considerable differences occur. The small differences in activity gradient in Fig. 2 are in fact magnified by the steepness of the curve in Fig. 3 for very high activity values close to one. It has been argued above that steady state conditions within the endocuticle require that activity gradients be curved. However calculations show that the curvature may be neglected since predicted water contents fall within 1 % of the straight line values, presumably because endocuticle activity gradients are so slight. Machin *et al.* (1985) have presented evidence for a small, irreversible decrease in cuticle water affinity following initial water content measurement. Since the discrepancy in cuticular water content extends to samples equilibrated at haemolymph activities, *in vivo* water contents can be modelled by assuming that the same general *in vitro* form of the water affinity relationship applies, except that the *in vivo* slope is slightly greater. Modelled cuticular water contents are compared with observed values in Table 2. Data of Machin *et al.* (1985) were measured at 20 °C with a haemolymph or Ringer

Table 2. *Comparison of observed and modelled cuticular water contents under gradient conditions*

Ambient a_w	*N*	Cuticle water contents ($g H_2O g^{-1}$ dry mass) Observed ± S.E.	Modelled
Machin, Lampert & O'Donnell (1985)			
In vitro			
0.9931 (Ringer)	16	0.299 ± 0.006	[0.299]
0.85	18	0.307 ± 0.008	0.296
0.56	17	0.295 ± 0.012	0.294
0.20	18	0.243 ± 0.006	0.291
0.046	18	0.220 ± 0.008	0.290
In vivo			
0.9931 (haemolymph)	16	0.366 ± 0.009	[0.366]
0.85	18	0.357 ± 0.011	0.362
0.56	17	0.357 ± 0.014	0.359
0.20	18	0.286 ± 0.006	0.356
0.046	18	0.281 ± 0.012	0.354
Winston & Beament (1969)			
In vivo			
1.00	14	0.299 ± 0.090	0.330
0.85	28	0.251 ± 0.028	0.326
0.75	20	0.351 ± 0.028	0.325
0.42	5	0.330 ± 0.021	0.321
0.01	24	0.299 ± 0.043	0.317

Values in square brackets are equilibrated values on which the model values are based.

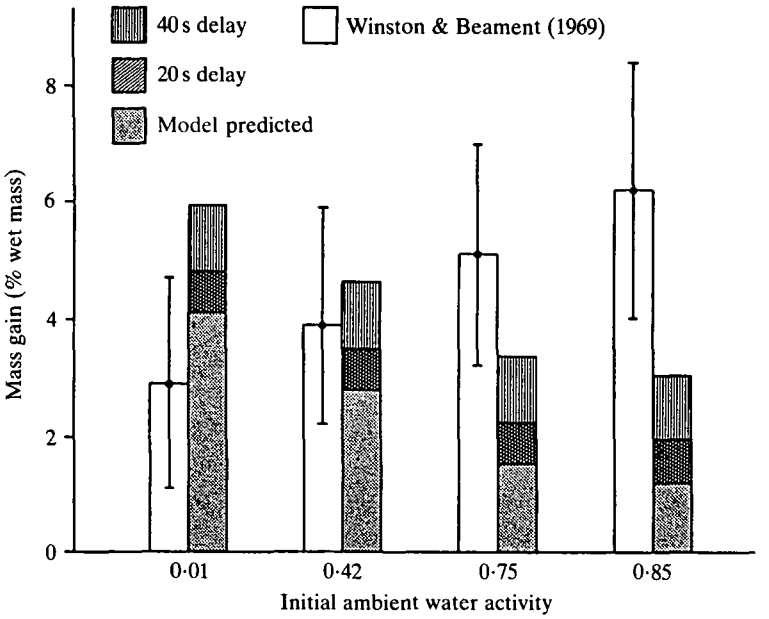

Fig. 5. Histograms comparing mean pronotal mass gains (± S.E.) following exposure to haemolymph water activities observed by Winston & Beament (1969) and those attributed by the present study to modelled cuticle activity gradients and evaporation errors. Cuticles were initially under gradient conditions with different ambient activities as indicated.

activity of 0·9931 (383 mosmol l^{-1}) while Winston & Beament (1969) made their determinations at 25 °C with activities of 0·9941 (328 mosmol l^{-1}). Model calculations adjust for the different activities but are based on permeabilities and water affinities measured at 20 °C. It can be seen that the agreement between observed and modelled water contents is good at high ambient activities and poor at activities below 0·20. The fit with Winston & Beament's (1969) values is good.

DISCUSSION

We interpret the results of modelling as evidence that cuticle water contents can be largely accounted for by purely passive mechanisms. This conclusion is based on the prediction by the model of the significant drop in cuticle water contents in ambient activities below that of the haemolymph. Since modelled water contents all show a decline with decreasing ambient activity from maximum values equilibrated to Ringer or haemolymph, it is reasonable to conclude that the occasional departure from this trend in observed values is due to measuring error.

The model has been shown to overestimate water contents at low ambient activities both *in vivo* and *in vitro*. It is important to point out, however, that this cannont be attributed to the poor fit of the water content equation at low activity because modelled values are based entirely on the narrow range of extremely high activities characteristic of the endocuticle. Over this range the fit of the equation to the observed

points is very good. Nevertheless, despite deficiencies in the model at low ambient activity, modelled water contents still appear to account for most of Winston & Beament's (1969) observations by passive mechanisms. Modelled water contents can therefore be used to simulate their mass measurement experiment following re-exposure of cuticle samples to water activities equivalent to the haemolymph. Modelled mass gains, expressed in their paper as a percentage of wet mass, were calculated by assuming that the cuticle in different gradient conditions would regain the water contents observed when equilibrated over Ringer. Water absorption would be further increased if cuticle samples had been previously subjected to significant evaporation. The estimated range of these errors has also been included in Fig. 5. The histograms show there is a considerable degree of correspondence between the percentage mass gains observed by Winston & Beament (1969) and those derived from modelled values plus estimated evaporation errors. Mass gains based on observed *in vivo* and *in vitro* values of Machin *et al.* (1985) and corresponding modelled values show essentially the same results. A discrepancy does however exist between the 0·85 activity values. The trend of the modelled values and those observed by Riddle (1981) is opposite to those of Winston & Beament (1969). Their large overlapping standard errors suggest that their differences may not be significant.

Thus it can be concluded that cuticular mass gains over Ringer can largely be attributed to the effects of passively generated activity gradients in the cuticle together with evaporation errors. We suggest Winston & Beament may have been deceived by the relative insensitivity of water content to ambient activity because their values were expressed as a percentage of water mass. In addition, without investigating the actual form of the water affinity relationship, they automatically assumed that small differences in vapour pressure would lead to small differences in water content in the hydrated endocuticle. Quite to the contrary, the non-linear nature of water affinity demonstrates that water content is very sensitive to small vapour pressure differences particularly at the high activities, close to one, found in the endocuticle. It follows, therefore, that significant water activity deficits should be expected whenever the ambient activity falls below the haemolymph level, even when only passive forces are in operation.

We thank M. J. O'Donnell for helpful discussions at various stages of this work. This study was financially supported by the Natural Sciences and Engineering Research Council, Canada Operating Grant A1717, which is gratefully acknowledged.

REFERENCES

Beament, J. W. L. (1961). The water relations of insect cuticle. *Physiol. Rev.* **36**, 281–320.

Machin, J., Lampert, G. J. & O'Donnell, M. J. (1985). Component permeabilities and water contents in *Periplaneta* integument: role of the epidermis re-examined. *J. exp. Biol.* **117**, 155–169.

Riddle, W. A. (1981). Cuticle water affinity and water content of beetles and scorpions from xeric and mesic habitats. *Comp. Biochem. Physiol.* **68**A, 231–235.

Winston, P. W. & Beament, J. W. L. (1969). An active reduction of water level in insect cuticle. *J. exp. Biol.* **50**, 541–546.

J. exp. Biol. 117, 1–14 (1985)
Printed in Great Britain © *The Company of Biologists Limited 1985*

GILL AND BODY SURFACE AREAS OF THE CARP IN RELATION TO BODY MASS, WITH SPECIAL REFERENCE TO THE METABOLISM-SIZE RELATIONSHIP

BY SHIN OIKAWA AND YASUO ITAZAWA
Department of Fisheries, Kyushu University 46–04, Hakozaki, Fukuoka 812, Japan

Accepted 15 January 1985

SUMMARY

The relationships of resting metabolism per unit mass of body to gill and body surface areas were examined by measuring gill, body surface and fin areas of carp ranging from 0·0016 to 2250 g. There was a triphasic allometry for the relationship between gill area and body mass: during the prelarval (0·0016–0·003 g) and postlarval (0·003–0·2 g) stages there was a positive allometry (slopes of 7·066 and 1·222, respectively), during the juvenile and later stages (0·2–2250 g) there was a negative allometry with a slope of 0·794. There was a diphasic negative allometry for the relationship between surface area of the body or the fins and body mass, with a slope of 0·596 or 0·523 during the larval stage and 0·664 or 0·724 during the juvenile and later stages, respectively. Except for the 3rd phase (juvenile to adult) of gill area, these slopes were significantly different ($P < 0·01$) from the slope for the relationship between resting metabolism and body mass of intact carp (0·84; value from Winberg, 1956). It is considered, therefore, that gill, body surface and fin areas do not directly regulate the resting metabolism of the fish, in the larval stage at least.

INTRODUCTION

The mass-specific rate of basal metabolism decreases with increasing body mass. This phenomenon has been widely observed and repeatedly discussed in various animals including fishes (Winberg, 1956; Hemmingsen, 1960; Kleiber, 1961; Paloheimo & Dickie, 1966; Schmidt-Nielsen, 1970; Brett & Groves, 1979; Heusner, 1982; Feldman & McMahon, 1983; Hughes, 1984*a*; Wieser, 1984; and many others). The relationship between basal metabolic rate of animals (M) and the body mass (W) is expressed, both intraspecifically and interspecifically, by the allometric equation, $M = aW^b$, where a and b are constants. Because the mass exponent b is smaller than unity, the mass-specific metabolic rate (M/W) decreases with increasing body mass.

This phenomenon was formerly explained by the so-called 'surface rule' in terms of homoiothermy (Rubner, 1883). However, a similar relationship was also shown for poikilotherms. The mass exponent b was later found to be not 2/3, which is the mass

Key words: Gill area, body surface area, fin area, metabolism-size relationship, carp.

exponent of the body surface, but 3/4 in mammals and birds (Kleiber, 1932) and about 0·85 in fishes (Ricker, 1973, calculated from the data of Winberg, 1956; Brett & Groves, 1979).

It was later suggested that the phenomenon was the result of a decrease in mass-specific rate of tissue respiration (Q_{O_2}) with increasing body mass; however, the slopes of the relationships between Q_{O_2} and body mass in most tissues are not large enough to explain the phenomenon in intact animals (Krebs, 1950; Von Bertalanffy & Pirozynski, 1953; Girard & Grima, 1980; Oikawa & Itazawa, 1984*a*).

On the other hand, the slopes for the respiratory area-body mass relationship have been argued to be similar to the slopes for the metabolism-body mass relationship (Ludwig, 1956; Balke, 1957; Von Bertalanffy, 1957; Whitford & Hutchison, 1967; Ultsch, 1973, 1976). In fishes, morphometric studies on the relationship between gill area and body mass have been carried out in many species (Price, 1931; Byczkowska-Smyk, 1961; Ursin, 1967; Muir, 1969; Muir & Hughes, 1969; Suzuki, 1969; Hughes, 1970, 1978; Hughes, Dube & Munshi, 1973; Hughes *et al.* 1974; De Silva, 1974; Holeton, 1976; Hakim, Munshi & Hughes, 1978), and there have been excellent morphological studies on the development of the gill system (Byczkowska-Smyk, 1961; Morgan, 1974*a,b*). Most of these studies, however, were devoted to limited stages in the life history of the fish, although Price (1931) examined the dimensions of the gill sieve in small-mouthed black bass of 0·33–840 g. There have been few measurements of the area of the body surface that is considered to play an important role in gas exchange during early development.

We here present the results of morphometric studies on the allometric relationships of gill, body surface and fin areas to body mass of carp ranging from 2-day-old larvae of 0·0016 g to the adults of 2250 g, and we discuss the relationship between surface area and metabolism.

MATERIALS AND METHODS

Measurements of gill, body surface and fin areas were carried out on 32 carp, *Cyprinus carpio*, ranging from 0·0016 g (2 days after hatching and at the stage at which the gill secondary lamellae became clearly recognisable) to 2250 g. The fish smaller than 30 g were raised at 20 °C in our laboratory and were fed on live water fleas, *Daphnia pulex*, for a week beginning 2 days after hatching and then on marketed carp diet made from fish meal, wheat flour, soybean cake, vitamins and minerals as well as water fleas. The fish larger than 30 g were raised at a commercial fish farm and transported to our laboratory.

The fish of under 100 g were fixed whole in formalin Cortland saline made from one part of concentrated formalin and nine parts of Cortland saline (Wolf, 1963). With the fish of over 100 g, the gills together with the gill arches were excised and fixed in the formalin Cortland saline. The results of measurements with the fixed materials were converted to the figures with the fresh ones based on the average shrinking coefficients estimated from carp of 0·054–200 g; i.e. 2·9 % for filament length, 4·3 % for body length, 5·7 % for gill area, 7·3 % for body surface and fin areas, and − 2·4 % (2·4 % increase) for body mass.

The gill area or the total bilateral area of the secondary lamellae (A) was estimated,

after Hughes (1966, 1984*b*), by the formula

$$A\ (\mathrm{mm}^2) = (2L/d')bl,$$

where L is the total length of all the filaments (mm), $1/d'$ is the average spacing of the secondary lamellae on one side of the filaments (mm^{-1}) and bl is the average bilateral area of the secondary lamellae (mm^2). It should be noted that bl is not $b \times l$ both of which are described later.

The total length of all the filaments (L) was determined by doubling the estimate of the filament length of all the gill arches on the left side of the body, obtained by measuring the length of every filament from small fish of 0·0016–1·3 g and every third or fifth filament from fish of 2·2–2250 g.

The spacing of the secondary lamellae on one side of the filaments was determined from measurements of all the lamellae on the filaments of average length in the dorsal, middle and ventral parts of all the gill arches on the left side of the body in small fish of 0·0016–0·33 g. In fish of 1·3–2250 g, the second left arch was examined. The average spacing was estimated by the weighted mean method, which takes into account the difference in length of different filaments, although the spacing was not very different among different filaments and among different regions on a filament.

The area of the secondary lamellae was determined with the lamellae chosen at almost regular intervals on the filaments of average length in the dorsal, middle and ventral parts of the second gill arch on the left side of the body, except for very small fish of 0·0016–0·014 g in which all the left gill arches were used. The number of lamellae chosen for the measurement ranged from 9 in the fish of 0·0016 g to 236 in the fish of 2250 g, with exceptional cases in which 380 and 1475 lamellae were chosen from the fish of 532 g and 660 g, respectively. Twice the value of a lamellar area was regarded as the area of the lamella, considering both sides of the lamella to function as the site for gas exchange. The average value of the bilateral lamellar area was estimated by the weighted mean method, which takes account of the lengths of different filaments, because the area and shape of the lamellae varied considerably among different filaments and among different regions on a filament.

The area of a lamella was determined by both or either one of the following two methods, depending on fish size. In the triangle method, as used by Price (1931) but not Hughes (1966, 1984*b*), applied to small fish of 0·0016–6·5 g, the area of a lamella was calculated, assuming it to be a triangle, from the maximum height (b) and the base length (l) of the lamella measured from a magnified figure traced on paper by means of a microscope and a *camera lucida*. In very small fish of 0·0016–0·014 g, it was difficult to measure the base length, and so this was estimated from the maximum height and body mass (W) using the formula, obtained with nine fish of 0·0028–1·3 g, $l/b = 2{\cdot}01W^{0{\cdot}130}$ [the correlation coefficient between log (l/b) and log W was 0·897]. In fish of 2·2–2250 g, the area of a lamella was directly measured using a section of 90–150 μm cut by the freezing method from a filament embedded in gelatine and stained with diluted Giemsa solution. The lamellar area was obtained by tracing, with a planimeter, the outline of a magnified figure of the sectioned lamella. The apparent value of the lamellar area obtained by this method was converted to the real value, allowing both for angular bias of the section from the lamellar axis and for shrinkage of the lamella by fixing.

J. exp. Biol. **117**, 319–333 (1985)
Printed in Great Britain © *The Company of Biologists Limited 1985*

RENAL EXCRETION OF MAGNESIUM IN A FRESHWATER TELEOST, *SALMO GAIRDNERI*

BY A. O. J. OIKARI* AND J. C. RANKIN

Division of Physiology, Department of Zoology, University of Helsinki, Arkadiankatu 7, SF–00100 Helsinki, Finland and *School of Animal Biology, University College of North Wales, Bangor, Gwynedd, LL57 2UW, U.K.*

Accepted 18 January 1985

SUMMARY

Infusion of magnesium salts into the body cavity of freshwater-adapted rainbow trout led to elevated plasma magnesium concentrations and to stimulation of renal tubular secretion of magnesium. The majority of the infused load was excreted renally, no net branchial excretion being detected. Magnesium sulphate infusion led to increased tubular secretion of sulphate. Magnesium chloride infusion led to reduced tubular reabsorption of chloride. Magnesium could either be reabsorbed or secreted in control freshwater-adapted trout, apparently as a function of nutritional status. Fish could switch from reabsorption to secretion in response to magnesium loading. It is suggested that freshwater fish eliminate excess dietary magnesium renally.

INTRODUCTION

Whilst a number of studies have been carried out on the control of plasma sodium and chloride concentrations in teleosts, relatively little attention has been paid to the regulation of magnesium and sulphate levels. This is perhaps not surprising since, as stated in a recent review of magnesium transport in the mammalian kidney (Quamme & Dirks, 1980), 'little is known of the mechanisms that regulate magnesium conservation and excretion' and even less is known about sulphate. Fish plasma magnesium concentrations are maintained within the range 1–4 mmol l^{-1}, being higher in marine than in freshwater teleosts (Evans, 1979). In the euryhaline European eel, *Anguilla anguilla*, plasma levels are higher when in sea water than when in fresh water (Chester Jones, Chan & Rankin, 1969) but the difference is relatively small (4 mmol l^{-1} compared to 2 mmol l^{-1}).

Magnesium concentrations of fresh water are approx. 200 μmol l^{-1} or less; in ocean water, it is the third most abundant ion with a concentration of more than 50 mmol l^{-1} (Rankin & Davenport, 1981). In marine fish, branchial osmotic losses must be replaced by drinking, and this leads to continual intestinal absorption of

* Present address: Department of Biology, University of Joensuu, P.O. Box 111, SF–80101 Joensuu, Finland.
Key words: Magnesium, sulphate, urine, renal, excretion/secretion, rainbow trout.

magnesium and sulphate ions; these are thought to be eliminated exclusively by the kidneys (Hickman & Trump, 1969; Evans, 1979).

Freshwater fish must obtain magnesium and sulphate ions either by active uptake or in the diet. There is no evidence for active branchial uptake and only indirect evidence of absorption from the alimentary canal (Cowley *et al.* 1977). Dietary loads will be highly variable depending on the feeding habits of the species. Breakdown of tissues and their proteins will release large quantities of magnesium and sulphate ions, for example. In the few studies carried out on freshwater fish, ultrafiltered magnesium appears to be reabsorbed (Hickman & Trump, 1969), although experiments on starved fish would obviously not reveal the mechanisms responsible for the elimination of magnesium loads. Infusion of magnesium salts stimulates renal secretion of magnesium ions in marine southern flounder (Hickman, 1968), freshwater-adapted Japanese eels, *Anguilla japonica* (Hirano, 1979) and river lampreys, *Lampetra fluviatilis* (Rankin, Henderson & Brown, 1983).

Euryhaline fish may need to be able to initiate renal magnesium secretion rapidly. The Baltic teleost *Myoxocephalus quadricornis*, a species living and surviving only in dilute salinities, seems to possess a huge overcapacity to secrete magnesium ions in relation to the salinity range in which it is able to osmoregulate (Oikari, 1978*a*). Such a capability may be only a relict from marine ancestors or it may have some ionoregulatory function in freshwater teleosts. The responses of a freshwater-acclimated euryhaline fish, the rainbow trout *Salmo gairdneri*, to experimental magnesium loading were therefore studied.

MATERIALS AND METHODS

Animals

Rainbow trout (*Salmo gairdneri* Richardson), weighing 140–190 g, were obtained from a local hatchery (Upper Mills Trout Farm, Clwyd). After transfer to Bangor they were acclimated in well-aerated, dechlorinated, copper-free tap water (Na 0·15; Cl 0·18; Mg 0·022 mmol l^{-1}; pH 6·8; temperature 11·5 ± 1 °C) for at least 2 weeks with a 12 : 12 light : dark regime (L : 08·00 to 20·00). Fish were fed daily (except as specified later) *ad libitum* with commercial trout food (Shell Salmon Food, ∅3 mm).

Most trout were starved for the last 4–6 days before operation (= fish in postabsorptive stage). A few (= fish in absorptive stage) were fed to satiation 25–30 h before urine collections were started. These nutritional stages were also monitored as absence and presence of faecal pellets on the bottom of the test chamber. A separate batch of trout was gradually – over a 5-day period – transferred to full strength Menai Straits sea water (980 mosmol kg^{-1}) and acclimatized in it at 13 °C for 3 weeks.

Surgical techniques

Urinary catheters were made from 3- to 4-cm pieces of the perforated tips of infant feeding tubes (Argyle® Cat. no. AR–33R, size 5) fitted to 40-cm length of PP 50 (Portex) polypropylene tubing shaped into an 'S' at the proximal end. Intraperitoneal cannulae were made from 30-cm lengths of PP 50 tubing with the internal end formed into a short spiral in hot (90 °C) water. This design, with appropriate ligatures,

prevented the cannula from sliding out. In both types of tubing two or three bubbles were made by heating with a loop of tungsten wire heated by a 4·5 V d.c. current. When stitching the tubing to the body wall all sutures were made distally to these anchoring bubbles.

Trout were anaesthetized in aerated solution of MS222 (ethyl-*m*-aminobenzoate methane sulphonic acid salt, Sigma, 100 mg l^{-1}) and kept upside down in a V-shaped trough with the head immersed in an aerated solution of anaesthetic at the minimum concentration needed to maintain anaesthesia (less than 50 mg l^{-1}). The perforated tip of the catheter was pushed 10–15 mm inside the the urinary papilla, tied in with a ligature around the papilla and then anchored to the skin by three sutures. The intraperitoneal cannula was inserted, with the aid of a sharpened steel wire inside the tubing, into the body cavity – first under the skin for 10–13 mm and then through the latero-abdominal muscles – and was fixed in place with two sutures. *Post mortem* examination showed that the tip of the cannula was adjacent to connective and fatty tissues surrounding the small intestine.

Urine collections

Operated trout were allowed to recover in the experimental chamber, a partially black-painted Perspex box, sufficiently small (26 × 3·8 × 7 cm) to prevent most swimming activity and turning, with a water flow of 1·3–1·5 l min^{-1}. Within 3 h the trout had adjusted to the box, and steady urine output was obtainable for 8–12 h.

The box was connected by siphon to a 100-l recirculation tank with 95 % replacement every 10 h. Experimental water temperatures (T_w) varied during the study period (February–March) from 12·5 to 13·6 °C, but for each fish T_w was adjusted to within ± 0·3 °C or less. The urinary catheter led to a fraction collector (LKB Ultrarack) about 10 cm below the fish. Collection periods generally lasted 60 or 90 min and, when urine volumes were small, as in seawater fish, were made under water-saturated liquid paraffin to prevent evaporation. Prepared tubes were weighed to the nearest 0·5 mg, and urine flow rates ($\dot{V}$ in ml kg^{-1} h^{-1}) was calculated on a weight basis. All samples were either kept at 2–4 °C or frozen at −20 °C before analysis.

Glomerular filtration rate (GFR) was measured as inulin clearance (C_{in}). About 20 μCi of ^{3}H-inulin (> 300 mCi $mmol^{-1}$; Amersham International) in 0·5 ml distilled water was injected intraperitoneally *via* a cannula (freshwater fish) or by hypodermic needle (seawater fish) at least 12 h before each experiment. Three blood samples were collected at 12- to 16-h intervals from minimally anaesthetized (150 mg MS222 l^{-1}) fish by puncturing the caudal vein and were immediately centrifuged. Aliquots of 25 or 50 μl of plasma were counted in a liquid scintillation counter (Beckman LS 7000) with correction for quenching. Plasma radioactivity decayed in a linear manner (generally with a correlation coefficient, $r = 1{\cdot}00$) when plotted on semilogarithmic paper. The d.p.m. at the midpoint of each urine collection period was calculated and C_{in} was calculated as urine d.p.m./plasma d.p.m. × $\dot{V}$. As a first approximation, filtered ionic loads were taken as the product of C_{in} and plasma ultrafiltrate concentration, i.e. ignoring the Donnan equilibrium (see Discussion). Net reabsorption or secretion of an ion was calculated as the difference between filtered and excreted amounts.

Ionic infusions and analyses

All infusions were made at a constant rate *via* the intraperitoneal cannula using a calibrated infusion pump ('perfusor', Braun), usually for 60 min. As preliminary experiments showed that distilled water (DW) infusions from 0·8 to 10·2 ml h^{-1} per 150–160 g fish did not evoke diuresis, a rate of 1·62 ml h^{-1} per fish (approx 10·5 ml kg^{-1} h^{-1}) was adopted in most cases. This rate was found to lead to efficient uptake of an infused magnesium load into the blood plasma (cf. Fig. 1), whereas lower rates yielded slower distribution. The salts infused ($MgCl_2$, $MgSO_4$, Na_2SO_4; 50–100 mmol l^{-1}, analytical reagent quality, British Drug House) were dissolved in DW or in freshwater (FW) teleost Ringer (Rankin & Maetz, 1971) if very low doses of magnesium were needed.

Electrolyte (Mg^{2+}, SO_4^{2-}, Cl^-, Na^+) concentrations of plasma and urine were determined as described by Logan, Morris & Rankin (1980). Osmolalities were measured by freezing point depression using a Knauer Halbmikro-Osmometer. The magnesium concentration of commercial salmon food was analysed by atomic absorption spectroscopy (AAS) after extraction of duplicate 100-mg samples in 5-ml aliquots of 0·1 mol l^{-1} HCl for 5 days.

Access of dietary magnesium to the bloodstream was demonstrated as follows: dried salmon food (Shell) was soaked in 1 mol l^{-1} $MgCl_2$ solution and minced; the meal was force-fed, with the aid of flexible silicone tubing (5 mm radius), directly into the stomach of an anaesthetized trout; blood samples were taken as described above during the following 22 h and plasma magnesium concentrations were measured and compared to the pre-feeding level.

Net extrarenal magnesium flux was measured as follows: catheterized, cannulated trout were allowed to recover in the experimental chamber in the usual manner, except that the water in the chamber was also directly aerated; the inflow was then turned off and serial water samples from the well-aerated bath were collected for up to 2 h and their magnesium concentrations analysed by AAS. Net fluxes of more than 1 μmol kg^{-1} h^{-1} could be measured by this technique.

Magnesium binding in plasma

Eight rainbow trout (130–320 g, both sexes) from a Finnish Hatchery (Savon Taimen) were acclimated for 2–3 weeks in dechlorinated Helsinki tap water at 12 °C. Blood was taken from lightly anaesthetized (75 mg MS222 l^{-1}) fish and a single intraperitoneal injection of 0·25 mol l^{-1} $MgCl_2$ calculated to give a dose of 1300–2000 μmol Mg kg^{-1} was given. After 1·4 h another blood sample was taken. Plasma was immediately separated by centrifugation. A part of the plasma was ultrafiltered through dialysis tubing (A. H. Thomas Co., approximate pore size 4·8 nm) in a centrifuge (approx. 250 × ***g*** for 4 h at 12 °C; further centrifugation after 20 h gave identical results). Magnesium concentrations of the plasma and its ultrafiltrate were determined by AAS. The mean binding values obtained were used to calculate filtered loads of magnesium before and during peak excretion periods following infusions.

RESULTS

Magnesium binding in plasma

Ultrafiltration experiments revealed that an appreciable portion of the total plasma magnesium was bound to macromolecules. In control plasma samples 44 ± 10 % (mean ± S.D., $N = 8$) of the magnesium was non-dialysable; 1·4 h after magnesium chloride injection this had fallen to 31 ± 9 %. These mean values were used in all calculations of net renal secretion or reabsorption. Although the percentage bound fell in magnesium-loaded fish, the total amount bound increased, suggesting that control plasma contains more binding sites than are normally occupied.

Control urine flow rate ($\dot{V}$) and ionic composition

$\dot{V}$ varied from 2·80 to 5·61 ml kg^{-1} h^{-1} at 13 ± 1 °C (mean ± S.D. = 4·25 ± 0·90, $N = 9$). Variation between samples in individual fish was less than that between fish (standard deviations ranging from 12·7 to 20·6 % of mean, $N = 10$ fish), indicating that each trout maintained a relatively constant urine output. $\dot{V}$ was not related to the nutritional status of the fish (cf. control trout of Table 2) but was increased by even the smallest disturbances in the animal's surroundings.

Normal urine composition in trout 4–10 days after feeding is given in Table 1. Urinary magnesium concentrations of freshwater individuals were highly variable, ranging from 0·05 to 0·98 mmol l^{-1}. Sulphate concentrations were almost six times as high. Seawater fish showed much higher magnesium than sulphate concentrations. The other values in Table 1 are similar to those reported previously (Hickman & Trump, 1969; Beyenbach & Kirschner, 1975; Schmidt-Nielsen & Renfro, 1975;) for teleost fish. Plasma values are given for comparison.

Renal elimination of infused magnesium ion

Elevated plasma magnesium concentrations were attained rapidly following intraperitoneal administration and were maintained during the next hour (Fig. 1A) with a concomitant rapid increase in magnesium excretion (Figs 1B, 3) so that 15–42 % of the injected dose was eliminated within 1 h and 70–80 % within 3 h after cessation of infusion. (In the majority of experiments, plasma levels were not monitored since this involved additional periods of anaesthesia for blood sampling.) The time course of the peak excretion rate of magnesium was very similar whether magnesium sulphate of chloride was infused.

The peak magnesium excretion rate in freshwater-adapted trout during the first or second hour following a 60-min infusion was positively and linearly correlated to the dose infused up to approximately 900 μmol kg^{-1} h^{-1} (Fig. 2). Thus, no T_m (transport maximum) was observed; that is, if one does exist, it must equal or exceed 200 μmol kg^{-1} h^{-1} which is about twice the excretion rate of a seawater-adapted trout. Occasionally urine flow rate increased following magnesium loading (as in Fig. 3), but overall there was no significant increase and the increases that were observed were not related to dose administered (Table 2). Antidiuresis was never observed. During and after a 14-h continuous magnesium sulphate infusion (160–250 μmol kg^{-1} h^{-1}), magnesium excretion was maintained at between 18 and 50 times the control rate for 18 h.

Table 1. *Urine and plasma osmolality and ionic concentrations in rainbow trout in fresh water and following 3 weeks adaptation to sea water*

	Freshwater-adapted trout		Seawater-adapted trout	
	Urine	Plasma	Urine	Plasma
Osmolality (mosmol kg^{-1} water)	29·7 ± 8·7 (22)	269 ± 13 (9)	369 ± 22 (3)	373 ± 39 (3)
Magnesium (mmol l^{-1})	0·49 ± 0·30 (18)	0·66 ± 0·17 (7)	141 ± 3 (3)	2·02 ± 1·01 (3)
Sulphate (mmol l^{-1})	2·88 ± 0·40 (9)		33·2 ± 19·5 (3)	
Chloride (mmol l^{-1})	7·7 ± 3·0 (22)	124 ± 13 (10)	210 ± 34 (3)	157 ± 11 (3)
Sodium (mmol l^{-1})	6·2 ± 3·5 (9)		32 ± 21 (3)	

Means ± S.D. of mean. $N = 8$ freshwater fish except for sulphate and sodium where $N = 3$, and $N = 3$ for seawater fish. Number of urine samples analysed in parentheses.

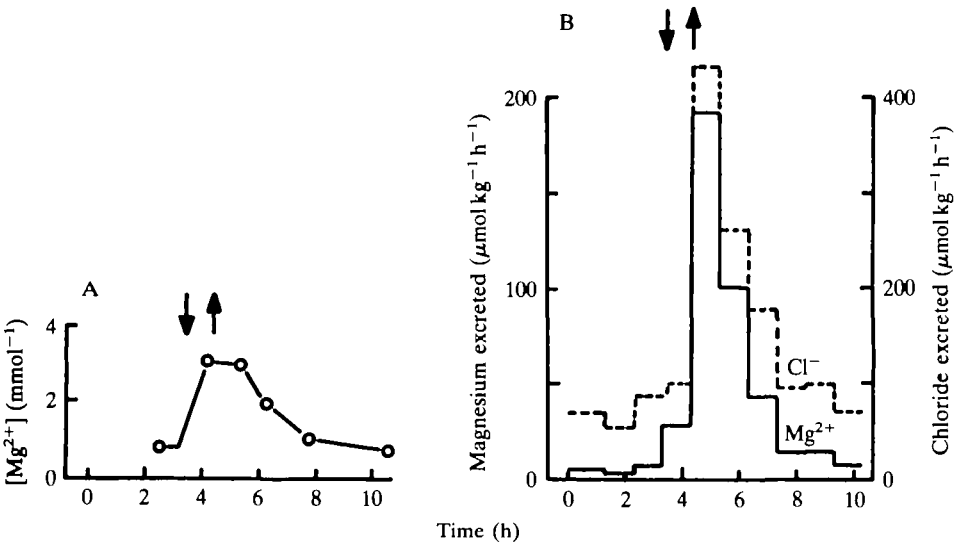

Fig. 1. Effects of infusion of magnesium chloride solution (440 μmol kg^{-1}, intraperitoneal) on (A) plasma magnesium concentration and (B) renal magnesium (solid line) and chloride (broken line) excretion rates in a rainbow trout adapted to fresh water. Arrows mark beginning and end of 1-h infusion period. Additional magnesium excretion in the 4-h period following the start of the infusion was equal to 76 % of the amount infused.

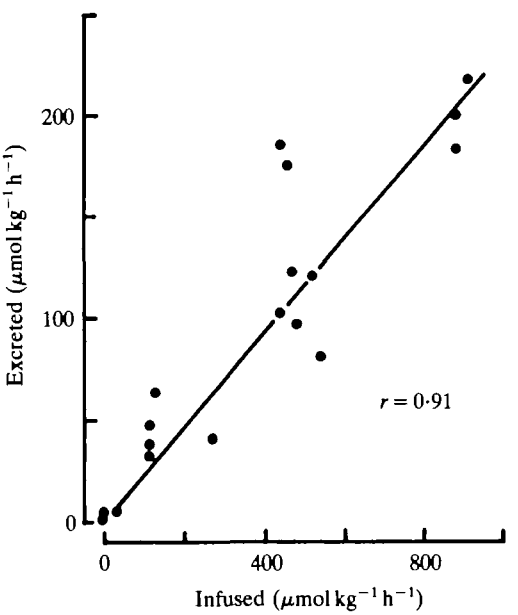

Fig. 2. Correlation between amount of intraperitoneally infused magnesium and maximum increase (over pre-infusion mean control rate) in urinary magnesium excretion rate in freshwater-adapted rainbow trout. Data are from 11 fish. All infusions and urine collection periods lasted for 1 h.

Extrarenal net flux of magnesium

It was not possible to measure any extrarenal net flux in control ($N = 7$) or magnesium-loaded (approx. 450 μmol kg^{-1} h^{-1}; $N = 6$; water temperature 14·5 °C) trout. Branchial net fluxes must therefore be less than the detection limit (1 μmol kg^{-1} h^{-1}), which is negligible (< 1 %) compared to the amounts excreted renally.

Excretion of sulphate and chloride

The peak rate of sulphate excretion during magnesium sulphate infusion closely paralled that of magnesium ($N = 4$ experiments; for example see Fig. 3). In most, but not all, cases urine chloride concentration also increased. Thus all three ions could contribute to the higher urine osmolality which invariably resulted. Sulphate excretion rate increased from 15 to 32 μmol kg^{-1} h^{-1} for 3 to 4 h following sodium sulphate infusion (275 μmol kg^{-1} h^{-1}) with no change in excretion of sodium or chloride ions. No changes in urinary sulphate excretion were observed following magnesium chloride infusion. Sulphate excretion thus can be independent of magnesium excretion and chloride can serve as an additional counterion with sulphate in the magnesium secretion process.

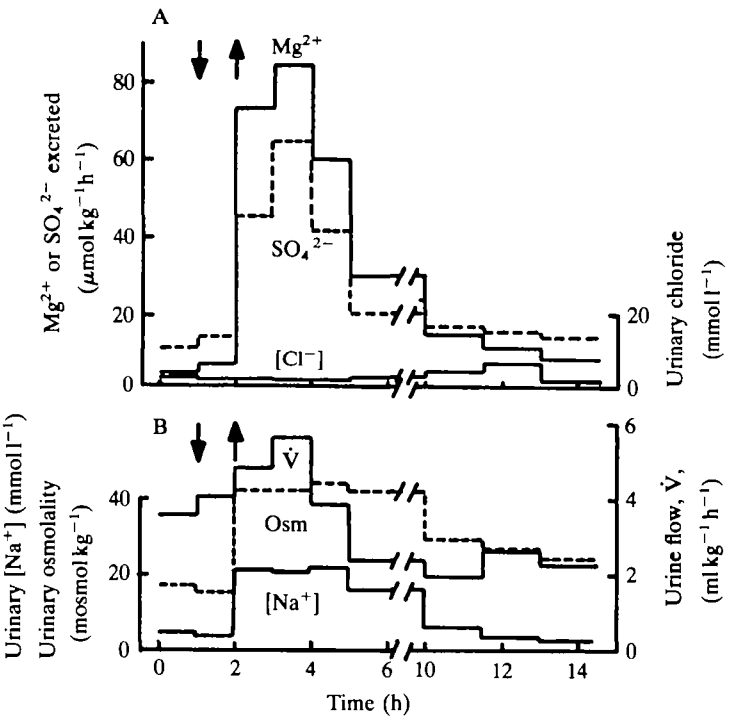

Fig. 3. Effects of infusion of 545 μmol kg^{-1} h^{-1} magnesium sulphate solution (0·8 ml h^{-1} into a 150-g trout adapted to fresh water) on (A) magnesium (solid line) and sulphate (broken line) renal excretion rates (in μmol kg^{-1} h^{-1}) and urinary chloride concentration (in mmol l^{-1}) and (B) rate of urine flow ($\dot{V}$ in ml kg^{-1} h^{-1}), urinary sodium concentration (solid line; in mmol l^{-1}) and urinary osmolality (Osm, broken line; in mosmol kg^{-1}). Arrows indicate beginning and end of infusion.

Table 2. *Effects of magnesium chloride infusions on urine flow and magnesium excretion rates in freshwater-adapted rainbow trout*

Dose of magnesium (μmol kg^{-1} h^{-1})	Urine flow rate (ml kg^{-1} h^{-1})	Inulin clearance (ml kg^{-1} h^{-1})	Peak Mg^{2+} excretion (μmol kg^{-1} h^{-1})	Mg secretion (% of amount excreted)
0 (control)	4·31 ± 1·03	10·67 ± 2·11	5·13 ± 3·73	22·8 ± 59·4†
451 ± 20	5·32 ± 1·81	13·44 ± 3·76*	139 ± 43***	90·4 ± 4·2**
898 ± 16	4·60 ± 1·23	12·52 ± 2·61	180 ± 38***	84·0 ± 5·2**
SW fish	0·77 ± 0·07***	2·00 ± 0·50***	109 ± 9***	97·7 ± 0·8**

Values for seawater-adapted (SW) fish are given for comparison.
† Three fish showed reabsorption; four showed secretion.
Means ± S.D. of mean. $N = 7$ (control), 5 (Mg-infused) or 3 (SW) fish.
Comparison with freshwater controls: * = $P < 0{\cdot}05$, ** = $P < 0{\cdot}01$, *** = $P < 0{\cdot}001$.

Infusions of magnesium chloride (0·9 and 1·8 mmol chloride $kg^{-1} h^{-1}$) did not cause significant differences in urine flow rate but did cause small increases in inulin clearance which were, however, only significant ($P < 0·05$) at the lower infusion rate (Table 2). During excretion of infused $MgCl_2$, calculated filtered loads of chloride increased but the net reabsorption rates were unchanged (Table 3). The percentage of the filtered chloride reabsorbed, however, decreased significantly ($P < 0·01$), leading to highly significant ($P < 0·001$) increases in urinary chloride concentrations at both infusion rates. (Chloride was not bound in plasma to any significant extent, so no corrections were needed in calculating filtered loads.) The chloride which acted as the counterion during magnesium secretion could therefore have come from the filtered load, rather than from any tubular Mg^{2+}/Cl^- co-transport mechanism. Whatever the site of magnesium secretion, the net result is that magnesium-chloride-loaded trout increase the molar chloride excretion to double that of magnesium (Fig 1; Tables 2, 3).

It is interesting to note that no statistically significant changes of the plasma chloride concentration occurred in magnesium-chloride-infused trout (control, 124 ± 13; high infusion rate, 122 ± 16 mmol l^{-1}, $N = 5$ fish) in contrast to the highly significant ($P < 0·0001$, $N = 10$) increase in plasma magnesium concentration.

Reabsorption and secretion of magnesium in fresh water

Control trout displayed either net reabsorption of filtered magnesium or net secretion (cf. Table 2). The renal status maintained was clearly associated with the nutritional status of the trout (Fig. 4) and we noted that it was possible to shift from net secretion to net reabsorption within 2 h of reaching the postabsorptive phase. The peak Mg^{2+} excretion following $MgCl_2$ infusion was predominantly caused by tubular secretion, the slight increase in filtered load being of negligible importance. Because GFR (C_{in}) was more than five times that of seawater-adapted trout, the filtered magnesium loads were higher, and thus the tubular secretion (as a percentage of total excretion) was lower, in freshwater trout. The results demonstrate that the freshwater trout kidney possesses active magnesium secretory mechanisms adequate to account for up to 90 % of the excreted amount.

Because plasma levels of sulphate were not measured, it was not possible to determine whether urinary sulphate of magnesium-sulphate-infused trout originated predominantly from secretion or filtration (Fig. 3). In unloaded controls, however, urinary sulphate concentrations (Table 1) were fairly high compared to salmonid plasma concentrations (0·4–2·0 mmol l^{-1}) reported by Holmes & Donaldson (1969), giving U/P ratios of between 1·5 and 7. This indicates that very little, if any, of the filtered sulphate is reabsorbed and that trout resort to net secretion to eliminate sulphate loads.

Dietary magnesium loading

Loading with magnesium chloride by stomach tube, like intraperitoneal infusion, increased plasma magnesium concentration, for example from 0·6 to 2·1 mmol l^{-1} in 30 min in response to 5 mmol kg^{-1}, remaining more than double the control value for at least 3–4 h. This demonstrated that the wall of the alimentary canal of freshwater trout is permeable to magnesium ions. In contrast to force feeding, digestion

Table 3. *Effects of magnesium chloride infusions on renal chloride excretion in freshwater-adapted rainbow trout*

Dose of chloride administered (N) (μmol kg^{-1} h^{-1})	Urinary chloride concentration (mmol l^{-1})	Peak excretion rate of chloride (μmol kg^{-1} h^{-1})	Net chloride reabsorption (μmol kg^{-1} h^{-1})	Net reabsorption of filtered chloride (%)
0 (control) (10)	8·9 ± 3·4	38 ± 16	1187 ± 178	97·0 ± 1·2
902 ± 40 (5)	55 ± 7***	291 ± 109***	1289 ± 313	81·3 ± 3·3**
1796 ± 32 (5)	72 ± 24***	348 ± 134***	1249 ± 355	78·6 ± 3·8**
SW fish (3)	210 ± 34***	164 ± 34***	147 ± 86***	45·3 ± 18·1*

Values for seawater-adapted (SW) fish are given for comparison.
For other details see Table 1.
Comparison with freshwater controls: * = $P < 0{\cdot}05$; ** = $P < 0{\cdot}01$; *** = $P < 0{\cdot}001$.

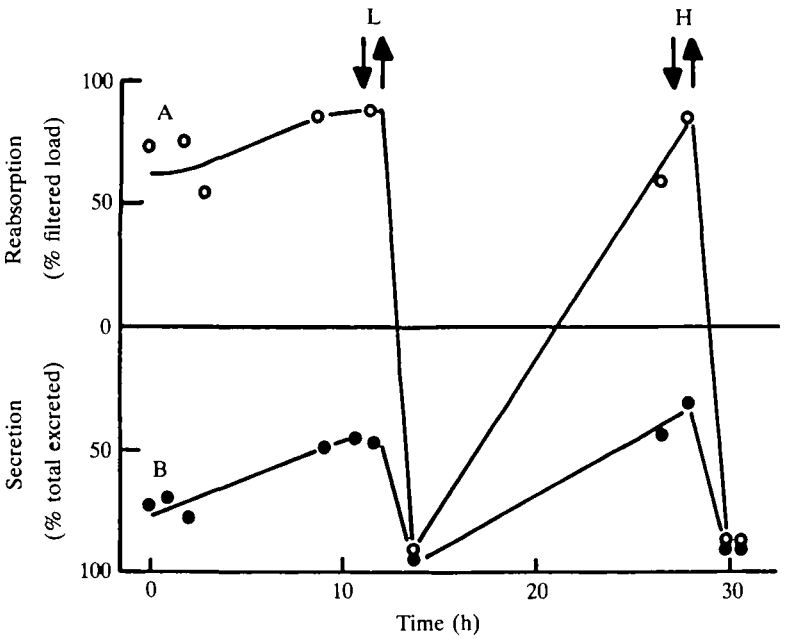

Fig. 4. Renal magnesium reabsorption/secretion in two freshwater-adapted trout loaded with low ($L = 445\ \mu mol\ kg^{-1}\ h^{-1}$) and high ($H = 890\ \mu mol\ kg^{-1}\ h^{-1}$) intraperitoneal infusions of magnesium chloride solution. Arrows indicate beginning and end of infusions. Typical examples are given from a fish in the absorptive (fish B; closed circles) and postabsorptive (fish A; open circles) phases (see Materials and Methods). Estimated filtered loads of magnesium were based on data for plasma magnesium concentrations before, during and after magnesium chloride infusions (see for example Fig. 2A) including an allowance for binding to plasma proteins.

of salmon pellets (containing $193\ \mu mol\ kg^{-1}$ magnesium) resulted in a much slower release and absorption of magnesium ions, which entered the circulation during the absorptive phase, producing a long-lasting increase in renal magnesium secretion (e.g. fish B in Fig. 4). This rate must be sufficient to prevent any significant increases in plasma magnesium concentration. Later, during the postabsorptive phase, trout kidneys switch from net secretion to net reabsorption (e.g. fish A in Fig. 4).

DISCUSSION

Methodology

Results were obtained on resting fish after recovery from the diuresis evoked by the operations. Some variations in urine output can be considerd normal (Hickman & Trump, 1969) and the highest coefficient of variation of any individual was 20·6%. Ureteral urine was siphoned continuously through the catheter, i.e. the role of the bladder (Beyenbach & Kirschner, 1975; Schmidt-Nielsen & Renfro, 1975) was absent or negligible.

Several markers, e.g. inulin, polyethylene glycol (PEG), glofil and ^{51}Cr-EDTA, have been used to measure GFR in teleosts. It seems possible that ^{3}H-inulin underestimates GFR by about 20% relative to PEG in the Americal eel (Schmidt-Nielsen & Renfro, 1975; Beyenbach & Kirschner, 1976). However, the usefulness of

these markers has not been substantiated in teleosts by micropuncture studies. In the lamprey, *Lampetra fluviatilis* (the only fish in which the reliability of any glomerular marker has been investigated using micropuncture techniques), PEG and ^{3}H-inulin clearances were identical although there was some (17 %) reabsorption of the latter (Moriarty, Logan & Rankin, 1978). Possible deviation of C_{in} from the true GFR is likely therefore to have led to underestimation of the amount of plasma magnesium filtered. Estimation of the percentage of ultrafilterable magnesium was based on the assumption that the dialysis tubing used had the same characteristics as the glomerular filtration barrier; this may have led to some error, as would the failure to correct for any possible Donnan effect. The calculations of percentage reabsorption or secretion of magnesium are therefore not exact but the changes observed (e.g. see Fig. 4) were of such magnitude that it was possible to be certain whether magnesium was being secreted or reabsorbed in spite of the above potential sources of error.

Excretion of magnesium ions in freshwater trout

It has long been realized that an important function of the marine teleost kidney is elimination of magnesium and sulphate ions absorbed from sea water drunk to maintain body water balance (Hickman & Trump, 1969; Evans, 1979), enabling the fish to maintain plasma magnesium concentrations of around 1·5–3 % of the seawater level. Micropuncture studies of lampreys have demonstrated magnesium secretion in the proximal renal tubules (Rankin, Logan & Moriarty, 1980); in teleosts, active magnesium secretion is thought to occur in the cells of the second proximal segment of the nephron (Hickman & Trump, 1969; Beyenbach, 1982). Typically, about 98 % of the magnesium excreted is secreted (Table 2); this is fairly similar to the amount (95 %) secreted by two species of Baltic sculpin living in brackish water of about 9 mmol $Mg^{2+}\,l^{-1}$ (Oikari, 1978*b*).

The present results show that freshwater trout, although normally reabsorbing magnesium, are able to switch immediately to secretion when loaded. A similar phenomenon has been observed in the freshwater lamprey (Rankin *et al.* 1983). On the other hand, it is not known whether such mechanisms are involved in the excretion of excess dietary magnesium, even in stenohaline freshwater teleosts. However, present results suggest that the inability of the kidney to secrete magnesium ions is unlikely to be a limiting factor preventing the colonization of sea water by such fish. The factor triggering the tubular secretion mechanism is not known, but a likely candidate is a direct effect on the tubular cells of an increase in plasma magnesium concentration (Babiker & Rankin, 1979). In freshwater trout there was no inverse relationship between urinary sodium and magnesium concentrations as was found in the perfused *Lophius* kidney (Babiker & Rankin, 1979); sodium reabsorption was always high as expected in a freshwater fish. Electroneutrality could be maintained either passively, by reduced reabsorption of chloride or sulphate ions (or both), or perhaps actively by secretion of sulphate ions. Active magnesium transport was not obligatorily coupled to either anion.

Biological significance of magnesium excretion in freshwater trout

The primary function of renal magnesium excretion in freshwater fish would appear to be to maintain a more or less stable plasma magnesium concentration in constantly

varying nutritional situations. Feeding is followed by diffusion of magnesium ions across the wall of the alimentary canal for a variable period, depending on the quality and quantity of food eaten, to be eliminated renally. The dietary magnesium load in a carnivorous fish can be appreciable. For example a trout digesting a fish meal of 2% of its body weight is loaded, if all the magnesium is absorbed, with 240 μmol kg^{-1} (calculation based on muscle magnesium contents given by Oikari, 1975 and Lönn & Oikari, 1982). This amount falls within the range investigated in this study (Fig. 2). In the postabsorptive stage, the trout switches to reabsorption of filtered magnesium and urinary concentrations fall to low (approx. 0·1–0·2 mmol l^{-1}) levels. Because of the high urine flow rates this results in a loss of 0·5–1·0 mmol kg^{-1} h^{-1}, which, in trout fed on a magnesium-deficient diet, eventually leads to plasma hypomagnesaemia (Cowey *et al.* 1977). The large internal pool of bound magnesium in bones and muscles (Cowey *et al.* 1977; Lönn & Oikari, 1982) delays this process and the time lapse may well be much longer than a normally fed fish would ever encounter. It would be interesting to see if renal magnesium excretion increases during severe starvation, when intracellular energy reserves have to be mobilized, in order to eliminate intracellular magnesium. On the other hand, we may suppose that the magnesium secretion mechanism, necessary for a euryhaline fish in sea water, will always be switched on when the extracellular magnesium concentration increases above a preset level. The kidneys of freshwater trout seem to function to maintain optimal extracellular fluid magnesium concentrations by switching from net reabsorption to net secretion and *vice versa* in varying nutritional situations.

This study was supported by the Herman Rosenberg Fund (University of Helsinki) to AO and Science and Engineering Research Council research grant GR/B 38179 to JCR. Most of the work was carried out at UCNW, Bangor and all the generous help received, particularly from Valmai Griffiths, is cordially acknowledged.

REFERENCES

BABIKER, M. M. & RANKIN, J. C. (1979). Factors regulating the functioning of the *in vitro* perfused aglomerular kidney of the anglerfish, *Lophius piscatorius* L. *Comp. Biochem. Physiol.* **62**A, 989–993.

BEYENBACH, K. W. (1982). Direct demonstration of fluid secretion by glomerular renal tubules in a marine teleost. *Nature, Lond.* **299**, 54–56.

BEYENBACH, K. W. & KIRSCHNER, L. B. (1975). Kidney and urinary bladder functions of the rainbow trout in Mg and Na excretion. *Am. J. Physiol.* **229**, 389–393.

BEYENBACH, K. W. & KIRSCHNER, L. B. (1976). The unreliability of mammalian glomerular markers in teleostean renal studies. *J. exp. Biol.* **64**, 369–378.

CHESTER JONES, I., CHAN, D. K. O. & RANKIN, J. C. (1969). Renal function in the European eel (*Anguilla anguilla* L.): changes in blood pressure and renal function of the freshwater eel transferred to sea-water. *J. Endocr.* **43**, 9–19.

COWEY, C. B., KNOX, D., ADRON, J. W., GEORGE, S. & PIRIE, B. (1977). The production of renal calcinosis by magnesium deficiency in rainbow trout (*Salmo gairdneri*). *Br. J. Nutr.* **38**, 127–135.

EVANS, D. H. (1979). Fish. In *Comparative Physiology of Osmoregulation in Animals*, Vol 1., (ed. G.M.O. Maloiy), pp. 305–390. London, New York: Academic Press.

HICKMAN, C. P. (1968). Urine composition and kidney tubular function in southern flounder, *Paralichthys lethostigma*, in seawater. *Can. J. Zool.* **46**, 439–455.

HICKMAN, C. P. & TRUMP, J. (1969). The Kidney. In *Fish Physiology*, Vol. I, (eds W. S. Hoar & D. J. Randall), pp. 91–239. New York, London: Academic Press.

HIRANO, T. (1979). Effects of carp urohypophysial extract on renal function in the eel, *Anguilla japonica*. *Gunma Symp. Endocr.* **16**, 59–67.

HOLMES, W. N. & DONALDSON, E. M. (1969). The body compartments and the distribution of electrolytes. In *Fish Physiology*, Vol. 1, (eds W. S. Hoar & D. J. Randall), pp. 1–89. New York: Academic Press.

LOGAN, A. G., MORRIS, R. & RANKIN, J. C. (1980). A micropuncture study of kidney function in the river lamprey, *Lampetra fluviatilis*, adapted to sea water. *J. exp. Biol.* **88**, 239–247.

LÖNN, B.-E. & OIKARI, A. (1982). Determination of muscle ions from trout *Salmo gairdneri*, by a simple wet extraction technique. *Comp. Biochem. Physiol.* **72A**, 49–53.

MORIARTY, R. J., LOGAN, A. J. & RANKIN, J. C. (1978). Measurement of single nephron filtration rate in the kidney of the river lamprey, *Lampetra fluviatilis* L. *J. exp. Biol.* **77**, 57–69.

OIKARI, A. (1975). Hydromineral balance in some brackish-water teleosts after thermal acclimation, particularly at temperatures near zero. *Ann. Zool. Fennici* **12**, 215–229.

OIKARA, A. (1978*a*). Aspects of osmotic and ionic regulation in two Baltic teleosts: effects of salinity on blood and urine composition. *Mar. Biol.* **44**, 345–355.

OIKARI, A. (1978*b*). Effects of dilute media on renal hydromineral balance in the Baltic sculpins *Myoxocephalus scorpius* (L.) and *M. quadricornis*. *Ann. Zool. Fennici* **15**, 53–59.

QUAMME, G. A. & DIRKS, J. H. (1980). Magnesium transport in the nephron. *Am. J. Physiol.* **239**, F393–F401.

RANKIN, J. C. & DAVENPORT, J. (1981). *Animal Osmoregulation*. Glasgow: Blackie.

RANKIN, J. C., HENDERSON, I. W. & BROWN, J. A. (1983). Osmoregulation and the control of kidney function. In *Control Processes in Fish Physiology*, (eds J. C. Rankin, T. J. Pitcher & R. T. Duggan), pp. 66–88.

RANKIN, J. C., LOGAN, A. G. & MORIARTY, R. J. (1980). Changes in kidney function in the river lamprey, *Lampetra fluviatilis* L, in response to changes in external salinity. In *Epithelial Transport in the Lower Vertebrates*, (ed. B. Lahlou), pp. 171–184. Cambridge: Cambridge University Press.

RANKIN, J. C. & MAETZ, J. (1971). A perfused teleostean gill preparation. Vascular actions of neurohypophysial hormones and catecholamines. *J. Endocr.* **51**, 621–635.

SCHMIDT-NIELSEN, B. & RENFRO, J. L. (1975). Kidney function of the American eel *Anguilla rostrata Am. J. Physiol.* **228**, 420–431.

The area of the magnified figure of a sectioned lamella was measured by both the triangle and the direct methods, and the results were compared. The relationship of the value of the lamellar area determined by the direct method (bl) to the value estimated by the triangle method (bl') in seven fish of 2·2–2250 g was expressed by the formula, $bl/bl' = 1{\cdot}48W^{-0{\cdot}026}$ [the correlation coefficient between log (bl/bl') and log W was $-0{\cdot}805$]. The value of the lamellar area obtained by the triangle method was, therefore, converted to the real value based on this formula.

The basal part of the secondary lamella is embedded in the tissue bed of the gill filaments, and the part responsible for gas exchange is considered to be the exposed part of the lamella. The values of the lamellar area obtained by the triangle method in small fish of 0·0016–6·5 g were considered to be the values of the whole lamellae including the embedded part, although the boundary line between the exposed part and the embedded one was not clear, because the line showing the relationship between the lamellar area obtained by the triangle method and body mass was approximately on the extension of the line for the whole lamellar area-body mass relationship in bigger fish of 2·2–2250 g (Fig. 1). The values of the lamellar area obtained in the small fish were therefore converted to the values for the exposed part using the formula for the ratio of the exposed part to the whole lamella (R), $R = 0{\cdot}76W^{-0{\cdot}037}$, obtained with seven fish of 2·2–2250 g (the correlation coefficient between log$R$ and log$W$ was $-0{\cdot}680$).

Body surface area was obtained, in large fish above 100 g, by multiplying the body length by the average circumference of the body measured at ten evenly-spaced transverse sections of the body. In small fish under 100 g, the body surface area was estimated from body heights and body widths of the ten evenly-spaced parts using the following parabolic equation, assuming the circumference to be

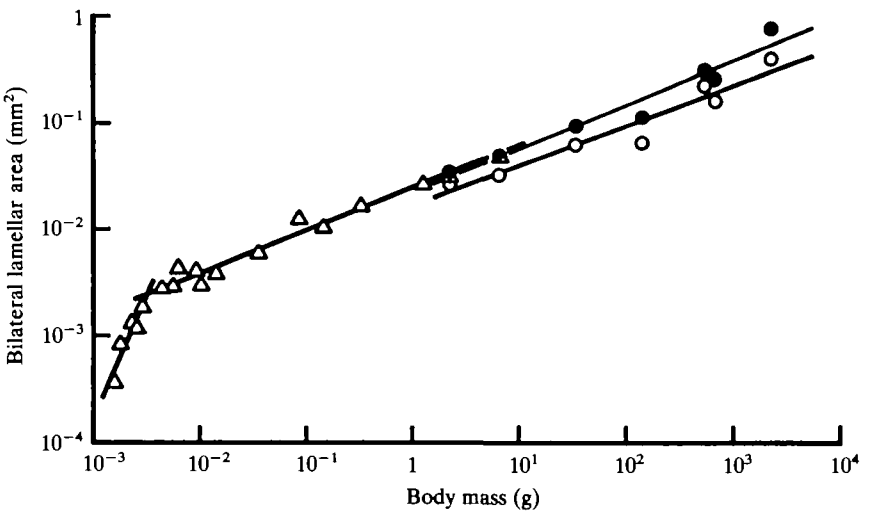

Fig. 1 Comparison between average bilateral areas of the gill secondary lamellae determined by two methods, the triangle method (△) and the direct method (● : whole area including the embedded part; ○ : area of the exposed part).

composed of two parabolas,

$$C = \sqrt{4H^2 + B^2} + \frac{B^2}{2H} \times \ln \frac{2H + \sqrt{4H^2 + B^2}}{B},$$

where C is circumferential length, H is body height, and B is body width. The body surface area estimated by this equation was found to be 8·3 % smaller than the directly measured area in fish of 140–2250 g. Therefore, the estimated values were multiplied by 1·09 to convert them to the real values. Fin area was directly measured by tracing, with a planimeter, the outline of the magnified figure of the fin fixed in formalin Cortland saline.

RESULTS

There was a triphasic allometry between gill area and body mass of the carp: the allometry was positive in the 1st and the 2nd phases and negative in the 3rd phase (Fig. 2). The fish developed from the 1st to the 2nd phase, when the larvae were about 7 days old, weighed about 0·003 g and when the yolk had been almost absorbed. They developed from the 2nd to the 3rd phase, when they were about 40 days old, weighed about 0·2 g, and when the fins had assumed the adult form and the scales had begun to appear. Therefore, we consider that the 1st phase corresponds to the prelarval

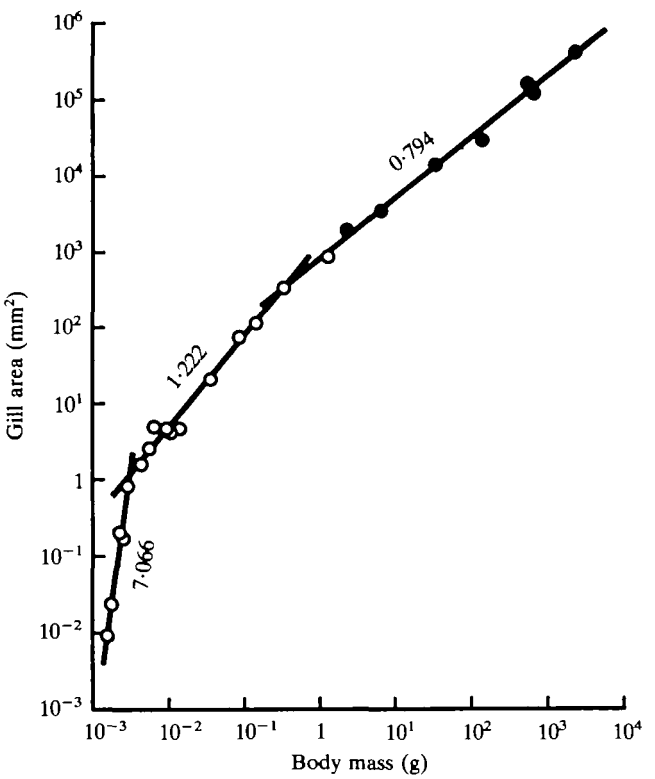

Fig. 2 Allometric relationships of the gill area to body mass. Open circles show the values estimated by the triangle method, and solid circles the values by the direct method. Figures by the regression lines indicate the slopes of the lines.

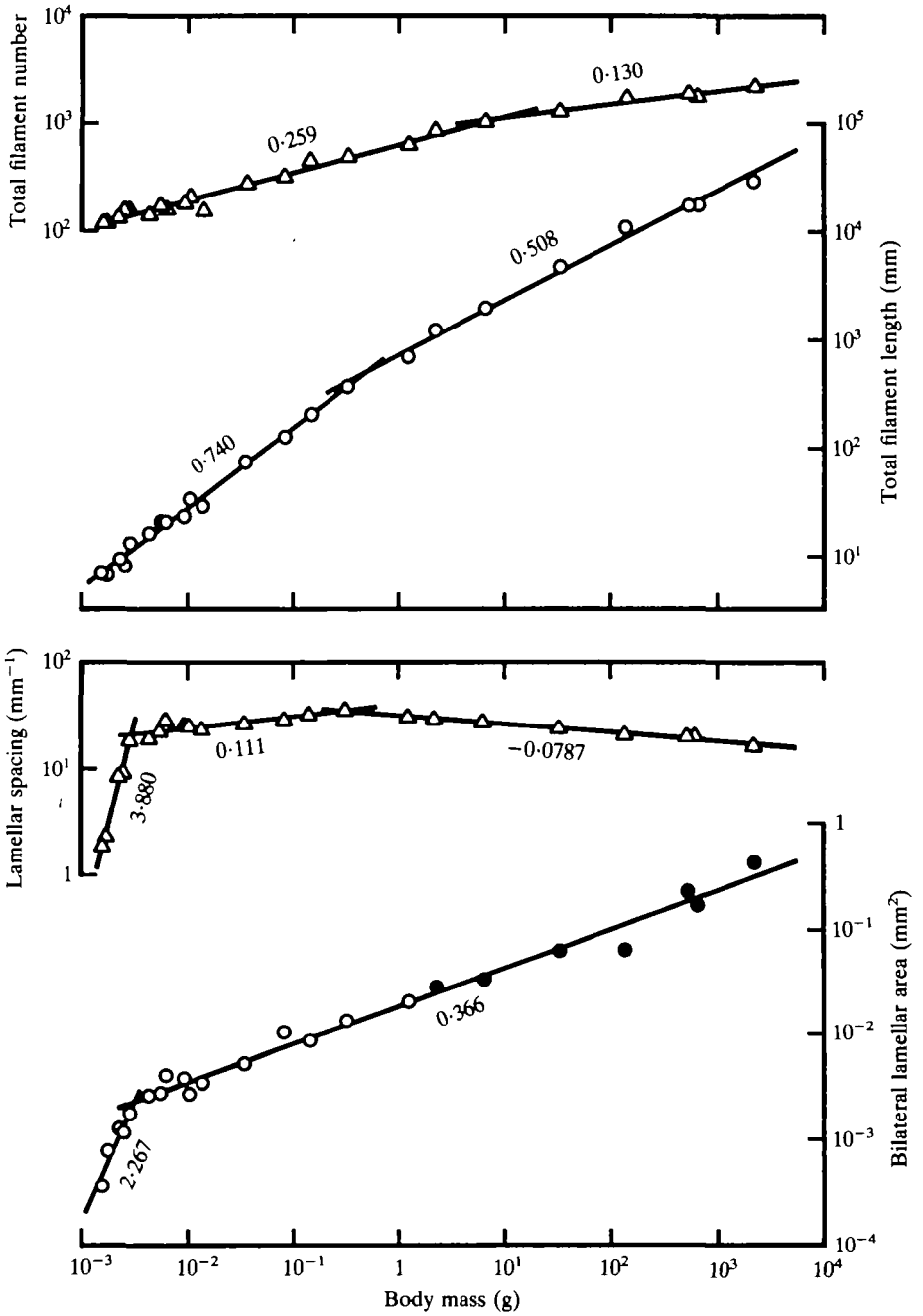

Fig. 3 Allometric relationships of the total filament number, the total filament length, the average spacing of the gill secondary lamellae on one side of the filament, and the average bilateral area of the lamellae, to body mass. Symbols for the lamellar area are the same as those in Fig. 2. Figures by the regression lines indicate the slopes of the lines.

J. exp. Biol. 117, 171–179 (1985)
Printed in Great Britain © *The Company of Biologists Limited 1985*

A PASSIVE TWO LAYER PERMEABILITY-WATER CONTENT MODEL FOR *PERIPLANETA* CUTICLE

BY J. MACHIN AND G. J. LAMPERT

Department of Zoology, University of Toronto, Toronto, Ontario, Canada M5S 1A1

Accepted 23 November 1984

SUMMARY

Two layers in *Periplaneta* pronotum, endocuticle and combined epicuticle and exocuticle were functionally distinguished by their permeabilities and water affinities. A passive model combining the permeabilities of these layers and the water content of the endocuticle was designed to predict pronotal water contents in a variety of ambient activities at 20 °C.

The model predicted cuticle water contents with acceptable accuracy above ambient activities of 0·56 but overestimated them in drier conditions. Despite universally high water activities in the endocuticle, differences in water content related to ambient activity were predicted. Cuticle water contents below haemolymph equilibrated values, represented in the literature as evidence of active water regulation, were largely attributed to passive activity gradients combined with evaporation errors.

INTRODUCTION

Mass gains, observed when excised cuticle samples are exposed to atmospheres of the same water activity as the haemolymph, have been put forward as evidence that the insect epidermis is capable of actively regulating cuticle water content (Winston & Beament, 1969). We suggest that Winston & Beament's (1969) active model might have arisen from faulty assumptions about the influence of water activity gradients on cuticle hydration, especially the inner, water-rich layers. Since the mass gains in question are small and the standard errors are relatively high, Winston & Beament could also have underestimated the importance of evaporative loss during preparation of cuticle samples, by dismissing the time taken as 'only a few seconds'.

It is therefore appropriate to examine the evidence supporting a greater epidermal role more closely. Both the data in the preceding paper (Machin, Lampert & O'Donnell, 1985) and those of Winston & Beament (1969) are suitable for this purpose because these studies employed essentially the same methods of preparing *Periplaneta* pronotal discs. However they came to widely differing conclusions about the forces governing the distribution of cuticular water.

Resolution of these diverging interpretations will rest on two different

Key words: *Periplaneta* cuticle, water content, permeability, passive model.

investigations. First, by reconstructing Winston & Beament's (1969) cuticle excision procedures, it has been possible to assess the magnitude of evaporation errors and their impact on subsequent rehydration. Second, the need to understand the forces governing the distribution of cuticular water at a quantitive level has led to the development of a passive model determined by ambient activity and the water affinities and permeabilities of component layers of the cuticle. The model interprets the water-holding characteristics of the cuticle components *in vitro* measured at equilibrium, in such a way that intact cuticular water content could be predicted for the range of water activity gradients experienced by living cockroaches. Most importantly the model can be used to simulate Winston & Beament's (1969) key experiment by predicting the amount of water the cuticle would possibly gain when returned to an atmosphere of the same water activity as the haemolymph.

METHOD AND RESULTS

Assessment of evaporation errors

The phases of preparing epidermis-free discs of cuticle from *Periplaneta* pronotum described by Machin *et al.* (1985) were timed with a stopwatch. As far as can be judged the technique was virtually identical to that used by Winston & Beament (1969), except that they wrapped their samples in foil prior to weighing on a torsion balance. To estimate the evaporative losses prior to wrapping, the masses of freshly excised discs were continuously recorded on a Mettler ME22 microbalance for several minutes. Air activity in the room was either 0·85 or 0·925 at a temperature of 22 °C. Winston & Beament prepared their cuticle samples in a humidified chamber with activities between 0·85 and 0·90. They are not clear on this point, but it seems likely that the chamber was at room temperature, presumably not greatly different from 22 °C.

Representative preparation times together with typical disc mass loss curves are shown in Fig. 1. The exponential equations best describing these curves are also indicated. Such equations were used to extrapolate the mass at the beginning of evaporation, considered to be the point at which epidermal and associated tissues were removed. As a result of our experience we estimate that the delay from the start of evaporation to the foil wrapping was probably between 20 and 40 s. This delay would account for a subsequent mass gain over Ringer to a minimum error (at 20 s delay at $0{\cdot}90a_w$) (a_w, water activity) of 0·70 and a maximum (at 40 s delay at $0{\cdot}85a_w$) of 1·83 % initial wet mass. Such gains represent a significant proportion of the gains interpreted by Winston & Beament (1969) as evidence of active regulation of cuticular water.

A passive model of cuticle water relations

Epidermal permeability has been shown to be insignificant so the model will concentrate on cuticle alone and is based on the two cuticular layers distinguished as endocuticle and combined exocuticle and epicuticle (Machin *et al.* 1985). The water content of any layer depends on its water affinity, expressed in terms of mass or volume, and the prevailing water activity. Water activity is determined, in turn, by the permeability of given layer in relation to the permeabilities of the others. If the

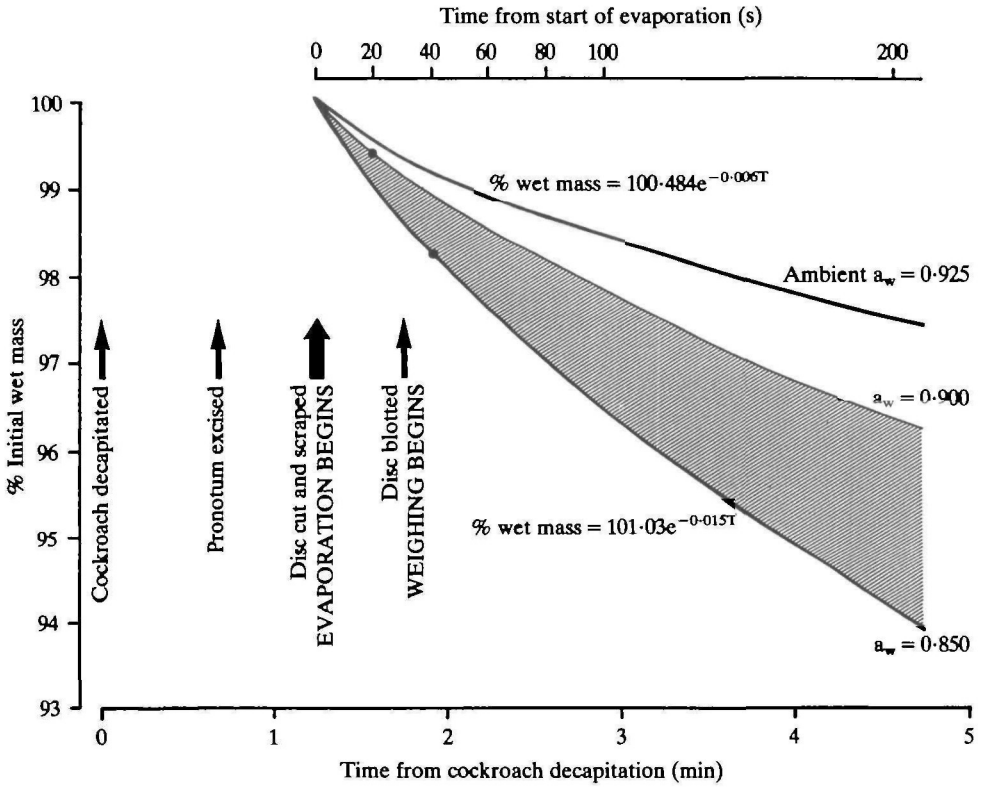

Fig. 1. Diagram to show the timing of the phases of disc preparation superimposed on observed pronotal water loss curves (heavy lines) at ambient water activities of 0·85 and 0·925 at 22 °C. Initial wet mass refers to fully hydrated cuticle discs. The parts of the curves preceding weighing were extrapolated using the least squares fitted exponential equations as indicated. The curves were used to construct a third (thin line) for 0·90 activity. The estimated range of potential evaporation error in conditions used by Winston & Beament (1969) is indicatd by the shaded area. The closed circles indicate minimum and maximum errors at 20 and 40 s delay in weighing, respectively.

properties within each of the two layers are uniform, the driving force of water flux, assumed to be vapour pressure or activity (a_w), would fall linearly across each layer.

For systems containing two barriers in series, the following general relationship enables a component permeability (P_2) to be calculated, knowing the overall permeability (P_O) and the permeability of the other component, (P_1):

$$\frac{1}{P_O} = \frac{1}{P_1} + \frac{1}{P_2}. \tag{1}$$

The gradients (Δa_w) for each layer in any conditions can then be obtained from their permeabilities by rearrangement of Fick's equation describing passive diffusion:

$$\Delta a_w = \frac{J}{PA}, \tag{2}$$

where J is equal to the total flux across the cuticle, A the area and P the permeability

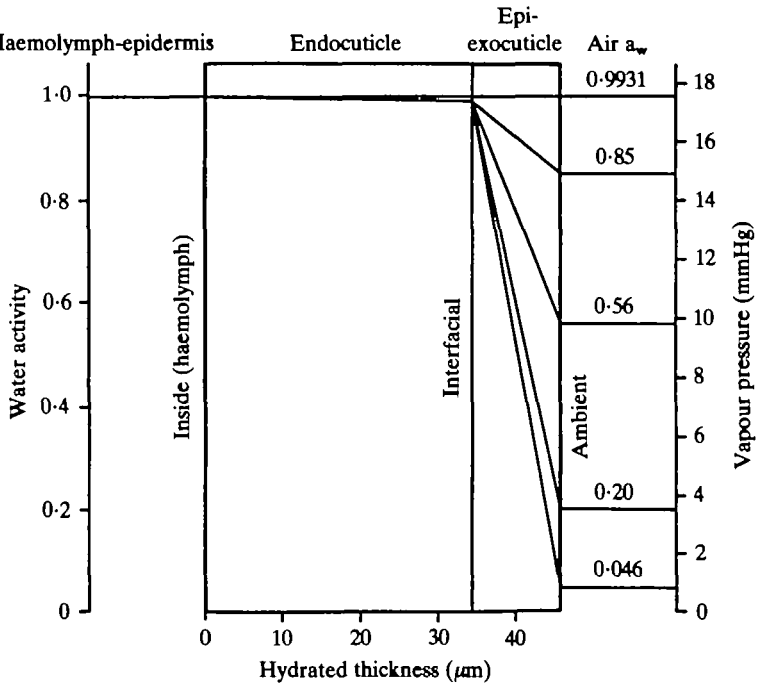

Fig. 2. Diagram showing steady state, *in vitro* water activity gradients across the cuticle in different ambient activities. The gradients were constructed by drawing straight lines between three fixed activities. Inside and ambient activities were measured and the steady state interfacial value between the two layers compatible with equal fluxes was calculated by progressive approximation.

of the layer in question. The total water held by the cuticle is then obtained by integrating water contents over the activity range existing in each layer.

Component permeabilities

Unfortunately, construction of a model is rather more difficult than the above account suggests because of the complex interdependence of permeability, water

Table 1. *Modelled* in vitro, *steady state permeabilities and interfacial vapour pressures at different ambient activities*

Water activity		Permeabilities ($mg\,h^{-1}\,cm^{-2}\,mm\,Hg^{-1}$)		
Ambient	Interfacial	Endocuticle	Epi-exocuticle	Total
0.85	0.9929	74.283	0.127	0.127
0.56	0.9927	72.692	0.067	0.067
0.20	0.9925	70.771	0.053	0.053
0.046	0.9924	69.873	0.050	0.050

Inside a_w was 0.9931, vapour pressure = 17.427 mmHg.

content and activity gradient in each of the layers (Machin *et al.* 1985). We would expect activity gradients within each of the layers to lead automatically to local differences in water content, and presumably permeability. Steady state conditions of regional equality of water flux would therefore require the activity gradient to be curved not linear. A workable solution to these problems appears to be offered by empirical permeability equations which take no account of the complexities within each layer. To determine how the properties of component layers combine in the intact cuticle, it is first necessary to determine the interfacial activity at the border of the endocuticle and epi-exocuticle so that the gradients across each layer can be determined separately. A calculator programme was used to determine which interfacial activity was compatible with a steady state from a series of approximations starting from any arbitrarily chosen value. The programme then averaged high and low interfacial values progressively until equality between endocuticle and epi-exocuticle water fluxes was reached. Fluxes, calculated from equation 2, were considered equal when they agreed to within 1 %. Under these steady state conditions no further changes to the water content of a layer or its permeability could take place.

The calculations were based upon the following empirical equations relating endocuticle and whole cuticle permeability with the reciprocal of vapour pressure lowering ($vp_s - vp_a$) at different ambient activities, obtained by Machin *et al* (1985):

$$\text{endocuticle } P = -0.892 + \frac{9.424}{vp_s - vp_a} \tag{3}$$

$$\text{epi-exocuticle } P = 0.0355 + \frac{0.263}{vp_s - vp_a}. \tag{4}$$

In vitro interfacial activities and component permeabilities calculated in this way are summarized in Table 1. Note that the very high endocuticle permeabilities are consistent with rapid, short-term evaporative loss in excised samples. In Fig. 2, which illustrates the corresponding linear activity gradients, it can be seen that all activity gradients in the endocuticle which fall within the width of the drawn line, are very close to the Ringer equilibrated ($a_w = 0{\cdot}9931$) line. Since interfacial activities are based directly on empirical results they are known with some certainty.

It is worth noting that the model confirms the traditional arrangement of an external water barrier maintaining the inner endocuticle in a hydrated state (Beament, 1961). Endocuticle hydration exaggerated the permeability difference of the two layers to a factor of between 550 and 1400. Beament (1961) speculated that lipid removal from the cuticle might result in a 100- to 300-fold permeability increase. The higher values for endocuticle are presumably due to corrections for unstirred layers which have not been made previously.

Water contents

Cuticle water contents (per gram dry mass of cuticle or per 0·633 g endocuticle) were calculated from endocuticle gradients alone since no significant difference was found between the water affinities of whole cuticle and of endocuticle (Machin *et al.* 1985). In Fig. 3 the calculated water affinity regression line for the whole cuticle, together with the data on which it was based, has been re-drawn with water activity

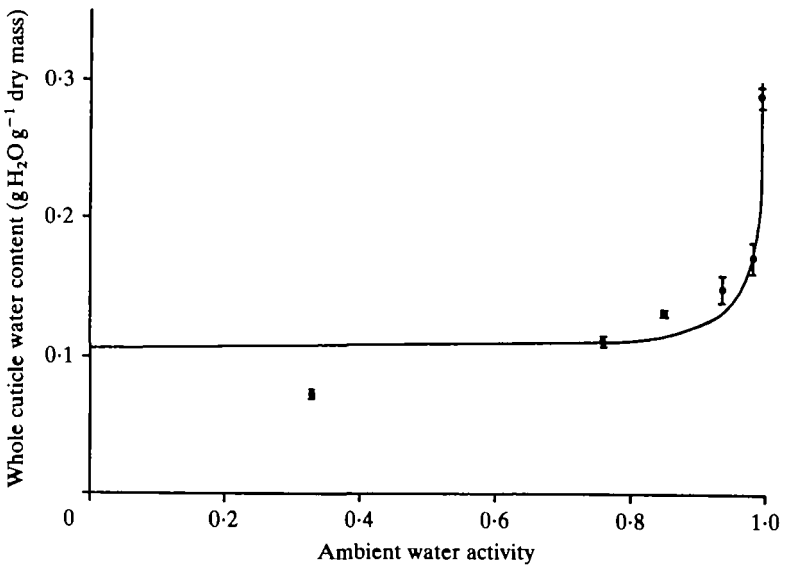

Fig. 3. Graph showing the relationship between whole cuticle water content and ambient water activity for *Periplaneta* pronotum at equilibrium. The line is the best least squares fit to the data of Machin, Lampert & O'Donnell (1985).

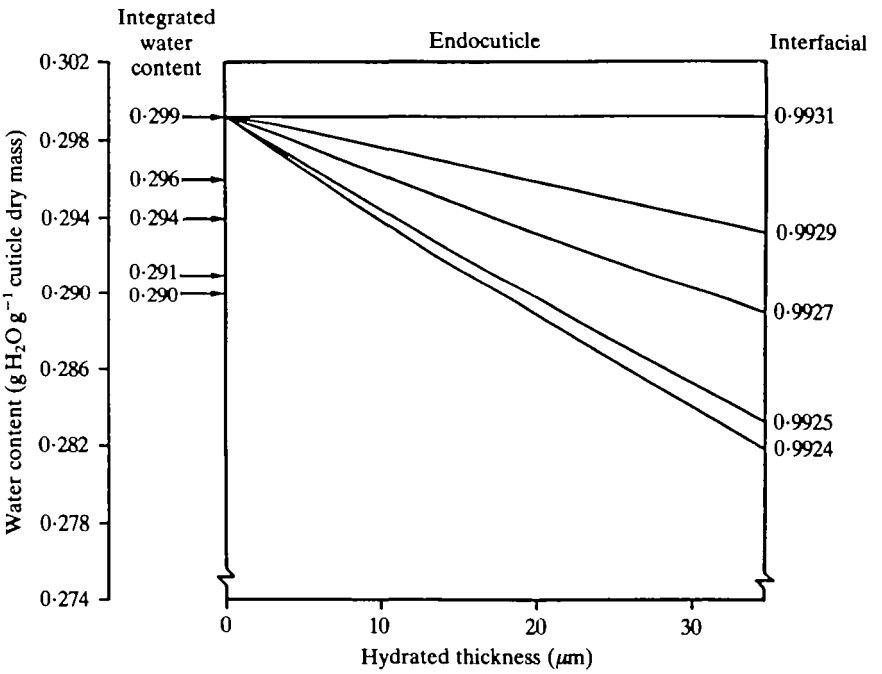

Fig. 4. Diagram demonstrating that endocuticle *in vitro* shows water content deficits even though activity gradients are very slight. The integrated total water contents determined by the model are also indicated on the left.

in place of the reciprocal of vapour pressure lowering on the abscissa. Total cuticle water contents were obtained by integrating the water content over the activity range existing across the endocuticle using the linear form of the water affinity relationship:

$$\text{whole cuticle water content (g g}^{-1}\text{ dry mass)} = 0.106 + \frac{0.0234}{vp_s - vp_a}. \quad (5)$$

When the actual distribution of water across the endocuticle is obtained from activity gradients (Fig. 4) it can be seen that considerable differences occur. The small differences in activity gradient in Fig. 2 are in fact magnified by the steepness of the curve in Fig. 3 for very high activity values close to one. It has been argued above that steady state conditions within the endocuticle require that activity gradients be curved. However calculations show that the curvature may be neglected since predicted water contents fall within 1 % of the straight line values, presumably because endocuticle activity gradients are so slight. Machin *et al.* (1985) have presented evidence for a small, irreversible decrease in cuticle water affinity following initial water content measurement. Since the discrepancy in cuticular water content extends to samples equilibrated at haemolymph activities, *in vivo* water contents can be modelled by assuming that the same general *in vitro* form of the water affinity relationship applies, except that the *in vivo* slope is slightly greater. Modelled cuticular water contents are compared with observed values in Table 2. Data of Machin *et al.* (1985) were measured at 20 °C with a haemolymph or Ringer

Table 2. *Comparison of observed and modelled cuticular water contents under gradient conditions*

Ambient a_w	*N*	Cuticle water contents ($g H_2O g^{-1}$ dry mass) Observed ± S.E.	Modelled
Machin, Lampert & O'Donnell (1985)			
In vitro			
0.9931 (Ringer)	16	0.299 ± 0.006	[0.299]
0.85	18	0.307 ± 0.008	0.296
0.56	17	0.295 ± 0.012	0.294
0.20	18	0.243 ± 0.006	0.291
0.046	18	0.220 ± 0.008	0.290
In vivo			
0.9931 (haemolymph)	16	0.366 ± 0.009	[0.366]
0.85	18	0.357 ± 0.011	0.362
0.56	17	0.357 ± 0.014	0.359
0.20	18	0.286 ± 0.006	0.356
0.046	18	0.281 ± 0.012	0.354
Winston & Beament (1969)			
In vivo			
1.00	14	0.299 ± 0.090	0.330
0.85	28	0.251 ± 0.028	0.326
0.75	20	0.351 ± 0.028	0.325
0.42	5	0.330 ± 0.021	0.321
0.01	24	0.299 ± 0.043	0.317

Values in square brackets are equilibrated values on which the model values are based.

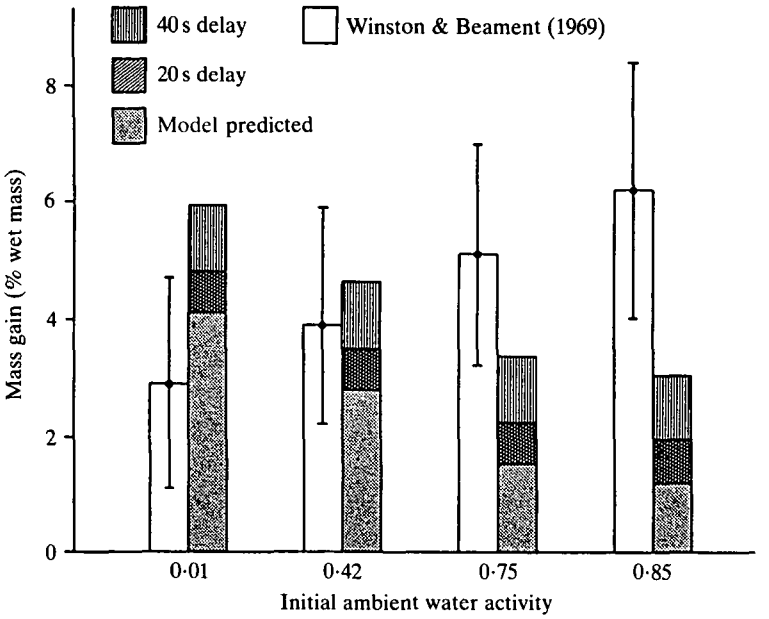

Fig. 5. Histograms comparing mean pronotal mass gains (± S.E.) following exposure to haemolymph water activities observed by Winston & Beament (1969) and those attributed by the present study to modelled cuticle activity gradients and evaporation errors. Cuticles were initially under gradient conditions with different ambient activities as indicated.

activity of 0·9931 (383 mosmol l^{-1}) while Winston & Beament (1969) made their determinations at 25 °C with activities of 0·9941 (328 mosmol l^{-1}). Model calculations adjust for the different activities but are based on permeabilities and water affinities measured at 20 °C. It can be seen that the agreement between observed and modelled water contents is good at high ambient activities and poor at activities below 0·20. The fit with Winston & Beament's (1969) values is good.

DISCUSSION

We interpret the results of modelling as evidence that cuticle water contents can be largely accounted for by purely passive mechanisms. This conclusion is based on the prediction by the model of the significant drop in cuticle water contents in ambient activities below that of the haemolymph. Since modelled water contents all show a decline with decreasing ambient activity from maximum values equilibrated to Ringer or haemolymph, it is reasonable to conclude that the occasional departure from this trend in observed values is due to measuring error.

The model has been shown to overestimate water contents at low ambient activities both *in vivo* and *in vitro*. It is important to point out, however, that this cannont be attributed to the poor fit of the water content equation at low activity because modelled values are based entirely on the narrow range of extremely high activities characteristic of the endocuticle. Over this range the fit of the equation to the observed

points is very good. Nevertheless, despite deficiencies in the model at low ambient activity, modelled water contents still appear to account for most of Winston & Beament's (1969) observations by passive mechanisms. Modelled water contents can therefore be used to simulate their mass measurement experiment following re-exposure of cuticle samples to water activities equivalent to the haemolymph. Modelled mass gains, expressed in their paper as a percentage of wet mass, were calculated by assuming that the cuticle in different gradient conditions would regain the water contents observed when equilibrated over Ringer. Water absorption would be further increased if cuticle samples had been previously subjected to significant evaporation. The estimated range of these errors has also been included in Fig. 5. The histograms show there is a considerable degree of correspondence between the percentage mass gains observed by Winston & Beament (1969) and those derived from modelled values plus estimated evaporation errors. Mass gains based on observed *in vivo* and *in vitro* values of Machin *et al.* (1985) and corresponding modelled values show essentially the same results. A discrepancy does however exist between the 0·85 activity values. The trend of the modelled values and those observed by Riddle (1981) is opposite to those of Winston & Beament (1969). Their large overlapping standard errors suggest that their differences may not be significant.

Thus it can be concluded that cuticular mass gains over Ringer can largely be attributed to the effects of passively generated activity gradients in the cuticle together with evaporation errors. We suggest Winston & Beament may have been deceived by the relative insensitivity of water content to ambient activity because their values were expressed as a percentage of water mass. In addition, without investigating the actual form of the water affinity relationship, they automatically assumed that small differences in vapour pressure would lead to small differences in water content in the hydrated endocuticle. Quite to the contrary, the non-linear nature of water affinity demonstrates that water content is very sensitive to small vapour pressure differences particularly at the high activities, close to one, found in the endocuticle. It follows, therefore, that significant water activity deficits should be expected whenever the ambient activity falls below the haemolymph level, even when only passive forces are in operation.

We thank M. J. O'Donnell for helpful discussions at various stages of this work. This study was financially supported by the Natural Sciences and Engineering Research Council, Canada Operating Grant A1717, which is gratefully acknowledged.

REFERENCES

Beament, J. W. L. (1961). The water relations of insect cuticle. *Physiol. Rev.* **36**, 281–320.

Machin, J., Lampert, G. J. & O'Donnell, M. J. (1985). Component permeabilities and water contents in *Periplaneta* integument: role of the epidermis re-examined. *J. exp. Biol.* **117**, 155–169.

Riddle, W. A. (1981). Cuticle water affinity and water content of beetles and scorpions from xeric and mesic habitats. *Comp. Biochem. Physiol.* **68**A, 231–235.

Winston, P. W. & Beament, J. W. L. (1969). An active reduction of water level in insect cuticle. *J. exp. Biol.* **50**, 541–546.

Table 1. *Regression analyses of the allometric relationships* ($Y=\alpha W^{\beta}$) *of the gill dimensions* (Y) *to body mass* (W)

Y	Range of body mass (g)	*N*	α	β ($\bar{X} \pm$ S.E.)	*r*
Gill area (mm^2)	0·0016–0·0028	5	$6{\cdot}74 \times 10^{17}$	7·066 ±0·934	0·975
	0·0028–0·33	11	1334	1·222 ±0·055	0·991
	0·33–2250	9	846	0·794 ±0·025	0.997
Total filament number	0·0016–6·5	18	635	0·259 ±0·0099	0·988
	6·5–2250	6	823	0·130 ±0·016	0·970
Total filament length (*L*, mm)	0·0016–0·33	15	835	0·740 ±0·021	0·995
	0·33–2250	9	719	0·508 ±0·017	0·996
Spacing of the secondary lamellae ($1/d'$, mm^{-1})	0·0016–0·0028	5	$1{\cdot}32 \times 10^{11}$	3·880 ±0·417	0·983
	0·0028–0·33	11	40·3	0·111 ±0·023	0·846
	0·33–2250	9	32·2	−0·0787 ±0·0039	−0·991
Average bilateral area of the secondary lamellae (*bl*, mm^2)	0·0016–0·0028	5	1053	2·267 ±0·515	0·931
	0·0028–2250	19	$1{\cdot}85 \times 10^{-2}$	0·366 ±0·012	0·991

stage, the 2nd phase to the postlarval stage, and the 3rd phase to the juvenile and later stages.

These transitions in the allometric relationships of gill area to body mass were closely correlated with changes following body mass increase in the total filament

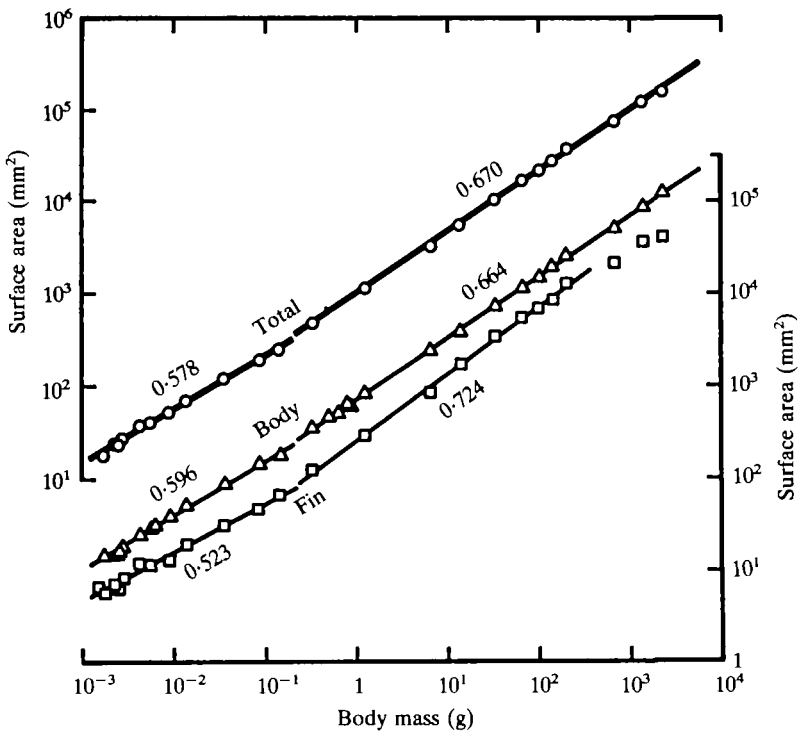

Fig. 4 Allometric relationships of body surface area (△), bilateral fin area (□) and the total surface area (○) to body mass. The total surface area means the sum of the body surface area and the bilateral fin area. Figures by the regression lines indicate the slopes of the lines.

Table 2. *Regression analyses of the allometric relationships* ($Y = \alpha W^{\beta}$) *of body surface, fin areas or total surface areas* (Y) *to body mass* (W)

Y	Range of body mass (g)	N	α	β ($\bar{X} \pm$ S.E.)	r
Body surface area (mm^2)	0·0018–0·14	12	616	0·596 ± 0·0077	0·999
	0·33–2250	16	719	0·664 ± 0·0032	0·9998
Bilateral fin area (mm^2)	0·0016–0·14	12	176	0·523 ± 0·0194	0·993
	0·33–200	9	255	0·724 ± 0·0133	0·999
Total surface area (mm^2)	0·0018–0·14	11	794	0·578 ± 0·0086	0·999
	0·33–2250	12	989	0·670 ± 0·0059	0·9996

length, the average spacing of the secondary lamellae on one side of the filaments, and the average area of the secondary lamellae (Fig. 3; Table 1).

Surface area of both body and fins showed diphasic negative allometry corresponding to the larval stage and the juvenile and later stages (Fig. 4; Table 2). Slopes for both body surface and fin areas in the larval stage were significantly smaller than 2/3 ($P < 0{\cdot}001$), while the slopes in the juvenile and later stages were nearly 2/3 for body surface area and larger than 2/3 for fin area ($P < 0{\cdot}01$).

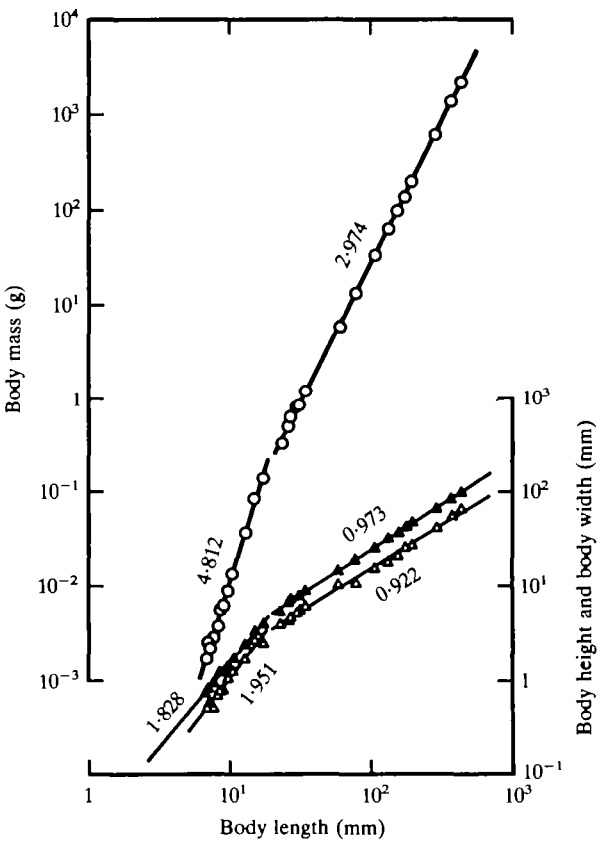

Fig. 5. Allometric relationships of body mass (○), the mean body height (▲) and the mean body width (△) to body length. Figures by the regression lines indicate the slopes of the lines.

Table 3. *Regression analyses of the allometric relationships* ($Y=\alpha L^{\beta}$) *of body mass, mean body height and mean body width* (Y) *to body length* (L)

Y	Range of body length (mm)	*N*	α	β ($\bar{X} \pm$ S.E.)	*r*
Body mass (g)	6·93–17·2	12	$1{\cdot}70 \times 10^{-7}$	$4{\cdot}812 \pm 0{\cdot}100$	0·998
	23·0–430	16	$3{\cdot}18 \times 10^{-5}$	$2{\cdot}974 \pm 0{\cdot}016$	0·9998
Mean body height (mm)	6·93–17·2	12	$2{\cdot}24 \times 10^{-2}$	$1{\cdot}828 \pm 0{\cdot}053$	0·996
	23·0–430	16	$2{\cdot}69 \times 10^{-1}$	$0{\cdot}973 \pm 0{\cdot}0093$	0·999
Mean body width (mm)	6·93–17·2	12	$1{\cdot}16 \times 10^{-2}$	$1{\cdot}951 \pm 0{\cdot}122$	0·981
	23·0–430	16	$2{\cdot}15 \times 10^{-1}$	$0{\cdot}922 \pm 0{\cdot}021$	0·996

The transition in the allometric relationships of body surface area to body mass was accompanied by a change in body form (Fig. 5). The results of regression analyses of the allometric relationships showing the body form are shown in Table 3. Body mass, mean body height and mean body width showed diphasic allometry, with an inflexion point at about 18 mm for body length and about 0·2 g for body mass. The slope in the 2nd phase was almost 3 for body mass and almost 1 for body height and body width, while the slopes in the 1st phase were much larger ($P < 0{\cdot}001$).

DISCUSSION

The morphometric results (Fig. 5; Table 3) indicate that the body form of the carp changes remarkably in the larval stage, but then changes little in the juvenile and later stages. The morphometry of the gills also showed the most remarkable changes in the early stages (Figs 2, 3). These observations are consistent with those of De Silva (1974), on herring and plaice, that the slope for the relationship of gill area to body mass and the slopes for the relationships of the total filament length, the lamellar spacing on the filaments, and the average area of the secondary lamellae to body mass are steeper before metamorphosis than after it. The observations are also consistent with those of McDonald & McMahon (1977), on Arctic char, that the gill area, the total number and the average area of the secondary lamellae, and the total filament number rapidly increase during the stages of 2–47 days old (0·067–0·099 g). The relationship of the total filament number to body mass is described as diphasic allometry in the present paper, but the rate of increase in filament number in the 2nd phase seems not to be constant but to diminish gradually, as described by Price (1931) in the small-mouthed black bass.

The gill area of the carp showed diphasic positive allometry with slopes of 7·066 and 1·222 during the larval stage (0·0016–0·33 g) and monophasic negative allometry with a slope of 0·794 during the juvenile and later stages (0·33–2250 g). Price (1931) described monophasic negative allometry with a slope of 0·785 in the gill area of small-mouthed black bass of 0·33–840 g. The slopes in fish larger than 0·33 g are almost the same in both species. The positive allometry with steep slopes during the larval stage of the carp means that the gill area per unit body mass is very small in the early larval stage and rapidly increases during the larval stage. The gill area per unit body mass calculated on the basis of the allometric equations (Table 1) is 7·4 $mm^2 g^{-1}$ at a body

mass of 0·0016 g, and increases to 370 $mm^2 g^{-1}$ at 0·003 g and 1100 $mm^2 g^{-1}$ at 0·35 g, and then decreases to 180 $mm^2 g^{-1}$ at 2000 g. The areas per unit body mass of the total surface (body surface and fin surface) are calculated from data in Table 2 to be 12 000, 9200, 1400 and 81 $mm^2 g^{-1}$ at the corresponding body masses of 0·0016, 0·003, 0·35 and 2000 g, respectively. We therefore consider that cutaneous respiration through the body and fin surfaces plays an important role during the early stages in the life history of fish. During the larval stage in the carp, the duct of Cuvier on the enlarged anterior part of the yolk and dense nets of vessels in the dorsal finfold have been considered to be important sites of gas exchange (Balon, 1975). In the prelarval stage, the yolk gradually diminishes in size as it is absorbed by the larva. At the same time, the gill area rapidly increases compensating for the loss of respiratory vessels in the yolk. In the postlarval stage, the relative importance of cutaneous respiration continues to decrease gradually, but at a slower rate than in the prelarval stage. In contrast, the relative importance of gill respiration increases with growth. For the body surface and fin areas, the slopes in the larval stage were smaller than 2/3. This means that smaller fish have larger mass-specific areas of body surface and fins which compensate for the smaller gill area in the earlier stage. The absence of scales during the larval stage probably facilitates gas exchange through the body surface. These features are consistent with the often emphasised phenomenon that the cutaneous gas exchange is relatively more important during the earlier stages in the life history of fish than in the later stages (Fry, 1957; Blaxter, 1969; De Silva, 1974; Balon, 1975; Iwai & Hughes, 1977; McDonald & McMahon, 1977; McElman & Balon, 1980).

Comparison of the results of morphometric study on carp gills by the present authors with those by Saunders (1962) and Hughes & Morgan (1973) is given, for fish of the same size, in Table 4. Although the values for lamellar spacing are not very different, the filament number is smaller, and both the lamellar number and the gill area are larger in the present study than in that of Saunders (1962) or Hughes & Morgan (1973), for fish of 184 g, 531 g or 878 g. The differences in the filament and lamellar numbers are probably caused by the different populations and the different rearing conditions, since they are gill dimensions that can be measured relatively accurately. The difference in the gill area is probably caused by the different populations and/or different technical procedures. If the gill areas of fish of 184 g, 531 g and 878 g in the present study are calculated ignoring the shrinkage coefficient (5·7 %) and the error in the triangle method (23 % for fish of 184 g, 20 % for one of 531 g and 19 % for one of 878 g estimated by the equation $bl/bl' = 1{\cdot}48W^{-0{\cdot}026}$), the values of the gill area become 210, 175 and 160 $mm^2 g^{-1}$, respectively, which are closer to the values obtained by Saunders (1962) and Hughes & Morgan (1973) than to our values in the present study.

In many species of fish, resting metabolism has been considered to be proportional to about the 0·85 power of body mass (Ricker, 1973; Brett & Groves, 1979). In carp, the exponent has been reported to be 0·84 in fish of 0·0032–3500 g (Winberg, 1956). We obtained a very similar figure, 0·832, in carp of 0·0019–620 g (Y. Itazawa & S. Oikawa, in preparation). On the other hand, the present study showed that the gill area was proportional to the 7·066, 1·222 or 0·794 power of body mass depending on the developmental stages, while the total surface area was proportional to the 0·578 or 0·670 power of body mass. The slopes for the surface areas are significantly

Table 4. *Comparison of the gill dimensions of carp in the present study and in previous reports*

Body mass (g)	Total no. of filaments	Secondary lamellae mm^{-1} filament of one side	Total no. of secondary lamellae	Average area of secondary lamellae (mm^2)	Gill area ($mm^2 g^{-1}$)	Reference
19	–	20·8	168 000	0·060†	526	Saunders (1962)
	1207	25·5	164 000	0·054	461	Present study
184	–	20·7	348 000	0·076†	145	Saunders (1962)
	1621	21·4	434 000	0·125	289	Present study
531	2567	20·0	491 000*	0·150†	139	Hughes & Morgan (1973)
	1861	19·7	685 000	0·184	232	Present study
878	–	17·9	634 000	0·189†	137	Saunders (1962)
	1986	18·9	850 000	0·221	209	Present study

* Arithmetic mean of 348 000 and 634 000, figures in Saunders (1962).
† Calculated by substituting figures in the original papers for the terms of the formula, gill area ($mm^2 g^{-1}$) × body mass (g)/total number of secondary lamellae.

different from the slope for metabolism-body mass relationship ($P < 0{\cdot}01$), except for the 3rd phase of gill area. We consider, therefore, that neither gill nor body surface areas directly regulate the resting rate of metabolism of the fish, in the larval stage at least.

The similarity of the slope for the gill area-body mass relationship during the juvenile and later stages to the slope for the resting metabolism-body mass relationship suggests that the mass-specific metabolic rate in these stages may be dependent on gill area. However, if other factors constrain the slope for the metabolic rate, in relation to body mass, to be approximately 0·85 throughout the whole range of body mass, this will give a better interpretation of the decline in mass-specific metabolic rate of the animal. We have previously (Itazawa & Oikawa, 1983) proposed that 'the decline in weight-specific rate of basal metabolism of an intact animal with increasing body size could be explained, partly at least, if tissues with low metabolic rates (Q_{O_2}) get larger with growth in weight in proportion to the whole body'. This hypothesis is now being examined, based on the Q_{O_2} values of various tissues (Oikawa & Itazawa, 1984*a*) and the relative growth of the tissues (Oikawa & Itazawa, 1984*b*) using carp of a wide range in body mass.

The gill area is considered to be concerned with the active metabolism rather than the resting metabolism. It has been reported in various animals that the slope for the active metabolism-body mass relationship is steeper than that for the resting metabolism-body mass relationship, and therefore larger animals have larger scope for activity (Brett, 1965, 1972; Hughes, Gaymer, Moore & Woakes, 1971; Brett & Glass, 1973; Hughes, 1984*a*). In sockeye salmon, the active metabolism has been reported to be proportional to the 0·97 power of body mass, while the resting metabolism is proportional to the 0·78 power of body mass (Brett, 1965). Hughes (1977) indicated that the slope for gill area-body mass relationship was larger than the slope for resting metabolism-body mass relationship, especially in salmon and trout.

The authors wish to thank Dr K. Yamamoto, Shimonoseki University of Fisheries, for providing carp eggs, and the anonymous referee of this paper for invaluable criticism and advice.

REFERENCES

BALKE, E. (1957). Der O_2–Konsum und die Tracheen-Innenfläche bei durch Tracheenkiemen atmenden Insektenlarven in Abhängigkeit von der Körpergrösse. *Z. vergl. Physiol.* **40**, 415–439.

BALON, E. K. (1975). Reproductive guilds of fishes: a proposal and definition. *J. Fish. Res. Bd Can.* **32**, 821–864.

BLAXTER, J. H. S. (1969). Development: eggs and larvae. In *Fish Physiology*, Vol. 3, (eds W. S. Hoar & D. J. Randall), pp. 177–252. New York: Academic Press.

BRETT, J. R. (1965). The relation of size to rate of oxygen consumption and sustained swimming speed of sockeye salmon (*Oncorhynchus nerka*). *J. Fish. Res. Bd Can.* **22**, 1491–1501.

BRETT, J. R. (1972). The metabolic demand for oxygen in fish, particularly salmonids, and a comparison with other vertebrates. *Respir. Physiol.* **14**, 151–170.

BRETT, J. R. & GLASS, N. R. (1973). Metabolic rates and critical swimming speeds of sockeye salmon (*Oncorhynchus nerka*) in relation to size and temperature. *J. Fish. Res. Bd Can.* **30**, 379–387.

BRETT, J. R. & GROVES, T. D. D. (1979). Physiological energetics. In *Fish Physiology*, Vol. 8, (eds W. S. Hoar, D. J. Randall & J. R. Brett), pp. 279–352. New York: Academic Press.

BYCZKOWSKA-SMYK, W. (1961). Development of the respiratory surface in the gills of the rainbow-trout (*Salmo irideus* Gibb.). *Acta Biol. Cracov., Ser. Zool.* **4**, 89–109.

DE SILVA, C. (1974). Development of the respiratory system in herring and plaice larvae. In *The Early Life History of Fish*, (ed. J. H. S. Blaxter), pp. 465–485. Berlin: Springer-Verlag.

FELDMAN, H. A. & MCMAHON, T. A. (1983). The 3/4 mass exponent for energy metabolism is not a statistical artifact. *Respir. Physiol.* **52**, 149–163.

FRY, F. E. J. (1957). The aquatic respiration of fish. In *The Physiology of Fishes*, Vol. 1, (ed. M. E. Brown), pp. 1–63. New York: Academic Press.

GIRARD, H. & GRIMA, M. (1980). Allometric relation between blood oxygen uptake and body mass in birds. *Comp. Biochem. Physiol.* **66**A, 485–491.

HAKIM, A., MUNSHI, J. S. D. & HUGHES, G. M. (1978). Morphometrics of the respiratory organs of the Indian green snake-headed fish, *Channa punctata*. *J. Zool., Lond.* **184**, 519–543.

HEMMINGSEN, A. M. (1960). Energy metabolism as related to body size and respiratory surfaces, and its evolution. *Rep. Steno meml Hosp.* **9**, 3–110.

HEUSNER, A. A. (1982). Energy metabolism and body size. I. Is the 0·75 mass exponent of Kleiber's equation a statistical artifact? *Respir. Physiol.* **48**, 1–12.

HOLETON, G. F. (1976). Respiratory morphometrics of white and red blooded antarctic fish. *Comp. Biochem. Physiol.* **54**A, 215–220.

HUGHES, G. M. (1966). The dimensions of fish gills in relation to their function. *J. exp. Biol.* **45**, 177–195.

HUGHES, G. M. (1970). Morphological measurements on the gills of fishes in relation to their respiratory function. *Folia morph., Praha* **18**, 78–95.

HUGHES, G. M. (1977). Dimensions and the respiration of lower vertebrates. In *Scale Effects in Animal Locomotion*, (ed. T. J. Pedley), pp. 57–81. New York: Academic Press.

HUGHES, G. M. (1978). On the respiration of *Torpedo marmorata*. *J. exp. Biol.* **73**, 85–105.

HUGHES, G. M. (1984*a*). Scaling of respiratory areas in relation to oxygen consumption of vertebrates. *Experientia* **40**, 519–524.

HUGHES, G. M. (1984*b*). Measurement of gill area in fishes: practices and problems. *J. mar. biol. Ass. U.K.* **64**, 637–655.

HUGHES, G. M., DUBE, S. C. & MUNSHI, J. S. D. (1973). Surface area of the respiratory organs of the climbing perch, *Anabas testudineus* (Pisces: Anabantidae). *J. Zool., Lond.* **170**, 227–243.

HUGHES, G. M., GAYMER, R., MOORE, M. & WOAKES, A. J. (1971). Respiratory exchange and body size in the Aldabra giant tortoise. *J. exp. Biol.* **55**, 651–665.

HUGHES, G. M. & MORGAN, M. (1973). The structure of fish gills in relation to their respiratory function. *Biol. Rev.* **48**, 419–475.

HUGHES, G. M., SINGH, B. R., GUHA, G., DUBE, S. C. & MUNSHI, J. S. D. (1974). Respiratory surface areas of an air-breathing siluroid fish *Saccobranchus* (=*Heteropneustes*) *fossilis* in relation to body size. *J. Zool., Lond.* **172**, 215–232.

ITAZAWA, Y. & OIKAWA, S. (1983). Metabolic rates in excised tissues of carp. *Experientia* **39**, 160–161.

IWAI, T. & HUGHES, G. M. (1977). Preliminary morphometric study on gill development in black sea bream (*Acanthopagrus schlegeli*). *Bull. Jap. Soc. scient. Fish.* **43**, 929–934.

KLEIBER, M. (1932). Body size and metabolism. *Hilgardia* **6**, 315–353.

KLEIBER, M. (1961). *The Fire of Life. An Introduction to Animal Energetics*, pp. 177–216. New York: John Wiley & Sons, Inc.

KREBS, H. A. (1950). Body size and tissue respiration. *Biochem. biophys. Acta* **4**, 249–269.

LUDWIG, W. (1956). Betrachtung über den Energiekonsum von Tieren mit Atmungsorganen von zweierlei Typ. *Z. vergl. Physiol.* **39**, 84–88.

MCDONALD, D. G. & MCMAHON, B. R. (1977). Respiratory development in Arctic char *Salvelinus alpinus* under conditions of normoxia and chronic hypoxia. *Can. J. Zool.* **55**, 1461–1467.

MCELMAN, J. F. & BALON, E. K. (1980). Early ontogeny of white sucker, *Catostomus commersoni*, with steps of saltatory development. *Env. Biol. Fish.* **5**, 191–224.

MORGAN, M. (1974*a*). The development of gill arches and gill blood vessels of the rainbow trout, *Salmo gairdneri*. *J. Morph.* **142**, 351–364.

MORGAN, M. (1974*b*). Development of secondary lamellae of the gills of the trout, *Salmo gairdneri* (Richardson). *Cell Tissue Res.* **151**, 509–523.

MUIR, B. S. (1969). Gill dimensions as a function of fish size. *J. Fish. Res. Bd Can.* **26**, 165–170.

MUIR, B. S. & HUGHES, G. M. (1969). Gill dimensions for three species of tunny. *J. exp. Biol.* **51**, 271–285.

OIKAWA, S. & ITAZAWA, Y. (1984*a*). Allometric relationship between tissue respiration and body mass in the carp. *Comp. Biochem. Physiol.* **77**A, 415–418.

OIKAWA, S. & ITAZAWA, Y. (1984*b*). Relative growth of organs and parts of the carp, *Cyprinus carpio*, with special reference to the metabolism-size relationship. *Copeia* **1984**, 800–803.

PALOHEIMO, J. E. & DICKIE, L. M. (1966). Food and growth of fish. II. Effects of food and temperature on the relation between metabolism and body weight. *J. Fish. Res. Bd Can.* **23**, 869–908.

PRICE, J. W. (1931). Growth and gill development in the small-mouthed black bass, *Micropterus dolomieu*, Lacépède. *Contrib. Franz Theodore Stone Lab. Ohio State Univ.* **4**, 1–46.

RICKER, W. E. (1973). Linear regressions in fishery research. *J. Fish. Res. Bd Can.* **30**, 409–434.

RUBNER, M. (1883). Ueber den Einfluss der Körpergrösse auf Stoff- und Kraftwechsel. *Z. Biol.* **19**, 535–562.

SAUNDERS, R. L. (1962). The irrigation of the gills in fishes. II. Efficiency of oxygen uptake in relation to respiratory flow activity and concentrations of oxygen and carbon dioxide. *Can. J. Zool.* **40**, 817–862.

SCHMIDT-NIELSEN, K. (1970). Energy metabolism, body size, and problems of scaling. *Fedn Proc. Fedn Am. Socs exp. Biol.* **29**, 1524–1532.

SUZUKI, N. (1969). Gill structure and its function on gas exchange in fresh water teleosts. *Physiol. Ecol. Japan* **15**, 79–100. (in Japanese).

ULTSCH, G. R. (1973). A theoretical and experimental investigation of the relationships between metabolic rate, body size, and oxygen exchange capacity. *Respir. Physiol.* **18**, 143–160.

ULTSCH, G. R. (1976). Respiratory surface area as a factor controlling the standard rate of O_2 consumption of aquatic salamanders. *Respir. Physiol.* **26**, 357–369.

URSIN, E. (1967). A mathematical model of some aspects of fish growth, respiration, and mortality. *J. Fish. Res. Bd Can.* **24**, 2355–2453.

VON BERTALANFFY, L. (1957). Quantitative laws in metabolism and growth. *Q. Rev. Biol.* **32**, 217–231.

VON BERTALANFFY, L. & PIROZYNSKI, W. J. (1953). Tissue respiration, growth, and basal metabolism. *Biol. Bull. mar. biol. Lab., Woods Hole* **105**, 240–256.

WHITFORD, W. G. & HUTCHISON, V. H. (1967). Body size and metabolic rate in salamanders. *Physiol. Zoöl.* **40**, 127–133.

WIESER, W. (1984). A distinction must be made between the ontogeny and the phylogeny of metabolism in order to understand the mass exponent of energy metabolism. *Respir. Physiol.* **55**, 1–9.

WINBERG, G. G. (1956). Rate of metabolism and food requirements of fishes. *Fish. Res. Bd Can.* (translation series No. 194).

WOLF, K. (1963). Physiological saline for fresh-water teleosts. *Prog. Fish-Cult.* **25**, 135–140.

the known effects of temperature on twitch contraction. Cooling decreases the rate of muscle relaxation and hence each muscle twitch is increased in size and prolonged (Hill, 1951; Wardle, 1980; Montgomery & Macdonald, 1984). The result of these changes is to produce summation at lower frequencies of stimulation, thereby increasing the slope of the stimulus-response curve; i.e. increasing gain at low temperature.

Large muscles have a slower twitch response (Wardle, 1980), which explains why the oculomotor responses of *D. mawsoni* (Fig. 2) exhibit a larger gain than those of the smaller antarctic fish *P. borchgrevinki*.

The large increase in gain observed in the antarctic fish at low temperature is likely to be of biological significance in offsetting reduced rates of CNS output, and lower sensory gain expected at low temperature (Montgomery & Paulin, 1984).

The authors wish to acknowledge grants from the Medical Research Council, the University Grants Committee, and the Auckland University Research Committee. We are grateful to the staff of New Zealand's Scott Base, Antarctica, and to the staff of the Leigh Marine laboratory.

REFERENCES

CARPENTER, R. H. S. (1977). *Movements of the Eyes*. London: Pion.

CLARKE, A. (1983). Life in cold water: the physiological ecology of polar marine ectotherms. *Oceanogr. mar. biol. A. Rev.* **21**, 341–453.

COLLINS, C. C. (1971). Orbital mechanics. In *The Control of Eye Movements*, (eds P. Bach-y-rita, C. C. Collins & J. Hyde), pp. 283–325. New York: Academic Press.

DEVRIES, A. L. (1980). Biological antifreezes and survival in freezing environments. In *Animals and Environmental Fitness*, (ed. R. Giles), pp. 583–607. Oxford, New York: Pergamon Press.

FRIEDLANDER, M. J., KOTCHABHAKDI, N. & PROSSER, C. L. (1976). Effects of cold and heat on behaviour and cerebellar function in goldfish. *J. comp. Physiol.* **112**, 19–45.

GESTRIN, P. & STERLING, P. (1977). Anatomy and physiology of goldfish oculomotor system. II. Firing patterns of neurons in abducens nucleus and surrounding medulla and their relation to eye movements. *J. Neurophysiol.* **40**, 573–588.

HELVERSEN, O. N. & ELSNER, N. (1977). The stridulatory movements of acridid grasshoppers recorded with an opto-electronic device. *J. comp. Physiol.* **122**, 53–64.

HELWIG, J. T. & COUNCIL, K. A. (1979). *The Statistical Analysis System User's Guide*. North Carolina: S.A.S. Institute.

HILL, A. V. (1951). The influence of temperature on the tension developed in an isometric twitch. *Proc. R. Soc. Lond. B* **138**, 349–354.

LITTLEPAGE, J. L. (1965). Oceanographic investigations in McMurdo sound, Antarctica. In *Biology of the Antarctic Seas*, Vol. 2, (ed. G. A. Llano), pp. 1–37. Washington: American Geophysical Union.

MCCARTHY, D. (1982). Temperature effects upon the Parore oculomotor system. MSc thesis, University of Auckland.

MACDONALD, J. A. (1981). Temperature compensation in the peripheral nervous system: antarctic vs. temperate poikilotherms. *J. comp. Physiol.* **142**, 411–418.

MACDONALD, J. A. & MONTGOMERY, J. C. (1982). Thermal limits of neuromuscular function in an antartic fish. *J. comp. Physiol.* **147**, 237–250.

MONTGOMERY, J. C. (1983). Eye movement dynamics in the dogfish. *J. exp. Biol.* **105**, 297–304.

MONTGOMERY, J. C. (1984). Low temperature increases gain in the fish oculomotor system. *J. Neurobiol.* **15**, 295–298.

MONTGOMERY, J. C. & MACDONALD, J. A. (1984). Performance of motor systems in antarctic fish. *J. comp. Physiol.* **154**, 241–248.

MONTGOMERY, J. C., MCVEAN, A. & MCCARTHY, D. (1983). Effects of lowered temperature on spontaneous eye movements in a teleost fish. *Comp. Biochem. Physiol.* **75A**, 363–368.

MONTGOMERY, J. C. & PAULIN, M. G. (1984). The effects of temperature on the characteristics of the dogfish oculomotor system. *J. exp. Biol.* **113**, 101–107.

PROSSER, C. L. & NELSON, D. O. (1981). The role of nervous system in temperature adaptation of poikilotherms. *A. Rev. Physiol.* **43**, 281–300.

ROBINSON, D. A. (1981). The use of control systems analysis in the neurophysiology of eye movements. *A. Rev. Neurosci.* **4**, 463–503.

STERLING, P. (1977). Anatomy and physiology of goldfish oculomotor system. I. Structure of abducens nucleus. *J. Neurophysiol.* **40**, 557–572.

WARDLE, C. S. (1980). Effects of temperature on the maximum swimming speed of fishes. In *Environmental Physiology of Fishes*, (ed. M. A. Ali), pp. 519–531. New York: Plenum Press.

ZUBER, B. L. (1968). Sinusoidal eye movements from brain stem stimulation in the cat. *Vision Res.* **8**, 1073–1079.

J. exp. Biol. 117, 133–154 (1985)
Printed in Great Britain © *The Company of Biologists Limited 1985*

VENTILATION, CIRCULATION AND THEIR INTERACTIONS IN THE LAND CRAB, *CARDISOMA GUANHUMI*

BY WARREN BURGGREN*, ALAN PINDER*, BRIAN McMAHON†, MICHELE WHEATLY†‡ AND MICHAEL DOYLE*

** Department of Zoology, University of Massachusetts, Amherst, MA 01003–0027, U.S.A.* and *† Department of Biology, University of Calgary, Calgary, Alberta T2V 1N4, Canada*

Accepted 10 January 1985

SUMMARY

Physiological variables for ventilation (scaphognathite frequency, branchial chamber pressure and branchial air flow) and for circulation (heart rate, intracardiac and pericardial haemolymph pressure) were measured in the land crab *Cardisoma guanhumi* (Latreille). Crabs were studied both in air alone and in air with access to a shallow layer of fresh, brackish or sea water.

During complete air exposure, forward scaphognathite beating predominated and reversed scaphognathite beating was very infrequent. Periods of apnoea were rare. When crabs were able to immerse the Milne-Edwards openings to the branchial chambers in water, scaphognathite reversal occurred much more frequently, and most air flow through the branchial chambers was generated by this mode of ventilation. Changes in water salinity had no effect on respiratory patterns. The cyclic variation between forward and reversed scaphognathite beating appears to serve not only to ventilate the branchial chambers with air, but also to flush water through the branchial chambers for non-respiratory purposes such as ion, water and acid-base regulation.

Haemolymph pressures were comparatively low (14 mmHg systolic, 6 mmHg diastolic). During diastole a pressure gradient of approximately 0·6 mmHg existed between the pericardial space and the heart lumen. Pauses in heart beat were never observed. Circulatory events were closely co-ordinated with adjustments in ventilation. Reversed scaphognathite beating produced a transient increase in systolic and diastolic haemolymph pressure due to the rise in branchial air pressure acting directly upon the large, haemolymph-filled spaces lining the branchial chambers. A transient bradycardia accompanied this brief rise in central haemolymph pressures. Possible mechanisms for the regulation of haemolymph pressure are discussed.

INTRODUCTION

The study of intertidal and terrestrial decapod Crustacea has burgeoned in recent years, partly because of the search for new insights into the evolution of air breathing,

‡ Present address: Department of Zoology, University of Florida, Gainesville, FL 32611, U.S.A.
Key words: Crab, ventilation, circulation.

and partly because of a specific interest in the adaptations of the land decapods *per se*. Regardless of habitat or degree of terrestrial adaptation, decapods that ventilate with air (i.e. use the paired scaphognathites to generate a flow of air through the branchial chambers) must still keep branchial respiratory structures moistened. Not only are hydrated respiratory membranes a requisite for adequate gas exchange, but in many aquatic and terrestrial decapods alike the gills are also of cardinal importance in hydromineral exchange between haemolymph and water passing through or residing within the branchial chambers (see Mantel & Farmer, 1983).

Water availability is an important limiting factor for terrestrial decapods, and numerous behavioural and morphological adaptations for water acquisition and retention are apparent. For example, many terrestrial brachyurans inhabit burrows, the lower chambers of which lie at or below the water table (Herreid & Gifford, 1963; Cameron, 1975, 1981). Thus, even though the crab may venture short distances from the burrow mouth, significant amounts of time are still spent in the presence of water at the bottom of the burrow. The ability to take a reservoir of water into an arid terrestrial environment is particularly well developed in some terrestrial hermit crabs, where a considerable volume of water may be retained in the inhabited mollusc shell (see DeWilde, 1973; McMahon & Burggren, 1979; Wheatly, Burggren & McMahon, 1984).

A number of studies have concentrated on the respiration and water relations of the land crab *Cardisoma*. Comprehensive accounts of the respiratory morphology of this genus have been provided by von Raben (1934), Gray (1957), Diaz & Rodriguez (1977), Cameron (1981) and Wood & Randall (1981). One noteworthy characteristic of *Cardisoma* is that the gills are quite small, occupying less than one-tenth of the volume of the branchial chamber. Much additional respiratory surface area is provided by extensive folding of the highly vascularized epithelial sheet lining the extensive branchial cavity.

Cardisoma is of considerable interest with respect to acquisition and retention of gill water. This genus not only makes frequent trips to burrows containing at least some water (Herreid & Gifford, 1963; Cameron, 1975, 1981), but also has been reported to retain significant quantities of water in the branchial chamber when active in air (Wood & Randall, 1981). When *Cardisoma* is completely air-exposed, it is not clear whether this branchial water reserve functions primarily as an O_2 source or a CO_2 sink (Wood & Randall, 1981), or whether its major respiratory function is to moisten the gills. Wood & Randall (1981) cut an observation port in the dorsal wall of the branchial chamber of completely air-exposed *Cardisoma carnifex* and observed that the mastigobranchs of the first, second and third maxilliped were in nearly constant motion, flicking water contained in the lower regions of the branchial chamber up over the gills. While this water was probably well aerated by this motion, forward scaphognathite beating simultaneously drew large volumes of air into the Milne-Edwards openings and expelled it out of the exhalant canals. Long periods of apnoea occurred and reversed scaphognathite beating was never observed. Similar observations of forward scaphognathite beating generating a large air flow, with very infrequent reversed beating, have also been previously reported for completely air-exposed *Cardisoma guanhumi* (Cameron, 1975; Herreid, O'Mahoney & Shah, 1979*b*; Herreid, Lee & Shah, 1979*a*).

Terrestrial migrations involving large numbers of *Cardisoma guanhumi* occur during seasonal transitions. Moreover, these crabs are frequently observed in areas with relatively dry surface soil. Thus, physiological studies of *Cardisoma* when completely air exposed, such as those mentioned above are, of course, of considerable interest and value. Unfortunately, such observations may have biased experimentation away from crabs in the natural amphibious setting. *Cardisoma guanhumi* spends considerable amounts of time in wet lowlands, and burrows excavated even in apparently dry areas often contain ground water at their deepest levels. With the progression of the dry season *Cardisoma* is rarely seen on open ground, and may even seal itself in its burrow (Herreid & Gifford, 1963). *Cardisoma* thus spends considerable time in proximity to water, but unfortunately little information exists on the respiratory or cardiovascular physiology of this genus in this normal amphibious state.

In this study on *Cardisoma guanhumi* we test the hypothesis that ventilatory patterns and performance are influenced by the available respiratory media. Additionally, we assess the extent of cardio-respiratory interactions under a variety of experimental conditions and measure basic cardiac variables to determine if the circulatory haemodynamics of land crabs differ from those of aquatic decapods.

MATERIALS AND METHODS

Experiments were performed on a total of 45 *Cardisoma guanhumi* (Latreille) (mean weight 127 ± 45 g, $\bar{x} \pm 1$ S.D.) captured on the Atlantic coast of Panama, and transported to and maintained at the Naos Marine Laboratory, Smithsonian Tropical Research Institute, on the Pacific coast of Panama. Crabs were maintained in shaded outdoor pens and experienced the normal temperature and humidity regime for the season (night temperature 25–26 °C, night humidity 75–95 %; day temperature 33–35 °C, day humidity 75–95 %). During this pre-experimental period all crabs had free access to 50 % sea water (SW) and were fed vegetable matter daily.

The experimental chamber consisted of an opaque box approximately 40 × 20 × 15 cm. The chamber, which was thermostatted to 30± 3 °C, was covered with a translucent lid to screen movements of the investigators. In some experiments, crabs were placed unrestrained in this box. In other experiments, crabs were partially restrained by using elastic bands to secure their legs and chelae to a 15 × 15 × 1 cm ceramic plate. Although restrained, such crabs could raise the carapace slightly above the plate and rotate the carapace dorso-ventrally. The restrained animal on the plate was then placed in the centre of the chamber described above. When a 2-cm water layer was placed in the chamber, voluntary rotational movements of the carapace allowed the crab either to immerse the openings to the branchial chambers at the bases of the legs, or raise these openings slightly above the water level (see below).

Ventilatory variables

Standard cannulation and measurement techniques for ventilatory pressures and impedance were employed (see Taylor, Butler & Sherlock, 1973; McDonald, McMahon & Wood, 1977). All pressure cannulae were 40-cm lengths of seawater-filled PE 160 tubing attached to Narco P–1000B pressure transducers, whose signals were displayed on a Narco MKIV rectilinear chart recorder. Each transducer was

J. exp. Biol 117, 87–110 (1985)
Printed in Great Britain © *The Company of Biologists Limited 1985*

THE ULTRASTRUCTURE OF THE EPICUTICULAR INTERFERENCE REFLECTORS OF TIGER BEETLES (*CICINDELA*)

BY T. D. SCHULTZ AND M. A. RANKIN
Department of Zoology, University of Texas, Austin, Texas 78712, U.S.A.

Accepted 4 December 1984

SUMMARY

Tiger beetles of the genus *Cicindela* exhibit iridescent structural coloration due to the presence of a non-ideal multilayer interference reflector located in the outermost 2 μm of the integument. The reflector is composed of alternating layers of electron-lucent and electron-dense material. This series of layers was distinguished from chitinous procuticle by its position, ultrastructure and solubility in dilute KOH. The reflector appears homologous with the inner epicuticle of current models. Measurements of surface reflectance, refractive index and the dimensions of the alternating layers suggests that the dense layer has a refractive index (RI) near 2·0 and may be a melanoprotein.

INTRODUCTION

The widespread occurrence of structural coloration in insect cuticle received vigorous attention in the early part of this century (Biederman, 1914; Onslow, 1920; Mason, 1927). These researchers ascribed the physical colours of the integument to the constructive interference of light reflected from thin layers within the exoskeleton. However, the exact anatomy of the reflector remained obscure, and proposals of morphologies varied widely. The advent of the electron microscope finally allowed ultrastructural studies of cuticular reflectors. The bulk of this work focused on interference reflectance by specialized structures such as insect cornea and lepidopteran wing scales (Bernard & Miller, 1968; Ghiradella *et al.* 1972). However, the most complete study of interference reflectance by whole cuticle was Neville & Caveney's (1969) work on scarab beetles. While that work elegantly described the exocuticular reflectors within that family, the morphologies of cuticular reflectors in other metallic-coloured insects have remained undescribed.

Coincidental with the early work on insect coloration, several authors described the elytral structure of several groups of beetles which exhibit interference reflectance (Buprestidae; Hass, 1916; Cicindelidae: Stegemann, 1930; Carabidae: Sprung, 1931). Stegemann (1930) described a superficial layer, the 'Sekretschicht', in tiger beetles (Cicindelidae) which dissolves in dilute KOH at 60 °C and pours from secretory glands after ecdysis. Mandl (1931) later ascribed the iridescence of *Cicindela* to

Key words: Interference colour, epicuticle, *Cicindela*.

this 'Sekretschicht'. Shelford (1917) independently suggested that a surface film reflects interference colours in *Cicindela*.

Many of the elytral structures described by early histological and morphological studies have not been re-examined rigorously under current concepts of cuticle structure. However, homologies have been proposed for these structures based upon more recent research involving other cuticles. Wigglesworth (1972) suggested that the 'Sekretschicht' may be analogous to the cement layer of other insects. Richards (1951) preferred the term 'tectocuticle' for this outermost layer presumed to be secreted by the dermal glands. A recent electron microscope study by Mossakowski (1980) identified an interference reflector in the outermost layers of cuticle in *Cicindela campestris*. He identified the reflective cuticle as exocuticle.

The following study attempts to locate the multilayer reflective system of cicindelid cuticle, to describe its ultrastructure, and to determine to what extent this cuticle conforms to the current models of insect morphology.

MATERIALS AND METHODS

Reflection from elytral surfaces was measured using a Cary 17D spectrophotometer. Elytra for reflectance measurements were taken from four species of tiger beetles, *Cicindela formosa* Say, *C. splendida* Hentz, *C. scutellaris rugata* Dejean and *C. repanda* Dejean. Adults of all four species were collected at Bastrop State Park, Bastrop County, Texas.

Samples of adult cuticle were cut or torn from the elytra and thoraces, and subjected to a variety of chemical treatments. They were then prepared for either scanning or transmission electron microscopy.

Chemical treatments of cuticle

In order to differentiate the epicuticle from the exocuticle, fragments of cuticle were immersed in 8 % KOH at 60 °C for periods of 4, 9, 12, 24, 48 h and 6 days. One set of samples was treated with concentrated KOH for 15 min at 160 °C. A second set was treated similarly, but followed with a 17-h immersion in 8 % KOH. Treatment with hot concentrated alkali is the initial step in the chitosan method of Campbell (1929) for detection of chitinous cuticle. All samples were rinsed with distilled water, dried, and any colour or gross textural change observed with a dissecting microscope. The fragments were cut to smaller size and prepared for either scanning or transmission electron microscopy.

In order to remove procuticular layers, elytra were immersed in concentrated H_2SO_4 for 1, 12, 24, 48 and 72 h. The elytra were rinsed with distilled water, dried, and any colour changes noted. The elytral fragments were then prepared for scanning electron microscopy (SEM).

Since H_2O_2 will bleach melanin and alter the interference colours if melanin is one component of the interference reflector, the role of melanin in cicindelid coloration was investigated by treating *C. formosa* and *C. scutellaris* elytral fragments for 6 days with 10 % H_2O_2 at 26 °C. When no colour change was observed, the samples were treated for a seventh day at 60 °C. Samples were dried, observed and prepared for transmission electron microscopy.

Preparation of cuticle for scanning or transmission electron microscopy

Dried strips of treated or untreated cuticle were mounted on edge, sputter-coated with 2·5 nm of gold-palladium, and examined with a Hitachi scanning electron microscope. This orientation provided a view of the torn edge perpendicular to the elytral surface with each cuticle layer exposed in relief.

For transmission electron microscopy, treated and untreated samples of cuticle were cut into extremely fine slivers (0·3 × 1 mm) with a tapering edge. Cuts were positioned between elytral tracheae to avoid trapped air bubbles. The cuticle was fixed in 2·5 % gluteraldehyde and post-fixed in 2 % OsO_4 for 2 h, dehydrated in a standard ethanol and propylene oxide series, and infiltrated in a long series of propylene oxide/Epon-Araldite mixes. Each infiltration step required agitation, and the final two immersions in pure Epon-Araldite were evacuated completely.

Thin sections were cut perpendicular to the elytral surface. Some sections from each treatment group were post-stained for 5 min in 1 % uranyl acetate in 50 % ethanol, followed by 5 min in lead citrate. Portions of the dorsal surface of *C. scutellaris* were also sectioned parallel to the plane of the elytral surface. All sections were examined under a Zeiss 10CA transmission electron miscroscope.

Thin sections of samples from each treatment group were mounted and reserved for interference and polarized light microscopy.

RESULTS

Elytral reflectance

The elytra and thorax of *C. formosa* are deep metallic red with white maculations – peak reflectance occurring at 655 nm, with a secondary peak near 360 nm (Fig. 1A). The Bastrop population of *C. formosa* exhibits the elytral coloration of the race *C. formosa pigmentosignata* Horn. While the maculae of Bastrop individuals are rarely reduced, many individuals exhibit a distal deep purple coloration on the elytron, which is characteristic of *C. formosa pigmentosignata* (Gaumer, 1977). For reflectance measurements and electron microscope studies, elytral fragments were selected from elytral areas which were homogeneously red.

The elytra of *C. splendida* are metallic brick red with a metallic green border. An elytron with the border removed shows maximal reflectance near 635 nm, with a very small secondary peak at 410 nm (Fig. 1B).

C. scutellaris rugata elytra reflect maximally at 499 nm in a relatively narrow band (Fig. 1C). *C. scutellaris* varies greatly in colour among its races, with *rugata* displaying an iridescent blue-green coloration. Both the intensity and the purity of this reflected colour exceed those of *C. formosa* and *C. splendida*.

The brown *C. repanda* elytron has a very different reflectance curve (Fig. 1D). Instead of a sharp peak in the visible wavelengths, the reflectance increases steadily towards the near-infrared.

The colour of tiger beetle elytra, like all interference colours, changes with the angle of viewing. As the angle of reflectance departs from the angle of incidence, the reflected wavelengths become shorter. The elytra of *Cicindela* are alveolate (Fig. 2)

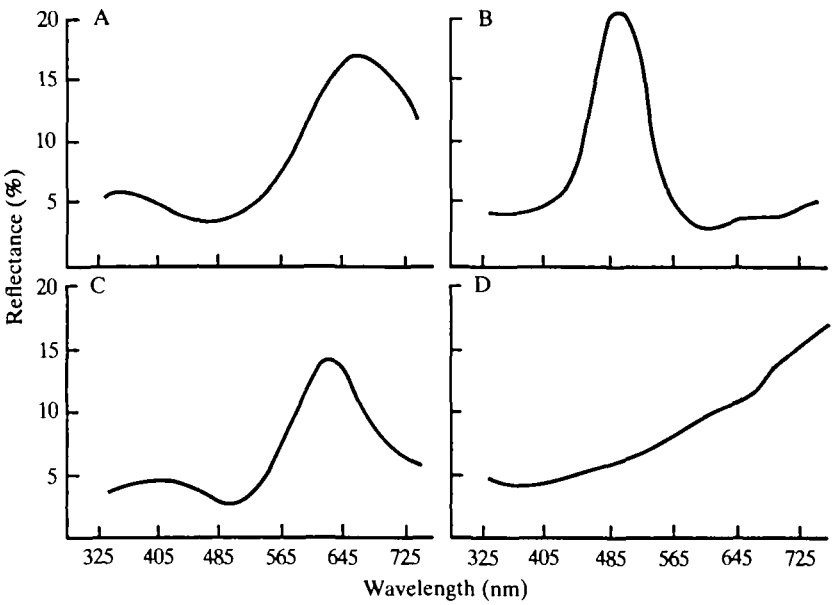

Fig. 1. Reflectance curves of four species of *Cicindela*. (A) *C. formosa pigmentosignata*, (B) *C. scutellaris rugata*, (C) *C. splendida* and (D) *C. repanda*.

with small ($10 \times 10\ \mu m$) hexagonal depressions. The alveoli are superimposed upon larger irregularities in the upper portion of the elytron. Light reflected from this surface is a composite of wavelengths reflected from a variety of angles. Not only would the total intensity of reflection be diminished, but the peak reflectance would be less sharply defined. Of the four species, *C. scutellaris* displays the most regular elytral surface with smooth, shallow alveoli. *C. repanda* and *C. splendida* possess the deepest alveoli and most acute ridges.

Elytral ultrastructure

The general features of elytral structure observed under SEM were consistent in the four species. Above the tracheae, the procuticular layers (region *D* in Fig. 2) are organized in the pseudo-orthogonal 'plywood' fashion that has been described for other Coleoptera (Hepburn, 1972). This region has been defined as endocuticle (Zelazny & Neville, 1972) or as mesocuticle (Hepburn, 1972), and is considered to be untanned or non-sclerotized.

Observed under the SEM, the outermost layer of *Cicindela* cuticle appears as a dense, solid material which bears the alveolate microsculpture of the integument (region *AB* in Fig. 2). This layer ranges in thickness from $3{\cdot}5\ \mu m$ at the bottom of a cell, to $7{\cdot}0\ \mu m$ at the top of an adjacent ridge. The torn vertical face of this layer appears less fibrous and more granular than the underlying cuticle (region *D* in Fig. 2). Occasionally, samples will tear obliquely and reveal two distinct portions of the outer layer in relief (Fig. 3). In these torn samples, a regular banding or lamination of 6–8 extremely even bands (150–200 nm thick) is visible in the outer $1–2\ \mu m$ of the layer (region *A* in Fig. 3B). These laminations appear in contrast to the rougher, non-laminated face of the inner portion (region *B* in Figs 3B and 4). Based upon their

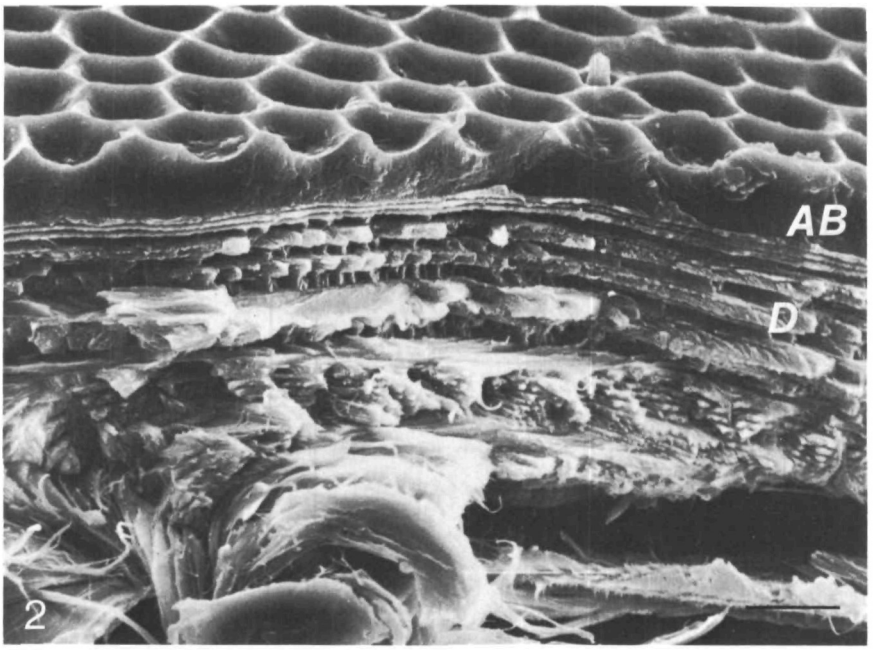

Fig. 2. Scanning electron microscope cross-section of exposed cuticular layers in the upper elytron of *Cicindela splendida*. Region *D* represents the pseudo-orthogonal procuticle. The composite layer *AB* (the presumptive epicuticle and exocuticle) conforms to the alveolate microsculpture of the elytral surface. Scale bar, 10 μm.

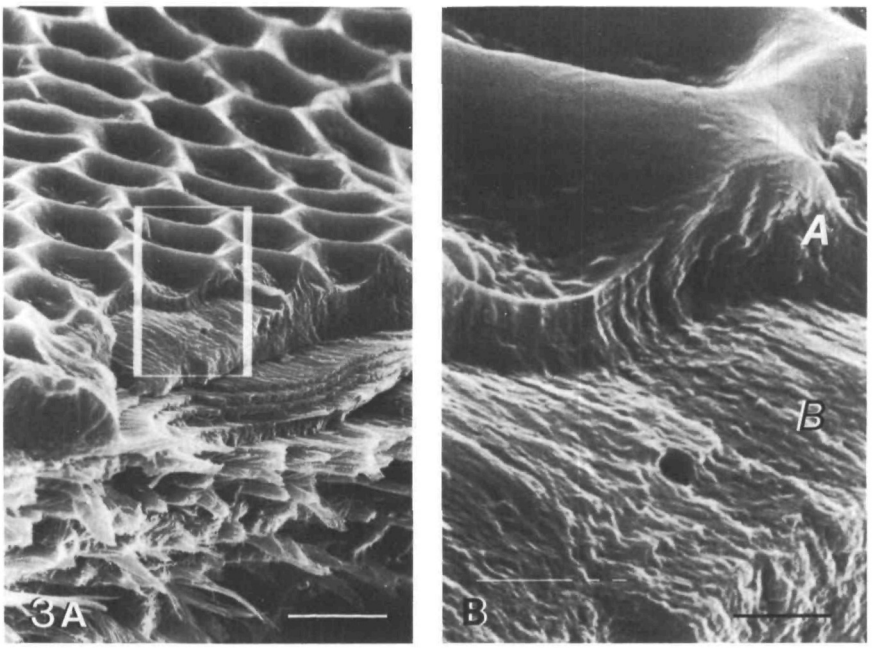

Fig. 3. Layer *A* (presumptive epicuticle) exposed separately from layer *B* (exocuticle). Horizontal laminations are visible in layer *A*. Scale bars: A, 10 μm; B, 2 μm.

ultrastructure, location, development and reaction to solvents, the outer and inner portions of the outer cuticle (layers *A* and *B* in Fig. 4) are here designated the epicuticle and outer exocuticle, respectively, and will be referred to as such throughout this report.

Dermal gland canals measure 0·8 μm in diameter and their orifices are distributed regularly over the surface of the elytron (Fig. 4, *dc*). The pattern of lamination is not disrupted around the canal opening. Epicuticular thickness is enhanced on the ridges, compared to the basins of the alveoli, but is not greater at the dermal gland opening than on adjacent ridges.

Transmission electron microscopy (TEM) reveals that the alveolate superficial layer of the scanning electron micrograph is indeed a composite of two complex layers (layers *A* and *B* in Fig. 5). Immediately below this composite, lie 2–3 thin exocuticular layers (layer *C* in Figs. 5, 6A) which exhibit the distinct arciform appearance of helocoidal cuticle as described by Bouligand (1972).

The outer exocuticle (layer *B* in Fig. 5) appears more electron-dense than the helicoidal or preferred layers below. This layer consists of 25–35 densely packed lamellae ranging in width from 0·055 to 0·1 μm. In some areas, electron-dense granules lie between or within lamellae. In post-stained sections, the horizontal lamellae are resolved into alternate patterns of microfibrils viewed in perpendicular and transverse orientations (Fig. 6B). This pattern closely resembles the description of the non-perfect helicoidal outer exocuticle of *Tenebrio* given by Filshie (1982).

Pore canals, 50–70 nm in diameter, traverse the outer exocuticle (Fig. 6C, *pc*). Within the exocuticle, they appear as segments of tubes containing material much denser than the surrounding fibrils. The pore canals extend into the epicuticle but appear much narrower in diameter (Fig. 6C, arrow). This pattern is similar to the branching of epicuticular filaments described in other insect cuticles (Filshie, 1982).

The epicuticle (Fig. 6D) is composed of a series of extremely dense bands (*D*) between 0·03 and 0·1 μm thick, regularly spaced by electron-lucent bands (*L*) of 0·06–0·125 μm. Each pair of electron-dense and electron-lucent layers corresponds to a single band observed in relief in the scanning electron micrographs. The number of bands varies between four dense layers at the base of a depression to nine layers within an adjacent ridge. Under high magnification, electron-dense layers appear to be composed of vertically aligned granules (Fig. 6D). Post-staining enhances this appearance. The electron-lucent bands exhibit no apparent ultrastructure. The outermost layer is always electron-lucent and 20–30 nm thicker than the other light bands. The outer 20–30 nm appears as a faint shadow of higher density, possibly representing a cuticulin layer (Fig. 6E, *cu*). Mossakowski (1980) identified the outer series of electron-dense and electron-lucent bands as exocuticle. He concluded that the banding was a diffraction pattern resulting from the structural organization of exocuticular fibrils.

Although there are occasional distortions, the organization of the epicuticular layers is exceedingly regular. One individual *L* or *D* layer may vary in thickness horizontally within a section. This is usually an artifact resulting from the section passing obliquely through the layer as it conforms to the alveolate surface. Each *L* or *D* layer may differ slightly in thickness from other *L*/*D* layers in that region of the stack. In *C. scutellaris*, the peripheral dense band is typically fragmented

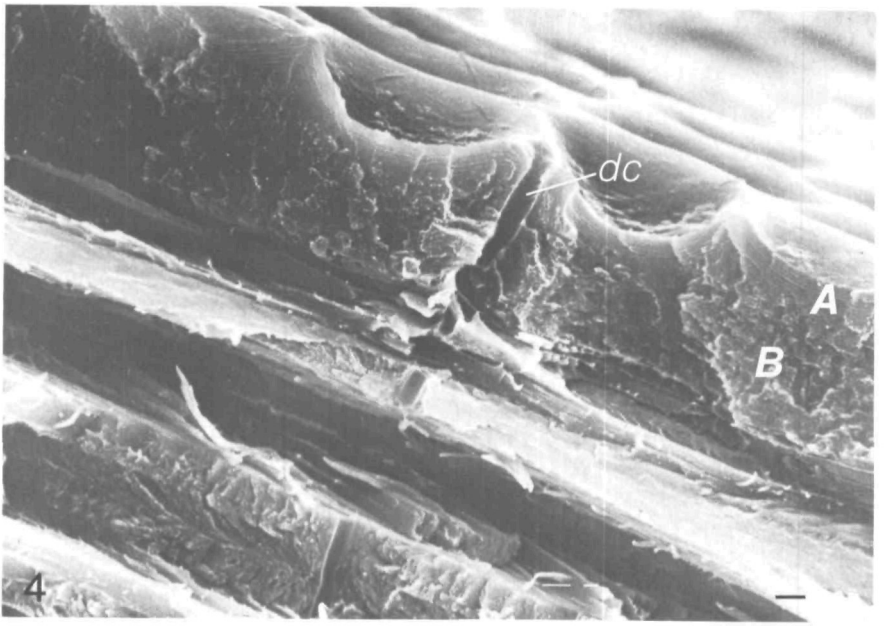

Fig. 4. Scanning electron microscope cross-section of the upper cuticular layers in *Cicindela splendida*. The laminated structure of layer *A* (presumptive epicuticle) distinguishes it from region *B* (presumptive outer exocuticle). *dc*, dermal gland canal. Scale bar, 1 μm

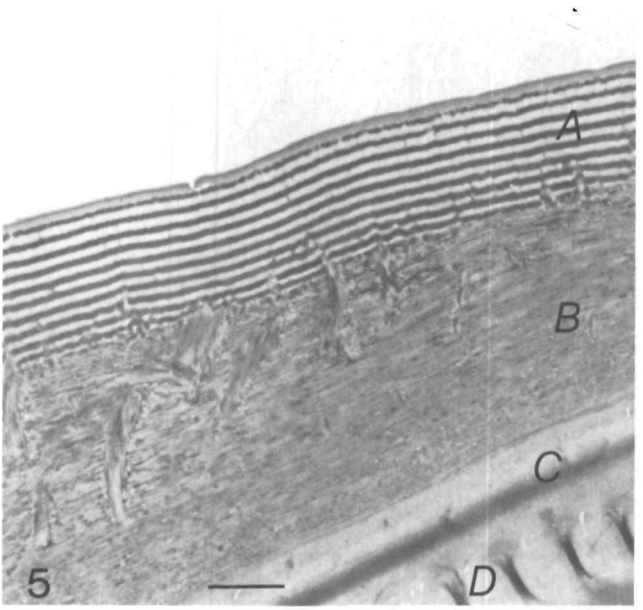

Fig. 5. Transmission electron microscope cross-section of the presumptive epicuticle (*A*) and the outer exocuticle (*B*) in the elytron of *Cicindela scutellaris*. Between the outer exocuticle and the underlying procuticle (*D*), lies a thin layer of helicoidal cuticle (*C*). Scale bar, 1 μm.

and particulate. Partially formed bands occur regularly at the outer exocuticular border.

When the honeycombed surface is sectioned horizontally, the section passes

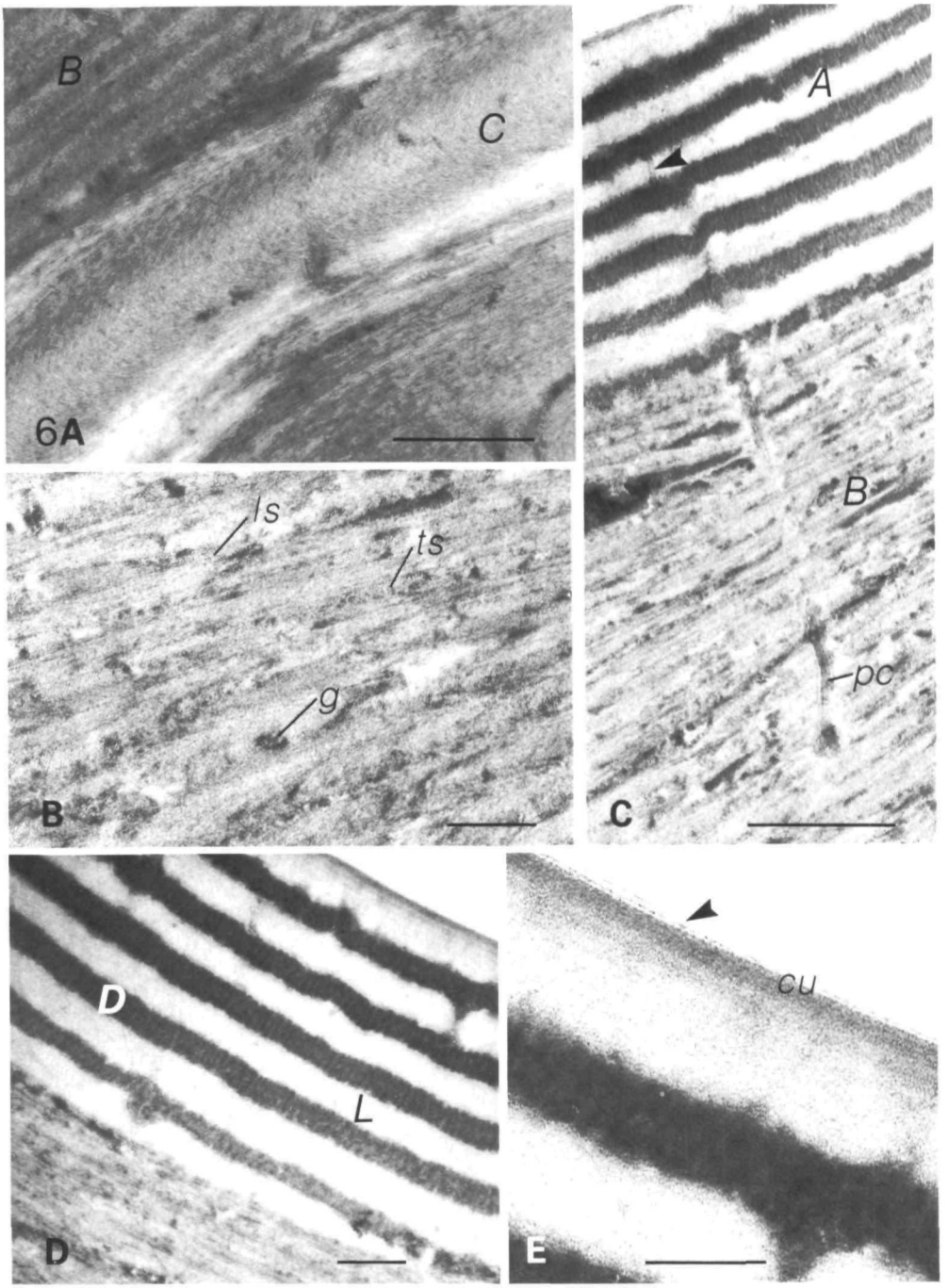

Fig. 6.

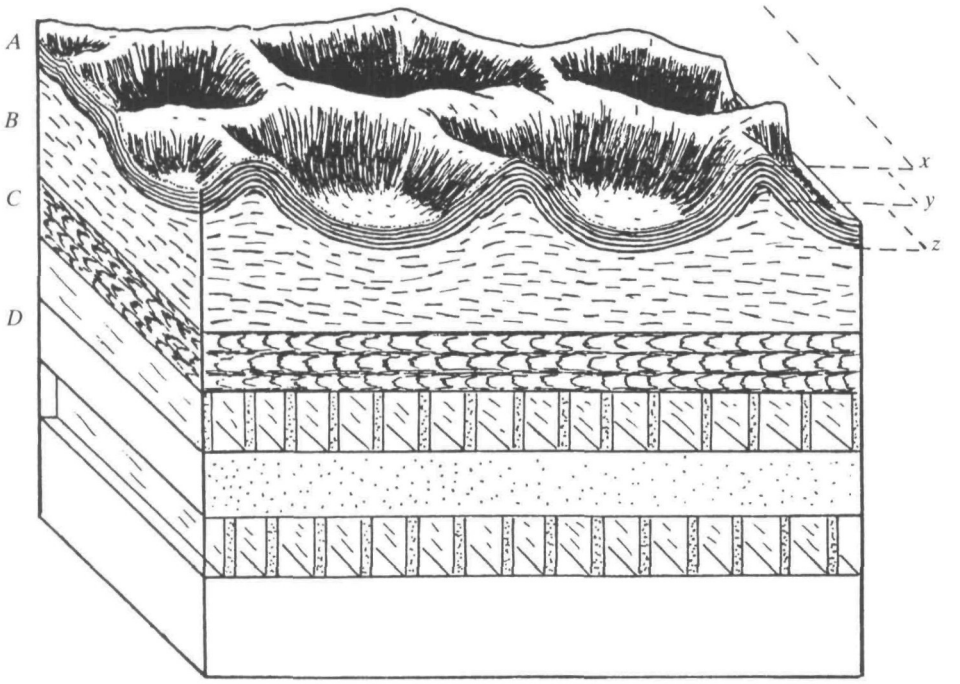

Fig. 7. Morphology and proposed terminology of the eltyral cuticle in *Cicindela*. (*D*) Endo- or mesocuticle. (*C*) Inner exocuticle. Two or three lamellae appear as a result of helicoidally oriented fibrils. (*B*) Outer exocuticle. Very fine lamellae result from the non-perfect helicoidal arrangements of fibrils. (*A*) Epicuticle. The layer assumes the outermost position and consists of alternating layers of electron-lucent and electron-dense material. No fibrillar structure is evident. Sections cut in the plane of the surface are represented by x, y and z (see text).

through the hexagonal ridges and across the intervening alveoli. Initial sections thus possess holes, surrounded by material from adjacent ridges (section x in Fig. 7). Within the ridge itself, the section passes obliquely across the outermost epicuticular layers, resulting in concentric rings around the hole. As the section intersects the ridge axis, it passes through the portion of an epicuticular layer that is oriented parallel to the section; this therefore appears as a continuous patch of either electron-dense or electron-lucent material. Deeper sections include the elevated portions of outer exocuticle within the base of a ridge (section y through region B in Fig. 7). Sections taken across the alveolar basin (section z in Fig. 7) result in a central spot of light or

Fig. 6. The ultrastructure of the outer cuticular layers in the elytron of *Cicindela formosa*. (A) Arcuate fibril pattern of layer *C* (presumptive inner exocuticle). Scale bar, 0·5 μm. (B) Fibril pattern of region *B* (presumptive outer exocuticle). Fine lamellae appear as the result of a semi-arcuate pattern of fibrils cut in longitudinal section (*ls*) and in transverse section (*ts*). Granules (*g*) of electron-dense material appear between lamellae. Scale bar, 0·2 μm. (C) Pore canal (*pc*) extending from the presumptive exocuticle (*B*) to the presumptive epicuticle (*A*). Narrow extensions of the canal are visible in layer *A* (arrow). Scale bar, 0·5 μm. (D) Ultrastructure of the presumptive epicuticle. The layer is composed of alternating layers of electron-lucent (*L*) and electron-dense (*D*) material. Scale bar, 0·2 μm. (E) High magnification of the outer edge of the presumptive epicuticle. An area of higher density in the outermost *L* layer represents the presumptive cuticulin layer (*cu*). An extremely thin (10 nm), electron-lucent layer appears between the cuticulin layer and the edge of the embedding medium (arrow). Scale bar, 0·1 μm.

dense epicuticular material ringed by obliquely sectioned layers. These islands of epicuticle are surrounded by exocuticle.

The horizontal sections demonstrate that electron-dense and electron-lucent layers have the same individual density and location when observed horizontally or vertically (Fig. 8A). The banding pattern is not, therefore, an artifact of diffraction. The layer

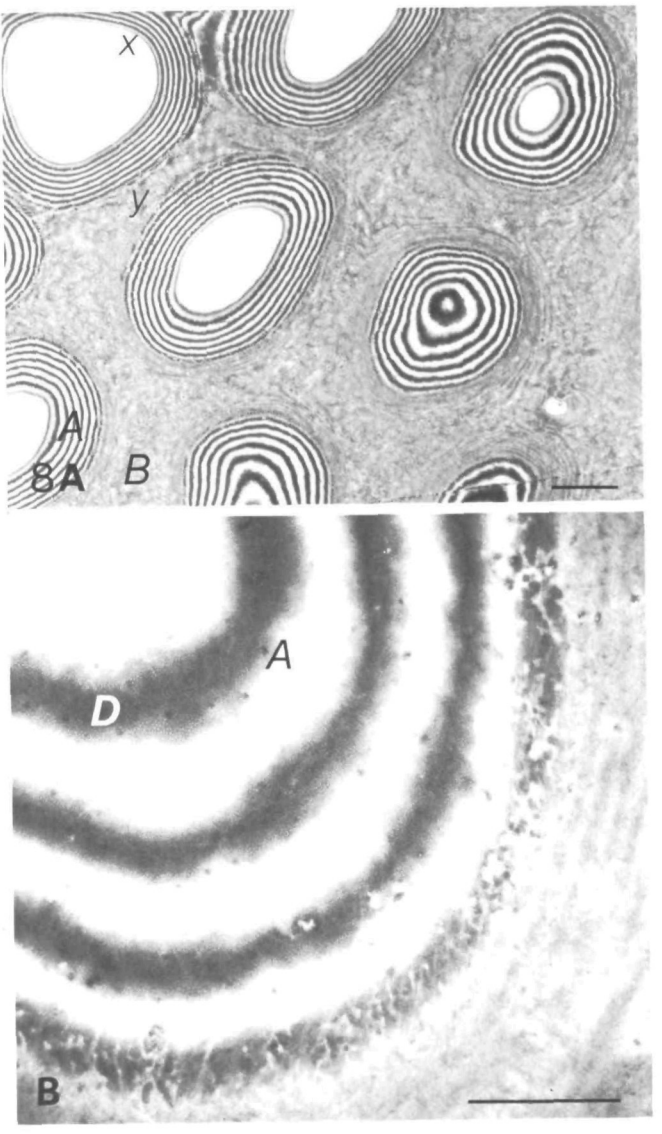

Fig. 8. (A) Transmission electron micrograph of the epicuticle (*A*) and the outer exocuticle (*B*) of *Cicindela scutellaris* sectioned in the plane of the elytral surface. Concentric rings of epicuticular material surround holes where the section did not include the basin of an alveolar cell (area *x*, see Fig. 7). The rings of epicuticle are surrounded by outer exocuticle in areas where the section includes tissues below the epicuticle within the alveolar ridges (area *y*, see Fig. 7). Note that the sequence of light and dense banding is the same as in cross-sections of the epicuticle (Fig. 5). Scale bar, 5 μm. (B) Planar section of an alveolar basin (see section *z*, Fig. 7). Note the particulate ultrastructure of the electron-dense layers (*D*) in the epicuticle (*A*). Scale bar, 1 μm.

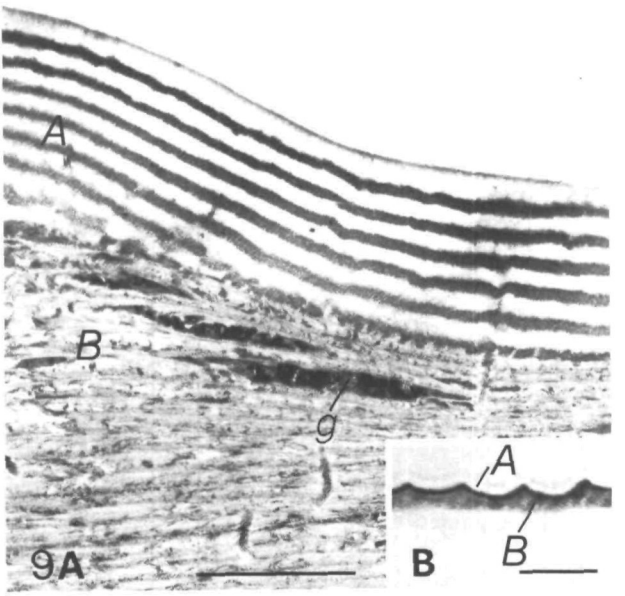

Fig. 9. (A) Transmission electron micrograph cross-section of the epicuticle (*A*) and outer exocuticle (*B*) of *Cicindela formosa*. The section was taken from a pigmented and iridescent area of the elytron. Granules (*g*) of electron-dense material appear in the exocuticle. Scale bar, 1 μm. (B) Photomicrograph of the same tissue. The epicuticle (*A*) and exocuticle (*B*) are pigmented and highly refractive. Scale bar, 10 μm.

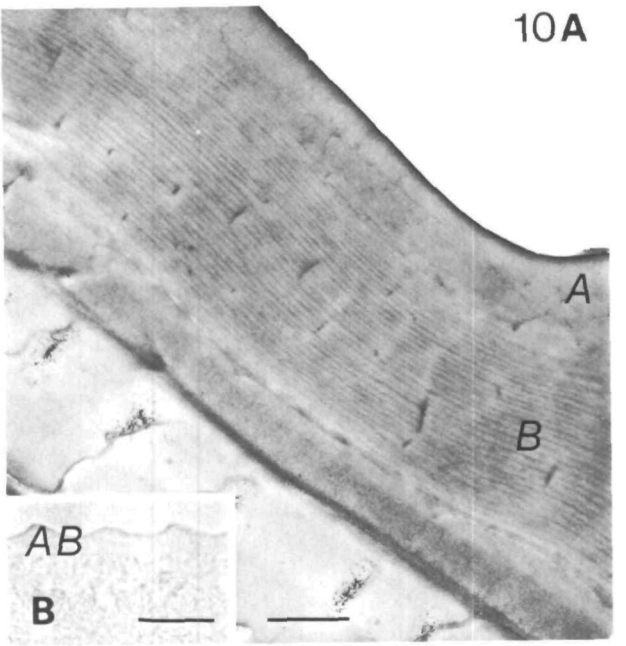

Fig. 10. (A) Transmission electron micrograph of a cross-section of elytral cuticle sectioned from the non-pigmented maculations of *Cicindela formosa*. Electron-dense layers are absent from the epicuticle (*A*). Scale bar, 1 μm. (B) Photomicrograph of the same non-pigmented tissue. The epicuticle and outer exocuticle (*AB*) show no pigmentation or higher refractivity than the underlying cuticle. Scale bar, 10 μm.

that borders the holes in horizontal sections is the outermost layer of the epicuticle, and is electron-lucent in both orientations. Furthermore, horizontal sections within a single epicuticular layer show continuous patches of electron-dense material. This material is very finely particulate when viewed perpendicular to the layer (Fig. 8B).

When thin sections are viewed through an optical microscope, the outer exocuticle and the epicuticle appear dark brown (Fig. 9B). This apparent pigmentation is confined to the outer 5 μm of the elytral cuticle. It is assumed that the dark brown appearance is due to the presence of melanin in this region, and that it is responsible for the dark opaque appearance of the elytron in transmitted light. The epicuticle and outer exocuticle display a greater retardation of light than the inner layers of procuticle under interference microscopy.

Sections of elytral cuticle were also cut from the white maculations of *C. formosa*. The white areas show no trace of either iridescent colour or brown or black pigmentation (Fig. 10B). Under interference microscopy, the sections of white cuticle show a uniformity in refractive index throughout the elytron. The epicuticle shows a refractive index of approximately 1·5 by the Becke line test (Neville, 1980).

Electron micrographs of this non-pigmented cuticle show an epicuticle which lacks the electron-dense bands (layer *A* in Fig. 10A). In general, this homogeneous epicuticle is thinner and lower in contrast than the laminated epicuticle of pigmented areas (layer *A* in Fig. 9A). SEM confirmed the absence of the epicuticular laminations in the region of the elytral maculations. The outer exocuticle of these sections lacks the electron-dense granules that were evident in the exocuticle of pigmented areas (layers *B* in Figs 9A and 10A).

Analysis of cuticle structure by chemical treatment

Tiger beetle cuticle treated with dilute KOH displayed a gradual loss of structural coloration, as well as pigmentation. Immersion in ethanol, xylene, acetone, sulphuric or nitric acid failed to produce any change in structural colour. Initially, structural colours became longer in wavelength as the solvent temporarily swelled the reflectance layers. After 4 h, however, the maroon portion of the elytron of *C. formosa* appeared blue-green. The anterior portion, originally red, became ochreous with slight orange-green reflections. The overall iridescence was reduced to a dull sheen. Scanning electron micrographs of the treated elytra revealed a distorted and heavily eroded surface microsculpture. Under transmission electron microscopy, the regular laminations at the periphery of the cuticle were disrupted and often stripped from the sample (Fig. 11).

With the exception of a few blue-green or violet reflections in the basins of punctures, elytra treated with KOH for 12–15 h were virtually devoid of structural colours. The surface had a flat, brown, darker appearance at the elytral base, which is assumed to be due to the residual presence of melanin in the exocuticle. The deep hexagonal depressions of the surface microsculpture were eroded to a shallow outline of the surface pattern. TEM micrographs revealed that the laminated epicuticle was completely removed from the surface of the outer exocuticle (Fig. 12). A light band, 0·29 μm thick, remained at the border of the exocuticle. The exocuticular lamination also became more obscure and fragmented.

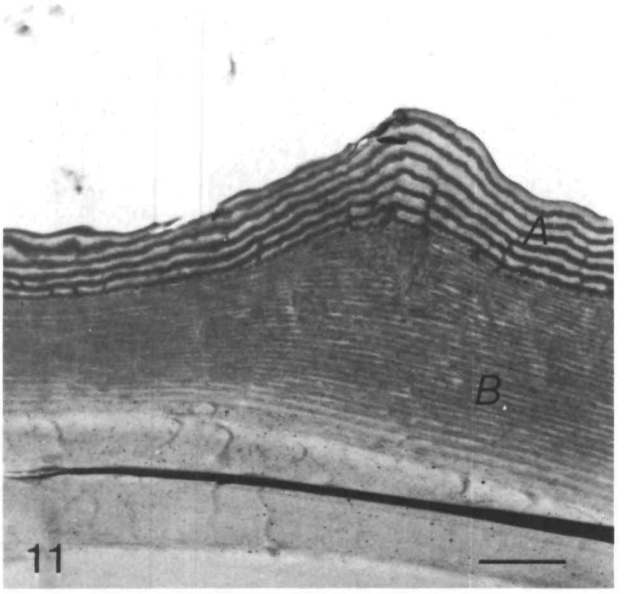

Fig. 11. Transmission electron micrograph of a cross-section of elytral cuticle of *Cicindela formosa* treated for 4 h with 8% KOH. The epicuticular layers are disrupted and partially dispersed. (*A*) epicuticle, (*B*) outer exocuticle. Scale bar, 1 μm.

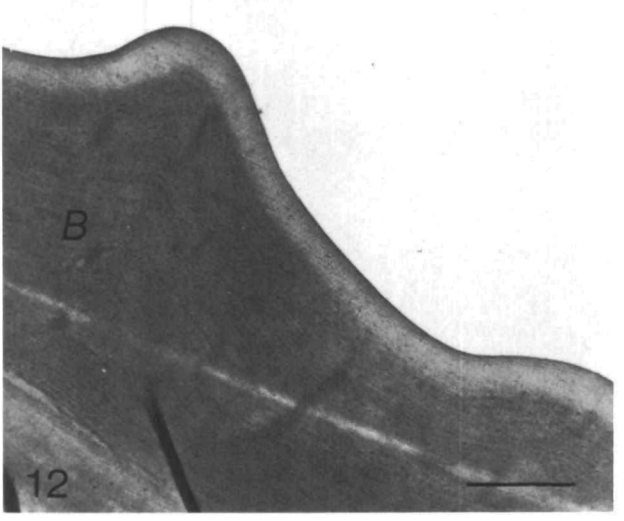

Fig. 12. Transmission electron micrograph cross-section of elytral cuticle of *Cicindela formosa* treated for 15 h with 8% KOH. The epicuticle is dissolved completely. An area of lower electron density appears near the exposed surface of the outer exocuticle (*B*). Scale bar, 1 μm.

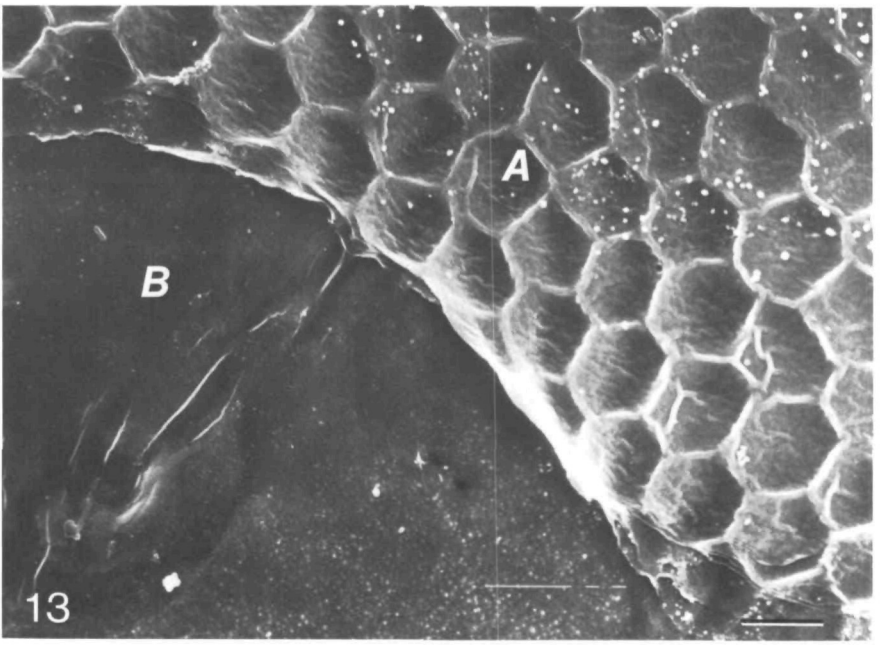

Fig. 13. Scanning electron microscope surface view of an elytron of *Cicindela scutellaris* treated for 15 min with concentrated KOH at 160 °C. In area *A*, the epicuticle is intact, but eroded. This area was still weakly iridescent. In area *B*, the epicuticle has been removed, exposing the surfaces of the exocuticle. This surface was non-iridescent. Scale bar, 10 μm.

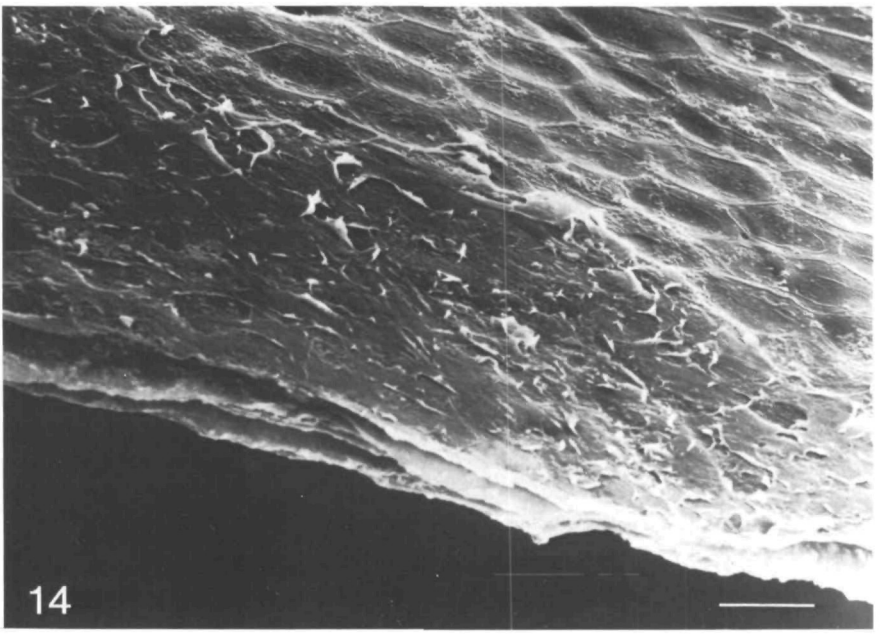

Fig. 14. Scanning electron microscope surface view of an elytron of *Cicindela formosa* treated for 15 min with concentrated KOH at 106 °C. The epicuticle has been dissolved. This sample was no longer iridescent. Scale bar, 10 μm.

Longer KOH treatments resulted in a progressive loss of the remaining brown colour. By 48 h, only a slight trace of the original maculation pattern was evident, and the elytron was a light straw colour. During this treatment, the outer exocuticle remained – the alveolate pattern was still visible in the surface. However, the thickness of this layer was reduced by 40 %, suggesting a leaching of exocuticular components.

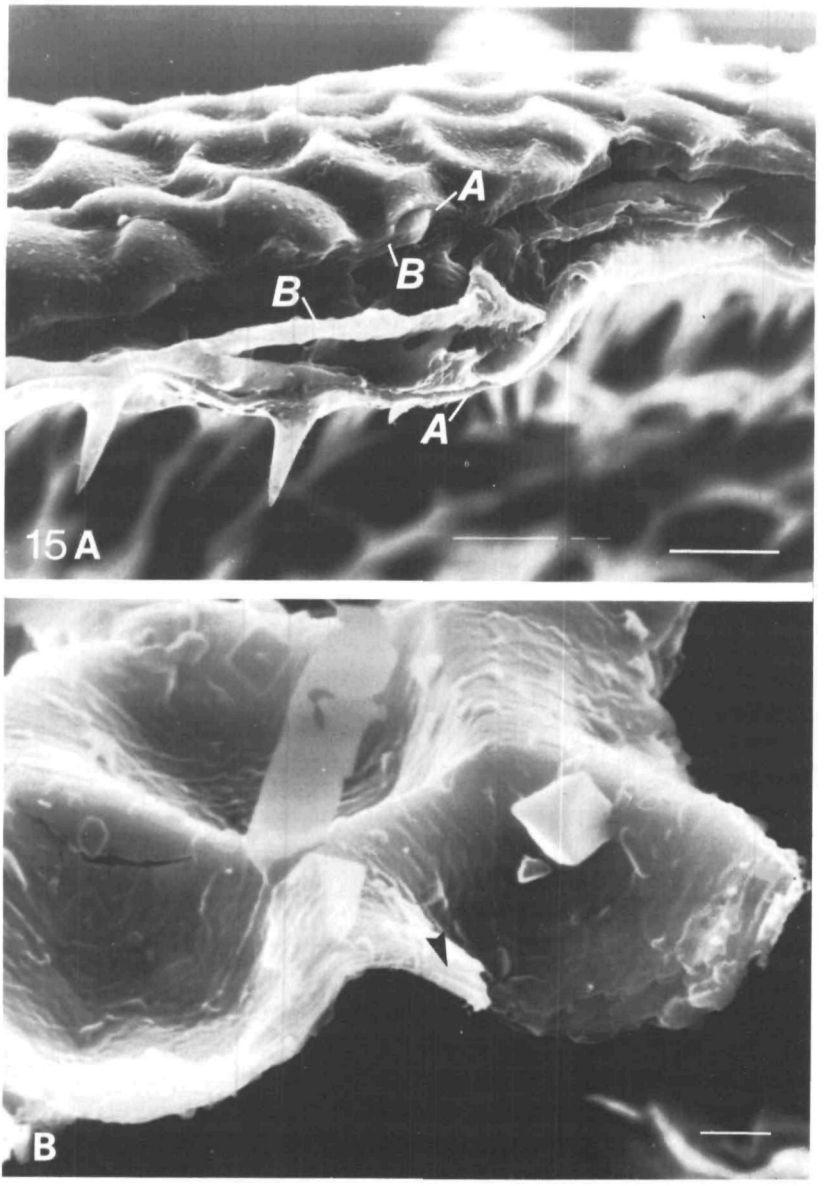

Fig. 15. Scanning electron microscope cross-section of an elytron of *Cicindela formosa* treated with concentrated H_2SO_4 for 48 h. (A) The endocuticle of the elytron has been dissolved, leaving a sleeve of epicuticle (*A*) and exocuticle (*B*). Scale bar, 10 μm. (B) A portion of the epicuticle separated from the outer exocuticle. Surface pattern and laminations are still intact (arrow). Scale bar, 2 μm.

The chitosan method of Campbell (1929) and van Wisselingh (1914) has long been used to distinguish chitinous from non-chitinous cuticle, although this technique is not conclusive (Richards, 1951). It requires the conversion of chitin to chitosan by treatment with concentrated KOH at 160 °C for 15 min. It is assumed that the non-chitinous elements of the exoskeleton (epicuticular components) are dissolved under

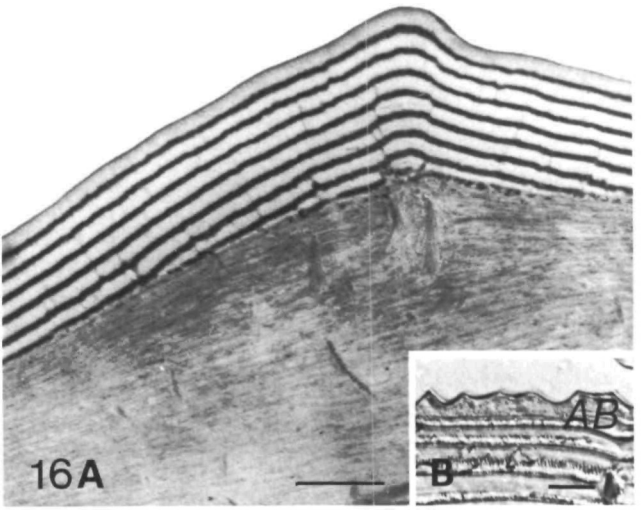

Fig. 16. (A) Transmission electron microscope cross-section of pigmented cuticle of *Cicindela formosa* treated with H_2O_2. The electron-dense layers of the epicuticle are reduced in thickness (compare with Fig. 9). Outer layers appear most reduced by the treatment. Scale bar, 1 μm. (B) Photomicrograph of the same tissue. The epicuticle and exocuticle (*AB*) are not strongly pigmented. Scale bar, 10μm.

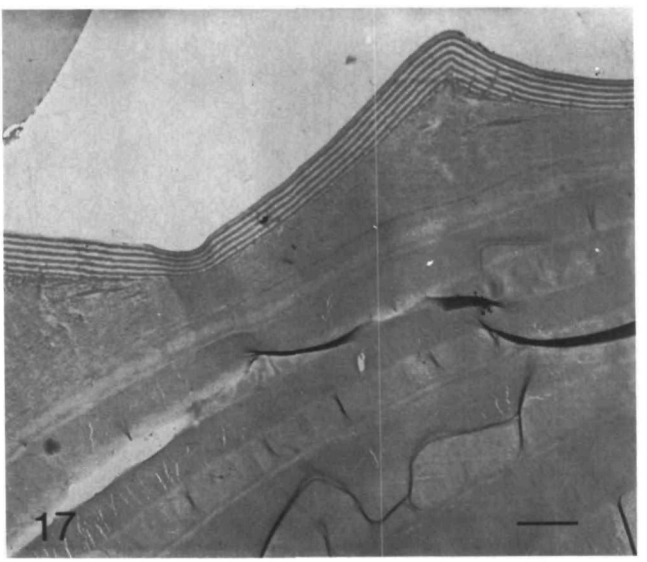

Fig. 17. Transmission electron micrograph cross-section of the elytral cuticle of *Cicindela repanda*. The epicuticle (*A*) is laminated, although no peak interference colour is reflected. Scale bar, 2 μm.

this alkali treatment. Samples of tiger beetle cuticle subjected to the chitosan test showed a severe break-up of the presumptive epicuticle. In *C. scutellaris*, an eroded epicuticle (area *A* in Fig. 13) was evident in some areas where a feebly iridescent sheen still appeared. If these treated samples were immersed in 8 % KOH for 18 h at room temperature, all traces of the presumptive epicuticle were removed, as well as the remaining pigmentation. In *C. formosa*, the epicuticle and iridescence were completely removed by the chitosan treatment (Fig. 14).

In contrast to the results of the alkali treatments, endocuticle is dissolved rapidly in concentrated sulphuric acid (Sprung, 1931; Wigglesworth, 1933; Hackman, 1974), whereas sclerotized exocuticle and epicuticle are said to remain intact. Tiger beetle elytra immersed in sulphuric acid showed a rapid dissolution of inner 'plywood' mesocuticle, leaving a thin, flexible sleeve of putative epicuticle and outer exocuticle, while the structural coloration of the elytron remained unaltered (Fig. 15A). SEM examinations of the treated cuticle revealed that the outer laminated layer (layer *A*) retained its ultrastructure intact (Fig. 15B). The outer exocuticle was also intact and pigmented through the first 48 h of treatment. The residual cuticle still appeared dark brown in transmitted light. Portions of the helicoidal exocuticle below could be seen adhering to the lower side of the outer exocuticle. Frequently, areas were observed in which the epicuticle had separated from the outer exocuticle, and these fragments were found floating on the surface of the acid. Even these isolated fragments maintained a laminated appearance under SEM, as well as an iridescence.

Treatments of elytral cuticle with H_2O_2 significantly altered the cuticle coloration. When observed in transmitted light, the brown coloration became more translucent. The outer exocuticle and epicuticle appeared either light brown or clear of pigment in microscopic sections (Fig. 16B). The structural colour of the cuticle surface became duller and shorter in principal wavelength. Similar results were obtained when samples were treated with 20 % H_2O_2 at 26 °C for 24–48 h.

TEM micrographs revealed a 40 % reduction in thickness of dense epicuticular layers in the H_2O_2-treated samples (Fig. 16A). The bands were progressively thinner towards the outer surface. The overall thickness of the epicuticle was not diminished significantly.

DISCUSSION

Cuticle histology

Probably because it is extremely thin, the epicuticle is the least understood portion of the insect integument. Its chemistry, structure and the terminology of epicuticular components have been controversial. Only a few, diverse arthropods have been studied intensively, and very little work has focused on the epicuticle of hard, adult exoskeletons (Delachambre, 1970). This is not surprising since hard cuticle is difficult to prepare and section for transmission electron microscopy.

The epicuticle, by definition, is non-chitinous or reacts negatively to tests for chitin (chitosan method). It is the first layer formed during the moult sequence and assumes the outermost position in the strata of the exoskeleton, bearing the surface microsculpture. The general model of epicuticle structure recognizes five components. These are the cuticulin layer, the inner epicuticle, the outer epicuticle, the wax layer

and the cement layer, listed in order of deposition (Filshie, 1982). The wax and cement layers are secreted upon the epicuticular surface by the epicuticular filaments and dermal glands, respectively. Filshie (1982) notes that the saturated lipids of wax layers do not survive conventional electron microscope preparations, and their supposed appearance in electron micrographs is probably an artifact or misidentification of other layers. Identifications of cement layers have been made by location only and remain unsupported by developmental studies.

The reflective layers of cicindelid cuticle are not a form of cement or tectocuticle. The so-called 'Sekretschicht'–the source of the structural colours–is formed preecdysially, not secreted from dermal glands (Schultz & Rankin, 1985). Furthermore, the very even pattern of layering over a contoured surface would be unlikely if it were formed from secretions of relatively dispersed glands. The layers remain evenly spaced around and even within the mouth of dermal glands (Fig. 4). Extraordinary properties of the two components and the dermal glands themselves would be required to produce such regular secretions over the entire cuticular surface.

The cuticulin layer (or outer epicuticle of Neville, 1975) is the first epicuticlar layer secreted by the epidermis during the moult sequence. It appears as a thin (10–20 nm), dense membrane at the outer edge of the cuticle in electron micrographs. In some insects (Locke, 1966; Delachambre, 1970), it initially appears laminated, but condenses to a uniform appearance. Micrographs of *C. formosa* show a dense region, 30–40 nm thick, at the edge of the outermost electron-lucent band (*cu* in Fig. 6E). The inner side of this region appears finely laminated, becoming more uniformly dense towards the surface of the cuticle. This region appears in all the *Cicindela* species and samples studied, including the pharate cuticle (see Schultz & Rankin, 1985), and is interpreted as the cuticulin layer. In mature cicindelid cuticle only, a very thin (10 nm), electron-lucent membrane appears above the cuticulin. This structure may represent the outer epicuticle that is thought to arise by separation from the cuticulin layer prior to ecdysis (Filshie, 1982).

The bulk of the epicuticle is composed of the inner epicuticle, 0·5–1 μm thick. Its appearance varies among species, and consequently, a wide range of chemical constituents have been proposed. These include protein, lipids, lipoprotein and dihydroxyphenols. This layer borders directly on the helicoidal exocuticle beneath it (Neville, 1975). Laminated inner epicuticles have been described, but these laminations have been transitory during the moult sequence (Delachambre, 1970), or have extremely short periods of less than 40 nm (Gupta & Smith, 1969; Gluud, 1968; Zacharuk, 1972).

The multilayered outer region of cicindelid cuticle is best described as inner epicuticle, due to its location, ultrastructure and solubility in KOH, in combination with a resistance to strong acid (Region *A* in Figs 2–7). Treatments with solvents demonstrate that this region is chemically distinct from the chitinous layers below. If it were exocuticle, the ultrastructure of the layers would survive the alkali treatment (Hackman, 1974). Furthermore, it lacks any indication of fibrillar architecture that is evident in the alkali-resistant layers or in the exocuticles of other insects.

The outermost layer of inner epicuticle, presumably secreted first, is always electron-lucent, while the innermost layer may be electron-lucent or electron-dense. More layers are produced at the borders of the epidermal cells than at their centres.

These borders are indicated by the hexagonal ridges in the surface microsculpture (Neville, 1975). Areas of elytral cuticle which lack pigmentation (i.e. the maculations), also lack electron-dense layers in the epicuticle. Perhaps the cicindelid inner epicuticle is described best as a homogeneous electron-lucent material, impregnated by electron-dense material at discrete intervals in those cuticles that are pigmented.

The epicuticle as an interference reflector

It appears that the epicuticle is the source of structural colours in *Cicindela*. Maceration or removal of the epicuticle with KOH results in the deterioration or loss of iridescent coloration. Conversely, removal of the other components of the integument produces no loss of colour. The change of hue under oblique incidence demonstrates that the structural colours result from constructive interference of reflected light.

The repetitive layering of two materials in the epicuticle, whose thicknesses are less than half the wavelength of visible light, is characteristic of a multilayer interference reflector. The two layers are distinct in their electron densities, and are not an artifact of the helicoidal arrangement of cuticle fibrils, as in the reflective exocuticle of optically active scarab beetles (Neville & Caveney, 1969). Multilayer reflectors have been described in a wide diversity of animal tissues, and the basic principles of interference in animal reflectors are reviewed by Land (1972).

In the 'ideal' case of thin film reflection, the wavelength of the first order maximum reflectance (λ max) depends on the thickness (d) and refractive index (n) of each layer such that

$$\lambda \max = 4nd \sin \theta, \tag{1}$$

where θ is the angle of incidence. Under 'ideal' conditions, the optical thicknesses of both layers are equivalent ($n_L d_L = n_D d_D$, where L indicates the lucent layer and D the dense layer). Each layer acts as a quarter-wavelength reflecting plane, with the reflections from all interfaces constructively interfering to produce the total coloration.

The optical thickness of each component is different ($n_L d_L \neq n_D d_D$) in a 'non-ideal' multilayer system. The first order reflectance peak occurs at

$$\lambda \max = 2(n_L d_L + n_D d_D) \tag{2}$$

under normal angle of incidence. Under 'non-ideal' conditions the peak reflectance and the band width of the first order peak are diminished. The result is a sharper peak and purer colour (Land, 1972). The reflecting layers of tiger beetle epicuticle are best described as a 'non-ideal' system. The thicknesses of the electron-dense (d_D) and the electron-lucent (d_L) layers vary considerably through a single point in the stack (Table 1). Assuming that the refractive indices (n_L and n_D) remain stable, the ratio d_L/d_D does not remain constant throughout the reflector.

A quarter-wave interference reflector has been described by Durrer & Villiger (1972) in the exocuticle of *Euchroma gigantea*, which consists of a series of electron-lucent and electron-dense bands similar to the epicuticle of *Cicindela*. The dimensions of the layers imply an average refractive index of 1·75 for the reflector. The authors propose that the multilayer system contains electron-dense melanin layers (RI = 2·0) separated by chitin (RI = 1·5), similar to the keratin-melanin interference

Table 1. *Average thickness of electron-lucent* (L) *and electron-dense* (D) *layers in four* Cicindela *species with predicted and experimental values of elytral reflectance*

Specimen	SEM bilayer thickness (nm)	Mean L layer thickness (nm)	Mean D layer thickness (nm)	Calculated λ max (nm) $n_L = 1{\cdot}5$; $n_D = 2{\cdot}0$	Experimental λ max (nm)
C. formosa					
ridge	188	106·59 ± 6.76	93·63 ± 11·756	694·31	655
alveolar basin		101·99 ± 5·292	74·974 ± 6·752	605·77	
C. scutellaris rugata	143	67·197 ± 4·08	72·147 ± 4·591	489·93	499
C. splendida	178	102·03 ± 14·907*	71·428 ± 6·563	591·8	635
C. repanda					
ridge	—	137·73 ± 18·233	110·65 ± 12·156	855·79	—
alveolar basin		81·22	88·035 ± 6·815	595·8	

Standard deviation values indicate the variation between successive layers in the epicuticle.
Calculations of λ max assume a refractive index (n) of 1·5 for L layers and 2·0 for D layers.
* The outermost L layer measured 130 nm in this sample.

reflectors of bird feathers (Durrer & Villiger, 1970). In their approach, the authors calculated the wavelength of maximum reflectance for each layer separately, in addition to determining the reflectance from the series of bilayers (equation 2). They concluded that a mixture of these reflected components results, producing the total colour.

Mossakowski (1980) examined interference reflectors in the cuticles of the buprestid, *Chrysocroa vittata*, and the tiger beetle, *Cicindela campestris*. Mossakowski calculated reflectances for a number of possible refractive indices using the theoretical treatment of Huxley (1968). He proposed that an average refractive index of 1·75 for the bilayers of *C. camprestis* would cause a total reflectance value far exceeding those determined experimentally. Mossakowski's measurements of total reflectance predicted refractive indices of 1·5 and 1·6 for the light and dense layers respectively. However, these values and the dimensions of the layers observed under electron microscopy predicted a wavelength of peak reflectance substantially below those recorded spectrophotometrically. Mossakowski assumed that the reflecting layers had experienced a 10–15 % shrinkage due to specimen preparation or exposure to the electron beam.

The dimensions of the interference layers of cicindelids presented in this paper suggest a relatively high average refractive index near 1·75 for the pairs of layers. Values of 1·5 and 2·0 for the light and dense layers predict peak wavelengths which approximate to the spectrophotometric results for *C. scutellaris* and *C. formosa* (Table 1). Refractive indices of 1·5 and 1·6 would predict substantially shorter wavelengths of peak reflectance. The epicuticle of *C. repanda* varied greatly in layer thickness and its reflectance exhibited no single peak within the visible wavelengths.

Even assuming an average refractive index of 1·75, calculations using the average thicknesses of epicuticular layers predict values of λ max well below the reflectance peak of *C. splendida*. Unlike the other specimens, the outermost electron-lucent layer of *C. splendida* is 40–50 nm thicker than all the underlying electron-lucent layers.

This layer makes a significant contribution to the large standard deviation in the average thickness of these layers. Variation in the thickness of the inner layers is less than that of *C. repanda* but greater than the variation in *C. scutellaris*. A λ max of 638 nm is predicted if calculations are based upon the superficial electron-lucent layer ($d_L = 130$ nm, $n_L = 1{\cdot}5$) and the underlying dense layer ($d_L = 62$ nm, $n_L = 2{\cdot}0$). This value is close to the experimental reflectance peak of 635 nm. Since the surface of *C. splendida* is so deeply sculptured with the alveolate pattern, the superficial epicuticular layers may contribute more to the peak reflectance than the underlying layers. Peak reflectances from deeper layers may occur at angles which depart from the angle of reflection that is sampled by the spectrophotometer.

In *C. scutellaris rugata* and the green form of *C. campestris* (Mossakowski, 1980), the thickness of the light and dense layers are roughly equivalent. In these cases, the average refractive index $\bar{n}$ may be estimated from the experimental peak wavelength and the thickness of each bilayer (d_{DL}):

$$\lambda \max = 2\bar{n}d_{DL} \tag{3}$$

$$\text{or } \bar{n} = \lambda \max/2d_{DL}. \tag{4}$$

For *C. scutellaris rugata*, an average refractive index of 1·74 is predicted.

No evidence of shrinkage appeared in the samples of cicindelid cuticle. The structural colours of specimens were observed unchanged within the embedding medium, indicating that shrinkage did not result from specimen preparation. SEM measurements of epicuticular bilayers corresponded well with bilayer measurements made from transmission electron micrographs. If bilayers measured from SEM micrographs were assumed to shrink 10% under the electron beam, they would appear 10–20 nm thinner than the average thickness of bilayers measured from TEM micrographs. If shrinkage had occurred under the electron beam, TEM measurements should fall below the thicknesses measured under SEM.

The relatively low total reflectance of cicindelid epicuticle may be due to its alveolate microsculpture. If the angle of incident light departs from normal, the wavelength of peak reflectance becomes shorter according to

$$\lambda \max = 4nd \cos \theta, \tag{5}$$

where θ is the angle of refraction within a single layer. In addition, each successive epicuticular layer conforms to the alveolate pattern of the surface. The wavelength of peak reflectance for multilayer reflectors at oblique incidence is then given by:

$$\lambda \max = 2(n_L d_L \cos \theta_L + n_D d_D \cos \theta_D), \tag{6}$$

where θ is the angle of incidence in the layer of lower density. Similarly, the reflectance at each interface is dependent upon the angle of refraction (Land, 1972). Thus, the wavelength and the intensity of reflection are affected by deviations in angle of incidence and refraction which occur continuously throughout the horizontal dimensions of the epicuticular layers. Due to these effects, and the scattering of reflected light by an alveolate surface, the spectrophotometric analysis of reflected light from the epicuticle must surely underestimate the reflectance predicted by normal theoretical conditions.

The peak reflectance is also dependent upon the constancy of layer thickness throughout the epicuticle. In *Cicindela*, the thicknesses of the bilayers vary both horizontally and vertically within the epicuticle (Table 1). The theoretical treatment of non-ideal, multilayer reflectors assumes that these dimensions remain constant. This non-uniformity in layer thickness and angle, with respect to incident light, clearly places the cicindelid epicuticle as an extremely complex example of a biological interference reflector. The epicuticle represents a non-ideal, multilayer system moulded into a shallow honeycomb form, and is not adequately described by theoretical treatments for regularly spaced, planar systems.

Correlations between electron microscope measurements and reflectance data should not be over-emphasized. The amount of cuticle sectioned is not comparable to the area of elytral material sampled for reflectance. The variability within the interference reflector has already been described. In addition, there is always uncertainty as to whether the section is precisely perpendicular to the interference layers.

With rare exceptions, the brown or black colours of insect cuticles are attributed to sclerotization and/or melanization of the cuticle (Richards, 1967). Eumelanins predominate as the brown or black pigments of insect integument (Hackman, 1974), and the pigmentation of *Cicindela* has been ascribed to melanin since the work of Shelford (1917). Unfortunately, it is exceedingly difficult to identify small amounts of melanin by staining or chemical analysis. Since the individual layers of dense material in the epicuticle are not resolvable under light microscopy, their optical properties cannot be examined separately. The treatment with KOH removes the epicuticle from the pigmented exocuticle, and produces a solution that is stained brown with dissolved epicuticle. But it is also possible that melanin may be leached from the exocuticle by the treatment (Richards, 1967).

Richards (1967) found that treatment with H_2O_2 will bleach melanin particles without removing them from the cuticle. Tiger beetle elytra were treated with H_2O_2 to determine the role of melanin in the elytral coloration. If melanin is involved simply as an absorbent background to the interference reflector, the iridescent colour should be reduced in intensity, but not altered in hue when the pigment is bleached (Mason, 1927). In treatments of *C. formosa*, a reduction in intensity and predominant wavelength resulted, as well as a thinning of pigmented colour in the cuticle. The change in reflected colour may be due to the bleaching of melanin within the structure of the reflecting epicuticle itself.

The structural dimensions of the two epicuticular layers, in conjunction with the experimental reflectance results, suggest that the epicuticular reflector is composed of an electron-lucent layer with a refractive index of 1·5 and a dense layer of 2·0. A refractive index of 1·5 is acceptable for insect cuticular proteins (Neville, 1975). This study proposes that the unusually high refractive index of 2·0 is provided by layers of melanin or melanoproteins. Precedents for such a system can be found in iridescent bird feather colouration (Greenwalt, Brandt & Friel, 1960; Rutschke, 1966; Durrer & Villiger, 1966, 1970). Additional melanin in the outer exocuticle provides an absorbent background for transmitted and extraneous wavelengths, hence purifying the reflected colour. Circumstantial evidence for the role of melanins is found in the restrictive co-occurence of pigmentation, iridescence and epicuticular lamination. Specific chemical analysis is still required to verify the identity of the electron-dense layer as melanin.

Structural coloration in Cicindela

The specific coloration of structurally-coloured tiger beetles depends upon the relative thicknesses of the epicuticular layers. In *C. formosa, C. scutellaris* and *C. splendida*, the dimensions of these layers are sufficient to cause the constructive interference of visible wavelengths of light. In epicuticles with regular laminations and a relatively smooth microsculpture, as in *C. scutellaris*, the reflectance colours are purer.

In some areas of *C. repanda* elytra, epicuticular laminations are too wide to reflect light at visible wavelengths (Fig. 17). However, visible wavelengths are reflected from areas where the layers are sufficiently thin in the highly variable epicuticle, e.g. within the alveoli. Furthermore, visible wavelengths may be reflected from thicker layers at oblique incidence due to the effect of angle of incidence on the wavelength of maximum reflectance. Thus, while the layers of *C. repanda* may reflect maximally above 760 nm, shorter red wavelengths will be reflected by the highly angled pattern of ridges in the microsculpture. The results of these factors is a relatively poor reflectance of any one visible wavelength, producing an overall flat brown appearance upon casual observation. Under the dissecting microscope, a wide range of reflected colours (predominantly red) can be observed from various points on the surface microsculpture. Although at first glance the elytra of *C. repanda* do not appear to be structurally coloured, the epicuticular structure is consistent with the epicuticular reflectors of other iridescent species.

Thus, tiger beetle structural coloration depends upon three variables: the thickness, uniformity and microsculpture of the reflecting layers. In species which reflect a narrow band of short wavelengths, the epicuticular bilayers are relatively thin and the intensity and purity of the colour depend upon the severity of the alveolate microsculpture. Several species which appear brown or coppery bear relatively thick and variable epicuticular bilayers. The deeply pitted microsculpture of the reflector further diminishes the intensity and purity of the reflected colour, resulting in a broad range of reflected wavelengths of low intensity. Small variations in the basic multilayer structure of the epicuticle are responsible for the wide variation in colour observed in the genus *Cicindela*.

The authors thank Dr S. Meier, University of Texas, for the use of the SEM, Dr Bird and K. Kotora of Rutgers University, for their assistance in the reflectance spectrophotometry, and the Texas Department of Parks and Wildlife for permission to collect specimens. We especially appreciate the assistance of Susan Houghton, MBL, Woods Hole, MA, who sectioned and photographed the TEM material. This study was supported partially by NSF Grant 2610711250.

REFERENCES

Bernard, G. D. & Miller, W. H. (1968). Interference filters in the corneas of Diptera. *Invest. Ophthamol.* **7**, 416–434.

Biedermann, W. (1914). Farbe und Zeichnung der Insecten. In *Handbuch Vergleichende Physiologie*, (ed. H. Winterstein), pp. 1657–1994.

Bouligand, Y. (1972). Twisted fibrous arrangements in biological materials and cholesteric mesophases. *Tissue Cell.* **4**, 189–217.

CAMPBELL, F. L. (1929). The detection and estimation of insect chitin; the irrelation of chitinization to hardness and pigmentation of the cuticula of the American cockroach, *Periplaneta americana*. *Ann. ent. Soc. Am.* **22**, 401–426.

DELACHAMBRE, J. (1970). Etudes sur l'épicuticle des insectes. La développement de l'épicuticle chez l'adulte de *Tenebrio molitor* L. (Insecta: Coleoptera). *Z. Zellforsch. mikrosk. Anat.* **108**, 380–396.

DURRER, H. & VILLIGER, W. (1966). Schillerfarben der Trogoniden. *J. Orn., Lpz* **107**, 1–36.

DURRER, H. & VILLIGER, W. (1970). Schillerfarben des Goldcuckucks, *Chysococcyx cupreous* Shaw, im Elektronenmikroskop. *Z. Zellforsch. mikrosk. Anat.* **109**, 407–413.

DURRER, H. & VILLIGER, W. (1972). Schillerfarben von *Euchroma gigantea* L., elektronenmikroskopische Untersuchung der Elytren. *Int. J. Insect. Morph. Embryol.* **1**, 233–240.

FILSHIE, B. (1982). Fine structure of the cuticle of insects and other arthropods. In *Insect Ultrastructure*, Vol. 1, (eds R. C. King & M. Akai), pp. 281–312. New York: Plenum Press.

GAUMER, G. C. (1977). The variation and taxonomy of *Cicindela formosa* Say (Coleoptera: Cicindelidae). Ph.D. thesis, Texas A & M University. 253 pp.

GHIRADELLA, H., ANESHANSLEY, D., EISNER, T., SILBERGLIED, R. E. & HINTON, H. E. (1972). UV reflection of male butterfly: interference colour caused by thin-layer elaboration of wing scales. *Science, N.Y.* **178**, 1214–1217.

GLUUD, A. (1968). Zur Feinstruktur der Insektencuticula. Ein Beitrag zur Frage des Eigengiftschutzes der Wanzencuticula. *Zool. Jb. (Anat.)* **85**, 191–227.

GREENWALT, C. H., BRANDT, W. & FRIEL, D. (1960). The iridescent colors of hummingbird feathers. *Proc. Am. Phil. Soc.* **104**, 249–253.

GUPTA, B. L. & SMITH, D. S. (1969). Fine structure organization of the spermatheca in the cockroach, *Periplaneta americana*. *Tissue Cell* **1**, 289–324.

HACKMAN, R. H. (1974). Chemistry of insect cuticle. In *The Physiology of Insecta*, Vol. 6, (ed. M. Rockstein), pp. 216–270. New York: Academic Press.

HASS, W. (1916). Ueber Metallfarben bei Buprestiden. *Sber. Ges. natur. Freunde Berl.* 332–343.

HEPBURN, H. R. (1972). Some mechanical properties of crossed fibrillar chitin. *J. Insect Physiol.* **18**, 815–820.

HUXLEY, A. F. (1968). A theoretical treatment of the reflexion of light by multilayer structures. *J. exp. Biol.* **48**, 227–245.

LAND, M. F. (1972). The physics and biology of animal reflectors. *Prog. Biophys. molec. Biol* **24**, 75–106.

LOCKE, M. (1966). The structure and formation of the cuticulin layer in the epicuticle of an insect, *Calpodes ethlius* (Lepidoptera: Hesperiidae). *J. Morph.* **118**, 461–494.

MANDL, K. (1931). Künstliche Veränderung der Farben an *Cicindela nitida* Licht und an anderen *Cicindela*-Arten. *Z. Morph. Okol. Tiere* **22**, 110.

MASON, C. W. (1927). Structural colors in insects. *J. phys. Chem.* **31**, 321–354.

MOSSAKOWSKI, D. (1980). Reflection measurements used in the analysis of structral colours of beetles. *J. Microscopy* **116**, 350–364.

NEVILLE, A. C. (1975). *Biology of the Arthropod Cuticle*. Berlin: Springer-Verlag.

NEVILLE, A. C. (1980). Optical methods in cuticle research. In *Cuticle Techniques in Arthropods*, (ed. T. A. Miller), pp. 45–89. New York: Springer-Verlag.

NEVILLE, A. C. & CAVENEY, S. (1969). Scarabeidae exocuticle as an optical analogue of cholesteric liquid crystals. *Biol. Rev.* **44**, 531–562.

ONSLOW, H. (1920). The iridescent colours of insects. 1. The colours of thin films. *Nature, Lond.* **106**, 149–152.

RICHARDS, A. G. (1951). *The Integument of Arthropods*. St. Paul: University of Minnesota Press.

RICHARDS, A. G. (1967). Sclerotization and the localization of brown and black colors in insects. *Zool. J. (Anat.)* **84**, 25–62.

RUTSCHKE, E. (1966). Submikroskopische Struktur schillernder Federn von Entenvögeln. *Z. Zellforsch. mikrosk. Anat.* **72**, 432–443.

SCHULTZ, T. D. & RANKIN, N. A. (1985). Developmental changes in the interference reflectors and colorations of tiger beetles (*Cicindela*). *J. exp. Biol.* **117**, 111–117.

SHELFORD, V. E. (1917). Color and color pattern mechanisms of tiger beetles. *Illinois. biol. Monogr.* **3**, 4.

SPRUNG, F. (1931). Die Flugeldecken der Carabidae. *Z. Morph. Ökol. Tiere* **24**, 435–490.

STEGMANN, F. (1930). Die Flugeldecken der Cicindelidae. Ein Beitrag zur Kenntnis der Insektcuticula. *Z. Morph. Ökol. Tiere* **18**, 1–73.

VAN WISSELINGH, C. (1914). Anwendung der in der organishen Chemie gebräuchlichen Reaktionen bei der phytomikrochemischen Untersuchungen. *Folia microbiol., Delft* **3**, 165–198.

WIGGLESWORTH, V. B. (1933). The physiology of the cuticle and of ecdysis in *Rhodnius prolixus* (Triatomidae: Hemiptera) with special reference to the function of the oenocytes and of the dermal glands. *Q. Jl microsc. Sci.* **76**, 269–315.

WIGGLESWORTH, V. B. (1972). *The Principles of Insect Physiology*. London: Chapman & Hall.

ZACHARUK, R. Y. (1972). Fine structure of the cuticle, epidermis, and fat body of larval Elateridae (Coleoptera) and changes acquainted with molting. *Can. J. Zool.* **50**, 1463–1487.

ZELAZNY, B. & NEVILLE, A. C. (1972). Quantitative studies on fibril orientation in beetle endocuticle. *J. Insect Physiol.* **18**, 1095–2122.

calibrated frequently and zeroed against the level of the catheter tip. The pressure cannulae were introduced through 10-mm square pieces of rubber dam glued to the carapace over 1-mm holes drilled through the dorsal surface of each branchial chamber. Impedance electrodes (for measurement of scaphognathite frequency) were constructed from 0·1 mm diameter insulated copper wire. The impedance leads were introduced through 0.5-mm holes drilled in the carapace lateral to the positions of the scaphognathite and held in place by gluing a 1-cm square of rubber dam over the hole in the carapace. In some additional preparations a 5-mm diameter hole was drilled in the carapace at the top of each branchial chamber. The edges of the hole were cauterized, and a removable rubber plug was fitted into the hole. Removal of the plugs eliminated pressure fluctuations in one or both branchial chambers.

With the varying combinations of implanted branchial impedance electrodes and pressure cannulae, ventilatory variables could be assessed for forward and reversed pumping in left and right branchial chamber. Symbols in the text representing variables measured during forward scaphognathite pumping have been assigned the superscript 'f', while the superscript 'r' has been used to designate variables measured during reversed scaphognathite beating. The variables measured, and the symbols used to represent them are given below.

F_R^f, scaphognathite frequency, forward pumping (beats min^{-1}),
P_{Br}^f, branchial pressure, forward pumping (mmHg),
P_P^f, branchial pulse pressure, forward pumping (mmHg),
F^r, frequency of reversal episodes (episodes min^{-1}),
F_R^r, scaphognathite frequency, reversed pumping (beats min^{-1}),
P_{Br}^r, branchial pressure, reversed pumping (mmHg),
P_P^r, branchial pulse pressure, reversed pumping (mmHg),
t_A, apnoea length (s).

Each of these variables could be measured independently for both left and right scaphognathite.

In five crabs ventilatory flow was measured by fitting a face mask, made from the base and neck of a rubber balloon, over the anterior portion of the carapace, as modified from McMahon & Wilkens (1977). The edges of the balloon were glued to the carapace with cyanoacrylate glue, ensuring a gas-tight seal. Inserted into the open end of the neck of the balloon was a 10-mm diameter T-connector. One open arm of the T-connector was directed ventrally to the bottom of the experimental chamber. The chamber contained a 2-cm layer of brackish water (50 % sea water), so that the ventral opening of the connector always rested below the water surface. This ventral arm of the connector provided a route by which any water pumped up into the face mask during forward pumping could be drained back to the chamber. However, since its opening was below the water surface, it could not serve as a site of air entry into the face mask. The dorsally directed arm of the connector, which provided a low resistance inlet for fresh air to flow into the face mask, also contained a hot-wire anemometer (HWA 104, Thermonetics Co., San Diego), the output of which was directed to one channel of the chart recording system. A catheter inserted into the connector between the hot wire anemometer and the face mask was attached to a suction pump drawing gas at a constant rate of 45 ml min^{-1}. When the crab was in a ventilatory pause, the signal from the anemometer indicated a constant gas flow

through the mask of 45 ml min^{-1}. When the crab pumped gas forward out of the exhalant canals into the mask, the flow of fresh air past the anemometer sensor and into the face mask generated by the suction pump was reduced by the exact amount of gas added to the face mask from the branchial chambers by forward scaphognathite pumping. During reversed scaphognathite pumping, gas from the face mask was being removed to ventilate the branchial chambers, as well as being removed by the suction catheter. This combined effect resulted in an increase in flow of fresh air past the hot-wire anemometer which was exactly proportional to the ventilatory volume during reversed beating. The frequency response of this system was extremely rapid, and allowed resolution on the recorder of individual movements of the scaphognathites. After each experiment the anemometer sensor was removed from the face mask and calibrated by directing known flows of air past it.

Circulatory variables

Typically, three or four 1-mm diameter holes were drilled through the carapace in the vicinity of the heart. Copper electrodes glued into two of these holes were used for measurement of heart beat by an impedance technique. The other holes were sealed with squares of rubber dam. A 40-cm long PE 160 catheter fitted with a PE 60 tip was used for recording intracardiac haemolymph pressures. The tip of this catheter was introduced through the dam at the midline of the carapace and advanced ventrally 3 mm into the lumen of the heart. This catheter was filled with filtered sea water and attached to a P–1000B pressure transducer and the rectilinear recorder described above. The pressure signal from the transducer was also sent to a Narco Biotachometer which computed and displayed instantaneous heart rate on the recorder. A similar catheter arrangement was used for measurement of pericardial pressure immediately outside of the heart, with the catheter tip advanced ventrally 2 mm through the carapace at a position 1 cm off the crab's midline. Cardiac and pericardial cannulation caused minimal disturbance to the crab (see Results).

Experimental protocols

In some preliminary experiments, crabs fitted only with impedance electrodes were allowed overnight recovery and acclimation to the experimental chamber before measurements were begun. In the remainder of the experiments, restrained crabs were allowed at least 1 h to recover from surgery and handling during restraint before measurements were begun. Animals in the latter experiments were clearly not 'undisturbed', but had stopped struggling against restraint during this period. If released from restraint, these crabs were immediately fully active and aggressive, indicating that they were not fatigued or otherwise severely disturbed by the experimental conditions.

Instrumented crabs were examined with an experimental protocol involving several experimental conditions. Cardio-ventilatory variables were measured during a 1-h period when air was the only available respiratory medium, and for additional 1-h periods when a 2-cm aerated layer of 100 % sea water, 50 % sea water or fresh water was placed in the bottom of the chamber. Crabs were never denied access to air, since we rarely observed voluntary total submergence in water in their natural habitat on the Atlantic coast of Panama.

Statistical analyses

All data were analysed for mean values ±1 S.E. Analysis of variance (ANOVA) was used to assess treatment effects. Where significant effects were found, Student's *t*-test for independent means (unless otherwise indicated) was used to determine the significance level of differences between particular means. A significance level of 0·05 was used in all statistical procedures.

RESULTS

The respiratory surfaces of *Cardisoma guanhumi* are ventilated by forward or reversed pumping by the scaphognathites located at the anterior margin of each branchial chamber. Whether water or air is the respiratory medium used by *Cardisoma* when it stands in shallow water depends largely upon the positioning of the Milne-Edwards openings and exhalant channels. During forward pumping in shallow (1–4 cm) water, an undisturbed crab adjusts its posture so that its horizontal plane is roughly parallel to the water surface. This usually places the openings of both the Milne-Edwards and exhalant channels at the air–water interface (Fig. 1A). Under these conditions much air in addition to water is drawn into the Milne-Edwards openings, and the gas exiting the exhalant canals anteriorly creates a constant stream of air bubbles at the water surface.

At the onset of a period of reversed scaphognathite beating in an undisturbed crab, a marked postural change occurs such that the plane of the carapace pivots upwards anteriorly (Fig. 1B). The crab lowers the limb bases and Milne-Edwards openings, completely submerging them in the water, and raises the openings of the exhalant channels well above the water surface. Air is drawn into the exhalant channels during reversed breathing, and a large stream of gas bubbles is forced out from the ventral region of the branchial chambers *via* the Milne-Edwards openings and rises to the water surface.

Effects of acclimation, restraint and cardiac cannulation

Since a variety of different techniques was used in this study, it was important first to define carefully the specific limitations of each technique, before discussing quantitative details of cardio-ventilatory patterns or experimental treatment effects.

Restraint

Ventilatory variables for both left and right scaphognathite as well as heart rate, all measured through impedance techniques, were measured 1–4 h after electrode attachment in both unrestrained and restrained crabs. All crabs had access either to air alone or to air and 50% sea water as indicated above. In air alone, none of the ventilatory parameters measured for either right or left scaphognathite nor heart rate were significantly altered by restraint ($P > 0{\cdot}10$).

When 2 cm of 50 % SW was placed in the chamber, heart rate and most parameters for forward pumping for either right or left scaphognathite were also not significantly different between restrained and unrestrained crabs. Only the length of the apnoeic

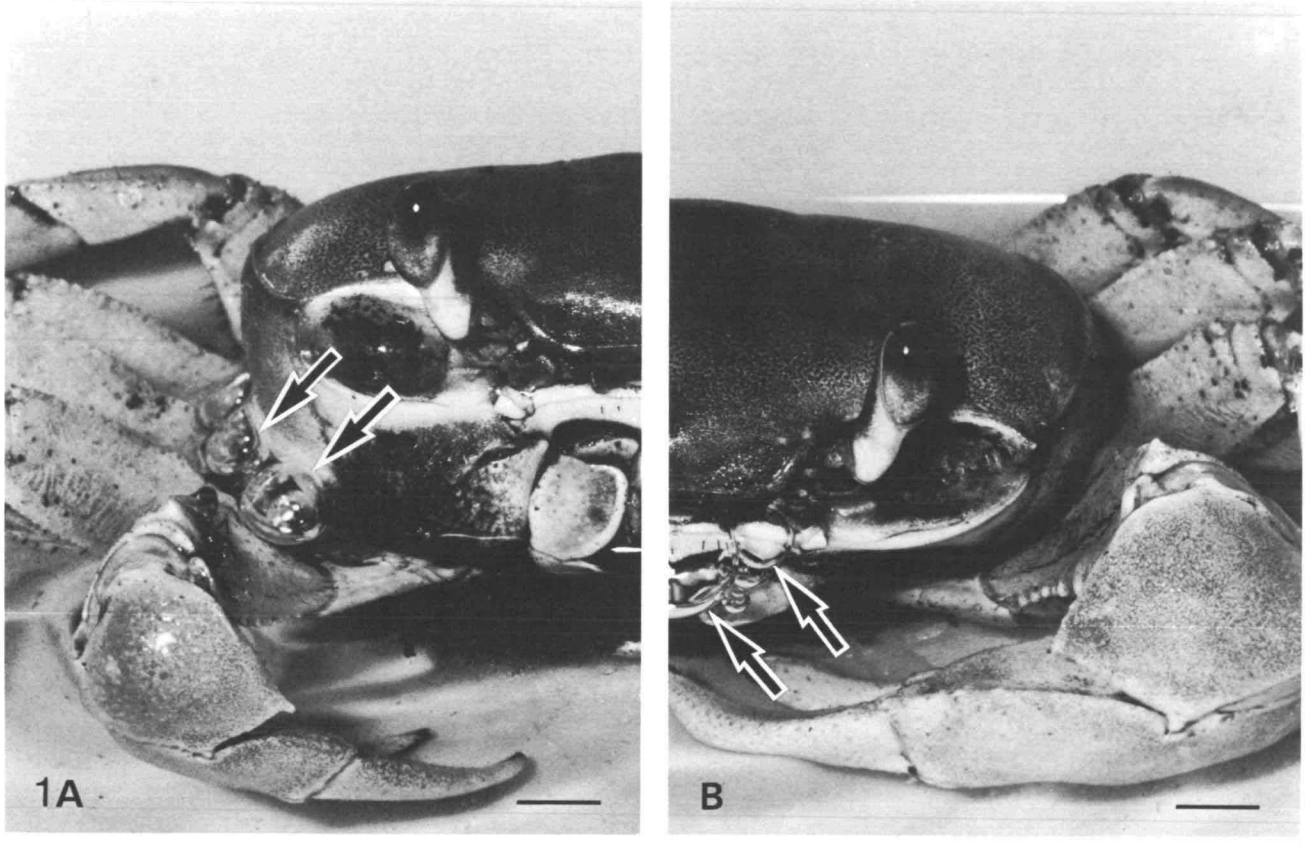

Fig. 1. Postural adjustments during branchial chamber ventilation in a land crab, *Cardisoma guanhumi*, resting in 3 cm of 50% SW. A and B were photographed from identical camera angles. (A) The posture during forward scaphognathite beating, in which the exhalant channels are held just at or below the water level. Note the bubbles of air (arrows) gathering around the exhalant channels. (B) The posture during reversed scaphognathite beating, in which the exhalant canals are elevated well above the surface of the water to allow air entry. Note the bubbles of air gathering around the Milne-Edwards openings (arrows). Scale bars, 1 cm. See Results for further details.

period of the right scaphognathite (but not the left) was significantly affected ($P<0{\cdot}05$), decreasing from $0{\cdot}5\pm0{\cdot}5$ min to $0{\cdot}1\pm0{\cdot}1$ min, but the effect was nonetheless not large enough to change significantly the beat frequency of the right scaphognathite. The frequency of reversal periods by both scaphognathites (3·3–4·9 periods min^{-1}) was not significantly influenced by restraint in crabs in 50 % SW, but the frequency of pumping within each period of reversed beating was significantly elevated ($P>0{\cdot}05$) in restrained crabs (23·1 beats min^{-1}) compared with unrestrained crabs (6·8 beats min^{-1}).

Patterns in left vs *right scaphognathite* (*i.e. 'handedness'*)

In some decapod Crustacea ventilatory patterns are characterized by very close coupling of left and right scaphognathite events, while in others the scaphognathites may drift in and out of phase, or even show unilateral pausing (Taylor, 1982; McMahon & Wilkens, 1983). In the present experiments, if cardiac and pericardial pressures were being measured simultaneously, the recorder channels remaining were sufficient only to monitor ventilatory events on one side of the crab. Since it was important to know whether the pattern of a single scaphognathite recorded under these circumstances was representative of both scaphognathites, a series of crabs was prepared in which both left and right scaphognathite patterns could be recorded.

Although there was very occasionally phase drifting or unilateral apnoea in *Cardisoma*, left and right scaphognathites were usually absolutely coupled under all experimental situations (i.e. unrestrained or restrained, in air or with access to 50 % sea water, before or after cardiac cannulation). In fact, the differences in mean values of all ventilatory parameters for right and left scaphognathites of each crab were not significantly different from zero ($P>0{\cdot}10$, Student's t-test for dependent means). Thereafter patterns of scaphognathite beating recorded from one side were assumed to be representative of both sides.

Cardiac cannulation

Ventilatory parameters and heart rate of restrained crabs with access to 50 % SW were measured immediately before and 30 min after cannulation of the heart. Cardiac cannulation caused no significant ($P>0{\cdot}10$) change in F^{f}_{R}, P^{f}_{Br}, P^{f}_{P}, F^{r}, P^{R}_{Br}, P^{R}_{P} or t_A of the right scaphognathite. Similarly, left scaphognathite pumping was not significantly affected by cardiac cannulation, with the exception of a significant but small decrease in F^{r} and rise in t_A. Importantly, heart rate was not significantly ($P>0{\cdot}10$) altered by cardiac cannulation.

In general, then, *Cardisoma guanhumi* tolerated restraint, instrument implantation and experimental manipulation very well. Since restraint or cannulation produced only small quantitative, rather than qualitative, changes in only a few of the respiratory and cardiac variables (and since unrestrained *Cardisoma* showed amazing ingenuity and dexterity in destroying implanted leads), the data which follow were recorded solely from restrained crabs unless otherwise indicated.

Ventilatory patterns and influence of respiratory medium

When ventilating with air alone, predominantly forward directed scaphognathite pumping generated subambient pressures in the branchial chamber. This produced

a ventilatory flow which was primarily forward through the branchial chamber and out of the exhalant canals (Fig. 2A). A quantitative analysis of ventilation (Fig. 3) reveals that scaphognathite frequencies during forward ventilation were about

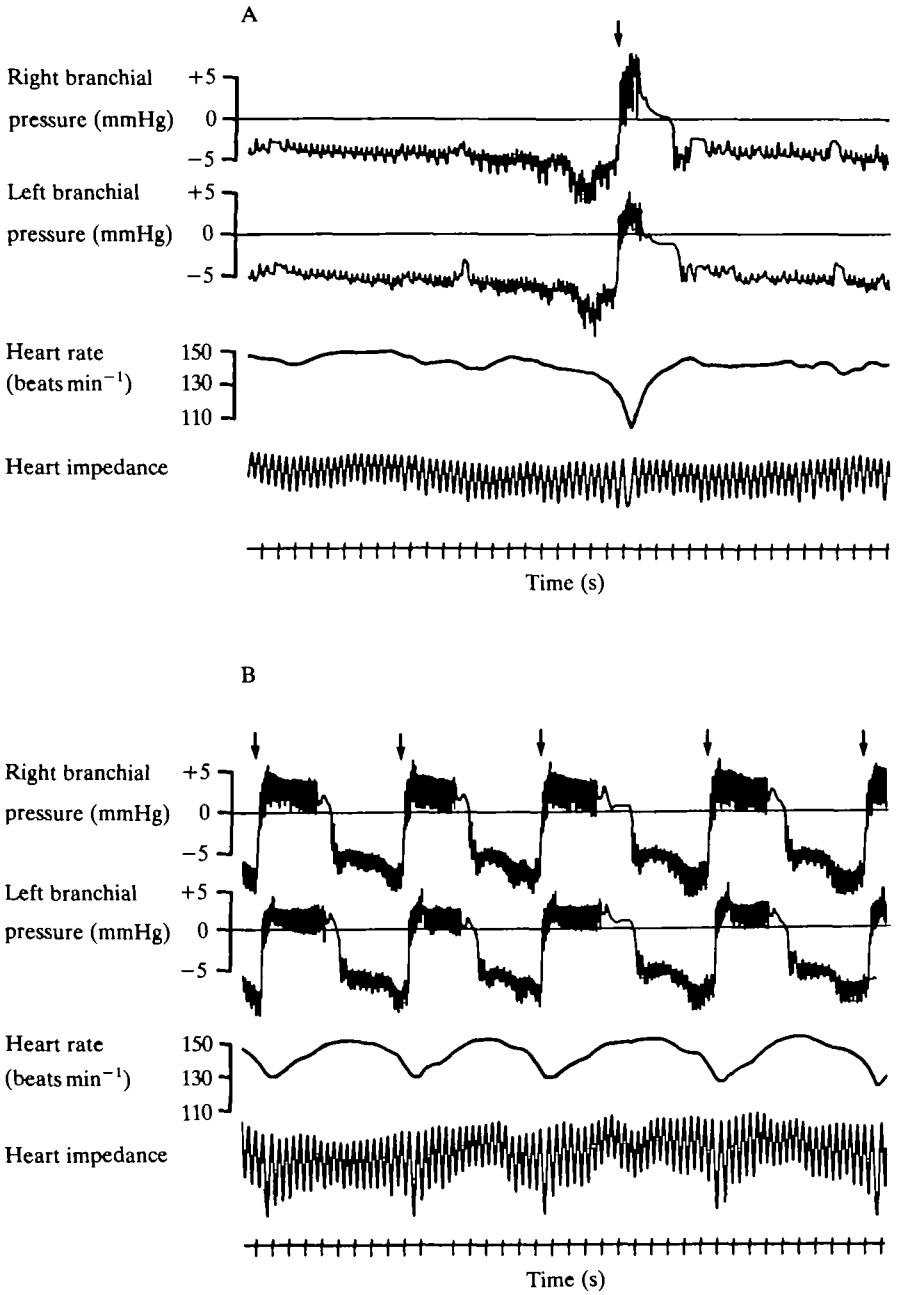

Fig. 2 Representative records of branchial pressures and heart impedance and rate in a restrained, 151 g *Cardisoma guanhumi*. (A) Patterns measured during total air exposure, which resulted in primarily forward scaphognathite beating. (B) Ventilatory patterns with frequent periods of reversals (arrows) stimulated by placement of the crab in 2 cm of 50 % SW.

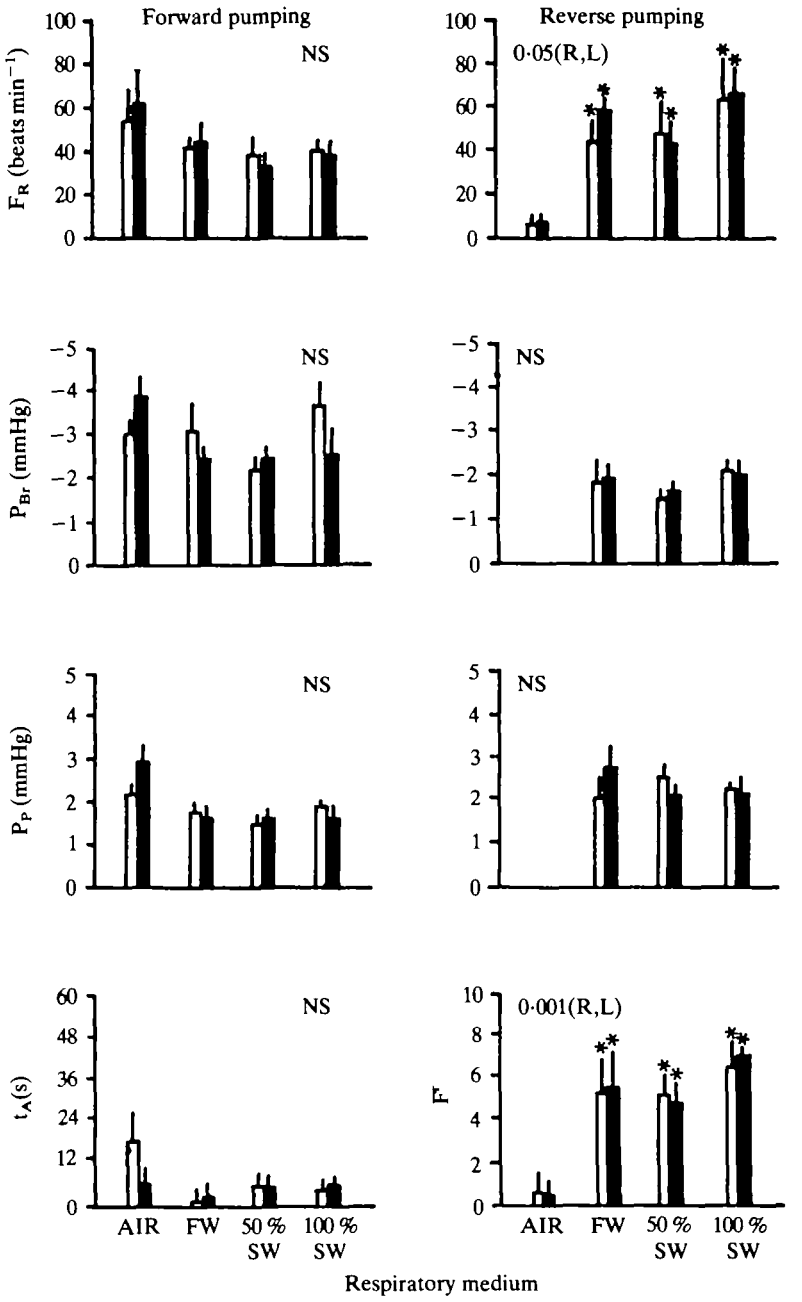

Fig. 3. Effect of ventilatory medium on scaphognathite frequency (F_R), branchial (P_{Br}) and branchial pulse (P_P) pressures, length of apnoea (t_A) and frequency of reversal episodes (F^r) during forward and reversed beating in *Cardisoma guanhumi*. Mean values ± 1 S.E. are presented for both left (L, white bars) and right (R, black bars) scaphognathites. Number of crabs analysed for each ventilatory medium are AIR = 8, FW (fresh water) = 7, 50 % SW = 8, and 100 % SW = 8. Results of analysis of variance for effect of ventilatory medium are shown in the upper region of each panel. Where significant treatment effects were indicated, *t*-tests were performed to reveal significant differences between ventilatory media. Thus, asterisks indicate significant differences from values measured with air as the ventilatory medium. *, $P<0·05$; **, $P<0·01$. See text for additional details. NS, not significant.

50–60 beats min^{-1}. Apnoeic episodes were infrequent and irregular (1 episode every 3–5 min) and lasted only 5–20 s. Intrabranchial pressures during forward beating were 3–4 mmHg subambient, with a pulse pressure of 2–3 mmHg. When ventilating with air, less than one reversal episode occurred per minute.

When *Cardisoma* was provided access to water and could thus partially submerge one or both of the Milne-Edwards openings, several important aspects of the ventilatory patterns were affected. Whereas F_R^F, P_{Br}^f, P_P^F and t_A remained unchanged, the frequency with which reversals occurred increased 10–15 times (Fig. 3). Not only did reversals occur more often, but the frequency of scaphognathite beating during these reversals was elevated several times compared with strictly aerial ventilation. Apnoeic episodes of significant length still occurred quite infrequently and irregularly when access to water was provided, although in some crabs a ventilatory pause of a few seconds occasionally followed a period of reversed scaphognathite beating.

Values for each ventilatory parameter measured when the crab had access to fresh water, 50 % sea water or 100 % sea water were statistically identical. Therefore, these changes in respiratory pattern were apparently related to use of water *versus* air as a respiratory medium, rather than to water quality *per se*.

Fig. 4 shows a representative recording of branchial pressures and gas flow at the exhalant canals during forward and reversed beating in a *Cardisoma* with access to both air and 50 % sea water. Mean values ($N = 5$ crabs) of right scaphognathite

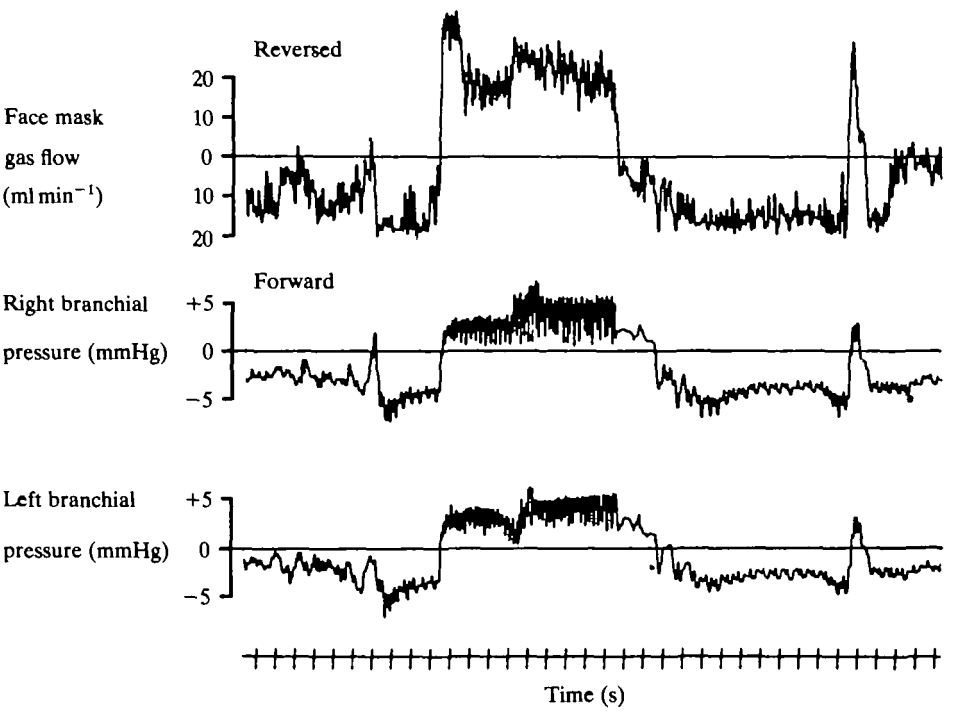

Fig. 4. Representative records of branchial pressures and of gas flow through the face mask of an 80 g *Cardisoma guanhumi* resting in approximately 2 cm of 50 % SW. Periods of reversed scaphognathite beating are characterized by positive branchial pressures and reversed gas flow through the face mask.

frequency, total gas flow into and out of the face mask during forward and reverse flow, respectively, and stroke volume of the scaphognathite pair (assuming equal frequency of left and right scaphognathites, see above) are presented in Fig. 5. Both stroke volume and gas flow were significantly greater during reversed beating than forward beating. From mean values for restrained crabs without face masks (Fig. 3),

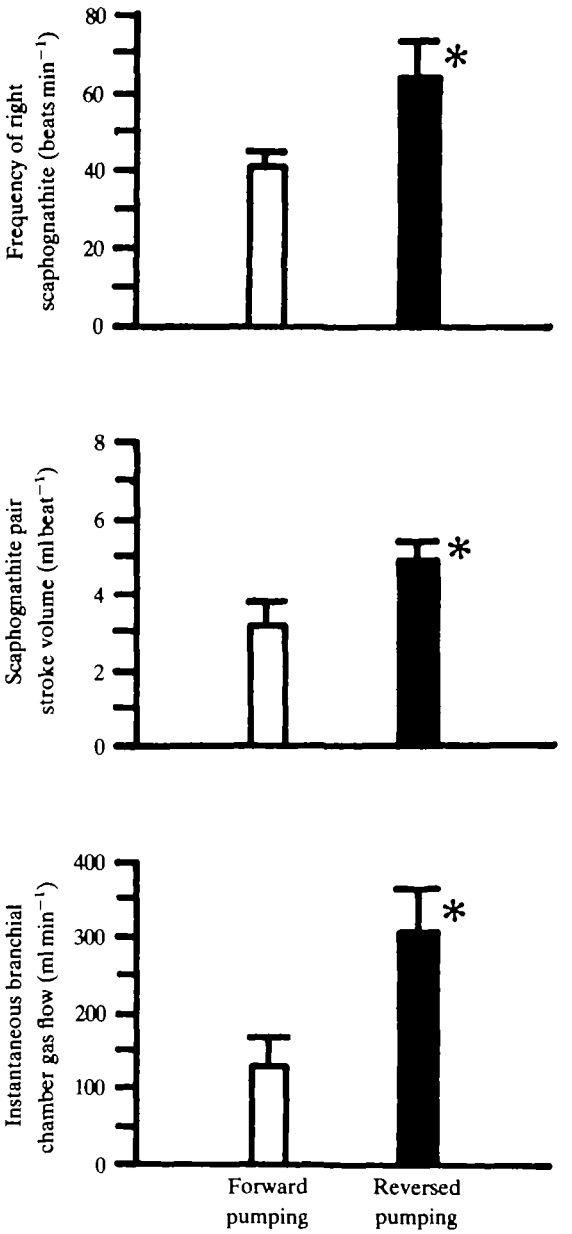

Fig. 5. Scaphognathite frequencies, stroke volumes and gas flows measured during forward and reversed pumping in five *Cardisoma guanhumi*. Mean values ± S.E. are given. Asterisks next to data for reversed pumping indicate significant difference ($P<0{\cdot}05$) from forward pumping.

it can be calculated that, during constant ventilation in *Cardisoma* with access to both 50% SW and air, forward ventilation occupies 36 s of every minute compared with 24 s for reversed ventilation. Given the differences in flow rates for the two directions of pumping (Fig. 5), this indicates that for every minute of scaphognathite ventilation approximately 125 ml kg^{-1} of gas are pumped out posteriorly from the Milne Edwards openings and 70 ml kg^{-1} of gas are pumped out anteriorly through the exhalant channels. This corresponds to 34% of total gas flow being generated by forward pumping compared with 66% by reversed pumping.

Measurements of forward and reversed gas flow were not made in crabs with access to air only, and we do not know if scaphognathite stroke volume changes under this condition. However, assuming an identical stroke flow to that measured when access to 50% SW was provided, and using the mean ventilatory rates and ratios of totally air-exposed crabs provided in Fig. 3, then estimated forward and reverse gas flow changed dramatically to approximately 98% and 2% of total flow, respectively.

Circulatory patterns and cardio-respiratory interaction

Circulatory variables, including haemolymph pressure, were measured in a total of 24 *Cardisoma guanhumi* exposed to air but with access to 50% SW. Mean values are

Table 1. *Circulatory variables measured in the land crab* Cardisoma guanhumi

	Mean ± 1 S.E.	Number of crabs measured
Heart rate (beats min^{-1})	134 ± 7	18
Intracardiac systolic pressure (mmHg)	14·1 ± 0·7	24
Intracardiac diastolic pressure (mmHg)	5·5 ± 0·7	24
Pericardial systolic pressure (mmHg)	8·4 ± 2·9	5
Pericardial diastolic pressure (mmHg)	6·1 ± 2·5	5

Crabs were restrained and had access to a 2-cm layer of 50% SW.

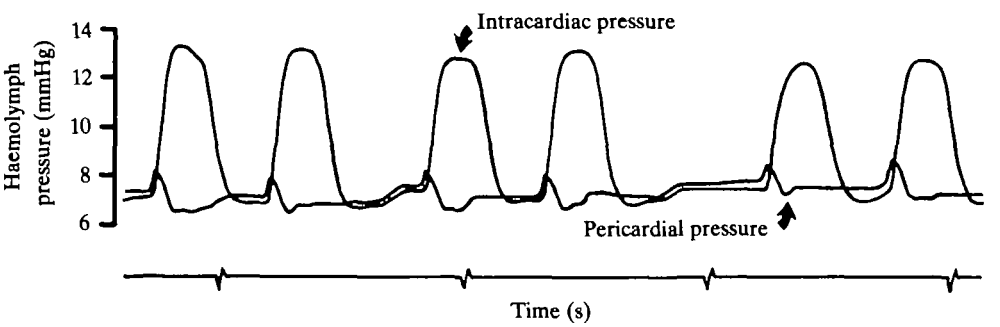

Fig. 6. Haemolymph pressure measured in the pericardial space and in the heart of a 159 g *Cardisoma guanhumi*.

given in Table 1, while Fig. 6 shows representative simultaneous recordings of intracardiac and pericardial pressures.

As is typical for the few decapod circulations investigated to date, intracardiac systolic pressure was generally below 20 mmHg and diastolic pressure several mmHg above ambient pressure. A pressure gradient from pericardial space to heart lumen of about 0·4–1·0 mmHg existed throughout diastole, and provided the driving pressure for cardiac filling. At the onset of systole, haemolymph pressure in the pericardium began to rise concomitantly with intracardiac pressure, suggesting open communication of the pericardium with the interior of the heart. After increasing by 1–3 mmHg, pericardial pressures fell back to diastolic levels while intracardiac pressures continued to rise, indicating effective closure of the ostial valves at this time.

Although mean circulatory variables were quite constant in individual crabs over an extended time period, both locomotor activity and changes in ventilatory patterns induced transient changes. The most consistent changes in circulatory parameters accompanied the transient changes from forward to reversed beating (Figs 7,8). Both systolic and diastolic intracardiac pressure began to increase within 0·5–2 s of the onset of a reversal, with both values having risen significantly (ANOVA, $P < 0{\cdot}001$) by approximately 2–3 mmHg by the end of the reversal period. A significant decrease in heart rate of about 10 beats min^{-1} occurred concomitantly with reversal of scaphognathite beat and rise in intracardiac haemolymph pressure. Immediately after the end of the reversal episode, both heart rate and intracardiac haemolymph pressure returned

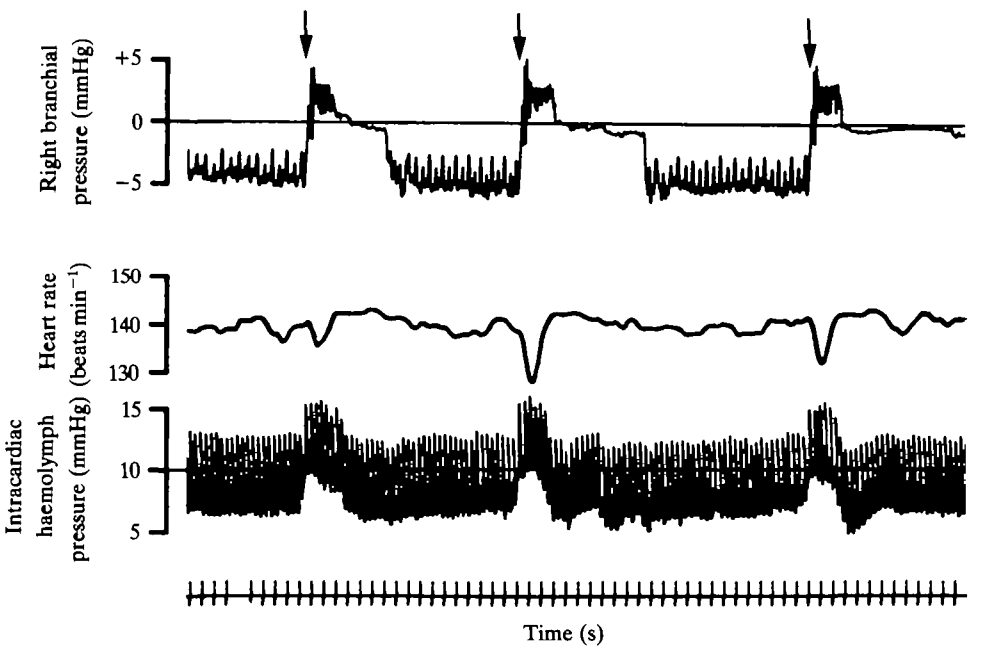

Fig. 7. Representative records of branchial gas pressure, intracardiac haemolymph pressure and heart rate during periods of both forward and reversed scaphognathite beat in a 142 g *Cardisoma guanhumi* with access to 50 % SW. Periods of reversed scaphognathite beating occur when branchial pressure swings to positive values (arrows).

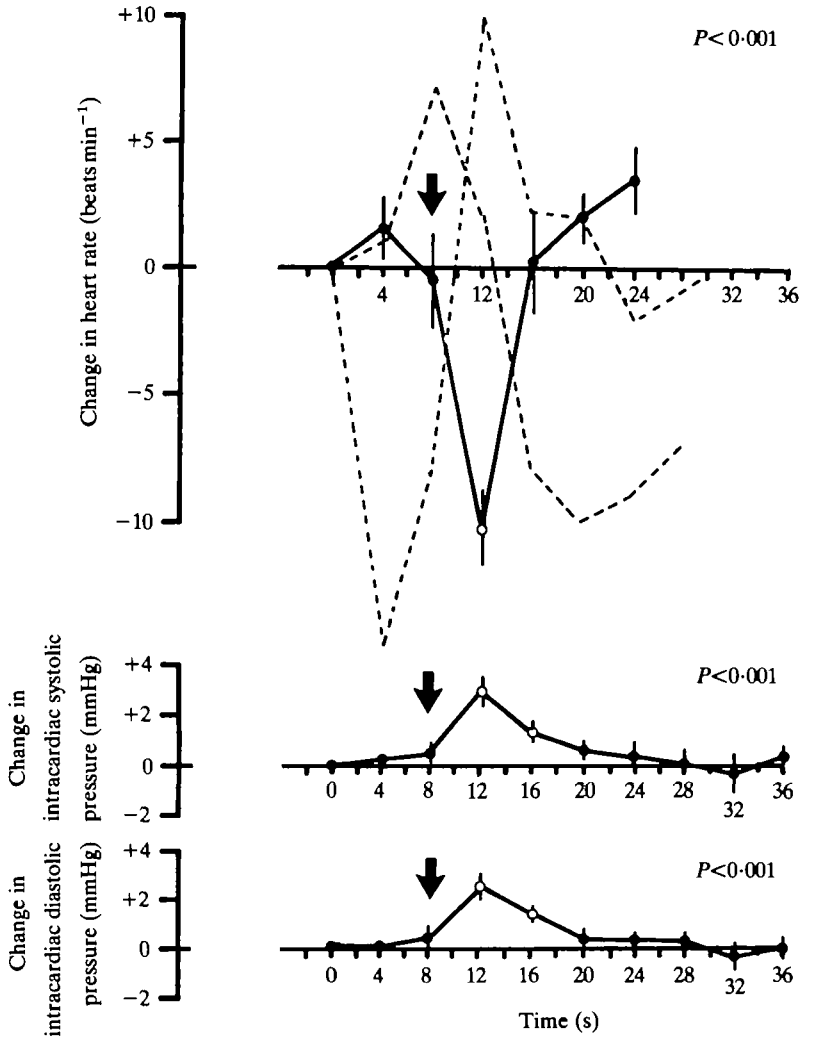

Fig. 8. Changes in heart rate and in intracardiac systolic and diastolic pressure before, during and after reversed scaphognathite beating in *Cardisoma guanhumi*. All crabs had access to 50% SW. Mean values ± 1 S.E. for five crabs are presented. Arrows indicate the onset of reversed beating, which lasted 4–10 s. Results of analysis of variance of means of each time class are shown in the upper right of each panel. Open circles represent means significantly different from values at time zero. The dashed lines indicate heart rate for two additional crabs showing atypical time courses associated with the onset of reversed scaphognathite beating.

to levels not significantly different ($P > 0{\cdot}10$) from before the onset of the reversal.

Interestingly, in two otherwise apparently normal crabs, quite different heart rate patterns were associated with spontaneous scaphognathite reversals (dashed lines, Fig. 8). In both these individuals, heart rate began to change 3–6 s before the onset of reversal, and in one crab the bradycardia was greatest about 10 s after the end of the reversal episode.

Additional experiments were performed on those *Cardisoma guanhumi* fitted with rubber plugs in the carapace. When the branchial plugs were in place, normal

pressures above and below ambient accompanied reversed and forward beating, respectively, and a transient bradycardia occurred during episodes of reversed beating. Removal of the rubber plugs inserted into the 5-mm diameter hole in the top of each branchial chamber, which opened the system to the atmosphere, eliminated

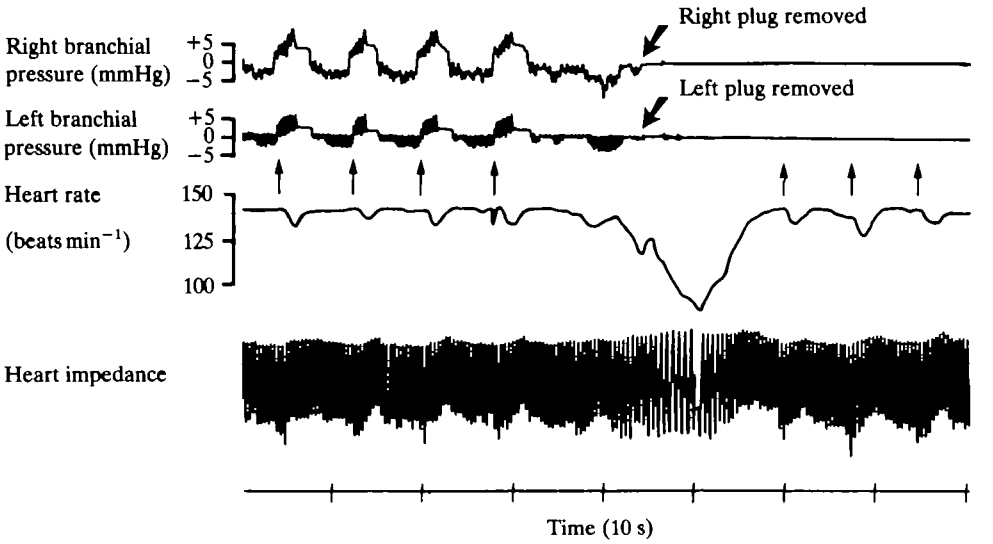

Fig. 9. Effects on branchial pressure and heart rate of *Cardisoma guanhumi* produced by removal of 'branchial plugs' from the carapace (large arrows). Small, upward pointing arrows indicate brief periods of reversed scaphognathite beating. Note that branchial gas pressure fluctuations disappear after the plugs are removed, but that the transient bradycardia associated with reversed scaphognathite beating persists. See text for details.

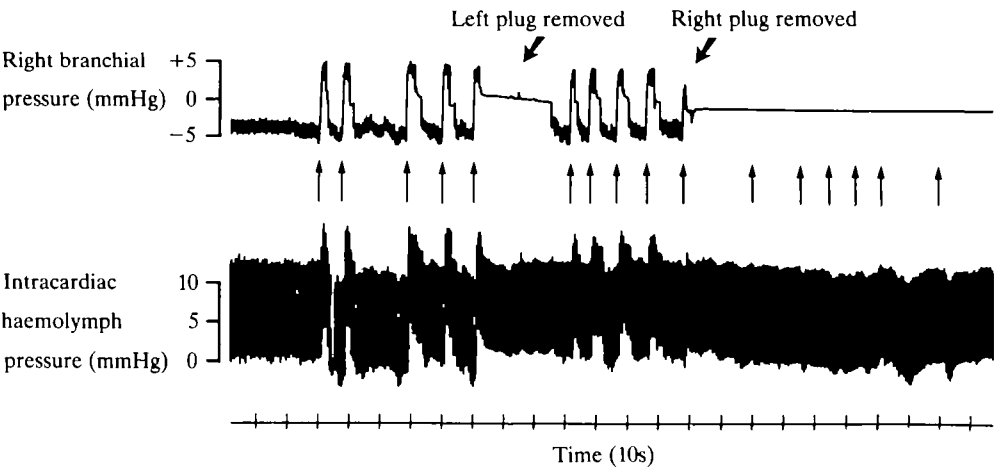

Fig. 10. Effects of sequential removal of left and right 'branchial plugs' on intracardiac haemolymph pressure in a 198 g *Cardisoma guanhumi* with access to 50% SW. Upward arrows indicate brief periods of reversed scaphognathite beat.

J. exp. Biol. **117**, 111–117 (1985)
Printed in Great Britain © *The Company of Biologists Limited 1985*

DEVELOPMENTAL CHANGES IN THE INTERFERENCE REFLECTORS AND COLORATIONS OF TIGER BEETLES (*CICINDELA*)

BY T. D. SCHULTZ AND M. A. RANKIN

Department of Zoology, University of Texas, Austin, Texas 78712, U.S.A.

Received 4 December 1984

SUMMARY

Samples of cicindelid cuticle were examined at various stages of adult ecdysis. The multilayered potential reflector was secreted in the initial stages of the moult, verifying that it is not tectocuticle and supporting the contention that it is a form of inner epicuticle. At early stages of ecdysis, the electron-dense layers were visible only when the section was post-stained. During post-ecdysial colour development, the dense layer increased in inherent electron density. Concurrently, the reflector increased in refractive index and the interference coloration increased in intensity and wavelength of maximum reflectance. Black pigment was also deposited simultaneously within the outer portion of the cuticle. It is proposed that electron-dense material was deposited *in situ* within the inner epicuticle after ecdysis, thereby increasing the wavelength and reflectance of interference colour.

INTRODUCTION

Schulze (1913) and Stegemann (1930) described the iridescent colour-producing layer of tiger beetle (Cicindelidae) cuticle as a 'Sekretschicht' or secretory layer produced by epidermal glands after ecdysis. This layer appeared as a superficial, thin, dark layer in cross-sections of elytra under optical microscopy (Stegemann, 1930). A gradual increase in thickness of this dark layer was interpreted as the discharge of a pigmented fluid over the surface of the pharate exoskeleton. Subsequently, the 'Sekretschicht' has been assumed to be a form of tectocuticle (Richards, 1951) or cement layer (Wigglesworth, 1972).

Detailed observations of post-ecdysial colour changes in cicindelids were made by Shelford (1917) and Willis (1967). In all of the species studied, the interference colours of the cuticle progressed from short to long wavelength colours during a 48-h period following emergence from the pupal exuvia. Simultaneously, the cuticle became pigmented and opaque to transmitted light. Histological or ultrastructural changes were not considered in these two studies.

Key words: Interference colour, epicuticle, *Cicindela*.

Schultz & Rankin (1985) identified the source of structural colours in tiger beetle (*Cicindela*) integument as epicuticular by virtue of its location, ultrastructure and reaction to solvents. The inner epicuticle consists of alternating layers of electron-dense and electron-lucent material which serve as a multilayer interference reflector. The reflective cuticle is located in the outer 2 μm of the exoskeleton. Cuticular layers below the reflective cuticle exhibit exocuticular characteristics.

In this study, the development of the cuticular reflector was investigated. Since the reflected colour directly relates to the optical thickness of the reflecting layers, development of these layers may be observed through the development of the interference coloration. The ultrastructure of developing cuticle was examined at different stages of colour development by transmission electron microscopy. The time of deposition of the reflecting layers also served to identify the layer according to current concepts of cuticle development and structure.

MATERIALS AND METHODS

Populations of larval and adult *C. scutellaris* Vaurie and *C. splendida* Hentz were counted over a period of 2 years (1979–1980) in Bastrop State Park, Texas. The approximate date of pupation was determined by census data and observations of larval activity.

Third instar larvae and pupae were excavated from their burrows and reared to adulthood in the laboratory. Larvae were placed in glass tubes, 70 cm × 30 mm. The extreme length was necessary for *C. scutellaris* whose burrows often exceed 50 cm. Tubes were packed with specific soils from oviposition sites in the field (Patilo soils for *C. scutellaris*, Axtell soils for *C. splendida*), and were placed vertically in a growth chamber with a photoperiod of 12·5 h light and 11·5 h dark. The sand was moistened every 6 days from the top of the tube. Larvae were fed *Tenebrio* larvae and adult *Tribolium confusum*.

Pupae were placed in opaque plastic cups. Each cup was padded with cotton, which formed an artificial pupal chamber. The artificial chamber was critical in ensuring that the imago would shed the pupal exuvia successfully. The cotton was moistened periodically with a solution of 1·5 % H_2O_2 to prevent mould developing. The development of adult colour was observed under a dissecting microscope.

Elytral cuticle was cut from developing *C. scutellaris* 4 days before ecdysis (10 days after pupation), 12 h after ecdysis, and 14 days after the moult. Strips of cuticle were prepared for transmission electron microscopy (TEM) as described previously (Schultz & Rankin, 1985). Sections of pharate and adult cuticle were both post-stained and left unstained. Post-staining consisted of 5 min in 1 % uranyl acetate in 50 % ethanol, followed by 5 min in lead citrate. All samples were examined under a Zeiss 10CA transmission electron microscope. Thin sections were also observed under optical microscopy.

RESULTS

The colour development of the tiger beetles, *C. splendida* and *C. scutellaris*, showed a progressive increase in peak reflected wavelength to the mature adult colour. Since the reflector is composed of multiple layers (Schultz & Rankin, 1985), there

must be either a gradual addition of layers which reflect longer wavelengths, or a gradual increase in the optimal thickness of the layers themselves. Electron microscopy, coordinated with observations of colour development, supported the latter interpretation. Since the ultimate colour of *C. splendida* is red, the sequence of colour development was longer, but essentially the same as that of *C. scutellaris*. For the sake of brevity, only the observations of *C. scutellaris* will be described.

The pharate elytron, 4 days prior to ecdysis, was pale white or cream with a slight violet iridescence. Electron micrographs revealed that the presumptive epicuticle (region *A*), and part of the exocuticle (region *B*), had already been deposited by this time (Fig. 1). The epicuticle was already composed of a full complement of bands, but the presumptive dense bands were thinner (15–40 nm thick) than they appear in mature cuticle, and were revealed only by post-staining (see Methods). In unstained sections, light 'negative shadows' appeared within the boundaries of the dark bands (layer *D* in Fig. 1). These could be distinguished from the grainy appearance of the potential electron-lucent bands (layer *L*). With post-staining, however, these areas appeared very dense, black and finely grained (Fig. 2). An electron-dense strip, 30 nm thick, was present in both stained and unstained sections at the outer border of the cuticle. The entire thickness of the epicuticle at this stage was 50–60 % thinner than in mature cuticle. No evidence of pigmentation was observable in optical cross-sections of the pharate elytron.

By the completion of ecdysis, the elytral colour had not changed substantially. Over the next 8 h, the basic colour of the cuticle darkened from white to a golden straw. The elytra were not yet pigmented, but displayed a distinctive violet hue. From 8 to 12 h after ecdysis, the iridescence became predominantly blue, and spread spatially over the elytron from base to apex. Simultaneously, the elytron blackened and became opaque. Pigmentation progressed through the elytron from base to apex, enhancing the lustre of the iridescence. By the 12th hour, all but the apical quarter of the elytron was pigmented, and it reflected a rich, blue colour. The apex was still violet and somewhat transparent.

Micrographs of cuticle 12 h after ecdysis showed that the epicuticle had assumed its surface microsculpture (Schultz & Rankin, 1985), and the outer exocuticle was fully formed (layers *A* and *B* in Fig. 3). Underlying layers of exocuticle (layer *C* in Fig. 3) were evident, but the formation of 'plywood' mesocuticle was yet to be initiated. The limits of the dense epicuticular bands were defined more clearly and expanded to approximately 80 % of their eventual thickness. However, they lacked the very dark granularity apparent in mature cuticle. Electron density decreased from outer to inner layers.

The elytra were entirely blue and pigmented 24 h after shedding the pupal exuvium. Over the following 6 h to 5 days the iridescent hue became progressively more green. All areas of the beetle became fully pigmented. The resistance of the elytron to superficial tears increased during this period, but the elytron did not become rigid and hardened for several days. In the field, this occurs after the adult has emerged from its pupal chamber. Drying undoubtedly facilitates elytral hardening. By the 14th day, the elytra and colour were developed fully.

Electron micrographs of mature cuticle show fully formed epicuticle, outer exocuticle and procuticular layers (Fig. 4). Although post-staining enhances the resolution

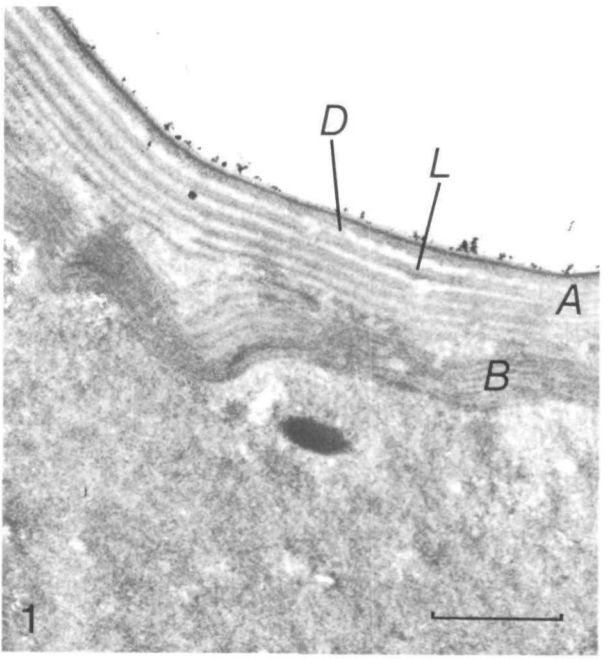

Fig. 1. Transmission electron micrograph of cross-section of pharate elytral cuticle 10 days after pupation. This section was not post-stained. The epicuticle (*A*) has been deposited and exhibits a multilayered ultrastructure. If not post-stained, the potential dense layers (*D*) appear less dense than the potential *L* layers. The outer exocuticle (*B*) has been partially deposited. Scale bar, 1 μm.

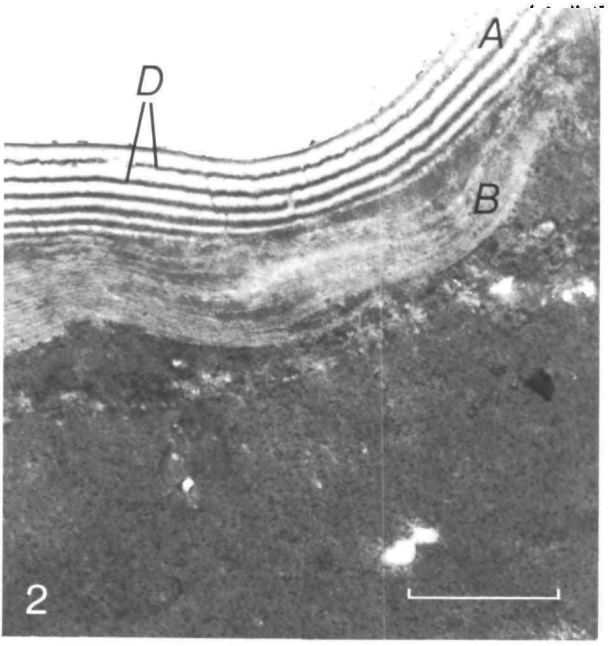

Fig. 2. Transmission electron micrograph of cross-section of pharate elytral cuticle 10 days after pupation. This section was taken from the same tissue as was the section in Fig. 1, but was post-stained with lead citrate and uranyl acetate. Structural features are the same, except that the potential *D* layers appear very dense and granulate. *A*, epicuticle; *B*, outer exocuticle. Scale bar, 1 μm.

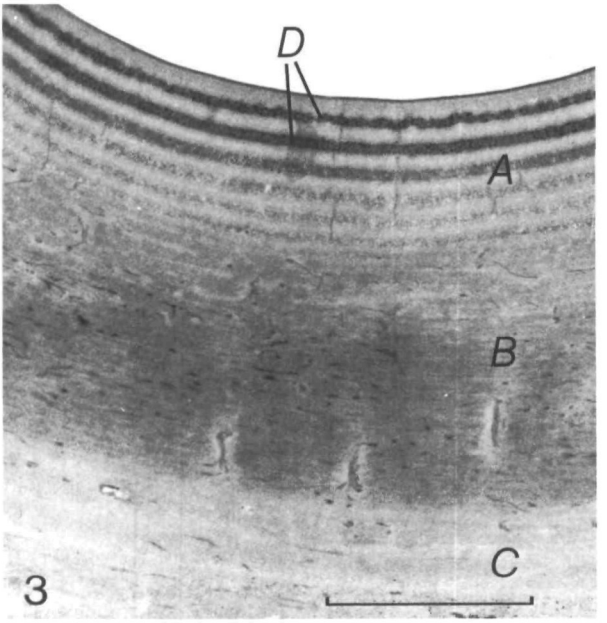

Fig. 3. Transmission electron micrograph of cross-section of elytral cuticle 12 h after ecdysis. The epicuticle (*A*) and outer exocuticle (*B*) are fully deposited. The inner exocuticle (*C*) is partially formed. The epicuticular *D* layers appear denser at this stage. Section was not post-stained. Scale bar, 1 μm.

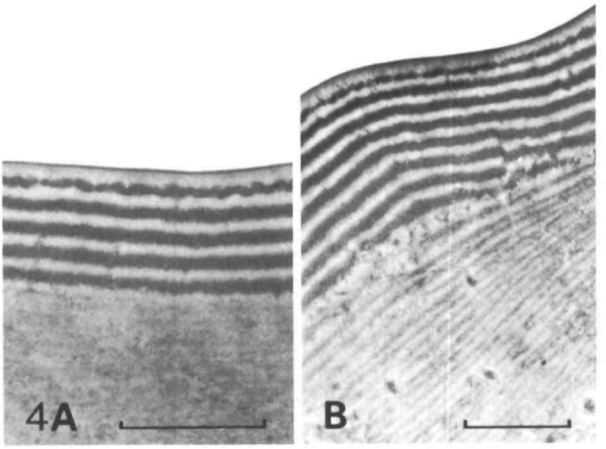

Fig. 4. Transmission electron micrograph of cross-sections of elytral cuticle 14 days after ecdysis. Epicuticular layers are fully developed and the electron density of the *D* layers is apparent in both unstained and post-stained sections. (A) Unstained; (B) post-stained. Scale bars, 1 μm.

of dense layers in the epicuticle (Fig. 4B), their high electron density is also apparent in micrographs of unstained sections (Fig. 4A).

DISCUSSION

The present study indicates that the potential cuticular reflector is formed prior to ecdysis, and therefore, cannot be considered as a dermal gland product. The early

deposition and location of the reflective layers indicate they are epicuticular. The first layer formed during a moult cycle is the cuticulin layer, followed by the inner epicuticle (Filshie, 1982). In pre-ecdysial samples of *C. scutellaris*, the potential reflective layers constitute the outer portion of newly formed cuticle, and display a thin, dense outer border, suggestive of a cuticulin layer. A partially deposited exocuticle appears below these layers and exhibits a helicoidal orientation of fibrils.

Micrographs of developing cuticle, and the continuity of dense layers produced by adjacent cells, indicate that a substrate or precursor is deposited during the initial formation of the epicuticle. The change in electron density of the dense layers suggests that a change in molecular chemistry occurs during the moult cycle. Either electron-dense material is deposited after formation of the epicuticle, or endogenous material within these layers is converted to compounds of higher electron density or affinity for OsO_4. Simultaneously, the colour of the newly emerged imago progresses from shorter to longer wavelengths, while dark pigmentation forms behind the reflecting layers. Although associated changes in refractive index cannot be determined, the increase in optical thickness of these layers must be responsible for the increasing wavelength of maximum reflectance observed during development.

In situ impregnations of developing cuticle have been reported previously. Wigglesworth (1976) described the spreading of a proteinaceous secretion within the epicuticle associated with sclerotization or melanization. It is generally assumed (Hackman, 1974) that a phenolic precursor of melanin is located in the integument at the site of pigmentation, perhaps as a by-product of sclerotization. This substrate is then assumed to be converted to melanin by an enzyme transported to this site *via* the pore canals.

Cicindelid pore canals contain materal substantially denser than the areas of exocuticle they traverse (Schultz & Rankin, 1985). Smaller extensions of the canals within the epicuticle possess electron-lucent lumina whose borders are dense. The dense contents of the pore canals may be substrates or enzymes dispersed in the exocuticle and epicuticle for sclerotization or pigmentation. If the dense epicuticular layers of cicindelids are melanoproteins formed *in situ*, the reaction entails a simultaneous increase in absorptivity and electron density.

These observations of colour development agree with those of Shelford (1917) and Willis (1967) for several *Cicindela* species. Shelford mistakenly assumed that the reflector was a single, thin layer containing materials with the properties of aniline dyes. He attributed the changing colours to changes in the chemical composition of the layer. While chemical characteristics of the reflector do appear to change during ecdysis, these changes occur within a multilayered ultrastructure that is formed during the initial stages of the adult moult.

The authors thank Susan Houghton of the Marine Biological Laboratory, Woods Hole, MA, for her considerable skill in sectioning and photographing this difficult material. Permission for the collection of specimens was provided by the Texas Department of Parks and Wildlife. This study was supported partially by graduate student subvention funds provided by the University of Texas and NSF Grant 2610711250.

REFERENCES

FILSHIE, B. (1982). Fine structure of the cuticle of insects and other arthropods. In *Insect Ultrastructure*, Vol. 1, (eds R. C. King & M. Akai), pp. 281–312. New York: Plenum Press.

HACKMAN, R. H. (1974). Chemistry of insect cuticle. In *The Physiology of Insecta*, Vol. 6, (ed. M. Rockstein), pp. 216–270. New York: Academic Press.

RICHARDS, A. G. (1951). *The Integument of Arthropods*. St. Paul: University of Minnesota Press.

SCHULZE, P. (1913). Chitin und andere Cuticularstrukturen bei Insekten. *Verh. dt. zool. Ges.* p. 165.

SCHULTZ, T. D. & RANKIN, M. A. (1985). The ultrastructure of the epicuticular interference reflectors of tiger beetles (*Cicindela*). *J. exp. Biol.* **117**, 87–110.

SHELFORD, V. E. (1971). Color and color pattern mechanisms of tiger beetles. *Illinois biol. Monogr.* **3**, 4.

STEGEMANN, F. (1930). Die Flugeldecken der Cicindelidae. Ein Beitrag zur Kenntnis der Insektcuticula. *Z. Morph. Ökol. Tiere* **18**, 1–73.

WIGGLESWORTH, V. B. (1972). *The Principles of Insect Physiology*. London: Chapman & Hall.

WIGGLESWORTH, V. B. (1976). The distribution of lipid in the cuticle of *Rhodnius*. In *The Insect Integument*, (ed. H. R. Hepburn), pp. 89–106. New York: Elsevier Scientific Publishing Co.

WILLIS, H. (1967). Bionomics and zoogeography of tiger beetles of saline habitats in the central United States. *Univ. Kansas Sci. Bull.* **47**, 145–313.

all transient changes in air pressure within the branchial chambers. When both plugs were removed simultaneously, the transient changes in intracardiac haemolymph pressure that accompanied reversals were also eliminated (Fig. 9). Removal of only the left plug, which eliminated branchial pressure fluctuations in the left branchial chamber only, reduced by approximately one-half the size of the transient change in intracardiac haemolymph pressure that had previously occurred during reversals (Fig. 10). Subsequent removal of the right plug essentially eliminated all fluctuations in haemolymph pressure normally associated with reversals. Although bilateral removal of plugs eliminated branchial and intracardiac pressure transients, a brief bradycardia accompanying reversed scaphognathite beating usually persisted.

DISCUSSION

Ventilation patterns

Qualitatively, the basic ventilatory patterns and mechanisms in *Cardisoma guanhumi* are similar to those found in other brachyuran crabs, both marine and semi- or fully terrestrial (see reviews by McMahon, 1981; Taylor, 1982; McMahon & Wilkens, 1983). However, the present study reveals many quantitative differences in ventilation in *Cardisoma guanhumi* which set this species apart from other brachyurans.

Unilateral beating of one scaphognathite, a common feature of branchial ventilation in brachyuran crabs (E.W. Taylor *et al.* 1973; McDonald *et al.* 1977; Butler, E.W. Taylor & McMahon, 1978; A.C. Taylor & Davies, 1982; McMahon & Wilkens, 1983), was observed only rarely in *Cardisoma guanhumi*, where coordinated bilateral ventilation definitely prevailed under all experimental conditions. Interestingly, Wood & Randall (1981) reported that unilateral scaphognathite beat was the normal mode of ventilation in air-exposed *Cardisoma carnifex* at 25 °C, with coordinated bilateral ventilation only occurring during exercise. It has been suggested that experimental disturbance or handling results in constant, bilateral ventilation in decapod crustaceans (see McDonald *et al.* 1977; Taylor, 1982; McMahon & Wilkens, 1983). However, disturbance does not appear to account for this pattern in *Cardisoma guanhumi* in the present study, since unrestrained, air-exposed crabs allowed overnight acclimation to experimental conditions in the present study still exhibited very close coordination of left and right scaphognathite beating. Interestingly, increased bilateral pumping was observed upon aerial exposure in the intertidal crab *Cancer productus* (DeFur & McMahon, 1984).

Another feature of branchial ventilation tending to set *Cardisoma guanhumi* apart from other brachyuran crabs and even from *Cardisoma carnifex* (Wood & Randall, 1981) is the infrequent occurrence and relatively brief duration of apnoeic periods. Even after overnight acclimation, undisturbed and unrestrained *Cardisoma guanhumi* ventilating with air but with access to 50 % sea water rarely stopped scaphognathite beating for more than 1 min. Given the high oxygen capacitance of air and the fact that at least in *Cardisoma carnifex* branchial chamber P_{O_2} rarely falls below 130 mmHg, even during periods of apnoea of several minutes (Wood & Randall, 1981), it is unlikely that continuous branchial ventilation in *Cardisoma guanhumi* is related to requirements for branchial O_2 uptake. Constant ventilation may instead

relate to non-respiratory processes that require water movement within the branchial chamber. Certainly, the complex ventilatory patterns seen when small amounts of water are available undoubtedly not only maintain gas flow through the upper regions of the branchial chamber, but also provide water irrigation of the gills in the lower regions of the branchial chambers. The gills and perhaps other structures in the branchial chamber of brachyurans are involved in water and ion regulation and acid-base balance (see Mantel & Farmer, 1983), and these functions would be facilitated by, if not totally dependent upon, turnover and agitation of water in the lower regions of the branchial chamber. Constant scaphognathite motion required primarily for non-respiratory, iono-regulatory functions may generate gas flow through the upper regions of the branchial chamber whether required for gas exchange at that time or not.

Interestingly, the ionic composition of the water available to *Cardisoma* had no significant influence on ventilatory patterns, at least during the relatively brief period of water exposure. Rather, the presence or absence of water *per se* was the important feature. This is quite unlike the effect of brief salinity stress in some euryhaline decapods (Taylor, Butler & Al-Wassia, 1977; Wheatly & McMahon, 1982). *Cardisoma guanhumi* is adept at regulating blood ion concentrations with water sources of varying salinities (Herreid & Gifford, 1963; M. Wheatly, unpublished) and apparently can achieve this without adjusting branchial ventilation pattern to water salinity.

Perhaps the most distinctive feature of branchial ventilation in *Cardisoma guanhumi* is the prominence of reversed scaphognathite beating. Most aquatic, intertidal or terrestrial brachyuran crabs maintained in normoxic, normocapnic environments may show a reversed beat or small group of reversed beats (see McMahon & Wilkens, 1983; E.W. Taylor, 1982; A.C. Taylor & Davies, 1982; DeFur & McMahon, 1984), but they are normally infrequent and in some species are apparently absent altogether (e.g. *Cardisoma carnifex*, Wood & Randall, 1981). However, scaphognathite reversal occurs frequently in *Cardisoma guanhumi* in air with access to water and, we believe, makes a major contribution not only to the turnover of gas but also of water within the branchial chambers. This may be important, not only for hydration of the respiratory membranes, but also for ion, water and acid-base regulation by the gills.

Increased reversed beating in other decapods has been observed with increased environmental temperature (Taylor & Butler, 1973), decreased environmental oxygen (Herreid *et al.* 1979*a,b*) and during burrowing activity (McDonald *et al.* 1977). The function of reversed scaphognathite beating in decapods has variously been attributed to cleaning of the branchial chamber, flushing poorly ventilated regions of the branchial chamber, and sampling water anterior to the animal (Hughes, Knights & Scammel, 1969; Johansen, Lenfant & Mecklenburg, 1970; Berlind, 1976; McDonald *et al.* 1977). In addition to the 'flushing' function for reversals which we propose for *Cardisoma guanhumi*, reversed scaphognathite beating and the positive branchial pressures it produces also may act to 'wring out' stagnant pools of haemolymph in poorly perfused regions of the gills and vascular bed lining the branchial chamber.

The large increase in net retrograde flow of gas through the branchial chamber when water becomes available occurs not only by increases in the number of reversal episodes in any given time period (Figs 2, 3), but also by increases in both frequency

and stroke volume of scaphognathite beat during reversal periods (Fig. 5). Increased scaphognathite frequency during reversed beating has also been reported for the marine crab, *Cancer magister* (McDonald *et al.* 1977), but in this crab scaphognathite stroke volume decreases rather than increases and so total ventilatory flow is reduced. Both acute and chronic adjustments in these aspects of scaphognathite performance have been reported for decapods (Burggren & McMahon, 1983; J.A. Mercier & J.L. Wilkens, unpublished), and adjustments in scaphognathite stroke volume or frequency reflect a particular set of physiological or environmental conditions rather than a species-specific characteristic.

Cardiovascular patterns

Heart rate in *Cardisoma guanhumi*, approximately 100–150 beats min^{-1} even in undisturbed, unrestrained crabs, was quite high compared with values which have been reported for other decapod Crustacea. However, most previous measurements on temperate marine or freshwater species or on tropical land crabs have been made at body temperatures of only 8–25 °C. Assuming a Q_{10} value for heart rate of approximately 2, *Cardisoma* would have a heart rate of 75–100 beats min^{-1} at 25 °C, which is comparable with heart rates for *Cardisoma carnifex* and *Cardisoma guanhumi* measured at that temperature (Herreid *et al.* 1979*a,b*; Wood & Randall, 1981). The high heart rates typical of *Cardisoma* at normal environmental temperatures indicate that filling of the heart with venous blood *via* the cardiac ostia must be a relatively rapid process, since the length of diastole (and thus the length of the time available for cardiac filling) will be correspondingly brief.

These experiments present the first measurements of haemolymph systolic pressures in a terrestrial decapod, and at 15–25 mmHg are comparable with systolic arterial pressures recorded for marine crabs (see Belman, 1976; McMahon & Wilkens, 1983). The relatively high diastolic intracardiac pressures in *Cardisoma*, usually several mmHg above ambient pressure (Fig. 6), indicate that post-branchial venous and pericardial pressures are similarly elevated above ambient. Simultaneous measurement of pericardial and intracardiac haemolymph pressures confirm this, and reveal that a gradient for haemolymph flow from the pericardium into the heart prevails for the entire diastolic period, or approximately half of the cardiac cycle. Since heart rates are high and diastolic periods consequently short (see above), a sustained pericardium-to-heart pressure gradient probably adds significantly to the effectiveness of cardiac filling in *Cardisoma* and may contribute to the high cardiac outputs calculated for this genus (C.M. Wood, R.G. Boutilier & D.J. Randall, unpublished data).

Pressure events in the pericardial space and heart during the earliest phases of systole – i.e. the near simultaneous rise in both compartments followed by a fall in pressure on the venous side as systole continues – resemble central cardiovascular events during similar cardiac phases in the vertebrate circulation. The ostial valves may well be closed by brief retrograde haemolymph flow from the heart just as the atrio-ventricular valves are closed in the vertebrate heart. Moreover, the valves remain closed against moderately high pressures, since no intracardiac pressure event is transmitted back to the pericardial space during systole.

Finally, although terrestrial and aquatic brachyurans have fundamentally the same

cardiovascular and respiratory arrangement, the effects of gravity imposed on terrestrial forms may introduce circulatory complexities to tissue perfusion. For example, branchial resistances may be higher in terrestrial forms, where there is no buoying effect of water to prevent partial collapse of the gill filaments. The gills of terrestrial crabs are structurally modified to help prevent collapse in air (see von Raben, 1934; Gray, 1957; Diaz & Rodriguez, 1977) and the net circulatory effects of these modifications to branchial blood flow are currently unknown. Gravity acting on terrestrial crabs may also interfere with circulatory function by causing venous haemolymph to pool in tissue sinuses, analogous to that occurring in man during prolonged standing without movement. Additionally, the typical threat posture of *Cardisoma guanhumi*, involving elevation of the large, heavy chelae high over the carapace, may introduce several haemodynamic adjustments (e.g. increased venous return, increased arterial impedance) that would not occur in a crab making similar postural adjustments under water.

Ventilatory-circulatory interactions

Correlation of ventilatory and cardiovascular performance is a general feature of gas transport physiology in crustaceans (Taylor, 1982; McMahon & Wilkens, 1983), but the extent and constancy of interaction of these physiological processes in *Cardisoma guanhumi* is remarkable. The most striking correlation is between heart rate and direction of scaphognathite beating. Most crabs that were examined showed a consistent and marked bradycardia concomitant with the onset of reversed beating (Figs 6, 7, 8). A bradycardia during reversed beating has also been described for the marine crab *Cancer magister* in normoxic conditions (McDonald *et al.* 1977), though a tachycardia accompanies reversed beating stimulated by hypoxia in the shore crab *Carcinus maenas* (Taylor *et al.* 1973).

Measurements of intracardiac pressure in *Cardisoma guanhumi* revealed that scaphognathite reversal also caused transient increases in haemolymph pressure. Perturbations in heart rate and haemolymph pressure coincident with scaphognathite reversal could be accounted for by at least three mechanisms: (1) direct mechanical effects on the haemolymph spaces by the elevated epibranchial pressures generated during reversed beating; (2) reflex interactions involving circulatory baroreceptors; and/or (3) direct interactions between respiratory and cardiac elements of the central nervous system. Experiments in which the branchial pressure transients produced by reversed scaphognathite beating were experimentally reduced or eliminated (Figs 9, 10) strongly indicate that the elevated branchial pressure resulting from reversals is directly transmitted through the thin branchial vascular wall into the haemolymph spaces. This phenomenon has been considered, though not demonstrated, to be a factor in ventilatory-circulatory interactions in other crustaceans (Blatchford, 1971; Taylor, 1982; McMahon & Wilkens, 1983). The elevation of central haemolymph pressure by scaphognathite reversal appears to be a mechanical event.

Why then does a bradycardia occur during these transient changes in haemolymph pressure induced by scaphognathite reversal? Preliminary (unpublished) evidence suggests that there is a baroreceptor reflex in *Cardisoma guanhumi*. Given a constant peripheral resistance, a decline in cardiac output due to a decline in heart rate – reflexly mediated or otherwise – might minimize any factors tending to increase

haemolymph pressure. Regulation of blood pressure in *Cardisoma guanhumi* may be vital in maintaining cardiac output, since a small pressure perturbation represents a proportionately much larger pressure adjustment in an animal with a comparatively low mean blood pressure.

Heart rate adjustments at the same time as scaphognathite reversal may also reflect some direct interaction of central neural elements controlling ventilation and circulation (Wilkens, Wilkens & McMahon, 1974; Taylor *et al.* 1973; Young, 1978; Young & Coyer, 1979; Pasztor & Bush, 1983*a*,*b*; Bush & Pasztor, 1983). Transient bradycardia associated with scaphognathite reversal persisted in some (but not all) crabs in the present experiments when the branchial chambers were opened to ambient pressure, eliminating all transient changes in haemolymph pressure (Figs 9,10). Thus, haemolymph pressure changes are not an absolute requisite for the bradycardia response. The time courses of the onset of reversals and bradycardia are also in support of some degree of central neural interaction of ventilatory and circulatory elements. Whereas changes in heart rate and haemolymph pressure were usually very closely linked in time, in a few crabs (dashed lines, Fig. 8), heart rate adjustments either began several seconds before reversed scaphognathite beating began, or persisted for several seconds after forward beating resumed. These atypical ventilatory-circulatory interactions nonetheless suggest that not all such phenomena are mediated by tightly linked 'cause-and-effect' events involving peripheral reflexes.

REFERENCES

Belman, B. W. (1976). New observations on blood pressure in marine Crustacea. *J. exp. Zool.* **196**, 71–78.

Berlind, A. (1976). Neurohormonal and reflex control of scaphognathite beating in the crab *Carcinus maenas*. *J. comp. Physiol.* **116**A, 77–90.

Blatchford, J. G. (1971). Hemodynamics of *Carcinus maenas* (L.). *Comp. Biochem. Physiol.* **39**A, 193–202.

Butler, P. J., Taylor, E. W. & McMahon, B. R. (1978). Respiratory and circulatory changes in the lobster (*Homarus vulgaris*) during long term exposure to moderate hypoxia. *J. exp. Biol.* **73**, 131–146.

Burggren, W. W. & McMahon, B. R. (1983). An analysis of scaphognathite pumping performance in the crayfish *Orconectes virilis*: compensatory changes to acute and chronic hypoxic exposure. *Physiol. Zoöl.* **56**, 309–318.

Bush, B. M. H. & Pasztor, V. M. (1983). Graded potential and spiking in single units of the oval organ, a mechanoreceptor in the lobster ventilatory system. II. Individuality of the three afferent fibres. *J. exp. Biol.* **107**, 451–464.

Cameron, J. N. (1975). Aerial gas exchange in the coconut crab *Birgus latro*, with some notes on *Gecardoidea lalandii*. *Comp. Biochem. Physiol.* **52**A, 129–134.

Cameron, J. N. (1981). Brief introduction to land crabs of the Palau Islands: stages in transition to air breathing. *J. exp. Zool.* **218**, 1–6.

DeFur, P. L. & McMahon, B. R. (1984). Physiological compensation to short-term air exposure in red rock crabs, *Cancer productus* Randall, from littoral and sublittoral habitats. I. Oxygen uptake and transport. *Physiol. Zoöl.* **57**, 137–150.

DeWilde, P. A. W. J. (1973). On the ecology of *Coenobita clypeatus* in Curacao. With reference to reproduction, water economy and osmoregulation in terrestrial hermit crabs. In *Studies on the Fauna of Curacao and Other Caribbean Islands*, Vol. 44. The Hague: Martinus Nijhoff.

Diaz, H. & Rodriguez, G. (1977). The branchial chamber in terrestrial crabs: a comparative study. *Biol. Bull. mar biol. Lab., Woods Hole* **153**, 485–503.

Gray, I. E. (1957). A comparative study of the gill area of crabs. *Biol. Bull. mar. biol. Lab., Woods Hole* **112**, 23–42.

Herreid, C. F., II & Gifford, C. A. (1963). The burrow habitat of the land crab, *Cardisoma guanhumi* (Latreille). *Ecology* **44**, 773–775.

Herreid, C. F., II, Lee, L. L. & Shah, G. M. (1979*a*). Respiration and heart rate in exercising land crabs. *Respir. Physiol.* **36**, 109–120.

Herreid, C. F., II, O'Mahoney, P. M. & Shah, G. M. (1979*b*). Cardiac and respiratory response to hypoxia in the land crab, *Cardisoma guanhumi* (Latreille). *Comp. Biochem. Physiol.* **63**A, 145–151.

J. exp Biol. **117**, 45–68 (1985)
Printed in Great Britain © *The Company of Biologists Limited 1985*

THE PHYSIOLOGY OF WANDERING BEHAVIOUR IN *MANDUCA SEXTA*
II. THE ENDOCRINE CONTROL OF WANDERING BEHAVIOUR

BY OLIVER S. DOMINICK* AND JAMES W. TRUMAN
Department of Zoology, University of Washington, Seattle, WA 98195, U.S.A.

Accepted 27 November 1984

SUMMARY

1. Removal of the prothoracic glands early during the 5th instar of *Manduca sexta* prevented the larvae from wandering and from further development. Infusion of 20-hydroxyecdysone (20-HE) into these larvae induced wandering behaviour.

2. In intact larvae, induction of precocious wandering behaviour required a 20-HE infusion lasting longer than 5 h. Infused 20-HE induced maximal response (90 %) when delivered at a rate of $0{\cdot}06\,\mu g\,g^{-1}$ body weight h^{-1}. At considerably higher concentrations ($0.25\,\mu g\,g^{-1}\,h^{-1}$ larvae performed brief, erratic behaviour or omitted wandering entirely.

3. The latency between appearance of 20-HE and the onset of wandering was dose-dependent with a minimum of 11 h following infusion at $0{\cdot}1\,\mu g\,g^{-1}\,h^{-1}$. Latency was not affected by the duration of 20-HE infusion.

4. The duration of induced wandering behaviour was proportional to the duration of 20-HE infusion. Minimal wandering behaviour lasted 2 h following 20-HE infusions at 5 h, while infusions lasting 11 h induced 9 h of wandering behaviour. Several lines of evidence suggest that the effects of 20-HE accumulate over time and directly determine the duration of wandering behaviour.

5. Many larvae exhibited a series of temporally distinct locomotor periods following various 20-HE infusion protocols, suggesting that a series of separate exposures to 20-HE can result in corresponding serial bouts of locomotion.

6. Responsiveness to 20-HE appeared to be principally modulated by juvenile hormone. Allatectomy of 2nd, 3rd and 4th instar larvae removed juvenile hormone (JH) precociously from these stages and was followed several days later by precocious wandering behaviour. Likewise, application of the JH mimic, EGS, prior to 20-HE exposure or at the start of it, could prevent the behavioural induction. During the 5th instar, 20-HE became increasingly effective in inducing wandering as larvae grew larger than 5 g, the size at which JH normally begins to disappear from the haemolymph. Allatectomized 5th instar larvae responded directly to 20-HE a day sooner than larvae with normal JH titres, but before day 2 the effects of 20-HE on wandering behaviour appear to be indirect, requiring a latency greater than

* Present address: Department of Entomology, Caldwell Hall, Cornell University, Ithaca, New York 14853, U.S.A.

Key words: Behaviour, steroid, endocrinology.

24 h. Several processes, of which the elimination of JH is the last, appear to be required before 20-HE can induce wandering behaviour.

7. Throughout the entire period when 20-HE was acting to induce wandering, the appearance of JH could prevent further induction of behaviour, but the effects of 20-HE which had already been established up to that time were expressed. Thus, application of EGS progressively later during the interval of 20-HE action was progressively less effective in reducing the length of wandering behaviour. The presence of EGS during wandering had no behavioural effect, indicating that only the induction of behaviour by 20-HE is sensitive to modulation by JH.

INTRODUCTION

In many animals steroid hormones have dual actions on the nervous system, and on non-neural tissues, such that changes in behaviour are coordinated with other physiological changes. This is well documented by numerous studies of modification of vertebrate reproductive behaviour by steroids in conjunction with the regulation of gonadal function (Davidson & Levine, 1972; Pfaff, 1980). Steroids also play a fundamental role in regulating invertebrate development (Highnam & Hill, 1977) but their roles in modulating invertebrate behaviour have not been examined closely.

Previous studies of the endocrine control of insect development suggest that the specialized larval behaviour typically preceding pupation might be released specifically by the hormonal environment which induces pupation. During the day prior to wandering in the tobacco hornworm, *Manduca sexta*, the titre of the steroid moulting hormone, 20-hydroxyecdysone (20-HE), rises (Bollenbacher, Vedeckis & Gilbert, 1975) in the absence of juvenile hormone (JH) (Fain & Riddiford, 1975). This unique endocrine milieu induces the characteristic premetamorphic changes in pigmentation (Nijhout, 1976; Hori & Riddiford, 1982) and cuticular commitment (Riddiford, 1978) of the epidermis. Administration of ecdysteroids to a larva of *Hyalophora cecropia* (Lounibos, 1976) and to larvae of *Ephestia* (Giebultowicz, Zdarek & Chroscikowska, 1980) have induced cocoon spinning, suggesting that ecdysteroids may regulate this behaviour.

In addition, several lines of evidence indicate that JH plays an important role in regulating premetamorphic behaviour. Application of JH causes aberrant cocoon spinning in caterpillars of *Hyalophora cecropia* (Riddiford, 1972), *Galleria* (Piepho, 1950) and *Pieris* (Benz, 1973). Furthermore, removal of the corpora allata (CA) from early instar larvae of the silkmoth, *Bombyx*, or the waxmoth, *Galleria*, causes precocious metamorphosis preceded by the construction of a complete, but miniature cocoon (Bounhiol, 1936; Piepho, 1938, 1939).

In this paper we have used *Manduca sexta* to examine the endocrine control of wandering behaviour, a period of continuous locomotion which accompanies the larva's developmental preparation for pupation. During wandering, the larva abandons its feeding habitat, burrows into the soil and constructs a pupation chamber underground (Dominick & Truman, 1984).

MATERIALS AND METHODS

Experimental animals

Larvae of the tobacco hornworm, *Manduca sexta*, were individually raised in the laboratory on an artificial diet as previously described (Truman 1972; Bel & Joachim, 1976) at 26 °C under a short day photoperiod (12L:12D). Lights off was arbitrarily designated as midnight (00.00). The locomotor activity of wandering behaviour in 5th instar larvae was monitored as previously described (Dominick & Truman, 1984) by placing individual larvae in tilt-sensitive actographs in which locomotion was recorded with an Esterline Angus chart recorder. The wandering behaviour of 3rd and 4th instar larvae was recorded with lightweight tilting actographs constructed from thin acetate sheets.

The temporal interval of the gate in which particular larvae would release prothoracicotropic hormone (PTTH) could be predicted on the basis of their weights during the preceding days of the 5th instar (Nijhout & Williams, 1974*a*). In the experiments reported here, larvae weighing more than 7·0 g at 17.00 on day 2 routinely released PTTH during the gate on day 3 (Gate I larvae), while those weighing 7·5–8·8 g on day 3 released PTTH during the gate on day 4 (Gate II). With animals younger than day 2 the errors in predicting the gate increased, but within a group of larvae which entered the 5th instar synchronously those larvae with weights in the top 20 % of a group were typically Gate I, while the smallest 20 % were usually Gate II.

Surgical procedures

The corpora allata (CA) were removed from 2nd, 3rd and 4th instar larvae which were anaesthetized by immersion in water for about 20 min, according to the method described by Kiguchi & Riddiford (1978). The head was flexed back under a thin piece of plastic and the neck membrane pierced laterally with sharpened no. 5 forceps. Each CA was removed from among the tracheae at the ventral lateral regions of the neck. Following allatectomy, the larvae were returned to their individual cups to feed.

The prothoracic glands were removed on day 1, through an incision slightly dorsal and posterior to the prothoracic spiracle from CO_2-anaesthetized 5th instar larvae which were immersed in saline (Ephrussi & Beadle, 1936). The clustered glandular tissue was found branching over the tracheae, and was carefully separated from its numerous fine tracheal attachments with no. 5 forceps. Particular care was needed to liberate the long branch which projects into the head region without breaking off the terminal lobe of that branch. The incision was subsequently closed with 6–0 gauge braided silk sutures, and the larvae were then returned to their feeding cups.

Ecdysteroid treatments

20-hydroxyecdysone (20-HE) (Rhoto Pharmaceutical, Osaka, Japan) was dissolved in *Manduca* saline (Cherbas, 1973) and concentrations were confirmed spectrophotometrically (E_{240}=12 670; Meltzer, 1971). Larvae were anaesthetized with CO_2 and either received an injection of 20-HE into an abdominal proleg or were infused with the 20-HE solution *via* a long polyethylene catheter (PE-10; Clay Adams)

inserted into the head capsule and stabilized with Tackiwax (Cenco). A 50-μl Hamilton syringe mounted on a syringe pump (Sage Instruments, model 355) was used to deliver the 20-HE solution through the tubing. Solutions were usually infused at a rate of 5 $\mu l\,h^{-1}$, and 20-HE concentration was varied accordingly. Larvae recovered from anaesthesia and remained in their feeding cups during the infusion and were subsequently placed in the actographs without food.

EGS treatment

The JH mimic, 6,7-epoxygeranyl-3′,4′–methylene dioxyphenyl ether (epoxygeranylsesamole, EGS) (Bowers, 1969) (Insert Control, Inc.) was dissolved in cyclohexane (Baker, Inc.) and 10 $\mu g\,\mu l^{-1}$ was applied to the dorsal intersegmental region of unanaesthetized larvae. Mosaic pupae produced by this treatment were scored using the method of Truman, Riddiford & Safranck (1974) in which 0 represents normal pupation and 5 indicates almost completely larval cuticle.

RESULTS

The role of ecdysteroids

Effects of prothoracic gland removal

Prothoracic glands (PTG) were completely removed from four larvae on day 0 of the 5th instar. These larvae grew slowly and continuously to a maximum weight of 15–18 g over the next 12 days, whereas sham-operated larvae wandered by day 6 and pupated by day 10. The PTG– larvae survived for nearly a month without ever showing wandering behaviour, the morphological changes associated with this behaviour, or any sign of pupation.

Sham-operated larvae wandered as usual, although the onset of wandering was often delayed by 1 or 2 days. Of 10 larvae in which removal of the PTG was unsuccessful (as determined by the presence of remnant PTG fragments as small as four cells during subsequent dissection) nine wandered in the gate following attainment of 7–9 g. Most of these wandered by the second gate (day 5) but three larvae grew unusually slowly following surgery and delayed wandering as late as day 8 (Gate V). Therefore, in subsequent experiments requiring PTG– larvae we used only those which reached 7–9 g by day 4 and which failed to wander by Gate III (day 6).

One such larva from which prothoracic glands had been completely removed on day 0 was infused with 50μg of 20-HE (1 $\mu g\,\mu l^{-1}$ at 5 $\mu l\,h^{-1}$) over 10 h on day 6. This treatment resulted in appearance of the dorsal vessel and a 6 h period of wandering beginning 13 h after the start of infusion. This larva never retracted its ocellar pigment or pupated, and, until it died several weeks later, it showed sustained locomotor activity lasting 1–2 h whenever disturbed.

In further experiments, larvae were allatectomized following PTTH release in the 4th instar so that, following removal of their prothoracic glands on day 0 of the 5th instar, there would be no post-surgical, JH-mediated effects on ecdysteroid sensitivity. All unsuccessfully operated larvae wandered by day 6 as described above. Those that showed no wandering were subsequently infused with dosages of 20-HE varying from 5–50 μg over 10 h beginning at 17.00 on day 6 ($N=11$). A wandering response

Table 1. *Effect of 20-HE infusions on wandering behaviour in larvae lacking corpora allata and prothoracic glands*

Dose (μg)	*N*	Latency (h ± S.E.M.)	Wandering duration (h)
5	2	17	6·5
40	5	11 ± 0	5 ± 1
50	2	12·5 ± 0·5	6 ± 0

Infusions were for 10 h at a rate of 5 μl h^{-1} for 50 μl of 20-HE solutions containing 0·1 μg μl^{-1}, 0·8 μg μl^{-1} or 1·0 μg μl^{-1}.
Latency is relative to start of infusion.

was induced in 80 % of the larvae (Table 1). With a relatively small 20-HE dose (5 μg delivered as 0·1 μg μl^{-1} at 5μl h^{-1} over 10 h) the latency between the start of infusion and behavioural onset was longer than that seen after the larger dosages (40–50 μg). Wandering duration in these larvae was 5-6 h regardless of 20-HE dose.

Parameters of ecdysteroid exposure

The effect of prothoracic gland removal clearly implicated ecdysteroids in the induction of wandering behaviour. The role of ecdysteroids was further explored by treating larvae with intact PTG with exogenous 20-HE on the day prior to PTTH and ecdysteroid secretion. Initial experiments involved injecting Gate II larvae with varying amounts of 20-HE (5–100 μg) at 20.00 on day 3. As had been noted earlier by Nijhout (1976), a single injection proved to be a poor mode of delivery for ecdysteroids. Only one larva out of 39 showed early wandering after such treatment. The remainder wandered at their expected time or were delayed for up to 1 day.

To imitate the prolonged exposure to 20-HE which occurs during endogenous hormone secretion (Bollenbacher *et al.* 1975), presumptive Gate II larvae were

Table 2. *The effects of infusing different dosages of 20-HE into presumptive gate II larvae*

Dose (μg)	*N*	% Early	Latency (h ± S.E.)	Duration of induced wandering (h ± S.E.)	% Repeat wandering	Duration of repeat wandering (h ± S.E.)
0*	10	0	(36 ± 2)	(20 ± 4)	0	0
0·30	10	10	14	4	100	16
0·75	8	0	–	0	0	0
1·5	10	70	20 ± 1	6 ± 1	71	7 ± 2
3·5	8	88	15 ± 1	9 ± 2	71	4 ± 1
7·0	8	88	18 ± 2	5 ± 1	89	9 ± 2
15	9	66	14 ± 1	7 ± 1	66	4 ± 1
25	10	90	13 ± 1	7 ± 1	89	9 ± 2
50	21	52	12 ± 1	3 ± 1	40	8 ± 3
100	8	63	11 ± 1	4 ± 1	20	3 ± 1

Solutions were infused over 10 h starting at 19.00 on day 3 using 20-HE concentrations to give the total dose indicated.
* Saline-infused controls with latency and duration for normal wandering in parentheses.

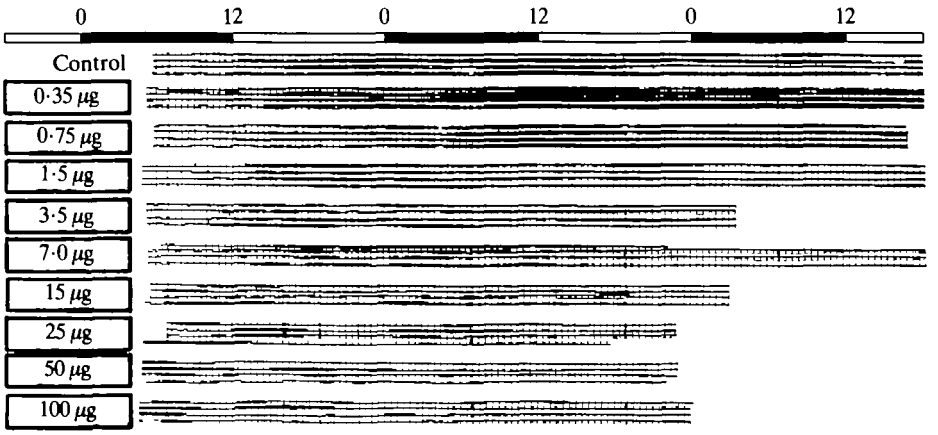

Fig. 1. Activity records of larvae infused with different dosages of 20-HE. Presumptive Gate II larvae were infused with varying dosages of 20-HE (from 0·35–100 μg, as marked) over a 10-h interval (delimited by box surrounding 20-HE dosage) beginning at 19.00 on day 3. For each treatment, the original tilt-dish activity records of four larvae showing typical responses to the hormone are shown. The 12L : 12D photoperiod is shown by the light and dark bars at the top of the figure.

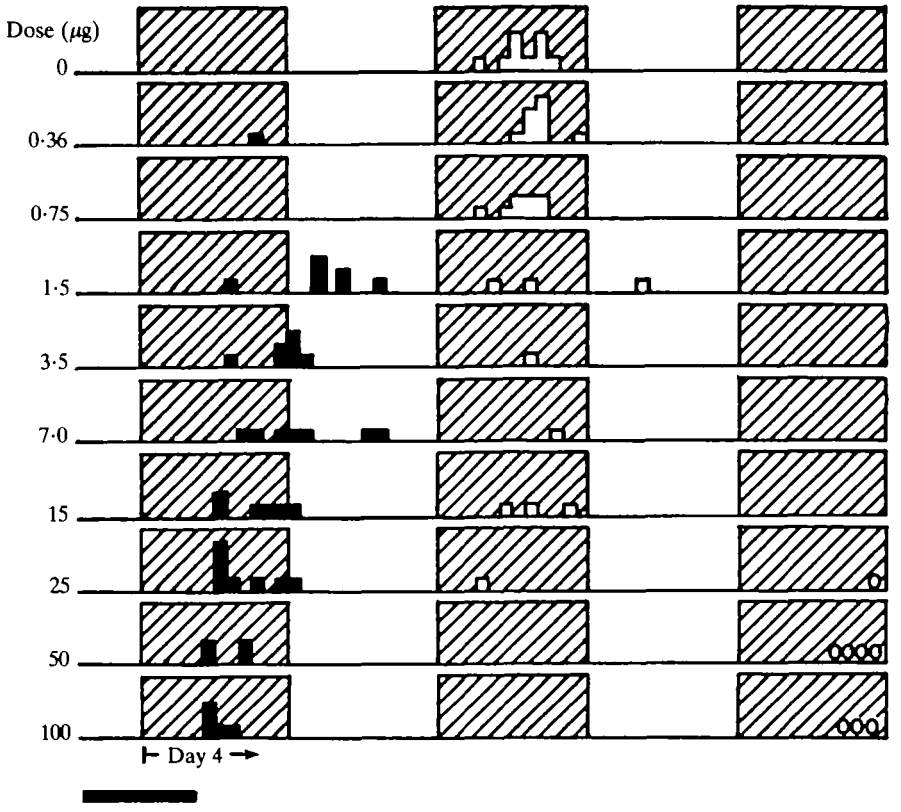

Fig. 2. Onset times of wandering in response to infusions of differing dosages of 20-HE. Data are from the experiment described in Fig. 1. The black bar represents the interval during which 20-HE was infused for each group of larvae. Histograms designate the starting times for wandering behaviour after each treatment. Onset times which are equivalent to Gate II controls are shown as open squares, and advanced onset times are shown as black squares. Larvae which failed to wander are indicated by an open circle to the right. The 12L : 12D photoperiod is represented by the light and cross-hatched background.

infused with varying amounts of 20-HE over a 9-h period beginning at 19.00 on day 3 (Table 2) to ensure that exogenous 20-HE appeared well before the time of endogenous ecdysteroid secretion. Animals infused with less than 1·5 μg of 20-HE were rarely observed to wander earlier than their expected gate (Figs 1, 2). With infusions of 1·5 μg or more, wandering began at progressively earlier times as the hormone dose increased, but even with extremely large doses (up to 100 μg), the minimal latency between the beginning of the infusion and behavioural onset was 11 h (Fig. 2). Indeed, at the larger doses, wandering was often delayed by 1 day or omitted. The duration of induced wandering varied from 3–9 h, independent of dose (Fig. 1; Table 2).

As seen in Fig. 3 there was a clear dosage optimum for the induction of wandering locomotion by 20-HE. In Gate II larvae the incidence of early wandering rose from 10 % to about 90 % as the infused 20-HE dose increased from 0 to 5 μg. Presumptive Gate I larvae showed essentially the same dose-response relationship but the proportion responding at each dose was 20–30 % lower (Fig. 3). At higher doses a gradually increasing number of animals omitted the behaviour, in spite of the appearance of the dorsal vessel, such that at 50 μg and above, between 40 % and 50 % of the infused larvae failed ever to show wandering locomotion.

In the ecdysteroid-infused larvae the dorsal vessel appeared prematurely (Fig. 4) as previously reported by Nijhout (1976). Interestingly, the induction of wandering

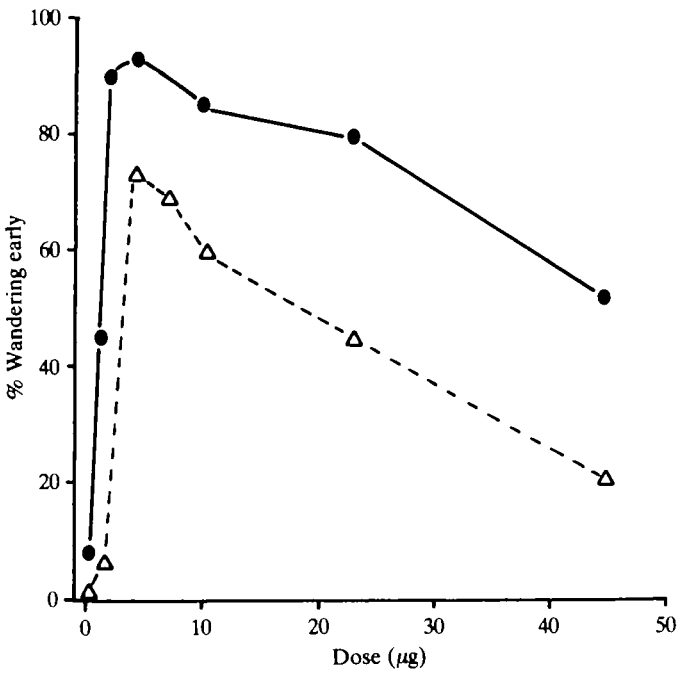

Fig. 3. The effectiveness of 20-HE infusions for inducing wandering behaviour as a function of hormone dose. After infusion with different dosages of 20-HE as described for Fig. 1, the proportion of Gate II larvae which began wandering earlier than the normal gate was noted (filled circles). In a parallel experiment, presumptive Gate I larvae were infused with 20-HE on day 2, and wandering response was observed (open triangles). The value of each point is based on 10–40 larvae.

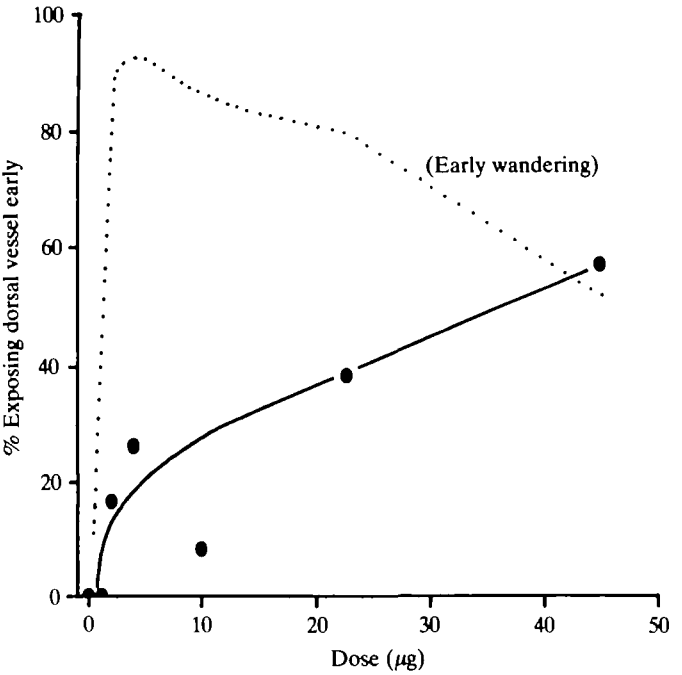

Fig. 4. The effect of infused 20-HE on heart exposure. The time when the heart was exposed following 20-HE infusion was noted for the Gate II larvae described in Fig. 1 ($N = 10$–40 per point). For each dose, the solid circles indicate the proportion of 20-HE infused larvae exposing their hearts earlier than usual. For comparison, the dotted line reiterates the behavioural response (Fig. 3) of these larvae at these dosages.

behaviour was more sensitive to the infused 20-HE than were the epidermal changes. Thus, the behavioural responses to 20-HE can occur in the absence of obvious peripheral changes that normally occur at the same time.

The relationship between dose and the apparent requirement for prolonged exposure to the hormone was examined by varying dosage and duration of 20-HE infusion over a wide range. Fig. 5 summarizes the results of an experiment in which Gate II larvae received a total dosage of 5 μg of 20-HE (as a 0·1 mg ml^{-1} solution) infused over time periods which varied from a single instantaneous injection to 10 h. The effectiveness of the 5 μg dosage in inducing early wandering increased abruptly as the length of exposure to hormone exceeded 4 h with 54 % of the larvae wandering in response to a 5-h infusion, and the maximal response of 80 % occurring after 8–10 h of infusion. The results (Figs 3–5; Table 3) indicate that the maximal behavioural effectiveness of 20-HE occurred under relatively limited conditions of low hormone dose (2–15 μg) and long infusion time (8–10 h).

Effects of 20-hydroxyecdysone on wandering duration

Possible relationships between the amount of ecdysteroid infused and the duration of wandering behaviour are complicated by the existence of overdosage effects which result in the omission of wandering behaviour. Consequently we examined temporal aspects of ecdysteroid exposure on the behaviour of the animal by infusing low dosages of 20-HE (0·5 μg h^{-1}) for varying amounts of time beginning at 19.00 on day 3.

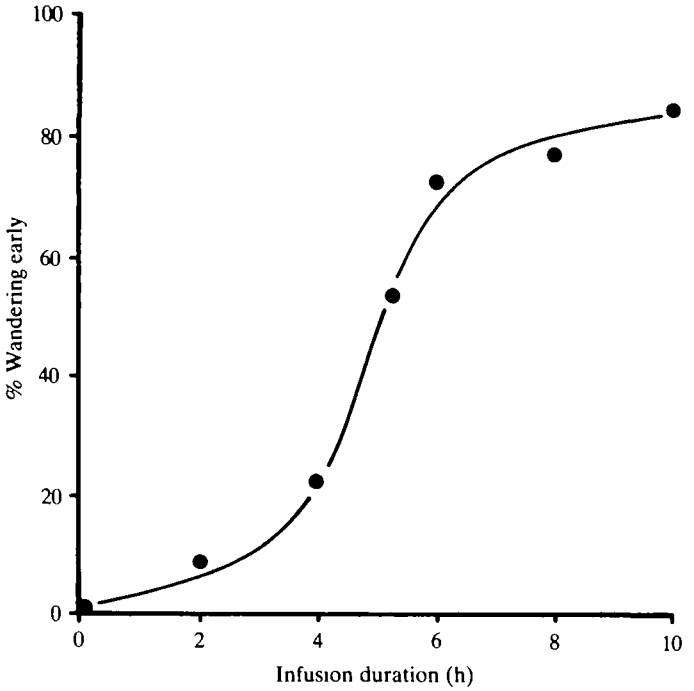

Fig. 5. The length of 20-HE infusion needed to induce wandering behaviour. A total dose of 5 μg of 20-HE was infused into presumptive Gate II larvae over a 0-(single injection) to 10-h period, beginning at 20.00 on day 3. The proportion of larvae wandering earlier than saline-infused controls is plotted for each infusion duration (N = 10–40 animals per point).

Infusions lasting 3 h or less were ineffective in inducing early wandering (Figs 6, 7).

As the length of the infusion increased to 5 h or more, precocious wandering appeared in increasing numbers of larvae. Importantly, the interval between the start of the infusion and behavioural onset was constant regardless of infusion duration, averaging 14±1 h (N=53), indicating that the initiation of wandering was not accelerated by increasing the duration of 20-HE exposure.

The systematic lengthening of the time of 20-HE infusion caused a proportional increase in the average duration of induced wandering behaviour, from a minimum

Table 3. *The effect of infusion of 20-HE for varying lengths of time*

Infusion duration (h)	Total dose (μg)	N	% Early	Latency (h ± S.E.M.)	Induced duration (h ± S.E.M.)	% Repeat	Repeat duration (h)
0(control)	0·0	25	0	(36 ± 2)	(20 ± 2)	0	0
1	0·5	7	0	–	–	–	–
3	1·5	19	0	–	–	–	–
5	2·5	16	50	16 ± 2	2 ± 0·5	100	9 ± 1
7	3·5	23	61	13 ± 1	5 ± 1	57	4 ± 1
9	4·5	26	73	13 ± 1	7 ± 1	63	9 ± 2
11	5·5	17	71	15 ± 1	9 ± 1	67	8 ± 2

Presumptive Gate II larvae were infused with 0·5 μg 20-HE h^{-1} beginning at 19.00 on day 3.

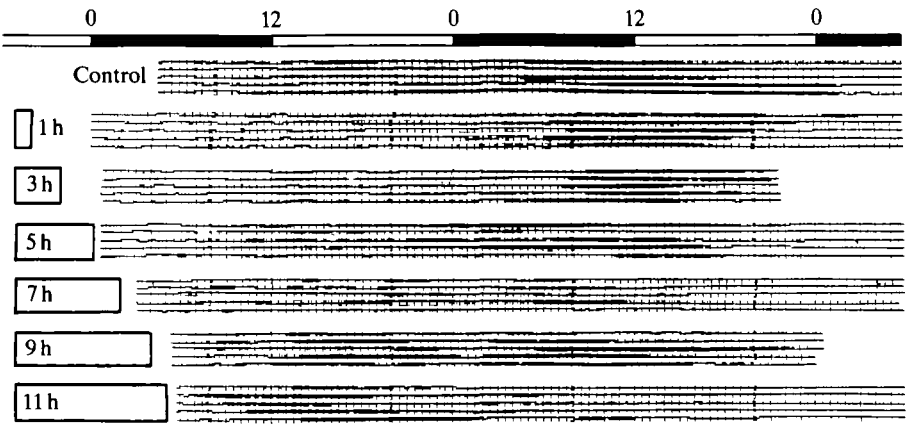

Fig. 6. Activity records of wandering behaviour induced by varying the length of infusion of a constant 20-HE concentration. Predicted Gate II larvae were infused with 20-HE at a rate of 0·5 μg h^{-1} for varying lengths of time from 1–11 h starting at 19.00 on day 3 (as indicated by the numbers and the white bars at the left side of the figure). Typical records from five larvae responding in each experimental group are shown. Records of uninfused control Gate II larvae are also shown. The 12L : 12D photoperiod is shown as light and dark bars at the top of the figure.

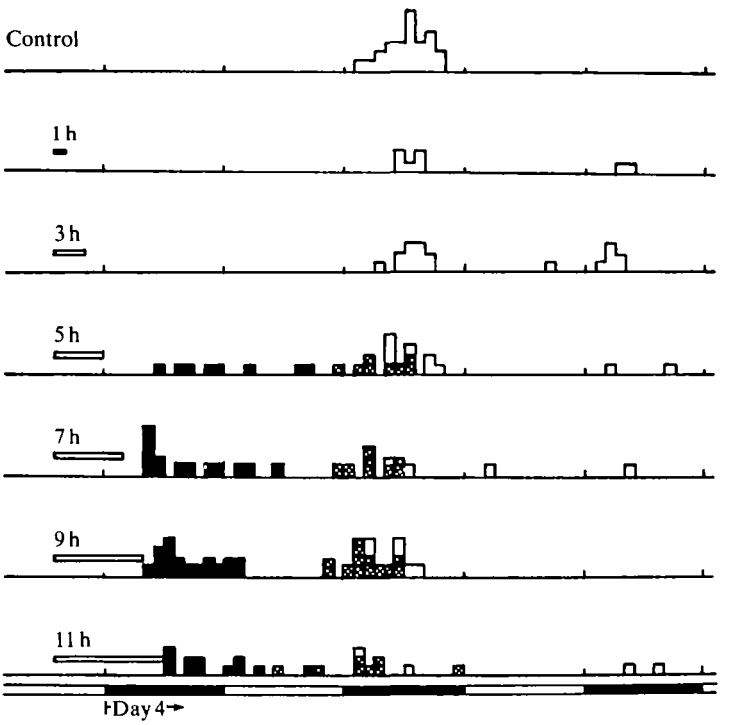

Fig. 7. Onset of wandering behaviour induced by 20-HE infusions of varying duration. Data represent the behaviour of all larvae infused in the experiment for which representative activity records were shown in Fig. 6. Each group of 20-HE infusions is illustrated as a thin white bar on the left side of the figure, and is labelled with the duration in hours. Black histograms represent onset times of wandering which were earlier than control Gate II times (which are shown as white histograms). The appearance of a second bout of wandering is shown as a cross-hatched histogram. The 12L : 12D photoperiod is shown below the figure.

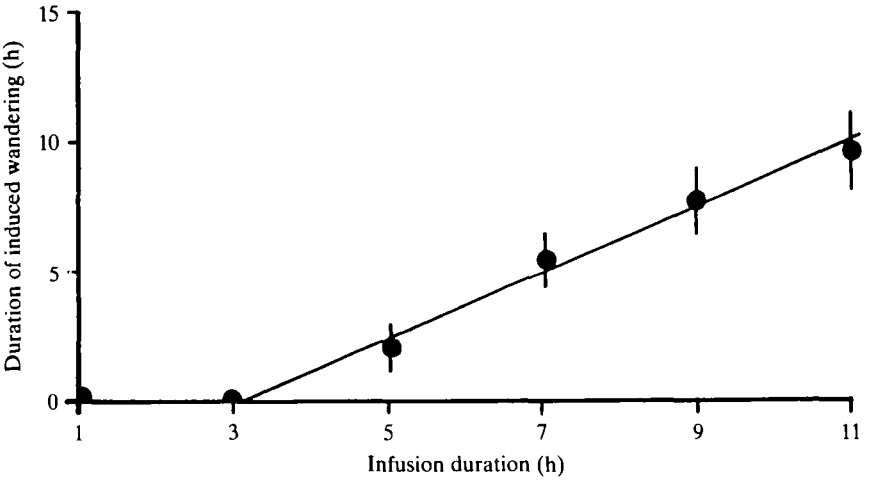

Fig. 8. The control of wandering duration by length of 20-HE infusion. The durations of early bouts of wandering behaviour induced by the 20-HE infusions of varying length (as described in Figs 6 and 7) were measured and plotted (mean ± S.E.) with reference to the length of the 20-HE infusion ($N = 7$–26 per point; see Table 3). The line calculated by linear regression ($y = 1{\cdot}2x + 3{\cdot}2$) represents a significant correlation ($r = 0{\cdot}9$; $P < 0{\cdot}01$).

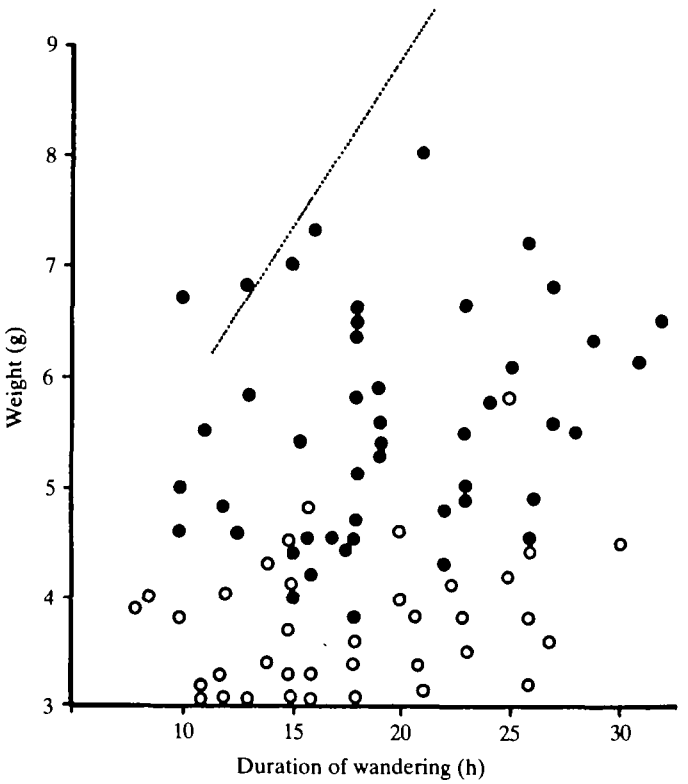

Fig. 9. Relationship between weight and wandering duration in allatectomized larvae. Weights were taken at 17.00 on day 1 and day 2 for Gate I (open circles) and Gate II (filled circles) larvae respectively. The correlation coefficient ($r = 0{\cdot}09$) is not significant. The dotted line indicates the regression line for Gate I and II larvae with intact CA (Dominick & Truman, 1984).

of 2 h in response to a 5-h infusion, to 9 h of locomotion after 11 h of 20-HE infusion (Fig. 8). Infusions longer than 11 h were impractical because wandering often started before the infusion was completed.

Following the period of early wandering induced by 20-HE, many of the larvae appeared to wander a second time, early in their normal wandering gate (Figs 1, 6; Table 2). The length of this second behavioural period was shorter than that of control animals, lasting less than 10 h, and bearing no relationship to the dose of hormone infused.

The role of juvenile hormone

Effects of removal of the corpora allata

A number of previous experiments indicate that the induction of cocoon spinning behaviour of various caterpillars is inhibited by JH secreted from the CA (Bounhiol, 1938; Piepho, 1939, 1950, 1960; Riddiford, 1972; Akai & Kobayashi, 1970; Benz, 1973). We initially examined the role of the CA in wandering of *Manduca* by removing these glands from 4th instar larvae on the day prior to ecdysis to the 5th instar (14–18 h after PTTH and ecdysone release). Under this protocol successful allatectomy was clearly indicated by melanization of the new 5th instar cuticle (Kiguchi & Riddiford, 1978). These larvae began wandering during gates on the third and fourth nights following ecdysis, 1 day earlier than the wandering gates for sham-operated larvae (Nijhout, 1975*b*; Kiguchi & Riddiford, 1978). As with the onset of wandering in sham-operated controls, the wandering gates for allatectomized larvae were about 8–9 h wide during the scotophase and showed a 'gating bias' (Pittendrigh & Skopik, 1970) such that larvae began wandering later during the first gate than they did during the second.

In contrast to the correlation between larval size and average wandering duration in normal larvae (Dominick & Truman, 1984) there was no correlation between larval size and the duration of wandering (average, 19·5 h) in allatectomized 5th instar larvae (Fig. 9). The observation supports the earlier suggestion (Dominick & Truman, 1984) that the correlation between larval size and wandering duration is based on JH effects.

Larvae were also allatectomized early in the 2nd, 3rd and 4th instars. These larvae wandered during a broad gate on the third scotophase following surgery for an average of 10 h (3rd instar) to 19 h (4th instar). Detailed data were not collected from the tiny 2nd instar larvae. These results indicate that wandering can be induced by the appearance of ecdysteroids in any larval instar following the elimination of JH.

Effects of exogenous juvenile hormone

The above results suggest that JH may inhibit the performance of wandering behaviour when early instars are exposed to ecdysteroids and it may modulate the expression of wandering behaviour by the last instar larvae. When the JH mimic, EGS, was applied to Gate II, 5th instar larvae at progressively later times up until about 05.00 during the scotophase of day 4, the wandering gate was delayed by 1–3 days (Fig. 10). Throughout this period, progressively later EGS applications became increasingly effective both in causing the retention of larval characteristics at pupation

Fig. 10. Effect of EGS on onset of wandering. EGS (10 μg) was applied topically to Gate II larvae at various times (arrows) during the day prior to wandering. Following EGS treatment, the onset times of wandering were recorded in tilt-dish actographs and are shown as black histograms. The starting times of a distinct second wandering period which occurred in many of these larvae are also shown (open histograms). The distribution of wandering onset times in untreated Gate II larvae is shown in the top panel. The cross-hatched areas represent scotophases, beginning with day 4.

(Truman *et al.* 1974; personal observations) and in reducing the duration of wandering in the delayed gates to as little as 1 h.

Between 05.00 and 06.30 there was an abrupt increase in the proportion of EGS-treated larvae which wandered in their expected gate, although the onset time within the gate was influenced by the treatment. Thus, the ability of EGS applications to postpone wandering declined sharply during this period, as did its effectiveness in causing the retention of larval features at pupation (Truman *et al.* 1974).

Fig. 10 also shows that in response to EGS applications over the 9-h period beginning at about 06.30, wandering in the normal gate was followed by a second gated period of wandering in about 25 % of the larvae. The onset times of the repeated behaviour usually coincided with the start of wandering for animals which had been delayed by 1 day. Furthermore, wandering behaviour in this gate was extremely short: 2 ± 1 h for repeats; 5 ± 2 h for delayed larvae.

Although treatment with EGS after 06.30 could no longer delay the onset of wandering, it still had a marked effect on the duration of the behaviour (Fig. 11). With application of EGS at 06.30, 63 % of the treated larvae wandered in their usual gate, but the average duration of locomotion was only 2 ± 1 h. As EGS was applied at progressively later times, the duration of wandering increased proportionately until 15–20 h later, at which time behavioural duration could no longer be affected by EGS. Thus, it appears that the duration of wandering behaviour is determined by the gradual accumulation of effects of a process sensitive to interference by JH over an approximately 20-h period on the day prior to wandering.

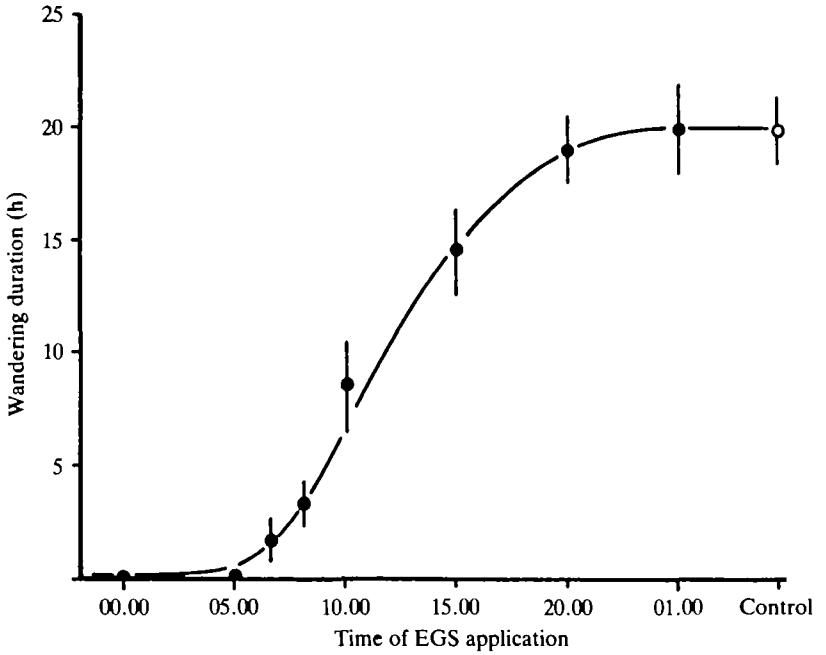

Fig. 11. Effect of EGS application on Gate II wandering duration. The duration (shown as mean ± S.E.) of wandering behaviour during the second gate (day 5) was measured in tilt-dish actographs following the EGS applications described in Fig. 10 ($N = 11–19$ per point).

Interaction between juvenile hormone and ecdysteroids

Effects of EGS application during 20-HE infusion

The above results show that appropriately timed applications of the JH analogue, EGS, during the period of endogenous 20-HE secretion, caused systematic changes in the duration of wandering. We examined whether this was due to the progressive interference with the 20-HE effects which normally lead to the 20 h long wandering behaviour. Gate II larvae were infused with 5 μg of 20-HE over 10 h starting at 00.00 on day 4, and 10 μg of EGS was administered either at the start of the infusion or 6 h later. As seen in Table 4, both EGS-treated groups of the larvae which wandered exhibited a duration of locomotion which was shorter than that seen when the 20-HE infusion was given alone. Those receiving EGS at the onset of ecdysteroid infusion

Table 4. *Effects of ECG treatment during 20-HE infusion into Gate II larvae*

EGS application time	*N*	% Early (*N*)	Induced duration (h ± S.E.M.)	Latency* (h ± S.E.M.)
00.00	29	38(11)	1·5 ± 0·5	15 ± 1
06.00	25	84(21)	5·5 ± 0·5	14 ± 0·5
none	20	85(17)	8·1 ± 1	14 ± 1

Gate II larvae were treated topically with 10 μg of EGS (1 μg EGS μl^{-1} cyclohexane) during 20-HE infusion (5 μg 20-HE over 10 h beginning at 00.00 on day 4).

* Latency is relative to start of 20-HE infusion.

only wandered for 2 h whereas those receiving EGS 6 h later spent 6 h wandering. Importantly, the time of EGS application did not alter the interval between the start of the infusion and the onset of induced wandering, which remained at 14–15 h.

In larvae receiving EGS during the period of endogenous or infused ecdysteroid action, wandering ended abruptly at about 16 h following the time of EGS application. The animals treated with EGS at the start of infusion showed a duration of wandering that was similar to larvae that had received 6 h of uninterrupted ecdysteroids. This relationship is consistent with the proposed 5-h equilibration period for topically applied EGS (Riddiford & Ajami, 1973).

The development of sensitivity to 20-HE

The effects of both allatectomy and EGS application on wandering behaviour are consistent with the idea that ecdysteroids must act in the absence of JH to induce wandering (Nijhout & Williams, 1974*b*; Truman *et al.* 1974). It was therefore important to determine when the 5th instar larvae acquired competence to wander in response to 20-HE, and to relate this to the normal fluctuation of the JH titre in larvae. When larvae were infused with 5 μg 20-HE over 10 h prior to 16.00 on day 2, wandering was not directly induced by 20-HE (Fig. 12). Many of these larvae (57 %) delayed

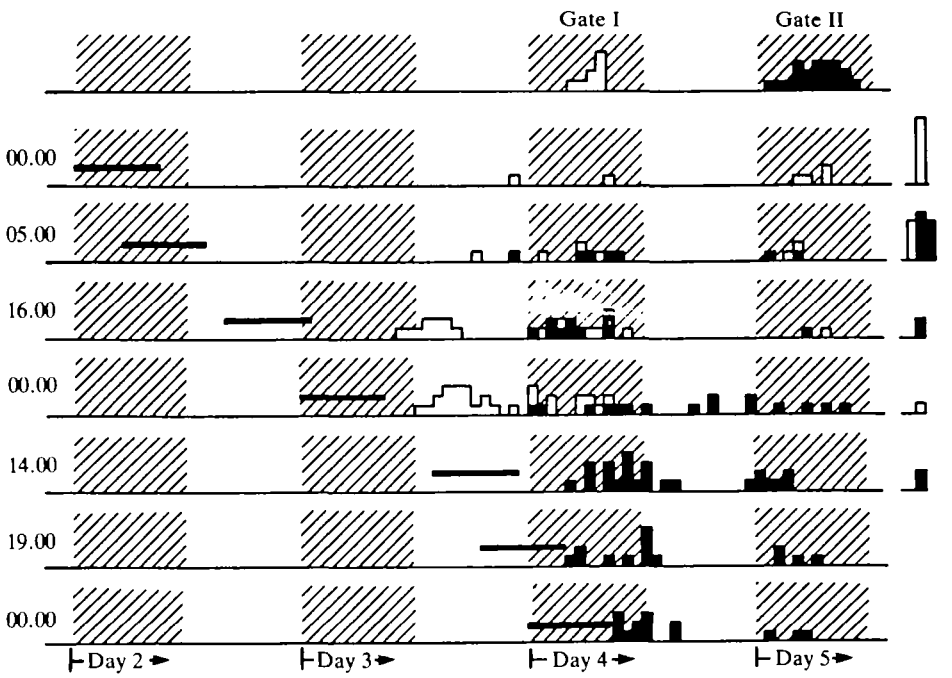

Fig. 12. The development of behavioural sensitivity to 20-HE during the 5th instar. Larvae were predicted to be either Gate I or Gate II by weight at different times during the 5th instar and were then infused with 20-HE (5 μg over 10 h) as indicated by the black bar to the left of each group. The subsequent wandering onset time was recorded in a tilt-dish actograph for each larva and is shown for predicted Gate I (white histograms) and Gate II (black histograms) larvae. The normal onset times for wandering in Gate I and Gate II larvae are shown at the top of the figure. Larvae wandering later than their normal gate are grouped to the right of each treatment.

wandering past the second gate as a result of starvation following the hormone treatment. By 16.00 on day 2, about 36 h before the first wandering gate was expected, infused 20-HE induced a clear wandering response in 67 % of the larger larvae with a mean latency of 25 ± 1 h. Most of the smaller, presumptive Gate II larvae were shifted to the first gate with a latency of more than 36 h from the start of the infusion. When 20-HE was infused into presumptive Gate I larvae starting at 00.00 on day 3 the response latency was further reduced to 16 ± 1 h. A similar pattern of declining latency associated with later infusions also occurred in the Gate II larvae. Therefore, once behavioural responsiveness to 20-HE had clearly appeared in one size class of larvae, later infusions decreased the interval between the start of infusion and the onset of behaviour from 20–25 h during the early stages of sensitivity, to 11–14 h when full sensitivity had been acquired.

The behavioural response to 20-HE was analysed in terms of larval size at the start of the infusion (Fig. 13). Prior to attaining a weight of 5·5 g, the onset time of wandering could not be advanced by 20-HE and was delayed by starvation following

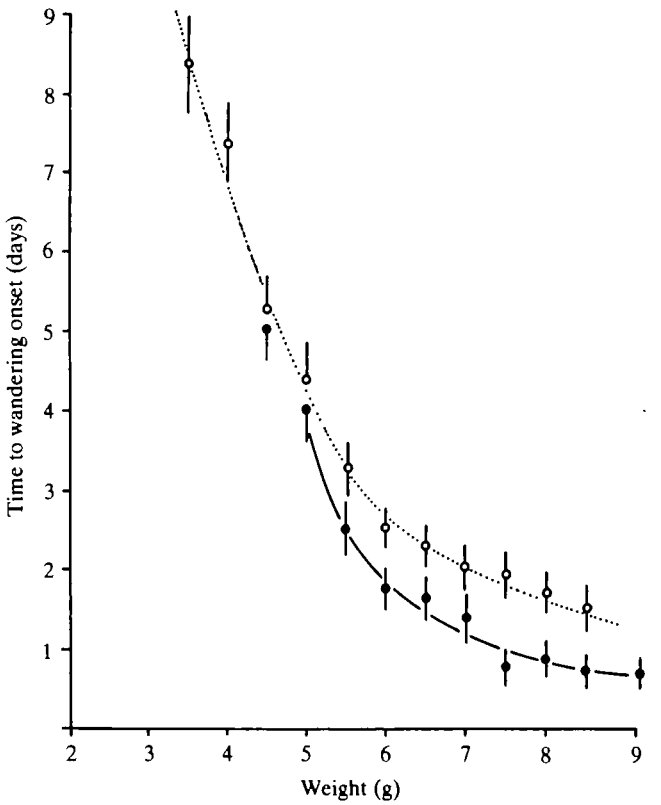

Fig. 13. Development of sensitivity to 20-HE as a function of larval weight during the 5th instar. Latencies to wandering were obtained from the results in Fig. 12 and were grouped according to weight at the time of 20-HE infusion. Open circles represent the latency (mean ± S.E., $N = 8–15$) to wandering of uninfused, starved control larvae; filled circles show the latency for larvae of each weight class ($N = 9–27$) following infusion with 20–HE (5 μg over 10 h).

20-HE infusion, as expected from the results of Nijhout & Williams (1974*a*). As larvae grew beyond 5·5 g, 20-HE infusion caused increasingly pronounced advancement of the behaviour relative to control larvae.

The appearance of sensitivity to 20-HE when the larvae attained a weight of 5·5 g supports the idea that the size-dependent decline of JH which begins at a critical weight of about 5 g (Nijhout & Williams, 1974*b*; Nijhout, 1975*a*) initiates competence for wandering in response to 20-HE. When allatectomized 5th instar larvae were infused with the standard dosage of 5 μg of 20-HE over 10 h, a slow but pronounced wandering response was evoked in 82% of the larvae by infused 20-HE as early as 14.00 on day 1, about 56 h prior to the expected wandering gate (Fig. 14). In these cases the latencies were exceptionally long, being 36 ± 4 h. Infusions before this time had a weaker, (but still significant) effect, in that larvae wandered in the normal gate 1 day earlier than fed, allatectomized controls. Such long latencies for response again suggest that very early 20-HE infusions had only an indirect effect on wandering even in allatectomized larvae. Later infusions required a shorter (13 h) latency, indicating direct induction of wandering by 20-HE.

The relationship between larval size and induction of wandering in these infused, allatectomized larvae is shown in Fig. 15. In the absence of JH, even 1·5-g larvae showed a behavioural response to 20-HE. Although the response had a very long latency (3·5 ± 0·5 days), these larvae wandered several days before the equivalent saline-infused controls. These exceptionally long latencies suggest that early 20-HE treatment might be acting indirectly by altering the normal timing mechanism for wandering rather than directly inducing the behaviour. Infusion of a much larger dose

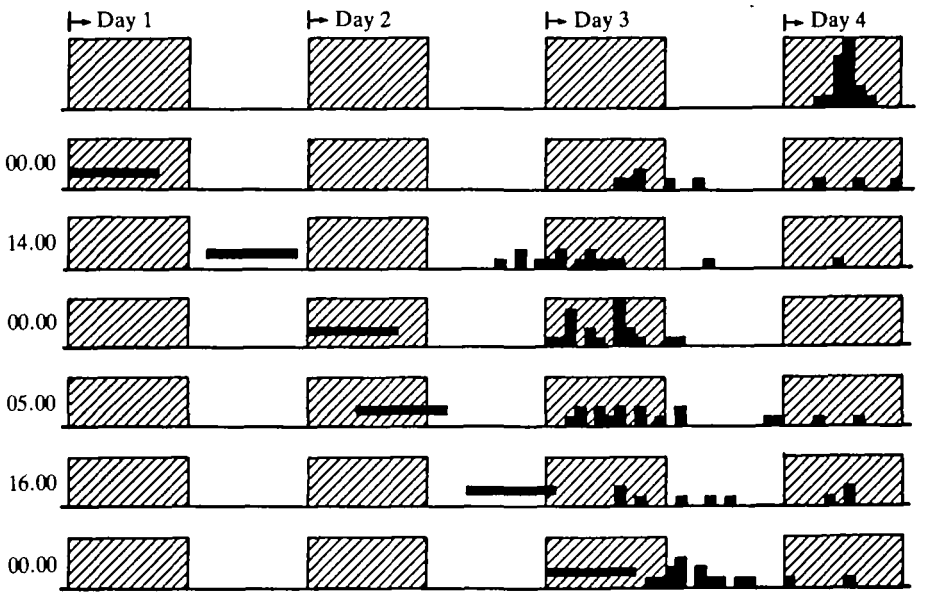

Fig. 14. Development of behavioural sensitivity to 20-HE in allatectomized larvae during the 5th instar. The time of wandering onset was recorded in tilt-dish actographs following 20-HE infusion (5 μg over 10 h) (black bars) into allatectomized larvae at various times during the 5th instar. The onset time for uninfused, allatectomized larvae is shown as a histogram at the top of the figure.

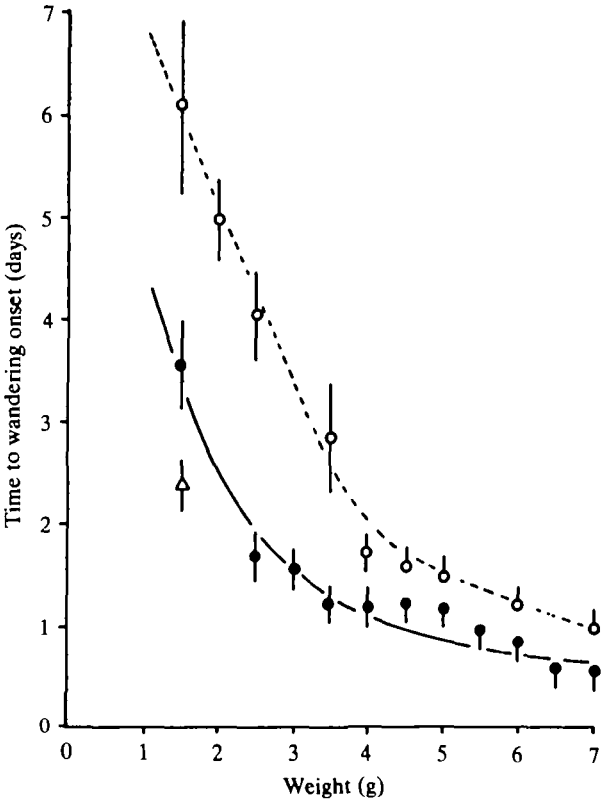

Fig. 15. Development of sensitivity to 20-HE as a function of weight during the 5th instar in allatectomized larvae. The latencies to wandering behaviour were obtained with respect to weight from the results shown in Fig. 15. Open circles show latency (mean ± S.E.) for uninfused, allatectomized controls ($N = 6$–12). Filled circles show the latency to wandering in each weight class following 20-HE infusion ($N = 9$–17). The open triangle represents the latency to wandering in response to a 20-HE infusion of 40 μg over 10 h ($N = 6$).

of 20-HE (40 μg) at this time resulted in a substantial reduction of the latency to 2·5 ± 0·2 days. As larvae grew past 1·5 g the latency following infusion of 5 μg over 10 h decreased rapidly, but it remained in excess of 24 h until, in 5- to 6-g larvae, the latency decreased to a minimum of about 15 h.

DISCUSSION

The role of ecdysteroids

Ecdysteroids have been implicated in the premetamorphic behaviour of the giant silkworm, *Samia cynthia* (Fujishita, Ohnishi & Ishizaki, 1982), *Hyalophora cecropia* (Lounibos, 1976) and *Ephestia kuhniella* (Giebultwicz *et al.* 1980). The results reported in this paper show that the wandering behaviour of *Manduca* larvae is induced by 20–HE. The requirement for ecdysteroids was shown by removing the prothoracic glands, the source of ecdysone, from larvae. This prevented the appearance of wandering behaviour as well as all other developmental changes known to require ecdysteroids. When these larvae were infused with 20-HE, wandering was induced,

followed by a state of quiescence from which bouts of locomotion could be briefly re-evoked by disturbance. This post-wandering excitability represented a distinct behavioural state of the larvae, persisting until the larvae died several weeks later without undergoing any further development.

The effectiveness of 20-HE in activating wandering was a function of the dose and duration of the hormone treatment as well as of the JH environment. Prolonging the exposure to 20-HE by multiple injections or continuous infusion has previously been shown to enhance the effect of this hormone compared with single injections (Ohtaki, Milkman & Williams, 1968; Zdarek & Fraenkel, 1970; Nijhout, 1976). The observation is particularly pertinent to the induction of wandering behaviour, where even large amounts (up to 100 μg) of injected 20-HE were unsuccessful in causing wandering. Prolonged exposure to 20-HE was necessary to induce a behavioural response. The maximal effectiveness of this treatment was reached with 9- to 10-h infusions of the steroid. The most effective infusion rate was 0.5 $\mu g\,h^{-1}$ or 0·06 $\mu g\,g^{-1}$ body weight h^{-1}. This rate of 20-HE delivery is consistent with the levels of ecdysteroid that are normally seen preceding wandering, ie. 0·07 $\mu g\,ml^{-1}$ (Wielgus, Bollenbacher & Gilbert, 1979).

Dosages greater than the optimal amount resulted in increasingly disrupted behaviour and at 5 $\mu g\,h^{-1}$ about 50 % of the larvae omitted wandering entirely (Fig. 3). In the silkmoth, *Samia cynthia*, large amounts of 20-HE caused an acceleration and compression of the early events of adult development (Williams, 1968). A similar effect of large infused dosages of 20-HE may accelerate the response of *Manduca* larvae such that they compress part or all of the spontaneous wandering period. Curiously, pupation was not noticeably advanced in such larvae. Thus, in order to activate the physiological process leading to wandering behaviour, an adequate, but not excessive, 20-HE concentration must be maintained in the larva for a sustained period of time.

Within the range of 20-HE infusions which induced wandering, the latency between the beginning of the infusion and behavioural onset varied with the rate of the infusion. A 20-h latency was seen when the 20-HE concentration was at the lower limit of effectiveness (0·15 $\mu g\,h^{-1}$) (Fig. 2; Table 2). This latency gradually shortened as dose increased, until at very high rates (5 and 10 $\mu g\,h^{-1}$) the minimal latency of about 11 h was observed. Infusions in the range of 0·2–0·5 $\mu g\,h^{-1}$ are thought to approximate the *in vivo* secretion of ecdysteroids. That these infusion rates resulted in an approximately 15-h latency suggests that the behaviourally relevant secretion of ecdysone is under way in normal animals by about 15 h prior to the onset of wandering behaviour. Photoperiod shift experiments (Dominick & Truman, 1984) also indicate an interval of about 15 h between a photoperiod-sensitive event and wandering behaviour. This time would coincide with the second pulse of PTTH proposed by Gilbert *et al.* (1981) which apparently elevates the ecdysteroid titre to a level leading to the induction of the behaviour.

An important feature of the wandering behaviour is that the duration of the spontaneous locomotor activity appears not to be a predetermined characteristic but instead is a function of the duration of ecdysteroid action which precedes the behaviour. Application of the JH mimic, EGS, at various times during exposure to endogenous or infused ecdysteroids resulted in behavioural durations proportional to the interval

of ecdysteroid action preceding the appearance of JH (Fig. 11). More directly, varying the duration of 20-HE infusion at 0·5 $\mu g\,h^{-1}$ resulted in a linear proportionality between the length of the infusion and the duration of the subsequently induced behaviour (Fig. 8). Thus, the duration of wandering behaviour is established as a direct consequence of the duration of ecdysteroid presence, and not as a preprogrammed repertoire which is simply triggered by a phasic hormonal signal.

In studies of vertebrate reproductive behaviour, relatively long but dose-dependent latencies similar to those reported here exist before the onset of lordosis behaviour induced in rabbits (30 h, McDonald, Vidal & Beyer, 1970) and in rats (16–22 h, Green, Luttge & Whalen, 1970). The long latency typically required for the induction of behavioural effects by steroids probably represents the time required for a sequence of hormonally stimulated RNA and protein synthetic steps which are thought to constitute the mechanism by which steroid mediated behavioural changes occur (McEwan, Davis, Parsons & Pfaff, 1979).

The duration or intensity of steroid-induced behaviour can be graded in vertebrates in response to varying the parameters of hormone exposure, as has been demonstrated with oestrogen-dependent mating behaviour in the rat (Aren-Engelbrektsson, Larsson, Sodersten & Wilhelmsson, 1970; Demassa, Smith, Tennent & Davidson, 1977), rabbit (McDonald *et al.* 1970), cat (Peretz, 1968) and guinea pig (Goy & Young, 1957). Therefore, the programming of the duration or intensity of induced behaviour as a cumulative steroid effect may be a phylogenetically widespread phenomenon.

Wandering latency and duration are controlled independently by different parameters of 20-HE exposure. The minimal effective 20-HE infusion lasts 4 h during which time the steroid probably acts by inducing primary biochemical changes such as mRNA and protein synthesis. Since the behavioural duration induced by such a short 20-HE infusion is also short (Fig. 11), the relevant biochemical changes would appear to have a relatively short half-life and quantitatively to support the behaviour. Thus, by increasing the duration of 20-HE exposure, the induced product might be synthesized over a longer period of time, thereby enabling the behaviour for a correspondingly extended period. Induction of new neurotransmitter or postsynaptic receptor species in the 20-HE target neurones are possible examples which would conform to this interpretation.

Although 4 h infusion with 20-HE was sufficient to induce wandering behaviour, a minimum latency of 11 h must intervene before the induced behaviour appears. Since this latency varies strictly as a function of 20-HE dose (Table 2) and is not influenced by infusion duration (Table 3) the rate of accumulation of the presumed induction product would be dose dependent as is typical with steroid hormones. In the simplest case the product might accumulate to a critical level (the threshold for wandering) at a rate proportional to the 20-HE concentration, thereby advancing the start of behaviour as 20-HE concentration increases. This accumulation would require at least 7 h in addition to the 4 h infusion of 20-HE (a total latency of 11 h at the highest effective hormone concentration. Alternatively, the dose-dependent accumulation of product to the threshold level may be more rapid but additional time could be required for a secondary, hormone-independent process which contributes significantly to the latency. Transport of induced neurotransmitter or receptor

molecules to appropriate pre- or postsynaptic regions of the putative 20-HE target neurones could provide such a delay.

Wandering behaviour induced by 20-HE infusion was often followed by a distinct second period of wandering which began early in the usual wandering gate (Figs 1, 7) and which was uniformly shorter than normal, averaging 7 h in length (Tables 2, 3). This reappearance of wandering was apparently due to the endogenous gated secretion of ecdysone, since second bouts of wandering behaviour were not observed in 20-HE-infused larvae lacking prothoracic glands. Evidently, the behavioural action of 20-HE does not necessarily include a programmed loss of behavioural sensitivity to subsequent re-induction as is true for eclosion hormone (Truman, 1978). Furthermore, varying the starting time and duration of 20-HE infusion into unoperated larvae greatly affected the onset time and duration of the induced behaviour, but had no effect on the initiation or duration of the repeat wandering. Indeed, when larvae were restrained and infused with 20-HE at the start of wandering about half of them entered a distinct second period of wandering extending well past the usual time when control larvae become inactive.

Juvenile hormone effects on wandering induction by 20-HE

The disappearance of JH from the tissues of the last instar larva of *Manduca* is a prerequisite for PTTH release (Nijhout & Williams, 1974*b*) and for ecdysteroids to induce premetamorphic changes in the epidermis (Riddiford, 1978). Allatectomy resulted in precocious wandering behaviour in earlier instars of *Manduca* as has been found for *Bombyx* (Bounhiol, 1938) and *Galleria* (Piepho, 1938). Thus, the requisite behavioural circuitry appears to be both present and responsive to its endocrine trigger from a time very early in post-embryonic development.

The release of PTTH and ecdysteroid necessary for wandering behaviour can be delayed if JH reappears before these secretory processes begin. Application of the JH mimic, EGS, to larvae during ecdysteroid infusion or during their normal time of release of ecdysteroid showed that JH can antagonize the action of 20-HE apparently at any time during the 24-h ecdysteroid release. Interestingly, any effects of ecdysteroid that have occurred prior to the application of EGS are subsequently manifest as the normal initiation and progression of the behaviour. Since applications of EGS just prior to the start of wandering had no effect, only the induction and not the expression of the behaviour is sensitive to JH. The spinning of very thin or flat cocoons by *H. cecropia* larvae which were treated with JH during the period when epidermal commitment could be disrupted (Riddiford, 1972) suggests that the endocrine activation of cocoon spinning is analogous to that of *Manduca* wandering in that the behavioural programme accumulates as a function of ecdysteroid action over time.

The ability of JH to modify the duration of wandering is probably the basis for the size-related variation of behavioural duration seen in *Manduca* larvae (Dominick & Truman, 1984). Wandering duration lengthens as larval weight increases in larvae with intact CA, but allatectomized 5th instar larvae show no such relationship. Therefore, it appears that following the elimination of measureable JH which starts when the larva reaches a critical size of about 5 g (Nijhout & Williams, 1974*b*), JH or its effects gradually decrease with time as the larva continues to grow. The residual JH effects may influence the behavioural action of 20-HE in proportion to their

J. exp. Biol. **117**, 29–43 (1985)
Printed in Great Britain © *The Company of Biologists Limited 1985*

PRESSURE-INDUCED CHANGES IN Ca^{2+}-CHANNEL EXCITABILITY IN *PARAMECIUM*

BY T. OTTER* AND E. D. SALMON

Department of Biology, University of North Carolina, Chapel Hill, North Carolina 27514, U.S.A.

Accepted 7 January 1985

SUMMARY

The behaviour of swimming *Paramecium* is markedly affected by hydrostatic pressure (50–200 atm, 1 atm = 101 325 Pa). To investigate whether pressure might alter behaviour by acting directly on specific ion channels that mediate the behavioural responses, we examined the effects of K^+, Na^+ and Ba^{2+} ions on swimming speed and the reversal response during pressurization and decompression. If pressure acted on the channels that transport these ions, then the pressure-induced responses of swimming *Paramecium* should be exaggerated or diminished, according to which ions were present in the experimental buffer. Pressurization to 100 atm in standard buffer inhibited the brief reversal of swimming direction that occurred at atmospheric pressure when a paramecium encountered the wall of the pressure chamber. To determine whether pressure impaired mechanoreceptor function or directly blocked the Ca^{2+}-channels that control ciliary reversal, we added Ba^{2+} or Na^+ to standard buffer to induce multiple spontaneous reversals. Pressurization blocked these reversals, suggesting that channel opening is directly inhibited by pressure. Decompression in standard buffer elicited momentary ciliary reversal and backward swimming. Buffers with a high ratio of K^+ to Ca^{2+} suppressed this response, and the decompression-induced reversal was exaggerated in the presence of Ba^{2+} or Na^+, consistent with the effects that these ions are known to have on *Paramecium*'s reversal response. These data imply that, upon decompression, the Ca^{2+}-channels that mediate ciliary reversal open transiently. In addition to blocking the reversal response, pressurization slowed forward swimming. By examining the response to pressurization of *Paramecium* immobilized by Ni^{2+}, we found that hydrostatic pressure apparently slows swimming by reorientating the direction of ciliary beat.

INTRODUCTION

Many types of excitable cells are sensitive to changes in hydrostatic pressure (reviewed by Wann & MacDonald, 1980). Kitching has described, in detail, the responses of a variety of ciliates and flagellates, including

*Present address: Cell Biology Group, Worcester Foundation for Experimental Biology, 222 Maple Avenue, Shrewsbury, MA 01545, U.S.A.
Key words: *Paramecium*, hydrostatic pressure, excitable membrane, cilia.

Paramecium and *Spirostomum*, to pressurization and decompression (Kitching, 1957, 1969; MacDonald & Kitching, 1976). His results demonstrated that the sensory behaviour of ciliates is impaired by pressurization. More recently, studies of voltage-clamped neurones under pressure have indicated that pressures of 200 atm or less can alter neuronal function and nerve excitability (Conti, Fioravanti, Segal & Stuhmer, 1982; Harper, MacDonald & Wann, 1981; Parmentier & Bennett, 1980; Wann, MacDonald & Harper, 1979).

We have used hydrostatic pressure to study the sensory and motor behaviour of *Paramecium*. Hydrostatic pressure is particularly well-suited for these studies because pressurization and decompression are rapid and the effects of pressure changes appear completely reversible up to about 280 atm (Otter & Salmon, 1979). Within this pressure range there are no obvious changes in *Paramecium*'s structure, and the cells respond instantaneously to changes in pressure. The pressure-sensitive components of *Paramecium*'s motility reside primarily in its electrically excitable plasma membrane (Otter & Salmon, 1979). In particular, the Ca^{2+}-channels that mediate ciliary reversal appeared to be sensitive to changes in hydrostatic pressure.

Sensory behaviour in the ciliate *Paramecium* is linked to the cell's motor response by its electrically excitable plasma membrane. Normally, a *Paramecium* swims forward because its cilia beat with their effective strokes directed toward the cell's posterior. Reversal of ciliary beat direction and backward swimming result from depolarization of the surface membrane. An inward flow of calcium ions through voltage-sensitive channels, located in the plasma membrane covering the cilia, depolarizes the cell, elevates the Ca^{2+} concentration around the ciliary axonemes and triggers reversed beating of the cilia. When the surface membrane re-establishes its resting electrical potential and the calcium concentration surrounding the axonemes falls, normal forward swimming resumes. This scenario of sensory-motor coupling in *Paramecium* has been deduced from a variety of experiments using genetic, biochemical, electrophysiological and microscopical techniques (Dunlap, 1977; Eckert & Brehm, 1979; Kung *et al.* 1975; Kung & Saimi, 1982; Machemer & Ogura, 1979; Naitoh & Kaneko, 1972). Nevertheless, relatively little is known about the molecular basis of *Paramecium*'s membrane excitation or the Ca^{2+}-dependent pathway in the cytoplasm that leads to reversal of ciliary beat direction.

In this paper, we describe the motility of *Paramecium* during pressurization and decompression in buffers of different ionic composition made by systematically varying the concentrations of Ca^{2+}, K^+, Na^+ and Ba^{2+} ions. Because these cations are known to induce alterations in the behaviour of *Paramecium* swimming at atmospheric pressure, we can make specific predictions regarding how substitution of cations might alter the responses of *Paramecium* to changes in hydrostatic pressure (Kung & Saimi, 1982). We have analysed the pressure-induced responses of *Paramecium* according to these predictions in order to understand how pressure alters the physiology of the excitable plasma membrane. In order to study ciliary movements under pressure, we have examined pressure-induced changes in orientation of cilia paralysed by nickel ions. Finally, we describe a new, enlarged microscope pressure chamber for studying cell movements under pressure. Portions of this work have been published in abstract form (Otter, 1980; Otter & Salmon, 1982).

MATERIALS AND METHODS

Growth media and harvesting cells

Paramecium caudatum (Carolina Biological Supply, Burlington, NC) were grown at room temperature in bacterized Cerophyl medium (Cerophyl Corp., Kansas City, MO) as described by Sonneborn (1970). *Paramecium* were transferred from culture medium to an experimental buffer (see below) by washing them three times at room temperature by gentle hand centrifugation (30–60 s, 150 × ***g***). Experiments described here concern swimming behaviour after an initial period of adjustment to the ions in the buffer. We allowed an equilibration period of at least 30 min before beginning experiments. *Paramecium* observed during a transfer from culture medium to buffer often swam backwards or forwards rapidly, but after several minutes of exposure this behaviour subsided.

Chemicals and experimental buffers

Our standard buffer (TECK) contained (in mmol l^{-1}): Tris, pH 7·2, 10·0; EDTA, 0·1; $CaCl_2$, 1·0; KCl, 4·0. Salts were purchased from Sigma Chemical Company, St. Louis, MO. To this buffer we added either: 10 mmol l^{-1} KCl (K^+-TECK), 10 mmol l^{-1} NaCl (Na^+-TECK) or 20 mmol l^{-1} KCl. To induce 'barium dancing' we added 4 mmol l^{-1} $BaCl_2$ to TECK, K^+-TECK or TEC buffer. TEC buffer is standard buffer without KCl.

Paralysis by nickel ions

The effective concentration of $NiCl_2$ for paralysis of cilia was determined by transferring about 100 μl of TECK containing about 50 *Paramecium* to a dish of TECK plus $NiCl_2$ at various concentrations. We chose a concentration of nickel that immobilized 90 % of the *Paramecium* within 10 min without obvious physical distortion of the cells. For *Paramecium* that had been preincubated in TECK, 0·2 mmol l^{-1} $NiCl_2$ proved effective; other concentrations were not suitable. Higher concentrations (0·5–1 mmol l^{-1} $NiCl_2$) lysed many cells and at 0·1 mmol l^{-1} $NiCl_2$ paralysis was complete in 2 h.

Hydrostatic pressure chamber for microscopy

We have designed and built a pressure chamber for observing *Paramecium* at pressures of 350 atm or less. The chamber is a larger, modified version of a miniature pressure chamber for microscopy described by Salmon & Ellis (1975; Fig. 1).

The microscope chosen for this study was a Leitz Diavert inverted microscope (Otter & Salmon, 1979; Otter, 1981). In order to record the orientation of paralysed cilia during pressurization and decompression, we fitted the Diavert with a Zeiss Model I long working distance phase contrast condensor and a Nikon 40× DML phase contrast objective with correction collar; paralysed specimens were pressurized in the miniature chamber (Salmon & Ellis, 1975). Illumination was routinely a tungsten filament bulb. For flash photography we used a Strobex model 136 power supply equipped with a Xenon arc flash tube (model 35 s). All triggering circuitry for driving the Strobex power supply was home-made.

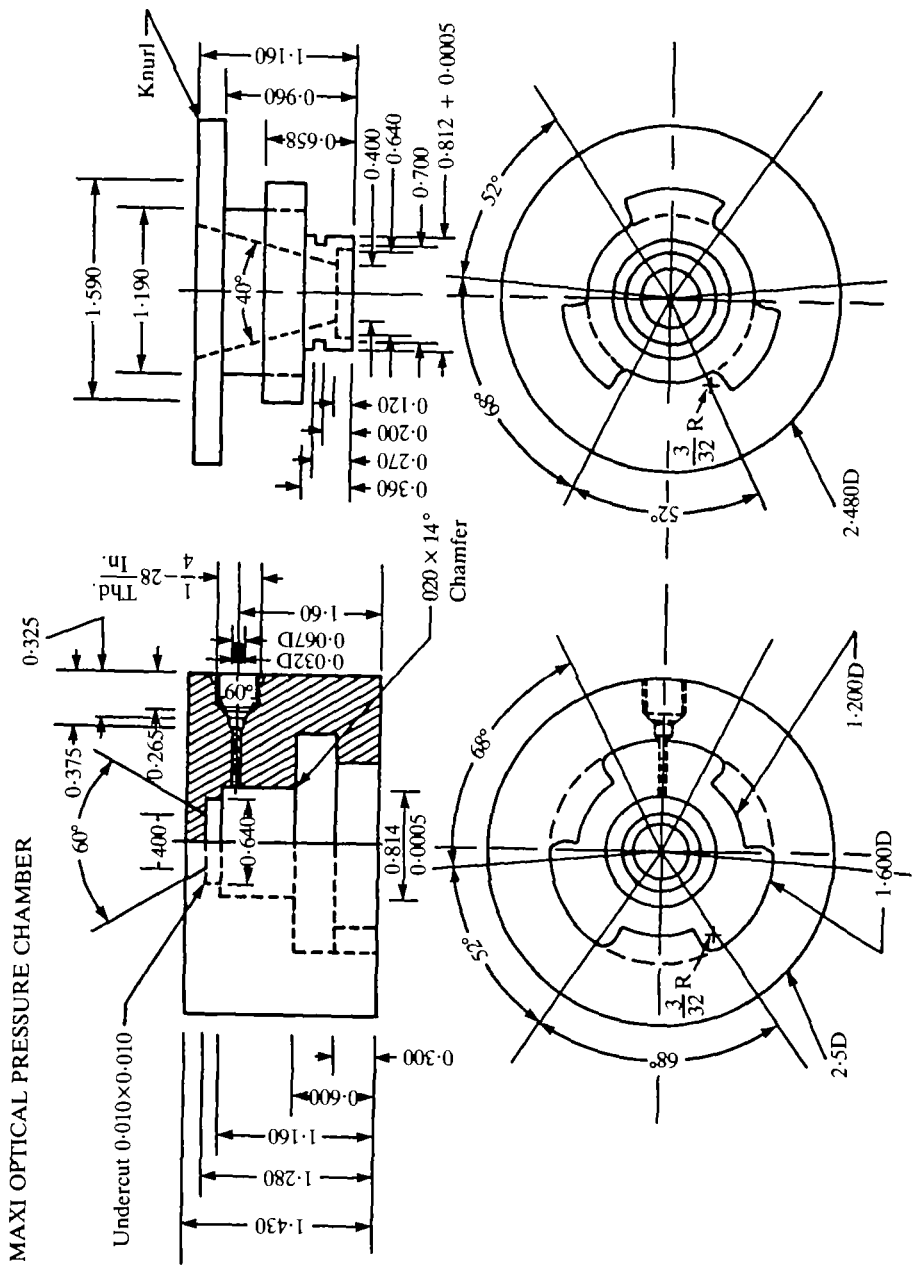

Fig. 1. Detailed drawings of large microscope pressure chamber. The material is 316 stainless steel. All dimensions are ± 0.001 inches unless otherwise noted. All sharp corners are broken. All surfaces machine finished with no burrs. The window seats should be turned flat within 0.0002 inches. The windows are 3 mm-thick optical glass. Substituting sapphire windows for glass would increase the working pressure range to 1000 atm.

Recording swimming behaviour

Qualitative observations on the responses of swimming *Paramecium* to step changes in pressure and counts of reversals were obtained by directly viewing *Paramecium* in the chamber. All measurements of swimming speed and ciliary orientation were taken from photographic records (Otter & Salmon, 1979). Swimming direction was deduced from the experimenter's written and mental records that a cell was swimming backward or forward and from the clearly-defined body shape of the *Paramecium* recorded on the film. Because the *Paramecium* moved about rapidly in the chamber, it was important to have a simple, highly-automated method to record swimming tracks. The strobe delivered a pre-set number of flashes at a predetermined interval, τ, usually 0·3 s. After the final flash, the trigger circuit closed the shutter, reset itself and advanced the film.

RESULTS

Pressurization in culture medium

Paramecium were highly sensitive to pressure when they were swimming in culture medium (Table 1). As little as 30 atm produced a noticeable decrease in both forward speed and in reversal frequency; at 70 atm many *Paramecium* came to rest against the lower cover-glass surface. On release of pressure, *Paramecium* backed up quickly and then swam actively.

Pressurization in standard buffer (TECK)

The pressure-induced responses of *Paramecium* swimming in TECK buffer were described briefly elsewhere (Otter & Salmon, 1979). At atmospheric pressure, *Paramecium* in TECK buffer swam in a series of relatively straight paths interrupted by brief reversals or 'avoiding reactions'. Normally, a *Paramecium* swam at about 1·4 mm s^{-1} and backed up about 7 times per minute (Table 2). Pressurization immediately slowed their forward speed; the higher the pressure the lower the average speed of swimming *Paramecium* (Figs 2,4,5). At 100 atm, they swam at about one-

Table 1. *Responses to pressurization and decompression*

	Pressurization		Decompression
Buffer	Slowing	Fewer reversals	Transient reversal
TECK	+	+	+
TEC	+	+	+
K^+-TECK	++	++	−−
Na^+-TECK	+	−	++
Ba^{2+}-TECK	+	−−	+++
Cerophyl	++	++	++

Responses to changes in hydrostatic pressure ranged from very weak (−−) to very strong (+++). The 'average' responses (+) were defined as those seen in TECK.

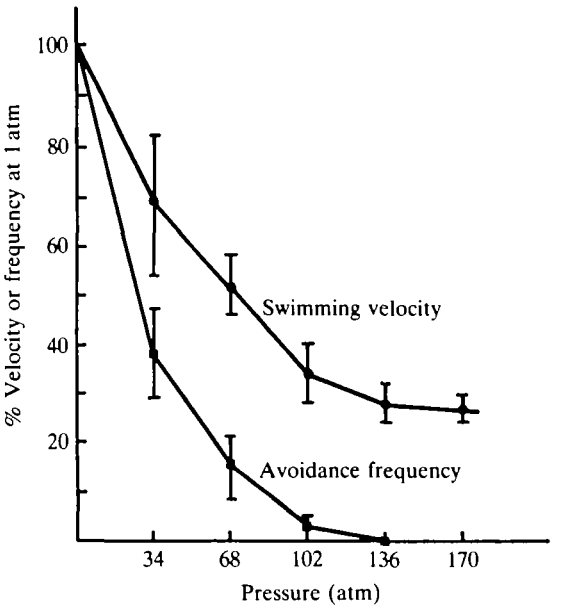

Fig. 2. Decrease in velocity of forward swimming (●) and frequency of avoiding reactions (■) with increasing pressure. Pressure was raised from atmospheric in steps of 34 atm at 5-min intervals. At each pressure, swimming speeds of 5–10 organisms were determined from photographs taken during each 5-min interval. Data from four such experiments were pooled and averaged for each pressure level. In five separate experiments, visual counts of the number of jerks, hesitations or reversals of four or five organisms were recorded at each pressure. Values plotted are the mean ± S.E. normalized to the initial value at atmospheric pressure.

Table 2. *Ion effects on swimming behaviour*

	Avoidance frequency Reversals ($cell^{-1} min^{-1}$)	Forward swimming speed ($mm\ s^{-1}$)
TECK	6·75 ± 0·76 (7)	1·37 ± 0·25 (102)
Na^+–TECK	11·48 ± 1·05 (7)	1·36 ± 0·16 (73)
K^+–TECK	2·51 ± 0·45 (4)	0·93 ± 0·09 (183)
TEC	9·4 ± 2·7 (7)	1·59 ± 0·38 (112)

Values are means ± S.D. (*N*).

third their initial speed, and many *Paramecium* were completely immobilized by this pressure. When the pressure was increased further, more *Paramecium* came to rest at the edge of the specimen enclosure, and the remaining cells slowed down. Pressurization also inhibited reversal of swimming direction that was observed at atmospheric pressure. Occasionally at 100 atm *Paramecium* hesitated briefly; above 100 atm, some continued to move forward slowly, but they did not back up.

Rapid decompression (within 2 s) to 13.6 atm elicited a transient reversal response similar to an avoiding reaction (Figs 3A, 5). Even if the pressure was reduced slowly ($\simeq 1{\cdot}5\ atm\ s^{-1}$), the *Paramecium* jerked backwards when the pressure reached 68 atm. The effects of pressurization and decompression appeared to be completely reversible up to about 300 atm. After the brief reversal upon decompression, the *Paramecium* swam in a manner characteristic for the lower pressure.

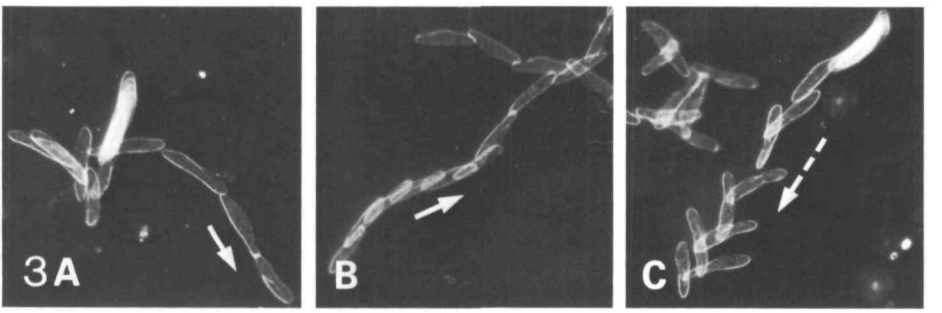

Fig. 3. Responses to abrupt decompression. Pressure was held at 170 atm during the first four strobe flashes and then quickly lowered to 13·6 atm. In TECK buffer (A), the *Paramecium* jerked backwards upon decompression and then swam forwards (arrow). Upon decompression in K^+-rich buffer (B), the *Paramecium* simply accelerated forwards (arrow). The response to decompression in Ba^{2+}-TECK (C) was prolonged backward swimming (dashed arrow). $\tau = 0{\cdot}3$ s. Magnification, ×40.

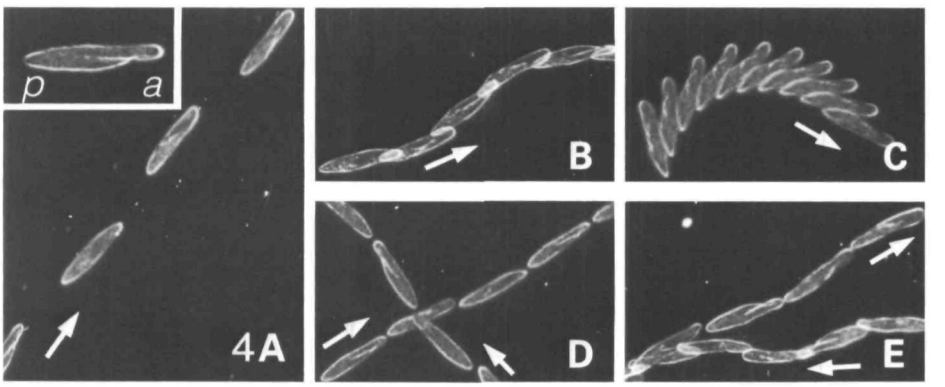

Fig. 4. Slowing of forward swimming induced by increasing pressure (A,B,C) or increasing [KCl] at atmospheric pressure (A,D,E). (A) TECK buffer at atmospheric pressure; (B) 68 atm in TECK: (C) 136 atm in TECK; (D) 10 mmol l^{-1} KCl added to TECK at atmospheric pressure; (E) 20 mmol l^{-1} KCl-TECK at atmospheric pressure. Inset (A) Posterior (*p*) and anterior (*a*) are easily distinguished. In all photographs, arrows indicate the direction of forward movement and $\tau = 0{\cdot}3$ s. Magnification, ×40.

Effect of pressure in K^+-rich buffer (K^+-TECK)

At atmospheric pressure, increasing the KCl concentration from 4 mmol l^{-1} (TECK buffer) to 10 or 20 mmol l^{-1} slowed swimming *Paramecium* (Table 2; Fig. 4). In 10 mmol l^{-1} K^+ buffer (K^+-TECK), the average speed of *Paramecium* was reduced by about 40 %, so that they travelled approximately one body length per flash interval; in 20 mmol l^{-1} K^+ buffer successive images of swimming *Paramecium* appeared slightly overlapped. At either KCl concentration the swimming paths of *Paramecium* appeared wavy or corkscrew-shaped compared to paths in TECK buffer, and the forward speed of individual *Paramecium* was more monotonous. They swam slowly from one side of the enclosure to the other, often without spontaneous hesitation or acceleration. When they reached the edge, they backed up weakly, turned and swam slowly in a new direction. The frequency of avoiding reactions was reduced in K^+-TECK buffer (Table 2). Many cells appeared noticeably flattened by

exosmosis in 20 mmol l^{-1} K^+ buffer, so we did not use this buffer for further experiments with hydrostatic pressure.

We compared the swimming behaviour of *Paramecium* in TECK buffer and in K^+-TECK during pressurization to 204 atm in 68-atm steps and during decompression (Fig. 5). In either buffer, after a step increase in pressure, the forward speed of an individual decreased immediately. In K^+-TECK at 68 atm nearly all *Paramecium* had stopped moving forwards. A few individuals continued to swim forward slowly, and they never backed up. In TECK buffer a pressure of 136 atm or above was required to produce the same effect. At a given pressure, *Paramecium* swimming in TECK changed speed more quickly and more often than *Paramecium* in K^+-TECK buffer (Fig. 5).

Paramecium in K^+-TECK did not reverse their ciliary beat during decompression to 13.6 atm; they hesitated briefly and then simply accelerated forward (Fig. 5). Reducing the Ca^{2+}-concentration from 1 mmol l^{-1} (in TECK) to 0·1 mmol l^{-1} produced the same result: no reversal occurred on decompression (Fig. 3B).

Removing K^+-ions from the external medium (TEC) changed the swimming behaviour of *Paramecium* only slightly compared to their behaviour in TECK. At atmospheric pressure, the forward speed and frequency of reversals increased, but the responses of *Paramecium* in TEC to changes in pressure were essentially identical to those in TECK (Tables 1,2).

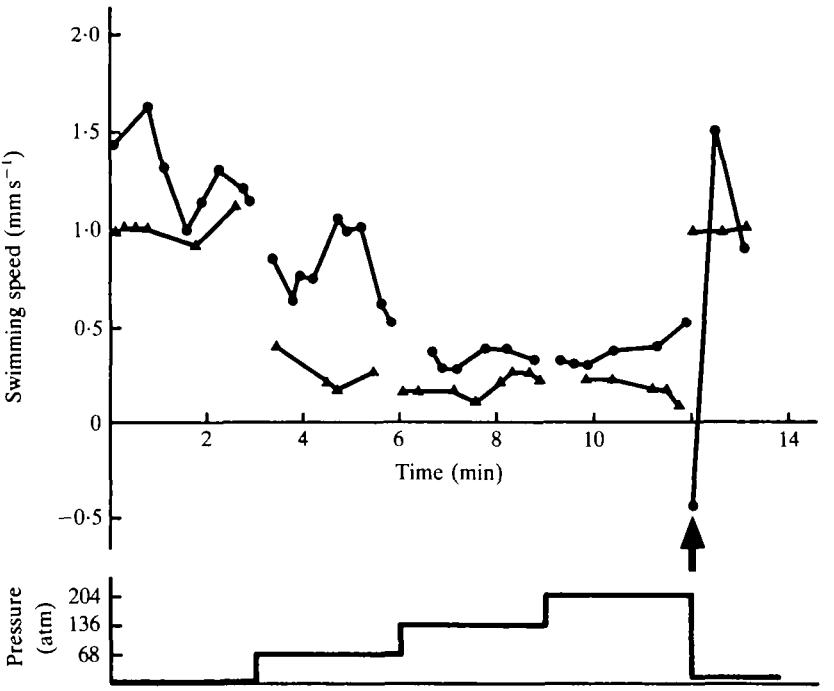

Fig. 5. Instantaneous velocity of typical individual *Paramecium* during stepwise pressurization in TECK (●) or K^+-TECK (▲). Pressure was increased from atmospheric in steps of 68 atm at 3-min intervals to 204 atm and then returned abruptly to 13·6 atm. Swimming velocity was determined from photographs taken during each interval. Decompression elicited an avoiding reaction (arrow) in TECK buffer, but not in K^+-TECK.

Effect of pressure in Na^+- or Ba^{2+}-rich buffer (Na^+-TECK or Ba^{2+}-TECK)

We examined the responses of swimming *Paramecium* to pressurization and decompression in Na^+-TECK containing 10 mmol l^{-1} NaCl (Table 1). At atmospheric pressure, adding NaCl slowed their forward speed slightly, but it increased their frequency of avoiding reactions 1·7-fold (Table 2). Occasionally, prolonged reversals (> 3 s duration) occurred in Na^+-TECK. Pressurization of *Paramecium* in Na^+-TECK to 68 atm slowed their forward movement. This pressure did not completely block reversals, but 136 atm did. Nearly all *Paramecium* were stopped at 136 atm. Decompression caused an exaggerated reversal, followed by rapid forward swimming punctuated by frequent reversals. This latter result contrasted strikingly with the weak hesitation that accompanied decompression in K^+-TECK.

Addition of 4 mmol l^{-1} $BaCl_2$ to TECK, TEC or K^+-TECK induced frequent repetitive avoiding reactions, a behaviour known as the 'barium dance' (Fig. 6). Many cells jerked backwards repeatedly and made no forward progress through the medium. For example, in TECK buffer the *Paramecium* backed up about three times as often with barium present. Additionally, most of the reversals occurred spontaneously, when no obvious physical stimulus was present.

Pressurization to 68 atm reduced the frequency of barium-induced reversals. In Ba^{2+}-TECK buffer or Ba^{2+}, K^+-TECK buffer, 204 atm blocked the barium-induced reversals completely, but in Ba^{2+}-TEC buffer, barium-induced reversals continued

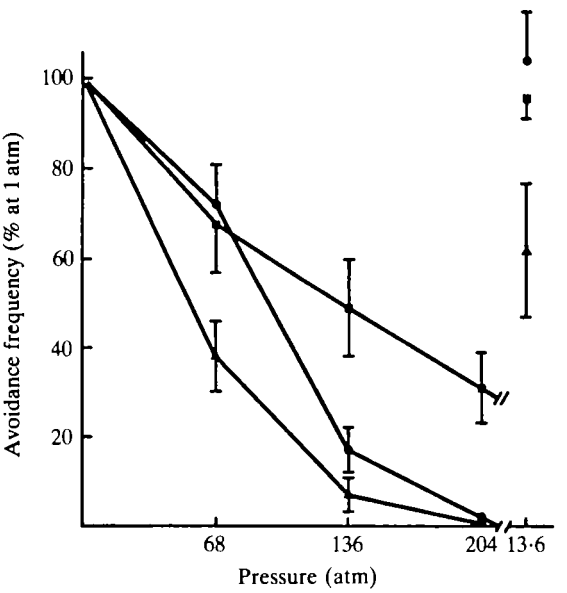

Fig. 6. Decreasing frequency of spontaneous reversals in Ba^{2+}-rich media with increasing pressure. (●) Ba^{2+}-TECK; (▲) Ba^{2+}, K^+-TECK; (■) Ba^{2+}-TEC. Pressure was increased from atmospheric in steps of 68 atm to 204 atm and then reduced in a single step to 13·6 atm. At each pressure, reversals of four or five *Paramecium* were counted for 3 min. The experiment was repeated four times for each buffer and the data for each pressure level were pooled and normalized to the initial value at atmospheric pressure. Values are the mean ± S.E. At atmospheric pressure, (●) = 15·8 ± 1·8; (▲) = 18·2 ± 2·9; (■) = 26·4 ± 1·3 reversals (cell^{-1} min^{-1}).

even at 204 atm. Reversals were more violent in Ba^{2+}-TEC than in the other two buffers at any pressure. *Paramecium* jerked backwards rhythmically and rotated rapidly about their long body axis. Even though the *Paramecium* made little or no forward progress at 204 atm, they still occasionally jerked backwards.

These decreases in Ba^{2+}-induced reversals under pressure appeared to be completely reversible within the pressure range studied. Upon decompression in any medium containing barium, many *Paramecium* reversed vigorously and then danced wildly for the next several minutes (Fig. 3C). Often during the few minutes following decompression in barium-containing media, the frequency of reversals was higher than it had been before pressurization (Fig. 6).

Pressure-induced changes in ciliary orientation and movement

In order to examine specifically if pressure induced changes in the orientation of cilary beat, we observed the behaviour of *Paramecium* immobilized by nickel ions during step pressurization and decompression. Nickel ions paralyse cilia so that they do not beat, but they retain the ability to reorientate in response to chemical, physical or electrical stimuli (Naitoh, 1966; Eckert & Naitoh, 1970). The orientation of cilia immobilized by nickel reflects the direction of the effective stroke that a normal beating cilium would have. To minimize the toxic effects of nickel, we performed all experiments within the first 40 min following incubation in 0·2 mmol l^{-1} $NiCl_2$-TECK. Gradually, over the next 30 min, the cilia assumed a resting position that was more or less at a right angle to the cell surface.

During the first 30 min of paralysis, the cilia appeared gently curved. They 'vibrated' and occasionally reversed spontaneously. When the nickel-paralysed *Paramecium* were transferred from TECK buffer plus nickel to 20 mmol l^{-1} K^+-TECK, their cilia reversed immediately and continued to point towards the anterior for tens of seconds, similar to K^+-induced reversal of swimming direction in unparalysed *Paramecium* (Fig. 7D; Naitoh, 1968). To interpret the pressure-induced changes in ciliary orientation (discussed below), we designated the normal orientation and the reversed orientation in 20 mmol l^{-1} K^+-TECK as two extremes.

Pressurization to 68 atm caused cilia paralysed by nickel ions to move from their normal, posteriorly-directed posture to nearly perpendicular to the *Paramecium*'s surface (Fig. 7). Increasing the pressure to 136 atm caused the cilia to point slightly toward the cell's anterior (Fig. 7C). Above 70 atm pressure, the paralysed cilia never reversed or pointed towards the posterior; they stuck out straight and vibrated weakly. As noted above, cells that had been incubated in nickel medium for over 30 min had many of their cilia pointing at a right angle to the cell surface at atmospheric pressure. These cells responded to pressure by shifting their cilia slightly towards the anterior, but this change was not nearly as striking as the pressure-induced reorientation in a freshly immobilized *Paramecium*.

Decompression caused a *Paramecium*'s paralysed cilia to swing towards the anterior transiently, similar to a spontaneous or K^+-induced reversal (Fig. 7E). In standard buffer containing nickel, the reversal was momentary and a recovery period of confused orientations of cilia followed (Fig. 7F). During recovery many of the cilia appeared to lie flat against the cell surface. The first recognizable position assumed by the cilia after decompression-induced reversal was directed towards the

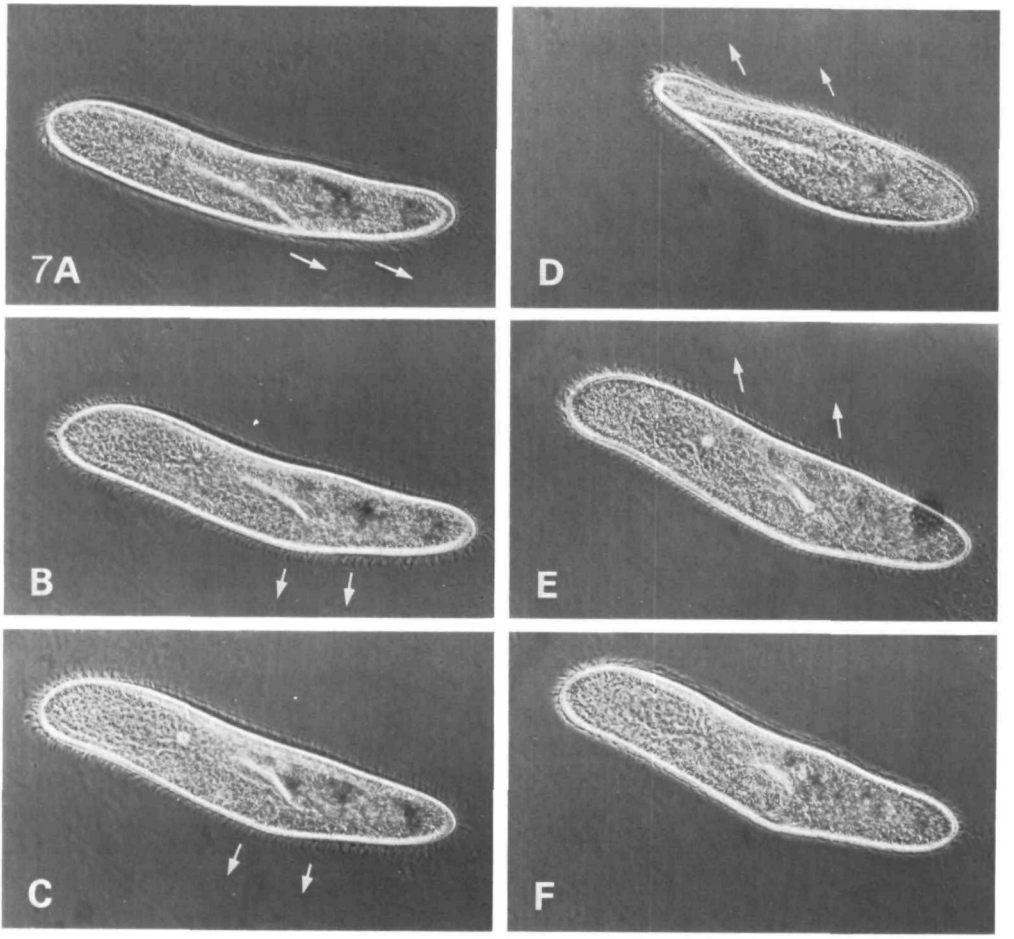

Fig. 7. Reorientation of nickel-paralysed cilia during pressurization and decompression. Orientation of lateral body cilia of an individual *Paramecium* (arrows) is shown at atmospheric pressure (A), 68 atm (B), 136 atm (C), during decompression (E) and immediately after decompression to 13·6 atm (F). Pressure was increased stepwise and held for several minutes at each pressure. For comparison, 'reversal' of paralysed cilia induced by 20 mmol l^{-1} KCl-TECK is shown (D). Magnification, ×220.

posterior, as in normal forward-swimming cells at the end of their effective stroke.

DISCUSSION

Pressure effects on the reversal response

The cilium and its Ca^{2+}-channels appeared to be specific targets of pressure action. Decompression-induced reversal apparently did not result from a global influx of Ca^{2+} across *Paramecium*'s surface; if this were the case, then 'pawn' mutants should have reversed during decompression, but they did not (Kung & Naitoh, 1973; Otter & Salmon, 1979). Rather, the response of *Paramecium* to decompression depended on the functional state of the Ca^{2+}-channels in their plasma membrane.

The excitability of the Ca^+-channels that mediate ciliary reversal can be altered by mutation or by changing the ionic composition of the medium surrounding the *Paramecium*. For example, barium ions facilitate Ca^{2+}-entry through the channels by inducing spontaneous and prolonged channel opening and so barium changes *Paramecium*'s Ca^{2+}-response from one graded with stimulus intensity to an all-or-none response (Naitoh & Eckert, 1968). 'Pawn' mutants have genetically altered Ca^{2+}-channels that do not open when electrically stimulated (Kung *et al.* 1975; Satow & Kung, 1980). As one might have predicted, the transient reversal upon decompression was absent in 'pawn' mutants (Otter & Salmon, 1979) and was exaggerated in media containing Ba^{2+} ions (Fig. 3C; Table 1). At atmospheric pressure, Na^+ induces spontaneous membrane depolarizations and frequent, brief reversals of ciliary beat in wild-type *Paramecium*, and elevated Na^+ causes prolonged reversals in 'paranoiac' mutants of *Paramecium* (Satow, Hansma & Kung, 1976; Table 2). Decompression elicited an exaggerated reversal response in the presence of Na^+, suggesting that Na^+ acts during decompression to prolong backward swimming. While the mechanism by which Na^+ alters *Paramecium*'s membrane excitation is unclear, our results are consistent with the observation that high Na^+ levels induce hyperexcitable behaviour in *Paramecium* (Kung & Saimi, 1982). On the other hand, buffers with high K^+ concentrations relative to Ca^{2+} inhibit ciliary reversal and attenuate the membrane's response to mechanical or electrical stimulation (Eckert, Naitoh & Friedman, 1972; Naitoh, 1968; Naitoh, Eckert & Friedman, 1972). It is not surprising, then, that the decompression-induced reversal response was weak or lacking in K^+-rich buffer (Fig. 3B; Table 1).

The above results suggest that decompression specifically opened the Ca^+-channels that normally mediate ciliary reversal and elicited a response physiologically similar to an avoiding reaction.

Pressurization immediately blocked avoiding reactions of swimming *Paramecium* (Fig. 2; Table 1); above 68 atm, *Paramecium* did not back up. As postulated earlier, pressure may have inhibited the anterior mechanoreceptors and so reduced the frequency of avoiding reactions that occurred when a *Paramecium* contacted the wall of the pressure chamber (Kitching, 1969; Otter & Salmon, 1979). However, our experiments in barium medium suggest that increased pressure directly inhibited the calcium channels from opening (Fig. 6). Barium-induced reversals are independent of contact with the chamber wall and their frequency decreased with increasing hydrostatic pressure. Substantially higher pressure was required to block barium-induced reversals (approx. 200 atm), so impairment of mechanoreceptor and channel function by pressurization may be additive.

Pressurization does not appear to block ciliary reversal by directly inhibiting the events in the ciliary axoneme or basal apparatus that cause reversed beating. Above 68 atm in TECK buffer *Paramecium* did not back up (Fig. 2), but if the buffer contained Na^+ or Ba^{2+}-ions, *Paramecium* occasionally backed up at a pressure of over 200 atm (Fig. 6). Abrupt decompression of 40 atm elicited a reversal response, even at 200 atm, and Triton-extracted *Paramecium* swam backwards under pressure when reactivated in 50 μmol l^{-1} $CaCl_2$ (Otter & Salmon, 1979). Similarly, Kitching (1969) reported that *Spirostomum* backed up in response to strong electrical, ionic or mechanical stimulation at 300 atm, a pressure sufficient to block all spontaneous

reversals. These observations suggest that cilia are able to reverse their direction of beating at a pressure that inhibits normal avoiding reactions.

Pressure effects on swimming speed

Pressurization altered the movement of cilia so that they were not effective for swimming. At a pressure of 68 atm or more, *Paramecium* slowed down or stopped, even though their cilia continued to beat rapidly (Figs 2,4,5). Pressure-induced reorientation of the direction of ciliary beat appears to be a major cause of slowing (Fig. 7). The laterally-directed position of cilia under pressure resembles 'ciliary inactivation' described by Machemer (1974).

A direct causal link between resting membrane potential (V_{rest}) and swimming speed has not been established, but slight membrane depolarization correlates strongly with a counterclockwise shift in beat direction (Machemer, 1974), anteriorly-directed reorientation of non-beating cilia (de Peyer & Machemer, 1983) and slowed forward swimming (Van Houten, 1979). Increased potassium concentrations depolarize V_{rest} (Machemer & Ogura, 1979) and slow swimming *Paramecium* at atmospheric pressure (Fig. 4; Table 2). Of the ions that we tested, only potassium acted synergistically with pressurization (Fig. 5). Thus, pressure-induced slowing of *Paramecium* closely resembles their response to small membrane depolarization (approx. 10 mV). Direct electrophysiological measurements on pressurized *Paramecium* would clarify whether V_{rest} changes under pressure.

Molecular basis of pressure action

In general, pressure effects on cellular processes can be understood qualitatively in terms of the Le Chatelier Principle. If a process is inhibited by pressure, then it proceeds with an increase in molecular volume; pressurization favours the low-volume state (Johnson, Eyring & Polissar, 1954). When ionizable groups are present, application of hydrostatic pressure favours dissociation of the ions, due to a volume decrease that accompanies 'electroconstriction' of water molecules around the dissociated species (Distèche, 1972). In *Paramecium*, for example, pressure-induced dissociation of ions bound to specific lipids near the mouth of the Ca^{2+}-channel might prevent channel 'gating' (Conti *et al.* 1982; Saimi & Kung, 1982).

Neither the molecular events of Ca^{2+}-channel opening nor the mechanism for transducing the Ca^{2+} influx into a change in ciliary beat direction is well-understood, so we cannot easily identify a particular biological reaction as pressure-sensitive. However, closing *Paramecium*'s Ca^{2+}-channels, reorientating the direction of ciliary beating and slowing of forward swimming are all Ca^{2+}-dependent processes: the calcium channels inactivate when intracellular Ca^{2+} rises, and an increase from 0·1 μmol l^{-1} Ca^{2+} to 1 μmol l^{-1} Ca^{2+} at the ciliary axoneme slows forward swimming (Brehm & Eckert, 1978; Mogami & Takahashi, 1982; Naitoh & Kaneko, 1972). Thus, the pressure-induced changes that we observed in *Paramecium*'s behaviour could be explained by alterations that resulted from a small rise in intracellular Ca^{2+} when the cells were pressurized. Since 'pawn' mutants slowed down under pressure and Ca^{2+} entry through the voltage-sensitive Ca^{2+}-channels is genetically blocked in 'pawn' mutants, it is unlikely that an inward leak of extracellular calcium through these channels causes pressure-induced slowing (Otter & Salmon, 1979;

Satow & Kung, 1980). Alternatively, pressurization may cause cellular Ca^{2+} receptor proteins to assume a 'Ca^{2+}-bound' configuration and thus produce a physiological state that mimics a rise in intracellular Ca^{2+}.

Our results are particularly striking because relatively low pressures produce drastic changes in *Paramecium*'s sensory-motor function. Calcium concentrations in cells are normally carefully regulated to low levels, and a small increment in cell calcium can markedly alter its physiology (Rose & Lowenstein, 1975; Baker, 1976). Further studies on excitable cells such as *Paramecium* may help to clarify whether cellular regulation of calcium ions is an important target of low levels of hydrostatic pressure.

Grant support: USPHS GM 23464 and NSF 76–09654 (EDS) and an NIH predoctoral traineeship (TO).

REFERENCES

BAKER, P. F. (1976). The regulation of intracellular calcium. *Symp. Soc. exp. Biol.* **30**, 67–88.

BREHM, P. & ECKERT, R. (1978). Calcium entry leads to inactivation of calcium channel in *Paramecium*. *Science, N.Y.* **202**, 1203–1206.

CONTI, F., FIORAVANTI, R., SEGAL, J. R. & STUHMER, W.(1982). Pressure dependence of the sodium currents of squid giant axon. *J. Membrane Biol.* **69**, 23–34.

DE PEYER, J. E. & MACHEMER, H. (1983). Threshold activation and dynamic response range of cilia following low rates of membrane polarization under voltage clamp. *J. comp. Physiol.* **150**, 223–232.

DISTÈCHE, A. (1972). Effects of pressure on the dissociation of weak acids. In *The Effects of Pressure on Living Organisms*. *Symp. Soc. exp. Biol.* **26**, 27–60.

DUNLAP, K. (1977). Localization of calcium channels in *Paramecium caudatum*. *J. Physiol., Lond.* **271**, 119–133.

ECKERT, R. & BREHM, P. (1979). Ionic mechanisms of excitation in *Paramecium*. *A. Rev. Biophys. Bioeng.* **8**, 353–383.

ECKERT, R. & NAITOH, Y. (1970). Passive electrical properties of *Paramecium* and problems of ciliary coordination. *J. gen. Physiol.* **55**, 467–483.

ECKERT, R., NAITOH, Y. & FRIEDMAN, K. (1972). Sensory mechanisms in *Paramecium*. I. Two components of the electric response to mechanical stimulation of the anterior surface. *J. exp. Biol.* **56**, 683–694.

HARPER, A. A., MACDONALD, A. G. & WANN, K. T. (1981). The action of high hydrostatic pressure on the membrane currents of *Helix* neurons. *J. Physiol., Lond.* **311**, 325–339.

JOHNSON, R. H., EYRING, H. & POLISSAR, M. (1954). *The Kinetic Basis of Molecular Biology*. New York: John Wiley & Sons, Inc.

KITCHING, J. A. (1957). Effects of high hydrostatic pressures on the activity of flagellates and ciliates. *J. exp. Biol.* **34**, 494–510.

KITCHING, J. A. (1969). Effects of high hydrostatic pressures on the activity and behaviour of the ciliate *Spirostomum*. *J. exp. Biol.* **51**, 319–324.

KUNG, C., CHANG, S. Y., SATOW, Y., VAN HOUTEN, J. & HANSMA, H. (1975). Genetic dissection of behavior in *Paramecium*. *Science, N.Y.* **188**, 898–904.

KUNG, C. & NAITOH, Y. (1973). Calcium-induced ciliary reversal in the extracted models of 'Pawn', a behavioral mutant of *Paramecium*. *Science, N. Y.* **179**, 195–196.

KUNG, C. & SAIMI, Y. (1982). The physiological basis of taxes in *Paramecium*. *A. Rev. Physiol.* **44**, 519–534.

MACDONALD, S. & KITCHING, J. A. (1976). The effect of partial pressures of inert gases on the behaviour and survival of the heterotrich ciliate *Spirostomum ambiguum*. *J. exp. Biol.* **64**, 615–624.

MACHEMER, H. (1974). Frequency and directional responses of cilia to membrane potential changes in *Paramecium*. *J. comp. Physiol.* **92**, 293–316.

MACHEMER, H. & OGURA, A. (1979). Ionic conductances of membranes in ciliated and deciliated *Paramecium*. *J. Physiol., Lond.* **296**, 49–60.

MOGAMI, Y. & TAKAHASHI, K. (1982). Effect of Ca^{2+} on the movement of single demembranated cilia of *Paramecium*. *Cell Motility Suppl.* **1**, 218.

NAITOH, Y. (1966). Reversal response elicited in nonbeating cilia of *Paramecium* by membrane depolarization. *Science, N.Y.* **154**, 660–662.

NAITOH, Y. (1968). Ionic control of the reversal response of cilia in *Paramecium caudatum*. A calcium hypothesis. *J. gen. Physiol.* **51**, 85–103.

NAITOH, Y. & ECKERT, R. (1968). Electrical properties of *Paramecium caudatum*: all-or-none electrogenesis. *Z. vergl. Physiol.* **61**, 453–472.

NAITOH, Y., ECKERT, R. & FRIEDMAN, K. (1972). A regenerative calcium response in *Paramecium*. *J. exp. Biol.* **56**, 667–681.

NAITOH, Y. & KANEKO, H. (1972). Reactivated Triton-extracted models of *Paramecium*: modification of ciliary movement by calcium ions. *Science, N. Y.* **176**, 523–524.

OTTER, T. (1980). Hydrostatic pressure depolarizes resting membrane potential in *Paramecium*. *J. Cell Biol.* **87**, 200a.

OTTER, T. (1981). Effects of hydrostatic pressure on membrane and ionic control of ciliary motility. Ph.D. dissertation, University of North Carolina at Chapel Hill, University Microfilms, Ann Arbor, MI., 138 pp.

OTTER, T. & SALMON, E. D. (1979). Hydrostatic pressure reversibly blocks membrane control of ciliary motility in *Paramecium*. *Science, N. Y.* **206**, 358–361.

OTTER, T. & SALMON, E. D. (1982). Hydrostatic pressure effects on paralyzed cilia in *Paramecium*. *Cell Motility Suppl.* **1**, 219.

PARMENTIER, J. L. & BENNETT, P. B. (1980). Hydrostatic pressure does not antagonize halothane effects on single neurons of *Aplysia californica*. *Anaesthesiology* **53**, 9–14.

ROSE, B. & LOWENSTEIN, W. R. (1975). Calcium ion distribution in cytoplasm visualized by aequorin: diffusion in cytosol restricted by energized sequestering. *Science, N.Y.*, **190**, 1204–1206.

SAIMI, Y. & KUNG, C. (1982). Are ions involved in the gating of calcium channels? *Science, N. Y.* **218**, 153–156.

SALMON, E. D. & ELLIS, G. W. (1975). A new miniature hydrostatic pressure chamber for microscopy. *J. Cell Biol.* **65**, 587–602.

SATOW, Y., HANSMA, H. G. & KUNG, C., (1976). The effect of sodium on 'paranoiac' – a membrane mutant of *Paramecium*. *Comp. Biochem. Physiol.* **54**A, 323–329.

SATOW, Y. & KUNG, C. (1980). Membrane currents of pawn mutants of the pwA group in *Paramecium tetraurelia*. *J. exp. Biol.* **84**, 57–71.

SONNEBORN, T. M. (1970). Methods in *Paramecium* research. *Meth. Cell Physiol.* **4**, 241–339.

VAN HOUTEN, J. (1979). Membrane potential changes during chemokinesis in *Paramecium*. *Science, N. Y.* **204**, 1100–1103.

WANN, K. T. & MACDONALD, A. G. (1980). The effects of pressure on excitable cells. *Comp. Biochem. Physiol.* **66**A, 1–12.

WANN, K. T., MACDONALD, A. G. & HARPER, A. A. (1979). The effects of high hydrostatic pressure on the electrical characteristics of *Helix* neurons. *Comp. Biochem. Physiol.* **64**A, 149–159.

magnitude. Presumably, in smaller larvae the level of covert JH effects is somewhat greater at the time of ecdysteroid release than in larger larvae, resulting in a slightly diminished ecdysteroid effect, and consequently in a shorter behaviour. Another interpretation is that the level of residual JH effects regulates the dynamics of ecdysteroid secretion from the prothoracic glands (Safranek, Cymborowski & Williams, 1980) and the altered ecdysteroid titre results in a modified behaviour.

Infusions of 20-HE into larvae with intact CA at various times during the 5th instar showed that responsiveness to infused hormone appears by the time larvae have reached 5·5 g (Fig. 13), a weight close to that described for 20-HE sensitivity of heart exposure (Nijhout, 1976). At this time the JH titre of the animals is rapidly declining as the CA become inactive (Granger *et al.* 1979) and JH-specific esterase appears (Vince & Gilbert, 1977; Beckage & Riddiford, 1982). As the effects of JH are erased during the period of growth beyond 5 g, the response to 20-HE becomes more rapid. The acquisition of a minimal latency at 7·5 probably represents maximal ecdysteroid sensitivity as a consequence of the virtual elimination of JH. This correlation of sensitivity with weight suggests that elimination of JH during the feeding stage of the 5th instar is the primary factor determining the ability of the larva to wander in response to 20-HE.

In larvae which had been allatectomized just prior to the 5th instar, wandering was induced to start only about 12 h earlier than the earliest 20-HE infused larvae with intact CA (Fig. 14 *vs* 12). Here, too, the infused 20-HE became increasingly effective with time, demonstrating that responsiveness to 20-HE improves over several days, even in the absence of measurable JH. Thus, endocrine events at the beginning of the instar, as well as at the 5 g size, are probably important to developing sensitivity to 20-HE.

In summary, wandering behaviour in *Manduca*, and the probably analogous prepupal behaviour patterns of many other Lepidoptera, are quantitatively determined by effects of ecdysteroids. These effects are prevented by the relatively high JH titres accompanying ecdysteroid action prior to the last instar, and may be subtly modified by the persistence of slight JH effects in the larval tissues during the period of ecdysteroid action which induces the behaviour.

We thank Professors Lynn M. Riddiford and Henry H. Hagedorn for reading an earlier draft of the manuscript. The work was supported by grants from NSF (PCM-8020975) and NIH (RO1 NS 13079) to JWT.

REFERENCES

AKAI, H. & KOBAYASHI, M. (1971). Induction of prolonged larval instar by the juvenile hormone in *Bombyx mori*. *Appl. Entomol. Zool.* **6**, 138–139.

AREN-ENGELBREKTSSON, B., LARSSON, K., SOLDERSTEN, P. & WILHELMSSON, M. (1970). The female lordosis pattern induced in male rats by estrogen. *Horm. Behav.* **1**, 181–188.

BECKAGE, N. E. & RIDDIFORD, L. M. (1982). Effects of parasitism by *Apanteles congragatus* on the endocrine physiology of the tobacco hornworm, *Manduca sexta*. *Gen. comp. Endocrin.* **407**, 308–322

BELL, R. A. & JOACHIM, F. G. (1976). Techniques for rearing laboratory colonies of tobacco hornworms and pink bollworms. *Ann. ent. Soc. Am.* **69**, 365–373.

BENZ, G. (1973). Reversal of spinning behavior in last instar larvae of *Pieris brassicae* treated with juvenile hormone derivatives. *Experientia* **29**, 1437–1438.

BOLLENBACHER, W. E., VEDECKIS, W. V. & GILBERT, L. I. (1975). Ecdysone titers and prothoracic gland activity during the larval-pupal development of *Manduca sexta*. *Devl Biol.* **44**, 46–53.

BOUNHIOL, J. J. (1938). Récherches experimentales sur le determinisme de la metamorphose chez les Lepidopteres. *Bull biol. Fr. Belg.* (Suppl.) **24**, 1–199.

BOWERS, W. S. (1969). Juvenile hormone: activity of aromatic terpenoid ethers. *Science, N. Y.* **164**, 323–325.

CHERBAS, P. T. (1973). Biochemical studies of insecticyanin. Ph.D. thesis, Harvard University, Cambridge, U.S.A.

DEMASSA, D. A., SMITH, E. R., TENNENT, B. & DAVIDSON, J. M. (1977). The relationship between circulating testosterone levels and male sexual behavior in rats. *Horm. Behav.* **8**, 275–286.

DAVIDSON, J. M. & LEVINE S. (1972). Endocrine regulation of behavior. *A. Rev. Physiol.* **34**, 375–408.

DOMINICK, O. S. & TRUMAN, J. W. (1984). The physiology of wandering behaviour in *Manduca sexta*: temporal organization and the influence of the internal and external environments *J. exp. Biol.* **110**, 35–51.

EPHRUSSI, B. & BEADLE, G. W. (1936). A technique for transplantation for *Drosophila*. *Am. Nat.* **70**, 218–225.

FAIN, M. J. & RIDDIFORD, L. M. (1975). Juvenile hormone titers in the hemolymph during late larval development of the tobacco hornworm, *Manduca sexta* (L.). *Biol. Bull. mar. biol. Lab., Woods Hole* **49**, 506–521.

FUJISHITA, M., OHNISHI, E. & ISHIZAKI, H. (1982). The role of ecdysteroids in the determination of gut-purge timing in the saturniid, *Samia cynthia ricini*. *J. Insect Physiol.* **28**, 961–967.

GIEBULTOWICZ, J. M., ZDAREK, J. & CHROSCIKOWSKA, U. (1980). Cocoon spinning behavior in *Ephestia kuehniella*; correlation with endocrine events. *J. Insect Physiol.* **26**, 459–464.

GILBERT, L. I., BOLLENBACHER, W. E., AGUI, N., GRANGER, N., SEDLAK, B., GIBBS, D. & BUYS, C. (1981). The prothoracicotropes: source of the prothoracicotropic hormone. *Am. Zool.* **21**, 641–653.

GOY, R. W. & YOUNG, W. C. (1957). Strain differences in the behavioral responses of female guinea pigs to estradiol benzoate and progesterone. *Behavior* **10**, 340–352.

GRANGER, N. A., BOLLENBACHER, W. E., VINCE, R., GILBERT, L. I., BAEHR, J. C. & DRAY, F. (1979). *In vitro* biosynthesis of juvenile hormone by the larval corpora allata of *Manduca sexta*: quantification by radioimmunoassay. *Molec. cell. Endocr.* **16**, 1–17.

GREEN, R., LUTTGE, W. G. & WHALEN, R. E. (1970). Induction of receptivity in ovariectomized female rats by a single intravenous injection of estradiol 17B. *Physiol. Behav.* **5**, 137–141.

HIGHNAM, K. C. & HILL, L. (1977). *The Comparative Endocrinology of the Invertebrates*. London: Edward Arnold Ltd. 357pp.

HORI, M. & RIDDIFORD, L. M. (1982). Isolation of ommochromes and 3-hydroxykynurentine from the tobacco hornworm, *Manduca sexta*. *Insect Biochem* **11**, 507–513.

KIGUCHI, K. & RIDDIFORD, L. M. (1978). A role of juvenile hormone in pupal development of the tobacco hornworm, *Manduca sexta*. *J. Insect Physiol.* **24**, 673–680.

LOUNIBOS, L. P. (1976). Initiation and maintenance of cocoon spinning behaviour by saturniid silkmoths. *Physiol. Entomol.* **1**, 195–206.

MCDONALD, P. G., VIDAL, N. & BEYER, C. (1970). Sexual behavior in the ovariectomized rabbit after treatment with different amounts of gonadal hormones. *Horm. Behav.* **1**, 161–172.

MCEWEN, B. S., DAVIS, P. G., PARSONS, B. & PFAFF, D. W. (1979). The brain as a target for steroid action. *A. Rev. Neurosci.* **2**, 65–112.

MELTZER, Y. L. (1971). *Hormonal and Attractant Pesticide Technology*. Park Ridge, New Jersey: Noyes Data Corp.

NIJHOUT, H. F. (1975*a*). A threshold size for metamorphosis in the tobacco hornworm, *Manduca sexta* (L.). *Biol. Bull. mar. biol. Lab., Woods Hole* **149**, 214–225.

NIJHOUT, H. F. (1975*b*). Dynamics of juvenile hormone action in larvae of the tobacco hornworm, *Manduca sexta* (L.). *Biol. Bull. mar. biol. Lab., Woods Hole* **149**, 568–579.

NIJHOUT, H. F. (1976). The role of ecdysone in pupation of *Manduca sexta*. *J. Insect Physiol.* **22**, 453–463.

NIJHOUT, H. F. & WILLAMS, C. M. (1974*a*). Control of moulting and metamorphosis in the tobacco hornworm, *Manduca sexta* (L.): growth of the last-instar larva and the decision to pupate. *J. exp. Biol.* **61**, 481–491.

NIJHOUT, H. F. & WILLIAMS, C. M. (1974*b*). Control of moulting and metamorphosis in the tobacco hornworm, *Manduca sexta* (L.): cessation of JH as a trigger for pupation. *J. exp. Biol.* **61**, 493–501.

OHTAKI, T., MILKMAN, R. D. & WILLIAMS, C. M. (1968). Dynamics of ecdysone secretion and action in the flesh fly *Sarcophaga peregrina*. *Biol. Bull. mar. biol. Lab., Woods Hole* **135**, 322–334.

PERETZ, E. (1968). Estrogen dose and duration of the mating period in cats. *Physiol. Behav.* **3**, 41–43.

PFAFF, D. W. (1980). *Estrogens and Brain Function*. New York: Springer-Verlag.

PIEPHO, H. (1938). Wachsturn and totale Metamorphose an Hantimplantaten bei der Washsmotte *Galleria mellonella* L. *Biol. Zbl.* **58**, 356–366.

PIEPHO, H. (1939). Hemmung der Verpuppung durch Corpora allata von Jungraupen bei der Wachsmotte *Galleria mellonella* L. *Naturwissenschaften* **27**, 675–676.

PIEPHO, H. (1950). Hormonale grundlagen der Spinntatigkeit bei Schmetterlingsraupen. *Z. Tierpsyhol.* **7**, 424–434.

PIEPHO, H. (1960). Hormonal control of moulting behavior and scale development in insects. *Ann. N.Y. Acad. Sci.* **89**, 564–571.

PITTENDRIGH, C. S. & SKOPIK, S. D. (1970). Circadian systems. V. The driving oscillation and the temporal sequence of development. *Proc. natn. Acad. Sci. U.S.A.* **65**, 500–507.

RIDDIFORD, L. M. (1972). Juvenile hormone in relation to the larval-pupal transformation of the Cecropia silkworm. *Biol. Bull. mar. biol. Lab., Woods Hole* **142**, 310–325.

RIDDIFORD, L. M. (1978). Ecdysone induced change in cellular commitment of the epidermis of the tobacco hornworm *Manduca sexta* at the initiation of metamorphosis. *Gen. comp. Endocr.* **34**, 438–446.

RIDDIFORD, L. M. & AJAMI, A. M. (1973). Juvenile hormone: its assay and effects on pupae of *Manduca sexta*. *J. Insect Physiol.* **19**, 749–767.

SAFRANEK, L., CYMBOROWSKI, B. & WILLIAMS, C. M. (1980). Effects of juvenile hormone on ecdysone dependent development in the tobacco hornworm, *Manduca sexta*. *Biol. Bull. mar. biol. Lab., Woods Hole* **158**, 248–256.

TRUMAN, J. W. (1972). Circadian organization of the endocrine events underlying the moulting cycle of larval tobacco hornworms. *J. exp. Biol.* **57**, 805–820.

TRUMAN, J. W. (1978). Hormonal release of stereotyped motor programmes from the isolated nervous system of the Cecropia silkmoth. *J. exp. Biol.* **74**, 151–173.

TRUMAN, J. W., RIDDIFORD, L. M. & SAFRANEK, L. (1974). Temporal patterns of response to ecdysone and juvenile hormone in the epidermis of the tobacco hornworm, *Manduca sexta*. *Devl Biol.* **39**, 247–262.

VINCE, R. K. & GILBERT, L. I. (1977). Juvenile hormone esterase activity in precisely timed last instar larvae and pharate pupae of *Manduca sexta*. *Insect Biochem.* **7**, 115–120.

WIELGUS, J. J., BOLLENBACHER, W. E. & GILBERT, L. I. (1979). Correlations between epidermal DNA synthesis and haemolymph ecdysteroid titre during the last larval instar of the tobacco hornworm, *Manduca sexta*. *J. Insect Physiol.* **25**, 9–16.

WILLIAMS, C. M. (1968). Ecdysone and ecdysone analogues: their assay and action on diapausing pupae of the cynthia silkworm. *Biol. Bull. mar. biol. Lab., Woods Hole* **134**, 344–355.

ZDAREK, J. & FRAENKEL, G. (1970). Overt and covert effects of endogenous and exogenous ecdysone in puparium formation of flies. *Proc. natn. Acad. Sci. U.S.A.* **67**, 331–337.

J. exp. Biol. **117**, 449–458 (1985)
Printed in Great Britain © *The Company of Biologists Limited 1985*

THE LOCATION OF CARDIAC VAGAL PREGANGLIONIC NEURONES IN THE BRAIN STEM OF THE DOGFISH *SCYLIORHINUS CANICULA*

BY D. J. BARRETT AND E. W. TAYLOR

Department of Zoology and Comparative Physiology, University of Birmingham, Birmingham B15 2TT, U.K.

Accepted 28 January 1985

SUMMARY

The locations, within the brain stem, of vagal efferent preganglionic neurones with axons in the two pairs of cardiac vagal rami of the dogfish have been defined by the retrograde intra-axonal transport of horseradish peroxidase (HRP). HRP was applied to the cardiac rami in one of two ways: either as crystals placed on the cut central end of the nerve or as a dried concentrated solution administered into the nerve on the tip of a fine pin. No difference was observed in the number of labelled cell bodies identified using either method. Labelled branchial cardiac vagal motoneurones were found ipsilaterally in the medial division of the vagal motor column, in the lateral division of the vagal motor column, and scattered between these two locations. In contrast, visceral cardiac vagal motoneurones were confined to the ipsilateral medial division of the vagal motor column. We suggest that the dual location of cell bodies supplying axons to the branchial cardiac branch of the vagus may represent a separation of function with respect to the two types of activity conducted by this nerve. Cardiac efferent fibres are confined in their exit from the brain to a middle group of vagal rootlets. This corresponds to the topographical representation of cardiac efferent somata within the extent of the vagal motor column.

INTRODUCTION

Elasmobranch fish are unusual amongst vertebrates in that nervous control of the heart is mediated solely by inhibitory tone exerted *via* branches of the vagus nerve. There is no accepted physiological evidence for sympathetic innervation of the heart of elasmobranchs (Young, 1933; Burnstock, 1969; Short, Butler & Taylor, 1977).

In the dogfish *Scyliorhinus canicula* the vagus nerve leaves the brain as a series of rootlets which are compressed together as they pass through the chondrocranium. Most proximally the vagus divides to form branchial branches 1, 2, 3 and 4, which contain motor fibres innervating the intrinsic respiratory muscles of gill arches 2, 3, 4 and 5 respectively, the 1st gill arch being supplied by the IXth (glossopharyngeal) nerve. The heart is supplied by two distinct pairs of vagal rami composed entirely of myelinated fibres (Short *et al.* 1977). The branchial cardiac branches arise from the

Key words: Cardiac vagal neurones, fish, horseradish peroxidase.

fourth branchial branches of the vagus (Norris & Hughes, 1920) and the visceral cardiac branches from the visceral branch of the vagus (Marshall & Hurst, 1905). The cardioinhibitory action of these cardiac vagi has been well described (Bottazzi, 1902; Lutz, 1930; Von Skramlik, 1938). The branchial cardiac branches are more effective in slowing the heart than the visceral cardiac branches (Short *et al.* 1977; Taylor, Short & Butler, 1977). No evidence for an inotropic influence on the heart has been reported for either of the two pairs of cardiac vagi.

Practically nothing is known about the position of the neuronal sub-populations of the vagal motor column that innervate specific target organs in elasmobranchs (Smeets, Niewenhuys & Roberts, 1983), although the gross location of the vagal motor column has been described, mainly in normal stained material, in a number of species (e.g. Black, 1917; Ariëns Kappers, 1920; Smeets & Niewenhuys, 1976; Smeets *et al.* 1983).

In the present study we have determined the distribution of preganglionic neurones giving rise to both pairs of vagal rami that innervate the heart of the dogfish. In addition the exit of cardiac efferent fibres from the brain was shown experimentally to be confined to the middle vagal rootlets. A preliminary account of part of this work has been published (Barrett, Roberts & Taylor, 1983).

METHODS

Retrograde labelling with horseradish peroxidase (HRP)

The results of this investigation were obtained from 13 dogfish, *Scyliorhinus canicula*, of either sex, with body length between 55 and 66 cm and supplied by the Marine Biological Association, Plymouth where the experiments were performed. The fish were maintained in large tanks of circulating sea water for at least 1 week before the start of the experiments. Prior to surgery each fish was anaesthetized with MS 222 dissolved in aerated sea water (Sandoz, $0{\cdot}17\,g\,l^{-1}$). When ventilatory movements became weak (after approximately 20 min) the fish was placed on an operating tray, covered with crushed ice, and left to cool for 5 min (Williamson & Roberts, 1981). The cardiac branches of the vagus were exposed on the floor of the anterior cardinal sinus (Short *et al.* 1977; Taylor *et al.* 1977), by making a 5-cm incision through the skin forward from the anterior margin of the pectoral girdle, 1 mm below and parallel to the lateral line. A cut perpendicular to the body axis was then made through the underlying muscle to the roof of the cardinal sinus which was opened to expose the required branch of the vagus nerve.

HRP (Sigma, type VI) was applied in one of two ways. In the first set of experiments (seven fish) the selected branch of the vagus was cut peripherally as it entered the ductus Cuveri, freed from connective tissue and lifted clear of the blood. The central cut end of the branch was placed on a small non-absorbent plastic strip and surface moisture removed by blotting. A few crystals of HRP were placed on the cut end of the branch and the preparation was left for 30 min. During this time the blood in the sinus was kept below the level of the severed nerve by manipulating the position of the anaesthetized fish. After 30 min, excess HRP was removed and a small amount of petroleum jelly applied around the cut end of the branch before replacing it on the floor of the sinus.

In the second set of experiments (six fish) the branch of the vagus was not cut peripherally. A concentrated solution of HRP was allowed to dry on the tip of a steel entomological pin (size A3). Approximately 2 mm of the required branch of the vagus was cleared of connective tissue. The cleared piece of nerve was carefully lifted above the level of the blood, dried and then punctured with the tip of the pin containing the dried HRP solution. The pin was then gently pushed 2 mm along the nerve towards the brain and was left in position for 30 s before being carefully withdrawn. To ensure that as many axons as possible were damaged, and allowed contact with the HRP, this procedure was repeated at least three times before a small amount of petroleum jelly was applied over the puncture in the nerve.

The post-operative survival (fish surviving until the processing date) was enhanced in those fish in which the pin technique was used. The pin technique involved the opening of the anterior cardinal sinus for less than 10 min (rather than for approximately 45 min which was necessary when using the other method) thus the danger of air being aspirated into the ductus Cuveri was greatly reduced. The pin technique also minimized the danger of HRP entering other nerves, damaged during surgery, which could lead to erroneous conclusions on the central origin of particular motoneurones (Kidd & McWilliam, 1979).

After the administration of HRP into the nerve the wound was sutured and covered with a patch of thin rubber membrane attached with cyanoacrylate adhesive. Each fish was then kept in a large recovery tank at 16–19 °C, for 4–10 days, depending on the temperature of the water, the body length of the fish and the length of the branch of the nerve from the point at which HRP had been applied to its junction with the brain.

When a fish was deemed ready for processing it was placed in sea water containing MS 222 (0·17 g l^{-1}) for 30 min. The fish was then injected with 1 ml of alphaxalone-alphadolone (Althesin, Glaxo Laboratories) *via* the sub-orbital sinus. The anaesthetized fish was perfused through the heart, first with dogfish Ringer solution for 3 min (during which time a further 1 ml of Althesin was injected), then with a mixture of 50 ml 25 % glutaraldehyde, 28·5 ml Analar formalin and 921·5 ml phosphate buffer (pH 7·4) as a fixative, for 20 min (Mesulam, 1978). The brain with surrounding cartilage was dissected out and placed in the fixative for approximately 4 h. The preparation was then dissected further until only the cerebellum, hindbrain and a small part of the spinal cord remained. This was placed in fresh fixative and left overnight at 4 °C. The following morning the preparation was transferred to cooled sucrose buffer and left for approximately 3 h prior to sectioning. Serial frozen sections were cut in the transverse plane at a thickness of 60 μm using a sledge microtome with a freezing platform.

Free-floating sections were reacted using tetramethylbenzidine (TMB) (Sigma) as the chromogen (Mesulam, 1978); 4 drops of 0·01 mol l^{-1} cobalt chloride were added at the start of the pre-reaction soak, and 3·5 ml of 0·3 % hydrogen peroxide (the 'incubation solution') added at the end of the pre-reaction soak. The observed cell bodies were accurately drawn, using a *camera lucida* attached to a Leitz microscope and the area of cells, in which the nucleus was clearly visible, measured from the drawings using a modified planimeter (Summagraphics). Photomicrographs were taken with a 35 mm Nikon camera attached to a Leitz microscope. The distribution of the labelled cell bodies was mapped with reference to the sulcus medianus inferior and obex.

The identification of vagal rootlets containing cardiac motor fibres

The investigation used four dogfish of either sex with body length between 58 and 62 cm. Each fish was anaesthetized in sea water containing MS 222 ($0{\cdot}17\,g\,l^{-1}$) and packed in ice during surgery. After decerebration the hindbrain was exposed as in the subsequent paper (Barrett & Taylor, 1985*b*). Two fine copper wires coated with varnish, with approximately 2 mm of the tips exposed, were inserted close to the pericardial cavity and held in position by a patch of thin rubber membrane secured to the skin of the fish with cyanoacrylate adhesive. These wires were attached to a pre-amplifier (Isleworth, type A101) and the ECG signal displayed on a pen recorder with rectilinear coordinates (Devices M19). The fish was then transferred to the experimental tank where it was clamped into a stereotaxic frame (Narishige Instruments) with a plate inserted into the mouth and clamped dorsally, and another lateral clamp holding the body of the fish posterior to the pectoral fins and dorsal to the midline to avoid constriction of the posterior cardinal sinus (Taylor & Butler, 1982). The gills were force ventilated with aerated sea water *via* a tube inserted into the mouth below the clamp. The fish was allowed 2 h to recover from the effects of anaesthesia before the start of the experiment. Tubocurarine (Tubarine, Wellcome) was then injected

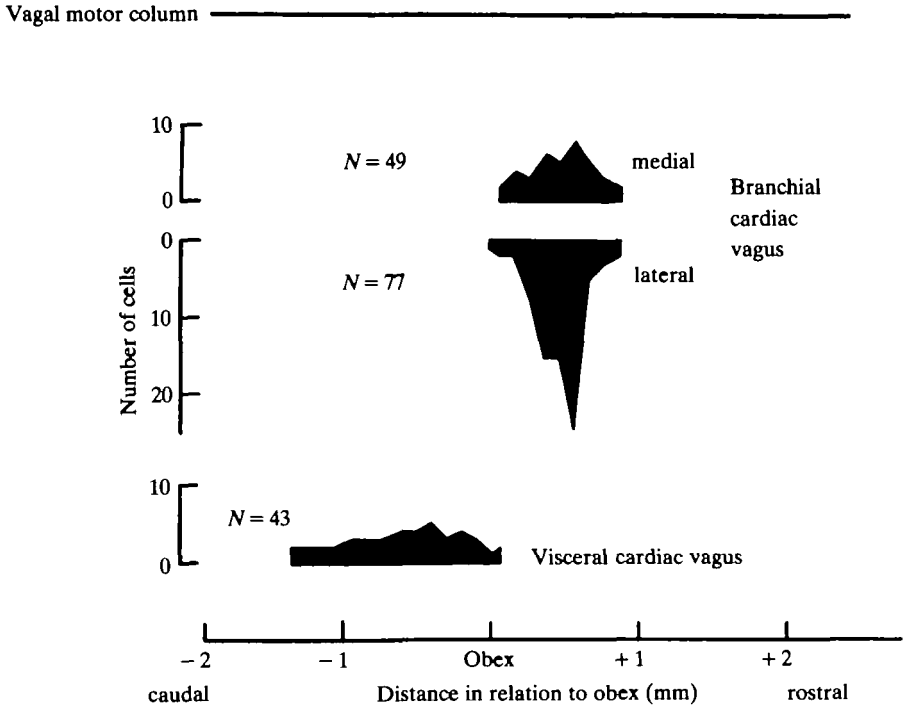

Fig. 1. A diagrammatic representation of the rostrocaudal distribution either side of obex of the visceral and branchial cardiac vagal motoneurones. The extent of the vagal motor column (top line) is taken from Barrett, Roberts & Taylor, 1984. Labelled cell bodies were counted (at 120-μm intervals) from the best backfills of each branch in single preparations. Labelled branchial cardiac motoneurones were found in two locations (medial and lateral); N is the number of cells identified in each location or, throughout the extent of the distribution (visceral cardiac vagus).

into the left sub-orbital sinus (7·5 mg kg^{-1}) and the fish was left for a further 1 h. The vagal rootlets on one side of the fish were severed and following 30 min recovery the vagal rootlets on the opposite side of the fish were cut sequentially, at 10-min intervals, just peripheral to the brain, either starting from the rostral or the caudal end of the brain. Heart rate was monitored continuously throughout the experiment.

Whenever possible measured variables are given as mean values ± S.E.M. with the number of observations in parentheses.

RESULTS

No difference was evident, in the number of labelled cells identified, between the two methods used for the application of the HRP into the branches of the vagus. For example, 42 visceral cardiac cell bodies were identified in one experiment using HRP applied to the central cut end of the nerve, and 43 visceral cardiac cell bodies were identified in an experiment using HRP applied on a pin into the intact nerve.

Cardiac vagal motoneurones

HRP was successfully applied to the branchial cardiac branch in nine fish and to the visceral cardiac branch in four fish.

Labelled visceral cardiac motoneurones were found in the caudal part of the vagal motor column from 1·06 mm caudal to 0·06 mm rostral to obex (Fig. 1) positioned medially close to the lateral edge of the 4th ventricle (Fig. 2). The rostrocaudal extent of their distribution (1·12 mm) belies the relatively small number of labelled cells. The maximum number of cells found in a single 60-μm section was seven, and

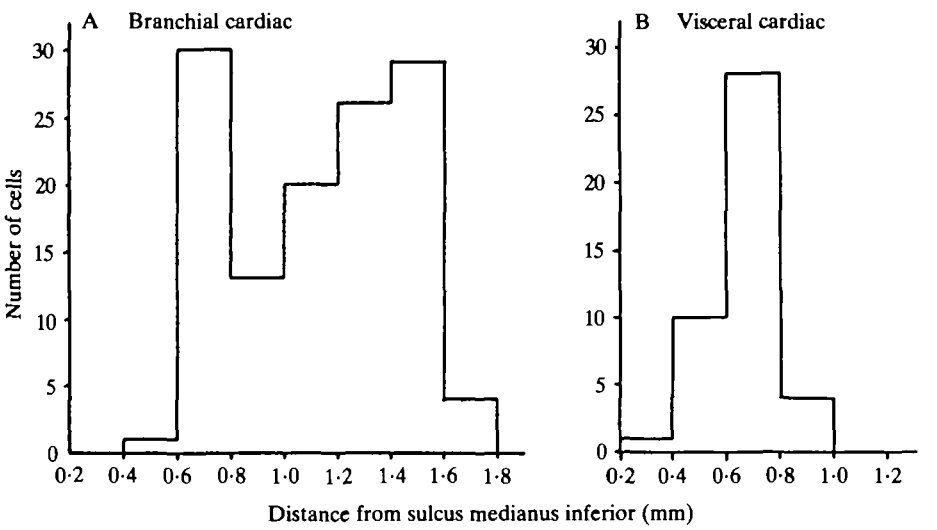

Fig. 2. Histograms of the mediolateral distribution in the hindbrain of labelled cell bodies from the best HRP backfills of the two cardiac vagi from separate preparations: (A) with axons in the branchial cardiac branch of the vagus and (B) with axons in the visceral cardiac branch of the vagus. Note the bimodal distribution of branchial cardiac motoneurones compared to visceral cardiac motoneurones.

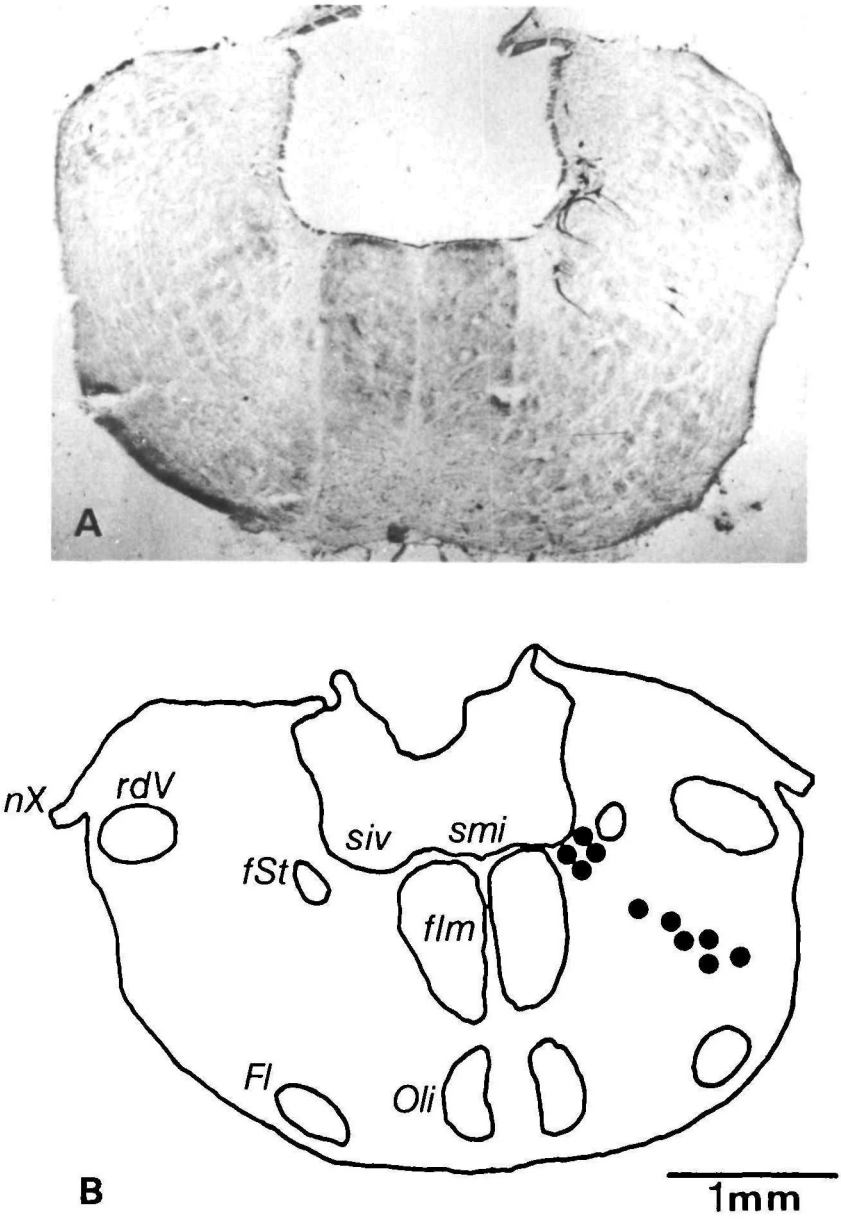

Fig. 3. (A) 60-μm transverse section through the hindbrain of a dogfish approximately 0·1 mm rostral to obex. Branchial cardiac motoneurones labelled with HRP are shown clearly on the right-hand side of the section. (B) A diagrammatic representation of a similar transverse section through the hindbrain to that shown in A. The locations of labelled branchial cardiac motoneurones(●) are shown in relation to other structures in the hindbrain *Fl*, nucleus funiculi lateralis; *flm*, fasiculus longitudinalis medialis; *fSt*, fasiculus medianus of Steida; *nX*, nervus vagus; *Oli*, oliva inferior; *rdV*, radix descendens nervi trigemini; *siv*, sulcus intermedius ventralis; *smi*, sulcus medianus inferior.

frequently only one or two labelled cells were identified (cf. Fig. 1). The number of labelled cells found from the application of HRP to the visceral cardiac vagus ranged from 17–43 cells in single fish.

Branchial cardiac motoneurones were found in the central part of the vagal motor column from 0·06 mm caudal to 0·78 mm rostral to obex (Fig. 1). The rostrocaudal extent of the branchial cardiac motoneurones (0·84 mm) was similar to the extent of the motoneurones supplying axons to each of the branchial branches (D. J. Barrett, B. L. Roberts & E. W. Taylor, in preparation) and was consistent with the fact that the branchial cardiac branch is the main post-trematic 4th branchial branch. Branchial cardiac neurones were found in the medial division of the vagal motor column close to the lateral edge of the 4th ventricle and also comprised a lateral division of the vagal motor column (Fig. 2). The spatial distribution of labelled cells characterized as either medial or lateral was continuous (Figs 2, 3) and both locations were occupied throughout the rostrocaudal extent of the branchial cardiac motoneurones (Fig. 1). The number of labelled cells identified ranged from 33 to 126 in a single fish. There was no obvious correlation between the number of labelled cells identified and the time the fish was left in the recovery tank or the length of the fish. The maximum number of cells found in a single 60-μm section was 18.

Branchial cardiac motoneurones overlap rostrally with motoneurones supplying axons to the 3rd branchial branch over a distance of approximately 330 μm. They overlap caudally with motoneurones supplying axons to the visceral branch of the vagus for most of their distribution (approximately 700 μm) (D. J. Barrett, B. L. Roberts & E. W. Taylor, in preparation).

The size of cardiac vagal preganglionic neurones

Cell area measurements were made of lateral and rostromedial branchial cardiac motoneurones from the same fish. The mean cell area of the lateral cardiac motoneurones was $741 \pm 39\ \mu m^2$ ($N = 45$), significantly different ($P < 0{\cdot}001 = t$-test) from that of the rostromedial cardiac motoneurones which was $650 \pm 36\ \mu m^2$ ($N = 34$). The mean cell area of the visceral cardiac motoneurones was not significantly different from that of the rostromedial branchial cardiac motoneurones.

Vagal rootlets containing cardiac motor fibres

In curarized preparations the control heart rate varied from 15 to 27 beats min^{-1} and a large increase was seen when all the vagal rootlets on one side were cut. The rate subsequently decreased to a value close to the control level. The rootlets on the other side of the fish were then cut sequentially in either a rostral or caudal direction.

The number of vagal rootlets that could be identified in each fish varied from 9 to 15. Wherever possible individual rootlets were cut, but the small size of some and their juxtaposition sometimes necessitated more than one rootlet being cut simultaneously. In fish in which 15, 11, 10 and 9 rootlets were identified, cutting rootlets 4–9, 4–8, 5–8 and 4–7 respectively, produced increases in heart rate. Cutting the other rootlets produced no significant change.

DISCUSSION

The branchial cardiac branch of the vagus receives axons from cells in two different locations in the medulla. Branchial cardiac motoneurones are found both rostromedially and solely comprise the lateral division of the vagal motor column (Barrett,

Roberts & Taylor, 1984). Cells are also found scattered between these locations. There is a morphological distinction between the two groups of cells, since the lateral cells are significantly larger than the two medial groups of cells.

In the elasmobranch *Squalus* an area lateral to the caudal part of the visceromotor column contains a distinct aggregation of large bipolar and triangular cells in Nissl, Klüver-Barrera and Bodian stained material (Smeets & Niewenhuys, 1976). These authors considered that this aggregation of cells represented a part of the motor nucleus of X and named it accordingly the nucleus motorius nervi vagi lateralis (Xml). The Xml extends from 2·00 mm rostral to approximately 4·0 mm caudal to obex. The vagal part of the visceromotor column was designated the nucleus motorius nervi vagi medialis (Xmm). The Xmm and the Xml, by virtue of their locations, may be the homologues of the mammalian dorsal vagal motor nucleus and the nucleus ambiguous respectively (Smeets & Niewenhuys, 1976). In *Squalus* the cells in the Xmm are somewhat larger than those in the Xml. These authors also described a medial vagal motor nucleus in *Scyliorhinus* but did not identify a lateral nucleus. The Xmm of *Scyliorhinus* extends from approximately 2·7 mm rostral to 2·25 mm caudal to obex (determined from the atlas provided by Smeets & Niewenhuys, 1976). More recently Barrett *et al.* (1984) have confirmed a similar rostrocaudal extent (4·83 mm) for the vagal motor column of *Scyliorhinus*.

It is interesting that of the two vagal rami that innervate the heart (the branchial cardiac and visceral cardiac branches) only motoneurones supplying axons to the branchial cardiac branch are found in two locations. The visceral cardiac motoneurones are confined to a medial position in the medulla. Peripheral stimulation of the cardiac branches in this species has indicated that the branchial cardiac branches were more effective in cardioinhibition than the visceral cardiac branches (Short *et al.* 1977) and selective transection of the branches indicated that the bradycardia during hypoxia was mediated predominantly *via* the branchial cardiac branches (Taylor *et al.* 1977). Recently, Taylor & Butler (1982) demonstrated that there are two types of nervous activity associated with the branchial cardiac branch; rhythmically bursting units, which are synchronous with ventilatory movements and sporadically active units. In the preceding paper it was shown that the bursting activity in paralysed fish is, at least partially, centrally generated (Barrett & Taylor, 1985*a*). It is suggested that the dual origin of branchial cardiac motoneurones may relate to the two types of nervous activity seen in peripheral recordings from this branch. Peripheral recordings from branchial branches of the vagus, which innervate the intrinsic respiratory muscles of the gill arches, contain predominantly rhythmic bursting units and respiratory vagal motoneurones are confined to the rostromedial division of the vagal motor column (Barrett *et al.* 1984). The medial branchial cardiac motoneurones could, by virtue of their location, be responsible for the rhythmically bursting units identified in peripheral recordings, whilst the lateral cells may be responsible for the sporadically active units that accelerate during hypoxia and possibly induce the reflex bradycardia (Taylor & Butler, 1982).

In the brain stem of some mammals the cell bodies of fibres which mediate the vagal bradycardia originate in the nucleus ambiguous (nA) (McAllen & Spyer, 1976, 1978). If the lateral division of the vagal motor column in *Scyliorhinus* can be regarded as the homologue of the nA then its functional role may be similar (Barrett & Taylor,

1985*a*,*b*). This possibility is supported by the observation that in the dogfish the branchial cardiac branches are more effective in cardioinhibition than the visceral cardiac branches (Short *et al.* 1977; Taylor *et al.* 1977) which arise solely from a medial location in the medulla.

It is interesting that, in the cat and the dog, the cell bodies of the cardiac motoneurones in the nA are larger than those in the dmnX (Geis, Kozelka & Wurster, 1981). This is similar to the situation in *Scyliorhinus* where the lateral cells (the nA homologue) are larger than the medial cells.

In *Squalus* which has 30 or more vagal rootlets, in contrast to the maximum of 15 identified in this study on *Scyliorhinus*, the majority are of mixed function, each comprising a wide sensory band and a narrow motor element (Norris & Hughes, 1920). This was confirmed for *Scyliorhinus* by cobalt backfills of the vagus nerve (Barrett, 1984), which indicated than an individual rootlet contained more sensory than motor fibres.

The rootlets containing cardiac motor fibres were found in the middle of the rostrocaudal distribution of the rootlets, a similar rostrocaudal location to that of the cardiac cell bodies in the vagal motor column (Barrett *et al.* 1984). Only cardiac fibres were shown to be localized in their exit from the brain in this study, but it seems plausible that the sequential representation of the peripheral distribution of the vagus in the vagal motor column may also be found in the exit of efferent fibres in the vagal rootlets, thus retaining some of the original morphological segmentation which is lost during development as the cranial segments fuse (cf. Young, 1950).

DJB was supported by a Science and Engineering Research Council CASE research studentship. The authors wish to acknowledge the contribution of the Director and Staff of the Laboratory of the Marine Biological Association, Plymouth, to this project and in particular the help and advice given by B. L. Roberts and R. M. Williamson.

REFERENCES

Ariëns Kappers, C. U. (1920). *Die Verglei Chende Anatomie de Nervensystems der Wirbeltiere und des Mensches* I. Haarlem: Bohn.

Barrett, D. J. (1984). The Xth cranial nerve (the vagus) in the elasmobranch fish *Scyliorhinus canicula* L. and its role in the control of the heart. Ph.D. thesis, University of Birmingham.

Barrett, D. J., Roberts, B. L. & Taylor, E. W. (1983). The identification of the cell bodies of cardiac vagal efferent fibres in the dogfish *Scyliorhinus canicula*. *J. Physiol., Lond.* **338**, 9P.

Barrett, D. J., Roberts, B. L. & Taylor, E. W. (1984). The topographical organisation of vagal motoneurones in the dogfish *Scyliorhinus canicula*. *J. Physiol., Lond.* **350**, 32P.

Barrett, D. J. & Taylor, E. W. (1985*a*). Spontaneous efferent activity in branches of the vagus nerve controlling ventilation and heart rate in the dogfish. *J. exp. Biol.* **117**, 433–448.

Barrett, D. J. & Taylor, E. W. (1985*b*). The characteristics of cardiac vagal preganglionic motoneurones in the dogfish. *J. exp. Biol.* **117**, 459–470.

Black, D. (1917). The motor nuclei of the cerebral nerves in physiology. I. Cyclostomi and pisces. *J. comp. Neurol.* **27**, 467–564.

Bottazzi, P. (1902). Untersuchungen uber das viscerale Nervensystem der Selachien. *Z. Biol.* **43**, 372.

Burnstock, G. (1969). Evolution of the autonomic innervation of visceral and cardiovascular systems in vertebrates. *Pharmac. Rev.* **21**, 247–324.

Geis, G. S., Kozelka, J. W. & Wurster, R. D. (1981). Organization and reflex control of vagal cardiomotor neurones. *J. auton. nerv. Syst.* **3**, 437–450.

Kidd, C. & McWilliam, P. N. (1979). The identification of the cell bodies of vagal efferent fibres of pulmonary and cardiac origin in the cat using horseradish peroxidase. *J. Physiol., Lond.* **290**, 9–10P.

LUTZ, B. R. (1930). Reflex cardiac and respiratory inhibition in the elasmobranch *Scyllium canicula*. *Biol. Bull. mar. biol. Lab., Woods Hole* **59**, 170–178.

MCALLEN, R. M. & SPYER, K. M. (1976). The location of cardiac vagal preganglionic motoneurones in the medulla of the cat. *J. Physiol., Lond.* **258**, 187–204.

MCALLEN, R. M. & SPYER, K. M. (1978). Two types of vagal preganglionic motoneurones projecting to the heart and lungs. *J. Physiol., Lond.* **282**, 343–364.

MARSHALL, A. H. & HURST, C. H. (1905). *Practical Zoology*. London: John Murray. p. 518.

MESULAM, M.-M. (1978). Tetramethyl benzidine for horseradish peroxidase neurohistochemistry. A non-carcinogenic blue reaction product with superior sensitivity for visualising neural afferents and efferents. *J. Histochem. Cytochem.* **26**, 106–117.

NORRIS, H. W. & HUGHES, S. P. (1920). The cranial, occipital and anterior spinal nerves of the dogfish, *Squalus acanthias*. *J. comp. Neurol.* **31**, 293–400.

SHORT, S., BUTLER, P. J. & TAYLOR, E. W. (1977). The relative importance of nervous, humoral and intrinsic mechanisms in the regulation of heart rate and stroke volume in the dogfish *Scyliorhinus canicula*. *J. exp. Biol.* **70**, 77–92.

SMEETS, W. J. A. J. & NIEWENHUYS, R. (1976). Topological analysis of the brain stem of the sharks *Squalus acanthias* and *Scyliorhinus canicula*. *J. comp. Neurol.* **165**, 333–368.

SMEETS, W. J. A. J., NIEWENHUYS, R. & ROBERTS, B. L. (1983). *The Central Nervous System of Cartilaginous Fishes*. Berlin: Springer-Verlag.

TAYLOR, E. W. & BUTLER, P. J. (1982). Nervous control of heart rate: activity in the cardiac vagus of the dogfish. *J. appl. Physiol.* **53**, 1330–1335.

TAYLOR, E. W., SHORT, S. & BUTLER, P. J. (1977). The role of the cardiac vagus in the response of the dogfish *Scyliorhinus canicula* to hypoxia. *J. exp. Biol.* **70**, 57–75.

VON SKRAMLIK, E. (1983). Uber der Kreishauf bei den Fishes. *Publs Staz. Zool., Napoli* **17**, 130.

WILLIAMSON, R. M. & ROBERTS, B. L. (1981). Body cooling as a supplement to anaesthesia for fishes. *J. mar. biol. Ass. U.K.* **61**, 129–131.

YOUNG, J. Z. (1933). The autonomic nervous system of Selachians. *Q. Jl microsc. Sci.* **15**, 571–624.

YOUNG, J. Z. (1950). *The Life of Vertebrates*. Oxford: Clarendon Press.

HUGHES, G. M., KNIGHTS, B. & SCAMMEL, C. A. (1969). The distribution of P_{O_2} and hydrostatic pressure changes within the branchial chambers of the shore crab *Carcinus maenas* L. *J. exp. Biol.* **51**, 203–220.

JOHANSEN, K., LENFANT, C. & MECKLENBURG, T. A. (1970). Respiration in the crab *Cancer magister*. *J. comp. Physiol.* **70**, 1–19.

MCDONALD, D. G., MCMAHON, B. R., & WOOD, C. M. (1977). Patterns of heart and scaphognathite activity in the crab *Cancer magister*. *J. exp. Zoöl.* **202**, 33–44.

MCMAHON, B. R. (1981). Oxygen uptake and acid-base balance during activity in decapod crustaceans. In: *Locomotion and Energetics in Arthropods*, (eds C. L. Herreid & C. R. Fourtner). New York: Plenum Press.

MCMAHON, B. R. & BURGGREN, W. W. (1979). Respiration and adaptation to the terrestrial habitat in the land hermit crab *Coenobita clypeatus*. *J. exp. Biol.* **79**, 265–281.

MCMAHON, B. R. & WILKENS, J. L. (1977). Periodic respiratory and circulatory performance in the red rock crab *Cancer productus*. *J. exp. Zoöl.* **202**, 363–374.

MCMAHON, B. R. & WILKENS, J. L. (1983). Ventilation, perfusion and oxygen consumption. In *The Biology of Crustacea*, Vol. 2, (eds L. H. Mantel & D. Bliss). New York: Academic Press.

MANTEL, L. H. & FARMER, L. H. (1983). Osmotic and ionic regulation. In *The Biology of Crustacea: Internal Anatomy and Physiological Regulation*, Vol. 5, (ed. L. H. Mantel). New York: Academic Press.

PASZTOR, V. M. & BUSH, B. M. H. (1983*a*). Graded potentials and spiking in single units of the oval organ, a mechanoreceptor in the lobster ventilatory system. I. Characteristics of dual afferent signalling. *J. exp. Biol.* **107**, 431–450.

PASZTOR, V. M. & BUSH, B. M. H. (1983*b*). Graded potentials and spiking in single units of the oval organ, a mechanoreceptor in the lobster ventilatory system. III. Sensory habituation to repetitive stimulation. *J. exp. Biol.* **107**, 465–472.

TAYLOR, A. C. & DAVIES, P. S. (1982). Aquatic respiration in the land crab, *Gecarcinus lateralis* (Freminville). *Comp. Biochem. Physiol.* **72A**, 683–688.

TAYLOR, E. W. (1982). Control and co-ordination of ventilation and circulation in crustacean: responses to hypoxia and exercise. *J. exp. Biol.* **100**, 289–319.

TAYLOR, E. W. & BUTLER, P. J. (1973). The behaviour and physiological responses of the shore crab *Carcinus maenas* during changes in environmental oxygen tension. *Neth. J. Sea Res.* **7**, 496–505.

TAYLOR, E. W., BUTLER, P. J. & AL-WASSIA, A. (1977). The effect of a decrease in salinity on respiration, osmoregulation and activity in the shore crab, *Carcinus maenas* (L.) at different acclimation temperatures. *J. comp. Physiol.* **119**, 155–170.

TAYLOR, E. W., BUTLER, P. J. & SHERLOCK, P. J. (1973). The respiratory and cardiovascular changes associated with the emersion response of *Carcinus maenas* (L.) during environmental hypoxia, at three different temperatures. *J. comp. Physiol.* **86**, 95–115.

YOUNG, R. E. (1978). Correlated activities in the cardiovascular nerves and ventilatory system in the Norwegian lobster, *Nephrops norvegicus* (L.). *Comp. Biochem. Physiol.* **61A**, 387–394.

YOUNG, R. E. & COYER, P. E. (1979). Phase co-ordination in the cardiac and ventilatory rhythms of the lobster *Homarus americanus*. *J. exp. Biol.* **82**, 53–74.

VON RABEN, K. (1934). Veranderungen im Kiemendeckel und in den Kiemen einiger Brachyuren (Decapoden) im Verlauf der Anpassung und die Feuchtluftatmung. *Z. wiss Zool.* **145**, 425–461.

WHEATLEY, M. G., BURGGREN, W. W. & MCMAHON, B. R. (1984). The effects of temperature and water availability on ion and acid-base balance in hemolymph of the land hermit crab *Coenobita clypeatus*. *Biol. Bull. mar. biol. Lab., Woods Hole* **166**, 427–445.

WHEATLY, M. G., & MCMAHON, B. R. (1982). Responses to hypersaline exposure in the euryhaline crayfish *Pacifastacus leniusculus* (Dana). I. The interaction between ionic and acid-base regulation. *J. exp. Biol.* **99**, 425–445.

WILKENS, J. L., WILKENS, L. A. & MCMAHON, B. R. (1974). Central control of cardiac and scaphognathite pacemakers in the crab *Cancer magister*. *J. comp. Physiol.* **90**, 89–104.

WOOD, C. M. & RANDALL, D. J. (1981). Oxygen and carbon dioxide exchange during exercise in the land crab (*Cardisoma carnifex*). *J. exp. Zoöl.* **218**, 7–22.

J. exp. Biol. **117**, 401–413 (1985)
Printed in Great Britain © *The Company of Biologists Limited 1985*

INNERVATION PATTERNS OF INHIBITORY MOTOR NEURONES IN THE THORAX OF THE LOCUST

BY J. P. HALE AND M. BURROWS

Department of Zoology, University of Cambridge, Downing Street, Cambridge CB2 3EJ, England

Accepted 20 December 1984

SUMMARY

The innervation pattern of inhibitory motor neurones of the locust has been revealed by intracellular recording from their cell bodies in the meso- and metathoracic ganglion and simultaneous recording from muscle fibres in a middle, or in a hind leg.

Three neurones in each ganglion, the common inhibitor ($CI = CI_1$), the anterior inhibitor ($AI = CI_2$), and the posterior inhibitor ($PI = CI_3$) innervate several muscles in one leg and are thus common inhibitory neurones. Metathoracic CI innervates 13 muscles in one hind leg and mesothoracic CI innervates 12 muscles in one middle leg. The muscles are all in the proximal parts of the legs and move the coxa, the trochanter and the tibia. Metathoracic AI and PI innervate four muscles in the more distal parts of one hind leg that move the tibia, the tarsus and the unguis. None of these muscles is innervated by CI. Each inhibitor innervates muscles that have different and often antagonistic actions during movements of a leg.

AI and PI receive many synaptic inputs in common and show similar patterns of spikes during imposed movements of a tibia. Tests fail, however, to reveal evidence for any electrical or synaptic coupling between them. A revised scheme of nomenclature for these inhibitory neurones is proposed.

INTRODUCTION

Motor neurones that cause inhibition of the axial or limb muscles that they innervate occur in several invertebrate phyla, but they have been most widely studied in the arthropods. In these animals, two types of inhibitory motor neurones have been recognized on the basis of their patterns of innervation. There are common inhibitors which innervate several muscles, often with distinct functions, and specific inhibitors which innervate one muscle or a small group of functionally similar muscles.

In crustaceans, common inhibitors innervate muscles in the legs and claws (Wiersma & Ripley, 1952; Hill & Lang, 1979), swimmerets (Davis, 1971) and antennae (Clarac & Vedel, 1975). In insects, common inhibitors innervate leg muscles (Pearson & Bergman, 1969; Pearson & Iles, 1971; Graham & Wendler, 1981) and neck muscles (Shepheard, 1974). The existence of neurones with wide fields of innervation makes it necessary to assess with caution the existence of specific inhibitors whose field of

Key words: Insect, central nervous system, inhibition.

innervation has not yet been revealed fully. Even the common inhibitory neurones themselves may have wider fields of innervation than previously suspected, as is now suggested for crayfish (Cooke & Macmillan, 1983) and crab limbs (Bevengut, Simmers & Clarac, 1983). Specific inhibitors have nevertheless been reported in crustacean limbs (Wiersma, 1961), uropods (Larimer & Kennedy, 1969) and abdomen where they are shared by two or more functionally similar muscles (Kennedy & Takeda, 1965; Parnas & Atwood, 1966). They also occur in some insect spiracles (Miller, 1969), in some abdominal muscles (Tyrer, 1971; Lewis, Miller & Mills, 1973) and possibly in some flight muscles (Piek & Mantel, 1970; Ikeda & Boettiger, 1965).

More than one inhibitory neurone may innervate a single muscle fibre in insects (Iles & Pearson, 1969; Pearson & Iles, 1971) and in crustaceans they can exert both pre- and postsynaptic effects. In this way the inhibitors can modulate the force produced by the action of the excitatory motor neurones (Burns & Usherwood, 1979). In addition, their own effectiveness can be modified by activity in other neurones. The inhibitory potential produced in the extensor tibiae muscle of the locust by a common inhibitory neurone is depressed by octopamine and therefore is also likely to be depressed by activity in the dorsal unpaired median neurone to that muscle (Evans & O'Shea, 1977).

The role of these inhibitory neurones in the behaviour of the animal, however, remains difficult to rationalize (see Pearson, 1973, for review) because the problem is to understand the action of a neurone that innervates many muscles which have different functions. The approach that we have taken here is to define the patterns of innervation of two sets of three inhibitory neurones to muscles in a middle and a hind leg of a locust. In the metathoracic segment, one of these neurones is known to be a common inhibitory neurone (CI) innervating at least two muscles (Pearson & Bergman, 1969), but the other two are known only to innervate the flexor tibiae muscle (Burrows & Horridge, 1974; Heitler & Burrows, 1977). In this paper we show that all three are common inhibitory neurones.

MATERIALS AND METHODS

Experiments were performed on adult *Schistocerca gregaria* (Forskal) of both sexes taken from our crowded culture about 2–8 days after their final moult. To map the innervation patterns of the meso- and metathoracic inhibitory neurones, three different preparations, ventral, dorsal and side, were used to gain access to muscles of the thorax, and a hind or middle leg. For the ventral preparation (Hoyle & Burrows, 1973), a locust was restrained, ventral surface uppermost, and the muscles exposed by removing appropriate parts of the ventral thoracic, coxal or femoral cuticle. For the dorsal preparation, a locust was secured dorsum uppermost and was opened by a midline incision. The two sides of the body were pulled apart and the gut was removed to expose the thoracic muscles. The side preparation, in which the cuticle overlying the coxal abductor muscles was removed, was used only for access to muscles 125 and 126 (metathoracic coxal abductors) and their homologues in the mesothorax (94, 95 and 96). These muscles could also be reached in a dorsal preparation by removing the overlying muscles. Similarly, muscles 133a or 103a

(trochanteral depressors) had to be removed to record from the trochanteral levators (131, 132, and 102).

The ventral preparation was used when intracellular recordings were to be made from neurones in thoracic ganglia. A small, wax-covered platinum platform was manoeuvred beneath the meso- and metathoracic ganglia to isolate them from movement. Before recording, the ganglia were treated with a 1% solution of protease (Sigma Type VI) for 2–3 min: care was taken to keep the protease away from the muscles. Intracellular recordings from muscle fibres and neurones were made with microelectrodes filled with 2 mol l^{-1} potassium acetate and with resistances of 30–50 MΩ. The tips of the electrodes were made more visible by dipping them in Indian ink. The preparations were perfused throughout with locust Ringer (Usherwood & Grundfest, 1965) at room temperature.

The metathoracic tibiae were moved in a controlled way with a servo-motor controlled by a microprocessor. Recordings were stored on magnetic tape for later analysis and filming. The numbering of muscles used throughout is that of Snodgrass (1929).

RESULTS

The innervation pattern of the metathoracic common inhibitor

The axon of the common inhibitory neurone (CI) branches as it emerges from the metathoracic ganglion to send axons into lateral nerves 3, 4 and 5 (Burrows, 1973). Within each of these main lateral nerves, an axon may divide again. No other leg motor neurones have this pattern of axonal branches. Therefore, this unique anatomy makes it possible to stimulate an axon of CI in one nerve and then search for muscles innervated by the other axons. Inhibitory junctional potentials (IPSPs) recorded with an intracellular microelectrode can be correlated with the stimulus pulses (Fig. 1). The nerve chosen for stimulation was the extensor nerve ($N5b_2 + N3b_2c$) within the femur, because it is known that CI innervates the extensor tibiae muscle (Pearson & Bergman, 1969), and this was readily confirmed in these experiments. Moreover, this nerve does not contain an axon of either of the other two inhibitory neurones that innervate muscles of the hind leg. These results could then be supplemented by observing the effects of the sporadic spikes that occur spontaneously in CI without imposed or voluntary movements by a hind leg. The muscles were usually explored in pairs with muscle 130 (coxal adductor), which is known to receive CI input (Hoyle, 1966), or one of the other muscles in which innervation could be readily established, as the reference member of the pair (Fig. 1B,H). This was an additional check that the stimulation was effective in evoking an antidromic spike. A failure to find CI input to a muscle fibre could then be attributed with some certainty to the failure of CI to innervate it and not to a failure of CI activation.

The metathoracic CI innervates the following 13 muscles: 120 (second coxal remotor), 121 (anterior coxal rotator), 122, 123, 124 (posterior coxal rotators), 125, 126 (coxal abductors), 130 (coxal adductor), 131, 132 (trochanteral levators), 133a, 133d (trochanteral depressors) and 135 (extensor tibiae). The type of evidence for this conclusion is shown for 10 of the muscles in Fig. 1A–H. In all these muscles the IPSPs

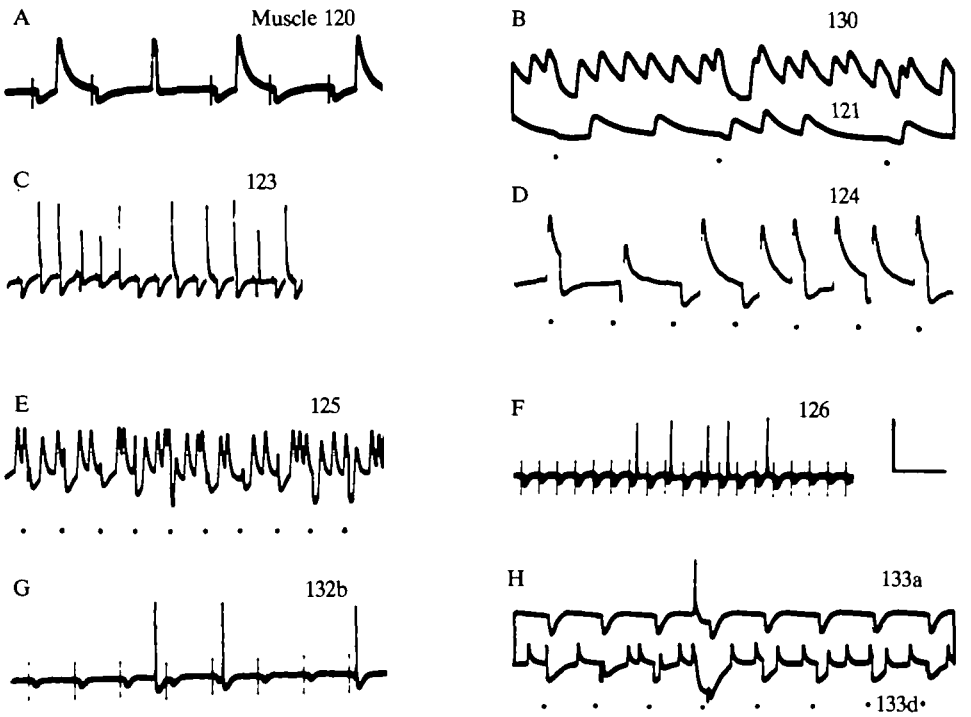

Fig. 1. Intracellular recordings from muscles innervated by the metathoracic common inhibitory neurone (CI). An axon of CI in the nerve to the extensor tibiae muscle within the femur is stimulated antidromically. Where the stimulus artefacts are not readily visible, stimuli are indicated by a dot. In B and H simultaneous recordings are made from two muscles. Calibration: voltage (A, B upper trace, D) 17 mV; (C) 10 mV; (E,G,H lower trace) 12·5 mV; (B lower trace) 33 mV; (F,H upper trace) 25 mV; time (A,C,E,G,H) 200 ms; (B) 50 ms; (D) 100 ms; (F) 400 ms.

would follow antidromic stimulation of an axon of CI at frequencies of at least 50 Hz. The field of innervation of CI is confined to muscles that move the proximal joints of a hind leg, the coxa, the trochanter and the tibia. Muscles moving the distal joints, the tarsus and the unguis, are not innervated. To determine which axon of CI innervates a particular muscle the nerve supply was traced by injecting locusts with reduced methylene blue. The nerve suspected of providing CI input to a particular muscle was then cut whilst recording from that muscle and antidromically stimulating the CI from the extensor nerve in the femur. The pattern of innervation is shown in Fig. 2.

No CI input was found, despite extensive searching, in muscles 113 (tergosternal), 118 (coxal promoter), 119 (first coxal remotor), 127 and 128 (pronator-extensors of the hindwing), 129 (depressor-extensor of the hindwing) or in 133b and c (bifunctional muscles which act as trochanteral depressors and hindwing elevators). There is a remote possibility that failure to find CI input to these muscles may have been due to failure of the CI spike in one of its axons.

The distribution and proportion of fibres receiving CI input differs in the various muscles. For example, in muscle 120 the innervated fibres are confined to a posterior

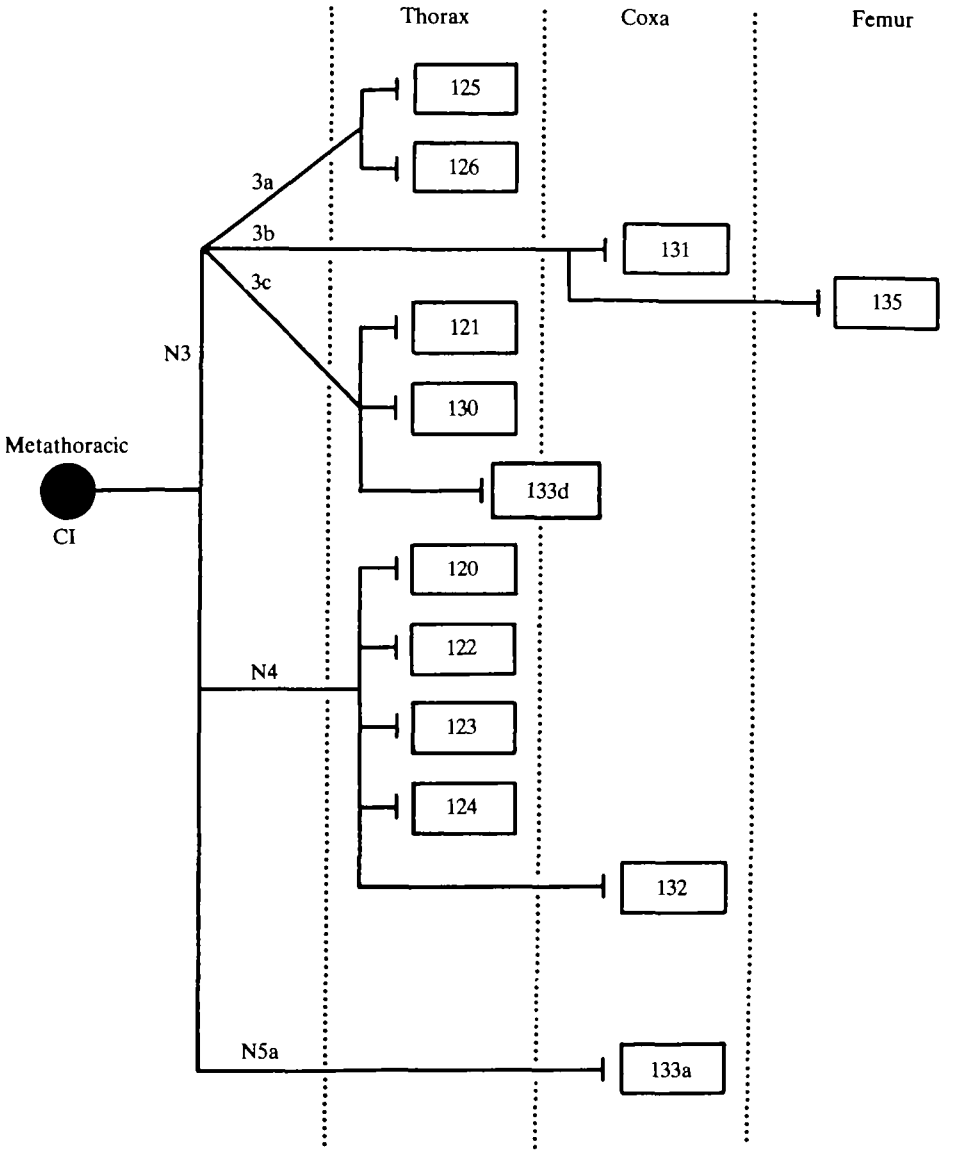

Fig. 2. Diagram of the innervation pattern of the metathoracic CI. Muscles that move the coxa, trochanter and femur are innervated by axons in nerves 3, 4 and 5.

region close to the apodeme (Fig. 1A). In muscle 123 the input is restricted to the more ventral part of the muscle (Fig. 1C). Recordings from this muscle were made in a dorsal preparation in which muscle 130 lies immediately ventral, so that it is possible that the electrode may have entered muscle 130. Cutting nerve 3c, which contains the CI axon to muscle 130, did not abolish the input to muscle 123. By contrast, in muscle 121 the distribution of CI innervation is more widespread.

The amplitude of an IPSP evoked by CI varies in different fibres of one muscle and in different muscles. IPSPs as large as 15 mV were recorded, although the majority

were less than 10 mV. No relationship between a particular muscle and the size of an IPSP was apparent. Occasionally depolarizing IPSPs were recorded, but usually from old preparations. The effect of the IPSP on an EPSP also varies; an EPSP could be reduced to as little as 10 % of its normal value, but again the variation within a muscle could be as large as the variation between muscles. One generalization that can be made, however, is that every fibre receiving CI input also receives an input from a tonic excitatory motor neurone.

The innervation pattern of the mesothoracic common inhibitor

The innervation pattern of mesothoracic CI was mapped using the same technique as for the metathoracic CI. Its axon in the extensor nerve in the mesothoracic femur

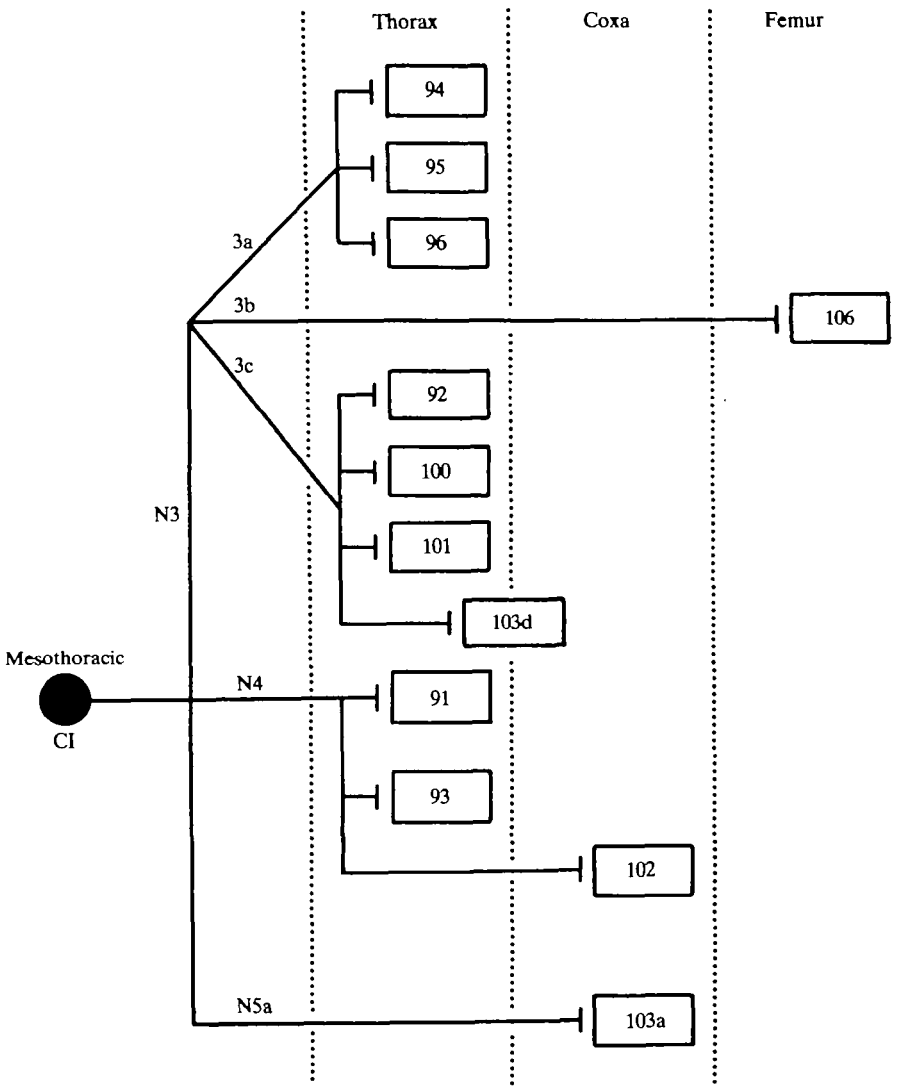

Fig. 3. Diagram of the innervation pattern of the mesothoracic CI. Note the similarity to that of the metathoracic CI.

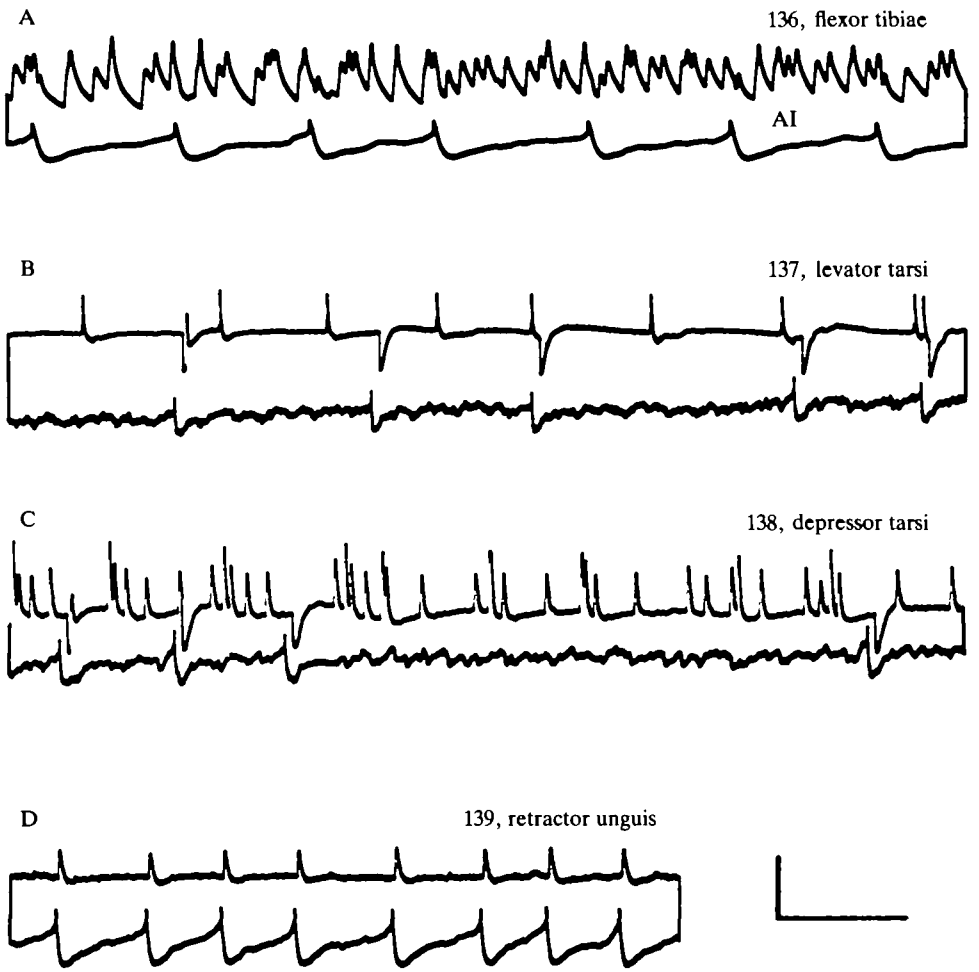

Fig. 4. Intracellular recordings from muscles innervated by the metathoracic anterior inhibitory neurone (AI). The recordings are made simultaneously from the soma of AI and from a fibre in the muscle indicated in (A–D). The spikes in AI occur spontaneously or after the application of depolarizing current through the recording microelectrode. Depolarizing potentials are recorded in the retractor unguis in the example shown (D). Calibration: voltage AI, (A) 10 mV; (B–D) 5 mV; muscle fibre (A,C) 10 mV; (B) 25 mV; (D) 5 mV; time (A) 200 ms; (B–D) 400 ms.

was stimulated antidromically, as it is known to innervate the extensor tibiae muscle (Burns & Usherwood, 1979). Alternatively, paired recordings were made from the muscle to be tested and from a muscle which had been shown to have CI input by the previous method. The CI was then excited by stroking the ipsilateral mesothoracic tarsus with a fine paint brush.

The mesothoracic CI innervates the following 12 muscles: 91 (second coxal remotor), 92 (anterior coxal rotator), 93 (posterior coxal rotator), 94, 95, 96 (coxal abductors), 100, 101 (coxal adductors), 102 (trochanteral levator), 103a, 103d (trochanteral depressors) and 106 (extensor tibiae) (Fig. 3). CI input was not found

in muscles 89 (coxal promotor), 90 (first coxal remotor), 103c (trochanteral levator) and 104 (femoral reductor, a muscle that is absent in the metathorax).

The innervation pattern of the metathoracic anterior and posterior inhibitors

The innervation pattern of these neurones was mapped by recording intracellularly from their somata in the metathoracic ganglion and, at the same time, exploring muscles in a hind leg with an intracellular electrode to look for IPSPs which corresponded 1:1 with the spikes (Fig. 4). The neurones were identified by the position of their somata in the ganglion and by their shape after injection of cobalt (A. H. D. Watson, M. Burrows & J. P. Hale, in preparation). The low frequency of spikes in these neurones could be increased by injecting depolarizing current into their cell bodies.

Both these inhibitors innervate the same four muscles which move the more distal segments of a hind leg, the femur, the tarsus and the unguis; 136 (flexor tibiae), 137 (tarsal levator), 138 (tarsal depressor) and 139 (retractor unguis) (Figs 4A–D, 5). Both neurones have a single axon that emerges from the metathoracic ganglion in nerve 5B (Fig. 5). Their axons do not divide to form branches in nerves 3B, 4 or 5A so that it is unlikely that they innervate any of the coxal or trochanteral muscles. Indeed, no IPSPs were recorded in these muscles which correlated with spikes in either the anterior (AI) or posterior (PI) inhibitors. Sometimes depolarizing potentials occurred in a muscle fibre whenever a spike of an inhibitory neurone was recorded in its soma (e.g. Fig. 4D). In other locusts the same arrangement of electrodes recorded conventional IPSPs. It is assumed that the depolarizing potentials are reversed IPSPs.

Reflex excitation of metathoracic inhibitors

AI and PI are both excited during imposed movements of the tibia about the femur. To discover whether the neurones are driven by common synaptic inputs during these responses, intracellular recordings were made simultaneously from AI and PI (Fig. 6). Each neurone was identified by the position of its cell body and by correlating spikes recorded from its cell body with IPSPs in the ipsilateral flexor tibiae muscle. In the absence of any imposed movements both neurones spike sporadically and at different times. Many of their synaptic inputs are common (Fig. 6A). Extension of the ipsilateral metathoracic tibia, starting from a femoro-tibial angle of 90°, causes an

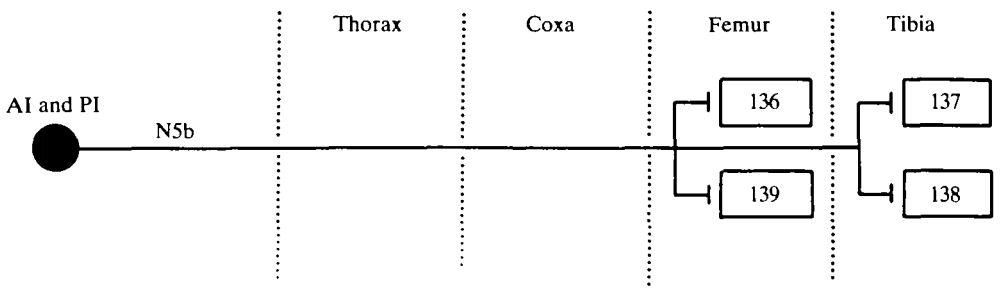

Fig. 5. Diagram of the innervation pattern of the metathoracic AI and PI. Muscles that move the tibia, tarsus and unguis are innervated.

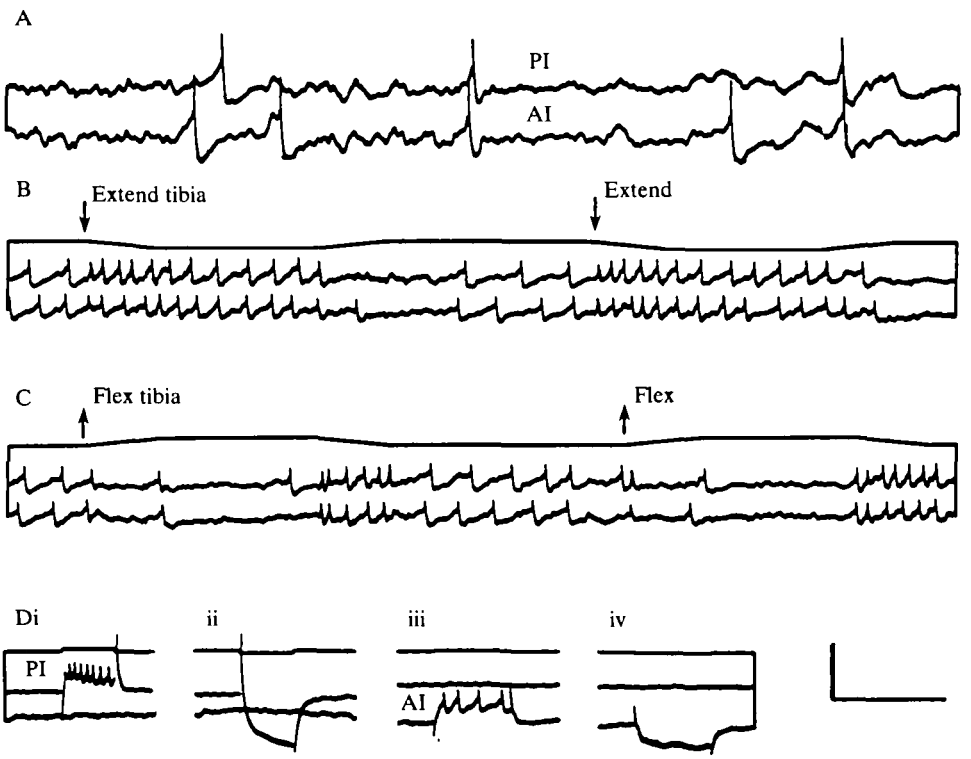

Fig. 6. Common synaptic potentials and reflex responses in AI and PI. Intracellular recordings are made simultaneously from the somata of the two neurones. (A) Spontaneous activity in which many of the synaptic potentials are common to both neurones. (B) The tibia is extended (arrows) about the femur from an initial femoro-tibial angle of 90° to 130°. Both neurones are excited, but their spikes are not synchronous. (C) The tibia is flexed (arrows) from 90°–50°. The spikes in both neurones decrease in frequency. (D) Tests for electrical coupling. Depolarizing (i,iii) and hyperpolarizing (ii,iv) current is injected into PI and then into AI. Upper traces, current; middle traces, PI; lower traces, AI. No coupling is revealed. Calibration: voltage (A) 4 mV; (B–D) 16 mV; current 30 nA; time (A) 200 ms; (B–D) 400 ms.

increase in the frequency of EPSPs and spikes in both AI and PI (Fig. 6B). By contrast, flexion of the tibia causes a decrease in the frequency of spikes in both neurones (Fig. 6C). Flexion or extension of the contralateral metathoracic tibia does not reliably affect the frequency of spikes in either neurone. Depolarizing current injected into PI to evoke spikes has no effect on the membrane potential of AI (Fig. 6Di). Hyperpolarizing current injected into PI is also without effect on AI (Fig. 6Dii). Similarly, current of either polarity injected into AI has no effect on PI (Fig. 6Diii, iv). These tests and the independent occurrence of the spikes during voluntary or imposed movements indicate that the two neurones are not coupled synaptically or by electrotonic junctions.

Other metathoracic inhibitory motor neurones

Other inhibitory motor neurones with cell bodies in the metathoracic ganglion innervate axial musculature through axons in nerve 6 or nerve 1. Intracellular recordings from muscles 117 (sixth ventral longitudinal), 141 (abdominal dorsal

longitudinal) and 143 (median internal ventral muscle) showed that they receive inhibitory innervation from nerve 6. One of these inhibitors to muscle 143 has been described (Yang & Burrows, 1983). Muscle 116 (fifth ventral longitudinal) also receives inhibitory input from metathoracic nerve 1A so the cell bodies may be in the meso- or metathoracic ganglion. Paired recordings have failed to provide evidence that the inhibitors are common to these muscles, although they do have a tendency to spike at the same time. This result does not necessarily mean that these inhibitors are specific ones, but probably indicates that all their target muscles have yet to be revealed.

DISCUSSION

Common inhibitory neurones

The three inhibitory neurones which innervate muscles in the hind or in the middle legs are all common inhibitory neurones. These neurones have been named in two different ways. CI was so named because it was shown to innervate two muscles (Pearson & Bergmann, 1969). AI and PI were named according to the position of their cell bodies in the metathoracic ganglion (AI anterior, PI posterior) (Burrows & Horridge, 1974). There was then no evidence to indicate whether these two neurones were specific or common inhibitors, so that names that implied nothing about the distribution of their terminals in the muscles were deemed appropriate. Now that they are also established as common inhibitory neurones it would seem sensible to name all inhibitors according to the same scheme. Our proposal therefore is that CI be called CI_1, AI to be called CI_2 and PI to be called CI_3. This scheme would then allow the other inhibitory neurones that we know to exist in the metathoracic ganglion (see also Yang & Burrows, 1983) to be incorporated by an appropriate subscript.

Braunig (1983) has recently described the innervation pattern of the metathoracic CI_1 in the locust, by recording its spikes in the various nerve branches that innervate known leg muscles. He found innervation to all the muscles described by us and in addition showed a consistent input to muscle 115 (pleurosternal), and in one locust he found an input to muscle 114 (pleuroalar, hindwing flexor). These small differences can probably be explained by the different methods used. Kutsch & Usherwood (1970) showed that muscle 90 in the mesothorax and its homologue, 120, in the metathorax both received inhibitory innervation. These inputs are here shown to be provided by CI_1 in the meso- and metathorax respectively. Siegler (1982) has also confirmed that two inhibitory neurones innervate the levator tarsi muscle. These are here identified as CI_2 and CI_3. The cockroach also has three common inhibitory neurones to the muscles of its hind legs (Pearson & Iles, 1971; Pearson & Fourtner, 1973). Like the locust, one has a more widespread field of innervation than the other two and has axons in more than one of the lateral nerves.

Role of inhibitory neurones in posture and locomotion

The difficulty in understanding the role of common inhibitors in the control of movement has always been in explaining why they should innervate muscles which must be active at different times. This paper has not addressed directly the issue of their functional role, but it has provided constraints for ideas about function by

demonstrating their wide fields of innervation.

CI_1 was known to innervate two muscles but now it is shown to innervate at least 13 that move a hind leg and at least 12 that move a middle leg. Its field of innervation is confined to muscles moving the coxa, the trochanter and the tibia, in other words the more proximal parts of a leg. It innervates antagonistic muscles that levate or depress the trochanter, muscles that rotate the coxa anteriorly and posteriorly and muscles that abduct and adduct the coxa, and a muscle that extends the tibia.

When a locust is motionless CI_1 spikes only sporadically. During walking, however, it spikes toward the end of the retraction, and the frequency of its spikes increases with the speed of locomotion (Burns & Usherwood, 1979). If its role is to accelerate the relaxation of force between the rhythmic contractions of the many muscles it innervates, then an improved performance by one muscle might well be counterbalanced by a degraded performance of another. Moreover, the many movements performed by a leg are achieved by participation of the same muscles in different combinations. The rigidity of action imposed by innervation from a common motor neurone would seem inappropriate for the required flexibility.

CI_2 and CI_3 have a more restricted field of innervation in the more distal parts of a leg. They both innervate the flexor tibiae muscle, and muscles which move the tarsus and the unguis. None of these muscles is innervated by CI_1. All three inhibitors, however, innervate muscles in the femur which move the tibia. The extensor tibiae is innervated by CI_1 and the flexor by both CI_2 and CI_3. For these two muscles at least there is the possibility that the separate action of the inhibitors could promote their more rapid relaxation between the rhythmic contractions they might undergo during walking. There is, however, little information on the action of CI_2 and CI_3 in movement. During imposed movements of a tibia, both receive a similar pattern of synaptic potentials, many of which are common, and have similar patterns of spikes. During walking, nothing is known of the activity of these neurones. During kicking, both are excited at the same time as the excitatory motor neurones to the flexor tibiae muscle are inhibited (Heitler & Burrows, 1977). The concurrent excitation of inhibitory neurones and inhibition of excitatory ones should lead to a rapid fall in force in the flexor muscle and allow the tibia to extend quickly. The effects on the muscles which move the tarsus must now be considered because they are also innervated by these same common inhibitors. When the kick is to occur and thrust must be applied to the offending object or to the ground, these muscles will receive an inhibitory input.

These attempts to suggest a role for the inhibitors are based on two assumptions; first that the inhibitor innervates all fibres in a particular muscle, and second that all fibres in a muscle have the same mechanical, electrical and biochemical properties. These assumptions are false. First, the extensive sampling with microelectrodes that has furnished the patterns of innervation shows that not all fibres in a muscle are innervated by the inhibitors. Some muscles have only small and restricted regions innervated by an inhibitor. For example, in the metathoracic extensor tibiae only 10% of the fibres are innervated by CI_1 (Usherwood & Grundfest, 1965). All the muscle fibres that are innervated by the various inhibitors are, however, also supplied by tonically active (slow) excitatory motor neurones (extensor tibiae muscle, Usherwood & Grundfest, 1965; other muscles this paper). Second, the diversity of types of fibres within an arthropod muscle is a well established fact (see Hoyle, 1983 for

review). The function of an inhibitor may thus reside in its ability to abolish or promote the relaxation of force only in those fibres that are particularly slow at contracting and relaxing, or which show catch-like properties (Usherwood, 1967; Usherwood & Runion, 1970). Such fibres would be ideal for the maintenance of posture or for slow adjustments of posture, but their slow responses would impede rapid movements during walking or jumping. Their exclusion from rapid movements could be achieved by the inhibitors, whose pattern of spikes would not need to be linked precisely to the underlying rhythm of the movement. In addition, the effectiveness of inhibitory action may be modified by the local release of chemicals from the terminals of particular dorsal unpaired median neurones.

What has emerged from this study is the realization that the sphere of influence of the inhibitory neurones is large. By comparison all the excitatory motor neurones to a leg innervate but a single muscle. This work has emphasized the need to correlate the patterns of innervation with the properties of the individual muscle fibres. It has also highlighted the inadequacies of descriptions of the action of the inhibitors and of most of the excitatory motor neurones to muscles which move proximal parts of a leg. These descriptions, though likely to be difficult to obtain, should now become a priority.

JPH was supported by an MRC (UK) studentship. Some of the experimental work was supported by NIH grant 16058 to MB.

REFERENCES

BEVENGUT, M., SIMMERS, A. J. & CLARAC, F. (1983). Central neuronal projections and neuromuscular organization of the basal region of the shore crab leg. *J. comp. Neurol.* **221**, 185–198

BRAUNIG, P. (1983). Morphology and physiology of locust hind leg proprioceptors and their influence on its motor system. Doctoral thesis, University of Konstanz, F.R.G. (in German).

BURNS, M. D. & USHERWOOD, P. N. R. (1979). The control of walking in Orthoptera. II. Motor neurone activity in normal free-walking animals. *J. exp. Biol.* **79**, 69–98.

BURROWS, M. (1973). The morphology of an elevator and a depressor motorneuron of the hindwing of a locust. *J. comp. Physiol.* **83**, 165–178.

BURROWS, M. & HORRIDGE, G. A. (1974). The organization of inputs to motoneurones of the locust metathoracic leg. *Phil. Trans. R. Soc. Ser. B.* **269**, 49–94.

CLARAC, F. & VEDEL, J. P. (1975). Neurophysiological study of the antennal motor patterns in the rock lobster *Palinurus vulgaris*. *J. comp. Physiol.* **102**, 201–221.

COOKE, I. R. C. & MACMILLAN, D. L. (1983). The common inhibitory innervation of the pereiopods of the crayfish *Cherax destructor*. *J. exp. Zool.* **225**, 513–517.

DAVIS, W. J. (1971). Functional significance of motorneuron size and soma position in swimmeret system of the lobster. *J. Neurophysiol.* **34**, 274–288.

EVANS, P. D. & O'SHEA, M. (1977). The identification of an octopaminergic neurone which modulates neuromuscular transmission in the locust. *Nature, Lond.* **270**, 257–259.

GRAHAM, D. & WENDLER, G. (1981). The reflex behaviour and innervation of the tergo-coxal retractor muscles of the stick insect *Carausius morosus*. *J. comp. Physiol.* **143**, 81–91.

HEITLER, W. J. & BURROWS, M. (1977). The locust jump. I. The motor programme. *J. exp. Biol.* **66**, 203–219.

HILL, R. H. & LANG, F. (1979). A revision of the inhibitory innervation pattern of the thoracic limbs of crayfish and lobster. *J. exp. Zool.* **208**, 129–135.

HOYLE, G. (1966). Functioning of the inhibitory conditioning axon innervating insect muscles. *J. exp. Biol.* **44**, 429–453.

HOYLE, G. (1983). *Muscles and Their Neural Control*. New York: Wiley.

HOYLE, G. & BURROWS, M. (1973). Neural mechanisms underlying behavior in the locust *Schistocerca gregaria*. I. Physiology of identified motorneurons in the metathoracic ganglion. *J. Neurobiol.* **4**, 3–41.

IKEDA, K. & BOETTIGER, E. G. (1965). Studies on the flight mechanism of insects. II. The innervation and electrical activity of the fibrillar muscles of the bumble bee, *Bombus*. *J. Insect Physiol.* **11**, 779–789.

J. exp. Biol. 117, 193–213 (1985)
Printed in Great Britain © *The Company of Biologists Limited 1985*

POSTSYNAPTIC POTENTIALS OF LIMITED DURATION IN VISUAL NEURONES OF A LOCUST

BY PETER J. SIMMONS

Department of Zoology, University of Newcastle upon Tyne, Newcastle upon Tyne, NE1 7RU

Accepted 27 November 1984

SUMMARY

Large, second-order neurones of locust ocelli ('L-neurones') make both excitatory and inhibitory connections amongst each other. A single L-neurone can be presynaptic at both types of connection. At the excitatory connections, transmission can be maintained for long periods without decrement. In contrast, inhibitory postsynaptic potentials (IPSPs) never last for more than 15–35 ms. This paper examines mechanisms which could limit the duration of these IPSPs.

1. An IPSP begins 4·5 ms after a presynaptic neurone starts to depolarize from its resting potential, and the time-to-peak is 7 ms.

2. The amplitude of an IPSP depends both upon the amplitude of the peak presynaptic potential and upon the potential at which a presynaptic neurone is held before it is depolarized.

3. The rate at which a postsynaptic neurone hyperpolarizes to produce an IPSP is proportional to the rate at which the presynaptic neurone depolarizes, independent of the potential from which the presynaptic depolarization starts. A maximum rate of postsynaptic hyperpolarization is reached when the presynaptic neurone depolarizes at $10\,mV\,ms^{-1}$.

4. Once an IPSP has occurred, both the amplitudes and the rates of hyperpolarization of subsequent IPSPs are depressed. The connection recovers its full ability to transmit over a period of 1·5 s. Larger IPSPs are followed by initially greater depression than smaller IPSPs.

5. A connection can begin to recover from depression while the presynaptic neurone is held depolarized from resting.

6. Transmission fails when a presynaptic neurone is depolarized by pulses shorter than 2 ms.

7. The most likely reason why the duration of the IPSPs is limited is that calcium channels in the presynaptic terminal inactivate within 7 ms of first opening.

INTRODUCTION

Large, second-order neurones of locust ocelli ('L-neurones') provide useful subjects for investigations on the transmission of signals both within a single neurone, and across synapses between neurones. Pairs of microelectrodes can be inserted into single

Key words: Postsynaptic potential, spike, ocellus, *Schistocerca*.

L-neurones to study the origin and transmission of signals within them (Wilson, 1978*b*), or, combined with a further microelectrode in a postsynaptic neurone, to study the operating characteristics of output connections from an L-neurone (Simmons, 1981, 1982*a*). Signals decrement very little throughout the length of an L-neurone (Wilson, 1978*b*; Simmons, 1982*a*), and L-neurones have very simple geometries (C. S. Goodman, 1976; L. J. Goodman, Patterson & Mobbs, 1975; Simmons, 1982*a*). This means that an electrode placed in the axon of an L-neurone will record fairly accurately the amplitudes and waveforms of potential changes which occur at pre- or postsynaptic sites.

The output connections which L-neurones make are of particular interest because two types of them, which have contrasting properties, have been found. A single L-neurone can make both types of output connection. L-neurones make excitatory connections with some large brain neurones which descend in the nerve cord (Simmons, 1981), and make both excitatory and inhibitory connections laterally amongst each other (Simmons, 1982*a*). At the excitatory connections, small, slowly changing variations in presynaptic potential are transmitted to the postsynaptic neurone, as long as the presynaptic neurone is depolarized from a threshold potential. Because the normal resting potential of an L-neurone is depolarized above the threshold for release of transmitter at the excitatory connections, small hyperpolarizations, such as those that occur when ocellar illumination is increased, are communicated across these connections (Simmons, 1981, 1982*a*). Transmission at the excitatory connections can be sustained for long periods without decrement. In contrast, at the inhibitory connections which L-neurones make amongst each other, the postsynaptic potential (PSP) has a duration limited to less than 35 ms, no matter for how long the presynaptic terminal is held depolarized (Simmons, 1982*a*). Two of the possible mechanisms which would limit the duration of these PSPs are that presynaptic transmitter becomes depleted, or that postsynaptic receptors desensitize. If either of these processes occurred rapidly, then slow changes in presynaptic potential would not be transmitted across the inhibitory connections, and fast depolarizing potentials, such as spikes, would be required to effect transmission. L-neurones produce single spikes, or, rarely, short bursts of spikes when illumination is reduced (Chappell & Dowling, 1972; Patterson & Goodman, 1974; Wilson, 1978*a*) or when a pulse of hyperpolarizing current injected into an L-neurone ends (Wilson, 1978*b*). The amplitude of a spike in an L-neurone depends on both the amplitude and duration of the preceding hyperpolarization (Simmons, 1982*a*) and L-neurones do not produce trains of spikes when depolarized. In this paper it is shown that neither transmitter depletion, nor desensitization of postsynaptic receptors is likely to occur at the inhibitory connections among L-neurones. Instead, transmission may be limited in duration by properties of calcium channels in the presynaptic membrane. The importance of rapid depolarization, such as a spike provides, in effective transmission at these connections is demonstrated.

METHODS

Experiments were performed on *Schistocerca gregaria* (Forskål), taken from culture at least 4 days after their final moult. Mouthparts were removed, the wounds were

sealed with wax, and the locust was fixed upright on a plasticene block. The lateral ocellar nerves and the dorsal surface of the brain were exposed. The head was stabilized against movement by inserting pins through the genae into the plasticene. A constant supply of saline (Eibl, 1978) bathed the brain. The tracheae of the brain were not disturbed, and ventilation was provided by the animal's own continual pumping movements. The laboratory was darkened as much as possible during an experiment. The temperature of the preparation was 18–22 °C.

In most preparations, to ease the passage of electrodes through the connective tissue sheath of the ocellar nerves and brain, a 1 % solution of protease in saline was applied for 2 min. Routinely, up to three independent glass microelectrodes were employed. They were filled with $2\,\text{mol}\,\text{l}^{-1}$ potassium acetate and had d.c. resistances of 40–80 MΩ. Each electrode was connected to a d.c. amplifier which incorporated a bridge circuit, allowing current to be injected through the electrode. Current was measured by using a virtual ground amplifier, which measured current flowing along the chloridized silver wire which was employed as the indifferent electrode. This electrode lay along the inside of the thorax, with its free end placed as close as possible to the brain. Results were recorded with an FM tape recorder and were analysed later with the aid of a North Star Horizon microcomputer, fitted with a Comart 7A + D analogue/digital converting card. Pre-triggered displays on the oscilloscope screen and signal averaging were achieved by use of programmes written in Pascal M/T (Simmons, 1985). The figures in this paper were drawn by an X-Y plotter, driven by the microcomputer.

L-neurones were identified as such by the waveform of their responses to light, delivered from a green light emitting diode (for justification of this method see Simmons, 1982*a*). Particular care was taken to ensure that the neurones were not damaged by penetration with microelectrodes. A number of observations were used to check for damage. The most direct was to observe any change in membrane potential recorded by one electrode as a second was inserted into the same neurone. A second method was to monitor the responses of L-neurones to pulses of light, delivered at frequent intervals to the ocellus from a green light emitting diode. In the dim light in which the experiments were conducted, undamaged L-neurones showed a constant barrage of distinct hyperpolarizing potentials, at least some of which probably corresponded to the capture of single photons by photoreceptors (Wilson, 1978*c*). Changes in the amplitude of these proved to be a sensitive and convenient measure of the health of a neurone. In most experiments, at least one pair of L-neurones connected by an inhibitory connection was found. Observations of IPSPs have been made in over 150 locusts, and in about half of these, two electrodes were inserted into the presynaptic neurone while a third recorded postsynaptic potential. Measurements were made from about one in three of these latter experiments. In the remaining experiments, measurements were not made for reasons which included: damage to neurones, small amplitudes of IPSPs relative to other postsynaptic events, and unacceptable coupling artefacts between electrodes. Where graphs were constructed, measurements were made from single sweeps and were later averaged. All the observations reported in this paper were made in at least three different preparations, with the exception of that in Fig. 6D, which was repeated twice.

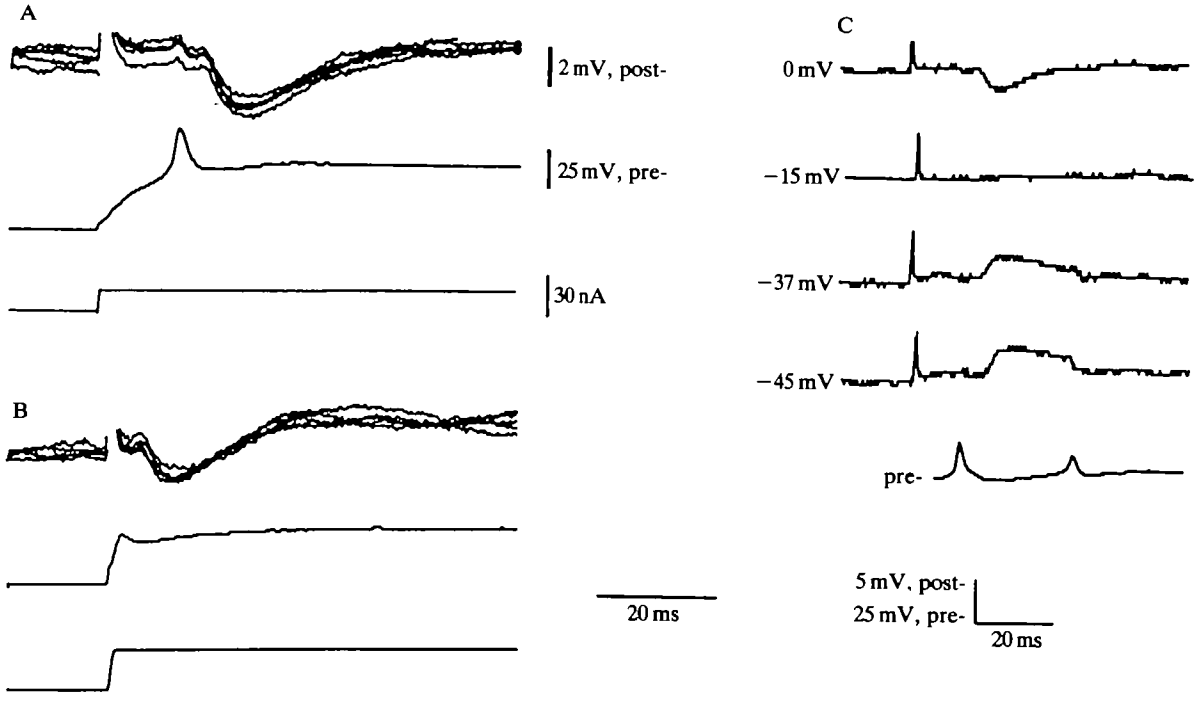

Fig. 1. (A,B) IPSPs mediated by spikes and by longer depolarizing potentials in a presynaptic neurone. Traces are: top, five superimposed sweeps showing IPSPs; second, presynaptic potential; bottom, current injected into the presynaptic neurone through a separate electrode. In A, the spike was triggered at the end of a pulse of hyperpolarizing current, 300 ms long, injected into the presynaptic neurone. In B, the pulse of current depolarized the presynaptic neurone from its normal resting potential. The apparent depolarization in postsynaptic membrane potential, when the ends of these traces are compared with the beginnings, is due to d.c. coupling between microelectrodes, the extent of which varied from preparation to preparation. In addition, a transient coupling artefact always accompanied a change in current injection. (C) Two electrodes were inserted into the postsynaptic neurone, one to inject hyperpolarizing current and the other to record potential. A single electrode in the presynaptic neurone was used both to inject hyperpolarizing current pulses and to record spikes. When the postsynaptic neurone was hyperpolarized to 15 mV from resting, no IPSP was recorded, and the IPSP became depolarizing when the postsynaptic neurone was hyperpolarized further. The potential of the postsynaptic neurone relative to resting is indicated with each trace (the traces are not aligned precisely with these holding potentials).

RESULTS

The time course of the inhibitory postsynaptic potential

The inhibitory postsynaptic potential (IPSP) at a connection between two L-neurones was examined by producing in the presynaptic neurone either a spike (Fig. 1A) or a more long-lasting depolarization (Fig. 1B). A spike was produced by switching off a hyperpolarizing current and lasted 4 ms, measured between departure from and return to resting potential (Fig. 1A). Resting potential was -30 to -35 mV (Simmons, 1981). To produce an IPSP by long depolarization, the presynaptic neurone was first held hyperpolarized by 4 mV, before a depolarization lasting 200 ms (Fig. 1B)

Latency was measured from the time the presynaptic neurone depolarized from resting potential, and was always 4·5 ms. Time-to-peak was 7 ms. Duration was 10–35 ms, varying with the amplitude of the IPSP, probably as a function of the membrane time constant.

Pulses of current injected to depolarize an L-neurone from resting were never observed to produce discrete spikes. However, such pulses did appear to activate regenerative channels in L-neurones, as the rate of potential change of an L-neurone was greater when the neurone was depolarized from resting than when it was repolarized back to resting potential. In addition, following the initial peak depolarization, there was usually a slight hyperpolarization in the membrane potential of an L-neurone, before it climbed again to a more sustained plateau depolarization, e.g. Fig. 1B. In 20 experiments, the potential was recorded at two different locations of an L-neurone while current was injected through a third electrode. The response recorded in the ocellar neuropile had a very similar waveform to that recorded in the axon in the brain. Measurements from five of these experiments gave values for the space constant of an L-neurone of 2·5 to 3·5 times the length of one of the lateral L-neurones (Goodman, 1976; Simmons, 1982*a*). In contrast to the statement in the summary of Wilson's (1978*b*) paper, spikes were conducted with little attenuation along L-neurone axons (some of Wilson's paired recordings may have been from two L-neurones linked by an excitatory connection rather than from a single axon; see also Simmons, 1982*a*). All recordings in this paper were made from L-neurone axons within 200 μm of the junction of the ocellar nerve with the brain. Because of the simple geometry (C.S. Goodman, 1976; L. J. Goodman *et al.* 1975; Simmons, 1982*b*) and the large space constants of L-neurones, the potentials recorded from this location were probably at least 70% of the value of the potentials occurring at any other location in an L-neurone, except for the cell body and its neurite. In ultrastructural studies, synapses have been found between large axons in ocellar nerves near to the brain (Goodman, Mobbs & Guy, 1977; Koontz & Edwards, 1984), although a detailed description of the distribution of synapses made by an L-neurone has not been made.

An IPSP could be reduced in amplitude, and then reversed in polarity, by injecting progressively greater amounts of hyperpolarizing current into the postsynaptic neurone (Fig. 1C). This is to be expected if the IPSP is generated by an increase in postsynaptic conductance to one or more species of ion. There was no indication of any late excitatory PSP (EPSP), which might be invisible at the normal postsynaptic

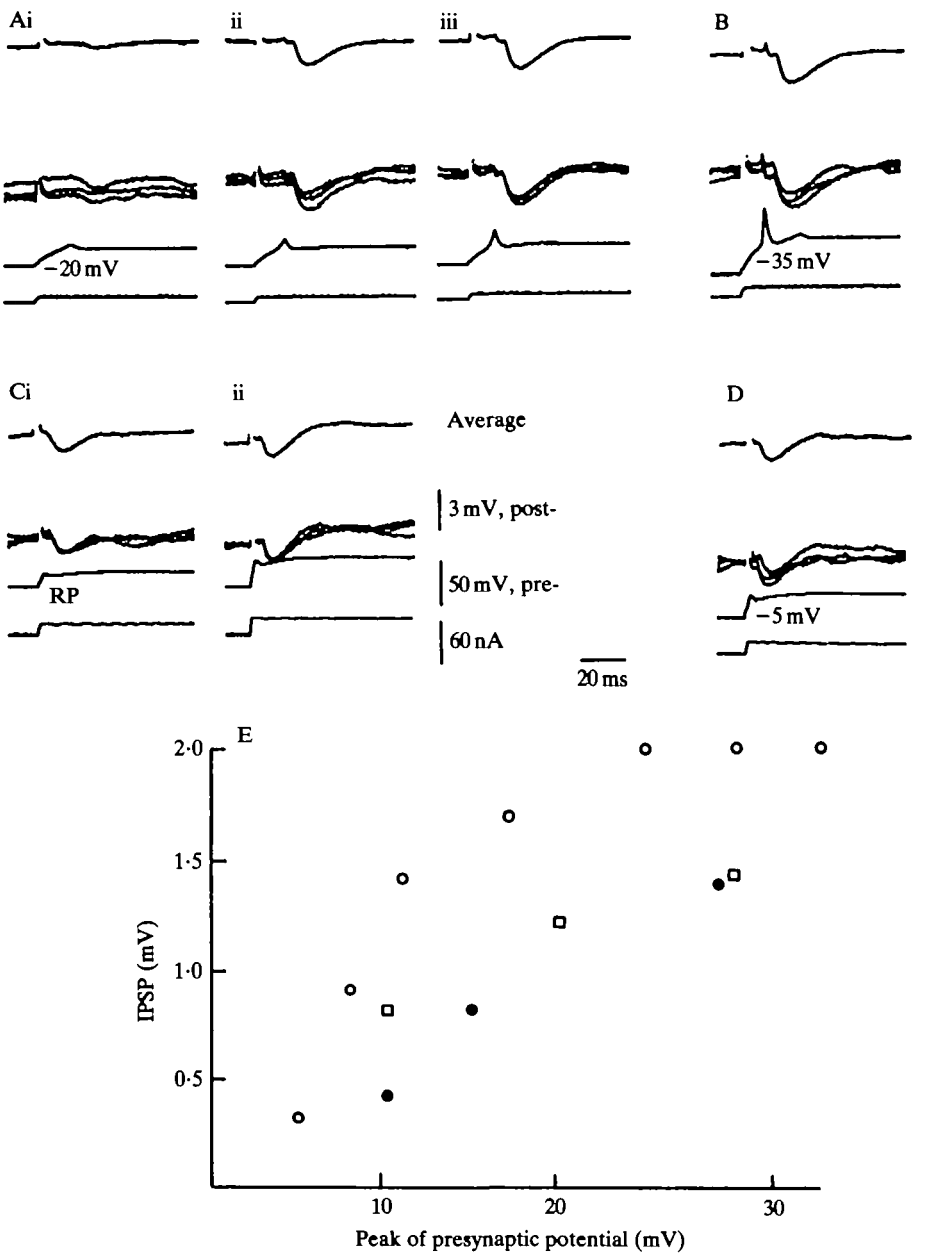

Fig. 2

resting potential, but which could terminate an IPSP and limit its duration. No sign of such an EPSP was seen, whether the IPSP was mediated by a presynaptic spike or by a more prolonged presynaptic depolarization. The time taken for an IPSP to reach its peak amplitude was unaffected by the membrane potential at which the postsynaptic membrane was held, but as the neurone was hyperpolarized by progressively greater amounts, the total duration of the IPSP increased. This was probably due to

the increase in PSP amplitude and to an increase in membrane resistance (Wilson, 1978*b*). The decay of an IPSP had a similar waveform and duration to the decay in potential at the end of a small pulse of hyperpolarizing current injected through an electrode into an L-neurone. In six experiments, the conductance of a postsynaptic neurone was measured both before and 40 ms following the start of an IPSP by injecting a 5 ms current pulse into the neurone. No conductance change following an IPSP was found.

The relationship between pre- and postsynaptic potentials

The amplitude of the IPSP was influenced by the potential at which the presynaptic neurone was held before depolarizing current was injected into it as well as by the peak of the presynaptic depolarizing potential (Fig. 2). In Fig. 2A, spikes were initiated in the presynaptic neurone by terminating pulses of hyperpolarizing current. These pulses hyperpolarized the neurone by 20 mV from its resting potential, and spikes of different amplitudes were produced by varying the duration of the hyperpolarizing pulses (Simmons, 1982*a*). For spikes reaching between 5 and 10 mV above resting potential, each 1-mV increase in spike amplitude caused an increment of 0·2 mV in IPSP amplitude (open circles, Fig. 2E). For larger spikes, the proportionate increase in IPSP amplitude fell off until, for spikes of 25 mV and greater, the IPSP reached its maximum amplitude of 2 mV. In Fig. 2C depolarizing pulses of current were injected to depolarize the presynaptic neurone from its resting potential. These presynaptic potentials (filled circles, Fig. 2E) produced smaller IPSPs than did presynaptic spikes reaching equivalent potentials from resting (open circles, Fig. 2E). For the depolarizations from resting, each 1-mV increase in peak depolarization of the presynaptic neurone caused an increment of 0·1 mV in IPSP amplitude, between presynaptic potentials of 10 and 20 mV. Fig. 2D and the open squares in Fig. 2E show IPSPs produced when the presynaptic neurone was hyperpolarized 5 mV from resting potential between depolarizing pulses. These IPSPs were intermediate in amplitude between those produced by spikes and those produced when the presynaptic potential returned to resting between pulses.

There was considerable variation in the maximum amplitudes of IPSPs which could be elicited in different preparations, although a detailed statistical analysis was not made. A few IPSPs reached 10 mV in amplitude, but most studies were made of IPSPs between 2 and 3 mV high. Often smaller IPSPs were recorded,

Fig. 2. The relationship between pre- and postsynaptic potentials. In A–D the traces are: top, the average from ten repetitions of an IPSP; second, the first three IPSPs from which the average was derived are superimposed; third, presynaptic potential; bottom, current that was injected presynaptically through a separate electrode. In A, each spike was initiated at the end of a pulse of hyperpolarizing current. Each current pulse hyperpolarized the presynaptic neurone by 20 mV, and spike amplitude was altered by varying the duration of the hyperpolarizing pulses. The lengths of the hyperpolarizing pulses had been: (i) 40 ms, (ii) 60 ms and (iii) 150 ms. In B, each current pulse (300 ms long) hyperpolarized the presynaptic neurone by 35 mV, and produced a spike which rose 35 mV from resting potential. In C, the presynaptic neurone was initially at its resting potential, and pulses of current were injected to depolarize it from this. D shows a pulse which depolarized the presynaptic neurone from an initial potential of − 5 mV. In E, the initial peak presynaptic potential caused by each depolarizing pulse of current is plotted against IPSP amplitude. The presynaptic potential is measured relative to resting potential (RP). Each point is plotted from ten repetitions. Starting potential: ○, − 20 mV; □, − 5 mV; ●, resting potential.

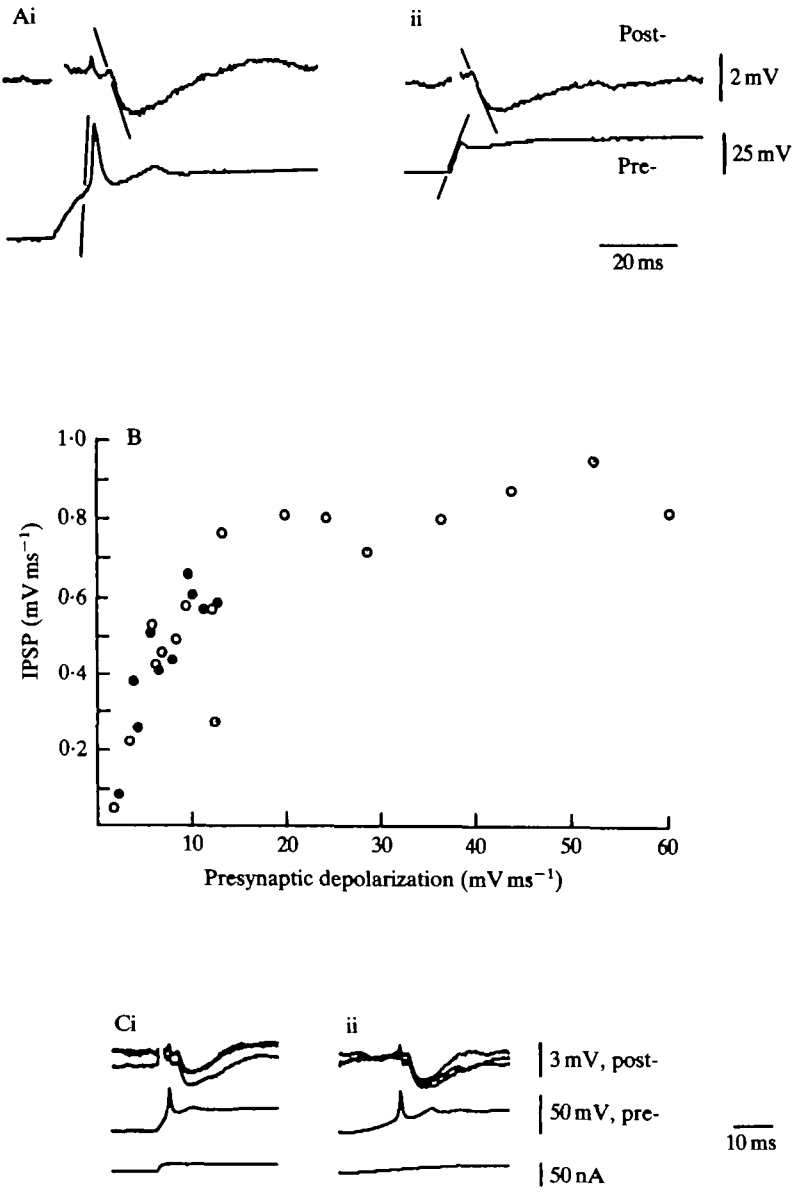

Fig. 3. Relationship between the rates of change in presynaptic and in postsynaptic potentials. In Ai, the spike and the IPSP it mediated are from Fig. 2A, and in Fig. Aii, the presynaptic depolarizing pulse and the IPSP it mediated, are from Fig. 2C. The lines drawn on each trace show the gradients that were measured. The small initial rapid phase of depolarization is probably an artefact due to coupling between electrodes. (B) A plot of the rate of presynaptic depolarization against rate of postsynaptic hyperpolarization, taken from the same experiment; O, spikes; ●, depolarizing pulses. In C, which was from a different experiment, the presynaptic neurone was initially hyperpolarized 12 mV from its resting potential, and a ramp of current depolarized it above resting. The rates of current change were different in i and ii. In each, the presynaptic neurone spiked, and spikes mediated IPSPs. Three examples of the IPSPs are superimposed in each record.

but measurements on these were difficult as they are about the same amplitude as fluctuations in potential caused by the random arrival of photons at photoreceptors (Wilson, 1978*c*).

The relationship between rates of change in pre-and postsynaptic potentials

The reason why the starting potential of the presynaptic neurone influences IPSP amplitude became clear when the rates of change of pre- and postsynaptic potentials were measured. For the experiment shown in Fig. 2, the rates of potential change in the two neurones were plotted (Fig. 3A), and the rates of presynaptic depolarization were plotted against rates of postsynaptic hyperpolarization both for presynaptic spikes and for more long lasting depolarizations (Fig. 3B). The rate of postsynaptic hyperpolarization, causing an IPSP, depended on the rate of presynaptic depolarization, and was independent of the initial potential of the presynaptic neurone. When a pulse of depolarizing current was injected into an L-neurone, the neurone depolarized more rapidly if it was initially hyperpolarized than if it was initially at resting potential. In the plot of Fig. 3B, for each 1 mV ms^{-1} increase in the rate of presynaptic depolarization up to a rate of 10 mV ms^{-1}, the rate of postsynaptic hyperpolarization increased by 0·08 mV ms^{-1}. For more rapid presynaptic depolarizations, which were achieved only by spikes, there was little or no increase in the rate of postsynaptic hyperpolarization beyond a maximum of 0·8 mV ms^{-1}. The maximum recorded rate of hyperpolarization during an IPSP was 3 mV ms^{-1}, and the amplitude of an IPSP was linearly proportional to its rate of rise. In a total of five experiments of this type, similar results were obtained. The rate of presynaptic depolarization at which the maximum rate of postsynaptic hyperpolarization was achieved was always within 2 mV ms^{-1} of 10 mV ms^{-1}. The rate of postsynaptic hyperpolarization, as well as the maximum amplitude of an IPSP, varied from experiment to experiment.

When gradual ramps of current were injected into a presynaptic neurone to depolarize it from an initially hyperpolarized potential, the neurone usually spiked and the spike mediated an IPSP (Fig. 3C). Judged from the inflection in the rate of depolarization, spikes were always initiated as the membrane potential was depolarized to resting, no matter how rapid the depolarization. Attempts to determine the minimum rate of presynaptic depolarization that would mediate an IPSP were thwarted by the tendency of L-neurones to spike. Ramps of current which produced depolarizations at less than 1 mV ms^{-1} produced neither spikes nor detectable IPSPs.

Recovery of the ability of inhibitory connections to transmit

When one IPSP had been produced, the ability of an inhibitory connection to transmit was depressed, and full recovery took about 1·5 s. Larger spikes caused a more pronounced depression (Fig. 4A) than did smaller spikes (Fig. 4B). Separate pulse generators and current sources were used to trigger the two spikes of a pair in order to ensure that the two spikes were of equal amplitude. Similar results were obtained in two experiments where pulses of depolarizing current were injected into the presynaptic neurone (not shown). Depression could be expressed as the amplitude of a second IPSP relative to the first (Fig. 4C) and the results were essentially similar to those obtained by plotting reduction in the rate of hyperpolarization which produced an IPSP (not shown).

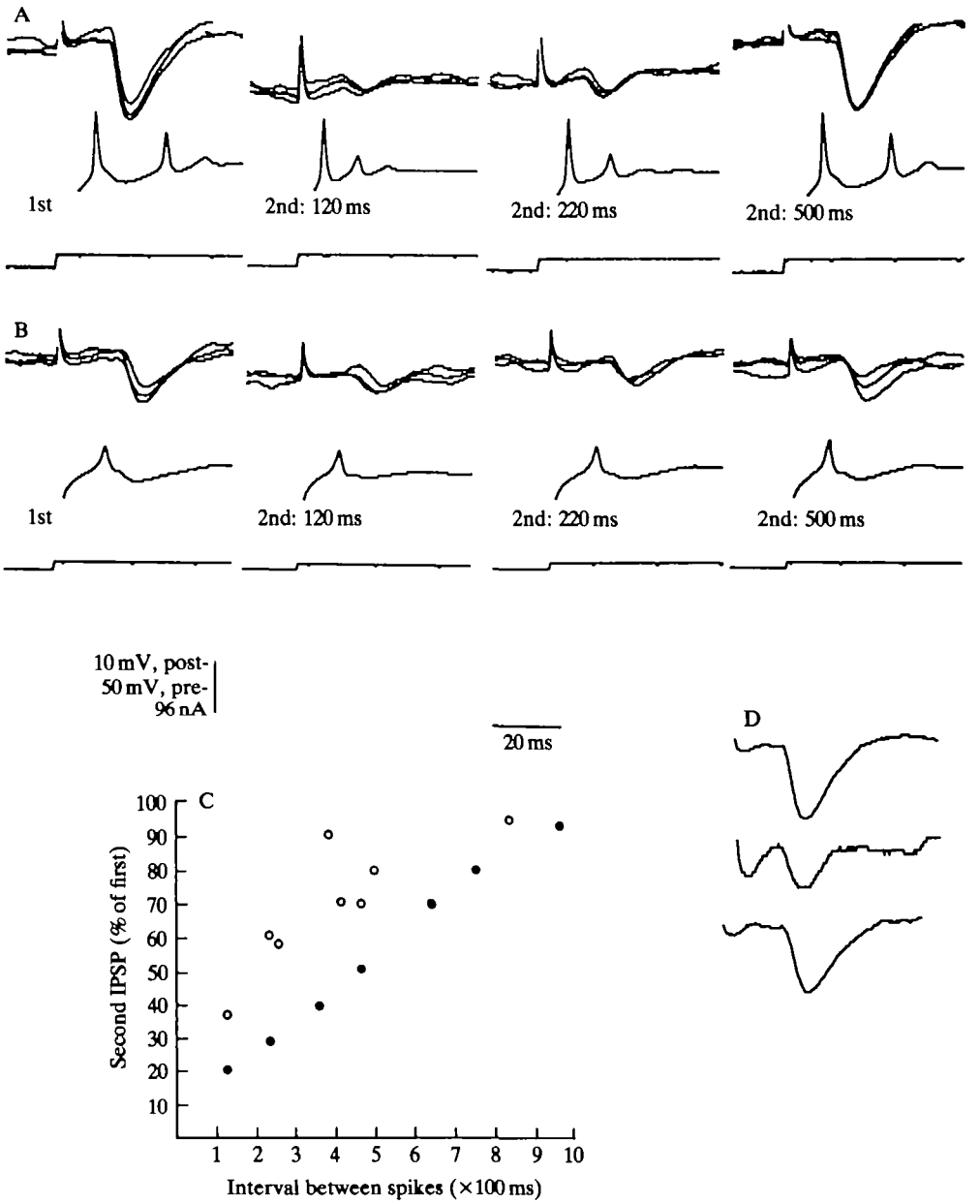

Fig. 4

Both the latency of an IPSP, and the time taken for it to reach its peak hyperpolarization, were the same for first or second IPSPs of a pair, or for IPSPs following large or small spikes. This is illustrated in Fig. 4D, where the traces are aligned with each other according to the times of the presynaptic spikes.

A connection could recover most of its ability to transmit while the presynaptic neurone was held depolarized from resting potential (Fig. 5). In Fig. 5A, pairs of spikes, separated by 100 ms, were produced by delivering pairs of hyperpolarizing

current pulses to the presynaptic neurone. The first spike of each pair produced an IPSP 2·2 mV in amplitude, and the second spike produced an IPSP of 0·8 mV, or 36 % of the amplitude of the first IPSP. In Fig. 5B, pairs of depolarizing pulses were injected into the presynaptic neurone. In each pair, the first pulse lasted for 48 ms, and the start of the second pulse occurred 100 ms after the start of the first pulse. The IPSP caused by each first pulse was 1·9 mV in amplitude, and the amplitude of the IPSP caused by each second pulse was 0·7 mV, or 37 % of the amplitude of the first IPSP. Therefore, the connection was recovering some of its ability to transmit before the presynaptic potential returned to resting at the end of the first pulse. The depolarizing pulses caused no more long-lasting depression than did single spikes. Similar results were obtained with much longer lasting pulses of depolarizing current injected into the presynaptic neurone (not shown). However, in three experiments, there was a relatively short interval between the end of the first pulse and the start of the second, and the second IPSP was usually reduced or absent. The reduction in IPSP amplitude was accompanied by a change in the shape of the initial depolarizing potential in the presynaptic neurone, which indicates that the short interval between pulses probably provided insufficient time for the conductance of the presynaptic membrane to return to its resting value. For example, in Fig. 5C, the interval between the start of the first and second pulses of each pair was 450 ms. The first pulse of each pair (Fig. 5Ci) produced an IPSP 1·4 mV in amplitude. IPSPs produced by the second pulses, when the duration of the first pulse was 390 ms, had amplitudes of 1·1 mV, or 79 % of the amplitudes of the first IPSPs (Fig. 5Cii). When the first pulse was lengthened to 410 ms, no IPSP was detected following each second pulse (Fig. 5Ciii). Here, the rate of depolarization of the presynaptic neurone at the start of the second pulse was reduced, as was the amplitude of the hyperpolarization which followed the initial peak depolarizing potential.

PSPs following short depolarizing pulses in presynaptic neurones

As pulses of current injected presynaptically were reduced to a length of 4 ms and less, both the IPSPs and EPSPs they mediated became smaller (Fig. 6). The pulse was 50 ms long in Fig. 6Ai, raising the presynaptic potential by 4 mV, and mediated and IPSP of 2·5 mV. In Fig. 6Aii, the presynaptic pulse reached an amplitude of 4 mV

Fig. 4. Following an IPSP, the ability of a connection to transmit is depressed and gradually recovers. Single microelectrodes were inserted into each neurone here. Spikes were initiated in the presynaptic neurone when pulses of hyperpolarizing current ended. In each recording in A and B, three superimposed IPSPs are shown for each spike. Pairs of spikes were produced, and an example of the first spike of a pair, together with IPSPs it mediated, is shown on the left of each sequence of recordings. The remaining recordings in each line show second spikes, and examples of the IPSPs they mediated. The interval between the first and second spikes of a pair is indicated. Three seconds separated the second spike of one pair and the first spike of the next pair. In A, the spikes peaked at 50 mV from resting potential, and in B the spikes peaked at 17 mV from resting potential. In C the amplitude of the second IPSP, expressed as a percentage of the amplitude of the first IPSP of a pair, is plotted against the interval between the two spikes which mediated the IPSPs. Each point is plotted as the average of ten repetitions of each pair; ○, smaller spikes; ●, larger spikes. In D, three IPSPs, at various voltage gains, are shown in order to illustrate latency and time to reach peak. The IPSPs are aligned according to the times of the spikes that mediated them (not shown in D). The top IPSP was produced by a large 1st spike, from A; the middle IPSP is also from A, and is the 2nd IPSP of a pair, mediated by large spikes separated by 120 ms; and the bottom IPSP is the 1st IPSP mediated by a smaller spike, from B.

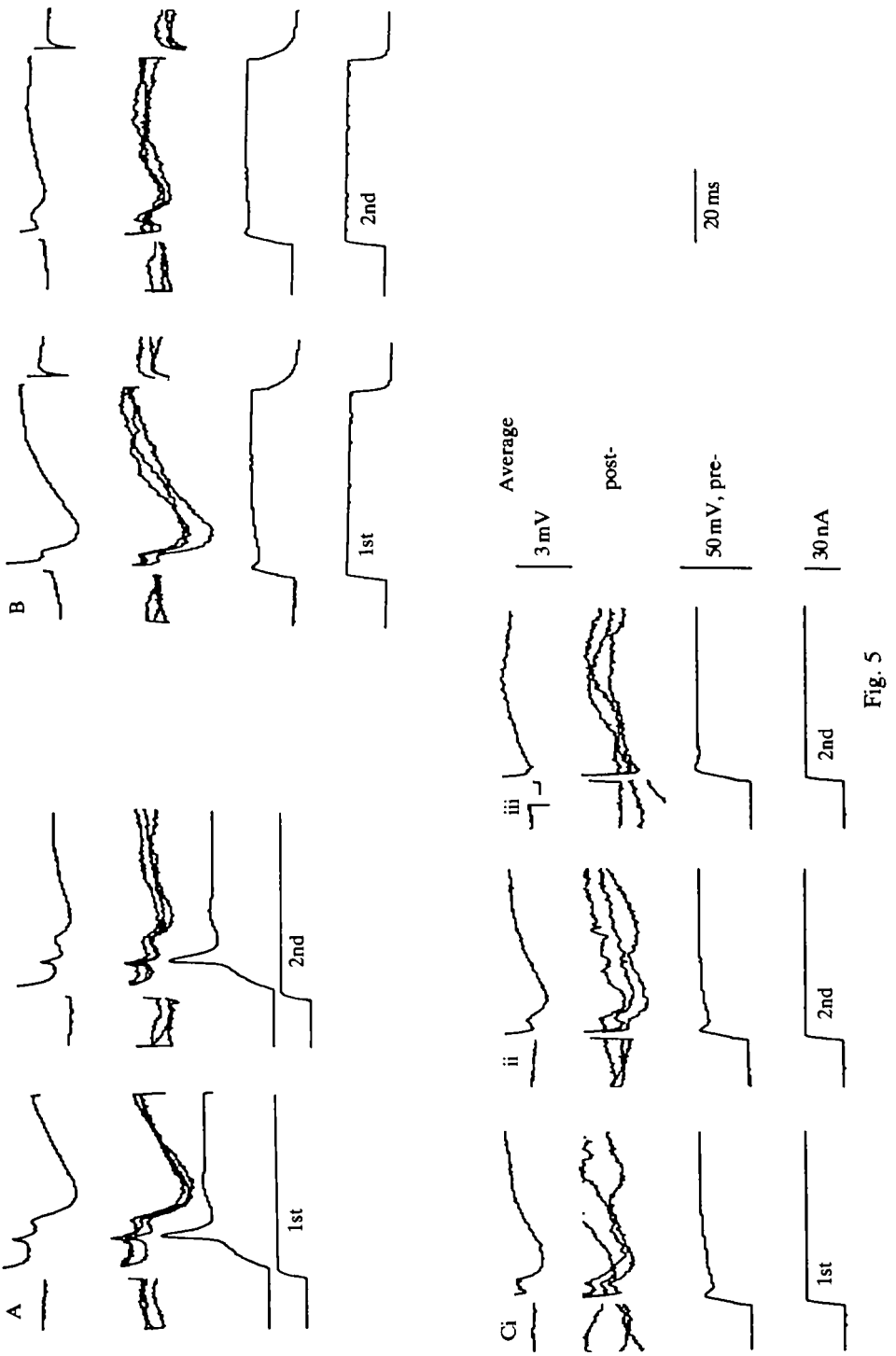
A
1st
2nd
B
1st
2nd
Ci
ii
iii
Average
3 mV
post-
50 mV, pre-
30 nA
20 ms
1st
2nd
2nd

Fig. 5

for 3 ms, and mediated an IPSP of 1·5 mV. With a shorter pulse (Fig. 6Aiii) the presynaptic neurone was depolarized to a maximum of 2 mV for 0·7 ms. There was no detectable IPSP following this depolarization.

Further evidence that presynaptic depolarizations shorter than 4 ms are less effective than longer pulses at mediating transmission was provided by examining the recovery of connections from depression. When two presynaptic stimuli, each longer than 4 ms, were separated by 100 ms, the amplitude of the second IPSP was reduced to 20–35 % of its value in a non-depressed connection (Fig. 4C). The reduction could be expected to be less if transmission during the first IPSP were to be reduced. This was examined by following each of the presynaptic pulses in Fig. 6A, after 100 ms, by a 50-ms test pulse (Fig. 6C). The amplitudes of the IPSPs elicited by these test pulses were compared with those of IPSPs elicited by single presynaptic pulses of the same amplitude and duration (Fig. 6B). The presynaptic pulses in Fig. 6B reached an amplitude of 12 mV, and elicited IPSPs of amplitude 4·5 mV. The ability of the electrode to depolarize the neurone declined during the last part of the experiment (Fig. 6Ciii), but this did not affect the results adversely. Following a first pulse 50 ms long (Fig. 6Ai), the test IPSP (Fig. 6Ci) had an amplitude of 2·5 mV, or 55 % of the amplitude of the IPSP in Fig. 6B. As the length of the first pulse decreased (Fig. 6Aii, iii) the amplitudes of the test IPSPs (Fig. 6Cii, iii) increased to 90 % and 100 % of the amplitude of the control IPSP in Fig. 6B. The IPSPs which followed presynaptic pulses 5 ms long had the same amplitude as those which followed longer presynaptic pulses, and 5-ms presynaptic pulses caused the same decrement in test IPSPs as did longer pulses.

Reduction in efficiency of transmission as presynaptic pulses were reduced in length was also observed at excitatory connections between L-neurones. In all three recordings of Fig. 6D current pulses depolarized the presynaptic neurone to 15 mV from resting. In Fig. 6D the pulse lasted for 50 ms, and the postsynaptic neurone depolarized to 2 mV above resting. The peak presynaptic depolarization of 15 mV lasted for 2·5 ms in Fig. 6D, and the postsynaptic potential reached 1 mV above resting. For a shorter depolarizing pulse, where the presynaptic membrane returned towards resting as soon as the peak depolarization was arrived at, the postsynaptic potential had an amplitude of 0·4 mV (Fig. 6Diii).

Fig. 5. Comparison of depression caused by spikes with depression following more long-lasting presynaptic depolarizing potentials. A and B are from one experiment, and C is from a different one. In each recording the traces are: top, an averaged IPSP, derived from ten repetitions; second, the first three IPSPs used in deriving the average are superimposed; third, presynaptic potential; bottom, current that was injected presynaptically through a separate electrode. (A) Recordings when a pair of presynaptic spikes were separated by 100 ms. (B) The presynaptic neurone was initially at its resting potential, and the IPSPs were produced by pulses of depolarizing current injected presynaptically. The starts of the 1st and 2nd depolarizing pulses were separated by 100 ms. Although the 1st pulse lasted for 48 ms, the 2nd IPSP was no smaller than the 2nd IPSP in Fig. 5A. (C) 1st and 2nd IPSPs were separated by 450 ms. 1st IPSPs are shown in Ci, and 2nd IPSPs in Cii and Ciii. For Cii, the length of the 1st presynaptic stimulus had been 390 ms; and for Ciii, the length of the presynaptic stimulus had been 410 ms. Note that the rate of presynaptic depolarization was less in Ciii than in Cii, and that the brief hyperpolarization which followed the initial peak was also reduced.

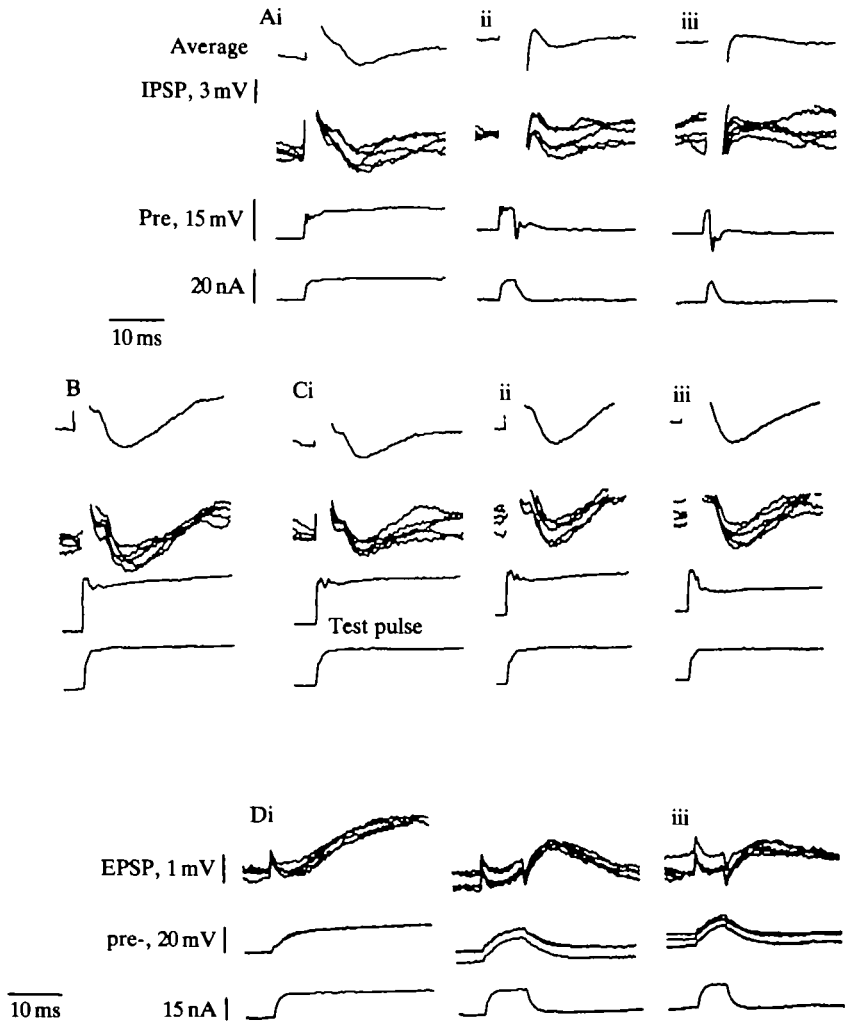

Fig. 6. IPSPs and EPSPs mediated by short depolarizing pulses injected into the presynaptic neurone. Separate electrodes injected current into and recorded potential from the presynaptic neurone. An inhibitory connection is shown in Fig. 6A–C. The traces are: top, IPSP averaged from ten sweeps; second, five single IPSPs superimposed; third, presynaptic potential; bottom, current which was injected presynaptically. Coupling artefacts on the IPSP recordings are particularly marked in these recordings. The presynaptic neurone was hyperpolarized by 7 mV from resting between depolarizing pulses, in order to produce a reasonably rapid rate of depolarization, and so to increase IPSP size. (A) Progressively shorter pulses of depolarizing current were injected into the presynaptic neurone, as described in the text. The size of a presynaptic potential was ultimately limited by the time constants of the membrane and electrode. (B) 50-ms depolarizing pulses were injected into the presynaptic neurone, and depolarized it by 12 mV from resting potential. Similar pulses were injected presynaptically in C in order to test whether the pulses in A had caused any depression, as described in the text. The start of a test pulse (Ci, ii, iii) followed the start of the corresponding first pulse (Ai, ii, iii) by 100 ms. (D) Progressively shorter stimuli were delivered to the presynaptic neurone at an excitatory connection. Traces are: top, five EPSPs superimposed; middle, presynaptic potential; bottom, current injected presynaptically. The presynaptic neurone was at its resting potential between stimuli.

DISCUSSION

Possible mechanisms for limiting the duration of a PSP are: (1) that stores of transmitter in the presynaptic neurone become depleted; (2) that postsynaptic receptors for the transmitter desensitize; (3) that the PSP is followed by a second PSP of opposite sign, curtailing it; and (4) that prolonged entry of calcium ions into the presynaptic sites is impossible, for reasons discussed below. At the inhibitory connections between L-neurones the first three mechanisms can be discounted. It is unlikely that stores of transmitter become depleted at presynaptic sites of L-neurones because if a presynaptic L-neurone remains depolarized for some time following an IPSP, the connection starts to recover its ability to transmit during this depolarization (Fig. 5). If transmitter stores did become rapidly depleted, the connection would not start to recover its ability to transmit until the end of the depolarizing pulse. Transmitter depletion has been demonstrated at a synapse between large neurones in the hatchetfish (Highstein & Bennett, 1975), when fairly intense trains of spikes are elicited presynaptically, and depletion may occur in some circumstances at synapses between giant neurones in the squid (Charlton, Smith & Zucker, 1982). However, there is no instance where depletion has been demonstrated to occur when naturally-occurring bursts of spikes invade presynaptic sites, and it has not been shown to occur at any synapse where the presynaptic neurone operates without producing trains of spikes. In some synapses, a spike is thought to cause the release of a single vesicle of transmitter from a presynaptic bouton (Korn, Mallet, Triller & Faber, 1982; Neale *et al.* 1983), and when such small stores are held ready for release at presynaptic terminals, depletion could play a role in shaping PSPs. The experiments to study the recovery from depression following long presynaptic depolarizing pulses (Fig. 5) also show that desensitization of postsynaptic receptors does not play an important role in limiting the duration of these IPSPs. If desensitization were important, transmitter would have to be released throughout the duration of a presynaptic depolarization, and the receptors would not begin to resensitize until the pulse ended. The possibility that the postsynaptic receptors would desensitize if exposed to transmitter for some time cannot be excluded, since the presynaptic neurone may not be able to release transmitter continually. A way to test for densitization would be to apply the transmitter directly to the postsynaptic membrane, as has been done at a neuromuscular junction in a frog (Katz & Thesleff, 1957), and with some neurones in *Aplysia* (Gardner & Kandel, 1977). The time courses both of desensitization and of resensitization in these two examples are considerably slower than the time courses of decrement and recovery of transmission at the inhibitory connections between L-neurones.

No evidence for a PSP which follows and curtails an IPSP has been found in the connections between L-neurones. Such a PSP would be expected to have a time course to match the recovery of a connection from depression, which occurs over a period of several hundred milliseconds (Fig. 4). A late PSP could have a reversal potential around the resting potential of the neurone, and curtail the IPSP by short-circuiting the membrane. Neither hyperpolarizing of the postsynaptic membrane (Fig. 1C) nor depolarization ever revealed a PSP which followed an IPSP. Also, no PSP was revealed by measurements of L-neurone conductance following an IPSP, and it has been shown previously (Simmons, 1982*a*) that an IPSP mediated by one

connection does not influence the amplitude of an IPSP mediated by a different connection onto the same postsynaptic L-neurone. Mixed synapses, where one type of PSP is followed by a second, both PSPs mediated by the same presynaptic neurone, have been reported for nudibranch molluscs (e.g. Wachtel & Kandel, 1967; Getting, 1981).

One mechanism which could reduce or eliminate prolonged entry of calcium ions into a presynaptic neurone is closure of the calcium channels by hyperpolarization of the membrane. This hyperpolarization could be caused by an increase in potassium conductance triggered by a depolarizing potential, or by synaptic feedback onto the L-neurone. Following a rapid depolarization, an L-neurone does produce a hyperpolarizing potential (Fig. 1A,B). However, this hyperpolarization is relatively small throughout the length of an L-neurone, and it is much less prolonged than the depression in the ability of an inhibitory connection to transmit following the production of an IPSP (Fig. 4). After a spike, changes in L-neurone conductance can persist for several tens of milliseconds, and for this reason care was taken to ensure that the two spikes were of equal amplitude, when pairs of spikes were produced in studying the recovery of the ability of a connection to transmit (Fig. 4). No difference in the duration of two spikes of such pairs was found, as would be expected if a long-lasting increase in potassium conductance was reducing transmitter release caused by the second spike. Because a good correlation between rates of pre- and postsynaptic potential change during transmission has been observed (Fig. 3B), and because changes in the shape of a presynaptic depolarization can be correlated with changes in IPSP amplitude (Fig. 5C), it is likely that any important hyperpolarizing potential that did occur at the presynaptic sites would have been recorded. Synaptic feedback onto the presynaptic neurone is unlikely because, if it occurred, a connection would not start to recover its ability to transmit until the end of a long depolarizing pulse applied to the presynaptic neurone. These inhibitory connections do start to recover their ability to transmit while the presynaptic neurone is depolarized from resting (Fig. 5).

The most likely explanation for the limited duration of the IPSPs described here is that calcium channels at the presynaptic sites inactivate after a few milliseconds, limiting the time for which transmitter can be released. At a synapse between two giant neurones in the stellate ganglion of the squid, it has been shown that the release of transmitter from the presynaptic neurone is proportional to the calcium current which enters it during a spike (Llinás, Steinberg & Walton, 1981; Llinás, Sugimori & Simon, 1982). When long depolarizing currents are injected into presynaptic terminals of the squid preparation, no reduction in calcium current is recorded (Llinás *et al.* 1981). In contrast, in a skin sensory neurone of *Aplysia*, repeated spikes cause progressive reduction in the calcium current which enters the neurone during each spike, and this reduction in calcium current is also found in isolated cell bodies when potassium and sodium currents have been blocked (Klein & Kandel, 1980). Patch clamping of single calcium channels has been performed in some snail neurones (Lux & Nagy, 1981; Lux & Brown, 1984*a*,*b*) and some of these channels inactivate (Lux & Brown, 1984*b*), but it is unknown whether these are the same calcium channels which mediate release of transmitter from these neurones. It is, therefore, possible that the calcium channels in some presynaptic sites inactivate, in a similar way to the

inactivation of voltage-gated sodium channels in the membrane of squid giant axons (Hodgkin & Huxley, 1952*a,b*), and at other presynaptic sites calcium channels do not inactivate, behaving more like potassium channels which cause the hyperpolarizing phase of the action potential in the squid giant axon (Hodgkin & Huxley, 1952*a,b*).

L-neurones possibly have at least two types of calcium channel: inactivating calcium channels, which mediate transmitter release at inhibitory connections to other L-neurones; and non-inactivating calcium channels, which mediate the release of transmitter at excitatory connections to other L-neurones (Simmons, 1982*a*) or to large, descending brain neurones (Simmons, 1981). In the leech, different output synapses of a single neurone have been found to facilitate at different rates, and the most likely explanation for this is that the neurone contains two different types of calcium channel (Muller & Nicholls, 1974). A number of non-spiking neurones make connections at which transmission can apparently be maintained for long periods without decrement (for example – vertebrate retina: Dowling & Ripps, 1973; Toyoda & Kujiraoka, 1982; arthropod central ganglia: Burrows & Siegler, 1978; Siegler, 1981; Blight & Llinás, 1980) and the presynaptic membrane of these neurones probably contains calcium channels which do not inactivate. Vertebrate photoreceptors have been shown to possess a non-inactivating calcium conductance (Bader, Bertrand & Schwartz, 1982), in contrast to horizontal cells maintained in culture, which produce a calcium current that inactivates after about 2 s (Tachibana, 1983). At some other synapses where the presynaptic neurone normally does not spike, a long pulse of depolarizing current injected presynaptically produces a PSP which has an initial peak amplitude, followed by a more sustained, lower plateau level of potential (spiny lobster stomatogastric ganglion, Graubard, 1978; dragonfly ocellar photoreceptors to L-neurones, Simmons, 1982*b*). At these synapses, the presynaptic neurones may contain an intermediate type of calcium channel, or else a mixture of calcium channels, some of which do and some of which do not inactivate.

If the hypothesis that the calcium channels inactivate at presynaptic sites of the inhibitory connections between L-neurones is correct, the operation of these connections is probably as follows. The rate at which transmitter is released depends upon the rate at which the calcium channels open. This is determined by the rate of depolarization of the presynaptic membrane. The calcium channels in the presynaptic membrane inactivate within 7 ms of opening, and the amplitude of an IPSP is limited to the potential reached in this time. The calcium channels recover from inactivation over a period of 1·5 s. The effect of inactivation is to reduce the rate at which transmitter can be released from a presynaptic site. There is probably a threshold potential for transmitter release, but it was not possible to produce suitable presynaptic potentials to measure this. Excitatory connections made by L-neurones have presynaptic threshold potentials 10–15 mV hyperpolarized from resting (Simmons, 1981, 1982*a*).

Two lines of experiment can be envisaged to test the hypothesis that calcium channels in the presynaptic membrane at the inhibitory connections inactivate. One involves the injection of calcium ions into presynaptic neurones directly. If IPSPs are short-lived because of inactivation of the channels through which calcium ions normally enter the presynaptic membrane, direct injection of calcium should cause unusually prolonged IPSPs. To perform this experiment, the calcium injection must be made precisely at a presynaptic site, and the locations of these must first be

established. This experiment also relies on the commonly accepted assumption that all neurotransmitter release is mediated by calcium entry, although some neurones, when isolated from the vertebrate retina, can release a neurotransmitter when depolarized in the absence of the entry of calcium ions (Schwartz, 1982). The second line of experiments is to measure the flow of ionic currents across the membrane of an L-neurone. The eventual aim would be to measure the entry of calcium into a presynaptic neurone, and correlate this with the production of PSPs. The following predictions about this calcium current can be made. First, its rate will be determined by the rate at which the presynaptic membrane depolarizes, and the current will reach a maximum value when the membrane depolarizes at $10\,mV\,ms^{-1}$. Second, it will inactivate within 7 ms, and recover from this over about 1·5 s. It will recover even if the presynaptic neurone is held depolarized.

A further prediction is that the presynaptic calcium channels will open relatively slowly. At the synapse between giant neurones in the squid, most of the synaptic delay (0·7 ms out of slightly less than 1 ms) is due to the time taken for the calcium channels in the presynaptic membrane to open (Llinás *et al.* 1981). The latency for transmission at output connections made by L-neurones is four times greater than that at the squid giant synapse. One possible explanation is that the connections are polysynaptic, but this is unlikely from the following considerations of structure and physiology. In ultrastructural studies, synapses between large neurones in the ocellar nerve and in the ocellus have been seen (Goodman *et al.* 1977; Goodman, Mobbs & Kirkham, 1979; Koontz & Edwards, 1984 make the same observation in a cricket). The only large axons in the ocellar nerves belong to L-neurones, as judged from sections and from cobalt back-fills from the ocellus (Goodman, 1976; Wilson, 1978*a*; Goodman *et al.* 1975). A synapse between a pair of L-neurones stained by intracellular injection of horseradish peroxidase has been found (A. H. D. Watson & P. J. Simmons, unpublished observations). In considering the following physiological observations, it should be borne in mind that physiological criteria which have been established previously (Berry & Pentreath, 1976; Getting, 1981) apply to presynaptic neurones that operate with trains of spikes. The first observation is from the experiments where presynaptic neurones were depolarized by short pulses of current (Fig. 6), and these lend strong support to the suggestion that presynaptic calcium channels open slowly. Many connections in the locust central nervous system have latencies of about 1 ms. If the connections between L-neurones were polysynaptic, involving a chain of connections which transmit with a latency of 1 ms, then presynaptic pulses 2 ms in duration should produce PSPs just as large as those produced by longer presynaptic depolarizations. Second, the smooth relationships between pre- and postsynaptic potential at excitatory connections (Simmons, 1981, 1982*a*), or between the rates of change in pre- and postsynaptic potential (Fig. 3), would probably not be found if additional neurones were interposed between the connected L-neurones. Finally, no suitable intermediary neurones have been found in over 100 recordings from pairs of interconnected neurones in the ocellar nerves of locusts. In a number of other animals, connections have been reported which are believed to be monosynaptic, but which have latencies of several milliseconds, even allowing for delay in propagation between the synaptic sites and recording sites. These include connections made by leech neurones in culture, where there is no doubt the connections are monosynaptic

(Fuchs, Henderson & Nicholls, 1982; Henderson, Kuffler, Nicholls & Zhang, 1983), synapses in the stomatogastric ganglion of the spiny lobster (Graubard, 1978), synapses in *Tritonia* (Getting, 1981) and synapses between photoreceptors and L-neurones in dragonfly ocelli (Chappell & Dowling, 1972; Dowling & Chappell, 1972; Simmons, 1982*b*). In their patch clamp study on single calcium channels in the cell body of a snail neurone, Lux & Brown (1984*b*) found that there could be a waiting time of 4–5 ms between the onset of a depolarization applied across the membrane and the opening of a calcium channel. Calcium channels in presynaptic membranes may well vary in the time they take to open, as well as in whether or not they inactivate.

One function of the spike in L-neurones is to ensure that these neurones can produce the rapid depolarizations that are required for transmission at the inhibitory connections between L-neurones. The ionic basis of this spike remains to be investigated. Similar spikes in second-order neurones of barnacle ocelli are mediated by calcium ions (Stuart & Oertel, 1978). In locust L-neurones, the channels which produce the rising phase of a spike are probably not the same channels through which calcium ions enter the presynaptic membrane to mediate transmitter release. The reasons for this suggestion are: first, there is a relatively long latency, of 4·5 ms, between the start of a spike and the start of a PSP; and second, when a pair of spikes, separated by a few 100 ms, are produced in the presynaptic neurone, the rate of hyperpolarization during the second IPSP is less than the rate during the first IPSP, although the rates of depolarization during the two spikes are the same (Fig. 4). In a crab, the flow of currents across the membrane of a non-spiking stretch receptor have been studied (Mirolli, 1983). Here, there is a fast initial transient to depolarizing potentials, which is mediated by sodium ions and is sensitive to tetrodotoxin, in segments of the neurone that are isolated from presynaptic membrane. In presynaptic regions of these neurones, fast transient depolarizing potentials may also be produced by the entry of calcium ions (Blight & Llinás, 1980; Mirolli, 1983). Fast depolarizing transients may well be necessary for transmission at other synapses, besides that described in this paper, which produce PSPs of limited duration. The reason why such PSPs have been found between at connections between L-neurones is that it is feasible to record pre- and postsynaptic potentials simultaneously. Possibly PSPs of limited duration are quite common in nervous systems, but the experiments needed to reveal them might rarely be feasible.

This work was supported by a grant from The Science and Engineering Research Council. I would like to thank Claire Rind for help and encouragement.

REFERENCES

BADER, C. R., BERTRAND, D. & SCHWARTZ, E. A. (1982). Voltage-activated and calcium-activated currents studied in solitary rod inner segments from the salamander retina. *J. Physiol., Lond.* **331**, 253–284.

BERRY, M. S. & PENTREATH, V. W. (1976). Criteria for distinguishing between monosynaptic transmission. *Brain Res.* **105**, 1–20.

BLIGHT, A. R. & LLINÁS, R. (1980). The non-impulsive stretch receptor complex of the crab: a study of depolarisation-release coupling at a tonic sensorimotor synapse. *Phil. Trans. R. Soc. B.* **290**, 219–276.

BURROWS, M. & SIEGLER, M. V. S. (1978). Graded synaptic transmission between local interneurones and motor neurones in the metathoracic ganglion of the locust. *J. Physiol., Lond.* **285**, 231–255.

CHAPPELL, R. L. & DOWLING, J. E. (1972). Neural organisation of the median ocellus of the dragonfly. I. Intracellular electrical activity. *J. gen. Physiol.* **60**, 121–147.

CHARLTON, M. P., SMITH, S. J. & ZUCKER, R. S. (1982). Role of presynaptic calcium ions and channels in synaptic facilitation and depression at the squid giant synapse. *J. Physiol., Lond.* **323**, 173–193.

DOWLING, J. E. & CHAPPELL, R. L. (1972). Neural organisation of the median ocellus of the dragonfly. II. Synaptic structure. *J. gen. Physiol.* **60**, 148–165.

DOWLING, J. E. & RIPPS, H. (1973). Effect of magnesium on horizontal cell activity in the skate retina. *Nature, Lond.* **242**, 101–103.

EIBL, E. (1978). Morphology of the sense organs in the proximal parts of the tibiae of *Gryllus campestris* and *Gryllus bimaculatus* de Geer (Insecta, Ensifera). *Zoomorphologie* **89**, 185–205.

FUCHS, P. A., HENDERSON, L. P. & NICHOLLS, J. G. (1982). Chemical transmission between individual Retzius and sensory neurones of the leech in culture. *J. Physiol., Lond.* **323**, 195–210.

GARDNER, D. & KANDEL, E. R. (1977). Physiological and kinetic properties of cholinergic receptors activated by multiaction interneurons in buccal ganglia of *Aplysia*. *J. Neurophysiol.* **40**, 333–348.

GETTING, P. A. (1981). Mechanisms of pattern generation underlying swimming in *Tritonia*. I. Neuronal network formed by monosynaptic connexions. *J. Neurophysiol.* **46**, 65–79.

GOODMAN, C. S. (1976). Anatomy of the ocellar neurones of Acridid grasshoppers. I. The large interneurones. *Cell Tissue Res.* **175**, 203–225.

GOODMAN, L. J., MOBBS, P. G. & GUY, R. G. (1977). Information processing along the course of a visual interneuron. *Experientia* **33**, 748–750.

GOODMAN, L. J., MOBBS, P. G. & KIRKHAM, J. B. (1979). The fine structure of the ocelli of *Schistocerca gregaria*. The neural organisation of the synaptic plexus. *Cell Tissue Res.* **196**, 487–510.

GOODMAN, L. J., PATTERSON, J. A. & MOBBS, P. G. (1975). The projections of ocellar neurons within the brain of the locust. *Cell Tissue Res.* **157**, 467–492.

GRAUBARD, K. (1978). Synaptic transmission without action potentials: input-output properties of a non-spiking presynaptic neuron. *J. Neurophysiol.* **41**, 1014–1025.

HENDERSON, L. P., KUFFLER, D. P., NICHOLLS, J. & ZHANG, R.-J. (1983). Structural and functional analysis of synaptic transmission between identified leech neurones in culture. *J. Physiol., Lond.* **340**, 347–358.

HIGHSTEIN, S. M. & BENNETT, M. V. L. (1975). Fatigue and recovery of transmission at the Mauthner-giant fiber synapse of the hatchetfish. *Brain Res.* **98**, 229–242.

HODGKIN, A. L. & HUXLEY, A. F. (1952*a*). Currents carried by sodium and potassium ions through the membrane of the giant axon of *Loligo*. *J. Physiol., Lond.* **116**, 449–472.

HODGKIN, A. L. & HUXLEY, A. F. (1952*b*). A quantitative description of membrane and current and its application to conduction and excitation in nerve. *J. Physiol., Lond.* **117**, 500–544.

KATZ, B. & THESLEFF, S. (1957). A study of the 'desensitization' produced by acetylcholine at the motor end-plate. *J. Physiol., Lond.* **138**, 63–80.

KLEIN, M. & KANDEL, E. R. (1980). Mechanism of calcium current modulation underlying presynaptic facilitation and behavioral sensitization in *Aplysia*. *Proc. natn. Acad. Sci. U.S.A.* **77**, 6912–6916.

KOONTZ, M. A. & EDWARDS, J. S. (1984). Central projections of first-order interneurons in two orthopteroid insects. *Cell Tissue Res.* **236**, 133–146.

KORN, H., MALLET, A., TRILLER, A. & FABER, D. S. (1982). Transmission at a central inhibitory synapse. II. Quantal description of release, with a physical correlate for binomial *n*. *J. Neurophysiol.* **48**, 679–707.

LLINÁS, R., STEINBERG, I. Z. & WALTON, K. (1981). Relationship between presynaptic calcium current and postsynaptic potential in squid giant synapse. *Biophys. J.* **33**, 323–351.

LLINÁS, R., SUGIMORI, M. & SIMON, S. M. (1982). Transmission by presynaptic spike-like depolarisation in the squid giant synapse. *Proc. natn. Acad. Sci. U.S.A.* **79**, 2415–2419.

LUX, H. D. & BROWN, A. M. (1984*a*). Patch and whole cell calcium currents recorded simultaneously in snail neurons. *J. gen. Physiol.* **83**, 727–750.

LUX, H. D. & BROWN, A. M. (1984*b*). Activation and inactivation of single calcium channels in snail neurons. *J. gen. Physiol.* **83**, 751–769.

LUX, H. D. & NAGY, K. (1981). Single channel Ca^{2+} currents in *Helix pomatia* neurons. *Pflügers Arch. ges. Physiol.* **391**, 252–254.

MIROLLI, M. (1983). Inward and outward currents in isolated dendrites of crustacean coxal receptors. *Cell. molec. Neurobiol.* **3**, 355–370.

MULLER, K. J. & NICHOLLS, J. G. (1974). Different properties of synapses between a single sensory neurone and two different motor cells in the leech C.N.S. *J. Physiol., Lond.* **238**, 357–369.

NEALE, E. A., NELSON, P. G., MACDONALD, R. L., CHRISTIAN, C. N. & BOWERS, L. M. (1983). Synaptic interactions between mammalian central neurons in cell culture. III. Morphological correlates of quantal synaptic transmission. *J. Neurophysiol.* **49**, 1459–1468.

NICHOLLS, J. & WALLACE, B. G. (1978). Modulation of transmission at an inhibitory synapse in the central nervous system of the leech. *J. Physiol., Lond.* **282**, 157–170.

PATTERSON, J. A. & GOODMAN, L. J. (1974). Intracellular recordings from receptor cells and second-order cells in the ocelli of the desert locust, *Schistocerca gregaria*. *J. comp. Physiol.* **95**, 237–250.

SCHWARTZ, E. A. (1982). Calcium-independent release of GABA from isolated horizontal cells of the toad retina. *J. Physiol., Lond.* **323**, 211–227.

J. exp. Biol. 117, 133–154 (1985)
Printed in Great Britain © *The Company of Biologists Limited 1985*

VENTILATION, CIRCULATION AND THEIR INTERACTIONS IN THE LAND CRAB, *CARDISOMA GUANHUMI*

BY WARREN BURGGREN*, ALAN PINDER*, BRIAN McMAHON†, MICHELE WHEATLY†‡ AND MICHAEL DOYLE*

** Department of Zoology, University of Massachusetts, Amherst, MA 01003–0027, U.S.A.* and *† Department of Biology, University of Calgary, Calgary, Alberta T2V 1N4, Canada*

Accepted 10 January 1985

SUMMARY

Physiological variables for ventilation (scaphognathite frequency, branchial chamber pressure and branchial air flow) and for circulation (heart rate, intracardiac and pericardial haemolymph pressure) were measured in the land crab *Cardisoma guanhumi* (Latreille). Crabs were studied both in air alone and in air with access to a shallow layer of fresh, brackish or sea water.

During complete air exposure, forward scaphognathite beating predominated and reversed scaphognathite beating was very infrequent. Periods of apnoea were rare. When crabs were able to immerse the Milne-Edwards openings to the branchial chambers in water, scaphognathite reversal occurred much more frequently, and most air flow through the branchial chambers was generated by this mode of ventilation. Changes in water salinity had no effect on respiratory patterns. The cyclic variation between forward and reversed scaphognathite beating appears to serve not only to ventilate the branchial chambers with air, but also to flush water through the branchial chambers for non-respiratory purposes such as ion, water and acid-base regulation.

Haemolymph pressures were comparatively low (14 mmHg systolic, 6 mmHg diastolic). During diastole a pressure gradient of approximately 0·6 mmHg existed between the pericardial space and the heart lumen. Pauses in heart beat were never observed. Circulatory events were closely co-ordinated with adjustments in ventilation. Reversed scaphognathite beating produced a transient increase in systolic and diastolic haemolymph pressure due to the rise in branchial air pressure acting directly upon the large, haemolymph-filled spaces lining the branchial chambers. A transient bradycardia accompanied this brief rise in central haemolymph pressures. Possible mechanisms for the regulation of haemolymph pressure are discussed.

INTRODUCTION

The study of intertidal and terrestrial decapod Crustacea has burgeoned in recent years, partly because of the search for new insights into the evolution of air breathing,

‡ Present address: Department of Zoology, University of Florida, Gainesville, FL 32611, U.S.A.
Key words: Crab, ventilation, circulation.

and partly because of a specific interest in the adaptations of the land decapods *per se*. Regardless of habitat or degree of terrestrial adaptation, decapods that ventilate with air (i.e. use the paired scaphognathites to generate a flow of air through the branchial chambers) must still keep branchial respiratory structures moistened. Not only are hydrated respiratory membranes a requisite for adequate gas exchange, but in many aquatic and terrestrial decapods alike the gills are also of cardinal importance in hydromineral exchange between haemolymph and water passing through or residing within the branchial chambers (see Mantel & Farmer, 1983).

Water availability is an important limiting factor for terrestrial decapods, and numerous behavioural and morphological adaptations for water acquisition and retention are apparent. For example, many terrestrial brachyurans inhabit burrows, the lower chambers of which lie at or below the water table (Herreid & Gifford, 1963; Cameron, 1975, 1981). Thus, even though the crab may venture short distances from the burrow mouth, significant amounts of time are still spent in the presence of water at the bottom of the burrow. The ability to take a reservoir of water into an arid terrestrial environment is particularly well developed in some terrestrial hermit crabs, where a considerable volume of water may be retained in the inhabited mollusc shell (see DeWilde, 1973; McMahon & Burggren, 1979; Wheatly, Burggren & McMahon, 1984).

A number of studies have concentrated on the respiration and water relations of the land crab *Cardisoma*. Comprehensive accounts of the respiratory morphology of this genus have been provided by von Raben (1934), Gray (1957), Diaz & Rodriguez (1977), Cameron (1981) and Wood & Randall (1981). One noteworthy characteristic of *Cardisoma* is that the gills are quite small, occupying less than one-tenth of the volume of the branchial chamber. Much additional respiratory surface area is provided by extensive folding of the highly vascularized epithelial sheet lining the extensive branchial cavity.

Cardisoma is of considerable interest with respect to acquisition and retention of gill water. This genus not only makes frequent trips to burrows containing at least some water (Herreid & Gifford, 1963; Cameron, 1975, 1981), but also has been reported to retain significant quantities of water in the branchial chamber when active in air (Wood & Randall, 1981). When *Cardisoma* is completely air-exposed, it is not clear whether this branchial water reserve functions primarily as an O_2 source or a CO_2 sink (Wood & Randall, 1981), or whether its major respiratory function is to moisten the gills. Wood & Randall (1981) cut an observation port in the dorsal wall of the branchial chamber of completely air-exposed *Cardisoma carnifex* and observed that the mastigobranchs of the first, second and third maxilliped were in nearly constant motion, flicking water contained in the lower regions of the branchial chamber up over the gills. While this water was probably well aerated by this motion, forward scaphognathite beating simultaneously drew large volumes of air into the Milne-Edwards openings and expelled it out of the exhalant canals. Long periods of apnoea occurred and reversed scaphognathite beating was never observed. Similar observations of forward scaphognathite beating generating a large air flow, with very infrequent reversed beating, have also been previously reported for completely air-exposed *Cardisoma guanhumi* (Cameron, 1975; Herreid, O'Mahoney & Shah, 1979*b*; Herreid, Lee & Shah, 1979*a*).

Terrestrial migrations involving large numbers of *Cardisoma guanhumi* occur during seasonal transitions. Moreover, these crabs are frequently observed in areas with relatively dry surface soil. Thus, physiological studies of *Cardisoma* when completely air exposed, such as those mentioned above are, of course, of considerable interest and value. Unfortunately, such observations may have biased experimentation away from crabs in the natural amphibious setting. *Cardisoma guanhumi* spends considerable amounts of time in wet lowlands, and burrows excavated even in apparently dry areas often contain ground water at their deepest levels. With the progression of the dry season *Cardisoma* is rarely seen on open ground, and may even seal itself in its burrow (Herreid & Gifford, 1963). *Cardisoma* thus spends considerable time in proximity to water, but unfortunately little information exists on the respiratory or cardiovascular physiology of this genus in this normal amphibious state.

In this study on *Cardisoma guanhumi* we test the hypothesis that ventilatory patterns and performance are influenced by the available respiratory media. Additionally, we assess the extent of cardio-respiratory interactions under a variety of experimental conditions and measure basic cardiac variables to determine if the circulatory haemodynamics of land crabs differ from those of aquatic decapods.

MATERIALS AND METHODS

Experiments were performed on a total of 45 *Cardisoma guanhumi* (Latreille) (mean weight 127 ± 45 g, $\bar{x} \pm 1$ S.D.) captured on the Atlantic coast of Panama, and transported to and maintained at the Naos Marine Laboratory, Smithsonian Tropical Research Institute, on the Pacific coast of Panama. Crabs were maintained in shaded outdoor pens and experienced the normal temperature and humidity regime for the season (night temperature 25–26 °C, night humidity 75–95 %; day temperature 33–35 °C, day humidity 75–95 %). During this pre-experimental period all crabs had free access to 50 % sea water (SW) and were fed vegetable matter daily.

The experimental chamber consisted of an opaque box approximately 40 × 20 × 15 cm. The chamber, which was thermostatted to 30± 3 °C, was covered with a translucent lid to screen movements of the investigators. In some experiments, crabs were placed unrestrained in this box. In other experiments, crabs were partially restrained by using elastic bands to secure their legs and chelae to a 15 × 15 × 1 cm ceramic plate. Although restrained, such crabs could raise the carapace slightly above the plate and rotate the carapace dorso-ventrally. The restrained animal on the plate was then placed in the centre of the chamber described above. When a 2-cm water layer was placed in the chamber, voluntary rotational movements of the carapace allowed the crab either to immerse the openings to the branchial chambers at the bases of the legs, or raise these openings slightly above the water level (see below).

Ventilatory variables

Standard cannulation and measurement techniques for ventilatory pressures and impedance were employed (see Taylor, Butler & Sherlock, 1973; McDonald, McMahon & Wood, 1977). All pressure cannulae were 40-cm lengths of seawater-filled PE 160 tubing attached to Narco P–1000B pressure transducers, whose signals were displayed on a Narco MKIV rectilinear chart recorder. Each transducer was

calibrated frequently and zeroed against the level of the catheter tip. The pressure cannulae were introduced through 10-mm square pieces of rubber dam glued to the carapace over 1-mm holes drilled through the dorsal surface of each branchial chamber. Impedance electrodes (for measurement of scaphognathite frequency) were constructed from 0·1 mm diameter insulated copper wire. The impedance leads were introduced through 0.5-mm holes drilled in the carapace lateral to the positions of the scaphognathite and held in place by gluing a 1-cm square of rubber dam over the hole in the carapace. In some additional preparations a 5-mm diameter hole was drilled in the carapace at the top of each branchial chamber. The edges of the hole were cauterized, and a removable rubber plug was fitted into the hole. Removal of the plugs eliminated pressure fluctuations in one or both branchial chambers.

With the varying combinations of implanted branchial impedance electrodes and pressure cannulae, ventilatory variables could be assessed for forward and reversed pumping in left and right branchial chamber. Symbols in the text representing variables measured during forward scaphognathite pumping have been assigned the superscript 'f', while the superscript 'r' has been used to designate variables measured during reversed scaphognathite beating. The variables measured, and the symbols used to represent them are given below.

F_R^f, scaphognathite frequency, forward pumping (beats min^{-1}),
P_{Br}^f, branchial pressure, forward pumping (mmHg),
P_P^f, branchial pulse pressure, forward pumping (mmHg),
F^r, frequency of reversal episodes (episodes min^{-1}),
F_R^r, scaphognathite frequency, reversed pumping (beats min^{-1}),
P_{Br}^r, branchial pressure, reversed pumping (mmHg),
P_P^r, branchial pulse pressure, reversed pumping (mmHg),
t_A, apnoea length (s).

Each of these variables could be measured independently for both left and right scaphognathite.

In five crabs ventilatory flow was measured by fitting a face mask, made from the base and neck of a rubber balloon, over the anterior portion of the carapace, as modified from McMahon & Wilkens (1977). The edges of the balloon were glued to the carapace with cyanoacrylate glue, ensuring a gas-tight seal. Inserted into the open end of the neck of the balloon was a 10-mm diameter T-connector. One open arm of the T-connector was directed ventrally to the bottom of the experimental chamber. The chamber contained a 2-cm layer of brackish water (50 % sea water), so that the ventral opening of the connector always rested below the water surface. This ventral arm of the connector provided a route by which any water pumped up into the face mask during forward pumping could be drained back to the chamber. However, since its opening was below the water surface, it could not serve as a site of air entry into the face mask. The dorsally directed arm of the connector, which provided a low resistance inlet for fresh air to flow into the face mask, also contained a hot-wire anemometer (HWA 104, Thermonetics Co., San Diego), the output of which was directed to one channel of the chart recording system. A catheter inserted into the connector between the hot wire anemometer and the face mask was attached to a suction pump drawing gas at a constant rate of 45 ml min^{-1}. When the crab was in a ventilatory pause, the signal from the anemometer indicated a constant gas flow

through the mask of 45 ml min^{-1}. When the crab pumped gas forward out of the exhalant canals into the mask, the flow of fresh air past the anemometer sensor and into the face mask generated by the suction pump was reduced by the exact amount of gas added to the face mask from the branchial chambers by forward scaphognathite pumping. During reversed scaphognathite pumping, gas from the face mask was being removed to ventilate the branchial chambers, as well as being removed by the suction catheter. This combined effect resulted in an increase in flow of fresh air past the hot-wire anemometer which was exactly proportional to the ventilatory volume during reversed beating. The frequency response of this system was extremely rapid, and allowed resolution on the recorder of individual movements of the scaphognathites. After each experiment the anemometer sensor was removed from the face mask and calibrated by directing known flows of air past it.

Circulatory variables

Typically, three or four 1-mm diameter holes were drilled through the carapace in the vicinity of the heart. Copper electrodes glued into two of these holes were used for measurement of heart beat by an impedance technique. The other holes were sealed with squares of rubber dam. A 40-cm long PE 160 catheter fitted with a PE 60 tip was used for recording intracardiac haemolymph pressures. The tip of this catheter was introduced through the dam at the midline of the carapace and advanced ventrally 3 mm into the lumen of the heart. This catheter was filled with filtered sea water and attached to a P–1000B pressure transducer and the rectilinear recorder described above. The pressure signal from the transducer was also sent to a Narco Biotachometer which computed and displayed instantaneous heart rate on the recorder. A similar catheter arrangement was used for measurement of pericardial pressure immediately outside of the heart, with the catheter tip advanced ventrally 2 mm through the carapace at a position 1 cm off the crab's midline. Cardiac and pericardial cannulation caused minimal disturbance to the crab (see Results).

Experimental protocols

In some preliminary experiments, crabs fitted only with impedance electrodes were allowed overnight recovery and acclimation to the experimental chamber before measurements were begun. In the remainder of the experiments, restrained crabs were allowed at least 1 h to recover from surgery and handling during restraint before measurements were begun. Animals in the latter experiments were clearly not 'undisturbed', but had stopped struggling against restraint during this period. If released from restraint, these crabs were immediately fully active and aggressive, indicating that they were not fatigued or otherwise severely disturbed by the experimental conditions.

Instrumented crabs were examined with an experimental protocol involving several experimental conditions. Cardio-ventilatory variables were measured during a 1-h period when air was the only available respiratory medium, and for additional 1-h periods when a 2-cm aerated layer of 100 % sea water, 50 % sea water or fresh water was placed in the bottom of the chamber. Crabs were never denied access to air, since we rarely observed voluntary total submergence in water in their natural habitat on the Atlantic coast of Panama.

Statistical analyses

All data were analysed for mean values ±1 S.E. Analysis of variance (ANOVA) was used to assess treatment effects. Where significant effects were found, Student's *t*-test for independent means (unless otherwise indicated) was used to determine the significance level of differences between particular means. A significance level of 0·05 was used in all statistical procedures.

RESULTS

The respiratory surfaces of *Cardisoma guanhumi* are ventilated by forward or reversed pumping by the scaphognathites located at the anterior margin of each branchial chamber. Whether water or air is the respiratory medium used by *Cardisoma* when it stands in shallow water depends largely upon the positioning of the Milne-Edwards openings and exhalant channels. During forward pumping in shallow (1–4 cm) water, an undisturbed crab adjusts its posture so that its horizontal plane is roughly parallel to the water surface. This usually places the openings of both the Milne-Edwards and exhalant channels at the air–water interface (Fig. 1A). Under these conditions much air in addition to water is drawn into the Milne-Edwards openings, and the gas exiting the exhalant canals anteriorly creates a constant stream of air bubbles at the water surface.

At the onset of a period of reversed scaphognathite beating in an undisturbed crab, a marked postural change occurs such that the plane of the carapace pivots upwards anteriorly (Fig. 1B). The crab lowers the limb bases and Milne-Edwards openings, completely submerging them in the water, and raises the openings of the exhalant channels well above the water surface. Air is drawn into the exhalant channels during reversed breathing, and a large stream of gas bubbles is forced out from the ventral region of the branchial chambers *via* the Milne-Edwards openings and rises to the water surface.

Effects of acclimation, restraint and cardiac cannulation

Since a variety of different techniques was used in this study, it was important first to define carefully the specific limitations of each technique, before discussing quantitative details of cardio-ventilatory patterns or experimental treatment effects.

Restraint

Ventilatory variables for both left and right scaphognathite as well as heart rate, all measured through impedance techniques, were measured 1–4 h after electrode attachment in both unrestrained and restrained crabs. All crabs had access either to air alone or to air and 50% sea water as indicated above. In air alone, none of the ventilatory parameters measured for either right or left scaphognathite nor heart rate were significantly altered by restraint ($P > 0{\cdot}10$).

When 2 cm of 50 % SW was placed in the chamber, heart rate and most parameters for forward pumping for either right or left scaphognathite were also not significantly different between restrained and unrestrained crabs. Only the length of the apnoeic

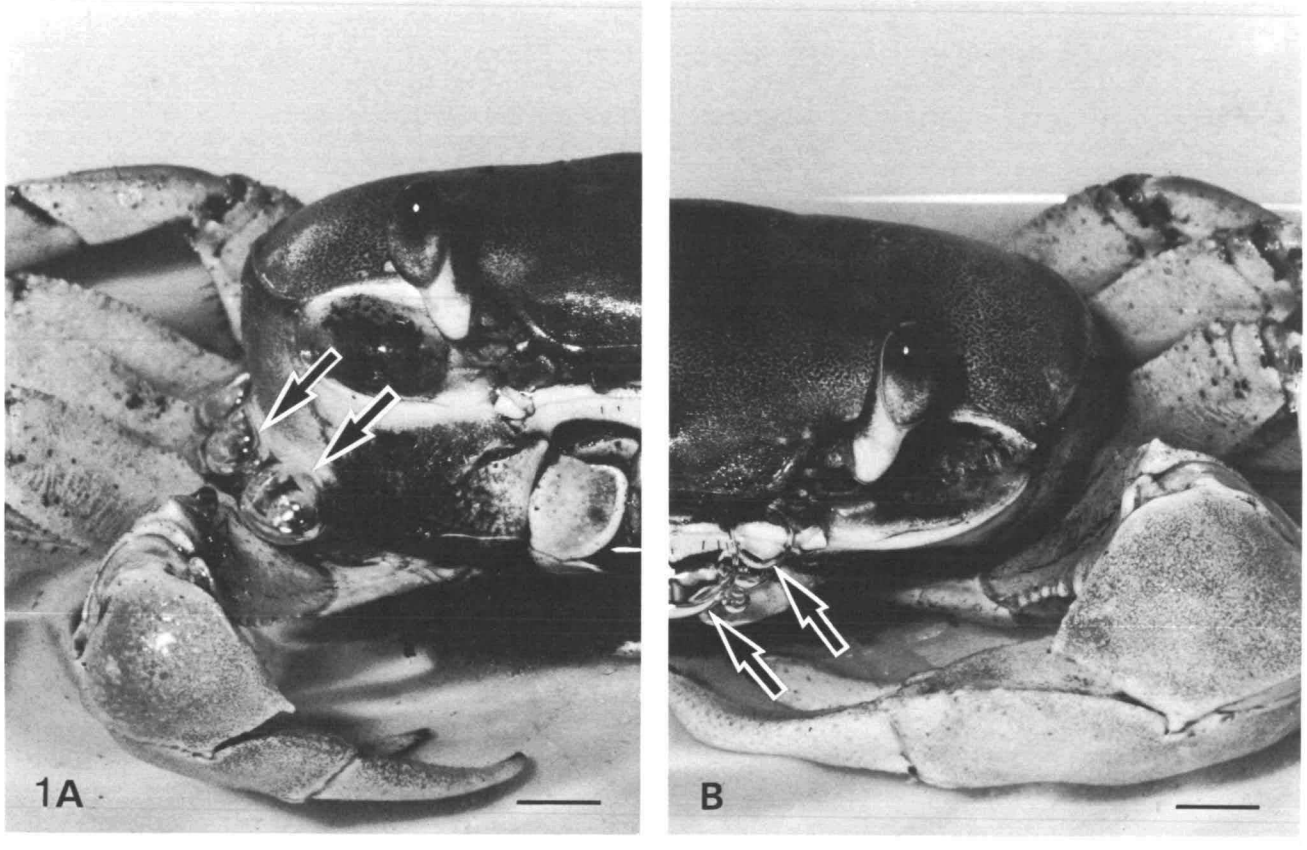

Fig. 1. Postural adjustments during branchial chamber ventilation in a land crab, *Cardisoma guanhumi*, resting in 3 cm of 50% SW. A and B were photographed from identical camera angles. (A) The posture during forward scaphognathite beating, in which the exhalant channels are held just at or below the water level. Note the bubbles of air (arrows) gathering around the exhalant channels. (B) The posture during reversed scaphognathite beating, in which the exhalant canals are elevated well above the surface of the water to allow air entry. Note the bubbles of air gathering around the Milne-Edwards openings (arrows). Scale bars, 1 cm. See Results for further details.

period of the right scaphognathite (but not the left) was significantly affected ($P<0{\cdot}05$), decreasing from $0{\cdot}5\pm0{\cdot}5$ min to $0{\cdot}1\pm0{\cdot}1$ min, but the effect was nonetheless not large enough to change significantly the beat frequency of the right scaphognathite. The frequency of reversal periods by both scaphognathites (3·3–4·9 periods min^{-1}) was not significantly influenced by restraint in crabs in 50 % SW, but the frequency of pumping within each period of reversed beating was significantly elevated ($P>0{\cdot}05$) in restrained crabs (23·1 beats min^{-1}) compared with unrestrained crabs (6·8 beats min^{-1}).

Patterns in left vs *right scaphognathite* (*i.e. 'handedness'*)

In some decapod Crustacea ventilatory patterns are characterized by very close coupling of left and right scaphognathite events, while in others the scaphognathites may drift in and out of phase, or even show unilateral pausing (Taylor, 1982; McMahon & Wilkens, 1983). In the present experiments, if cardiac and pericardial pressures were being measured simultaneously, the recorder channels remaining were sufficient only to monitor ventilatory events on one side of the crab. Since it was important to know whether the pattern of a single scaphognathite recorded under these circumstances was representative of both scaphognathites, a series of crabs was prepared in which both left and right scaphognathite patterns could be recorded.

Although there was very occasionally phase drifting or unilateral apnoea in *Cardisoma*, left and right scaphognathites were usually absolutely coupled under all experimental situations (i.e. unrestrained or restrained, in air or with access to 50 % sea water, before or after cardiac cannulation). In fact, the differences in mean values of all ventilatory parameters for right and left scaphognathites of each crab were not significantly different from zero ($P>0{\cdot}10$, Student's t-test for dependent means). Thereafter patterns of scaphognathite beating recorded from one side were assumed to be representative of both sides.

Cardiac cannulation

Ventilatory parameters and heart rate of restrained crabs with access to 50 % SW were measured immediately before and 30 min after cannulation of the heart. Cardiac cannulation caused no significant ($P>0{\cdot}10$) change in F^{f}_{R}, P^{f}_{Br}, P^{f}_{P}, F^{r}, P^{R}_{Br}, P^{R}_{P} or t_A of the right scaphognathite. Similarly, left scaphognathite pumping was not significantly affected by cardiac cannulation, with the exception of a significant but small decrease in F^{r} and rise in t_A. Importantly, heart rate was not significantly ($P>0{\cdot}10$) altered by cardiac cannulation.

In general, then, *Cardisoma guanhumi* tolerated restraint, instrument implantation and experimental manipulation very well. Since restraint or cannulation produced only small quantitative, rather than qualitative, changes in only a few of the respiratory and cardiac variables (and since unrestrained *Cardisoma* showed amazing ingenuity and dexterity in destroying implanted leads), the data which follow were recorded solely from restrained crabs unless otherwise indicated.

Ventilatory patterns and influence of respiratory medium

When ventilating with air alone, predominantly forward directed scaphognathite pumping generated subambient pressures in the branchial chamber. This produced

a ventilatory flow which was primarily forward through the branchial chamber and out of the exhalant canals (Fig. 2A). A quantitative analysis of ventilation (Fig. 3) reveals that scaphognathite frequencies during forward ventilation were about

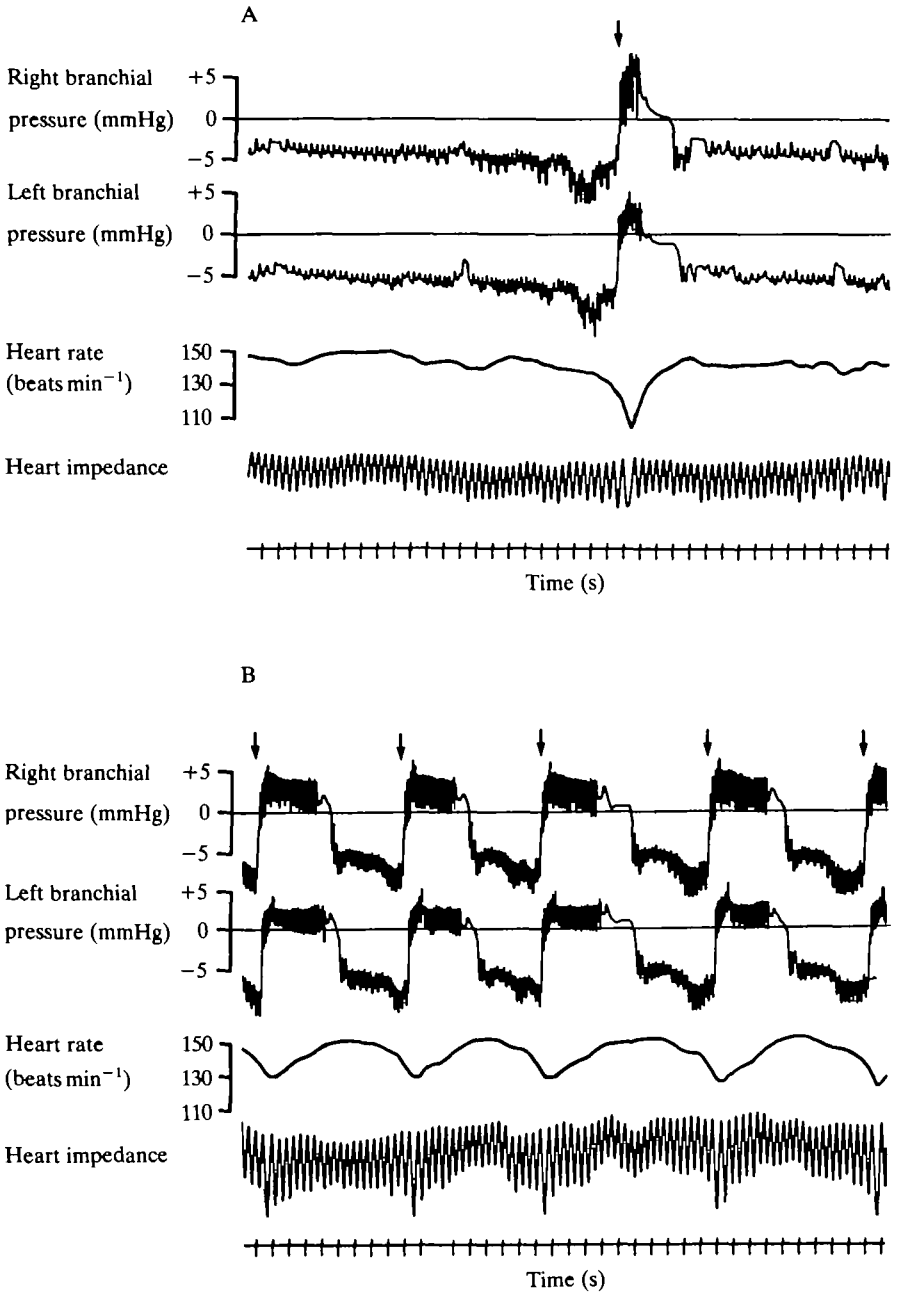

Fig. 2 Representative records of branchial pressures and heart impedance and rate in a restrained, 151 g *Cardisoma guanhumi*. (A) Patterns measured during total air exposure, which resulted in primarily forward scaphognathite beating. (B) Ventilatory patterns with frequent periods of reversals (arrows) stimulated by placement of the crab in 2 cm of 50 % SW.

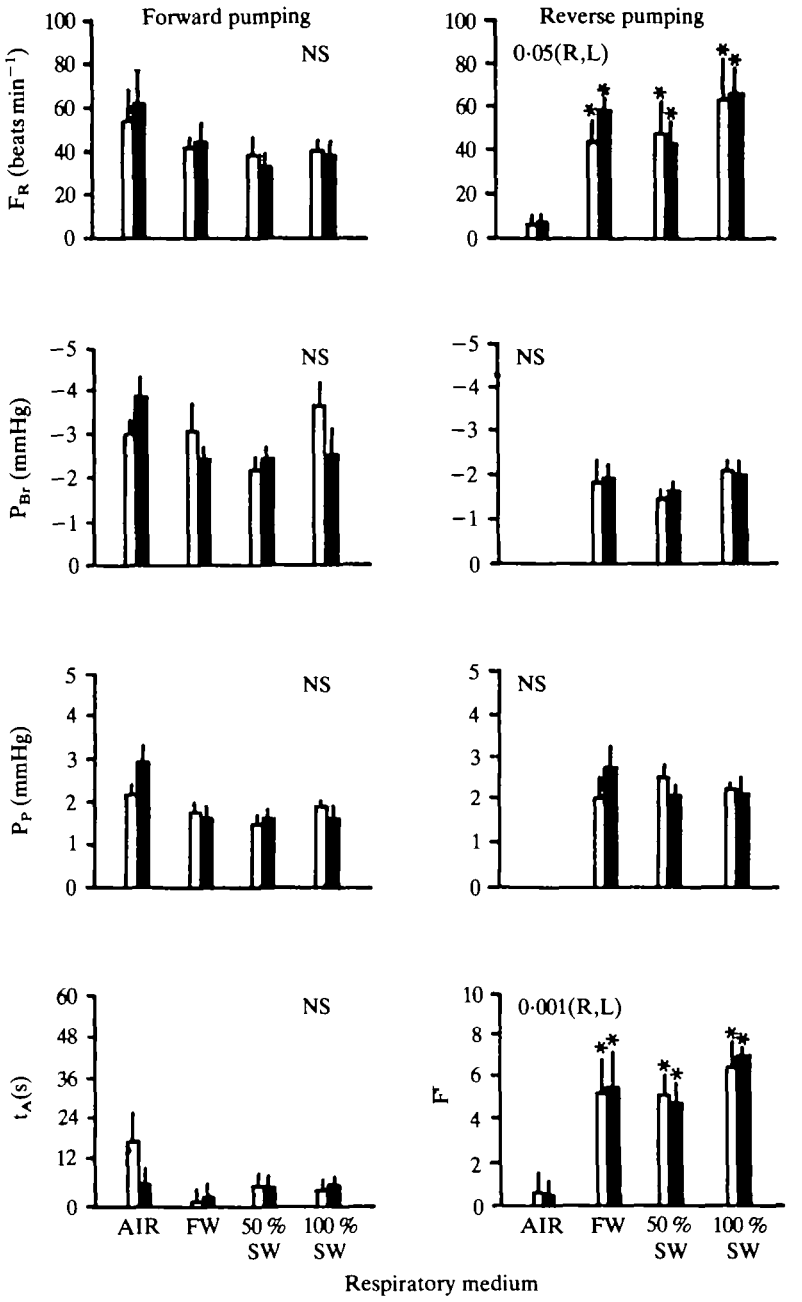

Fig. 3. Effect of ventilatory medium on scaphognathite frequency (F_R), branchial (P_{Br}) and branchial pulse (P_P) pressures, length of apnoea (t_A) and frequency of reversal episodes (F^r) during forward and reversed beating in *Cardisoma guanhumi*. Mean values ± 1 S.E. are presented for both left (L, white bars) and right (R, black bars) scaphognathites. Number of crabs analysed for each ventilatory medium are AIR = 8, FW (fresh water) = 7, 50 % SW = 8, and 100 % SW = 8. Results of analysis of variance for effect of ventilatory medium are shown in the upper region of each panel. Where significant treatment effects were indicated, *t*-tests were performed to reveal significant differences between ventilatory media. Thus, asterisks indicate significant differences from values measured with air as the ventilatory medium. *, $P<0·05$; **, $P<0·01$. See text for additional details. NS, not significant.

50–60 beats min^{-1}. Apnoeic episodes were infrequent and irregular (1 episode every 3–5 min) and lasted only 5–20 s. Intrabranchial pressures during forward beating were 3–4 mmHg subambient, with a pulse pressure of 2–3 mmHg. When ventilating with air, less than one reversal episode occurred per minute.

When *Cardisoma* was provided access to water and could thus partially submerge one or both of the Milne-Edwards openings, several important aspects of the ventilatory patterns were affected. Whereas F_R^F, P_{Br}^f, P_P^F and t_A remained unchanged, the frequency with which reversals occurred increased 10–15 times (Fig. 3). Not only did reversals occur more often, but the frequency of scaphognathite beating during these reversals was elevated several times compared with strictly aerial ventilation. Apnoeic episodes of significant length still occurred quite infrequently and irregularly when access to water was provided, although in some crabs a ventilatory pause of a few seconds occasionally followed a period of reversed scaphognathite beating.

Values for each ventilatory parameter measured when the crab had access to fresh water, 50 % sea water or 100 % sea water were statistically identical. Therefore, these changes in respiratory pattern were apparently related to use of water *versus* air as a respiratory medium, rather than to water quality *per se*.

Fig. 4 shows a representative recording of branchial pressures and gas flow at the exhalant canals during forward and reversed beating in a *Cardisoma* with access to both air and 50 % sea water. Mean values ($N = 5$ crabs) of right scaphognathite

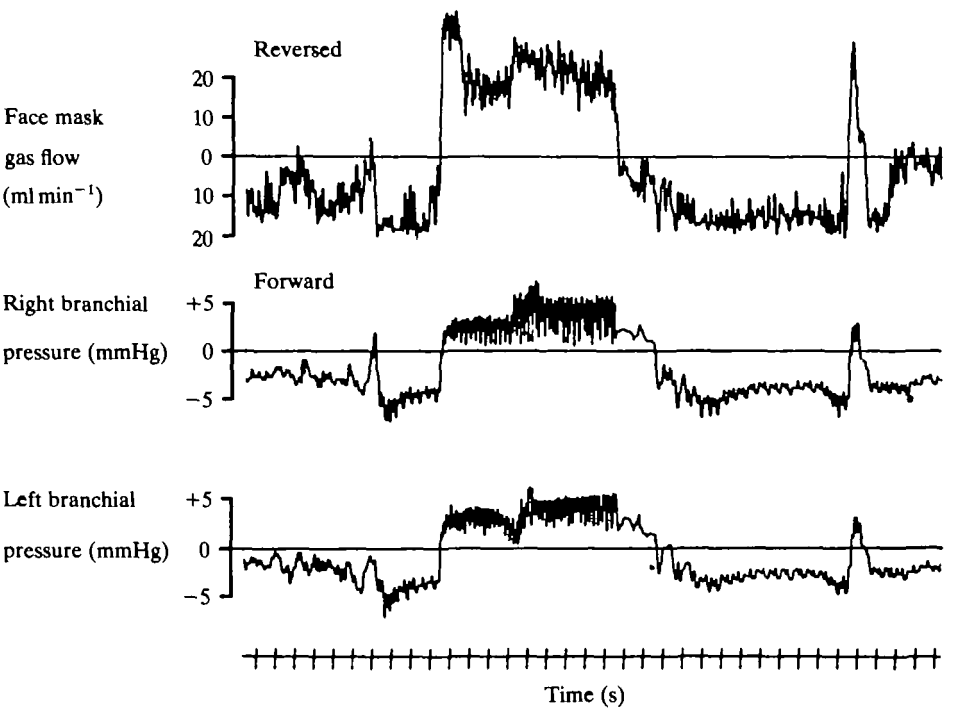

Fig. 4. Representative records of branchial pressures and of gas flow through the face mask of an 80 g *Cardisoma guanhumi* resting in approximately 2 cm of 50 % SW. Periods of reversed scaphognathite beating are characterized by positive branchial pressures and reversed gas flow through the face mask.

frequency, total gas flow into and out of the face mask during forward and reverse flow, respectively, and stroke volume of the scaphognathite pair (assuming equal frequency of left and right scaphognathites, see above) are presented in Fig. 5. Both stroke volume and gas flow were significantly greater during reversed beating than forward beating. From mean values for restrained crabs without face masks (Fig. 3),

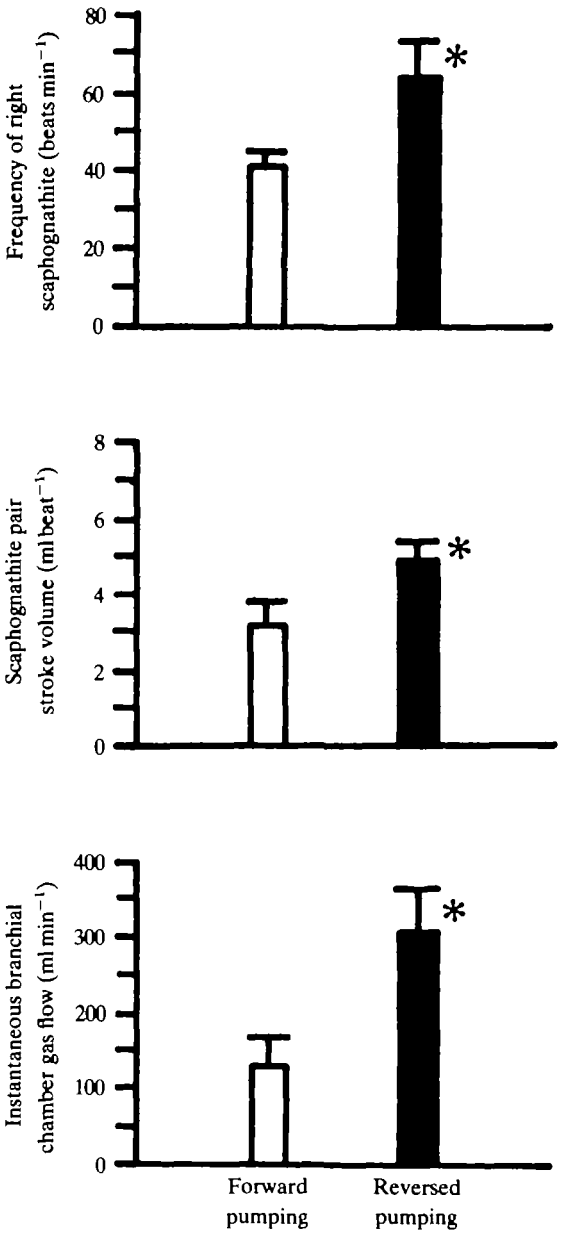

Fig. 5. Scaphognathite frequencies, stroke volumes and gas flows measured during forward and reversed pumping in five *Cardisoma guanhumi*. Mean values ± S.E. are given. Asterisks next to data for reversed pumping indicate significant difference ($P<0{\cdot}05$) from forward pumping.

it can be calculated that, during constant ventilation in *Cardisoma* with access to both 50% SW and air, forward ventilation occupies 36 s of every minute compared with 24 s for reversed ventilation. Given the differences in flow rates for the two directions of pumping (Fig. 5), this indicates that for every minute of scaphognathite ventilation approximately 125 ml kg^{-1} of gas are pumped out posteriorly from the Milne Edwards openings and 70 ml kg^{-1} of gas are pumped out anteriorly through the exhalant channels. This corresponds to 34% of total gas flow being generated by forward pumping compared with 66% by reversed pumping.

Measurements of forward and reversed gas flow were not made in crabs with access to air only, and we do not know if scaphognathite stroke volume changes under this condition. However, assuming an identical stroke flow to that measured when access to 50% SW was provided, and using the mean ventilatory rates and ratios of totally air-exposed crabs provided in Fig. 3, then estimated forward and reverse gas flow changed dramatically to approximately 98% and 2% of total flow, respectively.

Circulatory patterns and cardio-respiratory interaction

Circulatory variables, including haemolymph pressure, were measured in a total of 24 *Cardisoma guanhumi* exposed to air but with access to 50% SW. Mean values are

Table 1. *Circulatory variables measured in the land crab* Cardisoma guanhumi

	Mean ± 1 S.E.	Number of crabs measured
Heart rate (beats min^{-1})	134 ± 7	18
Intracardiac systolic pressure (mmHg)	14·1 ± 0·7	24
Intracardiac diastolic pressure (mmHg)	5·5 ± 0·7	24
Pericardial systolic pressure (mmHg)	8·4 ± 2·9	5
Pericardial diastolic pressure (mmHg)	6·1 ± 2·5	5

Crabs were restrained and had access to a 2-cm layer of 50% SW.

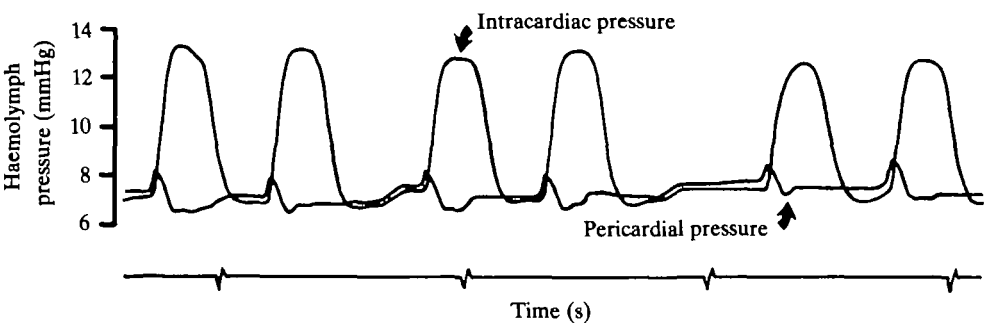

Fig. 6. Haemolymph pressure measured in the pericardial space and in the heart of a 159 g *Cardisoma guanhumi*.

given in Table 1, while Fig. 6 shows representative simultaneous recordings of intracardiac and pericardial pressures.

As is typical for the few decapod circulations investigated to date, intracardiac systolic pressure was generally below 20 mmHg and diastolic pressure several mmHg above ambient pressure. A pressure gradient from pericardial space to heart lumen of about 0·4–1·0 mmHg existed throughout diastole, and provided the driving pressure for cardiac filling. At the onset of systole, haemolymph pressure in the pericardium began to rise concomitantly with intracardiac pressure, suggesting open communication of the pericardium with the interior of the heart. After increasing by 1–3 mmHg, pericardial pressures fell back to diastolic levels while intracardiac pressures continued to rise, indicating effective closure of the ostial valves at this time.

Although mean circulatory variables were quite constant in individual crabs over an extended time period, both locomotor activity and changes in ventilatory patterns induced transient changes. The most consistent changes in circulatory parameters accompanied the transient changes from forward to reversed beating (Figs 7,8). Both systolic and diastolic intracardiac pressure began to increase within 0·5–2 s of the onset of a reversal, with both values having risen significantly (ANOVA, $P < 0{\cdot}001$) by approximately 2–3 mmHg by the end of the reversal period. A significant decrease in heart rate of about 10 beats min^{-1} occurred concomitantly with reversal of scaphognathite beat and rise in intracardiac haemolymph pressure. Immediately after the end of the reversal episode, both heart rate and intracardiac haemolymph pressure returned

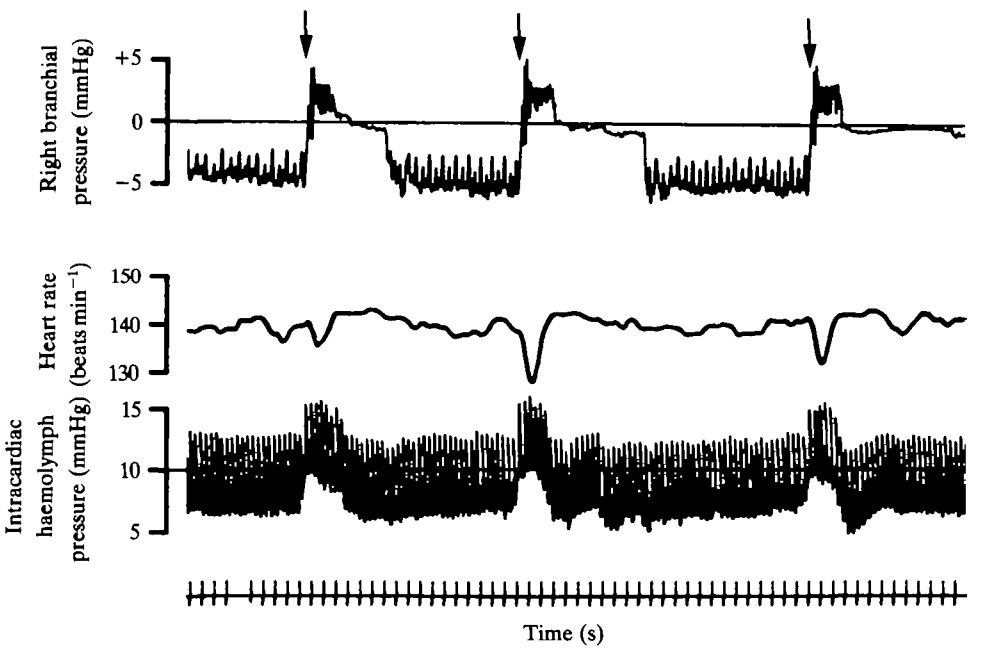

Fig. 7. Representative records of branchial gas pressure, intracardiac haemolymph pressure and heart rate during periods of both forward and reversed scaphognathite beat in a 142 g *Cardisoma guanhumi* with access to 50 % SW. Periods of reversed scaphognathite beating occur when branchial pressure swings to positive values (arrows).

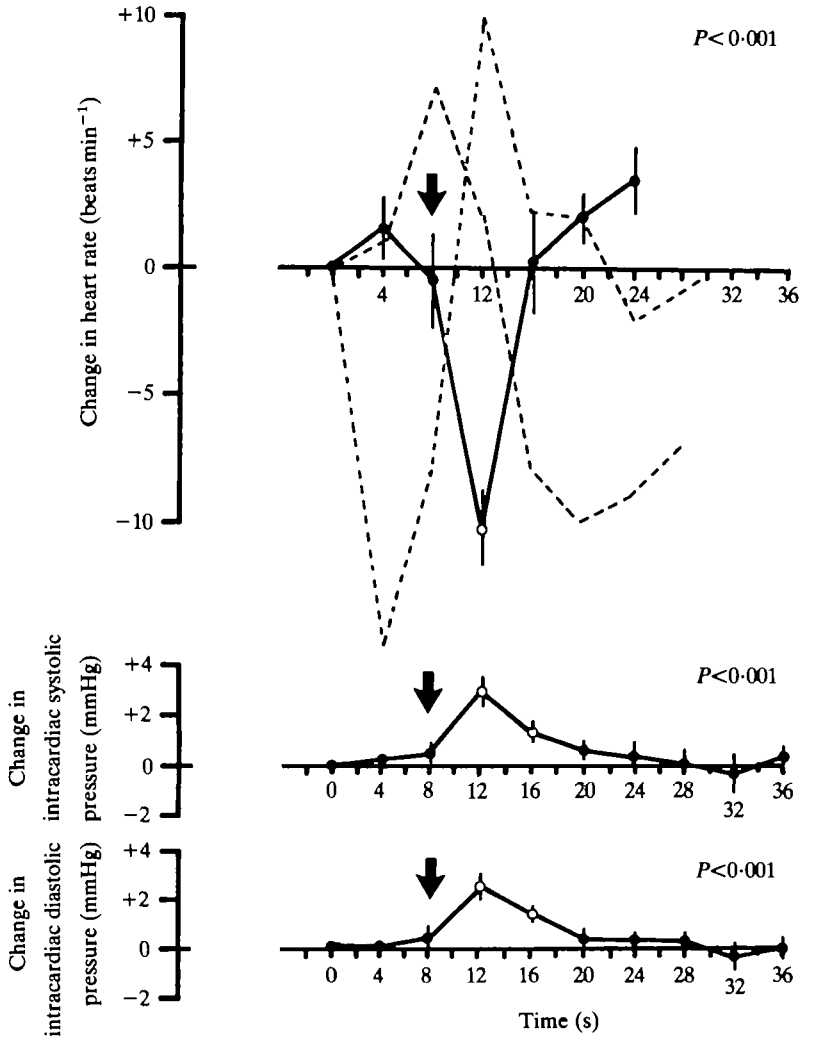

Fig. 8. Changes in heart rate and in intracardiac systolic and diastolic pressure before, during and after reversed scaphognathite beating in *Cardisoma guanhumi*. All crabs had access to 50% SW. Mean values ± 1 S.E. for five crabs are presented. Arrows indicate the onset of reversed beating, which lasted 4–10 s. Results of analysis of variance of means of each time class are shown in the upper right of each panel. Open circles represent means significantly different from values at time zero. The dashed lines indicate heart rate for two additional crabs showing atypical time courses associated with the onset of reversed scaphognathite beating.

to levels not significantly different ($P > 0{\cdot}10$) from before the onset of the reversal.

Interestingly, in two otherwise apparently normal crabs, quite different heart rate patterns were associated with spontaneous scaphognathite reversals (dashed lines, Fig. 8). In both these individuals, heart rate began to change 3–6 s before the onset of reversal, and in one crab the bradycardia was greatest about 10 s after the end of the reversal episode.

Additional experiments were performed on those *Cardisoma guanhumi* fitted with rubber plugs in the carapace. When the branchial plugs were in place, normal

pressures above and below ambient accompanied reversed and forward beating, respectively, and a transient bradycardia occurred during episodes of reversed beating. Removal of the rubber plugs inserted into the 5-mm diameter hole in the top of each branchial chamber, which opened the system to the atmosphere, eliminated

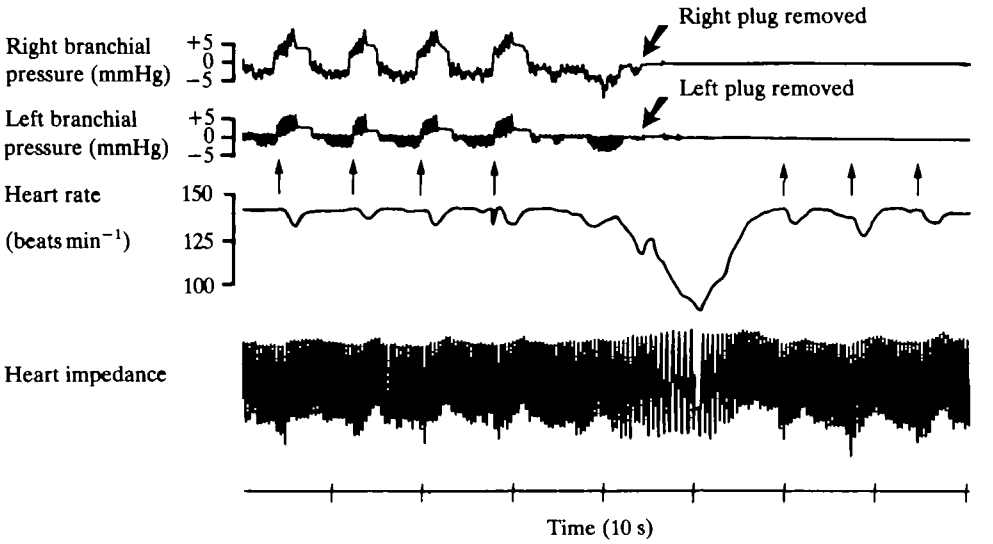

Fig. 9. Effects on branchial pressure and heart rate of *Cardisoma guanhumi* produced by removal of 'branchial plugs' from the carapace (large arrows). Small, upward pointing arrows indicate brief periods of reversed scaphognathite beating. Note that branchial gas pressure fluctuations disappear after the plugs are removed, but that the transient bradycardia associated with reversed scaphognathite beating persists. See text for details.

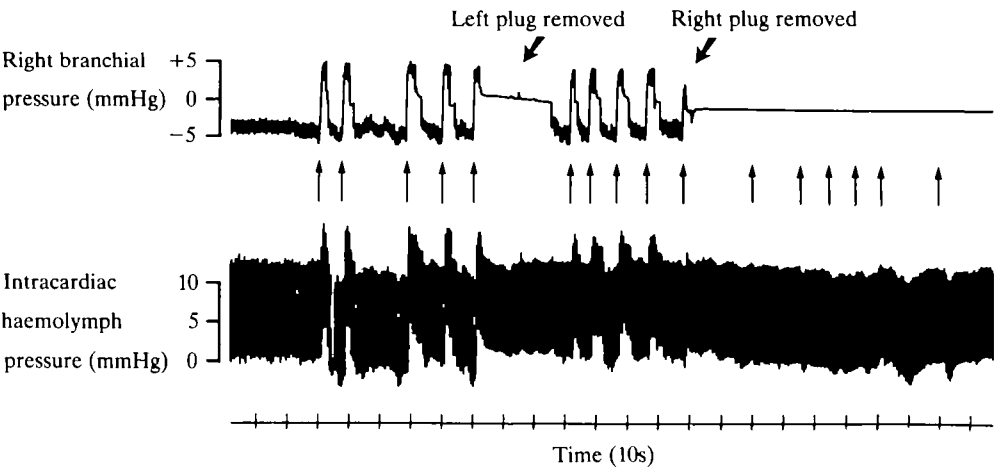

Fig. 10. Effects of sequential removal of left and right 'branchial plugs' on intracardiac haemolymph pressure in a 198 g *Cardisoma guanhumi* with access to 50% SW. Upward arrows indicate brief periods of reversed scaphognathite beat.

all transient changes in air pressure within the branchial chambers. When both plugs were removed simultaneously, the transient changes in intracardiac haemolymph pressure that accompanied reversals were also eliminated (Fig. 9). Removal of only the left plug, which eliminated branchial pressure fluctuations in the left branchial chamber only, reduced by approximately one-half the size of the transient change in intracardiac haemolymph pressure that had previously occurred during reversals (Fig. 10). Subsequent removal of the right plug essentially eliminated all fluctuations in haemolymph pressure normally associated with reversals. Although bilateral removal of plugs eliminated branchial and intracardiac pressure transients, a brief bradycardia accompanying reversed scaphognathite beating usually persisted.

DISCUSSION

Ventilation patterns

Qualitatively, the basic ventilatory patterns and mechanisms in *Cardisoma guanhumi* are similar to those found in other brachyuran crabs, both marine and semi- or fully terrestrial (see reviews by McMahon, 1981; Taylor, 1982; McMahon & Wilkens, 1983). However, the present study reveals many quantitative differences in ventilation in *Cardisoma guanhumi* which set this species apart from other brachyurans.

Unilateral beating of one scaphognathite, a common feature of branchial ventilation in brachyuran crabs (E.W. Taylor *et al.* 1973; McDonald *et al.* 1977; Butler, E.W. Taylor & McMahon, 1978; A.C. Taylor & Davies, 1982; McMahon & Wilkens, 1983), was observed only rarely in *Cardisoma guanhumi*, where coordinated bilateral ventilation definitely prevailed under all experimental conditions. Interestingly, Wood & Randall (1981) reported that unilateral scaphognathite beat was the normal mode of ventilation in air-exposed *Cardisoma carnifex* at 25 °C, with coordinated bilateral ventilation only occurring during exercise. It has been suggested that experimental disturbance or handling results in constant, bilateral ventilation in decapod crustaceans (see McDonald *et al.* 1977; Taylor, 1982; McMahon & Wilkens, 1983). However, disturbance does not appear to account for this pattern in *Cardisoma guanhumi* in the present study, since unrestrained, air-exposed crabs allowed overnight acclimation to experimental conditions in the present study still exhibited very close coordination of left and right scaphognathite beating. Interestingly, increased bilateral pumping was observed upon aerial exposure in the intertidal crab *Cancer productus* (DeFur & McMahon, 1984).

Another feature of branchial ventilation tending to set *Cardisoma guanhumi* apart from other brachyuran crabs and even from *Cardisoma carnifex* (Wood & Randall, 1981) is the infrequent occurrence and relatively brief duration of apnoeic periods. Even after overnight acclimation, undisturbed and unrestrained *Cardisoma guanhumi* ventilating with air but with access to 50 % sea water rarely stopped scaphognathite beating for more than 1 min. Given the high oxygen capacitance of air and the fact that at least in *Cardisoma carnifex* branchial chamber P_{O_2} rarely falls below 130 mmHg, even during periods of apnoea of several minutes (Wood & Randall, 1981), it is unlikely that continuous branchial ventilation in *Cardisoma guanhumi* is related to requirements for branchial O_2 uptake. Constant ventilation may instead

relate to non-respiratory processes that require water movement within the branchial chamber. Certainly, the complex ventilatory patterns seen when small amounts of water are available undoubtedly not only maintain gas flow through the upper regions of the branchial chamber, but also provide water irrigation of the gills in the lower regions of the branchial chambers. The gills and perhaps other structures in the branchial chamber of brachyurans are involved in water and ion regulation and acid-base balance (see Mantel & Farmer, 1983), and these functions would be facilitated by, if not totally dependent upon, turnover and agitation of water in the lower regions of the branchial chamber. Constant scaphognathite motion required primarily for non-respiratory, iono-regulatory functions may generate gas flow through the upper regions of the branchial chamber whether required for gas exchange at that time or not.

Interestingly, the ionic composition of the water available to *Cardisoma* had no significant influence on ventilatory patterns, at least during the relatively brief period of water exposure. Rather, the presence or absence of water *per se* was the important feature. This is quite unlike the effect of brief salinity stress in some euryhaline decapods (Taylor, Butler & Al-Wassia, 1977; Wheatly & McMahon, 1982). *Cardisoma guanhumi* is adept at regulating blood ion concentrations with water sources of varying salinities (Herreid & Gifford, 1963; M. Wheatly, unpublished) and apparently can achieve this without adjusting branchial ventilation pattern to water salinity.

Perhaps the most distinctive feature of branchial ventilation in *Cardisoma guanhumi* is the prominence of reversed scaphognathite beating. Most aquatic, intertidal or terrestrial brachyuran crabs maintained in normoxic, normocapnic environments may show a reversed beat or small group of reversed beats (see McMahon & Wilkens, 1983; E.W. Taylor, 1982; A.C. Taylor & Davies, 1982; DeFur & McMahon, 1984), but they are normally infrequent and in some species are apparently absent altogether (e.g. *Cardisoma carnifex*, Wood & Randall, 1981). However, scaphognathite reversal occurs frequently in *Cardisoma guanhumi* in air with access to water and, we believe, makes a major contribution not only to the turnover of gas but also of water within the branchial chambers. This may be important, not only for hydration of the respiratory membranes, but also for ion, water and acid-base regulation by the gills.

Increased reversed beating in other decapods has been observed with increased environmental temperature (Taylor & Butler, 1973), decreased environmental oxygen (Herreid *et al.* 1979*a,b*) and during burrowing activity (McDonald *et al.* 1977). The function of reversed scaphognathite beating in decapods has variously been attributed to cleaning of the branchial chamber, flushing poorly ventilated regions of the branchial chamber, and sampling water anterior to the animal (Hughes, Knights & Scammel, 1969; Johansen, Lenfant & Mecklenburg, 1970; Berlind, 1976; McDonald *et al.* 1977). In addition to the 'flushing' function for reversals which we propose for *Cardisoma guanhumi*, reversed scaphognathite beating and the positive branchial pressures it produces also may act to 'wring out' stagnant pools of haemolymph in poorly perfused regions of the gills and vascular bed lining the branchial chamber.

The large increase in net retrograde flow of gas through the branchial chamber when water becomes available occurs not only by increases in the number of reversal episodes in any given time period (Figs 2, 3), but also by increases in both frequency

and stroke volume of scaphognathite beat during reversal periods (Fig. 5). Increased scaphognathite frequency during reversed beating has also been reported for the marine crab, *Cancer magister* (McDonald *et al.* 1977), but in this crab scaphognathite stroke volume decreases rather than increases and so total ventilatory flow is reduced. Both acute and chronic adjustments in these aspects of scaphognathite performance have been reported for decapods (Burggren & McMahon, 1983; J.A. Mercier & J.L. Wilkens, unpublished), and adjustments in scaphognathite stroke volume or frequency reflect a particular set of physiological or environmental conditions rather than a species-specific characteristic.

Cardiovascular patterns

Heart rate in *Cardisoma guanhumi*, approximately 100–150 beats min^{-1} even in undisturbed, unrestrained crabs, was quite high compared with values which have been reported for other decapod Crustacea. However, most previous measurements on temperate marine or freshwater species or on tropical land crabs have been made at body temperatures of only 8–25 °C. Assuming a Q_{10} value for heart rate of approximately 2, *Cardisoma* would have a heart rate of 75–100 beats min^{-1} at 25 °C, which is comparable with heart rates for *Cardisoma carnifex* and *Cardisoma guanhumi* measured at that temperature (Herreid *et al.* 1979*a,b*; Wood & Randall, 1981). The high heart rates typical of *Cardisoma* at normal environmental temperatures indicate that filling of the heart with venous blood *via* the cardiac ostia must be a relatively rapid process, since the length of diastole (and thus the length of the time available for cardiac filling) will be correspondingly brief.

These experiments present the first measurements of haemolymph systolic pressures in a terrestrial decapod, and at 15–25 mmHg are comparable with systolic arterial pressures recorded for marine crabs (see Belman, 1976; McMahon & Wilkens, 1983). The relatively high diastolic intracardiac pressures in *Cardisoma*, usually several mmHg above ambient pressure (Fig. 6), indicate that post-branchial venous and pericardial pressures are similarly elevated above ambient. Simultaneous measurement of pericardial and intracardiac haemolymph pressures confirm this, and reveal that a gradient for haemolymph flow from the pericardium into the heart prevails for the entire diastolic period, or approximately half of the cardiac cycle. Since heart rates are high and diastolic periods consequently short (see above), a sustained pericardium-to-heart pressure gradient probably adds significantly to the effectiveness of cardiac filling in *Cardisoma* and may contribute to the high cardiac outputs calculated for this genus (C.M. Wood, R.G. Boutilier & D.J. Randall, unpublished data).

Pressure events in the pericardial space and heart during the earliest phases of systole – i.e. the near simultaneous rise in both compartments followed by a fall in pressure on the venous side as systole continues – resemble central cardiovascular events during similar cardiac phases in the vertebrate circulation. The ostial valves may well be closed by brief retrograde haemolymph flow from the heart just as the atrio-ventricular valves are closed in the vertebrate heart. Moreover, the valves remain closed against moderately high pressures, since no intracardiac pressure event is transmitted back to the pericardial space during systole.

Finally, although terrestrial and aquatic brachyurans have fundamentally the same

cardiovascular and respiratory arrangement, the effects of gravity imposed on terrestrial forms may introduce circulatory complexities to tissue perfusion. For example, branchial resistances may be higher in terrestrial forms, where there is no buoying effect of water to prevent partial collapse of the gill filaments. The gills of terrestrial crabs are structurally modified to help prevent collapse in air (see von Raben, 1934; Gray, 1957; Diaz & Rodriguez, 1977) and the net circulatory effects of these modifications to branchial blood flow are currently unknown. Gravity acting on terrestrial crabs may also interfere with circulatory function by causing venous haemolymph to pool in tissue sinuses, analogous to that occurring in man during prolonged standing without movement. Additionally, the typical threat posture of *Cardisoma guanhumi*, involving elevation of the large, heavy chelae high over the carapace, may introduce several haemodynamic adjustments (e.g. increased venous return, increased arterial impedance) that would not occur in a crab making similar postural adjustments under water.

Ventilatory-circulatory interactions

Correlation of ventilatory and cardiovascular performance is a general feature of gas transport physiology in crustaceans (Taylor, 1982; McMahon & Wilkens, 1983), but the extent and constancy of interaction of these physiological processes in *Cardisoma guanhumi* is remarkable. The most striking correlation is between heart rate and direction of scaphognathite beating. Most crabs that were examined showed a consistent and marked bradycardia concomitant with the onset of reversed beating (Figs 6, 7, 8). A bradycardia during reversed beating has also been described for the marine crab *Cancer magister* in normoxic conditions (McDonald *et al.* 1977), though a tachycardia accompanies reversed beating stimulated by hypoxia in the shore crab *Carcinus maenas* (Taylor *et al.* 1973).

Measurements of intracardiac pressure in *Cardisoma guanhumi* revealed that scaphognathite reversal also caused transient increases in haemolymph pressure. Perturbations in heart rate and haemolymph pressure coincident with scaphognathite reversal could be accounted for by at least three mechanisms: (1) direct mechanical effects on the haemolymph spaces by the elevated epibranchial pressures generated during reversed beating; (2) reflex interactions involving circulatory baroreceptors; and/or (3) direct interactions between respiratory and cardiac elements of the central nervous system. Experiments in which the branchial pressure transients produced by reversed scaphognathite beating were experimentally reduced or eliminated (Figs 9, 10) strongly indicate that the elevated branchial pressure resulting from reversals is directly transmitted through the thin branchial vascular wall into the haemolymph spaces. This phenomenon has been considered, though not demonstrated, to be a factor in ventilatory-circulatory interactions in other crustaceans (Blatchford, 1971; Taylor, 1982; McMahon & Wilkens, 1983). The elevation of central haemolymph pressure by scaphognathite reversal appears to be a mechanical event.

Why then does a bradycardia occur during these transient changes in haemolymph pressure induced by scaphognathite reversal? Preliminary (unpublished) evidence suggests that there is a baroreceptor reflex in *Cardisoma guanhumi*. Given a constant peripheral resistance, a decline in cardiac output due to a decline in heart rate – reflexly mediated or otherwise – might minimize any factors tending to increase

haemolymph pressure. Regulation of blood pressure in *Cardisoma guanhumi* may be vital in maintaining cardiac output, since a small pressure perturbation represents a proportionately much larger pressure adjustment in an animal with a comparatively low mean blood pressure.

Heart rate adjustments at the same time as scaphognathite reversal may also reflect some direct interaction of central neural elements controlling ventilation and circulation (Wilkens, Wilkens & McMahon, 1974; Taylor *et al.* 1973; Young, 1978; Young & Coyer, 1979; Pasztor & Bush, 1983*a*,*b*; Bush & Pasztor, 1983). Transient bradycardia associated with scaphognathite reversal persisted in some (but not all) crabs in the present experiments when the branchial chambers were opened to ambient pressure, eliminating all transient changes in haemolymph pressure (Figs 9,10). Thus, haemolymph pressure changes are not an absolute requisite for the bradycardia response. The time courses of the onset of reversals and bradycardia are also in support of some degree of central neural interaction of ventilatory and circulatory elements. Whereas changes in heart rate and haemolymph pressure were usually very closely linked in time, in a few crabs (dashed lines, Fig. 8), heart rate adjustments either began several seconds before reversed scaphognathite beating began, or persisted for several seconds after forward beating resumed. These atypical ventilatory-circulatory interactions nonetheless suggest that not all such phenomena are mediated by tightly linked 'cause-and-effect' events involving peripheral reflexes.

REFERENCES

Belman, B. W. (1976). New observations on blood pressure in marine Crustacea. *J. exp. Zool.* **196**, 71–78.

Berlind, A. (1976). Neurohormonal and reflex control of scaphognathite beating in the crab *Carcinus maenas*. *J. comp. Physiol.* **116**A, 77–90.

Blatchford, J. G. (1971). Hemodynamics of *Carcinus maenas* (L.). *Comp. Biochem. Physiol.* **39**A, 193–202.

Butler, P. J., Taylor, E. W. & McMahon, B. R. (1978). Respiratory and circulatory changes in the lobster (*Homarus vulgaris*) during long term exposure to moderate hypoxia. *J. exp. Biol.* **73**, 131–146.

Burggren, W. W. & McMahon, B. R. (1983). An analysis of scaphognathite pumping performance in the crayfish *Orconectes virilis*: compensatory changes to acute and chronic hypoxic exposure. *Physiol. Zoöl.* **56**, 309–318.

Bush, B. M. H. & Pasztor, V. M. (1983). Graded potential and spiking in single units of the oval organ, a mechanoreceptor in the lobster ventilatory system. II. Individuality of the three afferent fibres. *J. exp. Biol.* **107**, 451–464.

Cameron, J. N. (1975). Aerial gas exchange in the coconut crab *Birgus latro*, with some notes on *Gecardoidea lalandii*. *Comp. Biochem. Physiol.* **52**A, 129–134.

Cameron, J. N. (1981). Brief introduction to land crabs of the Palau Islands: stages in transition to air breathing. *J. exp. Zool.* **218**, 1–6.

DeFur, P. L. & McMahon, B. R. (1984). Physiological compensation to short-term air exposure in red rock crabs, *Cancer productus* Randall, from littoral and sublittoral habitats. I. Oxygen uptake and transport. *Physiol. Zoöl.* **57**, 137–150.

DeWilde, P. A. W. J. (1973). On the ecology of *Coenobita clypeatus* in Curacao. With reference to reproduction, water economy and osmoregulation in terrestrial hermit crabs. In *Studies on the Fauna of Curacao and Other Caribbean Islands*, Vol. 44. The Hague: Martinus Nijhoff.

Diaz, H. & Rodriguez, G. (1977). The branchial chamber in terrestrial crabs: a comparative study. *Biol. Bull. mar biol. Lab., Woods Hole* **153**, 485–503.

Gray, I. E. (1957). A comparative study of the gill area of crabs. *Biol. Bull. mar. biol. Lab., Woods Hole* **112**, 23–42.

Herreid, C. F., II & Gifford, C. A. (1963). The burrow habitat of the land crab, *Cardisoma guanhumi* (Latreille). *Ecology* **44**, 773–775.

Herreid, C. F., II, Lee, L. L. & Shah, G. M. (1979*a*). Respiration and heart rate in exercising land crabs. *Respir. Physiol.* **36**, 109–120.

Herreid, C. F., II, O'Mahoney, P. M. & Shah, G. M. (1979*b*). Cardiac and respiratory response to hypoxia in the land crab, *Cardisoma guanhumi* (Latreille). *Comp. Biochem. Physiol.* **63**A, 145–151.

J. exp. Biol. **117**, 119–132 (1985)
Printed in Great Britain © *The Company of Biologists Limited 1985*

AN INVESTIGATION OF HAEMOCYANIN OXYGEN AFFINITY IN THE SEMI-TERRESTRIAL CRAB *OCYPODE SARATAN* FORSK

BY S. MORRIS AND C. R. BRIDGES

Institut für Zoologie IV, Lehrstuhl für Stoffwechselphysiologie, Universität Düsseldorf, D-4000 Düsseldorf, F.R.G.

Accepted 21 December 1984

SUMMARY

The oxygen affinity of the haemocyanin in the supralittoral crab *Ocypode saratan* was investigated at temperatures between 20 and 35 °C. The effect of L-lactate on dialysed and undialysed haemolymph oxygen affinity was also examined.

In general, the temperature sensitivity of the haemocyanin was low: ΔH was $-3{\cdot}1\,kJ\,mol^{-1}$, between 25 and 30 °C. Temperature sensitivity was temperature-dependent, being larger at the extreme temperatures ($\Delta H = -26\,kJ\,mol^{-1}$). The Bohr effect ($\Delta \log P_{50}/\Delta pH$) was temperature-independent and averaged $-0{\cdot}67$.

No specific effect of CO_2 on oxygen affinity was observed but L-lactate increased oxygen affinity in both dialysed and undialysed haemolymph. The maximal effect of lactate on oxygen affinity was similar in dialysed and undialysed haemolymph, but was evident at a lower lactate concentration ($4\,mmol\,l^{-1}$) in dialysed, compared with undialysed, haemolymph ($7\,mmol\,l^{-1}$). Dialysed haemolymph showed a higher oxygen affinity than undialysed haemolymph at low lactate concentration ($<4\,mmol\,l^{-1}$). The Bohr effect and buffer value both decreased with increasing lactate concentration in both dialysed and undialysed haemolymph. The physiological implications of these findings are discussed.

INTRODUCTION

Although the ghost crabs, family Ocypodidae, have been the subject of numerous ecological studies (Bliss, 1968; Wolcott, 1978; see Powers & Bliss, 1983 for review) few studies have been made of the respiratory physiology of this group (Storch & Welsch, 1975; Burnett, 1979). Some characteristics of haemolymph gas transport in land crabs have been described by Redmond (1968), Young (1972) and Burnett & Infantino (1984). A significant contribution to the study of air breathing in crabs was made by a series of investigations during the *Alpha Helix* cruise of 1979 (cf. Cameron, 1981*a*). These investigations were, however, restricted to the genera present on the Palau islands and did not include any member of the Ocypodidae nor did they investigate extensively the oxygen-binding properties of the haemocyanin.

Key words: Land crabs, oxygen affinity, haemocyanin, temperature effect, lactate effect.

Since the work of Truchot (1980), the existence of specific, organic modulators of haemocyanin oxygen affinity has become an area of increasing interest. Some comparative information is available about the distribution of these modulating effects throughout the Crustacea (Mangum, 1983*a*; Bridges, Morris & Grieshaber, 1984), but to date no terrestrial decapod has been considered.

The subtropical land crab, *Ocypode saratan*, although not fully terrestrial, is confined to a supralittoral habitat (von Linsenmair, 1967) and can be found up to 1 km inland. The object of the present study was to characterize some of the oxygen-transporting properties of the haemolymph of this species and to investigate the specific modulation of haemocyanin O_2 affinity in a terrestrial decapod. The results of the investigation are discussed in terms of the possible physiological advantages to *Ocypode saratan*.

MATERIAL AND METHODS

Adult *Ocypode saratan* were collected from local beaches by personnel of the University of Jeddah, Saudia Arabia and individually packed for transport in cooled, moist styrofoam cases. The animals were then air freighted to the Department of Zoology in Glasgow and installed in a warm aquarium room at 25 ± 2 °C. The crabs were maintained for 2 weeks in tanks containing autoclaved sand dampened with sea water. Fresh water and sea water were both provided and the animals were fed with fresh salad/fruit twice each week and occasionally with chopped meat.

Blood sampling

Prior to sampling, intermoult male crabs of carapace width 35–49 mm (weight range 21–36 g) were maintained in separate polystyrene ice buckets, with moist sand, for a period of 1 day to ensure that L-lactate in the haemolymph was at resting levels. Venous haemolymph samples were then withdrawn, in less than 10 s, from the quiescent crabs *via* the arthrodial membrane at the base of the third walking leg. The samples were then pooled and frozen at − 70 °C prior to transport to Düsseldorf.

Initial measurements

The concentrations of the key inorganic ions were determined in the undialysed haemolymph samples. The concentrations of Mg^{2+} and Ca^{2+} were determined spectrophotometrically (Merkotest 3338, Darmstadt, F.R.G. and Roche, No. 1028, Basel Switzerland, respectively) and that of Cl^- using a chloride titrator (CMT 10, Radiometer, Copenhagen, Denmark). The concentration of L-lactate in the haemolymph samples and Ringer solutions used was estimated using the method of Gutmann & Wahlefeld (1974) modified according to Graham, Mangum, Terwilliger & Terwilliger (1983).

Haemolymph protein and haemocyanin concentrations were calculated from the absorbance peaks of spectrophotometric scans between 250–400 nm using 1 : 100 dilutions of haemolymph in Ringer solution. The absorbance maxima at 280 nm and 335 nm were used to determine concentrations of total protein and haemocyanin respectively using the extinction coefficients of 14·3 $E^{1\%}_{1\,cm}$ and 2·69 $E^{1\%}_{1\,cm}$ (Nickerson & van Holde, 1971).

Preparation

Native *Ocypode* haemolymph, in aliquots of 1 ml, was dialysed at 4 °C for 24 h against two changes (2 l) of *Ocypode* Ringer (pH = 8·2) with the following composition (in mmol l^{-1}): NaCl, 386; KCl, 7; $MgSO_4$, 10; $MgCl_2$, 5; and $NaHCO_3$, 22. Dialysis was carried out twice on two separate haemolymph aliquots (A and B). The different haemolymph lactate concentrations were achieved in the following manner. Samples (100 μl) from the appropriate test haemolymph were centrifuged at 136 000 ***g*** (Airfuge ultracentrifuge, Beckman, California, U.S.A.) for 30 min to pellet the haemocyanin. A portion of the plasma (5 μl) was then removed and replaced with 5 μl of neutralized (pH = 8·2) solutions of L-(+)-lactate (Boehringer, Mannheim, F.R.G.) of varying concentrations. The haemocyanin was then remixed with the plasma. The precise concentration of lactate in the haemolymph was subsequently determined by enzymatic assay. Control haemolymph solutions were made by using similar (5 μl) amounts of Ringer solution without lactate.

Construction of oxygen equilibrium curves

Oxygen equilibrium curves were constructed spectrophotometrically using 10 μl samples in a diffusion chamber (Sick & Gersonde, 1969) with the modifications of Lykkeboe, Johansen & Maloiy (1975) used by Bridges, Bicudo & Lykkeboe (1979). Gas mixtures were supplied to the chamber by serially connected Wösthoff gas mixing pumps (303 a/f Wösthoff, Bochum, F.R.G.). The pH of the haemolymph was varied by changing the partial pressure of CO_2 in the gas mixture (P_{CO_2} = 2–36 Torr). The pH of the haemolymph was measured in separate sub-samples (60 μl) tonometered in a BMS 2 (Radiometer) which was supplied with the same gas mixtures as the diffusion chamber. The pH of the equilibrated haemolymph was measured near the P_{50} using a microcapillary electrode (Type G299, Radiometer) thermostatted at the experimental temperature in BMS 2. These data were then used to calculate the magnitude of the Bohr shift.

Oxygen equilibrium curves were constructed for native, untreated *Ocypode saratan* haemolymph at temperatures of 20, 25, 30 and 35 °C to assess the effect of environmental temperature change (R. J. A. Atkinson, personal communication) on the O_2 binding of the haemocyanin. The changes in the heat of oxygenation (ΔH) of the pigment accompanying an increase in temperature, at a constant pH, were calculated according to the equation:

$$\Delta H = -2{\cdot}303R \frac{\Delta \log P_{50}}{\Delta(T^{-1})} \text{ (kJ mol}^{-1}\text{)},$$

where R is the gas constant and T is the absolute temperature.

Measurements on the effect of lactate were made at 30 °C. The P_{50} values were estimated from regression analyses of saturation values between 25 and 75 % according to the Hill equation. The cooperativity (n_{50}) was also determined from these points.

The possible existence of a specific effect of CO_2 on the affinity of *Ocypode saratan* haemocyanin was investigated by comparing the fixed acid and CO_2 Bohr effect for

native haemolymph at 30 °C. A similar method to that of Morris, Taylor, Bridges & Grieshaber (1985) was used to make these determinations. This technique involved first centrifuging the haemolymph and then replacing a small amount of the supernatant plasma (5 μl) with 0·1 mol l^{-1} HCl or 0·1 mol l^{-1} $NaHCO_3$ made up in Ringer solution. Control determinations were made using replacements of Ringer alone. Oxygen equilibrium curves were then constructed using two CO_2 concentrations, 0·4 % and 3 %, in order to compare the effects of changing pH with and without changes in CO_2.

Buffer values

Estimates of the buffer value of undialysed haemolymph and of dialysed haemolymph were made from CO_2 titration measurements. The P_{CO_2} was varied using gas mixing pumps (see above) and the pH measured. In each case the haemolymph bicarbonate concentration was calculated using the Henderson-Hasselbalch equation together with pK_1' and αCO_2 estimated from the nomograms of Truchot (1976) for 30 °C ($pK_1' = 5{\cdot}946$ and $\alpha CO_2 = 0{\cdot}334$ mol l^{-1} $Torr^{-1}$).

RESULTS

Calculations made using data from the spectrophotometric scans of the haemolymph of *Ocypode saratan* revealed a protein concentration of 53·3 mg ml^{-1} and a haemocyanin concentration that was virtually the same at 53·4 mg ml^{-1}. Using this information and assuming a molecular weight for haemocyanin of between 72 000 and 75 000 Da (Rochu & Fine, 1984) the oxygen-carrying capacity of the haemocyanin ($C^{max}_{HcyO_2}$) was calculated to be 0·72–0·74 mmol l^{-1} (1·59–1·62 vol%).

The concentration of Cl^- in the native haemolymph was 425 ± 15 mmol l^{-1} and the concentration of Mg^{2+} was 14·6 ± 0·8 mmol l^{-1} compared to 9·4 ± 2·3 mmol l^{-1} for Ca^{2+} ion concentration. The calculated concentration of HCO_3^- in the haemolymph after equilibration with 7·24 Torr CO_2 was, at 30 °C, 23·1 ± 1·8 mmol l^{-1}.

The effect of temperature on oxygen affinity

A large number of equilibrium curves resulted from this investigation and two typical sets of data for haemolymph at 20 and 35 °C are shown in Fig. 1. From these data it is apparent that the oxygen affinity of the haemolymph was temperature dependent; for example, the P_{50} at 35 °C was 12·2 Torr (pH = 7·91) but decreased to a value of 8·3 Torr at 20 °C (pH = 7·90). The same curves also clearly demonstrate the presence of a significant Bohr effect.

The CO_2 Bohr factor ($\varphi = \Delta \log P_{50}/\Delta pH$) was calculated for native *Ocypode* haemolymph at all experimental temperatures using the data presented in Fig. 2. The value of φ was found to be essentially temperature-independent (Fig. 2) and a mean CO_2 Bohr factor of $-0{\cdot}670 \pm 0{\cdot}02$ could be calculated for the temperature range 20–35 °C.

The temperature sensitivity of the haemocyanin was analysed further by comparing the ΔH values (Table 1) at two different pH values using data calculated from the regression lines presented in Fig. 2. The similarity of ΔH at the two pH values (7·4 and 7·8) confirms the low temperature sensitivity of φ. At a constant pH 7·8,

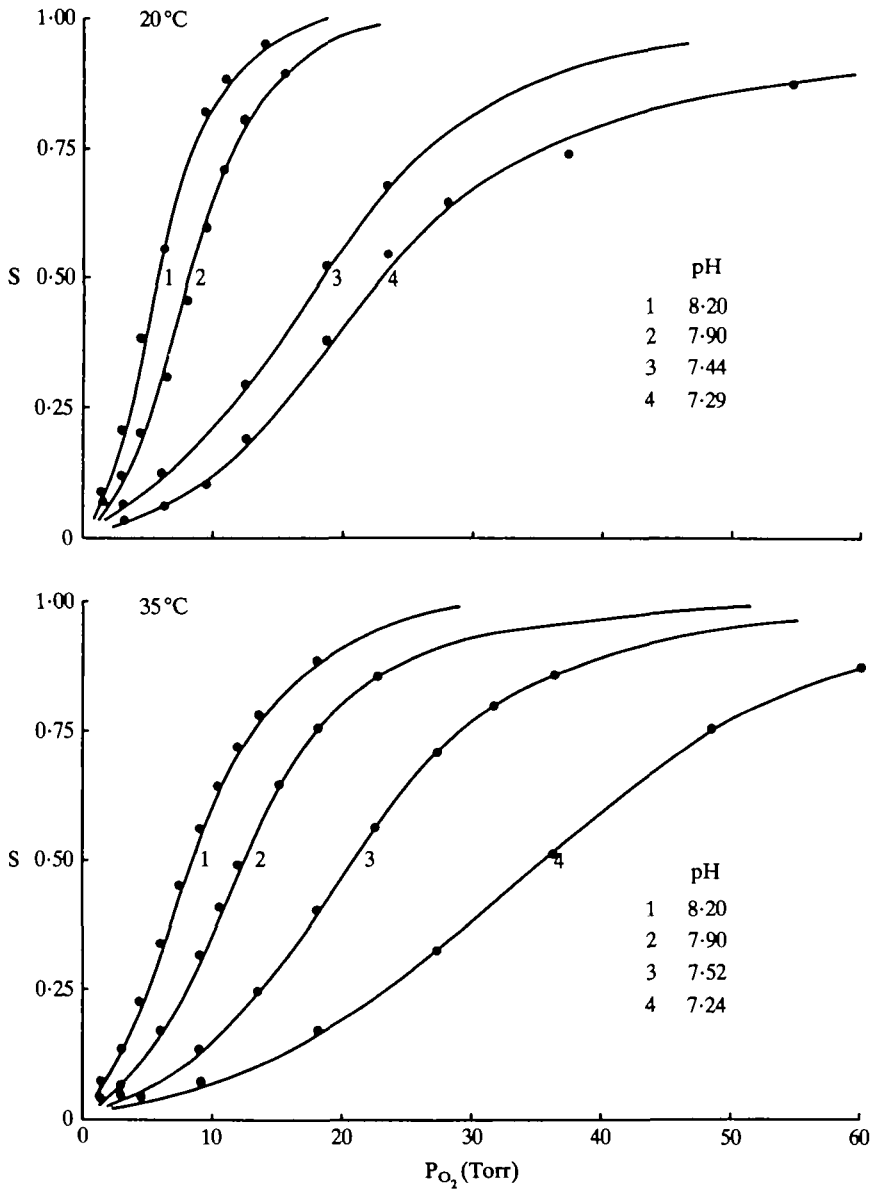

Fig. 1. Oxygen dissociation curves for *Ocypode saratan* haemocyanin constructed at 20 and 35 °C, using P_{CO_2} (2–36 Torr) to vary pH.

the change in the heat of oxygenation of the respiratory pigment accompanying a rise in temperature from 20 to 35 °C was found to be $-18{\cdot}4\,kJ\,mol^{-1}$. An examination of the change in ΔH accompanying increases of 5 °C within this temperature range showed, however, a distinct decrease in temperature sensitivity near to the normal environmental temperature. Increasing the temperature of the haemolymph from 25 to 30 °C produced a ΔH value of less than $-4\,kJ\,mol^{-1}$.

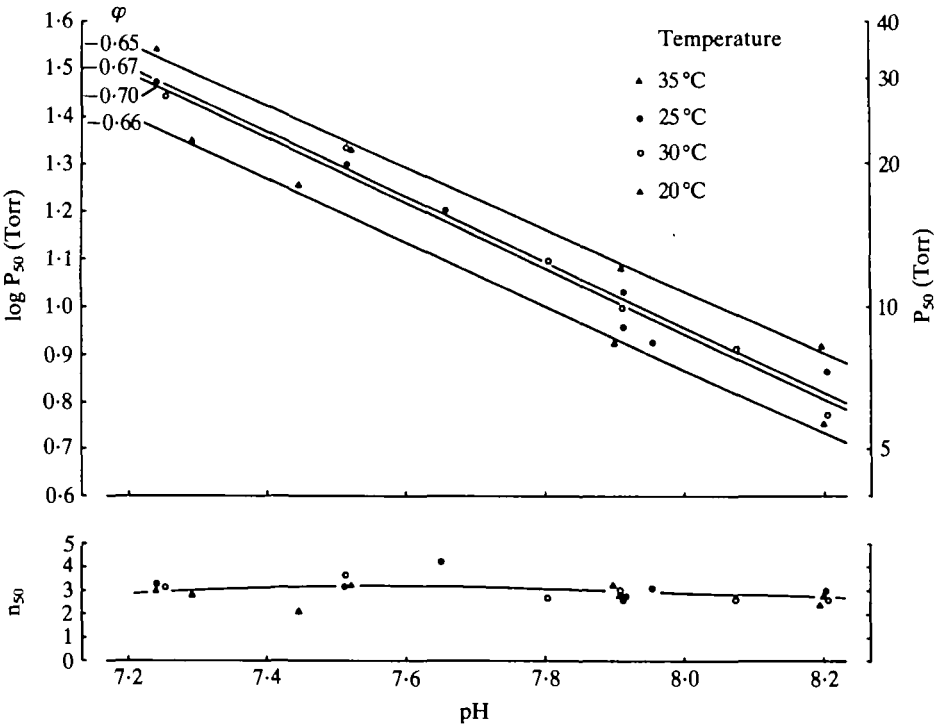

Fig. 2. The pH dependence of $\log P_{50}$ for *Ocypode saratan* haemolymph at 20, 25, 30 and 35 °C. The CO_2 Bohr values (φ) are the calculated slopes of the regression lines. The pH dependence of cooperativity measured at n_{50} is shown in the lower part of the figure.

Using P_{50} values from the O_2 equilibrium curves made at various temperatures an estimate was made for the temperature dependence of pH at a constant P_{CO_2}. This calculated *in vitro* value obtained at a P_{CO_2} of 7·4 ± 0·1 Torr (a CO_2 tension selected from the literature as being close to the *in vivo* tension) was extremely low (< 0·001 pH units °C^{-1}). Interestingly, the calculated n_{50} values exhibited no obvious dependence on temperature (Fig. 2) and changed minimally, if at all, with a change in haemolymph pH.

Table 1. *The effect of temperature on the binding of oxygen by the haemocyanin of* Ocypode saratan, *determined by the change in the heat of oxygenation (ΔH) accompanying temperature changes calculated for two constant pH values*

	ΔH (kJ mol^{-1})	
°C	pH 7·8	pH 7·4
20–25	− 25·75	− 32·10
25–30	− 3·11	− 1·04
30–35	− 26·45	− 22·87
20–35	− 18·43	− 18·09

$\Delta pH/\Delta T < 0{\cdot}001$ (*in vitro*, $P_{CO_2} = 7{\cdot}4 \pm 0{\cdot}1$).

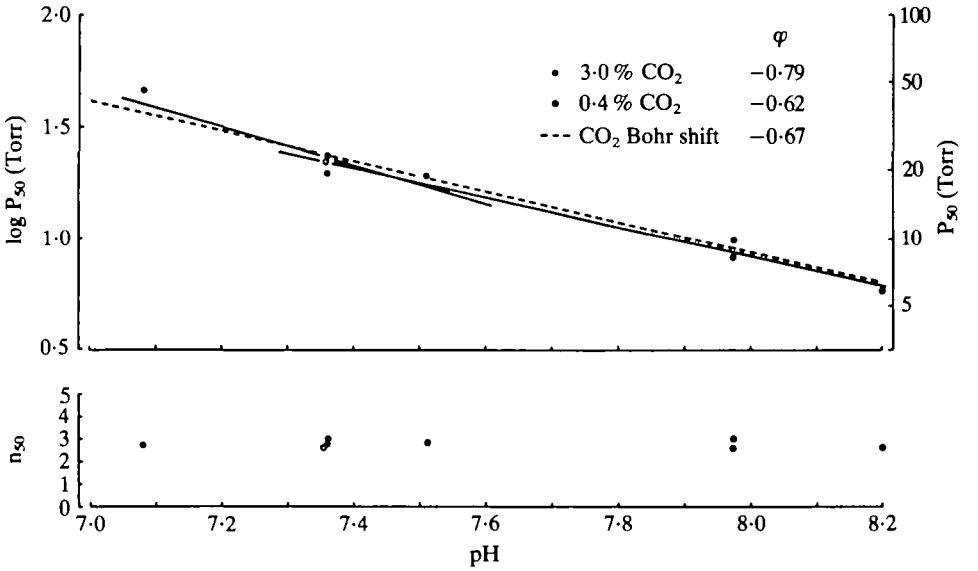

Fig. 3. Demonstration of the absence of a specific effect of CO_2 on the binding of oxygen by haemocyanin in *Ocypode saratan* at 30 °C. The slopes of the solid lines show fixed acid Bohr shifts at 0·4 % CO_2 (open symbols) and 3·0 % CO_2 (closed symbols). The CO_2 Bohr shift (P_{CO_2} = 2–36 Torr) is indicated by the broken line. The response of cooperativity (n_{50}) is shown in the lower part of the figure.

Specific effects on the binding of oxygen

Carbon dioxide

No detectable specific effect of carbon dioxide on O_2 binding by the haemocyanin of *Ocypode saratan* was found within the CO_2 concentration range 0·4–3·0 % (Fig. 3). The P_{50} values calculated from equilibrium curves made at these two concentrations and at different fixed acid concentrations were judged to describe one line for the relationship between pH and log P_{50} (the fixed acid Bohr shift). The calculated regression line for the combined data from the fixed acid determinations was; $\log P_{50} = 6{\cdot}31 - 0{\cdot}67\,\mathrm{pH}$ ($r = 0{\cdot}97$). A similar Bohr value was found for untreated haemolymph in which the Bohr shift was induced by CO_2 (see Figs 2, 3). The identity of the CO_2 and fixed acid Bohr shifts is clearly evident in Fig. 3, as is the absence of any effect of the small dilutions of the native plasma by the addition of acid or base.

L-(+)-*lactate*

The measured L-lactate concentration of native *Ocypode saratan* haemolymph was $1{\cdot}12 \pm 0{\cdot}01\ \mathrm{mmol\,l^{-1}}$, a value sufficiently low to permit the addition of neutralized L-lactate to give concentrations in the physiological range (Wood & Randall, 1981; Smatresk & Cameron, 1981; Taylor & Davies, 1982). The error of the lactate estimates was at all times less than 1 %. Increasing the lactate concentration of the undialysed haemolymph was found to increase the haemocyanin oxygen affinity (Fig. 4). Increasing the haemolymph lactate concentration to $9{\cdot}51\ \mathrm{mmol\,l^{-1}}$ resulted in a

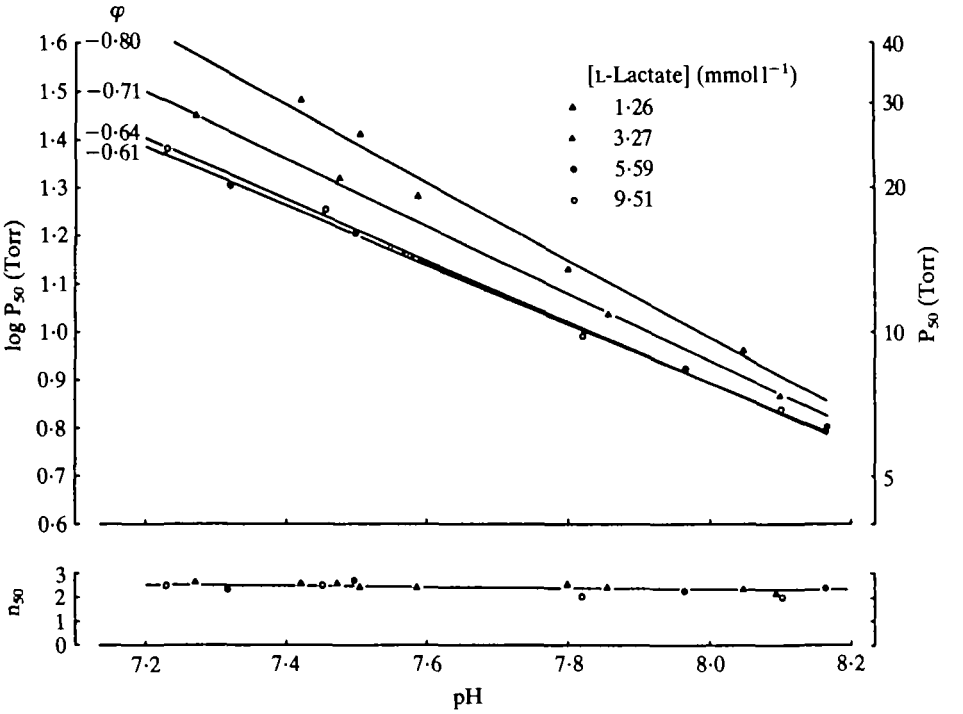

Fig. 4. The pH dependence of $\log P_{50}$ in *Ocypode saratan* whole haemolymph at varying lactate concentrations measured at 30 °C. The CO_2 Bohr values (φ) are the calculated slopes of the regression lines. The pH dependence of cooperativity measured at n_{50} and varying lactate concentrations is shown in the lower part of the figure.

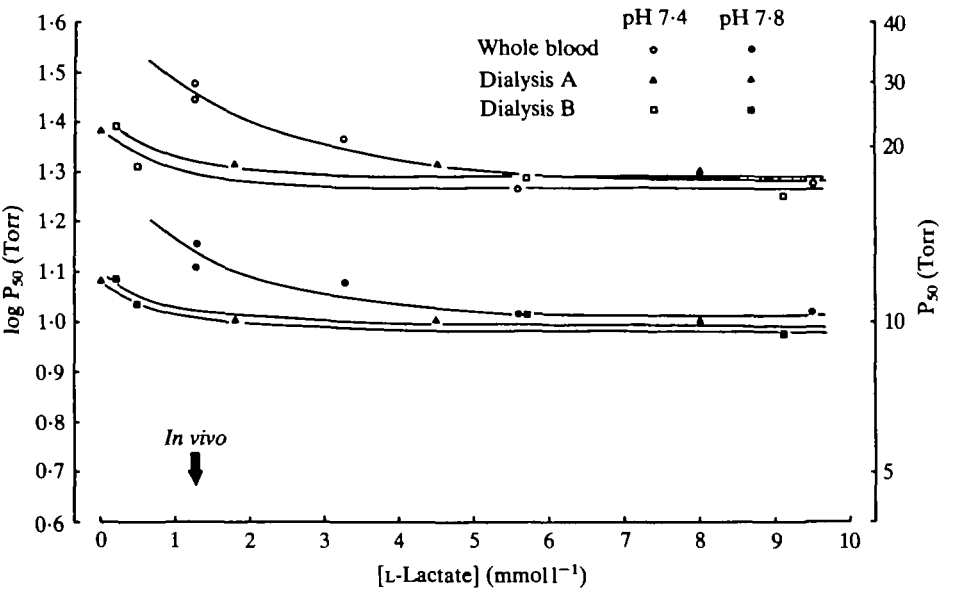

Fig. 5. The dependence of $\log P_{50}$ on L-lactate concentration for undialysed whole haemolymph and in the dialysed haemolymph (A and B) of *Ocypode saratan*, calculated for pH 7·4 (open symbols) and pH 7·8 (closed symbols) using the data shown in Fig. 3 together with similar data for dialysed haemolymph obtained at 30 °C. The dark arrow (⬇) indicates the measured *in vivo* lactate concentration of the undialysed whole haemolymph.

pH-dependent decrease in the log P_{50} value. For example $\Delta \log P_{50}$ is 0·123 at pH 7·8 ($\Delta P_{50} = 3{\cdot}7$ Torr) but increases to 0·195 at pH 7·4 ($\Delta P_{50} = 10{\cdot}5$ Torr) Increasing the concentration of haemolymph lactate not only increases affinity but also significantly (covariance analysis gives $0{\cdot}01 < P < 0{\cdot}05$) reduces the size of the Bohr factor (Fig. 4). The n_{50} values calculated from the same data showed no evidence of lactate-dependent cooperativity.

For the purposes of determining if other effectors of O_2 affinity were present in the haemolymph of *Ocypode saratan*, similar experiments were carried out on haemolymph dialysed against *Ocypode* Ringer. Lactate exponentially increased O_2 affinity in both dialysed and undialysed haemolymph. For comparison, plots of log P_{50} against log L-lactate concentration for dialysed and undialysed haemolymph have been presented in Fig. 5. The data were in all cases calculated using values from the regression lines for log P_{50} *vs* pH and include data shown in Fig. 4. The response of haemocyanin affinity to increasing lactate was dissimilar in dialysed and undialysed haemolymph. Firstly, the O_2 affinity of the undialysed haemolymph never exceeded that of haemolymph that had been dialysed and secondly, at lactate concentrations lower than approximately 7 mmol l^{-1}, the affinity of undialysed haemolymph became progressively lower. This effect resulted in a large difference in O_2 affinity between dialysed and undialysed haemolymph at low lactate concentrations. Near to the measured lactate concentration for the original native haemolymph, this difference was calculated to be 8·8 Torr and 3·5 Torr at pH 7·4 and pH 7·8, respectively. Similar results were obtained with the two separately dialysed aliquots (Fig. 5: A, B). The relationship between log P_{50} and log L-lactate concentration was calculated for native haemolymph and dialysed haemolymph by regression analysis (Table 2). The calculated coefficients in Table 2 indicate that dialysed haemolymph exhibited a reduced sensitivity to L-lactate when compared to that of undialysed haemolymph. A maximum effect of lactate was achieved at much lower concentrations (approx. 4 mmol l^{-1}) in dialysed blood than in undialysed blood (approx. 7 mmol l^{-1}). At concentrations greater than 7 mmol l^{-1} lactate, the effect was maximal in all preparations and the oxygen affinity was essentially the same at any given pH value.

Buffer values (β) calculated using pH and P_{CO_2} data from the oxygen equilibrium curves for undialysed blood are given in Table 3. It would appear that an increase in haemolymph lactate concentration results in a progressively decreasing buffer value. Furthermore, this relationship was not linear but exponential, like the

Table 2. *The relationship between haemocyanin oxygen affinity (log P_{50}) and haemolymph lactate concentration* (log [lactate$^-$]) *at 30 °C in* Ocypode saratan

	$\Delta \log P_{50}/\Delta \log$ [lactate$^-$]	
Blood treatment	pH 7.4	pH 7.8
Whole blood	−0·240	−0·162
Dialysis A	−0·035	−0·040
Dialysis B	−0·062	−0·048

Table 3. *Buffer values for the undialysed haemolymph of* Ocypode saratan *at 30 °C containing varying concentrations of* L-*lactate*

L-lactate (mmol l^{-1})	Buffer value (mmol pH $unit^{-1}$)
1·26	19·0
3·27	14·0
5·59	11·7
9·51	11·2

relationship between log P_{50} and lactate concentration. A regression equation calculated for these data by the method of least squares is given below:

$$\log[\text{lactate}^-] = 1{\cdot}296 - 0{\cdot}274\,\beta \; (r = -0{\cdot}979).$$

Dialysed haemolymph showed a similar trend with β decreasing with increasing lactate concentration.

DISCUSSION

Blood pH and oxygen affinity

Although no *in vivo* measurements were made during this study it would appear, from the literature, that the Ocypodidae might differ from other terrestrial decapods in at least one respect, the pH of the haemolymph. Data for *Ocypode quadrata,* which exhibits a similar mode of life to *Ocypode saratan* (von Linsenmair, 1967; Wolcott, 1978), indicate an *in vivo* pH value in excess of pH 7·9 (Burnett, 1979). Investigation of other semi-terrestrial crustaceans (Burggren & McMahon, 1981; McMahon & Burggren, 1981; Smatresk & Cameron, 1981; Cameron, 1981*b*; Wood & Randall, 1981; Taylor & Davies, 1982) all report pH values lower than 7·8. These workers agree, however, that haemolymph P_{CO_2} levels normally lie within the range 6–12 Torr. The *in vitro* pH 7·89 measured at a P_{CO_2} of 7·4 Torr (30 °C) in *Ocypode saratan* haemolymph is in close agreement with the data of Burnett (1979) and may be important in confirming that the Ocypodidae maintain a high haemolymph pH. This may be facilitated in *Ocypode saratan* through a high haemolymph bicarbonate level which can be up to 50 % higher than those reported in other land crabs (McMahon & Burggren, 1981; Cameron, 1981*b*; Wood & Randall, 1981; Taylor & Davies, 1982).

The maintenance of a high blood pH is of significance when estimating oxygen affinity *in vivo*. At pH 7·8 and near environmental temperatures (30 °C) the P_{50} is approximately 12 Torr. This is not an exceptionally high affinity in comparison with the P_{50} values from other terrestrial crabs, e.g. 3·9 Torr (pH 8·18) in *Cardisoma guanhumi* (Young, 1972) and 4·5 Torr (pH 7·53) in the same species (Redmond, 1962), 20 Torr (pH 7·3) in *Gecarcinus lateralis* (Taylor & Davies, 1981), 13 Torr (pH 7·46) and 25 Torr (pH 7·46) in *Cardisoma carnifex* and *Birgus latro*, respectively (Burggren & McMahon, 1981). The mean CO_2 Bohr factor of $-0{\cdot}67$ in *Ocypode saratan* is lower than the $-0{\cdot}76$ reported for *Ocypode quadrata* (Burnett, 1979) and the $-0{\cdot}95$ found for *Ocypode occidentalis* (Burnett & Infantino, 1984).

The effect of temperature

It is evident from Fig. 1 and Table 1 that oxygen affinity is temperature dependent in *Ocypode saratan*. The ΔH values in Table 1 are, however, low in comparison with values from other crustaceans ($\Delta H = -12$ to $-143\,kJ\,mol^{-1}$; Mangum, 1980). Young (1972) reports values, calculated at constant pH, of $-45\,kJ\,mol^{-1}$ for *Cardisoma*, $-43\,kJ\,mol^{-1}$ for *Gecarcinus* and $-46\,kJ\,mol^{-1}$ for *Goniopsis* within the temperature range 25–30 °C. Maximum values for ΔH (approx. $-26\ kJ\,mol^{-1}$) are observed in the present study at extreme temperatures. A similar temperature-dependent effect has been shown in *Palaemon elegans* (Morris *et al.* 1985), and low temperature sensitivity of oxygen binding has been reported in a number of crustaceans, including *Callianasa californiensis* (Miller & van Holde, 1974), *Pagurus bernhardus* (Jokumsen & Weber, 1982), *Euphasia superba* (Bridges *et al.* 1983) and *Palaemon elegans* (Morris *et al.* 1985). Values given for ΔH in the present study are calculated for a constant pH. *In vivo* pH values will change with temperature: McMahon & Burggren (1981) found a $\Delta pH/\Delta T$ of $-0{\cdot}023$ and $-0{\cdot}017$ in *Birgus latro* and *Cardisoma carnifex*, respectively. *In vitro* measurements in *Ocypode saratan*, however, indicate a far lower temperature sensitivity for pH. The Bohr effect may remain temperature-independent (Fig. 2), but if affinity is decreased at higher temperature then the same pH change will produce a more pronounced change in P_{50} (cf. $\log P_{50}$) than at lower temperatures.

Specific effects of CO_2 and L-lactate

Investigation of a specific CO_2 effect on oxygen binding by haemocyanin in *Ocypode saratan* did not reveal any changes in oxygen affinity, which is in agreement with other recent work (Burnett & Infantino, 1984; A. C. Taylor, S. Morris & C. R. Bridges, in preparation). Differences between fixed acid and CO_2 Bohr effects have seldom been reported (Truchot, 1973; Weber & Hagerman, 1981; Morris *et al.* 1985). Young (1972) has suggested, however, that his findings and those of Redmond (1955) possibly indicate the presence of a specific CO_2 effect in land crabs. No effect was detected in *Ocypode* (see also Burnett & Infantino, 1984), but this group (Ocypodidae) was not considered by Young and may well be phylogenetically different.

The recent finding (Truchot, 1980) that L-lactate increases the oxygen affinity of some haemocyanins has prompted more detailed investigations of this effect (Mangum, 1983*a*; Bridges *et al.* 1984). The calculated coefficients for the lactate effect ($\Delta \log P_{50}/\Delta \log [lactate^-]$) of $-0{\cdot}240$ and $-0{\cdot}162$ in undialysed haemolymph at pH 7·4 and pH 7·8, respectively (Table 2), represent a marked effect of lactate when compared to the known range of values of 0·00 to $-0{\cdot}630$ (Bridges *et al.* 1984). Some care should be taken when interpreting these values as the coefficient can be influenced by several parameters (Bridges *et al.* 1984). The coefficient does, however, demonstrate the pH sensitivity of the effect seen in some (see Bridges *et al.* 1984) but not all species (Truchot, 1980; Graham *et al.* 1983). The apparent reduction in the magnitude of the lactate effect in dialysed blood at low lactate concentration was unexpected. Although both sets of data (Fig. 5) show typical saturation kinetics the effect is near maximum at a much lower lactate concentration in dialysed haemolymph

(4 mmol l^{-1}) than in undialysed haemolymph (7 mmol l^{-1}). The cause of this difference is unclear.

The presence of an unidentified modulator of oxygen affinity has been shown in a number of crustaceans (Mangum, 1983*a,b*; Bridges *et al.* 1984), but these all increased the oxygen affinity. Lactate binding to haemocyanin does not show a 1 : 1 stoichiometry and lactate is thought to bind either between subunits or to a particular subunit (Johnson, Bonaventura & Bonaventura, 1984). It is possible that competitive inhibition could occur at either of these sites.

The exponential decrease in the buffer value with increasing lactate concentration (Table 3) also suggests an allosteric change in the structure of the haemocyanin such that the number of available proton buffering sites are decreased. This is corroborated by the decrease in the CO_2 Bohr effect with increasing lactate concentration. Much speculation surrounds the identity and mechanism of haemocyanin oxygen affinity modulators (Bridges *et al.* 1984; Johnson *et al.* 1984): the results for *Ocypode saratan* raise new questions which await further investigation at the molecular level.

Physiological implications

Exercise or environmental hypoxia may exert substantial demands on the oxygen transport system of crustaceans and in particular air-breathing species like *Ocypode saratan*. Cardiac output together with ventilation may control the efficiency of gas exchange and therefore modulate Pa_{O_2} (Wood & Randall, 1981), but venous oxygen tensions will depend upon the position of the equilibrium curve and on oxygen demand and supply.

A right shift of the curve, due to respiratory or metabolic acidosis, will aid unloading at the tissues to the detriment of arterial saturation, if Pa_{O_2} values are initially low due to gas exchange limitations or if the haemocyanin has an intrinsically low oxygen affinity. A left shift of the curve, due to respiratory alkalosis or to the presence of lactate, will enhance loading at the gill, if arterial saturation was previously impaired, and also defend the venous reserve, depending upon oxygen demand (Booth, McMahon & Pinder, 1982; Graham *et al.* 1983).

Inequalities in the efflux rates of protons and lactate from the tissues and their removal from the haemolymph after exercise have been reported in two species of land crab, *Cardisoma carnifex* (Wood & Randall, 1981) and *Gecarcinus lateralis* (Smatresk, Preslar & Cameron, 1979). Lactate was found to have a longer residence time in the haemolymph after exercise and may therefore play a significant role during recovery. This may represent an ideal adaptation for *Ocypode saratan*, which exhibits short periods of rapid locomotion and more sustained burrowing activity (von Linsenmair, 1967) the lactate effect would prevent the immediate depletion of haemolymph oxygen stores and could help maintain oxygen delivery under conditions of high oxygen demand.

The magnitude of both the Bohr and lactate effects together with the buffer value of the haemolymph, which is lactate-dependent in *Ocypode saratan* (Table 3), will all play a decisive role in determining the response of the oxygen transport system to both internal and external demands.

We are indebted to the personnel of the University of Jeddah, Saudi Arabia for supplying the animals for these experiments and we should like to thank Dr R. J. A. Atkinson and Dr A. C. Taylor for supervising the maintenance of the animals prior to sampling. Thanks are due also to Annette Lundkowski for technical assistance. Financial support was provided by the Heinrich-Hertz Stiftung, Nordrhein-Westfalen to SM and by the Deutsche Forschungsgemeinschaft (Gr 456/10-1) to CRB.

REFERENCES

Bliss, D. E. (1968). Transition from water to land in decapod crustaceans. *Am. Zool.* **8**, 355–392.

Booth, C. E., McMahon, B. R. & Pinder, A. W. (1982). Oxygen uptake and the potentiating effects of increased hemolymph lactate on oxygen transport during exercise in the blue crab *Callinectes sapidus*. *J. comp. Physiol.* **148**, 111–121.

Bridges, C. R., Bicudo, J. E. P. W. & Lykkeboe, G. (1979). Oxygen content measurement in blood containing haemocyanin. *Comp. Biochem. Physiol.* **62**A, 457–462.

Bridges, C. R., Morris, S. & Grieshaber, M. K. (1984). Modulation of haemocyanin oxygen affinity in the intertidal prawn *Palaemon elegans* (Rathke). *Respir. Physiol.* **57**, 189–200.

Bridges, C. R., Savel, A., Stöcker, W., Markl, J. & Linzen, B. (1983). Structure and function of Krill (*Euphausia superba*). Haemocyanin–adaptation to life at low temperature. In *Structure and Function of Invertebrate Respiratory Proteins*, (ed. E. J. Wood), pp. 353–356. Life Chemistry Reports, Suppl. 1, Chur, London, New York: Harwood Academic Publishers.

Burggren, W. W. & McMahon, B. R. (1981). Hemolymph oxygen transport, acid-base status and hydromineral regulation during dehydration in three terrestrial crabs, *Cardisoma, Birgus* and *Coenobita*. *J. exp. Zool.* **218**, 53–64.

Burnett, L. E. (1979). The effects of environmental oxygen levels on the respiratory function of haemocyanin in the crabs, *Libinia emarginata* and *Ocypode quadrata*. *J. exp. Zool.* **210**, 284–300.

Burnett, L. E. & Infantino, R. L. (1984). The CO_2-specific sensitivity of haemocyanin oxygen affinity in the decapod crustaceans. *J. exp. Zool.* **232**, 59–65.

Cameron, J. N. (1981*a*). Brief introduction to the land crabs of the Palau islands: stages in the transition to air breathing. *J. exp. Zool.* **218**, 1–5.

Cameron, J. N. (1981*b*). Acid-base responses to changes in CO_2 in two Pacific crabs: The Coconut crab, *Birgus latro*, and a Mangrove crab, *Cardisoma carnifex*. *J. exp. Zool.* **218**, 65–73.

Graham, R. A., Mangum, C. P., Terwilliger, R. C. & Terwilliger, N. (1983). The effect of organic acids on oxygen binding of haemocyanin from the crab *Cancer magister*. *Comp. Biochem. Physiol.* **74**A, 45–50.

Gutmann, I. & Wahlefeld, A. W. (1974). L-(+)-lactate determined with lactic dehydrogenase and NAD. In *Methods in Enzymatic Analysis* (2nd edition), (ed. H. U. Bergmeyer), pp. 1464. New York, London: Verlag Chemie Weinheim & Academic Press Inc.

Johnson, B. A., Bonaventura, C. & Bonaventura, J. (1984). Allosteric modulation of *Callinectes sapidus* hemocyanin by binding of L-lactate. *Biochemistry, N.Y.* **23**, 872–878.

Jokumsen, A. & Weber, R. E. (1982). Haemocyanin oxygen affinity in hermit crab blood is temperature independent. *J. exp. Zool.* **221**, 389–394.

Lykkeboe, G., Johansen, K. & Maloiy, G. M. O. (1975). Functional properties of haemoglobins in the teleost *Tilapia grahami*. *J. comp. Physiol.* **104**, 1–11.

McMahon, B. R. & Burggren, W. W. (1981). Acid-base balance following temperature acclimation in land crabs. *J. exp. Zool.* **218**, 45–52.

Magnum, C. P. (1980). Respiratory function of the haemocyanins. *Am. Zool.* **20**, 19–38.

Mangum, C. P. (1983*a*). On the distribution of lactate sensitivity among haemocyanins. *Mar. Biol. Lett.* **4**, 139–149.

Mangum, C. P. (1983*b*). Adaptability and inadaptability among HcO_2 transport systems: an apparent paradox. In *Structure and Function of Invertebrate Respiratory Proteins*, (ed. E. J. Wood), pp. 333–352. Life Chemistry Reports, Supp. 1, Chur, London, New York: Harwood Academic Publishers.

Miller, K. & van Holde, K. E. (1974). Oxygen binding by *Callianasa californiensis* haemocyanin. *Biochemistry, N.Y.* **13**, 1668–1674.

Morris, S., Taylor, A. C., Bridges, C. R. & Grieshaber, M. K. (1985). Respiratory properties of the haemolymph of the intertidal prawn *Palaemon elegans* (Rathke). *J. exp. Zool.* **233**, 175–186.

Nickerson, K. W. & van Holde, K. E. (1971). A comparison of molluscan and arthropod hemocyanin. I. Circular dichroism and absorption spectra. *Comp. Biochem. Physiol.* **39**B, 855–872.

Powers, L. W. & Bliss, D. E. (1983). Terrestrial adaptations. In *Environmental Adaptations, Biology of the Crustacea*, Vol. 8, (eds F. J. Vernberg & W. B. Vernberg), pp. 271–334. New York, London: Academic Press.

REDMOND, J. R. (1955). The respiratory function of haemocyanin in Crustacea. *J. cell. comp. Physiol.* **46**, 209–247.

REDMOND, J. R. (1962). The oxygen-haemocyanin relationships in the crab *Cardisoma guanhumi*. *Biol. Bull. mar. biol. Lab., Woods Hole* **122**, 252–262.

REDMOND, J. R. (1968). Transport of oxygen by the blood of the land crab *Gecarcinus lateralis*. *Am. Zool.* **8**, 471–479.

ROCHU, D. & FINE, J. M. (1984). The molecular weights of arthropod hemocyanin subunits: influence of Tris buffer in SDS-PAGE estimations. *Comp. Biochem. Physiol.* **79B**, 41–45.

SICK, H. & GERSONDE, K. (1969). Method for continuous registration of O_2-binding curves of hemoproteins by means of a diffusion chamber. *Analyt. Biochem.* **32**, 362–376.

SMATRESK, N. J. & CAMERON, J. N. (1981). Post-exercise acid-base balance and ventilatory control in *Birgus latro*, the Coconut crab. *J. exp. Zool.* **218**, 75–82.

SMATRESK, N. J., PRESLAR, A. J. & CAMERON, J. N. (1979). Post exercise acid-base disturbance in *Gecarcinus lateralis*, a terrestrial crab. *J. exp. Zool.* **210**, 205–210.

STORCH, V. & WELSCH, U. (1975). Über Bau und Funktion der Kiemen und Lungen von *Ocypode ceratophthalma* (Decapoda: Crustacea). *Mar. Biol.* **29**, 363–371.

TAYLOR, A. C. & DAVIES, P. S. (1981). Respiration in the land crab, *Gecarcinus lateralis*. *J. exp. Biol.* **93**, 197–208.

TAYLOR, A. C. & DAVIES, P. S. (1982). Aquatic respiration in the land crab, *Gecarcinus lateralis* (Freminville). *Comp. Biochem. Physiol.* **72A**, 683–688.

TRUCHOT, J.-P. (1973). Action specifique du dioxyde de carbone sur l'affinité pour l'oxygène de l'hémocyanine de *Carcinus maenas* (L.) (Crustacé Décapode Brachyoure). *C.R. hebd. Séanc. Acad. Sci., Paris.* **276**, 2965–2968.

TRUCHOT, J.-P. (1976). Carbon dioxide combining properties of the blood of the shore crab, *Carcinus maenas* (L.): carbon dioxide solubility coefficients and carbonic acid dissociation constants. *J. exp. Biol.* **64**, 45–57.

TRUCHOT, J.-P. (1980). Lactate increases the oxygen affinity of crab haemocyanin. *J. exp. Zool.* **214**, 205–208.

VON LINSENMAIR, K. E. (1967). Konstruktion und Signalfunktion der Reiterkrabbe *Ocypode saratan* Forsk (Decapoda, Brachyura, Ocypodidae). *Z. Tierpsychol.* **24**, 403–456.

WEBER, R. E. & HAGERMAN, L. (1981). Oxygen and carbon dioxide transporting qualities of haemocyanin in the hemolymph of a natant decapod *Palaemon adspersus*. *J. comp. Physiol.* **145**, 21–27.

WOLCOTT, T. G. (1978). Ecological role of ghost crabs, *Ocypode quadrata* (Fabricius) on an ocean beach: scavengers or predators. *J. exp. mar. Biol. Ecol.* **31**, 67–82.

WOOD, C. M. & RANDALL, D. J. (1981). Haemolymph gas transport, acid-base regulation and anaerobic metabolism during exercise in the land crab (*Cardisoma carnifex*). *J. exp. Zool.* **218**, 23–35.

YOUNG, R. E. (1972). The physiological ecology of haemocyanin in some selected cabs. II. The characteristics of haemocyanin in relation to terrestrialness. *J. exp. mar. Biol. Ecol.* **10**, 193–206.

HUGHES, G. M., KNIGHTS, B. & SCAMMEL, C. A. (1969). The distribution of P_{O_2} and hydrostatic pressure changes within the branchial chambers of the shore crab *Carcinus maenas* L. *J. exp. Biol.* **51**, 203–220.

JOHANSEN, K., LENFANT, C. & MECKLENBURG, T. A. (1970). Respiration in the crab *Cancer magister*. *J. comp. Physiol.* **70**, 1–19.

MCDONALD, D. G., MCMAHON, B. R., & WOOD, C. M. (1977). Patterns of heart and scaphognathite activity in the crab *Cancer magister*. *J. exp. Zoöl.* **202**, 33–44.

MCMAHON, B. R. (1981). Oxygen uptake and acid-base balance during activity in decapod crustaceans. In: *Locomotion and Energetics in Arthropods*, (eds C. L. Herreid & C. R. Fourtner). New York: Plenum Press.

MCMAHON, B. R. & BURGGREN, W. W. (1979). Respiration and adaptation to the terrestrial habitat in the land hermit crab *Coenobita clypeatus*. *J. exp. Biol.* **79**, 265–281.

MCMAHON, B. R. & WILKENS, J. L. (1977). Periodic respiratory and circulatory performance in the red rock crab *Cancer productus*. *J. exp. Zoöl.* **202**, 363–374.

MCMAHON, B. R. & WILKENS, J. L. (1983). Ventilation, perfusion and oxygen consumption. In *The Biology of Crustacea*, Vol. 2, (eds L. H. Mantel & D. Bliss). New York: Academic Press.

MANTEL, L. H. & FARMER, L. H. (1983). Osmotic and ionic regulation. In *The Biology of Crustacea: Internal Anatomy and Physiological Regulation*, Vol. 5, (ed. L. H. Mantel). New York: Academic Press.

PASZTOR, V. M. & BUSH, B. M. H. (1983*a*). Graded potentials and spiking in single units of the oval organ, a mechanoreceptor in the lobster ventilatory system. I. Characteristics of dual afferent signalling. *J. exp. Biol.* **107**, 431–450.

PASZTOR, V. M. & BUSH, B. M. H. (1983*b*). Graded potentials and spiking in single units of the oval organ, a mechanoreceptor in the lobster ventilatory system. III. Sensory habituation to repetitive stimulation. *J. exp. Biol.* **107**, 465–472.

TAYLOR, A. C. & DAVIES, P. S. (1982). Aquatic respiration in the land crab, *Gecarcinus lateralis* (Freminville). *Comp. Biochem. Physiol.* **72A**, 683–688.

TAYLOR, E. W. (1982). Control and co-ordination of ventilation and circulation in crustacean: responses to hypoxia and exercise. *J. exp. Biol.* **100**, 289–319.

TAYLOR, E. W. & BUTLER, P. J. (1973). The behaviour and physiological responses of the shore crab *Carcinus maenas* during changes in environmental oxygen tension. *Neth. J. Sea Res.* **7**, 496–505.

TAYLOR, E. W., BUTLER, P. J. & AL-WASSIA, A. (1977). The effect of a decrease in salinity on respiration, osmoregulation and activity in the shore crab, *Carcinus maenas* (L.) at different acclimation temperatures. *J. comp. Physiol.* **119**, 155–170.

TAYLOR, E. W., BUTLER, P. J. & SHERLOCK, P. J. (1973). The respiratory and cardiovascular changes associated with the emersion response of *Carcinus maenas* (L.) during environmental hypoxia, at three different temperatures. *J. comp. Physiol.* **86**, 95–115.

YOUNG, R. E. (1978). Correlated activities in the cardiovascular nerves and ventilatory system in the Norwegian lobster, *Nephrops norvegicus* (L.). *Comp. Biochem. Physiol.* **61A**, 387–394.

YOUNG, R. E. & COYER, P. E. (1979). Phase co-ordination in the cardiac and ventilatory rhythms of the lobster *Homarus americanus*. *J. exp. Biol.* **82**, 53–74.

VON RABEN, K. (1934). Veranderungen im Kiemendeckel und in den Kiemen einiger Brachyuren (Decapoden) im Verlauf der Anpassung und die Feuchtluftatmung. *Z. wiss Zool.* **145**, 425–461.

WHEATLEY, M. G., BURGGREN, W. W. & MCMAHON, B. R. (1984). The effects of temperature and water availability on ion and acid-base balance in hemolymph of the land hermit crab *Coenobita clypeatus*. *Biol. Bull. mar. biol. Lab., Woods Hole* **166**, 427–445.

WHEATLY, M. G., & MCMAHON, B. R. (1982). Responses to hypersaline exposure in the euryhaline crayfish *Pacifastacus leniusculus* (Dana). I. The interaction between ionic and acid-base regulation. *J. exp. Biol.* **99**, 425–445.

WILKENS, J. L., WILKENS, L. A. & MCMAHON, B. R. (1974). Central control of cardiac and scaphognathite pacemakers in the crab *Cancer magister*. *J. comp. Physiol.* **90**, 89–104.

WOOD, C. M. & RANDALL, D. J. (1981). Oxygen and carbon dioxide exchange during exercise in the land crab (*Cardisoma carnifex*). *J. exp. Zoöl.* **218**, 7–22.

SIEGLER, M. V. S. (1981). Posture and history of movement determine membrane potential and synaptic events in nonspiking interneurons and motor neurons of the locust. *J. Neurophysiol.* **46**, 296–309.

SIMMONS, P. J. (1981). Synaptic transmission between second- and third-order neurones of a locust ocellus. *J. comp. Physiol.* **145**, 265–276.

SIMMONS, P. J. (1982*a*). Transmission mediated with and without spikes at connexions between large second-order neurones of locust ocelli. *J. comp. Physiol.* **147**, 401–414.

SIMMONS, P. J. (1982*b*). The operation of connexions between photoreceptors and large second-order neurones in dragonfly ocelli. *J. comp. Physiol.* **149**, 389–398.

SIMMONS, P. J. (1985). Signal averaging by microcomputer using a program written in a high level language. *J. Neurosci. Methods* **12**, 235–240.

STUART, A. E. & OERTEL, D. (1978). Neuronal properties underlying processing of visual information in the barnacle. *Nature, Lond.* **275**, 287–290.

TACHIBANA, M. (1983). Solitary horizontal cells in culture. I. Their electrical properties. *Vision Res.* **23**, 1209–1216.

TOYODA, J.-I. & KUJIRAOKA, T. (1982). Analyses of bipolar cell responses elicited by polarization of horizontal cells. *J. gen. Physiol.* **79**, 131–6145.

WACHTEL, H. & KANDEL, E. R. (1967). A direct synaptic connection mediating both excitation and inhibition. *Science, N.Y.* **158**, 1206–1208.

WILSON, M. (1978*a*). The functional organisation of locust ocelli. *J. comp. Physiol.* **124**, 297–316.

WILSON, M. (1978*b*). Generation of graded potential signals in the second order cells of locust ocellus. *J. comp. Physiol.* **124**, 317–331.

WILSON, M. (1978*c*). The origin and properties of discrete hyperpolarising potentials in the second order cells of the locust ocellus. *J. comp. Physiol.* **128**, 347–358.

Iles, J. F. & Pearson, K. G. (1969). Triple inhibitory innervation of insect muscle. *J. Physiol., Lond.* **204**, 124P.

Kennedy, D. & Takeda, K. (1965). Reflex control of abdominal flexor muscles in the crayfish. *J. exp. Biol.* **43**, 211–227.

Kutsch, W. & Usherwood, P. N. R. (1970). Studies of the innervation and electrical activity of flight muscles in the locust, *Schistocerca gregaria*. *J. exp. Biol.* **52**, 299–312.

Larimer, J. L. & Kennedy, D. (1969). Innervation patterns of fast and slow muscle in the uropods of crayfish. *J. exp. Biol.* **51**, 119–133.

Lewis, G. W., Miller, P. L. & Mills, P. S. (1973). Neuro-muscular mechanisms of abdominal pumping in the locust. *J. exp. Biol.* **59**, 149–168.

Miller, P. L. (1969). Inhibitory nerves to insect spiracles. *Nature, Lond.* **221**, 171–173.

Parnas, I. & Atwood, H. L. (1966). Phasic and tonic neuromuscular systems in the abdominal extensor muscles of the crayfish and rock lobster. *Comp. Biochem. Physiol.* **18**, 701–723.

Pearson, K. G. (1973). Function of peripheral inhibitory axons in insects. *Am. Zool.* **13**, 321–330.

Pearson, K. G. & Bergman, S. J. (1969). Common inhibitory motorneurones in insects. *J. exp. Biol.* **50**, 445–471.

Pearson, K. G. & Fourtner, C. R. (1973). Identification of the somata of common inhibitory motorneurons in the metathoracic ganglion of the cockroach. *Can. J. Zool.* **51**, 859–866.

Pearson, K. G. & Iles, J. F. (1971). Innervation of coxal depressor muscles in the cockroach, *Periplaneta americana*. *J. exp. Biol.* **54**, 215–232.

Piek, T. & Mantel, P. (1970). A study of the different types of action potentials and miniature potentials in insect muscles. *Comp. Biochem. Physiol.* **34**, 935–951.

Shepheard, P. (1974). Control of head movement in the locust *Schistocerca gregaria*. *J. exp. Biol.* **60**, 735–767.

Siegler, M. V. S. (1982). Electrical coupling between supernumerary motor neurones in the locust. *J. exp. Biol.* **101**, 105–119.

Snodgrass, R. E. (1929). The thoracic mechanism of a grasshopper, and its antecedents. *Smithson.misc. Collns* **82**, 1–111.

Tyrer, N. M. (1971). Innervation of the abdominal intersegmental muscles in the grasshopper. II. Physiological analysis. *J. exp. Biol.* **55**, 315–324.

Usherwood, P. N. R. (1967). Insect neuromuscular mechanisms. *Am. Zool.* **7**, 553–582.

Usherwood, P. N. R. & Grundfest, H. (1965). Peripheral inhibition in skeletal muscle of insects. *J. Neurophysiol.* **28**, 497–518.

Usherwood, P. N. R. & Runion, H. I. (1970). Analysis of the mechanical responses of metathoracic extensor tibiae muscles of free-walking locusts. *J. exp. Biol.* **52**, 39–58.

Wiersma, C. A. G. (1961). The neuromuscular system. In *The Physiology of Crustacea*, Vol. 2, (ed. T. H. Waterman). New York: Academic Press.

Wiersma, C. A. G. & Ripley, S. H. (1952). Innervation patterns of crustacean limbs. *Physiologia comp. Oecol.* **2**, 391–405.

Yang, Q. Z. & Burrows, M. (1983). The identification of motor neurones innervating an abdominal ventilatory muscle in the locust. *J. exp. Biol.* **107**, 115–127.

J. exp. Biol 117, 87–110 (1985)
Printed in Great Britain © *The Company of Biologists Limited 1985*

THE ULTRASTRUCTURE OF THE EPICUTICULAR INTERFERENCE REFLECTORS OF TIGER BEETLES (*CICINDELA*)

BY T. D. SCHULTZ AND M. A. RANKIN
Department of Zoology, University of Texas, Austin, Texas 78712, U.S.A.

Accepted 4 December 1984

SUMMARY

Tiger beetles of the genus *Cicindela* exhibit iridescent structural coloration due to the presence of a non-ideal multilayer interference reflector located in the outermost 2 μm of the integument. The reflector is composed of alternating layers of electron-lucent and electron-dense material. This series of layers was distinguished from chitinous procuticle by its position, ultrastructure and solubility in dilute KOH. The reflector appears homologous with the inner epicuticle of current models. Measurements of surface reflectance, refractive index and the dimensions of the alternating layers suggests that the dense layer has a refractive index (RI) near 2·0 and may be a melanoprotein.

INTRODUCTION

The widespread occurrence of structural coloration in insect cuticle received vigorous attention in the early part of this century (Biederman, 1914; Onslow, 1920; Mason, 1927). These researchers ascribed the physical colours of the integument to the constructive interference of light reflected from thin layers within the exoskeleton. However, the exact anatomy of the reflector remained obscure, and proposals of morphologies varied widely. The advent of the electron microscope finally allowed ultrastructural studies of cuticular reflectors. The bulk of this work focused on interference reflectance by specialized structures such as insect cornea and lepidopteran wing scales (Bernard & Miller, 1968; Ghiradella *et al.* 1972). However, the most complete study of interference reflectance by whole cuticle was Neville & Caveney's (1969) work on scarab beetles. While that work elegantly described the exocuticular reflectors within that family, the morphologies of cuticular reflectors in other metallic-coloured insects have remained undescribed.

Coincidental with the early work on insect coloration, several authors described the elytral structure of several groups of beetles which exhibit interference reflectance (Buprestidae; Hass, 1916; Cicindelidae: Stegemann, 1930; Carabidae: Sprung, 1931). Stegemann (1930) described a superficial layer, the 'Sekretschicht', in tiger beetles (Cicindelidae) which dissolves in dilute KOH at 60 °C and pours from secretory glands after ecdysis. Mandl (1931) later ascribed the iridescence of *Cicindela* to

Key words: Interference colour, epicuticle, *Cicindela*.

this 'Sekretschicht'. Shelford (1917) independently suggested that a surface film reflects interference colours in *Cicindela*.

Many of the elytral structures described by early histological and morphological studies have not been re-examined rigorously under current concepts of cuticle structure. However, homologies have been proposed for these structures based upon more recent research involving other cuticles. Wigglesworth (1972) suggested that the 'Sekretschicht' may be analogous to the cement layer of other insects. Richards (1951) preferred the term 'tectocuticle' for this outermost layer presumed to be secreted by the dermal glands. A recent electron microscope study by Mossakowski (1980) identified an interference reflector in the outermost layers of cuticle in *Cicindela campestris*. He identified the reflective cuticle as exocuticle.

The following study attempts to locate the multilayer reflective system of cicindelid cuticle, to describe its ultrastructure, and to determine to what extent this cuticle conforms to the current models of insect morphology.

MATERIALS AND METHODS

Reflection from elytral surfaces was measured using a Cary 17D spectrophotometer. Elytra for reflectance measurements were taken from four species of tiger beetles, *Cicindela formosa* Say, *C. splendida* Hentz, *C. scutellaris rugata* Dejean and *C. repanda* Dejean. Adults of all four species were collected at Bastrop State Park, Bastrop County, Texas.

Samples of adult cuticle were cut or torn from the elytra and thoraces, and subjected to a variety of chemical treatments. They were then prepared for either scanning or transmission electron microscopy.

Chemical treatments of cuticle

In order to differentiate the epicuticle from the exocuticle, fragments of cuticle were immersed in 8 % KOH at 60 °C for periods of 4, 9, 12, 24, 48 h and 6 days. One set of samples was treated with concentrated KOH for 15 min at 160 °C. A second set was treated similarly, but followed with a 17-h immersion in 8 % KOH. Treatment with hot concentrated alkali is the initial step in the chitosan method of Campbell (1929) for detection of chitinous cuticle. All samples were rinsed with distilled water, dried, and any colour or gross textural change observed with a dissecting microscope. The fragments were cut to smaller size and prepared for either scanning or transmission electron microscopy.

In order to remove procuticular layers, elytra were immersed in concentrated H_2SO_4 for 1, 12, 24, 48 and 72 h. The elytra were rinsed with distilled water, dried, and any colour changes noted. The elytral fragments were then prepared for scanning electron microscopy (SEM).

Since H_2O_2 will bleach melanin and alter the interference colours if melanin is one component of the interference reflector, the role of melanin in cicindelid coloration was investigated by treating *C. formosa* and *C. scutellaris* elytral fragments for 6 days with 10 % H_2O_2 at 26 °C. When no colour change was observed, the samples were treated for a seventh day at 60 °C. Samples were dried, observed and prepared for transmission electron microscopy.

Preparation of cuticle for scanning or transmission electron microscopy

Dried strips of treated or untreated cuticle were mounted on edge, sputter-coated with 2·5 nm of gold-palladium, and examined with a Hitachi scanning electron microscope. This orientation provided a view of the torn edge perpendicular to the elytral surface with each cuticle layer exposed in relief.

For transmission electron microscopy, treated and untreated samples of cuticle were cut into extremely fine slivers (0·3 × 1 mm) with a tapering edge. Cuts were positioned between elytral tracheae to avoid trapped air bubbles. The cuticle was fixed in 2·5 % gluteraldehyde and post-fixed in 2 % OsO_4 for 2 h, dehydrated in a standard ethanol and propylene oxide series, and infiltrated in a long series of propylene oxide/Epon-Araldite mixes. Each infiltration step required agitation, and the final two immersions in pure Epon-Araldite were evacuated completely.

Thin sections were cut perpendicular to the elytral surface. Some sections from each treatment group were post-stained for 5 min in 1 % uranyl acetate in 50 % ethanol, followed by 5 min in lead citrate. Portions of the dorsal surface of *C. scutellaris* were also sectioned parallel to the plane of the elytral surface. All sections were examined under a Zeiss 10CA transmission electron miscroscope.

Thin sections of samples from each treatment group were mounted and reserved for interference and polarized light microscopy.

RESULTS

Elytral reflectance

The elytra and thorax of *C. formosa* are deep metallic red with white maculations – peak reflectance occurring at 655 nm, with a secondary peak near 360 nm (Fig. 1A). The Bastrop population of *C. formosa* exhibits the elytral coloration of the race *C. formosa pigmentosignata* Horn. While the maculae of Bastrop individuals are rarely reduced, many individuals exhibit a distal deep purple coloration on the elytron, which is characteristic of *C. formosa pigmentosignata* (Gaumer, 1977). For reflectance measurements and electron microscope studies, elytral fragments were selected from elytral areas which were homogeneously red.

The elytra of *C. splendida* are metallic brick red with a metallic green border. An elytron with the border removed shows maximal reflectance near 635 nm, with a very small secondary peak at 410 nm (Fig. 1B).

C. scutellaris rugata elytra reflect maximally at 499 nm in a relatively narrow band (Fig. 1C). *C. scutellaris* varies greatly in colour among its races, with *rugata* displaying an iridescent blue-green coloration. Both the intensity and the purity of this reflected colour exceed those of *C. formosa* and *C. splendida*.

The brown *C. repanda* elytron has a very different reflectance curve (Fig. 1D). Instead of a sharp peak in the visible wavelengths, the reflectance increases steadily towards the near-infrared.

The colour of tiger beetle elytra, like all interference colours, changes with the angle of viewing. As the angle of reflectance departs from the angle of incidence, the reflected wavelengths become shorter. The elytra of *Cicindela* are alveolate (Fig. 2)

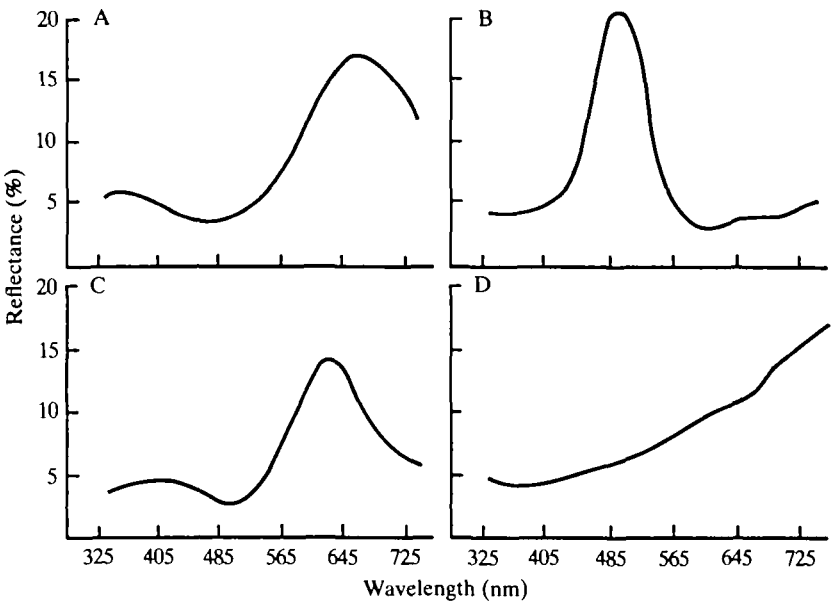

Fig. 1. Reflectance curves of four species of *Cicindela*. (A) *C. formosa pigmentosignata*, (B) *C. scutellaris rugata*, (C) *C. splendida* and (D) *C. repanda*.

with small ($10 \times 10\ \mu m$) hexagonal depressions. The alveoli are superimposed upon larger irregularities in the upper portion of the elytron. Light reflected from this surface is a composite of wavelengths reflected from a variety of angles. Not only would the total intensity of reflection be diminished, but the peak reflectance would be less sharply defined. Of the four species, *C. scutellaris* displays the most regular elytral surface with smooth, shallow alveoli. *C. repanda* and *C. splendida* possess the deepest alveoli and most acute ridges.

Elytral ultrastructure

The general features of elytral structure observed under SEM were consistent in the four species. Above the tracheae, the procuticular layers (region *D* in Fig. 2) are organized in the pseudo-orthogonal 'plywood' fashion that has been described for other Coleoptera (Hepburn, 1972). This region has been defined as endocuticle (Zelazny & Neville, 1972) or as mesocuticle (Hepburn, 1972), and is considered to be untanned or non-sclerotized.

Observed under the SEM, the outermost layer of *Cicindela* cuticle appears as a dense, solid material which bears the alveolate microsculpture of the integument (region *AB* in Fig. 2). This layer ranges in thickness from $3{\cdot}5\ \mu m$ at the bottom of a cell, to $7{\cdot}0\ \mu m$ at the top of an adjacent ridge. The torn vertical face of this layer appears less fibrous and more granular than the underlying cuticle (region *D* in Fig. 2). Occasionally, samples will tear obliquely and reveal two distinct portions of the outer layer in relief (Fig. 3). In these torn samples, a regular banding or lamination of 6–8 extremely even bands (150–200 nm thick) is visible in the outer $1–2\ \mu m$ of the layer (region *A* in Fig. 3B). These laminations appear in contrast to the rougher, non-laminated face of the inner portion (region *B* in Figs 3B and 4). Based upon their

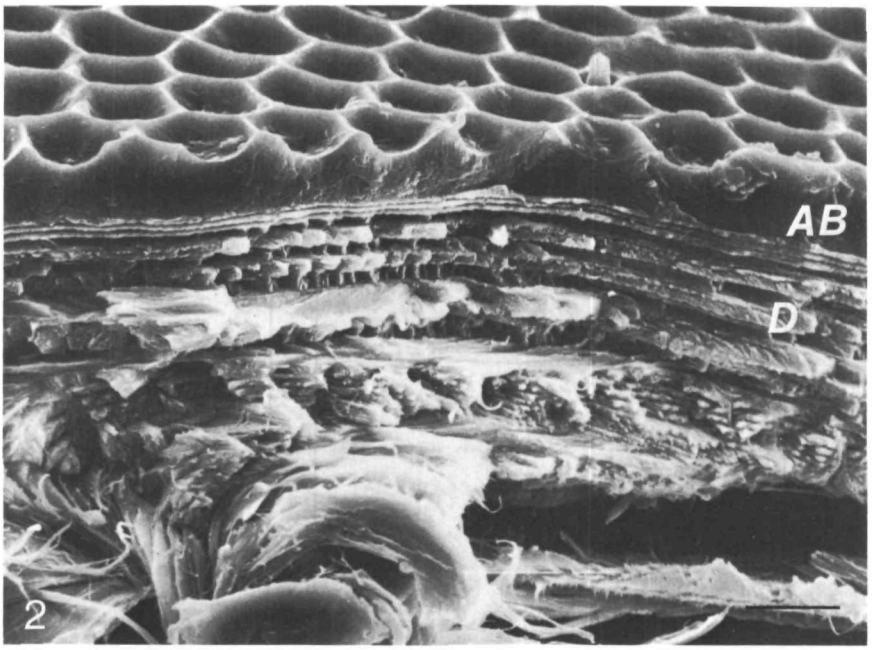

Fig. 2. Scanning electron microscope cross-section of exposed cuticular layers in the upper elytron of *Cicindela splendida*. Region *D* represents the pseudo-orthogonal procuticle. The composite layer *AB* (the presumptive epicuticle and exocuticle) conforms to the alveolate microsculpture of the elytral surface. Scale bar, 10 μm.

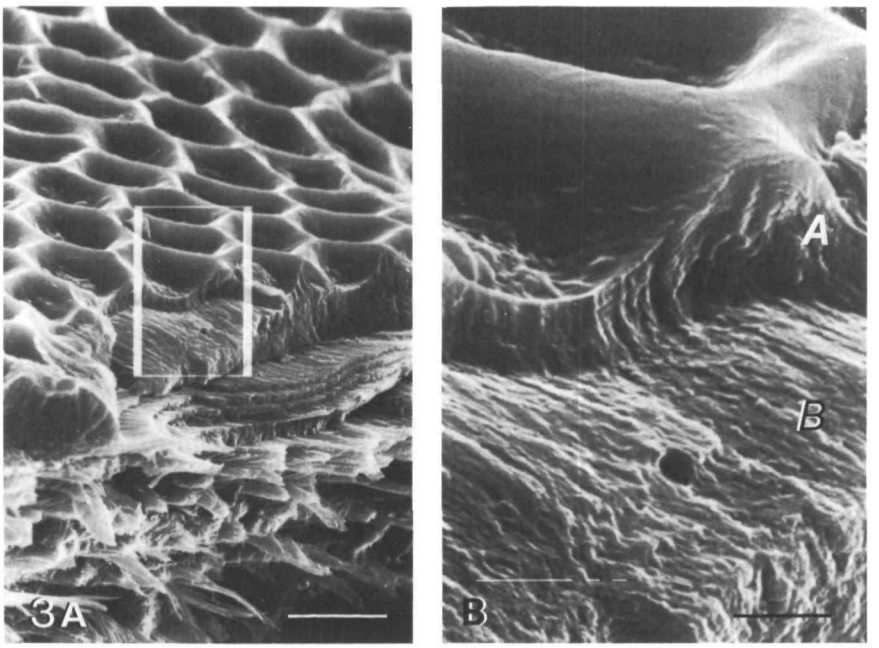

Fig. 3. Layer *A* (presumptive epicuticle) exposed separately from layer *B* (exocuticle). Horizontal laminations are visible in layer *A*. Scale bars: A, 10 μm; B, 2 μm.

ultrastructure, location, development and reaction to solvents, the outer and inner portions of the outer cuticle (layers *A* and *B* in Fig. 4) are here designated the epicuticle and outer exocuticle, respectively, and will be referred to as such throughout this report.

Dermal gland canals measure 0·8 μm in diameter and their orifices are distributed regularly over the surface of the elytron (Fig. 4, *dc*). The pattern of lamination is not disrupted around the canal opening. Epicuticular thickness is enhanced on the ridges, compared to the basins of the alveoli, but is not greater at the dermal gland opening than on adjacent ridges.

Transmission electron microscopy (TEM) reveals that the alveolate superficial layer of the scanning electron micrograph is indeed a composite of two complex layers (layers *A* and *B* in Fig. 5). Immediately below this composite, lie 2–3 thin exocuticular layers (layer *C* in Figs. 5, 6A) which exhibit the distinct arciform appearance of helocoidal cuticle as described by Bouligand (1972).

The outer exocuticle (layer *B* in Fig. 5) appears more electron-dense than the helicoidal or preferred layers below. This layer consists of 25–35 densely packed lamellae ranging in width from 0·055 to 0·1 μm. In some areas, electron-dense granules lie between or within lamellae. In post-stained sections, the horizontal lamellae are resolved into alternate patterns of microfibrils viewed in perpendicular and transverse orientations (Fig. 6B). This pattern closely resembles the description of the non-perfect helicoidal outer exocuticle of *Tenebrio* given by Filshie (1982).

Pore canals, 50–70 nm in diameter, traverse the outer exocuticle (Fig. 6C, *pc*). Within the exocuticle, they appear as segments of tubes containing material much denser than the surrounding fibrils. The pore canals extend into the epicuticle but appear much narrower in diameter (Fig. 6C, arrow). This pattern is similar to the branching of epicuticular filaments described in other insect cuticles (Filshie, 1982).

The epicuticle (Fig. 6D) is composed of a series of extremely dense bands (*D*) between 0·03 and 0·1 μm thick, regularly spaced by electron-lucent bands (*L*) of 0·06–0·125 μm. Each pair of electron-dense and electron-lucent layers corresponds to a single band observed in relief in the scanning electron micrographs. The number of bands varies between four dense layers at the base of a depression to nine layers within an adjacent ridge. Under high magnification, electron-dense layers appear to be composed of vertically aligned granules (Fig. 6D). Post-staining enhances this appearance. The electron-lucent bands exhibit no apparent ultrastructure. The outermost layer is always electron-lucent and 20–30 nm thicker than the other light bands. The outer 20–30 nm appears as a faint shadow of higher density, possibly representing a cuticulin layer (Fig. 6E, *cu*). Mossakowski (1980) identified the outer series of electron-dense and electron-lucent bands as exocuticle. He concluded that the banding was a diffraction pattern resulting from the structural organization of exocuticular fibrils.

Although there are occasional distortions, the organization of the epicuticular layers is exceedingly regular. One individual *L* or *D* layer may vary in thickness horizontally within a section. This is usually an artifact resulting from the section passing obliquely through the layer as it conforms to the alveolate surface. Each *L* or *D* layer may differ slightly in thickness from other *L*/*D* layers in that region of the stack. In *C. scutellaris*, the peripheral dense band is typically fragmented

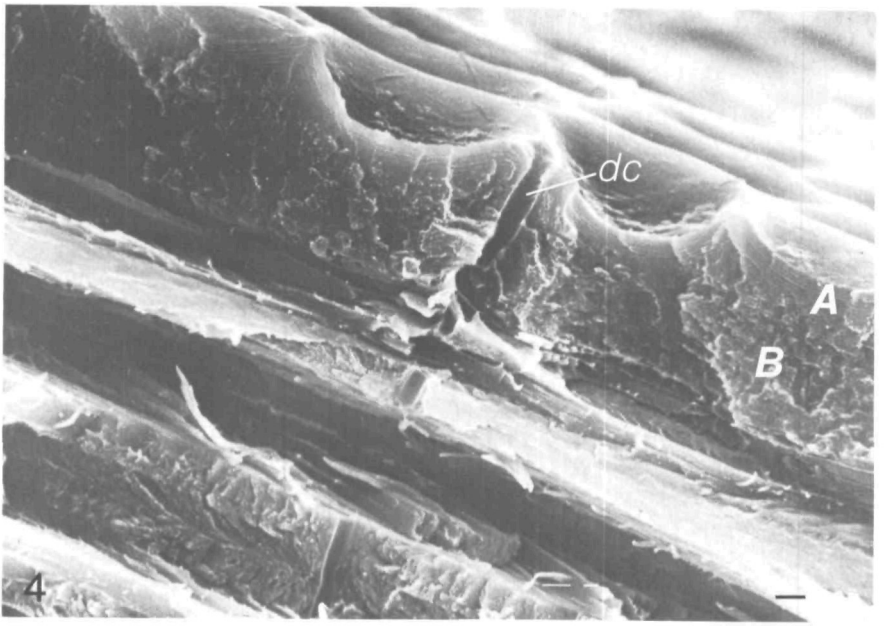

Fig. 4. Scanning electron microscope cross-section of the upper cuticular layers in *Cicindela splendida*. The laminated structure of layer *A* (presumptive epicuticle) distinguishes it from region *B* (presumptive outer exocuticle). *dc*, dermal gland canal. Scale bar, 1 μm

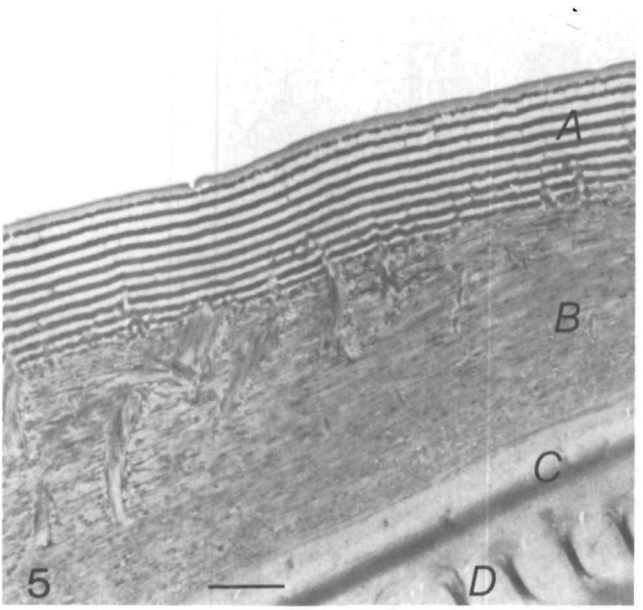

Fig. 5. Transmission electron microscope cross-section of the presumptive epicuticle (*A*) and the outer exocuticle (*B*) in the elytron of *Cicindela scutellaris*. Between the outer exocuticle and the underlying procuticle (*D*), lies a thin layer of helicoidal cuticle (*C*). Scale bar, 1 μm.

and particulate. Partially formed bands occur regularly at the outer exocuticular border.

When the honeycombed surface is sectioned horizontally, the section passes

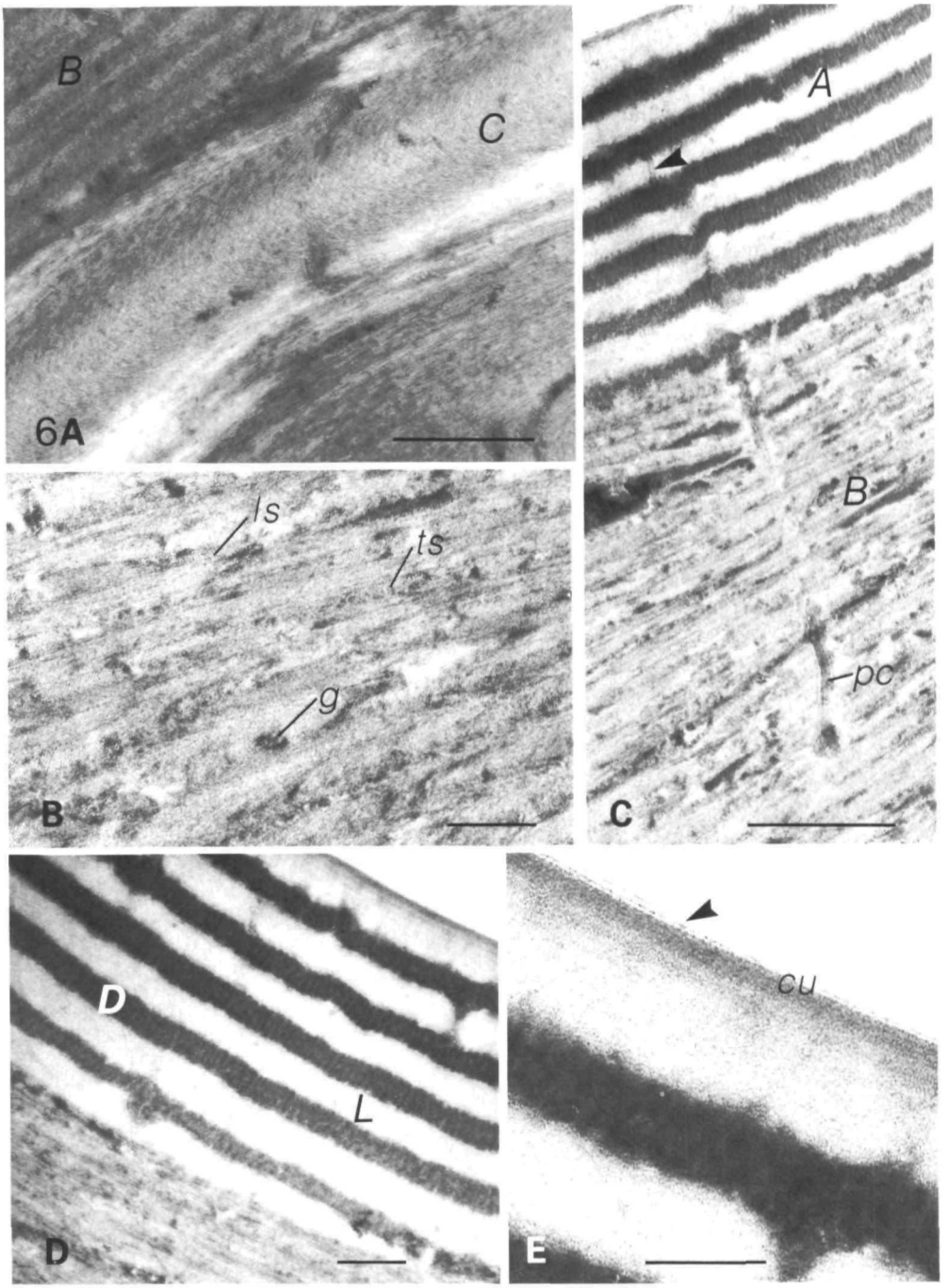

Fig. 6.

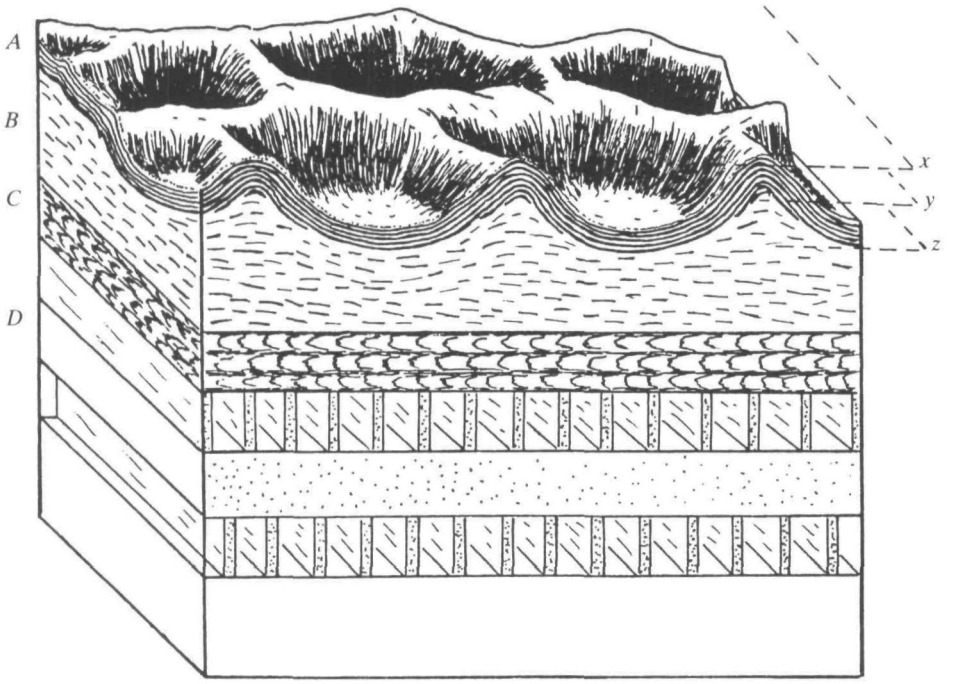

Fig. 7. Morphology and proposed terminology of the eltyral cuticle in *Cicindela*. (*D*) Endo- or mesocuticle. (*C*) Inner exocuticle. Two or three lamellae appear as a result of helicoidally oriented fibrils. (*B*) Outer exocuticle. Very fine lamellae result from the non-perfect helicoidal arrangements of fibrils. (*A*) Epicuticle. The layer assumes the outermost position and consists of alternating layers of electron-lucent and electron-dense material. No fibrillar structure is evident. Sections cut in the plane of the surface are represented by x, y and z (see text).

through the hexagonal ridges and across the intervening alveoli. Initial sections thus possess holes, surrounded by material from adjacent ridges (section x in Fig. 7). Within the ridge itself, the section passes obliquely across the outermost epicuticular layers, resulting in concentric rings around the hole. As the section intersects the ridge axis, it passes through the portion of an epicuticular layer that is oriented parallel to the section; this therefore appears as a continuous patch of either electron-dense or electron-lucent material. Deeper sections include the elevated portions of outer exocuticle within the base of a ridge (section y through region B in Fig. 7). Sections taken across the alveolar basin (section z in Fig. 7) result in a central spot of light or

Fig. 6. The ultrastructure of the outer cuticular layers in the elytron of *Cicindela formosa*. (A) Arcuate fibril pattern of layer *C* (presumptive inner exocuticle). Scale bar, 0·5 μm. (B) Fibril pattern of region *B* (presumptive outer exocuticle). Fine lamellae appear as the result of a semi-arcuate pattern of fibrils cut in longitudinal section (*ls*) and in transverse section (*ts*). Granules (*g*) of electron-dense material appear between lamellae. Scale bar, 0·2 μm. (C) Pore canal (*pc*) extending from the presumptive exocuticle (*B*) to the presumptive epicuticle (*A*). Narrow extensions of the canal are visible in layer *A* (arrow). Scale bar, 0·5 μm. (D) Ultrastructure of the presumptive epicuticle. The layer is composed of alternating layers of electron-lucent (*L*) and electron-dense (*D*) material. Scale bar, 0·2 μm. (E) High magnification of the outer edge of the presumptive epicuticle. An area of higher density in the outermost *L* layer represents the presumptive cuticulin layer (*cu*). An extremely thin (10 nm), electron-lucent layer appears between the cuticulin layer and the edge of the embedding medium (arrow). Scale bar, 0·1 μm.

dense epicuticular material ringed by obliquely sectioned layers. These islands of epicuticle are surrounded by exocuticle.

The horizontal sections demonstrate that electron-dense and electron-lucent layers have the same individual density and location when observed horizontally or vertically (Fig. 8A). The banding pattern is not, therefore, an artifact of diffraction. The layer

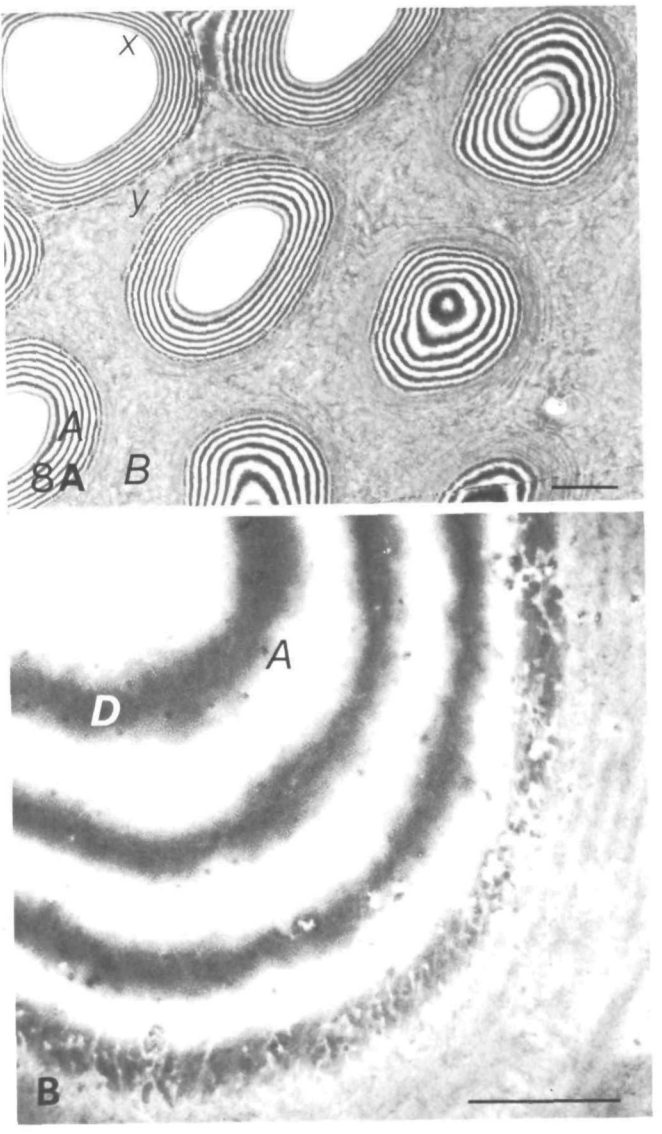

Fig. 8. (A) Transmission electron micrograph of the epicuticle (*A*) and the outer exocuticle (*B*) of *Cicindela scutellaris* sectioned in the plane of the elytral surface. Concentric rings of epicuticular material surround holes where the section did not include the basin of an alveolar cell (area *x*, see Fig. 7). The rings of epicuticle are surrounded by outer exocuticle in areas where the section includes tissues below the epicuticle within the alveolar ridges (area *y*, see Fig. 7). Note that the sequence of light and dense banding is the same as in cross-sections of the epicuticle (Fig. 5). Scale bar, 5 μm. (B) Planar section of an alveolar basin (see section *z*, Fig. 7). Note the particulate ultrastructure of the electron-dense layers (*D*) in the epicuticle (*A*). Scale bar, 1 μm.

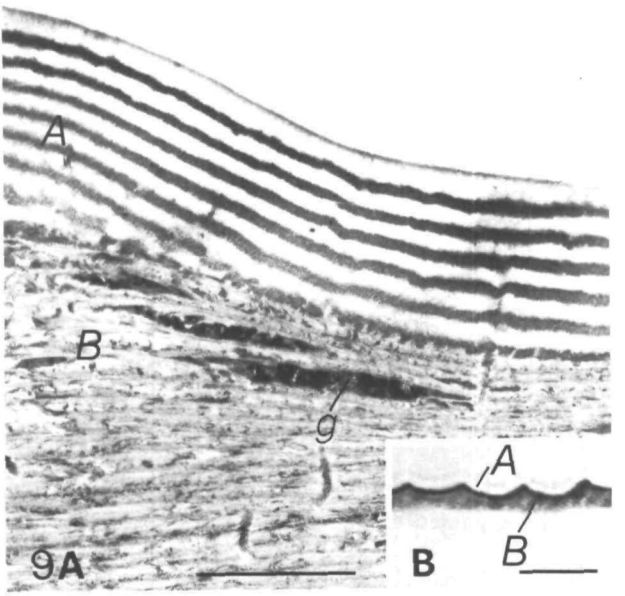

Fig. 9. (A) Transmission electron micrograph cross-section of the epicuticle (*A*) and outer exocuticle (*B*) of *Cicindela formosa*. The section was taken from a pigmented and iridescent area of the elytron. Granules (*g*) of electron-dense material appear in the exocuticle. Scale bar, 1 μm. (B) Photomicrograph of the same tissue. The epicuticle (*A*) and exocuticle (*B*) are pigmented and highly refractive. Scale bar, 10 μm.

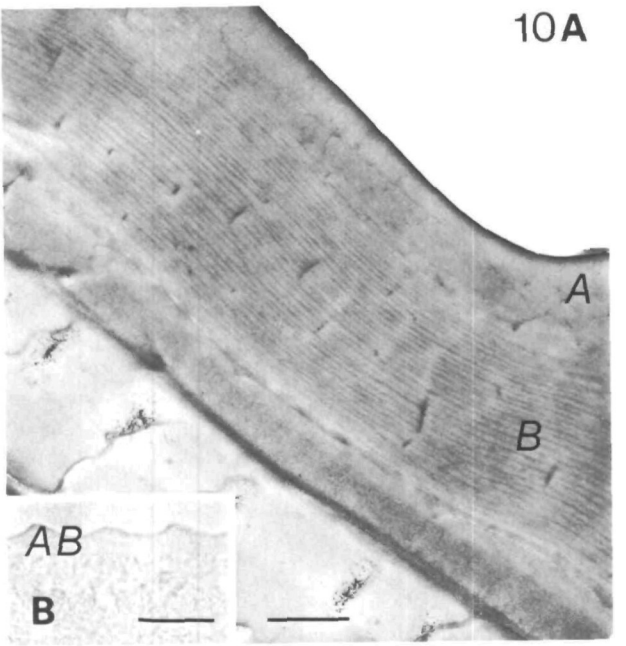

Fig. 10. (A) Transmission electron micrograph of a cross-section of elytral cuticle sectioned from the non-pigmented maculations of *Cicindela formosa*. Electron-dense layers are absent from the epicuticle (*A*). Scale bar, 1 μm. (B) Photomicrograph of the same non-pigmented tissue. The epicuticle and outer exocuticle (*AB*) show no pigmentation or higher refractivity than the underlying cuticle. Scale bar, 10 μm.

that borders the holes in horizontal sections is the outermost layer of the epicuticle, and is electron-lucent in both orientations. Furthermore, horizontal sections within a single epicuticular layer show continuous patches of electron-dense material. This material is very finely particulate when viewed perpendicular to the layer (Fig. 8B).

When thin sections are viewed through an optical microscope, the outer exocuticle and the epicuticle appear dark brown (Fig. 9B). This apparent pigmentation is confined to the outer 5 μm of the elytral cuticle. It is assumed that the dark brown appearance is due to the presence of melanin in this region, and that it is responsible for the dark opaque appearance of the elytron in transmitted light. The epicuticle and outer exocuticle display a greater retardation of light than the inner layers of procuticle under interference microscopy.

Sections of elytral cuticle were also cut from the white maculations of *C. formosa*. The white areas show no trace of either iridescent colour or brown or black pigmentation (Fig. 10B). Under interference microscopy, the sections of white cuticle show a uniformity in refractive index throughout the elytron. The epicuticle shows a refractive index of approximately 1·5 by the Becke line test (Neville, 1980).

Electron micrographs of this non-pigmented cuticle show an epicuticle which lacks the electron-dense bands (layer *A* in Fig. 10A). In general, this homogeneous epicuticle is thinner and lower in contrast than the laminated epicuticle of pigmented areas (layer *A* in Fig. 9A). SEM confirmed the absence of the epicuticular laminations in the region of the elytral maculations. The outer exocuticle of these sections lacks the electron-dense granules that were evident in the exocuticle of pigmented areas (layers *B* in Figs 9A and 10A).

Analysis of cuticle structure by chemical treatment

Tiger beetle cuticle treated with dilute KOH displayed a gradual loss of structural coloration, as well as pigmentation. Immersion in ethanol, xylene, acetone, sulphuric or nitric acid failed to produce any change in structural colour. Initially, structural colours became longer in wavelength as the solvent temporarily swelled the reflectance layers. After 4 h, however, the maroon portion of the elytron of *C. formosa* appeared blue-green. The anterior portion, originally red, became ochreous with slight orange-green reflections. The overall iridescence was reduced to a dull sheen. Scanning electron micrographs of the treated elytra revealed a distorted and heavily eroded surface microsculpture. Under transmission electron microscopy, the regular laminations at the periphery of the cuticle were disrupted and often stripped from the sample (Fig. 11).

With the exception of a few blue-green or violet reflections in the basins of punctures, elytra treated with KOH for 12–15 h were virtually devoid of structural colours. The surface had a flat, brown, darker appearance at the elytral base, which is assumed to be due to the residual presence of melanin in the exocuticle. The deep hexagonal depressions of the surface microsculpture were eroded to a shallow outline of the surface pattern. TEM micrographs revealed that the laminated epicuticle was completely removed from the surface of the outer exocuticle (Fig. 12). A light band, 0·29 μm thick, remained at the border of the exocuticle. The exocuticular lamination also became more obscure and fragmented.

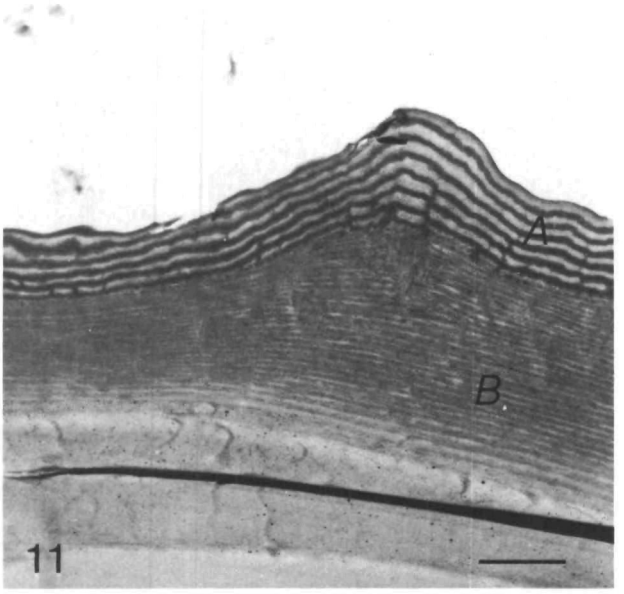

Fig. 11. Transmission electron micrograph of a cross-section of elytral cuticle of *Cicindela formosa* treated for 4 h with 8% KOH. The epicuticular layers are disrupted and partially dispersed. (*A*) epicuticle, (*B*) outer exocuticle. Scale bar, 1 μm.

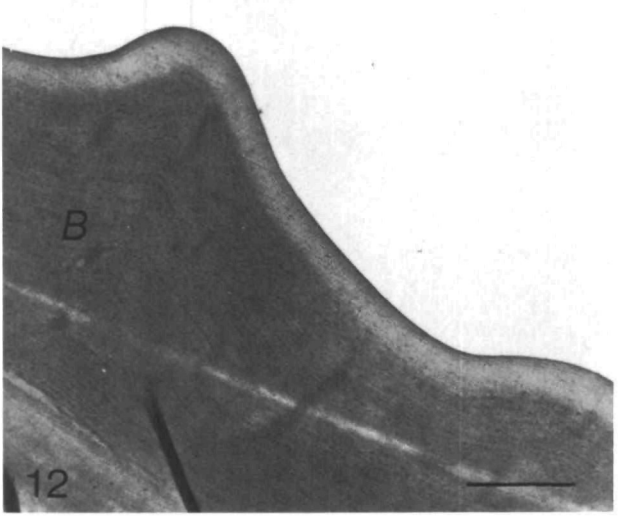

Fig. 12. Transmission electron micrograph cross-section of elytral cuticle of *Cicindela formosa* treated for 15 h with 8% KOH. The epicuticle is dissolved completely. An area of lower electron density appears near the exposed surface of the outer exocuticle (*B*). Scale bar, 1 μm.

J. exp Biol. **117**, 45–68 (1985)
Printed in Great Britain © *The Company of Biologists Limited 1985*

THE PHYSIOLOGY OF WANDERING BEHAVIOUR IN *MANDUCA SEXTA*
II. THE ENDOCRINE CONTROL OF WANDERING BEHAVIOUR

BY OLIVER S. DOMINICK* AND JAMES W. TRUMAN
Department of Zoology, University of Washington, Seattle, WA 98195, U.S.A.

Accepted 27 November 1984

SUMMARY

1. Removal of the prothoracic glands early during the 5th instar of *Manduca sexta* prevented the larvae from wandering and from further development. Infusion of 20-hydroxyecdysone (20-HE) into these larvae induced wandering behaviour.

2. In intact larvae, induction of precocious wandering behaviour required a 20-HE infusion lasting longer than 5 h. Infused 20-HE induced maximal response (90 %) when delivered at a rate of $0{\cdot}06\,\mu g\,g^{-1}$ body weight h^{-1}. At considerably higher concentrations ($0.25\,\mu g\,g^{-1}\,h^{-1}$ larvae performed brief, erratic behaviour or omitted wandering entirely.

3. The latency between appearance of 20-HE and the onset of wandering was dose-dependent with a minimum of 11 h following infusion at $0{\cdot}1\,\mu g\,g^{-1}\,h^{-1}$. Latency was not affected by the duration of 20-HE infusion.

4. The duration of induced wandering behaviour was proportional to the duration of 20-HE infusion. Minimal wandering behaviour lasted 2 h following 20-HE infusions at 5 h, while infusions lasting 11 h induced 9 h of wandering behaviour. Several lines of evidence suggest that the effects of 20-HE accumulate over time and directly determine the duration of wandering behaviour.

5. Many larvae exhibited a series of temporally distinct locomotor periods following various 20-HE infusion protocols, suggesting that a series of separate exposures to 20-HE can result in corresponding serial bouts of locomotion.

6. Responsiveness to 20-HE appeared to be principally modulated by juvenile hormone. Allatectomy of 2nd, 3rd and 4th instar larvae removed juvenile hormone (JH) precociously from these stages and was followed several days later by precocious wandering behaviour. Likewise, application of the JH mimic, EGS, prior to 20-HE exposure or at the start of it, could prevent the behavioural induction. During the 5th instar, 20-HE became increasingly effective in inducing wandering as larvae grew larger than 5 g, the size at which JH normally begins to disappear from the haemolymph. Allatectomized 5th instar larvae responded directly to 20-HE a day sooner than larvae with normal JH titres, but before day 2 the effects of 20-HE on wandering behaviour appear to be indirect, requiring a latency greater than

* Present address: Department of Entomology, Caldwell Hall, Cornell University, Ithaca, New York 14853, U.S.A.

Key words: Behaviour, steroid, endocrinology.

24 h. Several processes, of which the elimination of JH is the last, appear to be required before 20-HE can induce wandering behaviour.

7. Throughout the entire period when 20-HE was acting to induce wandering, the appearance of JH could prevent further induction of behaviour, but the effects of 20-HE which had already been established up to that time were expressed. Thus, application of EGS progressively later during the interval of 20-HE action was progressively less effective in reducing the length of wandering behaviour. The presence of EGS during wandering had no behavioural effect, indicating that only the induction of behaviour by 20-HE is sensitive to modulation by JH.

INTRODUCTION

In many animals steroid hormones have dual actions on the nervous system, and on non-neural tissues, such that changes in behaviour are coordinated with other physiological changes. This is well documented by numerous studies of modification of vertebrate reproductive behaviour by steroids in conjunction with the regulation of gonadal function (Davidson & Levine, 1972; Pfaff, 1980). Steroids also play a fundamental role in regulating invertebrate development (Highnam & Hill, 1977) but their roles in modulating invertebrate behaviour have not been examined closely.

Previous studies of the endocrine control of insect development suggest that the specialized larval behaviour typically preceding pupation might be released specifically by the hormonal environment which induces pupation. During the day prior to wandering in the tobacco hornworm, *Manduca sexta*, the titre of the steroid moulting hormone, 20-hydroxyecdysone (20-HE), rises (Bollenbacher, Vedeckis & Gilbert, 1975) in the absence of juvenile hormone (JH) (Fain & Riddiford, 1975). This unique endocrine milieu induces the characteristic premetamorphic changes in pigmentation (Nijhout, 1976; Hori & Riddiford, 1982) and cuticular commitment (Riddiford, 1978) of the epidermis. Administration of ecdysteroids to a larva of *Hyalophora cecropia* (Lounibos, 1976) and to larvae of *Ephestia* (Giebultowicz, Zdarek & Chroscikowska, 1980) have induced cocoon spinning, suggesting that ecdysteroids may regulate this behaviour.

In addition, several lines of evidence indicate that JH plays an important role in regulating premetamorphic behaviour. Application of JH causes aberrant cocoon spinning in caterpillars of *Hyalophora cecropia* (Riddiford, 1972), *Galleria* (Piepho, 1950) and *Pieris* (Benz, 1973). Furthermore, removal of the corpora allata (CA) from early instar larvae of the silkmoth, *Bombyx*, or the waxmoth, *Galleria*, causes precocious metamorphosis preceded by the construction of a complete, but miniature cocoon (Bounhiol, 1936; Piepho, 1938, 1939).

In this paper we have used *Manduca sexta* to examine the endocrine control of wandering behaviour, a period of continuous locomotion which accompanies the larva's developmental preparation for pupation. During wandering, the larva abandons its feeding habitat, burrows into the soil and constructs a pupation chamber underground (Dominick & Truman, 1984).

MATERIALS AND METHODS

Experimental animals

Larvae of the tobacco hornworm, *Manduca sexta*, were individually raised in the laboratory on an artificial diet as previously described (Truman 1972; Bel & Joachim, 1976) at 26 °C under a short day photoperiod (12L:12D). Lights off was arbitrarily designated as midnight (00.00). The locomotor activity of wandering behaviour in 5th instar larvae was monitored as previously described (Dominick & Truman, 1984) by placing individual larvae in tilt-sensitive actographs in which locomotion was recorded with an Esterline Angus chart recorder. The wandering behaviour of 3rd and 4th instar larvae was recorded with lightweight tilting actographs constructed from thin acetate sheets.

The temporal interval of the gate in which particular larvae would release prothoracicotropic hormone (PTTH) could be predicted on the basis of their weights during the preceding days of the 5th instar (Nijhout & Williams, 1974*a*). In the experiments reported here, larvae weighing more than 7·0 g at 17.00 on day 2 routinely released PTTH during the gate on day 3 (Gate I larvae), while those weighing 7·5–8·8 g on day 3 released PTTH during the gate on day 4 (Gate II). With animals younger than day 2 the errors in predicting the gate increased, but within a group of larvae which entered the 5th instar synchronously those larvae with weights in the top 20 % of a group were typically Gate I, while the smallest 20 % were usually Gate II.

Surgical procedures

The corpora allata (CA) were removed from 2nd, 3rd and 4th instar larvae which were anaesthetized by immersion in water for about 20 min, according to the method described by Kiguchi & Riddiford (1978). The head was flexed back under a thin piece of plastic and the neck membrane pierced laterally with sharpened no. 5 forceps. Each CA was removed from among the tracheae at the ventral lateral regions of the neck. Following allatectomy, the larvae were returned to their individual cups to feed.

The prothoracic glands were removed on day 1, through an incision slightly dorsal and posterior to the prothoracic spiracle from CO_2-anaesthetized 5th instar larvae which were immersed in saline (Ephrussi & Beadle, 1936). The clustered glandular tissue was found branching over the tracheae, and was carefully separated from its numerous fine tracheal attachments with no. 5 forceps. Particular care was needed to liberate the long branch which projects into the head region without breaking off the terminal lobe of that branch. The incision was subsequently closed with 6–0 gauge braided silk sutures, and the larvae were then returned to their feeding cups.

Ecdysteroid treatments

20-hydroxyecdysone (20-HE) (Rhoto Pharmaceutical, Osaka, Japan) was dissolved in *Manduca* saline (Cherbas, 1973) and concentrations were confirmed spectrophotometrically (E_{240}=12 670; Meltzer, 1971). Larvae were anaesthetized with CO_2 and either received an injection of 20-HE into an abdominal proleg or were infused with the 20-HE solution *via* a long polyethylene catheter (PE-10; Clay Adams)

inserted into the head capsule and stabilized with Tackiwax (Cenco). A 50-μl Hamilton syringe mounted on a syringe pump (Sage Instruments, model 355) was used to deliver the 20-HE solution through the tubing. Solutions were usually infused at a rate of 5 $\mu l\,h^{-1}$, and 20-HE concentration was varied accordingly. Larvae recovered from anaesthesia and remained in their feeding cups during the infusion and were subsequently placed in the actographs without food.

EGS treatment

The JH mimic, 6,7-epoxygeranyl-3′,4′–methylene dioxyphenyl ether (epoxygeranylsesamole, EGS) (Bowers, 1969) (Insert Control, Inc.) was dissolved in cyclohexane (Baker, Inc.) and 10 $\mu g\,\mu l^{-1}$ was applied to the dorsal intersegmental region of unanaesthetized larvae. Mosaic pupae produced by this treatment were scored using the method of Truman, Riddiford & Safranck (1974) in which 0 represents normal pupation and 5 indicates almost completely larval cuticle.

RESULTS

The role of ecdysteroids

Effects of prothoracic gland removal

Prothoracic glands (PTG) were completely removed from four larvae on day 0 of the 5th instar. These larvae grew slowly and continuously to a maximum weight of 15–18 g over the next 12 days, whereas sham-operated larvae wandered by day 6 and pupated by day 10. The PTG– larvae survived for nearly a month without ever showing wandering behaviour, the morphological changes associated with this behaviour, or any sign of pupation.

Sham-operated larvae wandered as usual, although the onset of wandering was often delayed by 1 or 2 days. Of 10 larvae in which removal of the PTG was unsuccessful (as determined by the presence of remnant PTG fragments as small as four cells during subsequent dissection) nine wandered in the gate following attainment of 7–9 g. Most of these wandered by the second gate (day 5) but three larvae grew unusually slowly following surgery and delayed wandering as late as day 8 (Gate V). Therefore, in subsequent experiments requiring PTG– larvae we used only those which reached 7–9 g by day 4 and which failed to wander by Gate III (day 6).

One such larva from which prothoracic glands had been completely removed on day 0 was infused with 50μg of 20-HE (1 $\mu g\,\mu l^{-1}$ at 5 $\mu l\,h^{-1}$) over 10 h on day 6. This treatment resulted in appearance of the dorsal vessel and a 6 h period of wandering beginning 13 h after the start of infusion. This larva never retracted its ocellar pigment or pupated, and, until it died several weeks later, it showed sustained locomotor activity lasting 1–2 h whenever disturbed.

In further experiments, larvae were allatectomized following PTTH release in the 4th instar so that, following removal of their prothoracic glands on day 0 of the 5th instar, there would be no post-surgical, JH-mediated effects on ecdysteroid sensitivity. All unsuccessfully operated larvae wandered by day 6 as described above. Those that showed no wandering were subsequently infused with dosages of 20-HE varying from 5–50 μg over 10 h beginning at 17.00 on day 6 ($N=11$). A wandering response

Table 1. *Effect of 20-HE infusions on wandering behaviour in larvae lacking corpora allata and prothoracic glands*

Dose (μg)	*N*	Latency (h ± S.E.M.)	Wandering duration (h)
5	2	17	6·5
40	5	11 ± 0	5 ± 1
50	2	12·5 ± 0·5	6 ± 0

Infusions were for 10 h at a rate of 5 μl h^{-1} for 50 μl of 20-HE solutions containing 0·1 μg μl^{-1}, 0·8 μg μl^{-1} or 1·0 μg μl^{-1}.
Latency is relative to start of infusion.

was induced in 80 % of the larvae (Table 1). With a relatively small 20-HE dose (5 μg delivered as 0·1 μg μl^{-1} at 5μl h^{-1} over 10 h) the latency between the start of infusion and behavioural onset was longer than that seen after the larger dosages (40–50 μg). Wandering duration in these larvae was 5-6 h regardless of 20-HE dose.

Parameters of ecdysteroid exposure

The effect of prothoracic gland removal clearly implicated ecdysteroids in the induction of wandering behaviour. The role of ecdysteroids was further explored by treating larvae with intact PTG with exogenous 20-HE on the day prior to PTTH and ecdysteroid secretion. Initial experiments involved injecting Gate II larvae with varying amounts of 20-HE (5–100 μg) at 20.00 on day 3. As had been noted earlier by Nijhout (1976), a single injection proved to be a poor mode of delivery for ecdysteroids. Only one larva out of 39 showed early wandering after such treatment. The remainder wandered at their expected time or were delayed for up to 1 day.

To imitate the prolonged exposure to 20-HE which occurs during endogenous hormone secretion (Bollenbacher *et al.* 1975), presumptive Gate II larvae were

Table 2. *The effects of infusing different dosages of 20-HE into presumptive gate II larvae*

Dose (μg)	*N*	% Early	Latency (h ± S.E.)	Duration of induced wandering (h ± S.E.)	% Repeat wandering	Duration of repeat wandering (h ± S.E.)
0*	10	0	(36 ± 2)	(20 ± 4)	0	0
0·30	10	10	14	4	100	16
0·75	8	0	–	0	0	0
1·5	10	70	20 ± 1	6 ± 1	71	7 ± 2
3·5	8	88	15 ± 1	9 ± 2	71	4 ± 1
7·0	8	88	18 ± 2	5 ± 1	89	9 ± 2
15	9	66	14 ± 1	7 ± 1	66	4 ± 1
25	10	90	13 ± 1	7 ± 1	89	9 ± 2
50	21	52	12 ± 1	3 ± 1	40	8 ± 3
100	8	63	11 ± 1	4 ± 1	20	3 ± 1

Solutions were infused over 10 h starting at 19.00 on day 3 using 20-HE concentrations to give the total dose indicated.
* Saline-infused controls with latency and duration for normal wandering in parentheses.

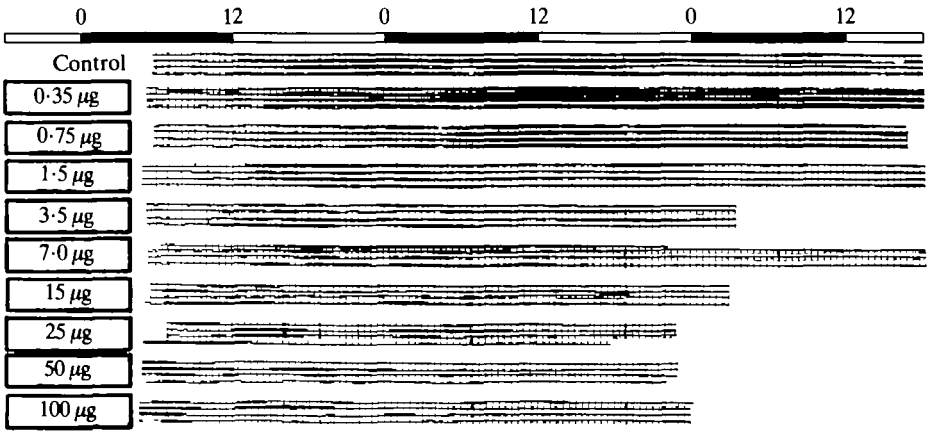

Fig. 1. Activity records of larvae infused with different dosages of 20-HE. Presumptive Gate II larvae were infused with varying dosages of 20-HE (from 0·35–100 μg, as marked) over a 10-h interval (delimited by box surrounding 20-HE dosage) beginning at 19.00 on day 3. For each treatment, the original tilt-dish activity records of four larvae showing typical responses to the hormone are shown. The 12L : 12D photoperiod is shown by the light and dark bars at the top of the figure.

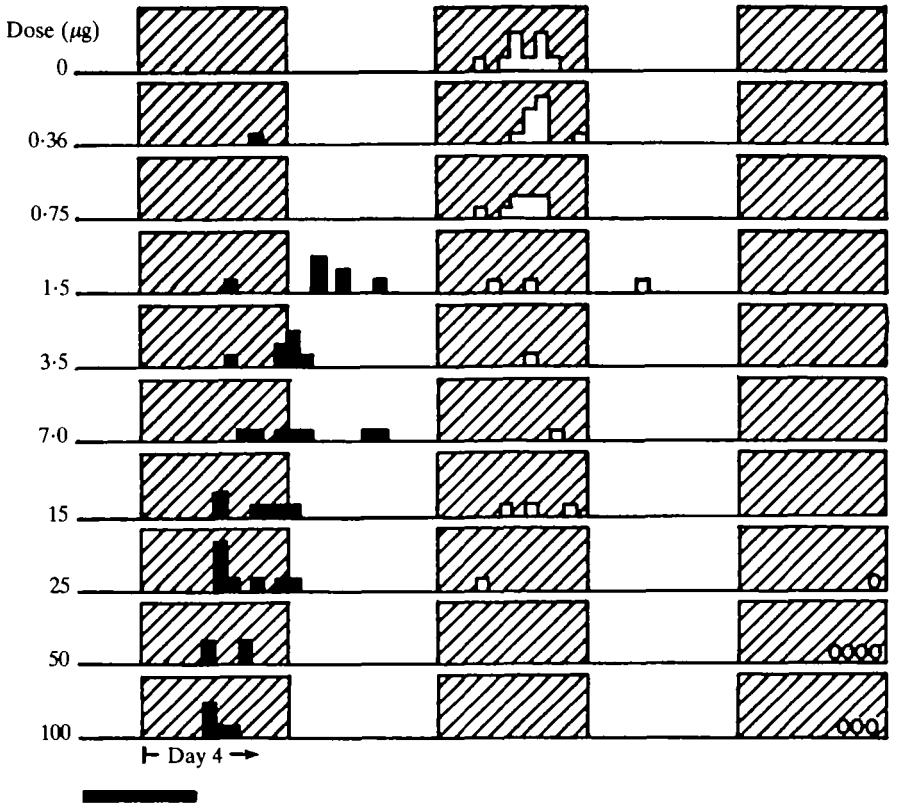

Fig. 2. Onset times of wandering in response to infusions of differing dosages of 20-HE. Data are from the experiment described in Fig. 1. The black bar represents the interval during which 20-HE was infused for each group of larvae. Histograms designate the starting times for wandering behaviour after each treatment. Onset times which are equivalent to Gate II controls are shown as open squares, and advanced onset times are shown as black squares. Larvae which failed to wander are indicated by an open circle to the right. The 12L : 12D photoperiod is represented by the light and cross-hatched background.

infused with varying amounts of 20-HE over a 9-h period beginning at 19.00 on day 3 (Table 2) to ensure that exogenous 20-HE appeared well before the time of endogenous ecdysteroid secretion. Animals infused with less than 1·5 μg of 20-HE were rarely observed to wander earlier than their expected gate (Figs 1, 2). With infusions of 1·5 μg or more, wandering began at progressively earlier times as the hormone dose increased, but even with extremely large doses (up to 100 μg), the minimal latency between the beginning of the infusion and behavioural onset was 11 h (Fig. 2). Indeed, at the larger doses, wandering was often delayed by 1 day or omitted. The duration of induced wandering varied from 3–9 h, independent of dose (Fig. 1; Table 2).

As seen in Fig. 3 there was a clear dosage optimum for the induction of wandering locomotion by 20-HE. In Gate II larvae the incidence of early wandering rose from 10 % to about 90 % as the infused 20-HE dose increased from 0 to 5 μg. Presumptive Gate I larvae showed essentially the same dose-response relationship but the proportion responding at each dose was 20–30 % lower (Fig. 3). At higher doses a gradually increasing number of animals omitted the behaviour, in spite of the appearance of the dorsal vessel, such that at 50 μg and above, between 40 % and 50 % of the infused larvae failed ever to show wandering locomotion.

In the ecdysteroid-infused larvae the dorsal vessel appeared prematurely (Fig. 4) as previously reported by Nijhout (1976). Interestingly, the induction of wandering

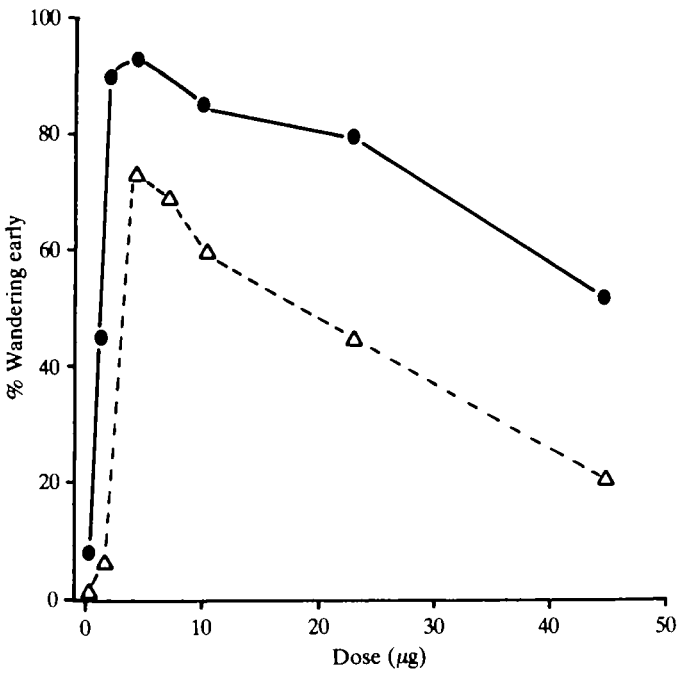

Fig. 3. The effectiveness of 20-HE infusions for inducing wandering behaviour as a function of hormone dose. After infusion with different dosages of 20-HE as described for Fig. 1, the proportion of Gate II larvae which began wandering earlier than the normal gate was noted (filled circles). In a parallel experiment, presumptive Gate I larvae were infused with 20-HE on day 2, and wandering response was observed (open triangles). The value of each point is based on 10–40 larvae.

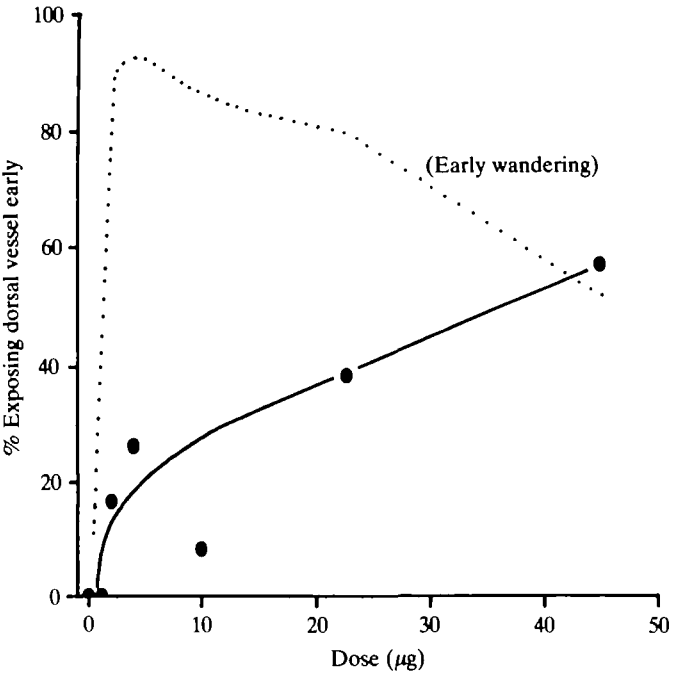

Fig. 4. The effect of infused 20-HE on heart exposure. The time when the heart was exposed following 20-HE infusion was noted for the Gate II larvae described in Fig. 1 ($N = 10$–40 per point). For each dose, the solid circles indicate the proportion of 20-HE infused larvae exposing their hearts earlier than usual. For comparison, the dotted line reiterates the behavioural response (Fig. 3) of these larvae at these dosages.

behaviour was more sensitive to the infused 20-HE than were the epidermal changes. Thus, the behavioural responses to 20-HE can occur in the absence of obvious peripheral changes that normally occur at the same time.

The relationship between dose and the apparent requirement for prolonged exposure to the hormone was examined by varying dosage and duration of 20-HE infusion over a wide range. Fig. 5 summarizes the results of an experiment in which Gate II larvae received a total dosage of 5 μg of 20-HE (as a 0·1 mg ml^{-1} solution) infused over time periods which varied from a single instantaneous injection to 10 h. The effectiveness of the 5 μg dosage in inducing early wandering increased abruptly as the length of exposure to hormone exceeded 4 h with 54 % of the larvae wandering in response to a 5-h infusion, and the maximal response of 80 % occurring after 8–10 h of infusion. The results (Figs 3–5; Table 3) indicate that the maximal behavioural effectiveness of 20-HE occurred under relatively limited conditions of low hormone dose (2–15 μg) and long infusion time (8–10 h).

Effects of 20-hydroxyecdysone on wandering duration

Possible relationships between the amount of ecdysteroid infused and the duration of wandering behaviour are complicated by the existence of overdosage effects which result in the omission of wandering behaviour. Consequently we examined temporal aspects of ecdysteroid exposure on the behaviour of the animal by infusing low dosages of 20-HE (0·5 μg h^{-1}) for varying amounts of time beginning at 19.00 on day 3.

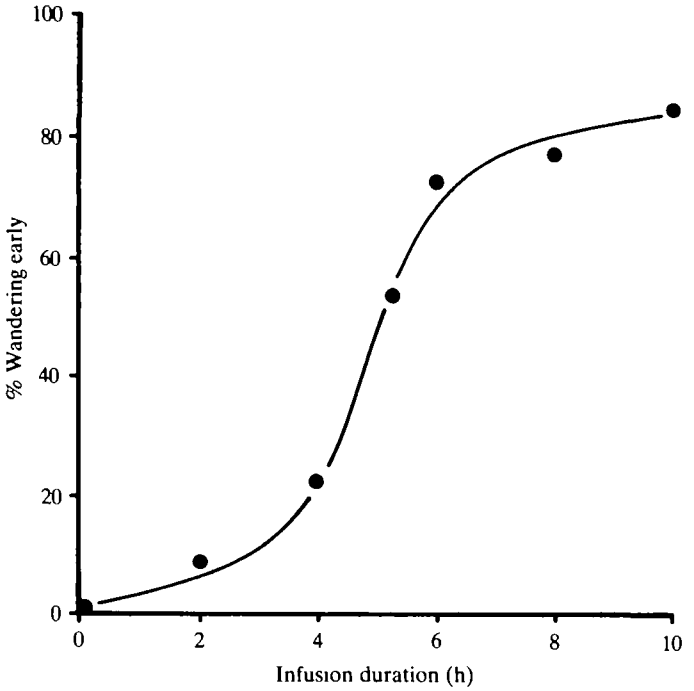

Fig. 5. The length of 20-HE infusion needed to induce wandering behaviour. A total dose of 5 μg of 20-HE was infused into presumptive Gate II larvae over a 0-(single injection) to 10-h period, beginning at 20.00 on day 3. The proportion of larvae wandering earlier than saline-infused controls is plotted for each infusion duration (N = 10–40 animals per point).

Infusions lasting 3 h or less were ineffective in inducing early wandering (Figs 6, 7).

As the length of the infusion increased to 5 h or more, precocious wandering appeared in increasing numbers of larvae. Importantly, the interval between the start of the infusion and behavioural onset was constant regardless of infusion duration, averaging 14±1 h (N=53), indicating that the initiation of wandering was not accelerated by increasing the duration of 20-HE exposure.

The systematic lengthening of the time of 20-HE infusion caused a proportional increase in the average duration of induced wandering behaviour, from a minimum

Table 3. *The effect of infusion of 20-HE for varying lengths of time*

Infusion duration (h)	Total dose (μg)	N	% Early	Latency (h ± S.E.M.)	Induced duration (h ± S.E.M.)	% Repeat	Repeat duration (h)
0(control)	0·0	25	0	(36 ± 2)	(20 ± 2)	0	0
1	0·5	7	0	–	–	–	–
3	1·5	19	0	–	–	–	–
5	2·5	16	50	16 ± 2	2 ± 0·5	100	9 ± 1
7	3·5	23	61	13 ± 1	5 ± 1	57	4 ± 1
9	4·5	26	73	13 ± 1	7 ± 1	63	9 ± 2
11	5·5	17	71	15 ± 1	9 ± 1	67	8 ± 2

Presumptive Gate II larvae were infused with 0·5 μg 20-HE h^{-1} beginning at 19.00 on day 3.

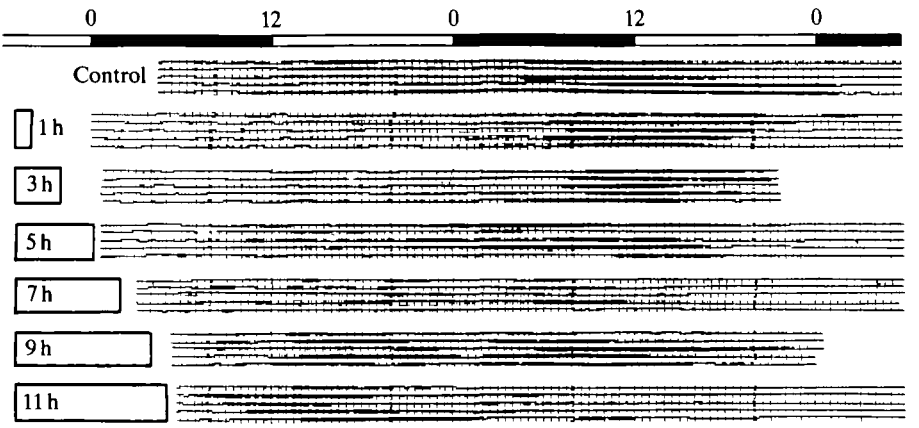

Fig. 6. Activity records of wandering behaviour induced by varying the length of infusion of a constant 20-HE concentration. Predicted Gate II larvae were infused with 20-HE at a rate of 0·5 μg h^{-1} for varying lengths of time from 1–11 h starting at 19.00 on day 3 (as indicated by the numbers and the white bars at the left side of the figure). Typical records from five larvae responding in each experimental group are shown. Records of uninfused control Gate II larvae are also shown. The 12L : 12D photoperiod is shown as light and dark bars at the top of the figure.

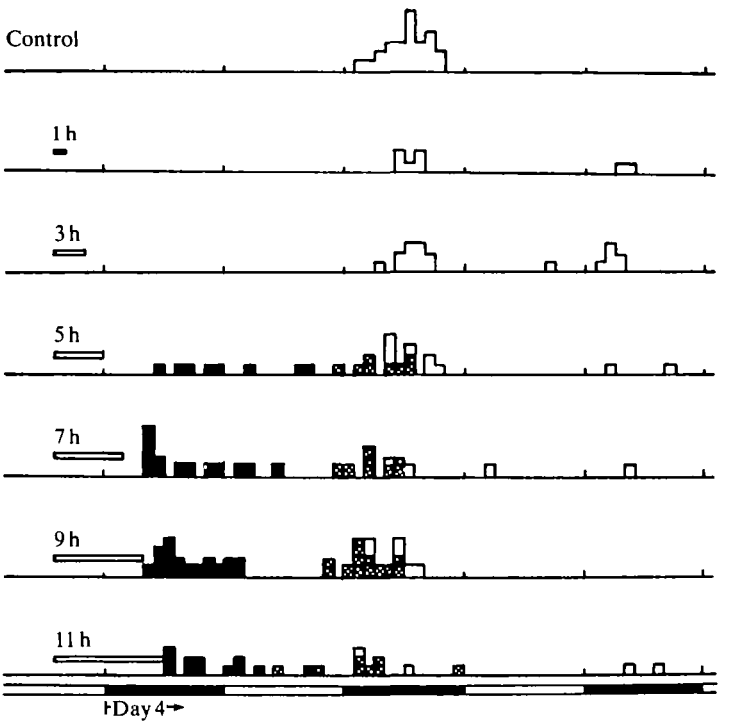

Fig. 7. Onset of wandering behaviour induced by 20-HE infusions of varying duration. Data represent the behaviour of all larvae infused in the experiment for which representative activity records were shown in Fig. 6. Each group of 20-HE infusions is illustrated as a thin white bar on the left side of the figure, and is labelled with the duration in hours. Black histograms represent onset times of wandering which were earlier than control Gate II times (which are shown as white histograms). The appearance of a second bout of wandering is shown as a cross-hatched histogram. The 12L : 12D photoperiod is shown below the figure.

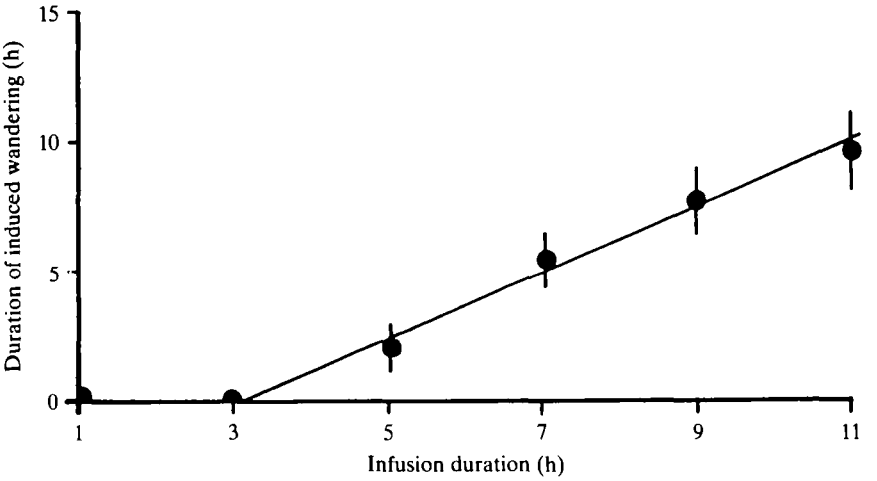

Fig. 8. The control of wandering duration by length of 20-HE infusion. The durations of early bouts of wandering behaviour induced by the 20-HE infusions of varying length (as described in Figs 6 and 7) were measured and plotted (mean ± S.E.) with reference to the length of the 20-HE infusion ($N = 7$–26 per point; see Table 3). The line calculated by linear regression ($y = 1{\cdot}2x + 3{\cdot}2$) represents a significant correlation ($r = 0{\cdot}9$; $P < 0{\cdot}01$).

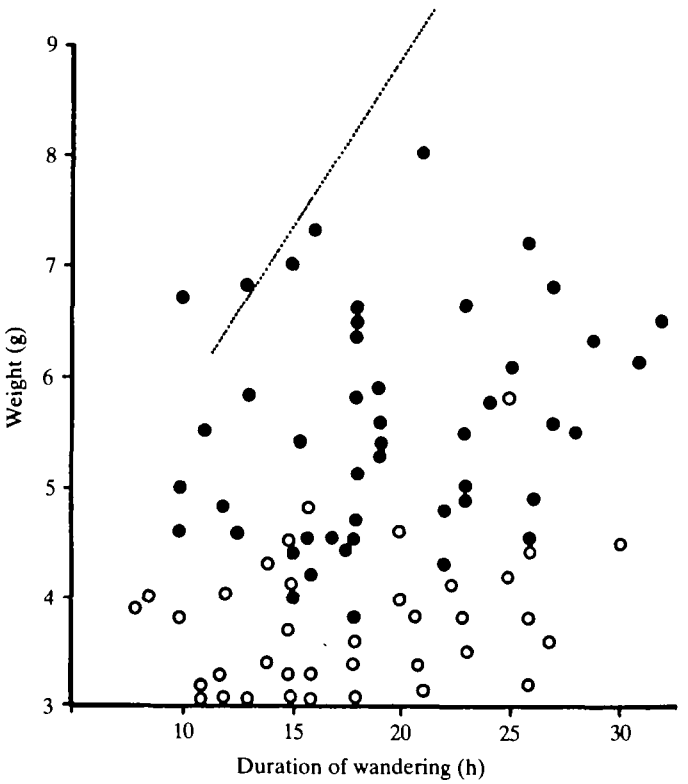

Fig. 9. Relationship between weight and wandering duration in allatectomized larvae. Weights were taken at 17.00 on day 1 and day 2 for Gate I (open circles) and Gate II (filled circles) larvae respectively. The correlation coefficient ($r = 0{\cdot}09$) is not significant. The dotted line indicates the regression line for Gate I and II larvae with intact CA (Dominick & Truman, 1984).

of 2 h in response to a 5-h infusion, to 9 h of locomotion after 11 h of 20-HE infusion (Fig. 8). Infusions longer than 11 h were impractical because wandering often started before the infusion was completed.

Following the period of early wandering induced by 20-HE, many of the larvae appeared to wander a second time, early in their normal wandering gate (Figs 1, 6; Table 2). The length of this second behavioural period was shorter than that of control animals, lasting less than 10 h, and bearing no relationship to the dose of hormone infused.

The role of juvenile hormone

Effects of removal of the corpora allata

A number of previous experiments indicate that the induction of cocoon spinning behaviour of various caterpillars is inhibited by JH secreted from the CA (Bounhiol, 1938; Piepho, 1939, 1950, 1960; Riddiford, 1972; Akai & Kobayashi, 1970; Benz, 1973). We initially examined the role of the CA in wandering of *Manduca* by removing these glands from 4th instar larvae on the day prior to ecdysis to the 5th instar (14–18 h after PTTH and ecdysone release). Under this protocol successful allatectomy was clearly indicated by melanization of the new 5th instar cuticle (Kiguchi & Riddiford, 1978). These larvae began wandering during gates on the third and fourth nights following ecdysis, 1 day earlier than the wandering gates for sham-operated larvae (Nijhout, 1975*b*; Kiguchi & Riddiford, 1978). As with the onset of wandering in sham-operated controls, the wandering gates for allatectomized larvae were about 8–9 h wide during the scotophase and showed a 'gating bias' (Pittendrigh & Skopik, 1970) such that larvae began wandering later during the first gate than they did during the second.

In contrast to the correlation between larval size and average wandering duration in normal larvae (Dominick & Truman, 1984) there was no correlation between larval size and the duration of wandering (average, 19·5 h) in allatectomized 5th instar larvae (Fig. 9). The observation supports the earlier suggestion (Dominick & Truman, 1984) that the correlation between larval size and wandering duration is based on JH effects.

Larvae were also allatectomized early in the 2nd, 3rd and 4th instars. These larvae wandered during a broad gate on the third scotophase following surgery for an average of 10 h (3rd instar) to 19 h (4th instar). Detailed data were not collected from the tiny 2nd instar larvae. These results indicate that wandering can be induced by the appearance of ecdysteroids in any larval instar following the elimination of JH.

Effects of exogenous juvenile hormone

The above results suggest that JH may inhibit the performance of wandering behaviour when early instars are exposed to ecdysteroids and it may modulate the expression of wandering behaviour by the last instar larvae. When the JH mimic, EGS, was applied to Gate II, 5th instar larvae at progressively later times up until about 05.00 during the scotophase of day 4, the wandering gate was delayed by 1–3 days (Fig. 10). Throughout this period, progressively later EGS applications became increasingly effective both in causing the retention of larval characteristics at pupation

Fig. 10. Effect of EGS on onset of wandering. EGS (10 μg) was applied topically to Gate II larvae at various times (arrows) during the day prior to wandering. Following EGS treatment, the onset times of wandering were recorded in tilt-dish actographs and are shown as black histograms. The starting times of a distinct second wandering period which occurred in many of these larvae are also shown (open histograms). The distribution of wandering onset times in untreated Gate II larvae is shown in the top panel. The cross-hatched areas represent scotophases, beginning with day 4.

(Truman *et al.* 1974; personal observations) and in reducing the duration of wandering in the delayed gates to as little as 1 h.

Between 05.00 and 06.30 there was an abrupt increase in the proportion of EGS-treated larvae which wandered in their expected gate, although the onset time within the gate was influenced by the treatment. Thus, the ability of EGS applications to postpone wandering declined sharply during this period, as did its effectiveness in causing the retention of larval features at pupation (Truman *et al.* 1974).

Fig. 10 also shows that in response to EGS applications over the 9-h period beginning at about 06.30, wandering in the normal gate was followed by a second gated period of wandering in about 25 % of the larvae. The onset times of the repeated behaviour usually coincided with the start of wandering for animals which had been delayed by 1 day. Furthermore, wandering behaviour in this gate was extremely short: 2 ± 1 h for repeats; 5 ± 2 h for delayed larvae.

Although treatment with EGS after 06.30 could no longer delay the onset of wandering, it still had a marked effect on the duration of the behaviour (Fig. 11). With application of EGS at 06.30, 63 % of the treated larvae wandered in their usual gate, but the average duration of locomotion was only 2 ± 1 h. As EGS was applied at progressively later times, the duration of wandering increased proportionately until 15–20 h later, at which time behavioural duration could no longer be affected by EGS. Thus, it appears that the duration of wandering behaviour is determined by the gradual accumulation of effects of a process sensitive to interference by JH over an approximately 20-h period on the day prior to wandering.

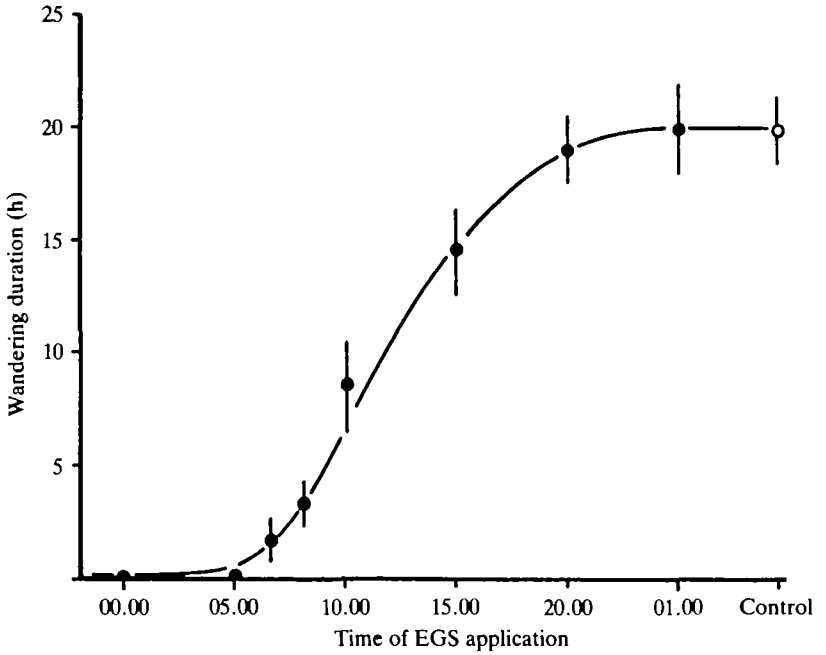

Fig. 11. Effect of EGS application on Gate II wandering duration. The duration (shown as mean ± S.E.) of wandering behaviour during the second gate (day 5) was measured in tilt-dish actographs following the EGS applications described in Fig. 10 ($N = 11–19$ per point).

Interaction between juvenile hormone and ecdysteroids

Effects of EGS application during 20-HE infusion

The above results show that appropriately timed applications of the JH analogue, EGS, during the period of endogenous 20-HE secretion, caused systematic changes in the duration of wandering. We examined whether this was due to the progressive interference with the 20-HE effects which normally lead to the 20 h long wandering behaviour. Gate II larvae were infused with 5 μg of 20-HE over 10 h starting at 00.00 on day 4, and 10 μg of EGS was administered either at the start of the infusion or 6 h later. As seen in Table 4, both EGS-treated groups of the larvae which wandered exhibited a duration of locomotion which was shorter than that seen when the 20-HE infusion was given alone. Those receiving EGS at the onset of ecdysteroid infusion

Table 4. *Effects of ECG treatment during 20-HE infusion into Gate II larvae*

EGS application time	*N*	% Early (*N*)	Induced duration (h ± S.E.M.)	Latency* (h ± S.E.M.)
00.00	29	38(11)	1·5 ± 0·5	15 ± 1
06.00	25	84(21)	5·5 ± 0·5	14 ± 0·5
none	20	85(17)	8·1 ± 1	14 ± 1

Gate II larvae were treated topically with 10 μg of EGS (1 μg EGS μl^{-1} cyclohexane) during 20-HE infusion (5 μg 20-HE over 10 h beginning at 00.00 on day 4).

* Latency is relative to start of 20-HE infusion.

only wandered for 2 h whereas those receiving EGS 6 h later spent 6 h wandering. Importantly, the time of EGS application did not alter the interval between the start of the infusion and the onset of induced wandering, which remained at 14–15 h.

In larvae receiving EGS during the period of endogenous or infused ecdysteroid action, wandering ended abruptly at about 16 h following the time of EGS application. The animals treated with EGS at the start of infusion showed a duration of wandering that was similar to larvae that had received 6 h of uninterrupted ecdysteroids. This relationship is consistent with the proposed 5-h equilibration period for topically applied EGS (Riddiford & Ajami, 1973).

The development of sensitivity to 20-HE

The effects of both allatectomy and EGS application on wandering behaviour are consistent with the idea that ecdysteroids must act in the absence of JH to induce wandering (Nijhout & Williams, 1974*b*; Truman *et al.* 1974). It was therefore important to determine when the 5th instar larvae acquired competence to wander in response to 20-HE, and to relate this to the normal fluctuation of the JH titre in larvae. When larvae were infused with 5 μg 20-HE over 10 h prior to 16.00 on day 2, wandering was not directly induced by 20-HE (Fig. 12). Many of these larvae (57 %) delayed

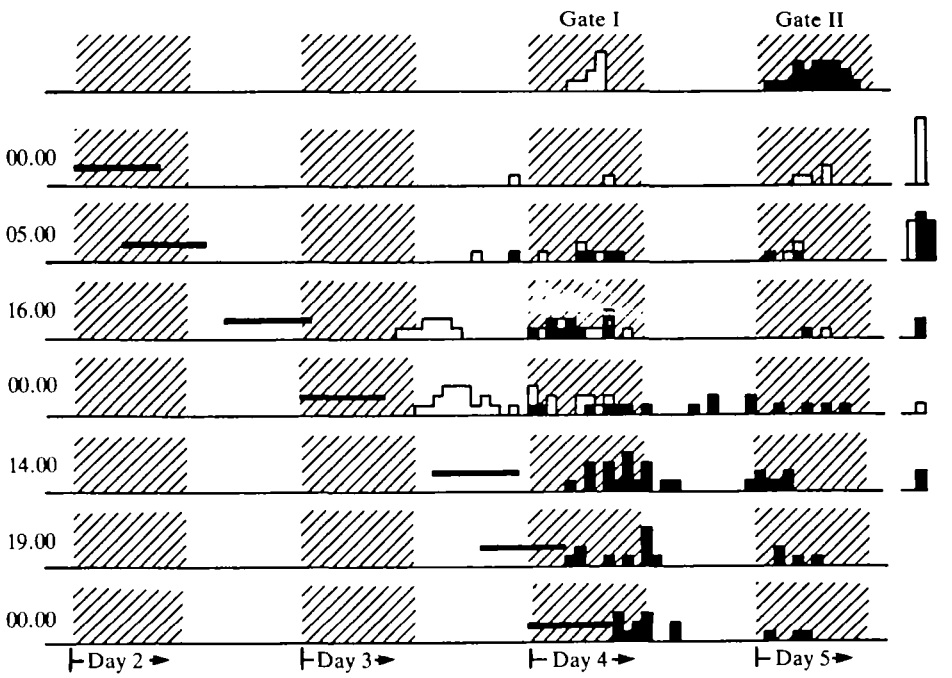

Fig. 12. The development of behavioural sensitivity to 20-HE during the 5th instar. Larvae were predicted to be either Gate I or Gate II by weight at different times during the 5th instar and were then infused with 20-HE (5 μg over 10 h) as indicated by the black bar to the left of each group. The subsequent wandering onset time was recorded in a tilt-dish actograph for each larva and is shown for predicted Gate I (white histograms) and Gate II (black histograms) larvae. The normal onset times for wandering in Gate I and Gate II larvae are shown at the top of the figure. Larvae wandering later than their normal gate are grouped to the right of each treatment.

wandering past the second gate as a result of starvation following the hormone treatment. By 16.00 on day 2, about 36 h before the first wandering gate was expected, infused 20-HE induced a clear wandering response in 67 % of the larger larvae with a mean latency of 25 ± 1 h. Most of the smaller, presumptive Gate II larvae were shifted to the first gate with a latency of more than 36 h from the start of the infusion. When 20-HE was infused into presumptive Gate I larvae starting at 00.00 on day 3 the response latency was further reduced to 16 ± 1 h. A similar pattern of declining latency associated with later infusions also occurred in the Gate II larvae. Therefore, once behavioural responsiveness to 20-HE had clearly appeared in one size class of larvae, later infusions decreased the interval between the start of infusion and the onset of behaviour from 20–25 h during the early stages of sensitivity, to 11–14 h when full sensitivity had been acquired.

The behavioural response to 20-HE was analysed in terms of larval size at the start of the infusion (Fig. 13). Prior to attaining a weight of 5·5 g, the onset time of wandering could not be advanced by 20-HE and was delayed by starvation following

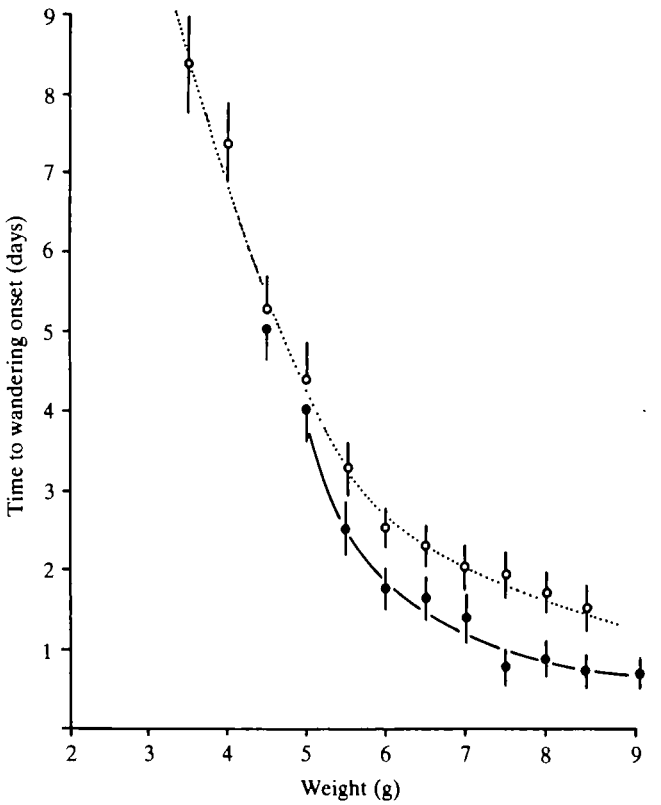

Fig. 13. Development of sensitivity to 20-HE as a function of larval weight during the 5th instar. Latencies to wandering were obtained from the results in Fig. 12 and were grouped according to weight at the time of 20-HE infusion. Open circles represent the latency (mean ± S.E., $N = 8–15$) to wandering of uninfused, starved control larvae; filled circles show the latency for larvae of each weight class ($N = 9–27$) following infusion with 20–HE (5 μg over 10 h).

20-HE infusion, as expected from the results of Nijhout & Williams (1974*a*). As larvae grew beyond 5·5 g, 20-HE infusion caused increasingly pronounced advancement of the behaviour relative to control larvae.

The appearance of sensitivity to 20-HE when the larvae attained a weight of 5·5 g supports the idea that the size-dependent decline of JH which begins at a critical weight of about 5 g (Nijhout & Williams, 1974*b*; Nijhout, 1975*a*) initiates competence for wandering in response to 20-HE. When allatectomized 5th instar larvae were infused with the standard dosage of 5 μg of 20-HE over 10 h, a slow but pronounced wandering response was evoked in 82% of the larvae by infused 20-HE as early as 14.00 on day 1, about 56 h prior to the expected wandering gate (Fig. 14). In these cases the latencies were exceptionally long, being 36 ± 4 h. Infusions before this time had a weaker, (but still significant) effect, in that larvae wandered in the normal gate 1 day earlier than fed, allatectomized controls. Such long latencies for response again suggest that very early 20-HE infusions had only an indirect effect on wandering even in allatectomized larvae. Later infusions required a shorter (13 h) latency, indicating direct induction of wandering by 20-HE.

The relationship between larval size and induction of wandering in these infused, allatectomized larvae is shown in Fig. 15. In the absence of JH, even 1·5-g larvae showed a behavioural response to 20-HE. Although the response had a very long latency (3·5 ± 0·5 days), these larvae wandered several days before the equivalent saline-infused controls. These exceptionally long latencies suggest that early 20-HE treatment might be acting indirectly by altering the normal timing mechanism for wandering rather than directly inducing the behaviour. Infusion of a much larger dose

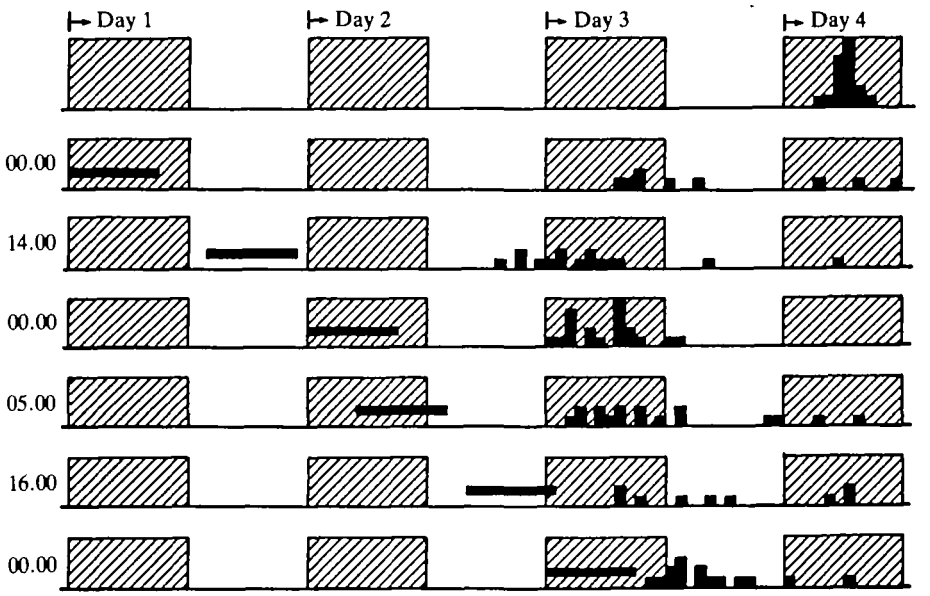

Fig. 14. Development of behavioural sensitivity to 20-HE in allatectomized larvae during the 5th instar. The time of wandering onset was recorded in tilt-dish actographs following 20-HE infusion (5 μg over 10 h) (black bars) into allatectomized larvae at various times during the 5th instar. The onset time for uninfused, allatectomized larvae is shown as a histogram at the top of the figure.

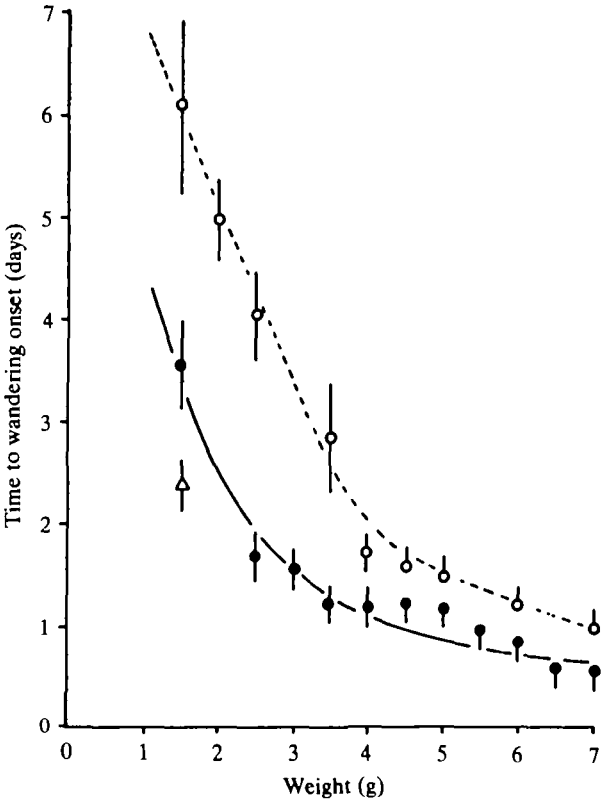

Fig. 15. Development of sensitivity to 20-HE as a function of weight during the 5th instar in allatectomized larvae. The latencies to wandering behaviour were obtained with respect to weight from the results shown in Fig. 15. Open circles show latency (mean ± S.E.) for uninfused, allatectomized controls ($N = 6$–12). Filled circles show the latency to wandering in each weight class following 20-HE infusion ($N = 9$–17). The open triangle represents the latency to wandering in response to a 20-HE infusion of 40 μg over 10 h ($N = 6$).

of 20-HE (40 μg) at this time resulted in a substantial reduction of the latency to 2·5 ± 0·2 days. As larvae grew past 1·5 g the latency following infusion of 5 μg over 10 h decreased rapidly, but it remained in excess of 24 h until, in 5- to 6-g larvae, the latency decreased to a minimum of about 15 h.

DISCUSSION

The role of ecdysteroids

Ecdysteroids have been implicated in the premetamorphic behaviour of the giant silkworm, *Samia cynthia* (Fujishita, Ohnishi & Ishizaki, 1982), *Hyalophora cecropia* (Lounibos, 1976) and *Ephestia kuhniella* (Giebultwicz *et al.* 1980). The results reported in this paper show that the wandering behaviour of *Manduca* larvae is induced by 20–HE. The requirement for ecdysteroids was shown by removing the prothoracic glands, the source of ecdysone, from larvae. This prevented the appearance of wandering behaviour as well as all other developmental changes known to require ecdysteroids. When these larvae were infused with 20-HE, wandering was induced,

followed by a state of quiescence from which bouts of locomotion could be briefly re-evoked by disturbance. This post-wandering excitability represented a distinct behavioural state of the larvae, persisting until the larvae died several weeks later without undergoing any further development.

The effectiveness of 20-HE in activating wandering was a function of the dose and duration of the hormone treatment as well as of the JH environment. Prolonging the exposure to 20-HE by multiple injections or continuous infusion has previously been shown to enhance the effect of this hormone compared with single injections (Ohtaki, Milkman & Williams, 1968; Zdarek & Fraenkel, 1970; Nijhout, 1976). The observation is particularly pertinent to the induction of wandering behaviour, where even large amounts (up to 100 μg) of injected 20-HE were unsuccessful in causing wandering. Prolonged exposure to 20-HE was necessary to induce a behavioural response. The maximal effectiveness of this treatment was reached with 9- to 10-h infusions of the steroid. The most effective infusion rate was 0.5 $\mu g\,h^{-1}$ or 0·06 $\mu g\,g^{-1}$ body weight h^{-1}. This rate of 20-HE delivery is consistent with the levels of ecdysteroid that are normally seen preceding wandering, ie. 0·07 $\mu g\,ml^{-1}$ (Wielgus, Bollenbacher & Gilbert, 1979).

Dosages greater than the optimal amount resulted in increasingly disrupted behaviour and at 5 $\mu g\,h^{-1}$ about 50 % of the larvae omitted wandering entirely (Fig. 3). In the silkmoth, *Samia cynthia*, large amounts of 20-HE caused an acceleration and compression of the early events of adult development (Williams, 1968). A similar effect of large infused dosages of 20-HE may accelerate the response of *Manduca* larvae such that they compress part or all of the spontaneous wandering period. Curiously, pupation was not noticeably advanced in such larvae. Thus, in order to activate the physiological process leading to wandering behaviour, an adequate, but not excessive, 20-HE concentration must be maintained in the larva for a sustained period of time.

Within the range of 20-HE infusions which induced wandering, the latency between the beginning of the infusion and behavioural onset varied with the rate of the infusion. A 20-h latency was seen when the 20-HE concentration was at the lower limit of effectiveness (0·15 $\mu g\,h^{-1}$) (Fig. 2; Table 2). This latency gradually shortened as dose increased, until at very high rates (5 and 10 $\mu g\,h^{-1}$) the minimal latency of about 11 h was observed. Infusions in the range of 0·2–0·5 $\mu g\,h^{-1}$ are thought to approximate the *in vivo* secretion of ecdysteroids. That these infusion rates resulted in an approximately 15-h latency suggests that the behaviourally relevant secretion of ecdysone is under way in normal animals by about 15 h prior to the onset of wandering behaviour. Photoperiod shift experiments (Dominick & Truman, 1984) also indicate an interval of about 15 h between a photoperiod-sensitive event and wandering behaviour. This time would coincide with the second pulse of PTTH proposed by Gilbert *et al.* (1981) which apparently elevates the ecdysteroid titre to a level leading to the induction of the behaviour.

An important feature of the wandering behaviour is that the duration of the spontaneous locomotor activity appears not to be a predetermined characteristic but instead is a function of the duration of ecdysteroid action which precedes the behaviour. Application of the JH mimic, EGS, at various times during exposure to endogenous or infused ecdysteroids resulted in behavioural durations proportional to the interval

of ecdysteroid action preceding the appearance of JH (Fig. 11). More directly, varying the duration of 20-HE infusion at 0·5 $\mu g\,h^{-1}$ resulted in a linear proportionality between the length of the infusion and the duration of the subsequently induced behaviour (Fig. 8). Thus, the duration of wandering behaviour is established as a direct consequence of the duration of ecdysteroid presence, and not as a preprogrammed repertoire which is simply triggered by a phasic hormonal signal.

In studies of vertebrate reproductive behaviour, relatively long but dose-dependent latencies similar to those reported here exist before the onset of lordosis behaviour induced in rabbits (30 h, McDonald, Vidal & Beyer, 1970) and in rats (16–22 h, Green, Luttge & Whalen, 1970). The long latency typically required for the induction of behavioural effects by steroids probably represents the time required for a sequence of hormonally stimulated RNA and protein synthetic steps which are thought to constitute the mechanism by which steroid mediated behavioural changes occur (McEwan, Davis, Parsons & Pfaff, 1979).

The duration or intensity of steroid-induced behaviour can be graded in vertebrates in response to varying the parameters of hormone exposure, as has been demonstrated with oestrogen-dependent mating behaviour in the rat (Aren-Engelbrektsson, Larsson, Sodersten & Wilhelmsson, 1970; Demassa, Smith, Tennent & Davidson, 1977), rabbit (McDonald *et al.* 1970), cat (Peretz, 1968) and guinea pig (Goy & Young, 1957). Therefore, the programming of the duration or intensity of induced behaviour as a cumulative steroid effect may be a phylogenetically widespread phenomenon.

Wandering latency and duration are controlled independently by different parameters of 20-HE exposure. The minimal effective 20-HE infusion lasts 4 h during which time the steroid probably acts by inducing primary biochemical changes such as mRNA and protein synthesis. Since the behavioural duration induced by such a short 20-HE infusion is also short (Fig. 11), the relevant biochemical changes would appear to have a relatively short half-life and quantitatively to support the behaviour. Thus, by increasing the duration of 20-HE exposure, the induced product might be synthesized over a longer period of time, thereby enabling the behaviour for a correspondingly extended period. Induction of new neurotransmitter or postsynaptic receptor species in the 20-HE target neurones are possible examples which would conform to this interpretation.

Although 4 h infusion with 20-HE was sufficient to induce wandering behaviour, a minimum latency of 11 h must intervene before the induced behaviour appears. Since this latency varies strictly as a function of 20-HE dose (Table 2) and is not influenced by infusion duration (Table 3) the rate of accumulation of the presumed induction product would be dose dependent as is typical with steroid hormones. In the simplest case the product might accumulate to a critical level (the threshold for wandering) at a rate proportional to the 20-HE concentration, thereby advancing the start of behaviour as 20-HE concentration increases. This accumulation would require at least 7 h in addition to the 4 h infusion of 20-HE (a total latency of 11 h at the highest effective hormone concentration. Alternatively, the dose-dependent accumulation of product to the threshold level may be more rapid but additional time could be required for a secondary, hormone-independent process which contributes significantly to the latency. Transport of induced neurotransmitter or receptor

molecules to appropriate pre- or postsynaptic regions of the putative 20-HE target neurones could provide such a delay.

Wandering behaviour induced by 20-HE infusion was often followed by a distinct second period of wandering which began early in the usual wandering gate (Figs 1, 7) and which was uniformly shorter than normal, averaging 7 h in length (Tables 2, 3). This reappearance of wandering was apparently due to the endogenous gated secretion of ecdysone, since second bouts of wandering behaviour were not observed in 20-HE-infused larvae lacking prothoracic glands. Evidently, the behavioural action of 20-HE does not necessarily include a programmed loss of behavioural sensitivity to subsequent re-induction as is true for eclosion hormone (Truman, 1978). Furthermore, varying the starting time and duration of 20-HE infusion into unoperated larvae greatly affected the onset time and duration of the induced behaviour, but had no effect on the initiation or duration of the repeat wandering. Indeed, when larvae were restrained and infused with 20-HE at the start of wandering about half of them entered a distinct second period of wandering extending well past the usual time when control larvae become inactive.

Juvenile hormone effects on wandering induction by 20-HE

The disappearance of JH from the tissues of the last instar larva of *Manduca* is a prerequisite for PTTH release (Nijhout & Williams, 1974*b*) and for ecdysteroids to induce premetamorphic changes in the epidermis (Riddiford, 1978). Allatectomy resulted in precocious wandering behaviour in earlier instars of *Manduca* as has been found for *Bombyx* (Bounhiol, 1938) and *Galleria* (Piepho, 1938). Thus, the requisite behavioural circuitry appears to be both present and responsive to its endocrine trigger from a time very early in post-embryonic development.

The release of PTTH and ecdysteroid necessary for wandering behaviour can be delayed if JH reappears before these secretory processes begin. Application of the JH mimic, EGS, to larvae during ecdysteroid infusion or during their normal time of release of ecdysteroid showed that JH can antagonize the action of 20-HE apparently at any time during the 24-h ecdysteroid release. Interestingly, any effects of ecdysteroid that have occurred prior to the application of EGS are subsequently manifest as the normal initiation and progression of the behaviour. Since applications of EGS just prior to the start of wandering had no effect, only the induction and not the expression of the behaviour is sensitive to JH. The spinning of very thin or flat cocoons by *H. cecropia* larvae which were treated with JH during the period when epidermal commitment could be disrupted (Riddiford, 1972) suggests that the endocrine activation of cocoon spinning is analogous to that of *Manduca* wandering in that the behavioural programme accumulates as a function of ecdysteroid action over time.

The ability of JH to modify the duration of wandering is probably the basis for the size-related variation of behavioural duration seen in *Manduca* larvae (Dominick & Truman, 1984). Wandering duration lengthens as larval weight increases in larvae with intact CA, but allatectomized 5th instar larvae show no such relationship. Therefore, it appears that following the elimination of measureable JH which starts when the larva reaches a critical size of about 5 g (Nijhout & Williams, 1974*b*), JH or its effects gradually decrease with time as the larva continues to grow. The residual JH effects may influence the behavioural action of 20-HE in proportion to their

magnitude. Presumably, in smaller larvae the level of covert JH effects is somewhat greater at the time of ecdysteroid release than in larger larvae, resulting in a slightly diminished ecdysteroid effect, and consequently in a shorter behaviour. Another interpretation is that the level of residual JH effects regulates the dynamics of ecdysteroid secretion from the prothoracic glands (Safranek, Cymborowski & Williams, 1980) and the altered ecdysteroid titre results in a modified behaviour.

Infusions of 20-HE into larvae with intact CA at various times during the 5th instar showed that responsiveness to infused hormone appears by the time larvae have reached 5·5 g (Fig. 13), a weight close to that described for 20-HE sensitivity of heart exposure (Nijhout, 1976). At this time the JH titre of the animals is rapidly declining as the CA become inactive (Granger *et al.* 1979) and JH-specific esterase appears (Vince & Gilbert, 1977; Beckage & Riddiford, 1982). As the effects of JH are erased during the period of growth beyond 5 g, the response to 20-HE becomes more rapid. The acquisition of a minimal latency at 7·5 probably represents maximal ecdysteroid sensitivity as a consequence of the virtual elimination of JH. This correlation of sensitivity with weight suggests that elimination of JH during the feeding stage of the 5th instar is the primary factor determining the ability of the larva to wander in response to 20-HE.

In larvae which had been allatectomized just prior to the 5th instar, wandering was induced to start only about 12 h earlier than the earliest 20-HE infused larvae with intact CA (Fig. 14 *vs* 12). Here, too, the infused 20-HE became increasingly effective with time, demonstrating that responsiveness to 20-HE improves over several days, even in the absence of measurable JH. Thus, endocrine events at the beginning of the instar, as well as at the 5 g size, are probably important to developing sensitivity to 20-HE.

In summary, wandering behaviour in *Manduca*, and the probably analogous prepupal behaviour patterns of many other Lepidoptera, are quantitatively determined by effects of ecdysteroids. These effects are prevented by the relatively high JH titres accompanying ecdysteroid action prior to the last instar, and may be subtly modified by the persistence of slight JH effects in the larval tissues during the period of ecdysteroid action which induces the behaviour.

We thank Professors Lynn M. Riddiford and Henry H. Hagedorn for reading an earlier draft of the manuscript. The work was supported by grants from NSF (PCM-8020975) and NIH (RO1 NS 13079) to JWT.

REFERENCES

AKAI, H. & KOBAYASHI, M. (1971). Induction of prolonged larval instar by the juvenile hormone in *Bombyx mori*. *Appl. Entomol. Zool.* **6**, 138–139.

AREN-ENGELBREKTSSON, B., LARSSON, K., SOLDERSTEN, P. & WILHELMSSON, M. (1970). The female lordosis pattern induced in male rats by estrogen. *Horm. Behav.* **1**, 181–188.

BECKAGE, N. E. & RIDDIFORD, L. M. (1982). Effects of parasitism by *Apanteles congragatus* on the endocrine physiology of the tobacco hornworm, *Manduca sexta*. *Gen. comp. Endocrin.* **407**, 308–322

BELL, R. A. & JOACHIM, F. G. (1976). Techniques for rearing laboratory colonies of tobacco hornworms and pink bollworms. *Ann. ent. Soc. Am.* **69**, 365–373.

BENZ, G. (1973). Reversal of spinning behavior in last instar larvae of *Pieris brassicae* treated with juvenile hormone derivatives. *Experientia* **29**, 1437–1438.

BOLLENBACHER, W. E., VEDECKIS, W. V. & GILBERT, L. I. (1975). Ecdysone titers and prothoracic gland activity during the larval-pupal development of *Manduca sexta*. *Devl Biol.* **44**, 46–53.

BOUNHIOL, J. J. (1938). Récherches experimentales sur le determinisme de la metamorphose chez les Lepidopteres. *Bull biol. Fr. Belg.* (Suppl.) **24**, 1–199.

BOWERS, W. S. (1969). Juvenile hormone: activity of aromatic terpenoid ethers. *Science, N. Y.* **164**, 323–325.

CHERBAS, P. T. (1973). Biochemical studies of insecticyanin. Ph.D. thesis, Harvard University, Cambridge, U.S.A.

DEMASSA, D. A., SMITH, E. R., TENNENT, B. & DAVIDSON, J. M. (1977). The relationship between circulating testosterone levels and male sexual behavior in rats. *Horm. Behav.* **8**, 275–286.

DAVIDSON, J. M. & LEVINE S. (1972). Endocrine regulation of behavior. *A. Rev. Physiol.* **34**, 375–408.

DOMINICK, O. S. & TRUMAN, J. W. (1984). The physiology of wandering behaviour in *Manduca sexta*: temporal organization and the influence of the internal and external environments *J. exp. Biol.* **110**, 35–51.

EPHRUSSI, B. & BEADLE, G. W. (1936). A technique for transplantation for *Drosophila*. *Am. Nat.* **70**, 218–225.

FAIN, M. J. & RIDDIFORD, L. M. (1975). Juvenile hormone titers in the hemolymph during late larval development of the tobacco hornworm, *Manduca sexta* (L.). *Biol. Bull. mar. biol. Lab., Woods Hole* **49**, 506–521.

FUJISHITA, M., OHNISHI, E. & ISHIZAKI, H. (1982). The role of ecdysteroids in the determination of gut-purge timing in the saturniid, *Samia cynthia ricini*. *J. Insect Physiol.* **28**, 961–967.

GIEBULTOWICZ, J. M., ZDAREK, J. & CHROSCIKOWSKA, U. (1980). Cocoon spinning behavior in *Ephestia kuehniella*; correlation with endocrine events. *J. Insect Physiol.* **26**, 459–464.

GILBERT, L. I., BOLLENBACHER, W. E., AGUI, N., GRANGER, N., SEDLAK, B., GIBBS, D. & BUYS, C. (1981). The prothoracicotropes: source of the prothoracicotropic hormone. *Am. Zool.* **21**, 641–653.

GOY, R. W. & YOUNG, W. C. (1957). Strain differences in the behavioral responses of female guinea pigs to estradiol benzoate and progesterone. *Behavior* **10**, 340–352.

GRANGER, N. A., BOLLENBACHER, W. E., VINCE, R., GILBERT, L. I., BAEHR, J. C. & DRAY, F. (1979). *In vitro* biosynthesis of juvenile hormone by the larval corpora allata of *Manduca sexta*: quantification by radioimmunoassay. *Molec. cell. Endocr.* **16**, 1–17.

GREEN, R., LUTTGE, W. G. & WHALEN, R. E. (1970). Induction of receptivity in ovariectomized female rats by a single intravenous injection of estradiol 17B. *Physiol. Behav.* **5**, 137–141.

HIGHNAM, K. C. & HILL, L. (1977). *The Comparative Endocrinology of the Invertebrates*. London: Edward Arnold Ltd. 357pp.

HORI, M. & RIDDIFORD, L. M. (1982). Isolation of ommochromes and 3-hydroxykynurentine from the tobacco hornworm, *Manduca sexta*. *Insect Biochem* **11**, 507–513.

KIGUCHI, K. & RIDDIFORD, L. M. (1978). A role of juvenile hormone in pupal development of the tobacco hornworm, *Manduca sexta*. *J. Insect Physiol.* **24**, 673–680.

LOUNIBOS, L. P. (1976). Initiation and maintenance of cocoon spinning behaviour by saturniid silkmoths. *Physiol. Entomol.* **1**, 195–206.

MCDONALD, P. G., VIDAL, N. & BEYER, C. (1970). Sexual behavior in the ovariectomized rabbit after treatment with different amounts of gonadal hormones. *Horm. Behav.* **1**, 161–172.

MCEWEN, B. S., DAVIS, P. G., PARSONS, B. & PFAFF, D. W. (1979). The brain as a target for steroid action. *A. Rev. Neurosci.* **2**, 65–112.

MELTZER, Y. L. (1971). *Hormonal and Attractant Pesticide Technology*. Park Ridge, New Jersey: Noyes Data Corp.

NIJHOUT, H. F. (1975*a*). A threshold size for metamorphosis in the tobacco hornworm, *Manduca sexta* (L.). *Biol. Bull. mar. biol. Lab., Woods Hole* **149**, 214–225.

NIJHOUT, H. F. (1975*b*). Dynamics of juvenile hormone action in larvae of the tobacco hornworm, *Manduca sexta* (L.). *Biol. Bull. mar. biol. Lab., Woods Hole* **149**, 568–579.

NIJHOUT, H. F. (1976). The role of ecdysone in pupation of *Manduca sexta*. *J. Insect Physiol.* **22**, 453–463.

NIJHOUT, H. F. & WILLAMS, C. M. (1974*a*). Control of moulting and metamorphosis in the tobacco hornworm, *Manduca sexta* (L.): growth of the last-instar larva and the decision to pupate. *J. exp. Biol.* **61**, 481–491.

NIJHOUT, H. F. & WILLIAMS, C. M. (1974*b*). Control of moulting and metamorphosis in the tobacco hornworm, *Manduca sexta* (L.): cessation of JH as a trigger for pupation. *J. exp. Biol.* **61**, 493–501.

OHTAKI, T., MILKMAN, R. D. & WILLIAMS, C. M. (1968). Dynamics of ecdysone secretion and action in the flesh fly *Sarcophaga peregrina*. *Biol. Bull. mar. biol. Lab., Woods Hole* **135**, 322–334.

PERETZ, E. (1968). Estrogen dose and duration of the mating period in cats. *Physiol. Behav.* **3**, 41–43.

PFAFF, D. W. (1980). *Estrogens and Brain Function*. New York: Springer-Verlag.

PIEPHO, H. (1938). Wachsturn and totale Metamorphose an Hantimplantaten bei der Washsmotte *Galleria mellonella* L. *Biol. Zbl.* **58**, 356–366.

PIEPHO, H. (1939). Hemmung der Verpuppung durch Corpora allata von Jungraupen bei der Wachsmotte *Galleria mellonella* L. *Naturwissenschaften* **27**, 675–676.

PIEPHO, H. (1950). Hormonale grundlagen der Spinntatigkeit bei Schmetterlingsraupen. *Z. Tierpsyhol.* **7**, 424–434.

PIEPHO, H. (1960). Hormonal control of moulting behavior and scale development in insects. *Ann. N.Y. Acad. Sci.* **89**, 564–571.

PITTENDRIGH, C. S. & SKOPIK, S. D. (1970). Circadian systems. V. The driving oscillation and the temporal sequence of development. *Proc. natn. Acad. Sci. U.S.A.* **65**, 500–507.

RIDDIFORD, L. M. (1972). Juvenile hormone in relation to the larval-pupal transformation of the Cecropia silkworm. *Biol. Bull. mar. biol. Lab., Woods Hole* **142**, 310–325.

RIDDIFORD, L. M. (1978). Ecdysone induced change in cellular commitment of the epidermis of the tobacco hornworm *Manduca sexta* at the initiation of metamorphosis. *Gen. comp. Endocr.* **34**, 438–446.

RIDDIFORD, L. M. & AJAMI, A. M. (1973). Juvenile hormone: its assay and effects on pupae of *Manduca sexta*. *J. Insect Physiol.* **19**, 749–767.

SAFRANEK, L., CYMBOROWSKI, B. & WILLIAMS, C. M. (1980). Effects of juvenile hormone on ecdysone dependent development in the tobacco hornworm, *Manduca sexta*. *Biol. Bull. mar. biol. Lab., Woods Hole* **158**, 248–256.

TRUMAN, J. W. (1972). Circadian organization of the endocrine events underlying the moulting cycle of larval tobacco hornworms. *J. exp. Biol.* **57**, 805–820.

TRUMAN, J. W. (1978). Hormonal release of stereotyped motor programmes from the isolated nervous system of the Cecropia silkmoth. *J. exp. Biol.* **74**, 151–173.

TRUMAN, J. W., RIDDIFORD, L. M. & SAFRANEK, L. (1974). Temporal patterns of response to ecdysone and juvenile hormone in the epidermis of the tobacco hornworm, *Manduca sexta*. *Devl Biol.* **39**, 247–262.

VINCE, R. K. & GILBERT, L. I. (1977). Juvenile hormone esterase activity in precisely timed last instar larvae and pharate pupae of *Manduca sexta*. *Insect Biochem.* **7**, 115–120.

WIELGUS, J. J., BOLLENBACHER, W. E. & GILBERT, L. I. (1979). Correlations between epidermal DNA synthesis and haemolymph ecdysteroid titre during the last larval instar of the tobacco hornworm, *Manduca sexta*. *J. Insect Physiol.* **25**, 9–16.

WILLIAMS, C. M. (1968). Ecdysone and ecdysone analogues: their assay and action on diapausing pupae of the cynthia silkworm. *Biol. Bull. mar. biol. Lab., Woods Hole* **134**, 344–355.

ZDAREK, J. & FRAENKEL, G. (1970). Overt and covert effects of endogenous and exogenous ecdysone in puparium formation of flies. *Proc. natn. Acad. Sci. U.S.A.* **67**, 331–337.

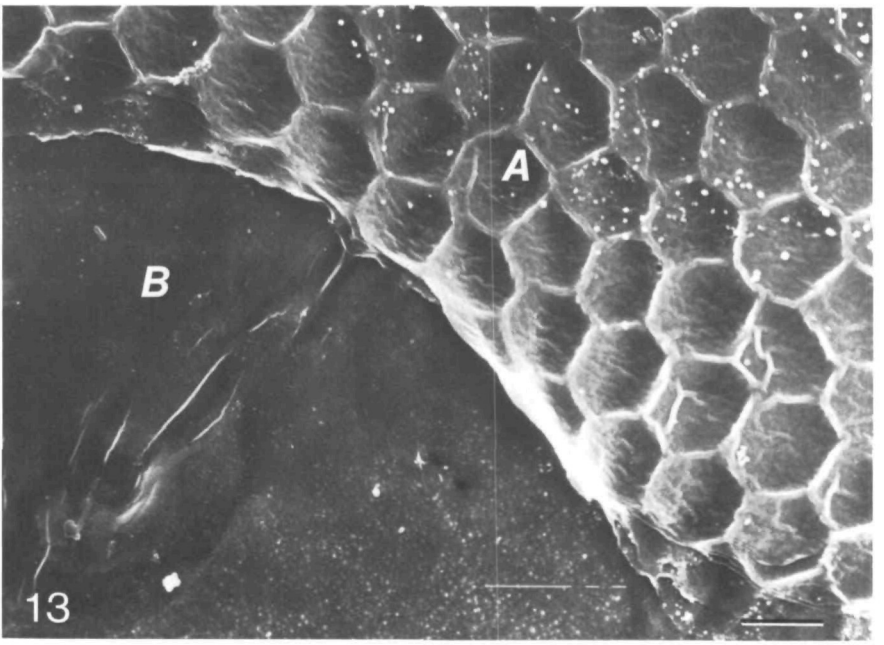

Fig. 13. Scanning electron microscope surface view of an elytron of *Cicindela scutellaris* treated for 15 min with concentrated KOH at 160 °C. In area *A*, the epicuticle is intact, but eroded. This area was still weakly iridescent. In area *B*, the epicuticle has been removed, exposing the surfaces of the exocuticle. This surface was non-iridescent. Scale bar, 10 μm.

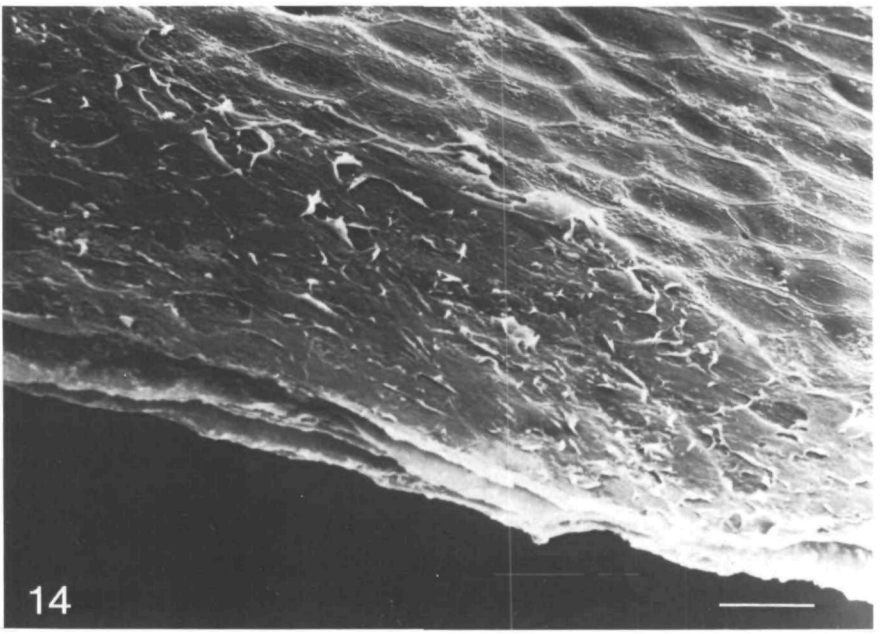

Fig. 14. Scanning electron microscope surface view of an elytron of *Cicindela formosa* treated for 15 min with concentrated KOH at 106 °C. The epicuticle has been dissolved. This sample was no longer iridescent. Scale bar, 10 μm.

Longer KOH treatments resulted in a progressive loss of the remaining brown colour. By 48 h, only a slight trace of the original maculation pattern was evident, and the elytron was a light straw colour. During this treatment, the outer exocuticle remained – the alveolate pattern was still visible in the surface. However, the thickness of this layer was reduced by 40 %, suggesting a leaching of exocuticular components.

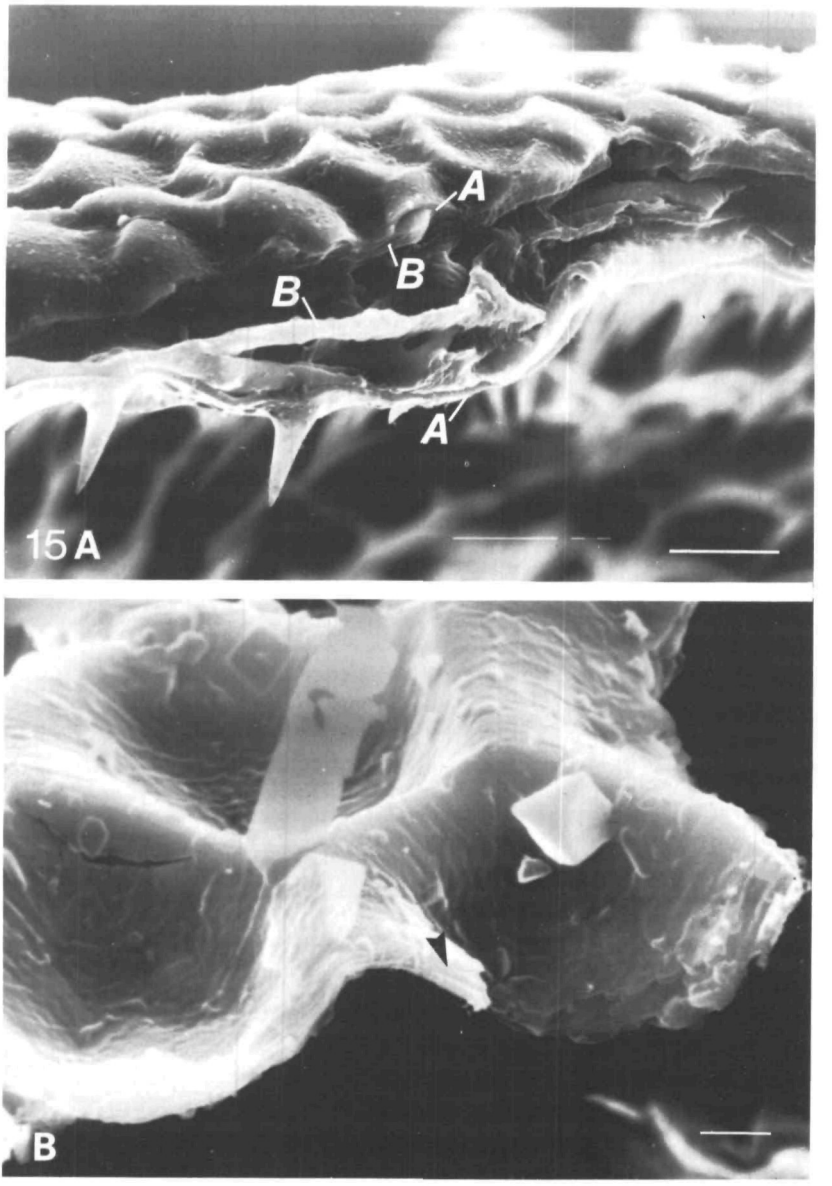

Fig. 15. Scanning electron microscope cross-section of an elytron of *Cicindela formosa* treated with concentrated H_2SO_4 for 48 h. (A) The endocuticle of the elytron has been dissolved, leaving a sleeve of epicuticle (*A*) and exocuticle (*B*). Scale bar, 10 μm. (B) A portion of the epicuticle separated from the outer exocuticle. Surface pattern and laminations are still intact (arrow). Scale bar, 2 μm.

The chitosan method of Campbell (1929) and van Wisselingh (1914) has long been used to distinguish chitinous from non-chitinous cuticle, although this technique is not conclusive (Richards, 1951). It requires the conversion of chitin to chitosan by treatment with concentrated KOH at 160 °C for 15 min. It is assumed that the non-chitinous elements of the exoskeleton (epicuticular components) are dissolved under

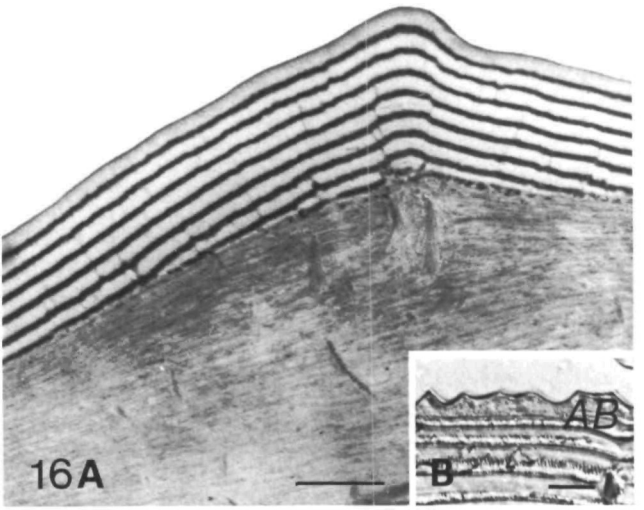

Fig. 16. (A) Transmission electron microscope cross-section of pigmented cuticle of *Cicindela formosa* treated with H_2O_2. The electron-dense layers of the epicuticle are reduced in thickness (compare with Fig. 9). Outer layers appear most reduced by the treatment. Scale bar, 1 μm. (B) Photomicrograph of the same tissue. The epicuticle and exocuticle (*AB*) are not strongly pigmented. Scale bar, 10μm.

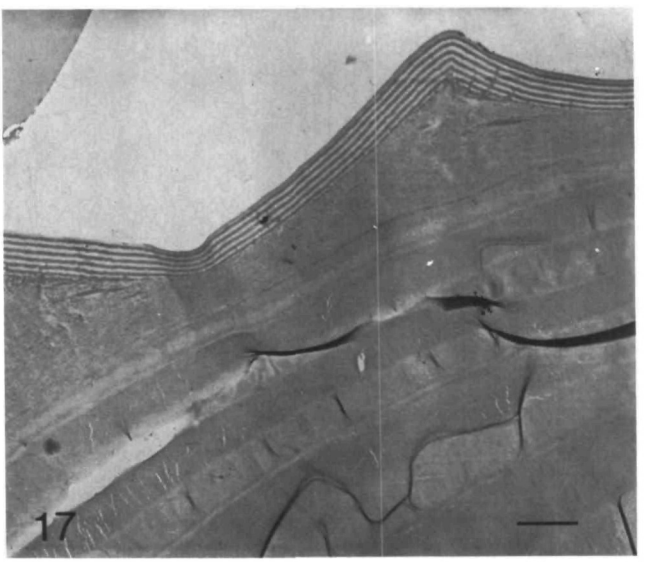

Fig. 17. Transmission electron micrograph cross-section of the elytral cuticle of *Cicindela repanda*. The epicuticle (*A*) is laminated, although no peak interference colour is reflected. Scale bar, 2 μm.

this alkali treatment. Samples of tiger beetle cuticle subjected to the chitosan test showed a severe break-up of the presumptive epicuticle. In *C. scutellaris*, an eroded epicuticle (area *A* in Fig. 13) was evident in some areas where a feebly iridescent sheen still appeared. If these treated samples were immersed in 8 % KOH for 18 h at room temperature, all traces of the presumptive epicuticle were removed, as well as the remaining pigmentation. In *C. formosa*, the epicuticle and iridescence were completely removed by the chitosan treatment (Fig. 14).

In contrast to the results of the alkali treatments, endocuticle is dissolved rapidly in concentrated sulphuric acid (Sprung, 1931; Wigglesworth, 1933; Hackman, 1974), whereas sclerotized exocuticle and epicuticle are said to remain intact. Tiger beetle elytra immersed in sulphuric acid showed a rapid dissolution of inner 'plywood' mesocuticle, leaving a thin, flexible sleeve of putative epicuticle and outer exocuticle, while the structural coloration of the elytron remained unaltered (Fig. 15A). SEM examinations of the treated cuticle revealed that the outer laminated layer (layer *A*) retained its ultrastructure intact (Fig. 15B). The outer exocuticle was also intact and pigmented through the first 48 h of treatment. The residual cuticle still appeared dark brown in transmitted light. Portions of the helicoidal exocuticle below could be seen adhering to the lower side of the outer exocuticle. Frequently, areas were observed in which the epicuticle had separated from the outer exocuticle, and these fragments were found floating on the surface of the acid. Even these isolated fragments maintained a laminated appearance under SEM, as well as an iridescence.

Treatments of elytral cuticle with H_2O_2 significantly altered the cuticle coloration. When observed in transmitted light, the brown coloration became more translucent. The outer exocuticle and epicuticle appeared either light brown or clear of pigment in microscopic sections (Fig. 16B). The structural colour of the cuticle surface became duller and shorter in principal wavelength. Similar results were obtained when samples were treated with 20 % H_2O_2 at 26 °C for 24–48 h.

TEM micrographs revealed a 40 % reduction in thickness of dense epicuticular layers in the H_2O_2-treated samples (Fig. 16A). The bands were progressively thinner towards the outer surface. The overall thickness of the epicuticle was not diminished significantly.

DISCUSSION

Cuticle histology

Probably because it is extremely thin, the epicuticle is the least understood portion of the insect integument. Its chemistry, structure and the terminology of epicuticular components have been controversial. Only a few, diverse arthropods have been studied intensively, and very little work has focused on the epicuticle of hard, adult exoskeletons (Delachambre, 1970). This is not surprising since hard cuticle is difficult to prepare and section for transmission electron microscopy.

The epicuticle, by definition, is non-chitinous or reacts negatively to tests for chitin (chitosan method). It is the first layer formed during the moult sequence and assumes the outermost position in the strata of the exoskeleton, bearing the surface microsculpture. The general model of epicuticle structure recognizes five components. These are the cuticulin layer, the inner epicuticle, the outer epicuticle, the wax layer

and the cement layer, listed in order of deposition (Filshie, 1982). The wax and cement layers are secreted upon the epicuticular surface by the epicuticular filaments and dermal glands, respectively. Filshie (1982) notes that the saturated lipids of wax layers do not survive conventional electron microscope preparations, and their supposed appearance in electron micrographs is probably an artifact or misidentification of other layers. Identifications of cement layers have been made by location only and remain unsupported by developmental studies.

The reflective layers of cicindelid cuticle are not a form of cement or tectocuticle. The so-called 'Sekretschicht'–the source of the structural colours–is formed preecdysially, not secreted from dermal glands (Schultz & Rankin, 1985). Furthermore, the very even pattern of layering over a contoured surface would be unlikely if it were formed from secretions of relatively dispersed glands. The layers remain evenly spaced around and even within the mouth of dermal glands (Fig. 4). Extraordinary properties of the two components and the dermal glands themselves would be required to produce such regular secretions over the entire cuticular surface.

The cuticulin layer (or outer epicuticle of Neville, 1975) is the first epicuticlar layer secreted by the epidermis during the moult sequence. It appears as a thin (10–20 nm), dense membrane at the outer edge of the cuticle in electron micrographs. In some insects (Locke, 1966; Delachambre, 1970), it initially appears laminated, but condenses to a uniform appearance. Micrographs of *C. formosa* show a dense region, 30–40 nm thick, at the edge of the outermost electron-lucent band (*cu* in Fig. 6E). The inner side of this region appears finely laminated, becoming more uniformly dense towards the surface of the cuticle. This region appears in all the *Cicindela* species and samples studied, including the pharate cuticle (see Schultz & Rankin, 1985), and is interpreted as the cuticulin layer. In mature cicindelid cuticle only, a very thin (10 nm), electron-lucent membrane appears above the cuticulin. This structure may represent the outer epicuticle that is thought to arise by separation from the cuticulin layer prior to ecdysis (Filshie, 1982).

The bulk of the epicuticle is composed of the inner epicuticle, 0·5–1 μm thick. Its appearance varies among species, and consequently, a wide range of chemical constituents have been proposed. These include protein, lipids, lipoprotein and dihydroxyphenols. This layer borders directly on the helicoidal exocuticle beneath it (Neville, 1975). Laminated inner epicuticles have been described, but these laminations have been transitory during the moult sequence (Delachambre, 1970), or have extremely short periods of less than 40 nm (Gupta & Smith, 1969; Gluud, 1968; Zacharuk, 1972).

The multilayered outer region of cicindelid cuticle is best described as inner epicuticle, due to its location, ultrastructure and solubility in KOH, in combination with a resistance to strong acid (Region *A* in Figs 2–7). Treatments with solvents demonstrate that this region is chemically distinct from the chitinous layers below. If it were exocuticle, the ultrastructure of the layers would survive the alkali treatment (Hackman, 1974). Furthermore, it lacks any indication of fibrillar architecture that is evident in the alkali-resistant layers or in the exocuticles of other insects.

The outermost layer of inner epicuticle, presumably secreted first, is always electron-lucent, while the innermost layer may be electron-lucent or electron-dense. More layers are produced at the borders of the epidermal cells than at their centres.

These borders are indicated by the hexagonal ridges in the surface microsculpture (Neville, 1975). Areas of elytral cuticle which lack pigmentation (i.e. the maculations), also lack electron-dense layers in the epicuticle. Perhaps the cicindelid inner epicuticle is described best as a homogeneous electron-lucent material, impregnated by electron-dense material at discrete intervals in those cuticles that are pigmented.

The epicuticle as an interference reflector

It appears that the epicuticle is the source of structural colours in *Cicindela*. Maceration or removal of the epicuticle with KOH results in the deterioration or loss of iridescent coloration. Conversely, removal of the other components of the integument produces no loss of colour. The change of hue under oblique incidence demonstrates that the structural colours result from constructive interference of reflected light.

The repetitive layering of two materials in the epicuticle, whose thicknesses are less than half the wavelength of visible light, is characteristic of a multilayer interference reflector. The two layers are distinct in their electron densities, and are not an artifact of the helicoidal arrangement of cuticle fibrils, as in the reflective exocuticle of optically active scarab beetles (Neville & Caveney, 1969). Multilayer reflectors have been described in a wide diversity of animal tissues, and the basic principles of interference in animal reflectors are reviewed by Land (1972).

In the 'ideal' case of thin film reflection, the wavelength of the first order maximum reflectance (λ max) depends on the thickness (d) and refractive index (n) of each layer such that

$$\lambda \max = 4nd \sin \theta, \tag{1}$$

where θ is the angle of incidence. Under 'ideal' conditions, the optical thicknesses of both layers are equivalent ($n_L d_L = n_D d_D$, where L indicates the lucent layer and D the dense layer). Each layer acts as a quarter-wavelength reflecting plane, with the reflections from all interfaces constructively interfering to produce the total coloration.

The optical thickness of each component is different ($n_L d_L \neq n_D d_D$) in a 'non-ideal' multilayer system. The first order reflectance peak occurs at

$$\lambda \max = 2(n_L d_L + n_D d_D) \tag{2}$$

under normal angle of incidence. Under 'non-ideal' conditions the peak reflectance and the band width of the first order peak are diminished. The result is a sharper peak and purer colour (Land, 1972). The reflecting layers of tiger beetle epicuticle are best described as a 'non-ideal' system. The thicknesses of the electron-dense (d_D) and the electron-lucent (d_L) layers vary considerably through a single point in the stack (Table 1). Assuming that the refractive indices (n_L and n_D) remain stable, the ratio d_L/d_D does not remain constant throughout the reflector.

A quarter-wave interference reflector has been described by Durrer & Villiger (1972) in the exocuticle of *Euchroma gigantea*, which consists of a series of electron-lucent and electron-dense bands similar to the epicuticle of *Cicindela*. The dimensions of the layers imply an average refractive index of 1·75 for the reflector. The authors propose that the multilayer system contains electron-dense melanin layers (RI = 2·0) separated by chitin (RI = 1·5), similar to the keratin-melanin interference

Table 1. *Average thickness of electron-lucent* (L) *and electron-dense* (D) *layers in four* Cicindela *species with predicted and experimental values of elytral reflectance*

Specimen	SEM bilayer thickness (nm)	Mean L layer thickness (nm)	Mean D layer thickness (nm)	Calculated λ max (nm) $n_L = 1{\cdot}5$; $n_D = 2{\cdot}0$	Experimental λ max (nm)
C. formosa					
ridge	188	106·59 ± 6.76	93·63 ± 11·756	694·31	655
alveolar basin		101·99 ± 5·292	74·974 ± 6·752	605·77	
C. scutellaris rugata	143	67·197 ± 4·08	72·147 ± 4·591	489·93	499
C. splendida	178	102·03 ± 14·907*	71·428 ± 6·563	591·8	635
C. repanda					
ridge	—	137·73 ± 18·233	110·65 ± 12·156	855·79	—
alveolar basin		81·22	88·035 ± 6·815	595·8	

Standard deviation values indicate the variation between successive layers in the epicuticle.
Calculations of λ max assume a refractive index (n) of 1·5 for L layers and 2·0 for D layers.
* The outermost L layer measured 130 nm in this sample.

reflectors of bird feathers (Durrer & Villiger, 1970). In their approach, the authors calculated the wavelength of maximum reflectance for each layer separately, in addition to determining the reflectance from the series of bilayers (equation 2). They concluded that a mixture of these reflected components results, producing the total colour.

Mossakowski (1980) examined interference reflectors in the cuticles of the buprestid, *Chrysocroa vittata*, and the tiger beetle, *Cicindela campestris*. Mossakowski calculated reflectances for a number of possible refractive indices using the theoretical treatment of Huxley (1968). He proposed that an average refractive index of 1·75 for the bilayers of *C. camprestis* would cause a total reflectance value far exceeding those determined experimentally. Mossakowski's measurements of total reflectance predicted refractive indices of 1·5 and 1·6 for the light and dense layers respectively. However, these values and the dimensions of the layers observed under electron microscopy predicted a wavelength of peak reflectance substantially below those recorded spectrophotometrically. Mossakowski assumed that the reflecting layers had experienced a 10–15 % shrinkage due to specimen preparation or exposure to the electron beam.

The dimensions of the interference layers of cicindelids presented in this paper suggest a relatively high average refractive index near 1·75 for the pairs of layers. Values of 1·5 and 2·0 for the light and dense layers predict peak wavelengths which approximate to the spectrophotometric results for *C. scutellaris* and *C. formosa* (Table 1). Refractive indices of 1·5 and 1·6 would predict substantially shorter wavelengths of peak reflectance. The epicuticle of *C. repanda* varied greatly in layer thickness and its reflectance exhibited no single peak within the visible wavelengths.

Even assuming an average refractive index of 1·75, calculations using the average thicknesses of epicuticular layers predict values of λ max well below the reflectance peak of *C. splendida*. Unlike the other specimens, the outermost electron-lucent layer of *C. splendida* is 40–50 nm thicker than all the underlying electron-lucent layers.

This layer makes a significant contribution to the large standard deviation in the average thickness of these layers. Variation in the thickness of the inner layers is less than that of *C. repanda* but greater than the variation in *C. scutellaris*. A λ max of 638 nm is predicted if calculations are based upon the superficial electron-lucent layer ($d_L = 130$ nm, $n_L = 1{\cdot}5$) and the underlying dense layer ($d_L = 62$ nm, $n_L = 2{\cdot}0$). This value is close to the experimental reflectance peak of 635 nm. Since the surface of *C. splendida* is so deeply sculptured with the alveolate pattern, the superficial epicuticular layers may contribute more to the peak reflectance than the underlying layers. Peak reflectances from deeper layers may occur at angles which depart from the angle of reflection that is sampled by the spectrophotometer.

In *C. scutellaris rugata* and the green form of *C. campestris* (Mossakowski, 1980), the thickness of the light and dense layers are roughly equivalent. In these cases, the average refractive index $\bar{n}$ may be estimated from the experimental peak wavelength and the thickness of each bilayer (d_{DL}):

$$\lambda \max = 2\bar{n}d_{DL} \tag{3}$$

$$\text{or } \bar{n} = \lambda \max/2d_{DL}. \tag{4}$$

For *C. scutellaris rugata*, an average refractive index of 1·74 is predicted.

No evidence of shrinkage appeared in the samples of cicindelid cuticle. The structural colours of specimens were observed unchanged within the embedding medium, indicating that shrinkage did not result from specimen preparation. SEM measurements of epicuticular bilayers corresponded well with bilayer measurements made from transmission electron micrographs. If bilayers measured from SEM micrographs were assumed to shrink 10% under the electron beam, they would appear 10–20 nm thinner than the average thickness of bilayers measured from TEM micrographs. If shrinkage had occurred under the electron beam, TEM measurements should fall below the thicknesses measured under SEM.

The relatively low total reflectance of cicindelid epicuticle may be due to its alveolate microsculpture. If the angle of incident light departs from normal, the wavelength of peak reflectance becomes shorter according to

$$\lambda \max = 4nd \cos \theta, \tag{5}$$

where θ is the angle of refraction within a single layer. In addition, each successive epicuticular layer conforms to the alveolate pattern of the surface. The wavelength of peak reflectance for multilayer reflectors at oblique incidence is then given by:

$$\lambda \max = 2(n_L d_L \cos \theta_L + n_D d_D \cos \theta_D), \tag{6}$$

where θ is the angle of incidence in the layer of lower density. Similarly, the reflectance at each interface is dependent upon the angle of refraction (Land, 1972). Thus, the wavelength and the intensity of reflection are affected by deviations in angle of incidence and refraction which occur continuously throughout the horizontal dimensions of the epicuticular layers. Due to these effects, and the scattering of reflected light by an alveolate surface, the spectrophotometric analysis of reflected light from the epicuticle must surely underestimate the reflectance predicted by normal theoretical conditions.

The peak reflectance is also dependent upon the constancy of layer thickness throughout the epicuticle. In *Cicindela*, the thicknesses of the bilayers vary both horizontally and vertically within the epicuticle (Table 1). The theoretical treatment of non-ideal, multilayer reflectors assumes that these dimensions remain constant. This non-uniformity in layer thickness and angle, with respect to incident light, clearly places the cicindelid epicuticle as an extremely complex example of a biological interference reflector. The epicuticle represents a non-ideal, multilayer system moulded into a shallow honeycomb form, and is not adequately described by theoretical treatments for regularly spaced, planar systems.

Correlations between electron microscope measurements and reflectance data should not be over-emphasized. The amount of cuticle sectioned is not comparable to the area of elytral material sampled for reflectance. The variability within the interference reflector has already been described. In addition, there is always uncertainty as to whether the section is precisely perpendicular to the interference layers.

With rare exceptions, the brown or black colours of insect cuticles are attributed to sclerotization and/or melanization of the cuticle (Richards, 1967). Eumelanins predominate as the brown or black pigments of insect integument (Hackman, 1974), and the pigmentation of *Cicindela* has been ascribed to melanin since the work of Shelford (1917). Unfortunately, it is exceedingly difficult to identify small amounts of melanin by staining or chemical analysis. Since the individual layers of dense material in the epicuticle are not resolvable under light microscopy, their optical properties cannot be examined separately. The treatment with KOH removes the epicuticle from the pigmented exocuticle, and produces a solution that is stained brown with dissolved epicuticle. But it is also possible that melanin may be leached from the exocuticle by the treatment (Richards, 1967).

Richards (1967) found that treatment with H_2O_2 will bleach melanin particles without removing them from the cuticle. Tiger beetle elytra were treated with H_2O_2 to determine the role of melanin in the elytral coloration. If melanin is involved simply as an absorbent background to the interference reflector, the iridescent colour should be reduced in intensity, but not altered in hue when the pigment is bleached (Mason, 1927). In treatments of *C. formosa*, a reduction in intensity and predominant wavelength resulted, as well as a thinning of pigmented colour in the cuticle. The change in reflected colour may be due to the bleaching of melanin within the structure of the reflecting epicuticle itself.

The structural dimensions of the two epicuticular layers, in conjunction with the experimental reflectance results, suggest that the epicuticular reflector is composed of an electron-lucent layer with a refractive index of 1·5 and a dense layer of 2·0. A refractive index of 1·5 is acceptable for insect cuticular proteins (Neville, 1975). This study proposes that the unusually high refractive index of 2·0 is provided by layers of melanin or melanoproteins. Precedents for such a system can be found in iridescent bird feather colouration (Greenwalt, Brandt & Friel, 1960; Rutschke, 1966; Durrer & Villiger, 1966, 1970). Additional melanin in the outer exocuticle provides an absorbent background for transmitted and extraneous wavelengths, hence purifying the reflected colour. Circumstantial evidence for the role of melanins is found in the restrictive co-occurence of pigmentation, iridescence and epicuticular lamination. Specific chemical analysis is still required to verify the identity of the electron-dense layer as melanin.

Structural coloration in Cicindela

The specific coloration of structurally-coloured tiger beetles depends upon the relative thicknesses of the epicuticular layers. In *C. formosa, C. scutellaris* and *C. splendida*, the dimensions of these layers are sufficient to cause the constructive interference of visible wavelengths of light. In epicuticles with regular laminations and a relatively smooth microsculpture, as in *C. scutellaris*, the reflectance colours are purer.

In some areas of *C. repanda* elytra, epicuticular laminations are too wide to reflect light at visible wavelengths (Fig. 17). However, visible wavelengths are reflected from areas where the layers are sufficiently thin in the highly variable epicuticle, e.g. within the alveoli. Furthermore, visible wavelengths may be reflected from thicker layers at oblique incidence due to the effect of angle of incidence on the wavelength of maximum reflectance. Thus, while the layers of *C. repanda* may reflect maximally above 760 nm, shorter red wavelengths will be reflected by the highly angled pattern of ridges in the microsculpture. The results of these factors is a relatively poor reflectance of any one visible wavelength, producing an overall flat brown appearance upon casual observation. Under the dissecting microscope, a wide range of reflected colours (predominantly red) can be observed from various points on the surface microsculpture. Although at first glance the elytra of *C. repanda* do not appear to be structurally coloured, the epicuticular structure is consistent with the epicuticular reflectors of other iridescent species.

Thus, tiger beetle structural coloration depends upon three variables: the thickness, uniformity and microsculpture of the reflecting layers. In species which reflect a narrow band of short wavelengths, the epicuticular bilayers are relatively thin and the intensity and purity of the colour depend upon the severity of the alveolate microsculpture. Several species which appear brown or coppery bear relatively thick and variable epicuticular bilayers. The deeply pitted microsculpture of the reflector further diminishes the intensity and purity of the reflected colour, resulting in a broad range of reflected wavelengths of low intensity. Small variations in the basic multilayer structure of the epicuticle are responsible for the wide variation in colour observed in the genus *Cicindela*.

The authors thank Dr S. Meier, University of Texas, for the use of the SEM, Dr Bird and K. Kotora of Rutgers University, for their assistance in the reflectance spectrophotometry, and the Texas Department of Parks and Wildlife for permission to collect specimens. We especially appreciate the assistance of Susan Houghton, MBL, Woods Hole, MA, who sectioned and photographed the TEM material. This study was supported partially by NSF Grant 2610711250.

REFERENCES

Bernard, G. D. & Miller, W. H. (1968). Interference filters in the corneas of Diptera. *Invest. Ophthamol.* **7**, 416–434.

Biedermann, W. (1914). Farbe und Zeichnung der Insecten. In *Handbuch Vergleichende Physiologie*, (ed. H. Winterstein), pp. 1657–1994.

Bouligand, Y. (1972). Twisted fibrous arrangements in biological materials and cholesteric mesophases. *Tissue Cell.* **4**, 189–217.

CAMPBELL, F. L. (1929). The detection and estimation of insect chitin; the irrelation of chitinization to hardness and pigmentation of the cuticula of the American cockroach, *Periplaneta americana*. *Ann. ent. Soc. Am.* **22**, 401–426.

DELACHAMBRE, J. (1970). Etudes sur l'épicuticle des insectes. La développement de l'épicuticle chez l'adulte de *Tenebrio molitor* L. (Insecta: Coleoptera). *Z. Zellforsch. mikrosk. Anat.* **108**, 380–396.

DURRER, H. & VILLIGER, W. (1966). Schillerfarben der Trogoniden. *J. Orn., Lpz* **107**, 1–36.

DURRER, H. & VILLIGER, W. (1970). Schillerfarben des Goldcuckucks, *Chysococcyx cupreous* Shaw, im Elektronenmikroskop. *Z. Zellforsch. mikrosk. Anat.* **109**, 407–413.

DURRER, H. & VILLIGER, W. (1972). Schillerfarben von *Euchroma gigantea* L., elektronenmikroskopische Untersuchung der Elytren. *Int. J. Insect. Morph. Embryol.* **1**, 233–240.

FILSHIE, B. (1982). Fine structure of the cuticle of insects and other arthropods. In *Insect Ultrastructure*, Vol. 1, (eds R. C. King & M. Akai), pp. 281–312. New York: Plenum Press.

GAUMER, G. C. (1977). The variation and taxonomy of *Cicindela formosa* Say (Coleoptera: Cicindelidae). Ph.D. thesis, Texas A & M University. 253 pp.

GHIRADELLA, H., ANESHANSLEY, D., EISNER, T., SILBERGLIED, R. E. & HINTON, H. E. (1972). UV reflection of male butterfly: interference colour caused by thin-layer elaboration of wing scales. *Science, N.Y.* **178**, 1214–1217.

GLUUD, A. (1968). Zur Feinstruktur der Insektencuticula. Ein Beitrag zur Frage des Eigengiftschutzes der Wanzencuticula. *Zool. Jb. (Anat.)* **85**, 191–227.

GREENWALT, C. H., BRANDT, W. & FRIEL, D. (1960). The iridescent colors of hummingbird feathers. *Proc. Am. Phil. Soc.* **104**, 249–253.

GUPTA, B. L. & SMITH, D. S. (1969). Fine structure organization of the spermatheca in the cockroach, *Periplaneta americana*. *Tissue Cell* **1**, 289–324.

HACKMAN, R. H. (1974). Chemistry of insect cuticle. In *The Physiology of Insecta*, Vol. 6, (ed. M. Rockstein), pp. 216–270. New York: Academic Press.

HASS, W. (1916). Ueber Metallfarben bei Buprestiden. *Sber. Ges. natur. Freunde Berl.* 332–343.

HEPBURN, H. R. (1972). Some mechanical properties of crossed fibrillar chitin. *J. Insect Physiol.* **18**, 815–820.

HUXLEY, A. F. (1968). A theoretical treatment of the reflexion of light by multilayer structures. *J. exp. Biol.* **48**, 227–245.

LAND, M. F. (1972). The physics and biology of animal reflectors. *Prog. Biophys. molec. Biol* **24**, 75–106.

LOCKE, M. (1966). The structure and formation of the cuticulin layer in the epicuticle of an insect, *Calpodes ethlius* (Lepidoptera: Hesperiidae). *J. Morph.* **118**, 461–494.

MANDL, K. (1931). Künstliche Veränderung der Farben an *Cicindela nitida* Licht und an anderen *Cicindela*-Arten. *Z. Morph. Okol. Tiere* **22**, 110.

MASON, C. W. (1927). Structural colors in insects. *J. phys. Chem.* **31**, 321–354.

MOSSAKOWSKI, D. (1980). Reflection measurements used in the analysis of structral colours of beetles. *J. Microscopy* **116**, 350–364.

NEVILLE, A. C. (1975). *Biology of the Arthropod Cuticle*. Berlin: Springer-Verlag.

NEVILLE, A. C. (1980). Optical methods in cuticle research. In *Cuticle Techniques in Arthropods*, (ed. T. A. Miller), pp. 45–89. New York: Springer-Verlag.

NEVILLE, A. C. & CAVENEY, S. (1969). Scarabeidae exocuticle as an optical analogue of cholesteric liquid crystals. *Biol. Rev.* **44**, 531–562.

ONSLOW, H. (1920). The iridescent colours of insects. 1. The colours of thin films. *Nature, Lond.* **106**, 149–152.

RICHARDS, A. G. (1951). *The Integument of Arthropods*. St. Paul: University of Minnesota Press.

RICHARDS, A. G. (1967). Sclerotization and the localization of brown and black colors in insects. *Zool. J. (Anat.)* **84**, 25–62.

RUTSCHKE, E. (1966). Submikroskopische Struktur schillernder Federn von Entenvögeln. *Z. Zellforsch. mikrosk. Anat.* **72**, 432–443.

SCHULTZ, T. D. & RANKIN, N. A. (1985). Developmental changes in the interference reflectors and colorations of tiger beetles (*Cicindela*). *J. exp. Biol.* **117**, 111–117.

SHELFORD, V. E. (1917). Color and color pattern mechanisms of tiger beetles. *Illinois. biol. Monogr.* **3**, 4.

SPRUNG, F. (1931). Die Flugeldecken der Carabidae. *Z. Morph. Ökol. Tiere* **24**, 435–490.

STEGMANN, F. (1930). Die Flugeldecken der Cicindelidae. Ein Beitrag zur Kenntnis der Insektcuticula. *Z. Morph. Ökol. Tiere* **18**, 1–73.

VAN WISSELINGH, C. (1914). Anwendung der in der organishen Chemie gebräuchlichen Reaktionen bei der phytomikrochemischen Untersuchungen. *Folia microbiol., Delft* **3**, 165–198.

WIGGLESWORTH, V. B. (1933). The physiology of the cuticle and of ecdysis in *Rhodnius prolixus* (Triatomidae: Hemiptera) with special reference to the function of the oenocytes and of the dermal glands. *Q. Jl microsc. Sci.* **76**, 269–315.

WIGGLESWORTH, V. B. (1972). *The Principles of Insect Physiology*. London: Chapman & Hall.

ZACHARUK, R. Y. (1972). Fine structure of the cuticle, epidermis, and fat body of larval Elateridae (Coleoptera) and changes acquainted with molting. *Can. J. Zool.* **50**, 1463–1487.

ZELAZNY, B. & NEVILLE, A. C. (1972). Quantitative studies on fibril orientation in beetle endocuticle. *J. Insect Physiol.* **18**, 1095–2122.